

ADVERTIMENT. L'accés als continguts d'aquesta tesi doctoral i la seva utilització ha de respectar els drets de la persona autora. Pot ser utilitzada per a consulta o estudi personal, així com en activitats o materials d'investigació i docència en els termes establerts a l'art. 32 del Text Refós de la Llei de Propietat Intel·lectual (RDL 1/1996). Per altres utilitzacions es requereix l'autorització prèvia i expressa de la persona autora. En qualsevol cas, en la utilització dels seus continguts caldrà indicar de forma clara el nom i cognoms de la persona autora i el títol de la tesi doctoral. No s'autoritza la seva reproducció o altres formes d'explotació efectuades amb finalitats de lucre ni la seva comunicació pública des d'un lloc aliè al servei TDX. Tampoc s'autoritza la presentació del seu contingut en una finestra o marc aliè a TDX (framing). Aquesta reserva de drets afecta tant als continguts de la tesi com als seus resums i índexs.

ADVERTENCIA. El acceso a los contenidos de esta tesis doctoral y su utilización debe respetar los derechos de la persona autora. Puede ser utilizada para consulta o estudio personal, así como en actividades o materiales de investigación y docencia en los términos establecidos en el art. 32 del Texto Refundido de la Ley de Propiedad Intelectual (RDL 1/1996). Para otros usos se requiere la autorización previa y expresa de la persona autora. En cualquier caso, en la utilización de sus contenidos se deberá indicar de forma clara el nombre y apellidos de la persona autora y el título de la tesis doctoral. No se autoriza su reproducción u otras formas de explotación efectuadas con fines lucrativos ni su comunicación pública desde un sitio ajeno al servicio TDR. Tampoco se autoriza la presentación de su contenido en una ventana o marco ajeno a TDR (framing). Esta reserva de derechos afecta tanto al contenido de la tesis como a sus resúmenes e índices.

WARNING. The access to the contents of this doctoral thesis and its use must respect the rights of the author. It can be used for reference or private study, as well as research and learning activities or materials in the terms established by the 32nd article of the Spanish Consolidated Copyright Act (RDL 1/1996). Express and previous authorization of the author is required for any other uses. In any case, when using its content, full name of the author and title of the thesis must be clearly indicated. Reproduction or other forms of for profit use or public communication from outside TDX service is not allowed. Presentation of its content in a window or frame external to TDX (framing) is not authorized either. These rights affect both the content of the thesis and its abstracts and indexes.

Early-Middle Pleistocene *Sus* and *Bison* from Western Palaeartic: Taxonomy, Paleobiology and Distribution

Leonardo Sorbelli

Ph.D. Dissertation 2023



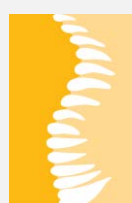
Supervisors: Joan Madurell-Malapeira,
Marco Cherin, Salvador Moyà-Solà

Academic tutor:
Salvador Moyà-Solà

Programa de Doctorat en Geologia, Universitat Autònoma de Barcelona

Institut Català de Paleontologia Miquel Crusafont

UAB
Universitat Autònoma
de Barcelona



ICP^R

Institut Català de Paleontologia
Miquel Crusafont



Early-Middle Pleistocene *Sus* and *Bison* from Western Palaeartic: Taxonomy, Paleobiology and Distribution

Leonardo Sorbelli

Ph.D. Dissertation

2023

Supervisors: Joan Madurell-Malapeira,
Marco Cherin, Salvador Moyà-Solà

Academic tutor:
Salvador Moyà-Solà

Programa de Doctorat en Geologia, Universitat Autònoma de Barcelona

Institut Català de Paleontologia Miquel Crusafont

UAB
Universitat Autònoma
de Barcelona

 **ICP**^R
Institut Català de Paleontologia
Miquel Crusafont

All that we can do is to keep steadily in mind that each organic being is striving to increase in a geometrical ratio; that each, at some period of its life, during some season of the year, during each generation, or at intervals, has to struggle for life and to suffer great destruction. When we reflect on this struggle, we may console ourselves with the full belief that the war of nature is not incessant, that no fear is felt, that death is generally prompt, and that the vigorous, the healthy, and the happy survive and multiply.

-Charles Darwin

The car's on fire and there's no driver at the wheel [...]

We're trapped in the belly of this horrible machine

and the machine is bleeding to death.

-Godspeed you! Black Emperor

ABSTRACT [English]

The Early Pleistocene is one of the most important periods for the evolution of the biosphere in the Western Palearctic. The climatic changes affecting the Northern Hemisphere from the mid-Pliocene deeply modified the ecosystems of Europe and settled the conditions for a major transition occurred during the latest stages of the Early Pleistocene. The long-term global cooling and the glacial dynamics intensified after ca. 3.0 Ma and, stronger, at ca. 1.4–1.2 Ma. The periodicity of Glacial-Interglacial (G-IG) cycles ultimately passed from ca. 41 ka to ca. 100 ka as non-linear response to the orbital parameters. This major turning point for the climate of the planet, constrained between ca. 1.4 and 0.4 Ma, has been called the Early-Middle Pleistocene Transition (EMPT). The consequences of these new dynamics exacerbated the cooling and aridification of the climate, eventually triggering the progressive shrinking of the forested habitats replaced by open landscapes, the harshening of temperatures, the more marked seasonality and, consequentially, a major renewal in the flora and fauna. The outcomes of this transition on the European environments and vertebrate communities have been largely studied and debated over the last centuries. In particular, the Early Pleistocene faunal assemblages' taxonomic composition and their response to the environmental change have been subject to numerous publications and have provided significant biochronological data. The deep effects of the EMPT on the mammal communities of Europe were recognized by many scholars, leading to several attempts of formalization of the Epivillafranchian biochron (ca. 1.2–0.8 Ma). This biochronological unit represents the 'transitional' timespan in which Europe was characterized by the co-occurrence of some Villafranchian relicts and the first Galerian taxa, mostly arrived in the continent from Asia and Africa.

Despite the increased interest in the paleontological community and the new discoveries, not all the representative faunal elements of the Epivillafranchian are well defined and this biochron is still poorly characterized. Among large mammal genera that appeared during the Plio-Pleistocene and that have a major role in the Epivillafranchian transition, *Sus* and *Bison* stand out. Their importance within the trophic chains of the Pleistocene and Holocene and their ecological adaptability and abundance in the fossil record made these two clades extremely useful both as environmental indicators and biochronological markers. Nonetheless, the taxonomic history of the early representatives of these clades is quite confused and their dispersal in western Eurasia is still relatively obscure. Therefore, the main aim of this PhD thesis is to better understand the taxonomy, paleobiology, and chrono-spatial distribution of these two iconic genera during the latest stages of Early Pleistocene.

The study performed on a rich suid record from the Epivillafranchian sites of Cal Guardiola and Vallparadís Estació (1.2–0.6 Ma, NE Iberian Peninsula) attests to the presence of the verrucosic boar *Sus strozzii* in the

Mediterranean area between 1.0 and 0.86 Ma, after the so-called ‘suid gap’, during which this group experienced a major demographic collapse. The study is extended to other samples of Suinae from Europe and reveals that, contrarily to what was commonly believed, *S. strozzi* did not disappear before the Jaramillo subchron (ca. 1.0) but persisted until the Early-Middle Pleistocene boundary (ca 0.8 Ma). The analyses suggest that some of the suid remains from European Epivillafranchian sites were erroneously referred to the extant boar *Sus scrofa* and actually belong to *S. strozzi*, which therefore, can be considered a marker for this biochron.

The rich bovid record from the late Villafranchian locality of Pietrafitta (central Italian Peninsula), originally attributed to *Leptobos*, is reappraised in this thesis and referred to the genus *Bison*. The primitive characters of the cranium, relatively small body size, and slender built indicate that the Pietrafitta sample can be referred to *Bison* (*Eobison*) *degiulii*, one of the earliest species of bison entering Europe after 1.8 Ma. The vague definition of the subgenus *Eobison* has triggered the reappraisal of its entire Eurasian record presented herein. The resulted emended diagnosis allows the recognition of, at least, three species of *Eobison*, spanning for more than 1.0 Ma in the whole Eurasia including: *Bison* (*Eobison*) *palaeosinensis* (eastern Asia), *Bison* (*Eobison*) *georgicus* (Caucasus), and *B. (E.) degiulii* (Mediterranean Europe).

The large bovid collection of the Vallparadís composite section provides new insights on the first ‘true’ bison entering Europe at the onset of the Epivillafranchian. This sample is here referred to the oldest member of the subgenus *Bison*, namely *Bison* (*Bison*) *schoetensacki*. A review of several *Bison* samples from Europe constrained between 1.2 and 0.6 Ma advocates the inclusion of this species among the major markers of the Epivillafranchian. Finally, the analyses performed on a large sample of *Leptobos* and *Bison* postcranial bones from the Quaternary of Eurasia reveals that these clades responded to the Pleistocene progressive climatic deterioration with changes in limb proportions and average body mass. Although the increase in metapodial stoutness and body size related to the progressive opening of the habitats is relatively constant over time, several fluctuations in these parameters are registered, according to punctual variations in the environmental conditions.

RESUM [Català]

El Pleistocè inferior és un dels períodes més importants per l'evolució de la biosfera al Paleàrtic occidental. Els canvis climàtics que afectaren l'hemisferi nord des de mitjans del Pliocè van modificar profundament els ecosistemes d'Europa i van establir les condicions per a una important transició que es va produir durant les últimes etapes del Pleistocè inferior. El progressiu refredament global i la dinàmica glacial es veieren intensificats després de ca. 3,0 Ma i especialment durant el període ca. 1,4-1,2 Ma. La periodicitat dels cicles Glacials-Interglacials (G-IG) va passar finalment de cicles de ca. 41 ka a cicles de ca. 100 ka com a resposta no lineal als paràmetres orbitals. Aquest important punt d'inflexió per al clima del planeta, limitat entre ca. 1,4 i 0,4 Ma, s'ha anomenat a la literatura Transició del Pleistocè Inferior i mitjà (EMPT). Les conseqüències d'aquestes noves dinàmiques van agreujar el refredament i l'aridificació del clima, provocant, finalment, la progressiva reducció dels hàbitats boscosos substituïts per paisatges oberts, una estacionalitat més marcada i, en conseqüència, un important recanvi en les associacions animals i vegetals. Els resultats d'aquesta transició sobre els ambients europeus i les comunitats de vertebrats han estat àmpliament estudiats i debatuts durant els últims segles. En particular, la composició taxonòmica dels conjunts faunístics del Pliocè inferior i la seva resposta al canvi ambiental han estat objecte de nombroses publicacions i han proporcionat dades biocronològiques importants. Els efectes de l'EMPT sobre les comunitats de mamífers d'Europa han sigut reconeguts per molts acadèmics, donant lloc a diversos intents de formalització de la biozona anomenada Epivillafranquià (ca. 1,2–0,8 Ma). Aquesta unitat biocronològica representa el període de temps "de transició" en què Europa es va caracteritzar per la co-aparició d'algunes espècies vिलाfranquianes i els primers tàxons galerians, arribats majoritàriament al continent procedents d'Àsia i Àfrica.

Malgrat l'augment de l'interès per la comunitat paleontològica i els nous descobriments, no tots els elements faunístics representatius de l'Epivillafranquià estan ben definits i aquesta biozona encara està poc caracteritzada. Entre els grans gèneres de mamífers apareguts durant el Plio-Pleistocè i que tenen un paper important en la transició de l'Epivillafranquià, destaquen *Sus* i *Bison*. La seva importància dins de les cadenes tròfiques del Pleistocè i l'Holocè i la seva adaptabilitat ecològica i abundància en el registre fòssil han fet que aquests dos clades siguin extremadament útils tant com a indicadors ambientals com a marcadors biocronològics. No obstant això, la història taxonòmica dels primers representants d'aquests clades és força confusa i la seva dispersió a l'oest d'Euràsia encara és relativament obscura. Per tant, l'objectiu principal d'aquesta tesi doctoral és entendre millor la taxonomia, la paleobiologia i la distribució crono-espacial d'aquests dos gèneres emblemàtics durant les últimes etapes del Pleistocè inferior.

L'estudi realitzat sobre el registre de suïds dels jaciments de l'Epivillafrancià de Cal Guardiola i Vallparadís Estació (1,2–0,6 Ma, NE Península Ibèrica) dona fe de la presència del senglar verrucós *Sus strozzi* a la zona mediterrània entre 1,0 i 0,86 Ma, després del l'anomenat 'suïd gap', durant la qual aquest grup va experimentar un important col·lapse demogràfic. L'estudi s'estén a altres mostres de Suïnae d'Europa i revela que, contràriament al que es creia comunament, *S. strozzi* no va desaparèixer abans del subcron Jaramillo (ca. 1,0Ma) sinó que va persistir fins al límit del Pleistocè inferior i mitjà (ca 0,8 Ma). Les anàlisis suggereixen que algunes de les restes de suïd dels jaciments europeus epivillafrancians es van referir erròniament al senglar actual *Sus scrofa* i que en realitat pertanyen a *S. strozzi*, que per tant, es pot considerar un marcador d'aquesta biozona.

En aquesta tesi es revalora el ric registre de bòvids de la localitat de Pietrafitta (Península italiana), atribuït originalment a *Leptobos*, i es refereix al gènere *Bison*. Els caràcters primitius del crani, la mida corporal relativament petita i la construcció esvelta indiquen que la mostra de Pietrafitta es pot referir a *Bison (Eobison) degiulii*, una de les espècies més primerenques de bisons que van entrar a Europa després d'1,8 Ma. La definició vaga del subgènere *Eobison* ha provocat la reavaluació de tot el seu registre eurasiàtic que es presenta aquí. El diagnòstic esmenat resultant permet el reconeixement d'almenys tres espècies d'*Eobison*, que abasten més d'1,0 Ma a tota Euràsia, incloent: *Bison (Eobison) paleosinensis* (Àsia oriental), *Bison (Eobison) georgicus* (Càucàs) i *B. (E.) degiulii* (Europa mediterrània). La gran mostra de bòvids de la secció composta de Vallparadís ofereix noves perspectives sobre els primers bisons que van entrar a Europa a l'inici de l'Epivillafrancià. Aquesta mostra es refereix aquí al primer membre del subgènere *Bison* que es dispersa al Paleàrtic Occidental, és a dir, *Bison (Bison) schoetensacki*. Una revisió de diverses mostres de bisons d'Europa restringides entre 1,2 i 0,6 Ma advoca per la inclusió d'aquesta espècie entre els principals marcadors de l'Epivillafrancià. Finalment, les anàlisis realitzades en una gran mostra d'ossos postcranials de *Leptobos* i *Bison* del Quaternari d'Euràsia revelen que aquests clades van respondre al deteriorament climàtic progressiu del Pleistocè amb canvis en les proporcions de les extremitats i la massa corporal mitjana. Tot i que l'augment de la robustesa metapodial i de la mida corporal relacionat amb l'obertura progressiva dels hàbitats és relativament constant en el temps, es registren diverses fluctuacions en aquests paràmetres, segons variacions puntuals de les condicions ambientals.

INDEX

Chapter 1.

INTRODUCTION

1.1. Early Pleistocene in Western Palaeartic: climate and palaeoenvironment	16
1.1.1. The intensification of Northern Hemisphere glaciations	16
1.1.2. The Early-Middle Pleistocene Transition	17
1.1.3. Palaeoenvironments before and during the EMPT	19
1.2. Early Pleistocene in Western Palaeartic: biochronology of large mammal fauna	22
1.2.1. European Land Mammal Ages: Villafranchian, Epivillafranchian and Galerian	23
1.2.2. Late Villafranchian large mammals	27
1.2.3. Epivillafranchian large mammals	29
1.2.4. Galerian large mammals	34
1.3. Suids and Bovids from their origins to the Pleistocene	38
1.3.1. European Suinae: paleobiogeography and biochronology	41
1.3.2. European Bovinae: paleobiogeography and biochronology	43

Chapter 2.

AIMS AND STRUCTURE, MATERIALS AND METHODS

2.1. Aims and scopes	50
2.2. Structure	51
2.3. Materials	52
2.3.1. Suidae sample	52
2.3.2. Bovidae sample	53
2.4. Methods	53
2.4.1. Suidae methodology	54
2.4.2. Bovidae methodology	56

Chapter 3.

SUS FROM THE EARLY PLEISTOCENE

3.	The persistence of <i>Sus strozzi</i> in Europe during the Epivillafranchian: evidence from the Vallparadís Section (NE Iberian Peninsula) and other coeval sites	67
-----------	--	-----------

Chapter 4.***EOBISON FROM THE EARLY PLEISTOCENE***

4.	Earliest bison dispersal in Western Palearctic: Insights from the <i>Eobison</i> record from Pietrafitta (Early Pleistocene, central Italy). Sorbelli et al. (2022)	73
-----------	--	-----------

Abstract	73
Introduction	73
The genus <i>Leptobos</i> and its historical and taxonomical background	73
Earliest Eurasian <i>Bison</i> in the paleontological literature, a review	74
Geological setting	74
Materials and methods	75
Results	77
Description	77
Comparisons and taxonomic assignment of the Pietrafitta sample	82
Discussion	90
<i>Leptobos</i> : state of the art	90
<i>Leptobos</i> : comments on the European taxa	94
<i>Eobison</i> and other “transitional” forms: state of the art	95
<i>Eobison</i> and other “transitional” forms: comments	97
Comments on the evolutionary trends in limb proportions and body mass	101
Conclusions	102
Acknowledgments	103
References	103

Chapter 5.***BISON FROM EARLY-MIDDLE PLEISTOCENE***

5.	A review on <i>Bison schoetensacki</i> and its closest relatives through the early-Middle Pleistocene transition: Insights from the Vallparadís Section (NE Iberian Peninsula) and other European localities. Sorbelli et al. (2021)	111
-----------	---	------------

Abstract	111
Introduction	111
The European record of <i>Leptobos</i>	112
Earliest Asian and European bison	112
The Vallparadis Composite Section	113
Materials and methods	113
Systematic paleontology	116
Referred specimens	116
Descriptions	116
Results	131
The VCS sample: taxonomy and morphological variation	131
The <i>Leptobos etruscus</i> - <i>Leptobos vallisarni</i> lineage	131
Early bison species	131
Other samples of <i>Bison schoetensacki</i>	133
Discussion	135
Metapodials variation within <i>Bison schoetensacki</i>	135
The metapodial morphology of <i>Bison schoetensacki</i>	136
Sexual dimorphism	136
Final remarks on the postcranial differences among <i>Leptobos</i> and <i>Bison</i>	136
Conclusions	137
Acknowledgments	137
References	137

Chapter 5.

GENERAL DISCUSSION

6.1.	The ‘suid gap’ debate and the persistence of <i>S. strozzii</i> in the Epivillafranchian	142
6.2.	The early bison, <i>Bison</i> (<i>Eobison</i>), their origin and dispersal in Europe	149
6.3.	The role of <i>Bison</i> s.s. as a marker of the Epivillafranchian and the <i>B. schoetensacki</i> issues	156
6.4.	Systematics of <i>Bison menneri</i>	162

Chapter 6.

CONCLUSIONS

7.	Conclusions	170
-----------	--------------------	------------

Chapter 7.**REFERENCES**

8.	References	175
-----------	-------------------	------------

SUPPLEMENTARY SECTION**Chapter S1.**

S1	The post-Jaramillo persistence of <i>Sus strozzii</i> (Suidae, Mammalia) in Europe: New evidence from the Vallparadís Section (NE Iberian Peninsula) and other coeval sites. Cherin et al. (2020) and Cherin et al. (2020) Supplementary material	207
-----------	--	------------

Introduction	207
Geographical and geological framework	208
Chronology	208
Materials and methods	209
Materials	209
Photogrammetry	210
Phylogenetic analysis	210
Systematic paleontology	211
Results	212
Description	212
Comparisons	216
Phylogenetic analysis	217
Discussion	218
The taxonomic importance of the lower canine morphology in suines	218
Quaternary suines from China	218
Epivillafranchian <i>Sus</i> from the Iberian Peninsula	219
Epivillafranchian <i>Sus</i> from France	220
Epivillafranchian <i>Sus</i> from Germany	220
Epivillafranchian <i>Sus</i> from Italy	222
Epivillafranchian <i>Sus</i> from eastern Europe	222

	Biochronological, paleobiogeographical, and paleoecological implications	223
	Conclusions	224
	Acknowledgments	225
	References	225
	Supplementary material (Cherin et al., 2020)	229
		Chapter S2.
S2	Sorbelli et al. (2022) Supplementary material	234
		Chapter S3.
S3	Sorbelli et al. (2021) Supplementary material	283
		ACKNOWLEDGMENTS
	Acknowledgements	344

Chapter 1.





1.1. Early Pleistocene in Western Palaeartic: climate and palaeoenvironment

At the end of the Pliocene, the glacial dynamics that were dominating the Earth's climate system gradually intensified, changing the Northern Hemisphere tropical-like ecosystems into more arid and seasonality marked environments (Etourneau et al., 2010). The two most important climatic events that characterized the Plio-Pleistocene are the intensification of the glacial dynamics (ca. 2.8 Ma) and the Early-Middle Pleistocene Transition (EMPT; 1.2-0.6 Ma), which marked a gradually sustained change in the Northern Hemisphere ecosystems in response to orbital forcing. Both of these events paced the long-term cooling that affected the Earth's climate system during the last 4 Ma. These events ultimately shaped the climate dynamics of the Quaternary in the Western Palaeartic, defining its environments and faunal associations (Fig. 1).

1.1.1. The intensification of Northern Hemisphere glaciations

The Late Pliocene Earth's climate system is strongly characterized by the start of a long-term global cooling. Between 3.6 and 3.0 Ma the earliest signs of glacial dynamics intensification emerged. By 2.7 Ma. the glacial-interglacial cycles (G-IG) settled to a 41-Ka periodicity (Fig. 1), characterized by a symmetrical waveform and low amplitude (Mudelsee and Raymo, 2005). It is commonly accepted that the main driving factor of the G-IG alternations are to be found in the orbital parameters of our planet (i.e., Milankovitch hypothesis). The three main orbital parameters, eccentricity, obliquity (or tilt) and precession, have a periodicity of 100 ka, 41 ka and 27 ka respectively (Maslin and Ridgwell, 2005). These features define the shape of Earth's orbit, the tilt of Earth's rotation axis with respect to the orbit's plane and its orientation (Maslin and Ridgwell, 2005). The dynamics expressed by the orbital geometry pace the seasonal cycles and strongly influence the annual insolation received, therefore, their periodical changes have a strong forcing effect on the G-IG cycles (Hays et al., 1976). It has been proven that the Early Pleistocene G-IG phases, at least until the onset of the EMPT, were correlated with a linear response of the climate dynamics to the 41-ka orbital obliquity (Imbrie et al., 1992). If it is widely accepted that the pacing of the cycles is given by the orbital parameters, the triggering mechanisms of their inception are still poorly understood. Several scholars tried to recognize the main causes of these dynamics, suggesting that most probably the decrease of the atmospheric CO₂ paired with large-scale tectonic and oceanic events would have settled, at 3.0–2.7 Ma the threshold at which the orbital forcing induced the intensification of the Northern Hemisphere G-IG alternations (Maslin et al., 1998; Bartoli et al., 2005; Haug et al., 2005; Lunt et al., 2008; Bartoli et al., 2011; Hayashi et al., 2020 among others). The linear response established between the G-IG cycles and the orbital obliquity will characterize the first part of the

Early Pleistocene until the onset of new non-linear dynamics, namely the EMPT, which from ca. 1.2 Ma, led to a progressive increase of G-IG periodicity and a widening of the amplitude in the global ice-volume variations.

1.1.2. The Early-Middle Pleistocene Transition

Since its first recognition, the EMPT has been considered one of the most important events that characterized the late Cenozoic (Maasch, 1988; Head and Gibbard, 2005; Clark et al., 2006; Lisiecki and Raymo, 2007; Head and Gibbard 2015; Chalk et al., 2017; among others). Previously known as the Mid-Pleistocene Transition, or Mid-Pleistocene Revolution (Maasch, 1988; Berger and Jansen, 1994; Maslin and Ridgwell, 2005), the EMPT settled new climate dynamics which led to a major environmental change at global scale, in the timespan comprised between the end of the Early Pleistocene and the first half of the Middle Pleistocene (Fig. 1). Over the years, many scholars tried to define the boundaries of the EMPT (e.g., Head and Gibbard, 2005; Head et al., 2008) which, in a broader sense, should be considered 1.4 and 0.4 Ma (Head and Gibbard, 2015), although the core of the transition is often restricted to 0.9–0.4 Ma, constrained by the so-called ‘900 ka event’ (Clark et al., 2006) and the ‘Mid-Brunhes Event’ or ‘Mid-Brunhes Transition’ (Jansen et al., 1986; Barth et al., 2018). The Earth’s climate, during this period, is largely characterized by the onset of a non-linear response to orbital forcing, including: a progressive increase in the amplitude of climatic oscillations with a shift towards a ca. 100-ka frequency, a declining of the mean sea-surface temperature and a long-term global ice-volume increase paired with a strong asymmetry in its cycles (i.e., long intervals of ice sheets growth followed by rapid intervals of deglaciation). These changes, given by the combined effect of orbital forcing and the consequent feedback mechanisms internal to climate system, eventually shaped both the Earth’s marine and terrestrial realms for the rest of the Quaternary (Head and Gibbard, 2015 and reference therein).

As already mentioned, the Early Pleistocene was characterized by 41-ka obliquity-forced cycles, with low amplitude and symmetrical wave form (Tiedemann et al., 1994; Clark et al., 2006; Elderfield et al., 2012). At around 1.4 Ma (MIS 45-46), the first precursors of the EMPT emerged with a decrease of relative interglacial durations and a weakening of the 41-ka periodicity response to orbital obliquity, testifying the increase of non-linear forcing and the approach of a major climatic transition (Lisiecki and Raymo, 2007). At 1.2 Ma (MIS 36), the onset of the EMPT core marked the gradual shift to ca. 100-ka rhythm and a passage from smooth to abrupt “saw-toothed” asymmetric G-IG cycles with a consequent increase in the amplitude of climatic oscillations as non-linear response to orbital parameters (Clark et al., 2006; Lisiecki and Raymo, 2007; Head and Gibbard, 2015 and reference therein). The causes of this non-linear response of the climate cycles to orbital forcing is still matter of debate. If it is commonly accepted that

eccentricity cannot be the major driving force (Maslin and Ridgwell, 2005), it is still not clear if the 100-ka periodicity represents bundles of 4-5 precession cycles (e.g., Maslin and Ridgwell, 2005), or 2-3 obliquity cycles (e.g., Hubers, 2006) or even if there is no consistent and reliable relationship between orbital parameters and G-IG cycles (e.g., Maslin and Brierley, 2015). It is indeed true that, although the orbital forcings are undoubtedly the main pacing factors of the G-IG climatic oscillations during the EMPT, it has been widely demonstrated that they are not enough to justify the periodicity shift (Ruddiman et al., 1986; Head and Gibbard, 2015 and references therein). For this reason, several long-term trends and internal feedback mechanisms have been proposed as potential triggers for amplification or threshold response (for a complete review see Head and Gibbard, 2015). Currently, there is still small consensus among scholars on this matter, which led to the conclusions for some authors, that the generic deterministic models relating G-IG cycles and astronomical forcing is too simplistic and the effect of the stochastic nature of the climate system might have been underestimated (e.g., Crucifix, 2012, 2013; Maslin and Brierley, 2015; Ditlevsen and Ashwin, 2018).

The EMPT features several events that mark the Earth's history between 1.4 and 0.4 Ma including, among the most significant: the intensification of glacial phases at ca. 1.2 Ma, the '900 ka event', the 'Mid-Brunhes Transition' and the two magnetostratigraphic markers of the Jaramillo subchron and Matuyama-Brunhes boundary (Fig. 1).

The subchron Jaramillo and the Matuyama-Brunhes reversal provide crucial magnetostratigraphic constraints for chronological studies dealing with the latest Early Pleistocene. The subchron C1r-1n, prosaically known as Jaramillo, is a normal polarity event within the upper part of Matuyama chron (Gradstein et al., 2012). Due to the timespan recorded, 1.07–0.99 Ma (MIS 31–28), Jaramillo is a significant marker of the early stages of the EMPT, reporting the first habitat change and faunal renewal triggered by the intensification of the G-IG cycles. On the other hand, the passage between the two major chrons Matuyama and Brunhes, dated to the upper part of MIS 19 (ca. 0.77 Ma), has been chosen as the boundary between the Early and Middle Pleistocene (Head and Gibbard, 2005).

The MIS 36, dated to 1.2 Ma, is regarded as the first prolonged glacial stage and marks the intensification in the cooling of sea surface and the increase of global ice-volume (Head and Gibbard, 2015). The so-called '900 ka event', lasted from ca. 0.94 to 0.87 Ma, includes two strong glacials (MIS 24, 22) and a weak interglacial (MIS 23). During this period the quasi-100-ka periodicity became dominant, the mean sea surface temperature dropped significantly and the sudden continental ice volume increase led to an abrupt eustatic fall (McClymont et al., 2013; Head and Gibbard, 2015). This major climatic reorganization triggered a series of changes at global scale including: the aridification of Africa, the increase of winter monsoon activity in Southeastern Asia and an increase of corrosivity in deep waters, paired with a stagnation and reduced productivity of Atlantic deep waters (Marino et al., 2009; Head

and Gibbard, 2015; Tachikawa et al., 2021). The ‘Mid-Brunhes Transition’ (MBT), at ca. 0.4 Ma (MIS 13–11), is considered the ending boundary of the EMPT, marking the onset of a more stable climatic condition due to the higher-amplitude interglacials (Head and Gibbard, 2015 and reference therein). The MBT is characterized by a step-like change in the intensity of the interglacial phases which features a relative increase of temperature and precipitation during the MIS 13 and 11 (Jansen et al., 1986; Candy and McClymont, 2013; Ao et al., 2020). The latter are, indeed, among the warmest and longest interglacials of the last 0.5 Ma interposed to a particularly strong and harsh glacial stage, namely MIS 12 (Lisiecki and Raymo, 2007; Candy et al., 2014). Although some evidence points out that MBT would not have been equally expressed in all the planet (e.g., Lang and Wolff, 2011; Candy and McClymont, 2013), the strong effects of this event in East Asia, Southern Hemisphere waters and Arctic territories set a major climatic threshold which reflected into an important environmental transition at global scale (Cronin et al., 2017; Barth et al., 2018; Ao et al., 2020).

1.1.3. Palaeoenvironments before and during the EMPT

The end of the Pliocene experienced a clear harshening of the climatic condition which progressively strengthened toward the Plio-Pleistocene boundary and became the dominant trend throughout the Pleistocene. During the Piacenzian (ca. 3.6–2.6 Ma) the world was warmer and wetter than today, with mean temperature higher by about 3 °C than the pre-industrial era (Dowsett, H. J. et al. 2013). These conditions allowed, in the Western Palaeartic, the expansion of tropical savannahs and forests, especially during the mid-Piacenzian warm optimum (Jiménez-Moreno et al., 2013; de la Vega et al., 2020). Although the first precursors of the G-IG cycles were present at 3.6 Ma (Mudelsee and Raymo, 2005), the first intensification of the glacial dynamics is dated at ca. 2.7 Ma (Mudelsee and Raymo, 2005; Bartoli et al., 2005, 2011; Hayashi et al., 2020 among others). This ‘climate crash’ (sensu Bartoli et al., 2005) not only exacerbated the cooling and the aridification processes of the climate, but also led to a more marked seasonality. The ecological consequences were testified by the progressive shrinking of the tropical and sub-tropical habitats replaced by more temperate ones (Fig. 1). Although this shift toward harsher conditions affected all Western Palaeartic, its timing and strength were not homogeneous in every area. Indeed, in Eastern and Southeastern Europe as well as in Asia Minor, the aridification trend started earlier than in other parts of Western Palaeartic, most probably due to a major action of the continentality (Kahlke et al., 2011). The Iberian Peninsula witnessed, before 3.0 Ma, the establishment of the Mediterranean seasonal precipitation rhythm (i.e., summer droughts) as also testified by the disappearance of most of the tropical-adapted plants and the shrinking of laurel forests in favour of many xerophytes (Postigo et al., 2009; Jimenez-Moreno et al., 2013). After 2.6 Ma, the cooling and aridification of the Iberian

Peninsula led to the opening-up of the habitats, which started to be dominated by the ‘*Artemisia steppes*’ (Jiménez-Moreno et al., 2010; Kahlke et al., 2011). The Italian Peninsula, from ca. 2.6 Ma, saw the progressive depletion of the thermophilus, deciduous plant taxa with the almost complete disappearance of the “Taxodiaceae” (e.g., *Taxodium*, *Glyptostrobus*) and the onset of a strong alternations of patched savannahs and wooded landscapes (Bertini, 2010; Magri et al., 2017 and references therein). The Aegean area witnessed the emergence of the Mediterranean-type flora at the expenses of the exotic taxa which, in some cases, survived in few refuge areas (Velitzelos et al., 2014). From 3.0 Ma the French territory showed a decrease of warm and humid habitats with the expansion of savannahs which became more common after 2.6 Ma, although woodlands were still a major presence in the environment of this area (Nomade et al., 2014). By 2.2-2.0 Ma, French landscape was mainly characterized by open habitats with patches of open forests in a temperate climate (Nomade et al., 2014).

After 1.8 Ma, the environmental conditions of Europe witnessed a further deterioration. In the whole Mediterranean area, from the Iberian Peninsula to the South-Eastern borders of the continent, both warmer and cooler phases are characterized by a decrease of temperature and humidity, leading to the expansion of savannahs alternated with woodlands influenced by continental/temperate climates (Kahlke, 2011 and reference therein). At 1.4 Ma the precursors of the EMPT started to model the European ecosystems. At 1.2 Ma, the 41-ka periodicity forcing decreased and a strong instability began to shape new climate dynamics (Fig. 1). All Western Palearctic witnessed the intensification of the cooler phases and a progressive opening of the landscapes with the complete disappearance of the subtropical humid forests (Head and Gibbard, 2015). The Italian Peninsula experienced rapid alternations between relatively warm steppes/coniferous forests and temperate deciduous forests given by the cool, temperate glacials and humid, warm interglacials (Bertini, 2010). The Iberian Peninsula featured a complex mosaic of environments marked by the increase of open savannahs and woodlands with emerging regional characteristics and strong differentiations of habitats given by the G-IG phases (González-Sampériz et al., 2010). Central Europe started to be strongly affected by continental conditions with warm and dry summers and a prevalence of grasslands habitats as testified by the dominance of Gramineae (Szymanek and Julienne, 2018). The forested areas were marked by the presence of boreal-subarctic vegetation during the colder phases and by mixed-deciduous taxa during the warmer periods (Szymanek and Julienne, 2018 and references therein). It has been pointed out that during the EMPT, although it is recognizable a general trend toward the aridification and the loss of diversity in the European flora, local and regional conditions (e.g., topography, continentality) strongly influenced the habitats and vegetational development (Head and Gibbard, 2015). It is true, indeed, that several areas of the continent (especially at the southern borders, but not only) represented temporary refugia for thermophilus plants of East Asian affinity (sensu Martinetto et al., 2017) and

densely forested-humid habitats during cold and arid glacial phases (Stewart and Lister, 2001; Bertini, 2010; González-Sampériz et al., 2010; Velitzelos et al., 2014). On the other hand, the opposite reaction is sometimes recorded in localities where steppe-like environment dominates at the beginning of deglaciation (e.g., the wooded steppe of southern Italy at the boundary MIS 20-19; Capraro et al., 2005). This discrepancy in timing and strength of environmental shift consequently affected the faunal turnovers which, although generally constrained in a roughly defined time and space, were subject to asynchronous triggering points through the EMPT (Fig.1).

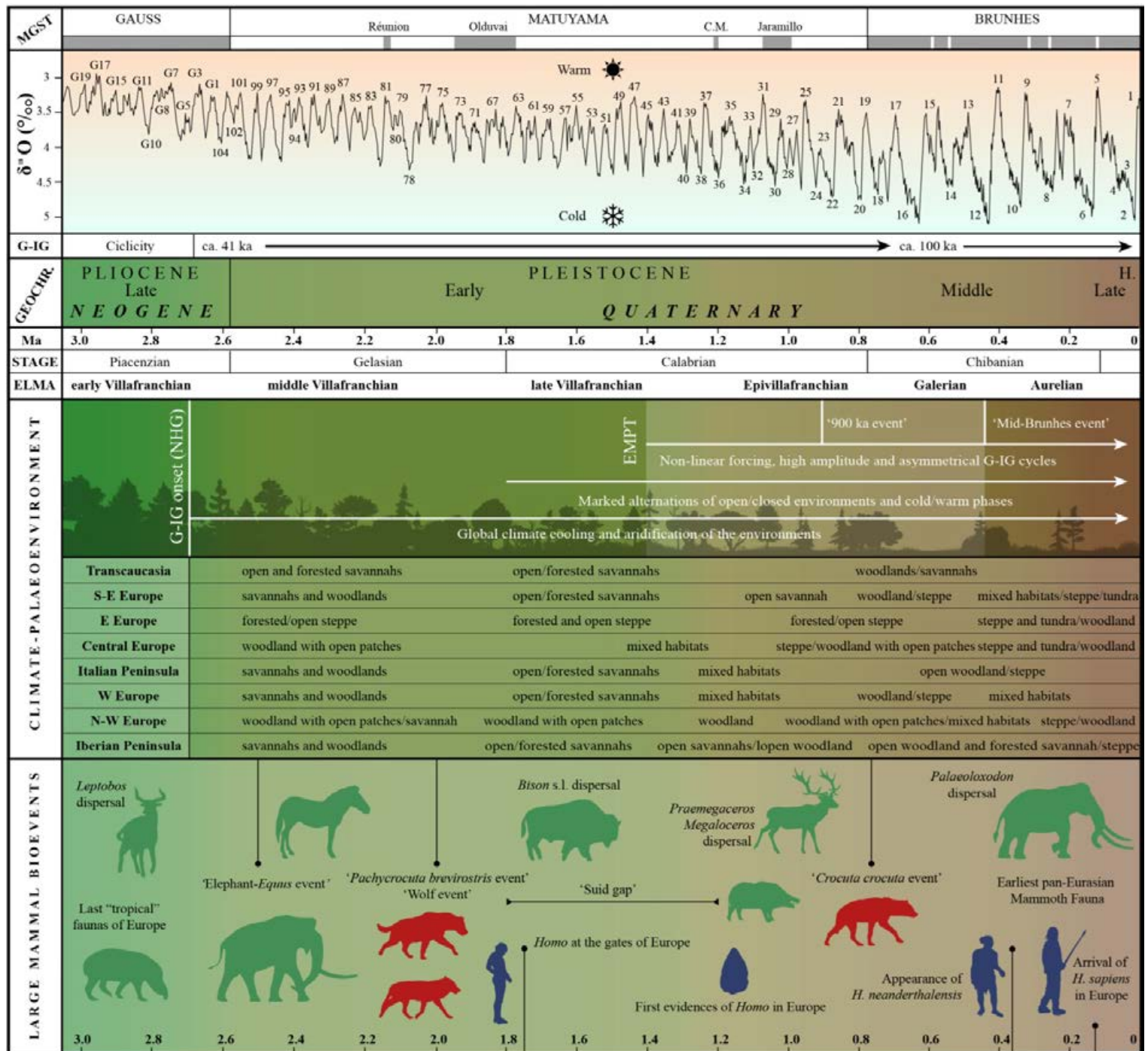


Fig. 1. Summarized and simplified scheme of main climatic, environmental and biotic events of the Quaternary correlated with geochronology, magnetostratigraphy and LR04 Benthic Stack (from Lisiecki and Raymo, 2005). Abbreviations: MGST, magnetostratigraphy; G-IG, glacial-interglacial cyclicality; Geochr., Geochronology; MA, mega annum; ELMA, European Land Mammal Age; H., Holocene.

1.2. Early Pleistocene in Western Palaeartic: biochronology of large mammal fauna

The Early Pleistocene large mammal associations are among the best-known faunal assemblages of all the Cenozoic. Their composition and evolution in response to environmental changes of the last 2.5 Ma were extensively studied and defined through various biochronological scales (Fig. 2).

Biochronology is the most used relative dating methods for continental deposits. Vertebrate palaeontologists divide geological periods in Land Mammal Ages (LMAs), *sensu* Lindsay (1990), i.e., chronological units defined by the succession of evolutionary stages of faunal assemblages and dispersal events. Thus, the biochrons are defined as elementary units of geological time based exclusively on palaeontological data, avoiding whatsoever reference to the lithostratigraphy of the sediments that contain the fossils (Berggren and Van Couvering, 1974). Although the term biochronology is already present in literature since the early years of 1900, its use in the European scientific community became widespread only after the pioneering works of the 1970s by Heintz (1968; 1970), Heintz et al. (1974), Mein (1975) and Azzaroli (1977; 1983), among others, from which the biochronological scale of European mammals has been widely developed. Although being a useful dating tool, biochronology is affected by issues related to the dispersal events which are, by their nature, diachronous and not homogeneous (Palombo, 2016). The geographical and environmental barriers, the distributional patterns of the organisms and their response to climatic changes, often hinder the correct definition of first and last appearances of taxa, especially in short period of time. Despite these problems, the concept of biochrons relies on the assumption that, at large scale (i.e., continental), in a given timespan, dispersal event of groups of organisms are roughly synchronous and homogeneous. During the last 70 years, several LMAs zone-systems were developed, providing an array of different biochronological scales, each often restricted to a regional scale use (Fig. 2). The Italian LMA scheme was one of the first to be developed and has been widely used in all Southern Europe, being among the better defined and well known across national borders.

Plio-Pleistocene LMAs of western Europe are often divided in biozones or faunal units. The MN and MNQ biozones (Fig. 2) were firstly developed for the Neogene (MN) by Mein (1975), then expanded by Guérin (1982, 1990) for the Pleistocene (MNQ). These biozones are based on the evolutionary stage of selected taxa lineages and the presence of particular associations of taxa in Europe, calibrated (when available) by magnetostratigraphic data (Nomade et al., 2014 and references therein). The Faunal Units (FU) were initially developed by Azzaroli (1977) for the Italian biochronological scheme and further expanded by other palaeontologists (Gliozzi et al., 1997; Petronio and Sardella, 1998 among others). The FU are defined on the basis of local faunas which correspond to a typical association and are named after a reference site (e.g., Farneta FU, Collocurto FU) (Fig. 2). These “low rank” biochronological units are

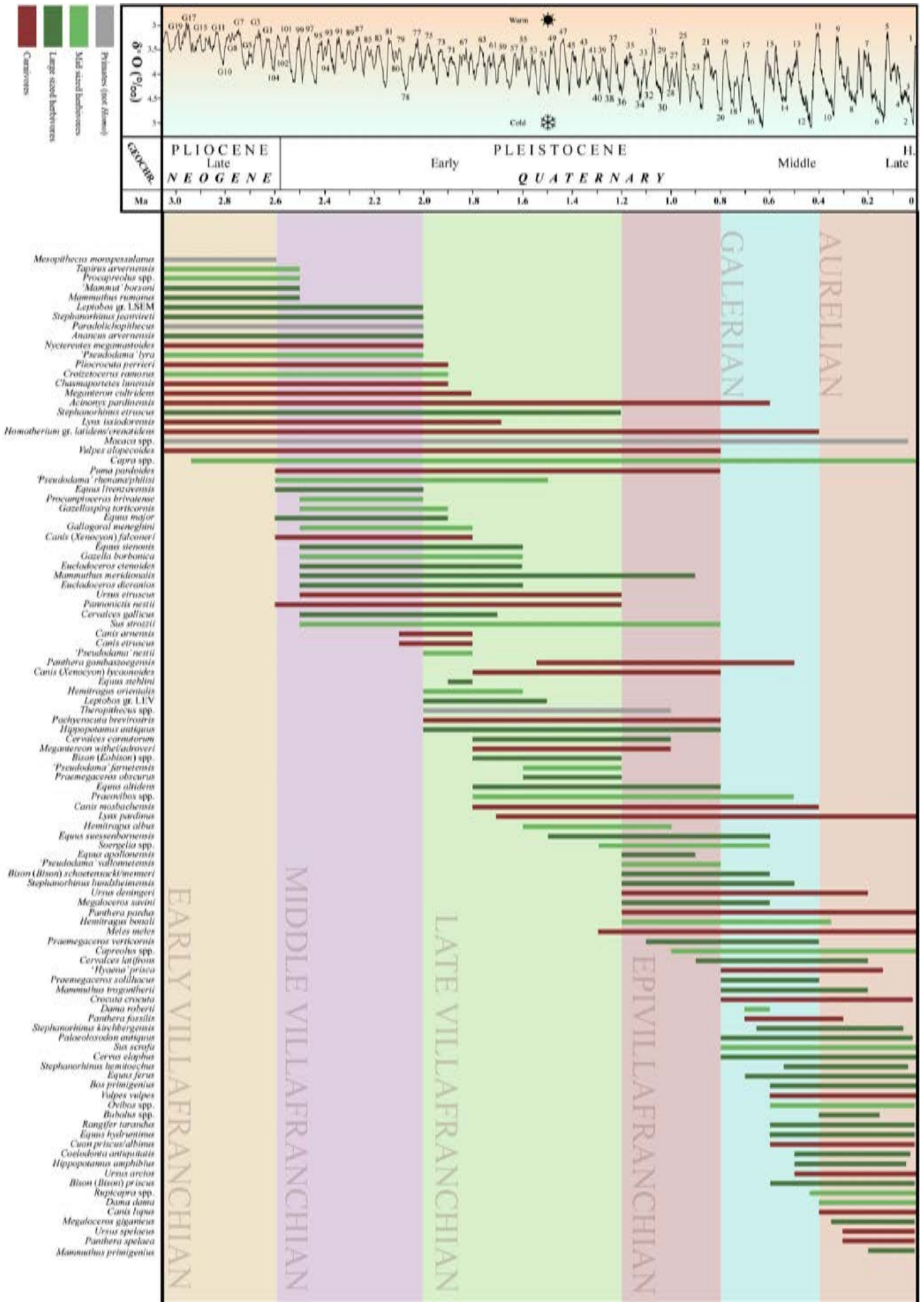
particularly useful at local scales, providing insight on the turnovers characterizing a concrete timespan and area, but less useful in a continental-scale study. Within this framework, during the decades several “events” were defined, including the ‘Elephant *Equus* event’, ‘Wolf event’, ‘*Pachycrocuta brevirostris* event’ (Azzaroli et al., 1988; Sardella and Palombo, 2007) (Fig. 1). However, most of the modern scholars agree on the poor liability of these definitions due to the diachronous nature of the turnovers/dispersals across Europe (e.g., Sardella and Palombo, 2007; Rook and Martínez-Navarro, 2010). For this reason, at present-day, these “events” are seldom used as global stratigraphic markers but only as local indicators of faunal renewals and paleoenvironmental proxies. Higher rank biochronological units such as the LMA encompass longer timespan and wider areas, thus, as stated before, partially solve the turnover heterogeneity issues and therefore are largely used in the modern biochronological studies at continental scale. For this reason, in this thesis I refer mainly to the European LMA biochronological scale (ELMA).

1.2.1. European Land Mammal Ages: Villafranchian, Epivillafranchian and Galerian

The Villafranchian LMA is a biochronological unit (or biochron) based on European large mammals and covering the interval comprised from the Late Pliocene to most of the Early Pleistocene (ca. 3.5–1.2 Ma). Pareto (1865), for the first time, coined the term Villafranchian to identify the fluvial and lacustrine sediments rich of mammalian remains in the surroundings of Villafranca d’Asti (north Italy) including also, in the definition, the faunal associations of Lower and Upper Valdarno basins (Central Italy; Rook and Martínez-Navarro, 2010). During the second half of the 1900, the term became common also outside the Italian borders and it is currently one of the most referred LMAs of Europe. Due to its widespread use, the chronological subdivision of the Villafranchian was extensively discussed and, as a result, a number of successive Faunal Units (see section above), were recognized and correlated with other European LMAs (Bout, 1960; Bourdier, 1961; Heintz et al., 1974; Mein, 1975; Guérin, 1990; Mein, 1990; Gliozzi et al., 1997; Guérin, 2007; Nomade et al., 2014 among others) (Fig. 2). In order to reduce the impact of the intrinsic issues given by the heterogeneous and diachronous nature of faunal assemblages, the Villafranchian has been divided in three main sub-units: early, middle and late Villafranchian, corresponding to the Late Pliocene (ca. 3.5–2.6 Ma), the first half of Early Pleistocene (ca. 2.6–2.0 Ma) and almost all the rest of Early Pleistocene (2.0 to 1.2 Ma), respectively (Fig. 3).

According to classic biochronology, the Villafranchian lasts until 1.0 Ma, succeeded by the Galerian (Rook and Martínez-Navarro, 2010). Nonetheless, the evidence of a major faunal turnover started at ca. 1.2 Ma, compelled the creation of a biochron that could identify the effect of the climatic instability given by the EMPT on the faunal associations of Europe. The period, spanning from ca. 1.2 to 0.8 Ma, is indeed, characterized by the persistence of

relicts of the Villafranchian faunas and the first occurrence of some Galerian taxa (Fig. 3). This transitional biochron has been named in various ways, including Protogalerian (Caloi and Palombo, 1996), latest Villafranchian (Koufos, 2001), Final Villafranchian (Spassov, 2003) and Epivillafranchian (Kahlke, 2001a, 2006, 2007). The latter term seems to have prevailed in the literature and, during the last decade, various attempts of formalization were provided (e.g., Kahlke, 2007; Rook and Martínez-Navarro, 2010; Kahlke et al., 2011; Madurell-Malapeira et al., 2014; Bellucci et al., 2015). Bourdier (1961) in its definition of “Epi-Villafranchien” based on the French sites of Saint-Cosme and Durfort, observed the presence of some faunal elements typical of the Middle Pleistocene with the occurrence of derived forms of elephants, bison, horses and reindeer. The term was forgotten until Kahlke (2001a) resurrected it as Epivillafranchian. From then on, this locution has been widely used for defining the timespan comprised between 1.2 and 0.8 Ma (thus including portions of both Villafranchian and Galerian) in which the European faunal assemblages feature the evidence of a major turnover leading to the Galerian faunas (e.g., Kahlke, 2006; Madurell-Malapeira et al., 2010; Martínez-Navarro et al., 2015; Brugal et al., 2020; Iannucci et al., 2021a). On the other hand, although some scholars attempted to properly formalize this biochron (e.g., Kahlke, 2007; Bellucci et al., 2015), others noticed that the lack of a homogeneous consistency in the fossil record (i.e., diachronous dispersal events, bias in the record) and the disagreement on the taxonomy among palaeontologists, hamper the correct definition of Epivillafranchian which should be revised (e.g., Palombo, 2016). The Galerian LMA was firstly defined by Ambrosetti et al. (1972) on the basis of the discoveries from Ponte Galeria, in Central Italy (ca. 0.75 Ma), as the timespan comprised between 1.0 and 0.4 Ma in which the Villafranchian taxa were progressively replaced by newcomers from Africa and Asia. As for the previous biochrons, several definitions and boundaries of Galerian were provided (e.g., Azzaroli, 1983; Petronio and Sardella, 1999; Petronio et al., 2011; Marra et al., 2014). Azzaroli (1983) and Azzaroli et al. (1988) refer to the early Galerian (ca. 1.0 Ma) as the ‘end-Villafranchian event’, a transitional period in which the last Villafranchian relict taxa were co-existing with representants of the Galerian. Marra et al. (2014) states that “the faunal turnover between the Villafranchian and Galerian species was completed around 0.6–0.5 Ma”, pointing out that, in the Italian Peninsula, this transition happened in a longer timespan due to the favourable climatic conditions and ‘cul-de-sac’ role played by the peninsula which could have helped some of the Villafranchian taxa to survive longer in the Middle Pleistocene. As aforementioned, during the last decades, several scholars started to consider that the biochronological implications given by this turnover compel the creation of a distinct biochron (i.e., Epivillafranchian) which could solve, definitely, one of the most controversial issues in the European biochronological framework (e.g., Kahlke, 2007; Rook and Martínez-Navarro, 2010; Madurell-Malapeira et al., 2010; Bellucci et al., 2015). For this reason, we follow Kahlke et al. (2011), Madurell-Malapeira et al. (2014) in postponing the beginning of the Galerian to the Early-Middle



1.2.2. Late Villafranchian large mammals

The late Villafranchian is possibly the best-known portion of the ELMA as it is represented by a large number of sites throughout Europe, including, among the most important: the *Homo*-bearing locality of Dmanisi (Georgia, ca. 1.8 Ma), the sites of Mygdonia Basin (Greece, ca. 1.7–1.2 Ma), Olivola, Tasso and Pietrafitta (Italy, ca. 2.0–1.8 Ma), Senèze (France, ca. 2.2 Ma) and the Iberian sites of Fonelas-1 and Venta Micena (Spain, ca. 1.8–1.6 Ma). For a comprehensive list of late Villafranchian sites with chronological and geographical positions see Fig. 4. After the middle to late Villafranchian transition (ca. 2.0 Ma), the marked drop in temperatures and progressive aridification of the habitats favoured the entrance of new species in Europe from Africa and Asia, especially among herbivores (Gliozzi et al., 1997; Rook and Martínez-Navarro, 2010; Kahlke et al., 2011) (Fig. 3).

The Villafranchian large bovids were mainly represented by the bovine *Leptobos* which appeared at the end of the Pliocene ('*Leptobos* event' sensu Azzaroli et al., 1988). At the very beginning of the late Villafranchian, the forest dweller species *L. stenometopon* and *L. merlai* (*Leptobos* gr. LSEM) were replaced by the stockier *L. etruscus* and *L. vallisarni* (*Leptobos* gr. LEV) (Rook and Martínez-Navarro, 2010; Cherin et al., 2019b; see also chapter 4). The latter were in turn succeeded by the first primitive forms of *Bison* (subgenus *Eobison*) which dispersed from Asia to Europe at ca. 1.8 Ma (Kahlke et al., 2011; Martínez-Navarro et al., 2011, see chapter 4). Among the small to mid-sized bovids, the most important newcomers are *Soergelia*, *Praeovibos*, and *Hemitragus* which, in some localities co-existed with the survivors of the middle-late Villafranchian transition such as *Gazellospira* and *Gazella* (Kahlke et al., 2011 and references therein). The late Villafranchian cervids are commonly divided in three groups: the '*Dama*-like' deer, the 'megalocerine' deer and the moose deer (see Azzaroli, 1992; Abbazzi, 2004; Croitor, 2006a, 2006b; Breda, 2008; Cherin et al., 2022; among others). Most of the species belonging to the former group are often assigned to the debated genus '*Pseudodama*' (sensu Cherin et al., 2022), which appeared before 3.0 Ma and evolved with an array of strictly related species during the middle-late Villafranchian (Cherin et al., 2022 and references therein). The Early Pleistocene 'megalocerine' deer are equally affected by several taxonomic issues, however, most scholars agree on the validity of the genus *Praemegaceros* (Abbazzi, 2004; Croitor, 2006b). The first representatives of this clade are among the most important newcomers of the late Villafranchian, replacing *Eucladoceros* as the dominant large deer after 1.6 Ma. The species *P. obscurus* is the commonest member of this group, present in various localities of the Mediterranean area and North Europe (Abbazzi, 2004; Croitor, 2006b). *Cervalces* is a genus of very large deer, related to the extant moose (*Alces*), which was common in the northern latitudes of the European continent since the middle Villafranchian (Breda and Marchetti, 2005; Breda, 2008).

The suids were represented solely by the genus *Sus* which already appeared during the Early Pliocene (Cherin et al., 2018; see chapters 3 and S1). The large verrucosic boar, *S. strozzi*, is a recurrent element in all the faunal assemblages of Europe until 1.8 Ma. After this interval, it became less common during the so-called ‘suid gap’, lasting from 1.8 to 1.2 Ma (Martínez-Navarro et al., 2015; see chapter 6).

Hippopotamus is a common element of Early-Middle Pleistocene assemblages in all Europe, from the Mediterranean area to, possibly, the British islands (Martino and Pandolfi, 2022; Adams et al., 2022). The first occurrence of the only Early Pleistocene hippo species, *H. antiquus*, is still controversial. Although already present in some Upper Valdarno sites (ca. 1.8 Ma), this taxon became widespread in the continent only after 1.2 Ma, being one of the most successful large herbivores of this period (Martino and Pandolfi 2022 and references therein).

Among the proboscideans, *Mammuthus meridionalis* was the only taxon able to survive the deforestation of the habitats of the middle Villafranchian. This large form of mammoth most probably emerged from the Late Pliocene *M. rumanus* and lasted for all the late Villafranchian, facing the extinction only at the end of Epivillafranchian when more advanced forms of elephants, better adapted to the post-EMPT steppe environments, replaced it (Kahlke et al., 2011). The rhino, *Stephanorhinus etruscus*, appeared slightly before 3.0 Ma, being a common element of the Villafranchian faunal assemblages from the Mediterranean to Central and North Europe (Guérin, 1980; Pandolfi et al., 2017). The Etruscan rhino at the end of Villafranchian, underwent to a shrinking of its habitat, surviving, until the end of Epivillafranchian, in some “refuge areas” of the Iberian and Italian Peninsulas (Pandolfi and Erten, 2017; Pandolfi et al., 2017). The horses (genus *Equus*) were already common elements of the European faunal assemblages since the middle Villafranchian (‘elephant-*Equus* event’ sensu Azzaroli, 1977). During the earliest stages of the late Villafranchian, the persistence of middle Villafranchian species, such as *Equus stenorhinus* and the large *Equus major*, is registered. After 1.8 Ma, the middle-sized *Equus altidens* replaced *Equus stehlini* and *Equus livenzovensis* as the most widespread horse in Europe until the Middle Pleistocene, sharing the habitats with the last *Equus stenorhinus* representatives (Cirilli et al., 2021, 2022 and references therein). At the end of the late Villafranchian (ca. 1.5–1.2 Ma), the occurrence of *Equus suessenbornensis* and *Equus apolloniensis* in the Mediterranean area may represent an early equid turnover for the large-sized horses of the EMPT (for a comprehensive review see Cirilli et al., 2022).

The late Villafranchian carnivore guilds are extraordinarily rich, showing heterogeneous assemblages with abundance of pack-hunters, scavengers, ambush and pursuit predators (Rodríguez-Gómez et al., 2015; Bartolini-Lucenti et al., 2022; Konidaris, 2022). Among large carnivorans, hyaenids and canids were the most affected by the middle-late Villafranchian turnover. The so-called ‘*Pachycrocuta brevirostris* event’ at ca. 2.0 Ma (Rook and Martínez-Navarro, 2010a) marks the dispersal of the giant bone-cracking hyaena in Europe. *Pachycrocuta*

brevirostris, due to its wide distribution and opportunistic behaviour, deeply shaped the faunal associations of all late Villafranchian and Epivillafranchian, being one of the major markers of the latest Villafranchian (Palombo et al., 2008; Martínez-Navarro et al., 2010a). Although the extinction of the two hyaenids *Pliocrocuta* and *Chasmaporthetes* is traditionally correlated to the arrival of *Pachycrocuta*, their survival until the latest Villafranchian is recorded in several sites of the Mediterranean Europe (Brugal et al., 2020; Koufos, 2022). The arrival of new Asian *Canis* species, including *Canis (Xenocyon) lycaonoides* and *C. mosbachensis*, replacing *C. etruscus*, *C. arnensis* and *C. (X.) falconeri*, characterized the pack-hunter guilds of Europe (Madurell-Malapeira et al., 2022). Among the large felids, the persistence of middle Villafranchian genera such as *Megantereon*, *Homotherium* and *Acinonyx* are registered in most Europe as well as the smaller *Lynx* and *Puma/Viretailurus*, which are joined by the newcomer *Panthera toscana* (Kahlke et al., 2011; Antón, 2013; Cherin et al., 2014; Konidaris, 2022). The Etruscan bear, *Ursus etruscus*, is the only ursid roaming the European continent, surviving until the very end of the late Villafranchian (Koufos et al., 2018).

Finally, the late Villafranchian is marked by the arrival of *Homo* in Europe (Fig. 1). Few sites of the continent bear the evidence of human passage, including the first occurrence of the genus at the gates of Europe in Dmanisi (Georgia) at ca. 1.8 Ma, and lithic artifacts from the Mediterranean area including the sites of Pirro Nord (Italy), Barranco León-D and Fuente Nueva 3 (Spain), dated between 1.7 and 1.2 Ma (Arzarello et al., 2007; Sirakov et al., 2010; Ferring et al., 2011; Toro-Moyano et al., 2013).

The late Villafranchian is a fundamental period for the ecosystem evolution of the European continent, due to its major faunal renewal, including a step-change in favour of taxa more adapted to the opening of the landscapes and drier conditions. The progressive aridification and shrinking of the subtropical environments, especially between 1.5 and 1.2 Ma, led to the extinction of all those animals which were suited to warm and closed habitats. It is noteworthy the overabundance of hypercarnivorous large predators, which strongly influenced the ecosystem by limiting the megaherbivore population sizes and reflected, perhaps, a high apport of scavengeable resources during this period (Konidaris, 2022 and references therein).

1.2.3. Epivillafranchian large mammals

After 1.2 Ma, the first effects of the EMPT started to model the faunal assemblages of Europe which were subjected to a major reorganization. The stronger and longer G-IG cycles strongly modified the environments with a shrinking of the forested habitats in favour of open ones. This led to the extinction of the last survivors of the middle-late Villafranchian transition, which were unable to adapt to the further harshening of the environmental conditions.

Fig. 4. Most important localities of the late Villafranchian of Europe with approximate chronology. Filled circles indicates more than one locality. 1, Dmanisi; 2, Tsalka; 3, Samarskoye; 4, Kamisli; 5, Yassigiime; 6, ‘Ubeidiyah; 7, Taurida Cave; 8, Salcia; 9, Fântâna lui Mitilan; 10, Grăunceanu; 11, Fântâna Alortitei; 12, La Pietriș 13, Milkovu din Vale; 14, Slivnitsa; 15, Krimni 3; 16, Apollonia 1; 17, Vasiloudi; 18, Gerakarou; 19, Tsiotra Vryssi; 20, Kalamoto 2; 21, Alykes; 22, Libakos; 23, Betfia VII/1, IX; 24, Trlica 10-11; 25, Kisláng; 26, Beremend (older sites); 27, Strmica; 28, Sandalja 1; 29, Olivola; 30, Tasso; 31, Matassino; 32, Torre Picchio; 33, Villa San Faustino; 34, Upper Valdarno (various localities); 35, Faella; 36, Farneta; 37, Mugello; 38, Pietrafitta; 39, Capena; 40, Fontana Acetosa; 41, Monte Argentario; 42, Pirro Nord; 43, Erpfinger Höhle; 44, Tegelen; 45, East Runton; 46, Westleton Beds; 47, Westbury-sub-Mendip (Siliceous Member); 48, Riège; 49, Montoussé; 50, Le Coupet; 51, Senèze; 52, Saint Privat d’Allier; 53, Chilhac; 54, Sainzelles; 55, Communac; 56, Ceysyssaquet; 57, Fonelas P-1; 58, Venta Micena; 59, Fuente Nueva 3; 60, Barranco León 5. Data taken from: Palombo, 2004; Breda et al., 2010; Rook and Martinez-Navarro, 2010; Kahlke et al., 2011; Madurell-Malapeira et al., 2014; Cherin et al., 2019a; Terhune et al., 2020; Brugal et al., 2020; Iannucci et al., 2021a.



MGST	GC.	Ma	ST.	ELMA	FU	MINQ	Transcaucasia Levant	East Europe	South-East Europe	Italian Peninsula	Central Europe	North-West Europe	West Europe	Iberian Peninsula				
MATUYAMA	Cobb Mountain	Early PLEISTOCENE	Calabrian	Late Villafranchian	Pirro	MINQ19	‘Ubeidiyah	Beremend	Kalamoto Krimni	Pietrafitta	Erfpinger Höhle	Westbury sub-Mendip (SM)	Ceyssagnet	Barranco León 5				
	Bjorn														Betfia VII/1, IX	Apollonia 1	Pirro Capena	Sainzelle Riège
	Gardar														Fântâna lui Mitilan	Pietrafitta	Monte Argentario	S. Privat d’Allier
	Giltsa														Trlica 10-11	Mugello	Communac	Fontana Acetosa
Olduvai	1.8	Gelasian	Late Villafranchian	Tasso	MINQ18	Dmanisi	Tsalka	Yassigiime	Tsiotra Vryssi	Upper Valdarno	East Runton	Le Coupet	Senèze	Venta Micena				
															Olivola	Alykes Libakos	Farneta	Fontana Acetosa
		2.0					Fântâna Alortitei	Gerakarou	Gerakarou	Faella Matassino		Westleton beds	Chillac					
							Sandalja 1	Vasiloudi	Vasiloudi	Torre Picchio								
							Slivnitsa	Kamisli	Kamisli									

The newcomers from Asia, better suited to face the onset of unstable dynamics, rapidly occupied the empty ecological niches as the first members of the upcoming dominant mammal guilds (Fig. 3). This transitional period in which there is a co-existence of both the remnants of late Villafranchian assemblages and the first Galerian representatives is commonly named Epivillafranchian (see above). Over the decades, the definition and the boundaries of Epivillafranchian had been a major point of interest for biochronology (Kahlke, 2007; Rook and Martínez-Navarro, 2010). These debates were fuelled by the discovery of several sites recording this biochron, including, among the most noticeable: Untermassfeld (Germany, ca. 1.1 Ma), Le Vallonnet and Durfort (France, ca. 1.2–0.8 Ma), Collecorti, Silvia, Cava Redicicoli and Frantoio (Italy, ca. 1.0 Ma) and the Iberian localities of Trinchera Elefante and Gran Dolina in Atapuerca (ca. 1.1–0.8 Ma), the Incarcial Complex (ca. 1.0–0.86 Ma) and the composite section of Vallparadís (ca. 1.2–0.8 Ma). For a comprehensive list of Epivillafranchian sites with chronological and geographical positions see Fig. 5.

The ungulate guilds were among the mostly affected by the Epivillafranchian transition. Some large bovids such as the primitive forms of *Bison* disappeared, replaced by larger and more robust species of the same genus such as *B. menneri* and *B. schoetensacki* (see chapters 5 and 6). The small bovids *Gazella*, *Gazellospira* and *Gallogoral* did not reach the final stages of late Villafranchian. On the contrary *Praeovibos*, *Soergelia* and *Hemitragus* were better adapted to the new arid conditions and thrived in most of the continent (Kahlke et al., 2011). Among the cervids, the small ‘*Pseudodama*’ *vallonnetensis* became the most widespread ‘*Dama*-like’ deer of the European faunal assemblages (De Lumley et al., 1988; Breda et al., 2020). During this period, the first occurrence of *Capreolus* in the Western Palearctic is also recorded (Breda et al., 2020). The Epivillafranchian ‘megalocerine’ and moose deer are represented by “advanced” versions of the late Villafranchian forms, such as *Praemegaceros verticornis*, which is most probably related to the Villafranchian *P. obscurus*, and *Cervalces carnutorum*, considered as deriving from a cladogenetic/anagenetic evolution of *C. gallicus* (Azzaroli and Mazza, 1993; Abbazzi, 2004; Breda, 2008). The first occurrence of the genus *Megaloceros*, with the species *M. savini* in many Western and Central Europe sites, has been considered a major marker of the biochron (Madurell-Malapeira et al., 2014).

After the late Villafranchian ‘suid gap’ in which the suid fossil record was scanty and non-continuous, *S. strozzi* re-appeared at the beginning of the Epivillafranchian (Martínez-Navarro et al., 2015; see also chapters 3, 6 and S1). After 1.2 Ma, the large hippo *H. antiquus* was widely distributed in the whole continent, spanning from the Mediterranean area to the high latitudes of Central and Northwestern Europe (Kahlke, 2001b, Martino and Pandolfi 2022; Adams et al., 2022). *Mammuthus meridionalis* was the dominant proboscidean during the late Villafranchian until the onset of the Epivillafranchian transition facilitated the dispersal of a more grazer-like elephants from Asia.

The arrival of *M. trogontherii* and *Palaeoloxodon antiquus* at the end of the Epivillafranchian are major bioevents of the transition from the Early to Middle Pleistocene (Ros-Montoya et al., 2018; Llaramendi et al., 2020). At ca. 1.2 Ma, the last *S. etruscus* were still populating few areas of Mediterranean Europe when the larger and more massive *S. hundsheimensis*, appeared and rapidly colonized all the continent (Lacombat, 2005; Pandolfi and Erten, 2017). The horses already faced an initial turnover between 1.5 and 1.2 with the arrival of the large-sized species *E. apolloniensis* and *E. suessenbornensis* which co-existed with the smaller *E. altidens*. Contrarily to the latter, which went extinct at the end of Epivillafranchian, these massive and long-legged forms thrived in most Europe until the Galerian (Cirilli et al., 2022 and reference therein).

The carnivore guilds of the earliest Epivillafranchian are characterized by the persistence of Villafranchian taxa such as the bone-cracking hyaena *P. brevirostris*, the wolves *C. (X.) lycaonoides* and *C. mosbachensis* and the large felids *Homotherium crenatidens*, *Megantereon adroveri*, *Panthera gombaszoegensis* and *Acinonyx pardinensis* (Kahlke et al., 2011; Antón, 2013; Madurell-Malapeira et al., 2014; Hemmer and Kahlke, 2022; Konidaris, 2022). At the end of the Early Pleistocene some large predators including: *Pachycrocuta*, *Canis (Xenocyon)*, *Megantereon* and *Puma/Viretailurus* faced extinction possibly because of the competition with some new African and Asian elements which were dispersing in Europe (Madurell-Malapeira et al., 2010, 2014, 2017; Konidaris, 2022). Among the new carnivoran taxa the most important are: the large ‘speloid bear’, *Ursus deningeri*, which replaced the Villafranchian *U. etruscus*, the first leopard *Panthera pardus*, and a large form of *Panthera*, possibly related to the giant *P. fossilis* of the Galerian (Moullé et al., 2006; Madurell-Malapeira et al., 2014; Sotnikova and Foronova, 2014; Prat-Vericat et al., 2022).

The Epivillafranchian is also marked by the spread of *Homo* across the continent. The peopling of Europe, which already started at the end of the Villafranchian, expanded furtherly as testified by the lithic industry found in various sites of the Mediterranean area such as: Monte Poggiolo, Le Vallonnet or Sima del Elefante (Peretto et al., 1998; Michel et al., 2017). This period is clearly marked by the record of the first acheulian artifacts at the Iberian site of La Boella (ca. 0.8 Ma; Vallverdú et al., 2014).

The Epivillafranchian biochron represents a pivotal point for the evolution of the faunas in Europe. The shrinking of the forested areas given by a strong decrease of humidity and the onset of new G-IG cycles with harshened and prolonged cold phases, led to step-change in the palaeoenvironmental conditions of the latest Early Pleistocene. This shift toward drier and more open habitats determined a series of ecological filters which wiped out most of the relict taxa of the Villafranchian age, unable to adapt to the progressive climatic deterioration and created niche space for other groups, better suited to face the newly formed conditions.



MGST	GC.	Ma	ST.	ELMA	FU	MNQ	Transcaucasia Levant	East Europe	South-East Europe	Italian Peninsula	Central Europe	North-West Europe	West Europe	Iberian Peninsula
MAT. Kamakitsura Santa Rosa	Early PLEISTOCENE	0.8	Calabrian	Epivillafranchian	Slivia	MNQ21	Evron Akhalkalaki	Trlica 6-5 Stránská Skála Gombasek	Manastirec	Silvia Promano	Würzburg- Schalksberg	Het-Gat	Trois Pigeons	Pontón de la Oliva Cueva Victoria Vallparadis 7-4 Cal Guardiola 4-8
		1.0												
Jaramillo	PLEISTOCENE	1.2												
Panaru														
Cobb Mountain														
Bjom														

Fig. 5. Most important localities of the Epivillafranchian of Europe with approximate chronology. Filled circles indicates more than one locality. 1, Akhalkalaki; 2, Evron; 3, Sarkel; 4, Semibalki 1; 5, Port Kraton; 6, Margaritovo 2; 7, Sinyaya Balka; 8, Nogaïsk; 9, Tsimbal; 10, Kairiy; 11, Chishmikiyoy; 12, Dealul Viilor; 13, Kunino (lower level); 14, Manastirec; 15, Ravine of Voulgarakis; 16, Gombasek; 17, Trlica 6-5; 18, Somssich Hill 2; 19, Stránská Skála; 20, Slivia; 21, Lefte 9; 22, Frantoio (Arda river); 23, Imola; 24, Promano; 25, Collecurti; 26, Monte Peglia; 27, Redicicoli; 28, Untermassfeld; 29, Würzburg-Schalksberg; 30, Het Gat; 31, Saint Prest; 32, Blassac-la-Girondie 33, Le Vallonnet; 34, Tour de Grimaldi; 35, Trois Pigeons; 36, Durfort; 37, Bois-de-Riquet; 38, Incarcal I-V; 39, Vallparadis Estació 12-4; 40, Cal Guardiola; 41, Barranc de la Boella; 42, Sima del Elefante TE7-TE14; 43, Gran Dolina TD3-7; 44, Pontón de la Oliva; 45, Quibas; 46, Cueva Victoria. Data taken from: Palombo, 2004; Breda et al., 2010; Rook and Martinez-Navarro, 2010; Kahlke et al., 2011; Madurell-Malapeira et al., 2014; Terhune et al., 2020; Brugal et al., 2020; Iannucci et al., 2021a and references therein.

1.2.4. Galerian large mammals

At the Early-Middle Pleistocene boundary, the EMPT already changed drastically the palaeoenvironments and, thus, the faunal associations of the Western Palaearctic. The old Villafranchian taxa mostly disappeared and the Epivillafranchian newcomers further dispersed and diversified. The Galerian biochron formally starts at this boundary and lasts until the late Middle Pleistocene (i.e., ca. 0.35 Ma), in which the Mid-Brunhes Transition marks the end of EMPT and the mammal guilds of Europe entered a new phase, namely the Aurelian LMA (Gliozzi et al., 1997). The Galerian, differently from the previous biochrons which are mostly recorded in the Mediterranean area, is well represented also at higher latitudes. It is worth mentioning the Cromer forest-bed sites of Boxgrove and Clacton (United Kingdom, ca. 0.8–0.4 Ma), Süssenborn, Voigtstedt, Mauer, Mosbach 2 and Hundsheim (Germany, ca. 0.7–0.5 Ma) in Central-North Europe, Sima de los Huesos and Trinchera Dolina TD8 (Spain, ca. 0.6–0.5 Ma), Soleilhac and Lunel-Viel (France, 0.7–0.4 Ma), Ponte Galeria, Isernia la Pineta and Fontana Ranuccio (Italy, ca. 0.8–0.4 Ma) in Southern Europe, and the Tiraspol complex (Moldavia, 0.9–0.4 Ma) in Eastern Europe. The complete list of the main Galerian localities with chronological and geographical positions is provided in Fig. 6.

The herbivore guild at the Matuyama-Brunhes boundary underwent to a partial reorganization with the extinction of some remnants of the Villafranchian age and the diversification of the Epivillafranchian newcomers. The large-sized bovid *B. schoetensacki* rapidly dispersed in the whole continent, reaching the Northern latitudes of Central Europe and British Isles (Flerov, 1972; Breda et al., 2010, see chapter 5). This form successfully adapted to the heterogeneous habitats of the European Middle Pleistocene and persisted until the end of the Galerian, after which, it was replaced by two other giant bovines, the steppe wisent (*B. priscus*) and the auroch (*Bos primigenius*), coming from Asia and Africa, respectively (Sala, 1986; Kahlke, 1999; Martínez-Navarro et al., 2007). During the interglacial phases of the latest Galerian, Europe was visited by the thermophilus bovine *Bubalus*, whereas during the colder stages, the large caprine *Ovibos* (musk-ox) sporadically appeared (Kahlke et al., 2011; Koenigswald et al., 2019; Ruff et al., 2020). The mid to small-sized bovids *Hemitragus*, *Hemibos* and *Praeovibos* evolved in forms which were better adapted to the strongly partitioned ecosystems of the Galerian (Kahlke et al., 2011). The ‘megalocerine’ deer like *P. verticornis* and *M. savini* became more common, while other large forms with palmed antlers, such as *P. solilhacus*, appeared (Pfeiffer, 2002; Croitor, 2006b; Breda et al., 2015 and reference therein). The moose genus *Cervalces* was represented by the very large species *C. latifrons* which firstly occurred at the Epivillafranchian-Galerian boundary (Breda, 2008). The reindeer *Rangifer tarandus* and the red deer *Cervus elaphus* (with several species/subspecies of a single phyletic lineage) have their first unambiguous appearance at the end of the Galerian (Abbazzi and Azzaroli,

1995; Moigne et al., 2006; Van der Made et al., 2017). During this biochron the smaller ‘*Dama*-like’ forms are poorly represented in terms of diversity and abundance (Breda and Lister, 2013). The first small deer with palmate antlers (genus *Dama*) appears around 0.7 Ma with the species *D. roberti*. This form will be replaced at the beginning of the Aurelian, by its relative *D. clactoniana* (Leonardi and Petronio, 1976; Breda and Lister, 2013). Regarding suids, the disappearance of the verrucosic boar *S. strozzi* just after the Jaramillo subchron, allows the dispersal of *Sus scrofa*, which adapted with various morphotypes to the heterogeneous ecosystems of the Western Palearctic (Kahlke et al., 2011; Van der Made et al., 2017; see chapter 3). *Hippopotamus antiquus* persisted in southern Europe until the Middle Pleistocene, being replaced by the modern species, *H. amphibius* after 0.5 Ma (Martino and Pandolfi, 2022 and references therein). The dominion of the gigantic proboscideans *M. trogontherii* and *P. antiquus* signs the whole Galerian age being among the commonest elements of the European record until the Late Pleistocene (Kahlke et al., 2011). The Epivillafranchian *S. hundsheimensis* was the only rhinoceros inhabiting the Western Palearctic until the early Middle Pleistocene, when other two species, *S. kirchbergensis* and *S. hemitoechus*, reached Europe, replacing the last Early Pleistocene rhinoceros (Van Asperen and Kahlke, 2015). At the end of the Galerian, the woolly rhinoceros (genus *Coelodonta*), typical element of the so-called *Mammuthus-Coelodonta* faunal complex, dispersed in the steppe environments of the Western Palearctic and persisted until the last interglacial (Kahlke, 1999; Kahlke and Lacomat, 2008). The horses *Equus ferus* and *E. hydruntinus*, respectively the ancestors of modern horses and asses, appeared around the mid-late Galerian and replaced the Epivillafranchian *E. suessenbornensis* (Cirilli et al., 2022).

The Galerian carnivorans underwent through an almost complete reorganization with the extinction of specialized Villafranchian-Epivillafranchian forms and the arrival of generalist and adaptable newcomers. The ‘*Crocota crocuta* event’ marks the passage from the Epivillafranchian to Galerian (ca. 0.8 Ma) in which the extinction of the bone-cracking hyaena *Pachycrocota* left empty a niche for the arrival of *C. crocuta* and ‘*Hyaena*’ *prisca* (Martínez-Navarro et al., 2010a; Palombo, 2014; Iannucci et al., 2021a). *C. mosbachensis* survived until the end of the Galerian when it was replaced by the modern wolf *Canis lupus* (Palombo, 2018; Iurino et al., 2022; Konidaris, 2022). The large felids experienced an important turnover with the last occurrence of the machairodontinae *Homotherium* and *Pa. gombaszoegensis*, (ca. 0.3 Ma) replaced by the large steppe lion *Pa. fossilis* and the leopard *Pa. pardus* (Madurell-Malapeira et al., 2014; Sotnikova and Foronova, 2014; Prat-Vericat et al., 2022; Konidaris, 2022). The speloid bear *U. deningeri*, appeared during the Epivillafranchian, persisted for all the Galerian, joined by the first forms of brown bear *U. arctos* which dispersed in Europe around 0.5 Ma (Moigne et al., 2006).

During the Galerian the human occupation of Western Palearctic started to be ubiquitous with a long list of sites scattered along the whole continent, from the Italian Peninsula to the British Isles, from the Levant to the Iberian

Peninsula (Muttoni et al., 2018 and references therein). According to the most recent reviews, the Galerian dispersal event of the genus *Homo* in the Western Palearctic is strictly related with the final results of the EMPT on environments and faunas (Muttoni et al., 2018). The decline of the carnivore guilds and the opening of the Po-Danube Gateway leading to the western dispersal of the Galerian large herbivores, might have favoured the first “mass” dispersal of humans in Europe (Palombo and Mussi, 2006; Muttoni et al., 2015, 2018).

The Galerian biochron represents the last stage of the EMPT effects on the faunas of European Pleistocene. The taxa appeared during the Epivillafranchian, thrived in a wide spectrum of forms and adaptations, progressively colonizing all the continent. The ecological niches left empty after the extinction of the last remnants of the Villafranchian age were occupied by these ascending groups as the precursors of the “modern” faunas which will be fully developed during the Aurelian LMA.

Next page. Fig. 6. Most important localities of the Galerian of Europe with approximate chronology. Filled circles indicates more than one locality. 1, Haykadzor; 2, Treugolnaya cave; 3, Girey 1; 4, Kagalnik; 5, Semibalki 2; 6, Gesher Benot Ya’aqov; 7, Tiraspol complex; 8, Araci-Cariëră; 9, Araci-Fântâna Fagului; 10, Feldioara; 11, Rotbav Silvestru; 13, Denzli; 14, Kunino (upper level); 15, Kozarnika B2-1; 16, Petralona cave; 17, Megalopolis; 18, Tarkő; 19, Vár-hegy; 20, Vértesszőlős; 21, Hundsheim; 22, Visogliano; 23, Brece di Soave; 24, Domegliara Selvavecchia; 25, Valdemino (lower layers); 26, Monte Oliveto; 27, Borgonuovo; 28, Cesi; 29, Beccia di Casal Selce; 30, Ponte Molle; 31, Ponte Galeria; 32, Fontana Ranuccio; 33, Cava Nera Molinario; 34, Pagliare di Sassa; 35, Isernia la Pineta; 36, Cimitero di Atella; 37, Notarchirico; 38, Venosa-Loreto; 39, Calorie; 40, Konéprusy C 718; 41, Schönebeck; 42, Voigtstedt; 43, Bad Frankenhausen; 44, Süssenborn; 45, Dorn-Dürkheim; 46, Mosbach 2; 47, Mauer; 48, Miesenheim 1; 49, Bruchsal-Büchenau; 50, Steinheim an der Murr; 51, Heppenloch; 52, West Runton; 53, Pakefield; 54, Ostend; 55, Waverly Wood; 56, Trimmingham; 57, Little Oakley; 58, Hoxne; 59, Clacton; 60, Swanscombe; 61, Westbury-sub-Mendip (Calcareous Member); 62, Boxgrove; 63, Terra Amata; 64, L’Escale; 65, Caune de l’Arago; 66, Soleilhac; 67, Pont-du-Château; 68, La Vayssiere; 69, Camp-de-Peyre; 70, Abbeville; 71, Gran Dolina TD 8; 72, Gran Dolina TD 10; 73, Sima de los Huesos; 74, Trinchera Galería TG 3; 75, Cúllar de Baza 1. Data taken from: Bon et al., 1991; Palombo, 2004; Breda et al., 2010; Rook and Martínez-Navarro, 2010; Kahlke et al., 2011; Madurell-Malapeira et al., 2014; Marra et al., 2014; Terhune et al., 2020; Brugal et al., 2020; Iannucci et al., 2021a and references therein.



MAT.	MGST	GC.	Ma	ST.	ELMA	FU	G.B.	Transcaucasia Levant	East Europe	South-East Europe	Italian Peninsula	Central Europe	North-West Europe	West Europe	Iberian Peninsula
BRUNHES <small>Big Lost</small>	Middle PLEISTOCENE	0.4	Chibanian	Galerian	Fontana Ranuccio	MNQ23		Feldioara Araci-Carieră Araci-Fântâna Fagului	Denzli Megalopolis		Fontana Ranuccio Visogliano	Selbnebeck Bad Frankenhäusern Bruchsal Büchenau Heppenheim Steinheim der Murr	Hoxne Clacton Swanscombe	Camp-de-Peyre Terra Amata	Trinchera Galeria 3
					0.6	Isernia	MNQ22	Treugolnaya cave	Rotbav Silvestru Uppony	Kagalnik	Cava Nera Ponte Molinario Molle	Mosbach 2	Waverly Wood Ostend	Abbeville Pont-du-Château Caune de l'Arago	Gran Dolina 10 Sima de los Huesos
MAT.	Early	0.8	Calab.	-----	Slivia	MNQ21	Gesher Benot Ya'aqov	Tarkó Vár-hegy Vertesszőlös Girey 1 Kozarnika B2-1 Tiraspol complex	Petralona cave	Cesi Cimitero di Aetia Casal Selce Biecece di Soave Calorie Pagliare di Sassa Borponovo Nortardirico Monte Oliveto Valderrino Ponte Galeria Venosus-Loreto	Hundsheim Miesenheim 1 Süssenborn Mauer	West Runtom Trimingham Pakefield	L'Escaie La Vayssiere Soleilhac	Cùllar de Baza 1 Gran Dolina 8	

1.3. Suids and Bovids from their origins to the Pleistocene

Bison and *Sus*, as testified by their extremely rich fossil records and historical/present geographic distribution, are two of the most widespread genera of Pleistocene and Holocene large herbivores (McDonald, 1981; Sipko, 2009; Barrios-Garcia and Ballari, 2012; Kerley et al., 2012; IUCN, 2022). Their adaptive radiations allowed them to populate most of Northern Hemisphere, facing successfully all the climate transitions of the last 1.5 Ma. *Bison* and *Sus*' importance in their ecosystems is renowned due to their position within the trophic web and their direct effects on the environments in which they live (Gunther and Haroldson, 1997; Melis et al., 2007; Barrios-Garcia and Ballari, 2012; Risch et al., 2021 among others). These two genera are among the most iconic taxa of their respective families, Bovidae and Suidae which, in turn, are among the most successful families of artiodactyls.

The order Artiodactyla (sensu Groves and Grubb, 2011), also commonly named 'even-toed ungulates' for their even number of functional toes on each limb, is the most diverse and widespread group of large mammals on Earth with 23 families, 131 genera and 335 species (IUCN, 2022). Their roots are found most probably in Dichobunoidea, a poorly-known paraphyletic group of small mammals of the early Eocene (Theodor et al., 2007; Orliac and O'Leary, 2014; Ducroq, 2019). From these small herbivores, not larger than a hare, the artiodactyls flourished during the Neogene with a variety of forms, adaptations and sizes which allowed them to conquer all the biomes and regions of the planet, including the oceans. The taxonomic history of Artiodactyla has been strongly discussed due to the apparent discrepancies between the traditional morphological analyses and the new molecular ones (for a complete review see Marcot, 2007 and references therein). Traditionally, Artiodactyla included the following extant major clades: Tayassuidae and Suidae (both in Suoidea, i.e., pigs and peccaries), Camelidae (in Tylopoda, i.e., camels and llamas), Hippopotamidae (in Ancodonta, i.e., hippos) and several families within Ruminantia (Fig. 7). To these, only in the last decades, was added the Cetacea (i.e., whales and dolphins), which has been proven by several molecular and morphological studies, to be deeply nested within Artiodactyla (Irwin and Arnason, 1994; Gatesy et al., 1996; Montgelard et al., 1997; Nikaido et al., 1999; Geisler and Uhen, 2003; Geisler et al., 2007; Zhou et al., 2011; Hassanin et al., 2012). For this reason, many authors prefer to refer to this group as Cetartiodactyla (e.g., Hassanin et al., 2012; Zurano et al., 2019). However, in this work, it has been decided to follow Groves and Grubb (2011) and Prothero et al. (2022) retaining the original nomenclature for the sake of consistency with centuries of taxonomic studies, but acknowledging that Cetacea is formally within the group. According to the paleontological record and the most recent time-calibrated molecular studies, Artiodactyla had various radiations during the Cenozoic including the abrupt diversification in three clades (Cetruminantia, Suina and Tylopoda) in the

earliest Eocene, the splitting of cetaceans in Mysticeti and Odontoceti close to the Eocene-Oligocene boundary and the explosive radiations of both Cetacea and Ruminantia between the Oligocene and Miocene (Hassanin et al., 2012; Zurano et al., 2019 and references therein) (Fig. 7).

Pigs, boars, warthogs and peccaries are included in Suoidea (also known as Suina), a superfamily of artiodactyls characterized by a robust body with relatively short legs, unfused metapodials, non-ruminant stomach, bunodont/brachydont dentition, large heads, short neurocranium and elongated splanchnocranium ending with a tubular snout (Groves and Grubb, 1993). Suoidea has been historically considered the sister taxon of Hippopotamidae (forming the suborder Suiformes), until recent years, when molecular analyses consistently placed Hippopotamidae and Cetacea in a monophyletic group called Cetancodonta or 'Whippomorpha' (Graur and Higgins 1994; Gatesy et al. 1996; Montgelard et al. 1997; Spaulding et al., 2009; Zurano et al., 2019 among others). At the current state of the art, Suoidea are considered among the most basal artiodactyls, being placed, alternately with Tylopoda, as sister group of Ruminantia (Spaulding et al., 2009; Zurano et al., 2019). Suoidea includes the extant Tayassuidae (tayassuids) and Suidae (suids) to which are added the debated extinct families of Palaeochoeridae and Sanitheridae (Van der Made and Hussain, 1992; Harris and Liu, 2007; Pickford, 2006; Orliac et al., 2010). The first suoids likely appeared during the middle-late Eocene in East Asia (Liu, 2001; Zurano et al., 2019). Suidae and Tayassuidae diverged sometimes later, during the late Eocene or early Oligocene in Asia and, whereas the latter colonized the Americas, the former dispersed in Eurasia becoming one of the most successful and widespread artiodactyl groups (Thenius, 1970; Orliac et al., 2010; Frantz et al., 2016; Gongora et al., 2017). The evolutionary history of Suidae is quite complex, characterized by a series of convergences in several morphological structures and an almost unknown Paleogene history (see Orliac et al., 2010). Although the first Suidae trace goes back to the Oligocene, the paucity of fossil record referable to this period might underestimate the diversity of this family which could have been already well developed before the Neogene (Orliac et al., 2010; Frantz et al., 2016). The first unambiguous recorded radiation of Suidae is registered during the Mio-Pliocene with multiple subfamilies colonizing the whole Old World (Frantz et al., 2016 and references therein). There is still little consensus among scholars but at least five subfamilies of Suidae emerged during the Miocene, namely Listriodontinae, Cainochoerinae, Hyotheriinae, Tetraconodontinae and Suinae, to which is sometimes added Babyrousiniae (Pickford, 1986; Orliac et al., 2010; Pickford, 2012; Frantz et al., 2016). It is worth mentioning that the relationships between the African and European suids are still controversial. Some authors (e.g., Groves, 1981a; Pickford, 2012) considered Eurasia as the area of origin of extant African suids, however, recent molecular studies suggest that the African clade is monophyletic and it might be evolved separately from the ancestors of modern-day Eurasian Suinae (Gongora et al., 2011). By the beginning of the Pliocene, most of the subclades of

Suidae went extinct with the exception of Suinae, Tetraconodontinae and the obscure group of Babyrousinae (Van der Made et al., 2006; Orliac et al., 2010; Frantz et al., 2016). Tetraconodontinae eventually disappeared sometime during the Pliocene, whereas Babyrousinae were restricted to remote areas of Southeastern Asia (Van der Made, 1998; Frantz et al., 2016). The ecological niches left empty by the loss of other suid competitors triggered the explosive radiation of Suinae, which reached their peak of diversity between the Late Miocene and Early Pliocene (Harris and White, 1979; Pickford, 1988; Geraads, 2004; Frantz et al., 2016; Pickford and Obada, 2016; Gongora et al., 2017). Suids, in their complex evolutionary history, were able to adapt their morphology and behaviour to the widest range of habitats and climates, being among the most common clades in the large mammal fossil records of Eurasia and Africa. Thanks to this richness, suids have been successfully used as biochronological tools for African records (White and Harris, 1977; Cooke, 1978) igniting a stimulating discussion about their usefulness in European stratigraphy (Van der Made and Moyà-Solà, 1989).

The crown group Ruminantia originated during the middle Eocene in Asia and includes Tragulina and Pecora (Zurano et al., 2019). This infraorder is the most diversified among the Artiodactyla with more than 190 species divided into six extant families (Hassanin and Douzery, 2003; Bibi, 2013; Zurano et al., 2019 and references therein). The members of this group share several adaptations in teeth (i.e., the lack of upper incisors and the presence of incisiform lower canine) and in limb bones (i.e., navicular and cuboid fused, magnum and trapezoid fused) and the presence of the ruminant digestive system which includes a four-chambered stomach, although Tragulina do not have a fully compartmentalized stomach (Hassanin and Douzery, 2003, Métais and Vislobokova, 2007; Prothero, 2017). Ruminantia is composed by the extant families Tragulidae, Moschidae, Giraffidae, Antilocapridae, Cervidae and Bovidae, to which are often added several extinct families of disputed validity (Hassanin and Douzery, 2003; Hassanin et al., 2012; Métais and Vislobokova, 2017; Zurano et al., 2019). The separation between Tragulina (represented by the only family Tragulidae) and Pecora (which includes all the remaining families) most probably happened sometime during the Eocene (Hassanin et al., 2012). The first radiation of crown Pecora is still strongly debated, happened either during the early Oligocene (Hassanin and Douzery, 2003), Oligocene-Miocene transition (Hassanin et al., 2012; Zurano et al., 2019) or Early Miocene (Meredith et al., 2011; Bibi, 2013). The available fossil record shows that, by the end of the Middle Miocene, all the families of Pecora were already fully developed (Bibi, 2013). Although Bovidae and Moschidae consistently result as sister taxa (e.g., Meredith et al., 2011; Hassanin et al., 2012; Bibi, 2013 among others), their splitting is still controversial being placed at the Early Miocene (Meredith et al., 2011; Bibi, 2013; Zurano et al., 2019) or slightly earlier, at the latest Oligocene (Hassanin and Douzery, 2003; Hassanin et al., 2012). The Early Miocene *Eotragus noyei* from Pakistan is considered the very first Bovidae

appearing in the fossil record, although it is still not clear if being part of stem or crown Bovidae (Bibi, 2013). Extant Bovidae includes two major clades, namely Bovinae and Antilopinae, made up by nine tribes: Bovini, Tragelaphini and Boselaphini, and Cephalophini, Reduncini, Antilopini, Alcelaphini, Hippotragini, and Caprini, respectively (Hassanin and Douzery, 2003; Bibi et al., 2009; Bibi, 2013; Hassanin et al., 2012; Zurano et al., 2019). According to Janis and Scott (1988), all these tribes share the presence of unbranched and non-deciduous cranial appendages, covered by a permanent keratin sheath, which differentiate them (i.e., Bovidae) from the other members of Pecora. The splitting between the two subfamilies, Bovinae and Antilopinae, must have been happened between the Middle and Late Miocene (Bibi, 2013; Zurano et al., 2019) or at the earliest stages of the Miocene (Hassanin et al., 2012). By the end of the Miocene, Bovini was already dispersing from Asia to Africa and Europe, becoming rapidly one of the most successful groups of artiodactyls of the Old World, subsequently reaching the North American continent at the end of the Pleistocene (Bibi et al., 2009; Froese et al., 2017).

1.3.1. European Suinae: paleobiogeography and biochronology

Suinae is the only extant suid subfamily with up to five genera, made by 17 species, living today (Frantz et al., 2016; Cherin et al., 2018). Suinae most likely appeared during the Late Miocene and, taking advantages of the extinction of other suid groups, rapidly colonized all the Old World with an abundance of morphologies and adaptations (Frantz et al., 2016; Gongora et al., 2017). Over the years several genera of Suinae from Africa and Eurasia were erected, including among the most widely recognized: *Propotamochoerus* (= *Korynochoerus*)† (Eurasia), *Hippopotamodon* (= *Microstonyx*)† (Eurasia), *Sus* (Eurasia), *Porcula* (Asia), *Celebochoerus*† (Asia), *Eumaiiochoerus*† (Europe), *Metridiochoerus*† (Africa), *Kolpochoerus*† (Africa), *Potamochoerus* (Africa), *Hylochoerus* (Africa), *Phacochoerus* (Africa) (Van der Made and Moyà-Solà, 1989; Harris and Liu, 2007; Gongora et al., 2017; Cherin et al., 2018). The African Miocene to Pleistocene suid guild is characterized by the presence of the Tetraconodontinae clade *Nyanzachoerus-Notochoerus* and the two Suinae clades *Metridiochoerus-Phacochoerus* and *Kolpochoerus-Hylochoerus*, all represented by several species whose phylogenetic relationships are still debated (Harris and White, 1979; Souron et al., 2015; Gongora et al., 2017; Cherin et al., 2018 among others). The Eurasian Suinae are commonly divided into two tribes, Dicoryphochoerini and Suini, on the basis of dental morphology (see Van der Made and Moyà-Solà, 1989). The former is composed by the three extinct genera *Hippopotamodon*, *Propotamochoerus* and *Eumaiiochoerus*, which most likely evolved from a common ancestor in southern Asia during the latest Middle Miocene and subsequently dispersed into Europe at the end of the Miocene (Pickford, 2015). Among these, the small-sized *Eumaiiochoerus* was endemic of the Tusco-Sardinian paleobioprovince (Hürzeler 1982; Mazza and Rustioni

1997), whereas the larger, and similar to each other, *Propotamochoerus* and *Hippopotamodon* were widespread in all Eurasia with a debated number of species (Kostopoulos et al., 2001; Pickford, 2015; Iannucci et al., 2021b; McKenzie et al., 2023). By the Mio-Pliocene boundary, the Dicoryphochoerini of Europe went extinct replaced by the Asian newcomers Suini. If the African suines are characterized by a large number of genera and species, the Eurasian lineage is mainly represented by the highly polymorphic and geographically widespread genus *Sus*.

The first representative of Eurasian Suini is most probably *Sus arvernensis* (= *S. minor*), whose first occurrence in Europe during the Pliocene has been commonly accepted as a marker of the beginning of the Ruscinian LMA (Van der Made 1990; Agustí et al. 2001; Iannucci et al., 2022). This small-sized species survived at least until the early Villafranchian (ca. 3.0 Ma, MN 16) and it has been recorded in many localities of Europe, Near East, China and Africa, although the taxonomic attribution of extra-European remains has been questioned (Iannucci et al., 2022 and references therein). *Sus arvernensis* has been considered as the ancestor of the ‘verrucosic canine’ clade (Azzaroli, 1954; Berdondini, 1992; Pickford, 2012; Cherin et al., 2018 among others) also grouped in the genus/subgenus *Dasychoerus* (Pickford, 2012; Pickford and Obada, 2016). This group of extinct and extant suids includes all species of *Sus*, with the exception of *S. scrofa* and possibly *S. lydekkeri*, featuring a lower male canine which in cross section is roughly equilateral (i.e., the labial and lingual sides are similar in size, and both larger than the distal one, Fig. 8) (Azzaroli, 1954; Hardjasasmita, 1987; Cherin et al., 2018 among others). The Early Pleistocene of Europe is marked by the arrival of *S. strozzi*, a large form of ‘verrucosic boar’, which most probably phylogenetically related with *S. arvernensis* and replaced it from the middle Villafranchian onward (Azzaroli, 1954; Berdondini, 1992; Cherin et al., 2018). *Sus strozzi* is a constant presence in the European fossil record until ca. 1.8 Ma, from when the remains of suids in the whole Western Palearctic become scanty and non-continuous (see also chapters 7 and S1). This ‘suid gap’ (Martínez-Navarro et al., 2015) has been questioned by Van der Made (2017). In spite of that, the evident bias of suids in the fossil record cannot be explained by taphonomic reasons (as the thick and robust bones and teeth of suids usually have a good probability of fossilization) or undersampling (as remains of suids during the ‘suid gap’ are absent even in localities which have yielded thousands of fossils remains; e.g., Dmanisi, Pietrafitta, Venta Micena, Fuente Nueva 3, or Apollonia). For a deeper discussion about this topic see chapter 6. At the beginning of the Epivillafranchian (ca. 1.2 Ma) this ‘suid gap’ seems to cease with the re-appearance of suids in Europe in many localities such as Untermassfeld, Le Vallonet, Vallparadís Section, La Boella and Frantoio among others (Moullé, 1992; Guérin and Faure, 1997; Bona and Sala, 2016; chapter S1). Until recent years, almost all the Epivillafranchian and Galerian remains of *Sus* were attributed the extant boar, *S. scrofa*, often referred to the primitive subspecies *S. s. priscus* (e.g., Kurten, 1968; Guérin and Faure, 1997; Van der Made, 1999; Van der Made et al., 2017). However, this

has been proved wrong by the work presented in this thesis (chapters 3 and S1) in which it is demonstrated that *S. scrofa* did not appear in Europe before the Middle Pleistocene and most of the Epivillafranchian suid records actually belong to the species *S. strozzi*. At the dawn of the Galerian, this species is among the large mammals that went extinct, replaced by the first representatives of *S. scrofa*. The origin of the latter species is still obscure, although it has been suggested that the Asian *S. lydekkeri* (with an intermediate scrofic-verrucosic canine) might be its ancestor (Fujita et al. 2000). *Sus scrofa*, indeed, is the only representative of the so-called ‘scrofic canine’ clade, in which the lower male canine section is scalene (i.e., the sides are all different in size and the lingual side is shorter than the distal one; Azzaroli, 1954; Cherin et al., 2018; Iannucci, 2022). By the Galerian LMA, the extant wild boar conquered all the temperate and sub-tropical environments of Eurasia and extirpated almost any competitor with the exception of some species belonging to the verrucosic clade surviving in Southeast Asia (e.g., *S. celebensis*, *S. verrucosus*, *S. barbatus*; Frantz et al., 2016; Cherin et al., 2018 and references therein).

1.3.2. European Bovinae: paleobiogeography and biochronology

Bovinae includes at least 23 extant and a much higher number of extinct species (Bibi, 2009). After the divergence from Antilopinae during the Miocene, Bovinae followed an independent evolutionary radiation into the tribes Bovini, Boselaphini and Tragelaphini (MacEachern et al., 2009; Bibi, 2013 among others). The latter two tribes represent all the spiral and four-horned ox like Bovinae (Bibi et al., 2009). Tragelaphini includes the extant genera *Tragelaphus* and *Taurotragus*, although the latter is often considered as a subgenus of the former (Bibi, 2009; Hassanin et al., 2018). The evolutionary history of this group is almost completely exclusive of the African continent (Bibi et al., 2009). Molecular and fossil evidence suggested that this group diverged before the Pliocene either in Africa or Eurasia but had its radiation in the former (Kostopoulos and Koufos, 2006; Bibi et al., 2009). The earliest African tragelaphine of the Mio-Pliocene boundary is most probably already a member of the crown group, although the recently discovered *Pheraios* from the Late Miocene of Greece may represent a possible stem clade of this group in Eurasia (Kostopoulos and Koufos, 2006; but see also Bibi, 2009). Whether the tribe emerged from an African forerunner or from a “pre-tragelaphine” Eurasian form which later dispersed in Africa, is still debated. However, if confirmed, the presence of a basal Tragelaphini in the terminal Miocene of Southeast Europe suggests the existence of two separated clades originated out of Africa before the Late Miocene (Kostopoulos and Koufos, 2006). Boselaphini, in its broader term, form a large and diverse tribe of bovids which includes the extant genera *Boselaphus* and *Tetracerus* and the Pleistocene *Duboisia* (Bibi, 2009; Rozzi et al., 2013). This group is currently considered a non-monophyletic clade being used, for many years, as a “wastebasket” for all the extinct taxa not conform to Tragelaphini

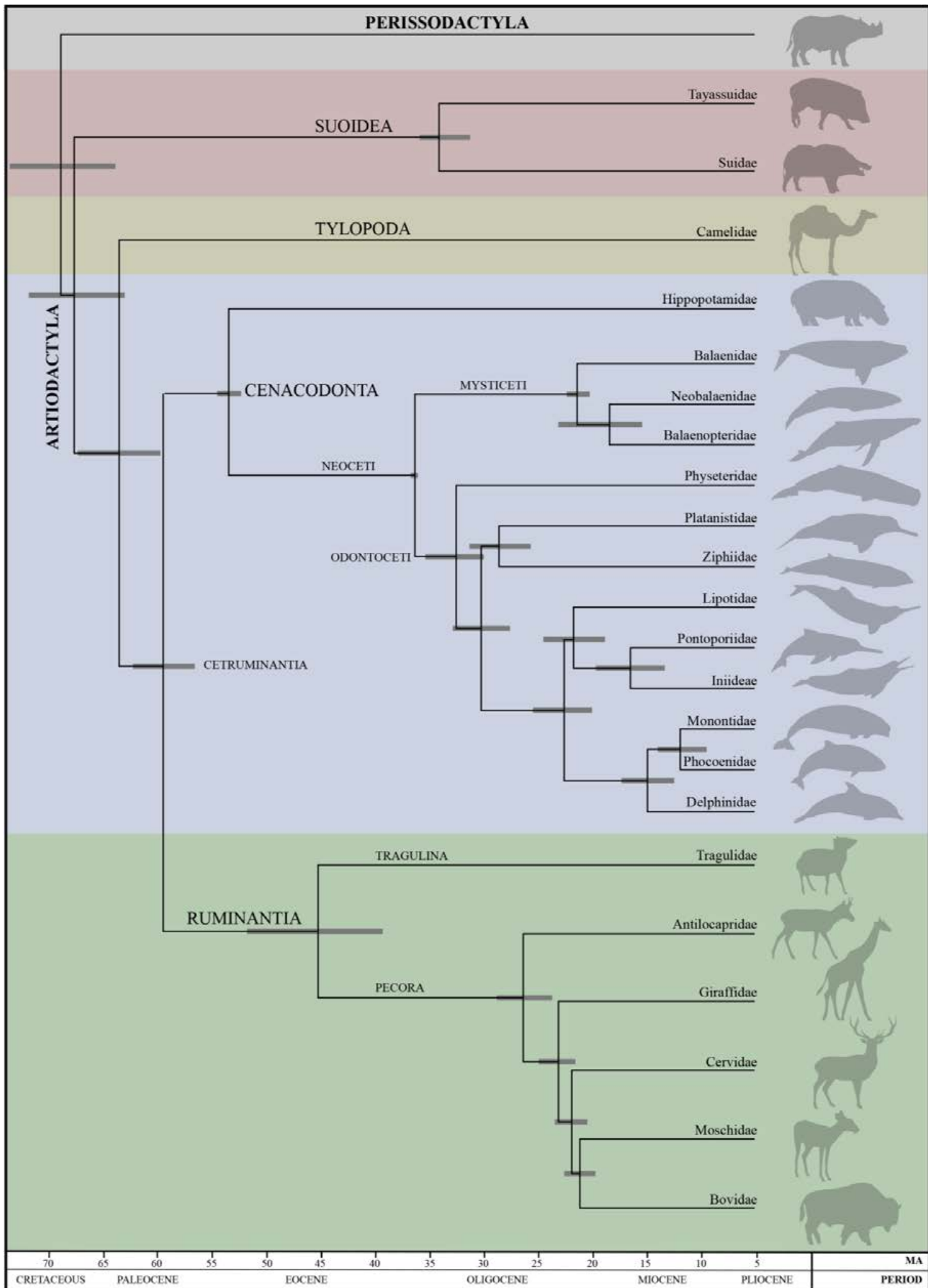
or Bovini (Bibi, 2009; Bibi et al., 2009). The earliest forms of “Boselaphini” are most probably not strictly related with the Asian crown Boselaphini whose origins are still obscure due to the lack of fossil record (Bibi et al., 2009). The Late Miocene and Early Pliocene of Eurasia is characterized by the presence of several genera (e.g., *Tragoportax*, *Miotragoceros*, *Protragoceros*), whose taxonomic status is still controversial, often lumped in “Boselaphini” (Moyà-Solà, 1983; Bibi et al., 2009). Bibi et al. (2009) suggested that most of these forms are actually either members of stem groups of one, or more, living bovid tribes or belong to independent non-Boselaphini clades. Sokolov (1953) erected Tragocerina in which these forms might be grouped, however, this clade is formally invalid, given that it is based on the synonymized taxon *Tragoceros* (Bibi, 2009).

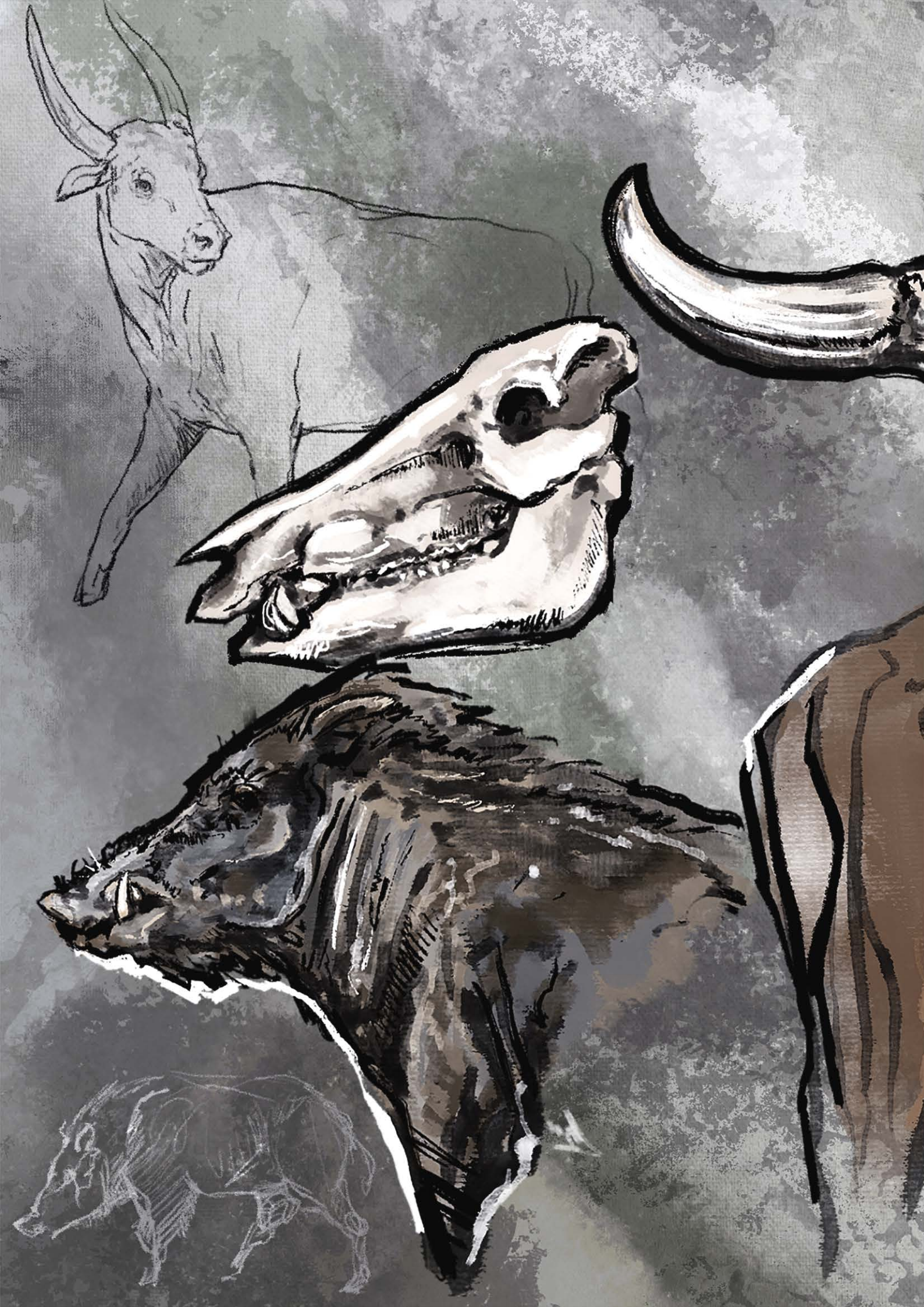
Stem Bovini most likely appeared during the early Late Miocene in Asia with *Selenoportax*, first, and *Pachyportax*, later (Bibi, 2007; Bibi et al., 2009). The dispersal event of early Bovini in Europe and Africa most likely happened right before the Mio-Pliocene boundary with the radiation in the subtribes Bubalina and Bovina (Geraads, 1992; Hassanin and Ropiquet, 2004; Ghassemi-Khademi et al., 2021). Bubalina, which is considered to have more ancestral traits than its sister-clade Bovina, probably appeared sometime during the Early Pliocene (Bibi, 2009). Traditionally, Bubalina includes the extant genera *Bubalus* (Asia) and *Syncerus* (Africa) and their putative ancestors *Prohamphibos* and *Ugandax*, respectively (Gentry and Gentry, 1978a, 1978b; Geraads, 1992; Bibi, 2009). Some authors include also *Hemibos* within the Asian clade, as an intermediate form between *Prohamphibos* and *Bubalus* (Pilgrim, 1939; Martínez-Navarro et al., 2011). For most of their history, Bubalina seldomly dispersed in Europe, although few taxa occasionally populated the continent during the warmer stages (Koenigswald et al., 2019). Bovina has a quite complex and debated history. This subtribe is traditionally composed by the extant genera *Bos* (auroch, oxen and cattle), *Bison* (bison and wisent), *Bibos* (banteg, gayal, gaur and kouprey) and *Poephagus* (yak), however, molecular studies widely support the inclusion of the latter three taxa into *Bos* as subgenera (e.g., Ritz et al., 2000; Verkaar et al., 2004). In this work, although recognizing this striking evidence, we follow Kostopoulos et al. (2018) and others in keeping the traditional nomenclature (with regard to *Bison*) in order to keep consistency with centuries of zoological and palaeontological studies (see chapter 4). Among the extinct taxa from Eurasia, *Leptobos*, *Epileptobos* and several other *Bison*-like and *Bos*-like genera of dubious validity (e.g., *Probison*, *Protobison*, *Adjiderebos*, *Ioribos*, *Proleptobos*) were often included in Bovina (Pilgrim, 1939; Sahni and Khan, 1968; Vekua, 1972; Burchak-Abramovich et al., 1980; Dubrovo and Burchak-Abramovich, 1986; Bibi, 2009; Masini et al., 2013). The African *Pelorovis* appeared during the latest Pliocene and survived until the Middle Pleistocene. Historically, *Pelorovis* was thought to derive from *Simatherium* (Gentry and Gentry, 1978a, 1978b; Vrba, 1987), however, this idea has lost approval and, instead, a close relationship between the former and *Bos* is supported, not without controversies

(Geraads, 1992; Martínez-Navarro et al., 2007, 2010b; Bibi, 2009). The European Pliocene is marked by the presence of *Parabos* and *Alephis*, two interesting taxa whose position within Bovinae is still not clearly resolved, having been considered either Boselaphini with Bovini-like morphology or very primitive forms of Bovini (Gromolard, 1980; Michaux, et al., 1991; Geraads, 1992; Montoya et al., 2006; Bibi, 2009; de Soler et al., 2012). *Leptobos* is the first Bovina entering Europe from Asia during the early Villafranchian (Pilgrim, 1937, 1939; Masini, 1989; Duvernois, 1990). This genus of large bovids includes several species from the Late Pliocene to the Early Pleistocene of Asia and Europe. Scholars divide the European forms into two lineages, sometimes referred to the subgenera *Smertiobos* and *Leptobos*, although this nomenclature is rarely used (see chapter 4). The origin of the genus and the relationships between the Asian and European species are still poorly understood due to the lack of data and confused taxonomy regarding the Pliocene forms of Siwaliks and Ponto-Caspian region. The genus *Bison* appeared for the first time in Asia during the latest Pliocene, most likely emerging from a derived stock of *Leptobos*, and reached Europe in the late Villafranchian (Masini, 1989; chapters 4, 5 and references therein). The earliest members of *Bison* were accommodated by Flerov (1972) in the subgenus *Eobison*, which became a “wastebasket” taxon for all the primitive forms of *Bison*-like bovids from the Early Pleistocene of Eurasia. In chapter 4 we provide a revision of this clade, re-defining the biochronology and taxonomy of these extremely interesting transitional forms. The larger and derived *Bison* (*Bison* s.s. in this thesis) do not occur in Europe before the beginning of the Epivillafranchian (Moullé, 1992; Brugal, 1995; Sher, 1997). The arrival of *Bi. menneri* and *Bi. schoetensacki* is discussed in chapter 5, with a focus on the record of the latter species. *Bison menneri*, whose record is restricted to a couple of Central-North European sites of the earliest Epivillafranchian, has been recently referred to the subgenus *Poephagus* (Bukhsianidze, 2020). By the Middle Pleistocene on, the steppe wisent *Bi. priscus* became one of the most representative elements of the faunal assemblages of Eurasia (Flerov, 1972; Sala, 1986; Kahlke, 1999; Vasiliev, 2008 among others). Unfortunately, not much is known about the origin of this species. At the end of the Pleistocene, it reached North America through Beringia and gave rise to the lineage which eventually led to the American ‘buffaloes’ (Flerov, 1972; McDonald, 1981; Froese et al., 2017). Molecular analysis widely demonstrated the *Bi. priscus* ancestry of the American bison; on the other hand, the relationships between the Pleistocene Eurasian forms and the European wisent *Bi. bonasus* are much more complex (Marsolier-Kergoat et al., 2015; Massilani et al., 2016; Soubrier et al., 2016; Froese et al., 2017; Palacio et al., 2017; Grange et al., 2018; Wang et al., 2018 among others). Recent studies discovered an unnamed species of *Bison* from the Middle to Late Pleistocene of Eurasia (often defined as ‘CladeX’ or ‘*Bison* Bb1’) genetically related to *Bi. bonasus* which, however, remained undetected by palaeontologists for decades due to its morphological similarities with the steppe wisent (Soubrier et al., 2016; Palacio et al., 2017; Grange et al., 2018). The

putative attribution of this “ghost taxon” to *Bi. schoetensacki* by Palacio et al. (2017), already questioned by Grange et al. (2018), is discussed in chapters 5 and 6. In addition to that, the evidence of a strong introgression of *Bo. primigenius* in the mitochondrial genome of *Bi. bonasus* led some authors to conclude that the latter is the product of hybridization between the steppe bison and auroch (Soubrier et al., 2016). Other studies on the nuclear genome, however, evidenced a much lesser degree of *Bos* gene flow into *Bison* and that the incomplete lineage sorting might be responsible of the “anomalous” mtDNA of the wisent (Wang et al., 2018). By the Middle Pleistocene, *Bo. primigenius* (i.e., the ancestor of modern cattle) started to populate the Eurasian woodlands and survived until historical times. The origins of this taxon are still quite controversial. Traditionally, auroch was thought to be evolved in Asia (Pilgrim, 1947; Groves, 1981b; Zong, 1984; van Vuure, 2005), however recent works evidence a close relationship between the giant African ‘buffalo’ *Pelorovis* and *Bos* (Geraads, 1992; Martínez-Navarro et al., 2007). The latter authors went further suggesting a direct ancestor-descendant relationship between the two taxa, even proposing that *Pelorovis* is synonym of *Bos*. The recent discovery of a primitive species of *Bos* with transitional characteristics from the earliest Middle Pleistocene of North Africa, seems to support this hypothesis (Martínez-Navarro et al., 2010b).

Next page. Fig. 7. Time-calibrated phylogenetic tree of extant Artiodactyla families. Horizontal grey bars represent the 95% highest posterior density of each node. Modified from Zurano et al. (2019).







Chapter 2.

2.1. Aims and scopes

Sus and *Bison* are among the most characterizing taxa of the Pleistocene period and persist as ones of the few large mammals still populating Eurasia after the Quaternary megafauna extinction outside Africa (Barnosky et al., 2004). Species belonging these two genera represent important markers of the faunal transitions that succeeded during the Pleistocene, often related with the first human dispersal events of the late Early Pleistocene (Kahlke et al., 2011; Van der Made, 2013; Head and Gibbard, 2015 among others). This period, characterized by a strong shift toward cooler and drier climates, is considered as crucial for the shaping of the first “modern” faunas of Europe. Environmental changes throughout the EMPT led to the arrival of several groups of large mammals from Asia to Europe, which co-existed, for a considerable timespan, with the last survivors of the Villafranchian age. Suines and bovines of this age, represented respectively by the genera *Sus* and *Bison*, have been matter of discussion among scholars as important markers for the definition of European biochrons. Unfortunately, their scattered fossil records and confused taxonomy strongly hindered the study of their evolutionary history, paleobiogeography and dispersal events which still remain obscure.

This thesis, therefore, aims to fill the gaps in this knowledge with a comprehensive reappraisal of the European fossil record attributed to these two groups, in the framework of a biochronological study. The main core of this work includes the systematic study of *Sus* and *Bison* remains from the most important late Villafranchian and Epivillafranchian localities of Europe. This, in order to re-define the chronological and geographical ranges of the species belonging to these taxa. Furthermore, a focus on their response to the climatic deterioration and consequent palaeoenvironmental changes during the EMPT is provided. To this end, three large collections (two of bovids and one of suids), from three of the most important paleontological localities of the late Early Pleistocene, were taken as case studies and compared with other coeval records. The final discussion of this thesis aims at integrating the systematic results with the biochronological scheme of Europe in order to provide new insights on the widely used Land Mammal Age framework.

2.2. Structure

This thesis seeks to achieve the specific objectives reported below, addressed in the respective chapters presented here, including:

- (I) **Chapters 3 and S1.** The systematic reappraisal of *Sus* from the Epivillafranchian of Europe. The case study is represented by the suid collection from the sites of Cal Guardiola and Vallparadís Estació (Epivillafranchian, Iberia), described in chapter S1. A focus on the ‘suid gap’ debate and its biochronological, paleobiogeographical and paleoecological implications of this study is provided in the general discussion (chapter 6) and in supplementary (chapter S1) sections. Chapter S1 is represented by a peer-reviewed paper published in the scientific journal *Quaternary Science Reviews*.
- (II) **Chapters 4 and S2.** The systematic reappraisal of primitive form of bison *B. (Eobison)* from the late Villafranchian of Europe. The case study is represented by the bovid collection from the site of Pietrafitta (late Villafranchian, Italy) described in chapter 4 and S2. Focuses on the limb proportions and body size changes of *Bison* and *Leptobos* in response to environmental change, and an overview on their dispersal in Western Palearctic are provided in chapters 4 and 6 respectively. Chapters 4 and S2 are represented by a peer-reviewed paper and its supplementary material published in the scientific journal *Quaternary Science Reviews*.
- (III) **Chapters 4 and S3.** The systematic reappraisal of the earliest *Bison* s.s. from the Epivillafranchian of Europe. The case study is represented by the bovid collection from the sites of Cal Guardiola and Vallparadís Estació (Epivillafranchian, Iberia). A focus on the morphometric and morphological differences between the metapodials of European Pleistocene large bovids, and an overview of the “true” *Bison* species taxonomy are provided in chapters 5 and 6 respectively. Chapters 5 and S3 are represented by a peer-reviewed paper and its supplementary material published in the scientific journal *Quaternary Science Reviews*.

2.3. Materials

The material which was studied and published for the first time in this thesis includes the samples of *Sus strozzii*, *Bison (Eobison) degiulii* and *Bison (Bison) schoetensacki*, from the sites of Cal Guardiola (Spain), Vallparadís Estació (Spain) and Pietrafitta (Italy), housed in the collections of the ICP and MPLB (see abbreviations in chapters 4, 5, S1). For the complete list of the specimens studied see chapters S1, S2 and S3. In order to provide the widest spectrum of comparison and compelled by the necessity of reappraising many records, the chosen comparative sample includes thousands of specimens referred to extant and fossil Suidae and Bovidae species from Eurasia and North America of the last 2.5 Ma. The data were either collected directly -by me or the co-authors/collaborators of the analyses- or retrieved from the available literature. Regarding the latter case, the references of the works from which the measurements were taken are cited in all the respective tables or in the text (Chapters 4, 5, S1, S2, S3).

2.3.1. Suidae sample

The comparative sample includes both extant and extinct taxa of suids. The study focused on the dentognathic remains which are commonly considered the most diagnostic elements in Suidae and, therefore, are widely represented in literature. The analysis of lower canines was performed only on adult male individuals whereas the study about other dentognathic element was extended to all adult specimens. The isolated lower canines without reliable sex attribution and juvenile individuals were not included in the analyses.

The comparative material which was directly studied is stored in the following institutions (see abbreviations in chapters 4, 5, S1): *Sus strozzii* Upper Valdarno (Italy) housed in the IGF, *S. strozzii* from Pantalla (Italy) housed in the SABAP UMB; *S. strozzii* from Slivia (Italy) housed in the MCSNT; *S. strozzii* from Le Vallonnet (France) housed in MPRM; *S. strozzii* from Untermassfeld (Germany) and *Sus scrofa* from Weimar-Ehringsdorf (Germany) housed in the IQW; *S. scrofa* from Gombaszög (Slovakia) housed in the NHM; *S. scrofa* from Mosbach housed in the NHM:MZ; *S. scrofa* from Lunel-Viel (France) housed in the ISEM; *S. scrofa* from undetermined localities of India and Italy housed in the MZUF; *S. scrofa*, *Sus barbatus*, *Sus verrucosus*, *Sus celebensis*, *Sus cebifrons* from undetermined localities of South-East Asia, China, Europe and Africa housed in the NHM; *S. barbatus* and *S. celebensis* from undetermined localities of South-East Asia housed in the NRM. For more information see the sections Material and Methods of chapters 4, 5 and S1.

2.3.2. Bovidae sample

The comparative sample includes both extant and extinct taxa, the analyses were performed on both female and male individuals whereas juvenile specimens were not included. The study concentrated on the most diagnostic and common skeletal elements of Bovidae in the fossil record, including skull, horn-cores, teeth and limb bones, with a focus on the anterior zygopodium and metapodials.

The comparative material which was directly studied is stored in the following institutions (see abbreviations in chapters 4, 5, S1): *Leptobos elatus* from Villarroya (Spain) housed in the ICP, *Leptobos etruscus*, *Leptobos vallisarni*, *Leptobos furtivus*, and *Bison (Eobison)* sp. from Olivola. Le Ville and other Upper Valdarno localities (Italy) housed in the IGF, *Leptobos merlai* from Pantalla and an undetermined locality of Umbria (Italy) housed in the SABAP UMB; *L. etruscus* from Upper Valdarno (Italy), *L. merlai* from Saint Vallier (France) and *Leptobos stenometopon* from Triversa (Italy) housed in the NHMB; *Bison (Eobison) degiulii* from Pirro Nord (Italy), housed in the DST and PF; *B. (E.) degiulii* from Mygdonia Basin (Greece) housed in the LGPUT and NHCK; *B. (E.) cf. degiulii* from Salita di Oriolo (Italy) housed in the MCSNF; *B. (E.) cf. degiulii* from Capena (Italy) and *Bison (Bison) cf. schoetensacki* from Cava Redicicoli (Italy) housed in the MUST; *B. (Eobison)* sp. from Mugello (Italy) housed in the MGCB; *B. (B.) schoetensacki* from Isernia La Pineta (Italy), housed in the MPPPL and IGF; *B. (B.) schoetensacki* from Cesi (Italy) housed in the, MuPA; *B. (B.) schoetensacki* from Le Vallonnet (France) housed in MPRM, *B. (B.) schoetensacki* from Cromerian localities of UK (United Kingdom) housed in NHM, BGS and YM; *Bison (Bison) priscus* from Siberia (Russia), housed in the Yakutia. The digital material studied includes the 3D models of *Bison (Eobison) georgicus* from Dmanisi (Georgia) housed in the GNM; *Bison (Bison) bonasus* from Białowieża (Poland) housed in the MRI PAS; *Bison (Bison) latifrons* from several North American sites housed in the IMNH. For more information see the sections Material and Methods of chapters 4, 5 and S1.

2.4. Methods

The Morphometric measurements of the studied sample were recorded to the nearest 0.1 mm with analogic and digital callipers. The measurements on the digital 3D models were taken with the aid of the software MeshLab (Cignoni et al., 2008). Statistical computations were made with the help of PAST v.3 and v.4 (Hammer et al., 2001) and R software (R Core Team, 2019). Here I provide a summarized list of the measurements taken and the statistical analyses performed for each group. For more detailed description of the study phases, and a better understanding of the tests computed in this work, see the Materials and Methods sections of the corresponding chapters.

2.4.1. Suidae methodology

The anatomical terminology used in chapter S1 follows Van der Made (1996) whereas the morphometric measurements are after Von den Driesch (1976) and Cherin et al. (2018) and are explained in Tab 1 and shown in Fig. 8. Lower canines are considered the most diagnostic teeth for distinguishing suids of Pleistocene in two informal groups (Cherin et al., 2018 and reference therein). The ‘scrofic group’, which nowadays includes only the living *Sus scrofa*, is characterized by a cross section in which the lingual side is the longest, and the distal side is longer than the labial one. On the other hand, the ‘verrucosic group’, including all the extant species of South-East Asia the extinct *Sus arvernensis* and *Sus strozzii*, the labial and lingual sides of the lower canine are roughly identical and broader than the distal one (see chapters 1, S1). The measurements of these elements were taken near the alveolus for the teeth which were still inserted in the mandible and at the level of their wider section for the isolated remains. The distal/labial and lingual/labial ratios of the two groups were compared with the analysis of variance (ANOVA) in R software (R Core Team, 2019) and visually represented in boxplots, in order to estimate the level of divergence between scrofic and verrucosic canines. In addition to that, Principal Component Analysis (PCA) was performed, with the help of the `prcomp` function in R on the Mosimann shape variables, i.e., the three canine measurements (labial, lingual, and distal diameters) were standardized by their geometric mean. Whenever possible, the three lengths were averaged between the left and right canines. A biplot of lower m3 comparing width vs length was produced in order to assess the intraspecific variability showed by the extant and extinct *Sus* species of Eurasia.

The Vallparadís Estació cranium IPS107041a was digitalized through photogrammetry, using the Structure-from-Motion technique (Remondino and El-Hakim, 2006). The pictures, manually taken, were transformed into a point cloud by the software Agisoft Photoscan v.1.2.6. and then adjusted with the help of Geomagic Design X. Finally, the polygonal surface was generated through the use of CloudCompare v. 2.10.2 and PhotoScan. For detailed information about these processes see chapter S1.

A cladistic phylogenetic analysis was performed using the data matrix by Cherin et al. (2018) with the exclusion of one species (*Sus lydekkeri*) and the inclusion of the Vallparadís CS sample as separated OTU (Operational Taxonomic Unit). Therefore, the final matrix was composed by 19 OTU and 52 craniomandibular and dental characters, unordered and unweighted. The phylogenetic reconstruction was performed in PAUP*4.0 (Swofford, 2002), under parsimony using heuristic searches with tree bisection reconnection branch-swapping algorithm and ACCTRAN optimization. Branch support was computed with 100,000 bootstrap replicates with random stepwise addition, and with Bremer index using the `bremer.run` script in TNT 1.5 (Goloboff and Catalano, 2016).

ABBREVIATION	DESCRIPTION OF THE MEASUREMENT
BAL	Basicranial axis: Basion – Hormion (cranium)
BSL	Basion – Staphylion (cranium)
CM3LL	Distance between distal border of c1 and distal border of m3 (mandible)
CWMAX	Max breadth occipital condyles (cranium)
DCLL	Length of c1-p1 diastema (mandible)
DET	Anteroposterior diameter of the distal epiphysis (tibia)
DEW	Mediolateral diameter of the distal epiphysis (tibia)
DPLL	Length of p1-p2 diastema (mandible)
DTW	Distal mediolateral diameter (astragalus)
EEL	Ectorbitale – Entorbitale (cranium)
EIL	Entorbitale – Infraorbitale (cranium)
FL	Frontal length: Bregma – Nasion (cranium)
FMW	Max breadth foramen magnum (cranium)
FWMAX	Max frontal breadth: Ectorbitale – Ectorbitale (cranium)
LCSMIN	Smallest length of the collum scapulae (scapula)
LGP	Greatest length of glenoid process (scapula)
LH	Height of the lacrimal (cranium)
LL	Lateral length (astragalus)
LM	Medial length (astragalus)
M1LH	Height of mandibular corpus at the mesial border of m1 (mandible)
M3LH	Height of mandibular corpus at the distal border of m3 (mandible)
MLL	Length of molar row (mandible)
MUL	Length of molar row (cranium)
MWMAX	Max mastoid breadth: Otion – Otion (cranium)
OSWMAX	Max breadth of the squamous part of the occipital bone (cranium)
OSWMIN	Min breadth of the squamous part of the occipital bone (cranium)
P2LH	Height of mandibular corpus at the mesial border of p2 (mandible)
PLLMAX	Length of premolar row, p1 included (mandible)
PLLMIN	Length of premolar row, p1 excluded (mandible)
PLWMAX	Max palatal breadth (cranium)
PPW	Max breadth at the base of paraoccipital processes (cranium)
PRL	Parietal length: Akrokranium – Bregma (cranium)
PRWMIN	Min breadth of the parietal: min breadth between temporal lines (cranium)
PTW	Proximal mediolateral diameter (astragalus)
PUL	Length of premolar row (cranium)

SFW	Min breadth between supraorbital foramina (cranium)
T	Anteroposterior diameter from the anterior border of the trochlea to the posterior border of the facet for calcaneum (astragalus)
TDMIN	Minimum anteroposterior diameter of the shaft (tibia)
TLLMAX	Length of tooth row, p1 included (mandible)
TLLMIN	Length of tooth row, p1 excluded (mandible)
UNL	Upper neurocranium length: Akrokranium – Supraorbitale (cranium)
WDMIN	Minimum mediolateral diameter of the shaft (tibia)
ZW	Zygomatic breadth (cranium)

Table 1. Abbreviations and descriptions of the measurements taken on *Sus* remains (chapter S1) and shown in Fig. 8.

2.4.2. Bovidae methodology

The anatomical terminology used in chapter 4 and 5 follows Heintz (1970), Sala (1986), Masini (1989), Kostopoulos et al. (2018) with minor changes. Linear measurements follow Masini (1989) with minor changes and are explained in Table 2 and shown in Fig. 9. Measurements taken in chapter 5 are slightly different from the ones presented here and taken in chapter 4 (see also chapter S2).

Chapter 4 includes the analysis of horn-cores compression which was defined by means of bivariate plot, comparing the anteroposterior and dorsoventral diameters of the bases. To assess the shape and size of the intertemporal bridge and frontal bones their length and width were plotted in bivariate diagrams (chapter 4). The Log10 diagram of teeth (Simpson, 1941) of chapter 4 was based on the average values of eight selected variables of *Leptobos* and *Bison* samples from Eurasia, using the record of *B. (B.) priscus* from Krasny Yar, ReW as a standard of comparison (data taken from Vasiliev, 2008). Chapter 5 features Z-scores analysis of selected dental measurements for the comparison of the bovid records. In addition to that, boxplots of the ratio (%) between tooth width and length and bivariate plots of length vs width were employed to determine the size and proportions of molars within *Bison* s.l. (see chapter S3). To assess the stoutness of limb bones, bivariate plots featuring the length vs the ratio between distal epiphyseal width and length (%) were performed on metapodials and astragali (chapter 4 and 5). The same plots, featuring length vs the ratio between proximal epiphysis width and length (%) were computed for the radii (chapter 4 and 5). To estimate the differences between *Leptobos* and *Bison* s.l. species with a multivariate approach, several Principal Component Analyses (PCAs) were performed and figured by bivariate diagrams. These tests were performed on both metapodials in chapter 4 and 5 and on cranial remains in chapter 4. These analyses rely on selected Mosimann Log-Shape variables (seven for the metapodials and six for the crania), obtained by log-transforming the ratio between each measurement and the geometric mean of the measurements for each specimen (Jungers et al., 1995).

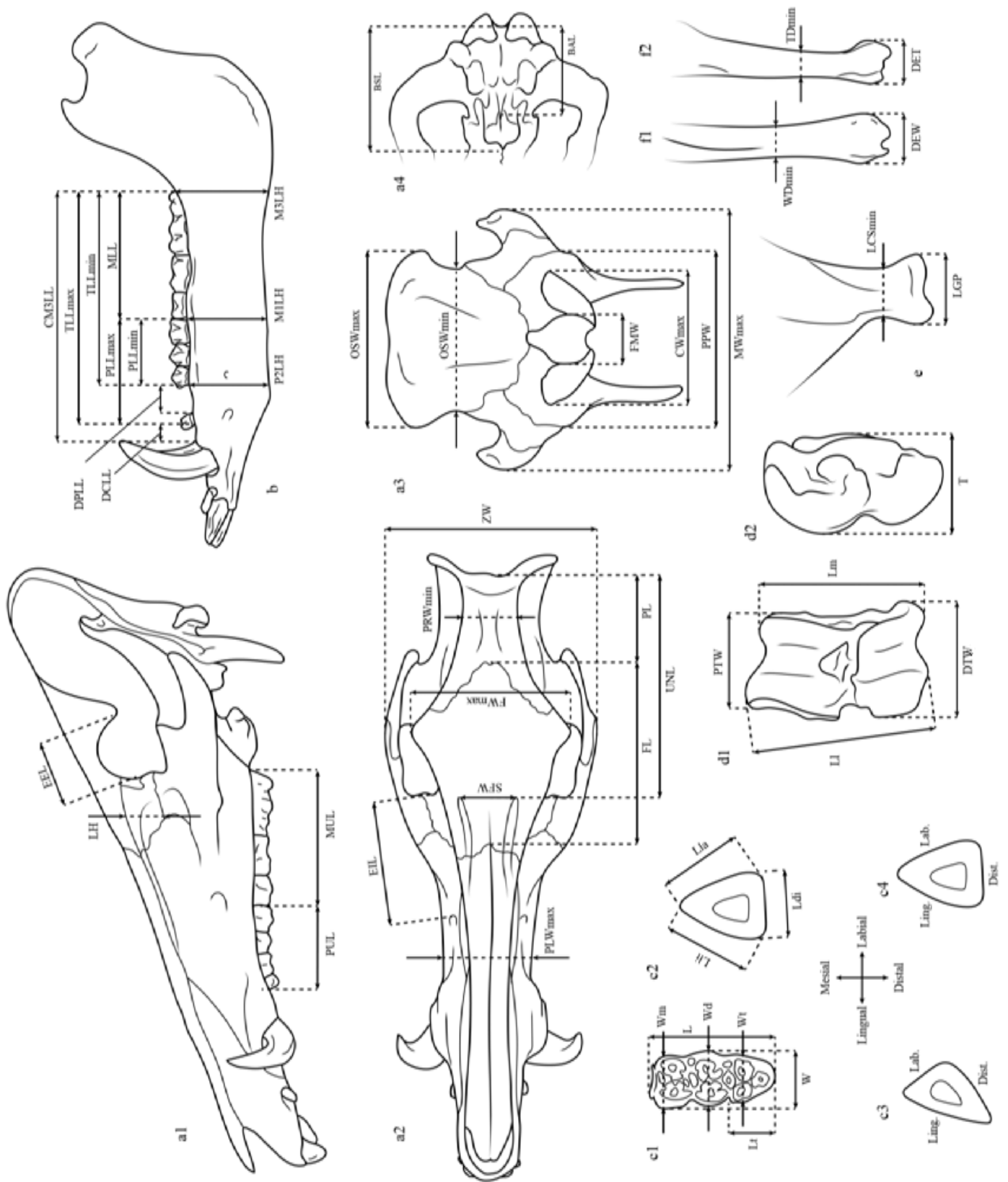


Fig. 8. Measurements taken for the *Sus* samples in chapter S1 and schematic representation of the two canine morphologies (transversal section): a, Cranium in lateral (a1), dorsal (a2), posterior (a3), and ventral (a4) views; b, Mandible; c, Teeth: molar (c1), canine (c2), section of scrofic (c3) and verrucosic (c4) canines; d1, astragalus in anterior (d1) and lateral (d2); e, scapula; f, Tibia in anterior (f1) and lateral (f2) views. Elements drawn not in scale. Abbreviations are explained in Table 1.

Chapter 5 includes a second set of eight variables for the metapodials, calculated following Scott and Barr (2014), i.e., adjusting each measurement as the log transformed ratio between the measurement and Scott's (2004) metapodial global size variable (MGSV, see chapter 5 for the formula). In order to enhance the statistical reliability of the results, a MANOVA test was computed on seven raw variables of the metapodials, setting the significance level at 0.05 (chapter 5). Log10 ratio diagrams were developed for the metacarpal sample of chapter 5, basing on the average values of seven selected variables of *Bison* records from Eurasia. The extant *B. (B.) bonasus* was used as a standard of comparison (data taken from Reshetov and Sukhanov, 1979). In chapter 4, the relative proportion of the limb bones elements was assessed by means of histograms presenting the average length of metatarsals and radii relatively to the metacarpals (%). Chapter 5 includes a series of tests for the quantitative distinction of leptobovine and bisontine groups (i.e., *Leptobos*, *Bison* s.l.) from taurine bovids (i.e., *Bos*), which are the following. The Stampfli's trochlea index (Stampfli, 1963), was performed on the distal humeri ends, computed as the ratio (%) between the distal trochlea width and the lateral epitrochlear width (chapter 5). For assessing the lateral tapering of distal humerus, the Lehmann trochlear index (Martin, 1987) was computed as the ratio (%) between the lateral and medial trochlear heights (chapter 5). *Bison* and *Leptobos* metapodials can be easily distinguished from the ones of *Bos* on the basis of the contact between the diaphysis and distal epiphysis. In order to define this feature, chapter 5 includes the ratio (%) between the distal epiphysis width and the distal diaphysis width. Chapter 5 features also the ratio (%) between the two facets of the proximal epiphysis, to recognize evolutionary trends among *Leptobos* and *Bison* in the relative size of the two articulations. The sexual dimorphism of large bovids is among the strongest for mammals. In order to quantify dimorphic features of metacarpals, the equation given by Schertz (1936) was applied on the putative males and females recognized (for the equation see chapter 5). The Body mass estimations of chapter 4 were obtained as the average of three estimations based on metapodials linear measurements following Scott (1983). Only complete specimens were considered in this analysis.

The Vallparadís composite section bovid remains were unearthed from layers which encompass about 0.5-0.6 Ma. Therefore, several tests were performed in order to verify the taxonomic homogeneity of the sample. For statistics reasons only the two main chronologies of the section were taken in account. To identify sources of significant biometric differences within the selected samples, univariate ANOVA test on eight variables for metacarpals and metatarsals were computed (see chapter 5). For the sake of consistency, a multivariate test (MANOVA) based on five variables was performed on the complete specimens. Finally, the teeth variability was assessed by means of an ANOVA test based on the ratio between width and length (%) of M2 and M3. For all the above-mentioned tests the significance level was set at 0.05.

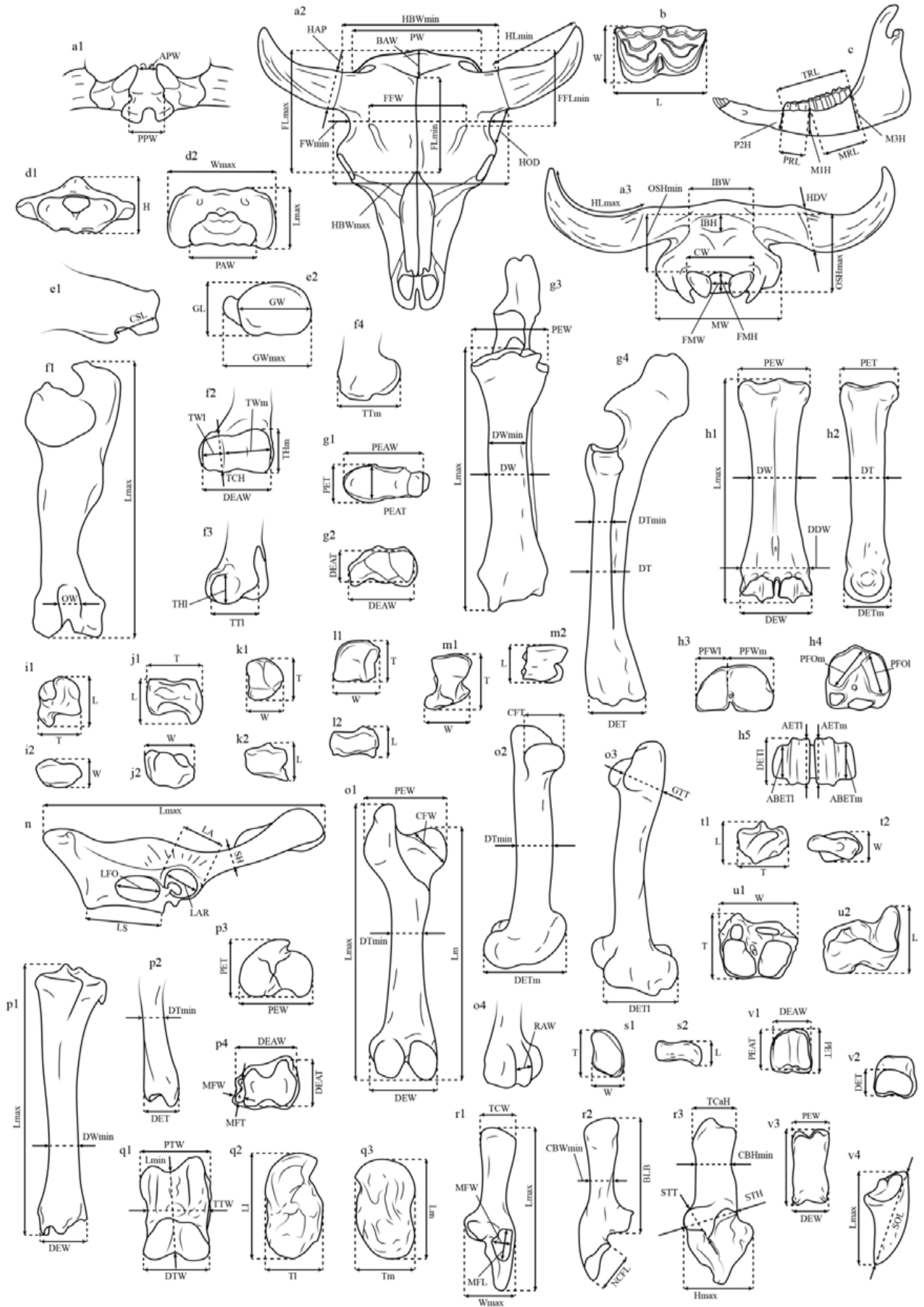
ABBREVIATION	DESCRIPTION OF THE MEASUREMENT
AAW	Anterior articular facet width (atlas)
ABETL	Abaxial hemicondyle thickness (metapodials)
ABETM	Abaxial hemicondyle thickness (metapodials)
AETM	Axial hemicondyle thickness (metapodials)
AL	Articular surface length
APW	Width of anterior processes (basioccipital)
AT	Articular surface thickness
BAW	Distance between bregma and akrocranium (temporo-parietal)
BLB	Body length (calcaneum)
BLMIN	Minimum length (calcaneum)
CBHMIN	Body minimum height (calcaneum)
CBWMIN	Body minimum width (calcaneum)
CFT	Capitis femoris thickness (femur)
CFW	Capitis femoris width (femur)
CSL	Collum scapulae length (scapulae)
CW	Condylar width (occipital)
DDT	Distal diaphysis thickness (metapodials)
DDW	Distal diaphysis width (metapodials)
DEAT	Distal end articular thickness (limb bones)
DEAW	Distal end articular width (limb bones)
DET	Distal end thickness (limb bones)
DETL	Distal end thickness of the lateral trochlear crest (metapodials and femur)
DETM	Distal end thickness of the medial trochlear crest (metapodials and femur)
DEW	Distal end width (limb bones)
DT	Diaphysis thickness at midshaft (limb bones)
DTMIN	Diaphysis minimum thickness (limb bones)
DTW	Distal trochlear width (astragalus)
DW	Diaphysis width at midshaft (limb bones)
DWMIN	Diaphysis minimum width (limb bones)
FFLMIN	Distance from supraorbital foramen to akrocranium (frontals)
FFW	Maximum distance between the supraorbital foramina (frontals)
FLMAX	Length from Nasion to akrocranium (frontals)
FLMIN	Frontal length from Nasion to Bregma (frontals)
FMH	Foramen magnum height (occipital)
FMW	Foramen magnum width (occipital)
FWMIN	Width of the postorbital constriction (frontals)

GL	Glenoid cavity length (scapula)
GMAX	Glenoid cavity maximum length (scapula)
GPL	Glenoid process length (scapulae)
GTT	Great trochanter thickness (femur)
GW	Glenoid cavity width (femur)
H	Height
HAP	Anteroposterior diameter at the base (horn)
HBWMAX	Distance between the anterior margins of the bases (horn)
HBWMIN	Distance between the posterior margins of the bases (horn)
HDV	Dorsoventral diameter at the base (horn)
HLMAX	Chord length following the maximum curve (horn)
HLMIN	Distance from the base to the tip (horn)
HMAX	Maximum height (calcaneum)
HOD	Distance between the horncore anterior margin and the orbit (frontals)
HS°	Angle between the mid-line of the horncore and the sagittal of the skull (cranium)
IBH	Intertemporal bridge height (occipital)
IBW	Intertemporal bridge width (occipital)
L	Left
LL	Lateral length (astragalus)
LM	Medial length (astragalus)
LMAX	Maximum length
LMIN	Minimum length (astragalus)
M1H	Height of the corpus at the first molar (mandible)
M3H	Height of the corpus at the third molar (mandible)
MFL	Malleolar facet length (tibia)
MFW	Malleolar facet width (tibia)
MRL	Molar row length (mandible)
MW	Mastoid width (occipital)
NCFL	Cubo-navicular articular facet length (calcaneum)
OSHMAX	Occipital squama maximum height (occipital)
OSHMIN	Occipital squama minimum height (occipital)
OW	Olecranon fossa width (humerus)
P2H	Height of the corpus at the second premolar (mandible)
PAW	Posterior articular facet width (atlas)
PEAT	Proximal end articular thickness (limb bones)
PEAW	Proximal end articular width (limb bones)
PET	Proximal end thickness (limb bones)

PEW	Proximal end width (limb bones)
PFOL	Proximo-lateral facet oblique diameter (metatarsal)
PFOM	Próximo-medial facet oblique diameter (metatarsal)
PFWL	Proximo-lateral articular facet width (metacarpal)
PFWM	Proximo-medial facet width (metacarpal)
PPW	Width of posterior processes (basioccipital)
PRL	Premolar row length (mandible)
PTW	Proximal trochlear width (astragalus)
PW	Postcornual width (temporo-occipital)
R	Right
RAW	Width of the rotula articulation
SOL	Oblique length of the sole (distal phalanx)
STH	Sustentaculum tali height (calcaneum)
STT	Sustentaculum tali thickness (calcaneum)
T	Thickness
TCAH	Tuber calcanei height (calcaneum)
TCRH	Trochlea crest height (humerus)
TCW	Tuber calcanei width (calcaneum)
THL	Lateral trochlear height (humerus)
THM	Medial trochlear height (humerus)
TL	Lateral thickness (astragalus)
TM	Medial thickness (astragalus)
TRL	Length of the teeth row (mandible)
TTL	Trochlea thickness of the lateral epicondyle (humerus)
TTM	Trochlea thickness of the medial epicondyle (humerus)
TTW	Intertrochlear width (astragalus)
TWL	Trochlear lateral articulation width (humerus)
TWM	Trochlear medial articulation width (humerus)
WMAX	Maximum width
WMIN	Minimum width

Table 2. Abbreviations and descriptions of the measurements taken on *Leptobos* and *Bison* remains (chapters 4 and 5) and shown in Fig. 9.

Next page. Fig. 9. Measurements taken for the Bison samples in chapters 5 and 6: a, Cranium in ventral (a1), dorsal (a2) and posterior (a3) views; b, Tooth; c, Mandible; d, Atlas in anterior (d1) and ventral (d2) views; e, Scapula in lateral (e1) and distal (e2) views; f, Humerus in posterior (f1), anterior (f2), lateral (f3) and medial (f4) views; g, Radius in proximal (g1), distal (g2), anterior (g3) and lateral (g4); h, Metapodials in anterior (h1), lateral (h2), proximal metacarpal (h3), proximal metatarsal (h4) and distal (h5) views; i, Pyramidal in lateral (i1) and posterior (i2) views; j, Scaphoid in lateral (j1) and proximal (j2) views; k, Unciform in proximal (k1) and lateral (k2) views; l, Magnum in proximal (l1) and lateral (l2) views; m, Semilunar in proximal (m1) and lateral (m2) views; n, Pelvis; o, Femur in posterior (o1), medial (o2), lateral (o3) and anterior (o4) views; p, Tibia in anterior (p1), medial (p2), proximal (p3) and distal (p4); q, Astragalus in anterior (q1), lateral (q2) and medial (q3) views; r, Calcaneum in anterior (r1), posterior (r2) and medial (r3) views; s, Cuneiform in proximal (s1) and lateral (s2) views; t, Malleolus in medial (t1) and proximal (t2) views; u, Cubonavicular in distal (u1) and anterior (u2) views; v, Phalanges in proximal (v1), distal (v2), anterior proximal phalanx (v3), anterior distal phalanx (v4). Elements drawn not in scale. Abbreviations are explained in Table 2.





Chapter 3.



The results of this chapter were published as:

Cherin, M., Alba, D.M., Crotti, M., Menconero, S., Moullé, P.É., Sorbelli, L. and Madurell-Malapeira, J., 2020. The post-Jaramillo persistence of *Sus strozzi* (Suidae, Mammalia) in Europe: new evidence from the Vallparadís Section (NE Iberian Peninsula) and other coeval sites. *Quaternary Science Reviews*, 233: 106234.

DOI: <https://doi.org/10.1016/j.quascirev.2020.106234>

Original paper and its supplementary material presented in **chapter S1**.

In this work, Leonardo Sorbelli contributed in:

- (I) Original conceptualization of the paper.
- (II) Direct observation and study of the fossil material.
- (III) Formal analysis of the data.
- (IV) Interpretation and discussion of the results.
- (V) Co-writing of the final draft.
- (VI) Review and editing of the final draft.
- (VII) Funding acquisition.

The persistence of *Sus strozzi* in Europe during the Epivillafranchian: evidence from the Vallparadís Section (NE Iberian Peninsula) and other coeval sites

After their radiation in the Miocene, Suidae of Europe experienced in the Plio-Pleistocene a major loss in diversity with the extinction of all the tribes except for Suina (Frantz et al., 2016). This last group was able to exploit the ecological niches left empty by the extinction of other suid competitors during the earliest Pliocene and, ultimately, conquered all the continent by the end of the Pleistocene. This prosperity, in Europe, was achieved by the single genus *Sus* with a chronological succession of species characterized by extreme ecological plasticity. It is indeed clear that, due to its abundance and wide distribution, *Sus* strongly marked each phase crossed by the everchanging mammal assemblages of the European Plio-Pleistocene, as some clades of Suinae and Tetraconodontinae did in Africa (White and Harris, 1977). Suines are, therefore, of high value for the biochronological studies of large mammal assemblages in Europe.

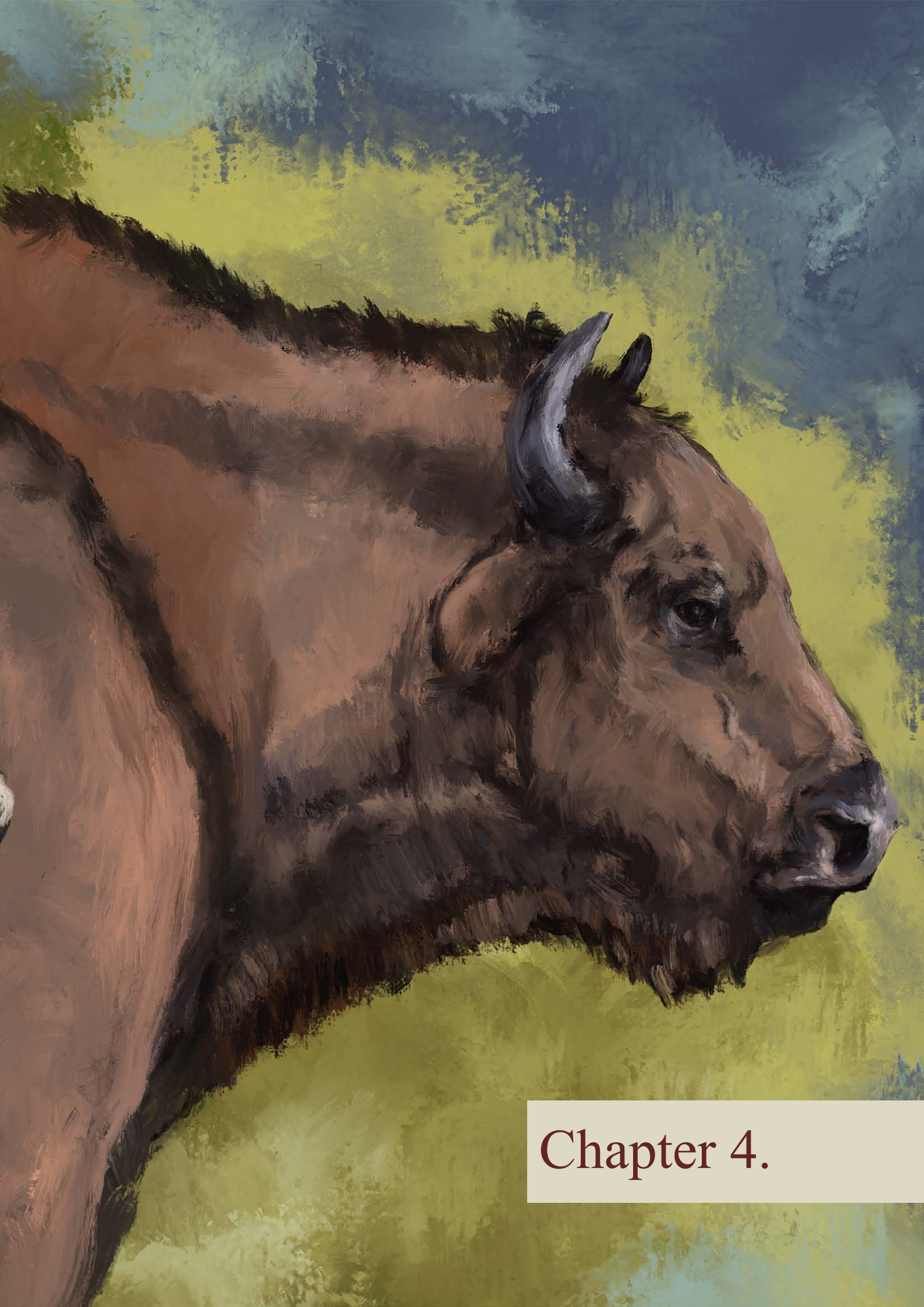
The first species of *Sus*, *S. arvernensis*, already appeared during the earliest stages of the Pliocene, marking the beginning of the Ruscinian ELMA (Agustí et al., 2001). This small suid, widespread in most of the European continent, is considered the ancestor of the larger verrucosic boar *S. strozzi* (Azzaroli, 1954; Berdondini, 1992; Iannucci et al., 2022). The latter replaced its putative ancestor at the onset of the middle Villafranchian and thrived in Europe for all the Early Pleistocene with a major loss in its distribution in the timespan comprised between 1.8 and 1.2 Ma (see chapter 6 for more detailed discussion). Until recent years, most of the remains of *Sus* younger than 1.2 Ma were attributed to the extant boar *Sus scrofa* (e.g., Guérin and Faure, 1997; Van der Made, 1999; Van der Made et al., 2017), thus the onset of Epivillafranchian was thought to be marked by the extinction of the late Villafranchian form *S. strozzi* and the arrival of *S. scrofa* (Kahlke et al., 2011; Bellucci et al., 2015; Martínez-Navarro et al., 2015).

The rich collection of suid from the sites of Cal Guardiola and Vallparadís Estació studied and described in chapter S1, evidences the presence of *S. strozzi* in Eastern Iberian Peninsula during the Epivillafranchian period. The Suidae material was analysed following the methodology presented in chapter 2 and the results were published as a peer-reviewed paper in the scientific journal Quaternary Science Reviews (for a detailed description of the fossil material see chapter S1). The cranial morphology of the Iberian suid, especially the verrucosic morphology of the canine (Fig. 8) allow the attribution of the sample to this late Villafranchian species of pig. The unexpected persistence of *S. strozzi* at 1.0 Ma, already suggested by the works of Moullé (1992) and Bona and Sala (2016), triggered the reappraisal of all suid records from the Epivillafranchian of Europe.

The analyses performed on this wide collection of *Sus* evidenced that several records of this genus, in some cases attributed to *S. scrofa*, are referable to the verrucosic boar *S. strozii*. These records include: Le Vallonnet (France), Untermassfeld (Germany, *S. scrofa priscus* in Guérin and Faure, 1997), Slivia (Italy, *S. scrofa* in Bon et al., 1992), Frantoio (Italy), Kozarnika (Bulgaria), Tsimbal (Russia, *S. tamanensis* in Vereshchagin, 1957). In addition to these, other few Suidae remains are reported from several European localities of Epivillafranchian which, according to the inferred age of the deposits, could be referred to *S. strozii* (e.g., Sima del Elefante TE9 and Gran Dolina TD3-5-8, Spain; Castagnone and Pagliare di Sassa, Italy). Nonetheless, the poor preservation and scanty nature of these record advice a cautious approach to this matter, and the *Sus* sp. attribution is preferred. On the other hand, this study revealed that, in those localities younger than 0.8 Ma, *S. strozii* is always replaced by *S. scrofa*, including: West Runton and Pakefield (United Kingdom), Mosbach 2 and Süssenborn (Germany), Gombaszög (Slovakia) among others (see chapter S1). For a detailed description and pictures of the studied samples see chapter S1.

The persistence of *Sus strozii* during the whole Epivillafranchian, evidenced in this thesis and supported by further study (Iannucci, 2022), can be considered a major bioevent of the Early Pleistocene (Fig. 10). Until the present, the arrival of *S. scrofa* was erroneously considered one of the markers of the Epivillafranchian (Bellucci et al., 2015; Martínez-Navarro et al., 2015 among others). The analysis performed in this work provided a new insight on the faunal associations of Pleistocene disproving an early occurrence of *S. scrofa* at ca. 1.0 Ma. The first, reliable estimation for the arrival of this taxon in Europe is thus not older than 0.8 Ma. Therefore, the dispersal of this species should be considered an indicator of the Galerian onset. On the other hand, the survival of *S. strozii* in European faunal associations of Epivillafranchian became one of the major markers of this biochron, which is added to the persistence of other Villafranchian taxa like *Homotherium crenatidens*, *Canis (Xenocyon) lycaonoides*, *Pachycrocuta brevirostris*, *Equus altidens* and *Mammuthus meridionalis* among others.





Chapter 4.

The results of this chapter were published as:

Sorbelli, L., Cherin, M., Kostopoulos, D.S., Sardella, R., Mecozzi, B., Plotnikov, V., Prat-Vericat, M., Azzarà, B., Bartolini-Lucenti, S. and Madurell-Malapeira, J., 2023. Earliest bison dispersal in Western Palearctic: Insights from the *Eobison* record from Pietrafitta (Early Pleistocene, central Italy). *Quaternary Science Reviews*, 301: 107923.

DOI: <https://doi.org/10.1016/j.quascirev.2022.107923>

Original paper presented in **chapter 4**. Supplementary material presented in **chapter S2**.

In this work, Leonardo Sorbelli contributed in:

- (I) Original conceptualization of the paper.
- (II) Direct observation and study of the fossil material.
- (III) Formal analysis of the data.
- (IV) Interpretation and discussion of the results.
- (V) Writing of the original draft.
- (VI) Review and editing of the final draft.
- (VII) Funding acquisition.



Contents lists available at ScienceDirect

Quaternary Science Reviews

journal homepage: www.elsevier.com/locate/quascirev

Earliest bison dispersal in Western Palearctic: Insights from the *Eobison* record from Pietrafitta (Early Pleistocene, central Italy)

Leonardo Sorbelli ^{a,*}, Marco Cherin ^b, Dimitris S. Kostopoulos ^c, Raffaele Sardella ^d,
Beniamino Mecozzi ^d, Valerii Plotnikov ^e, Maria Prat-Vericat ^a, Beatrice Azzarà ^b,
Saverio Bartolini-Lucenti ^{a,f}, Joan Madurell-Malapeira ^{f,g}

^a Institut Català de Paleontologia Miquel Crusafont, Universitat Autònoma de Barcelona, Edifici ICTA-ICP, c/ Columnes s/n, Campus de la UAB, 08193, Cerdanyola del Vallès, Barcelona, Spain

^b Dipartimento di Fisica e Geologia, Università degli Studi di Perugia, Via A. Pascoli, 06123, Perugia, Italy

^c Laboratory of Geology and Paleontology, School of Geology, Aristotle University of Thessaloniki, 54124, Thessaloniki, Greece

^d Dipartimento di Scienze della Terra (PaleoFactory), Sapienza Università di Roma, Piazzale A. Moro 5, 00185, Roma, Italy

^e Academy of Sciences of the Republic of Sakha (Yakutia), 677007, Yakutsk, Lenin Ave. 33, Russia

^f PaleoFab/Lab, Dipartimento di Scienze della Terra, Università degli Studi di Firenze, 50121, Firenze, Italy

^g Departament de Geologia, Universitat Autònoma de Barcelona, 08193, Cerdanyola del Vallès, Barcelona, Spain

ARTICLE INFO

Article history:

Received 14 July 2022

Received in revised form

17 November 2022

Accepted 14 December 2022

Available online xxx

Handling Editor: Danielle Schreve

Keywords:

Bison

Bovidae

Europe

Quaternary

Villafranchian

ABSTRACT

The late Villafranchian is one of the pivotal timespans in the succession of Pleistocene European faunal assemblages, setting the bases for the major faunal renewal that characterized the continent during the Epivillafranchian. *Bison* is one of the most important and successful large mammals to spread in Europe at the latest stages of the Early Pleistocene. Here we describe the remains of a large bovid from the late Villafranchian site of Pietrafitta (ca. 1.5 Ma), previously attributed to *Leptobos*. Our analyses allow to refer this sample to the genus *Bison*. The primitive characters featured by this sample suggest the attribution to the subgenus *Eobison*, a long-debated taxon which includes all the earliest forms of *Bison*. At Pietrafitta, thus, one of the largest and most complete record of primitive *Bison* is recorded. The vague diagnosis and confused taxonomic history of *Eobison* called for a reappraisal of its status. We present a re-definition of the diagnostic characters and a review of the Eurasian record of *Eobison* with a focus on the late Villafranchian samples from the Mediterranean area. We recognize at least three valid species of *Eobison* remarking, however, the extreme morphological variability of this group. The comparative analysis of *Eobison* and its closest relatives (i.e., *Leptobos* and *Bison* s.s.), confirms that both the leptobovine and bisontine clades underwent to an increase of stoutness of the appendicular skeleton in response to the shrinking of forested habitats and the onset of colder, arid climate during the Pleistocene.

© 2022 Elsevier Ltd. All rights reserved.

1. Introduction

1.1. The genus *Leptobos* and its historical and taxonomic background

According to most scholars the origin of *Bison* probably lies within the extinct genus *Leptobos* (McDonald, 1981; Duvernois and Guérin, 1989; Masini, 1989; Geraads, 1992; Martínez-Navarro et al., 2007; Tong et al., 2016; Cherin et al., 2019 among others). This

group of mid-to large-sized and slender bovines is a constant faunal element during the whole Villafranchian European Land Mammal Age (ELMA; about 3.3–1.2 Ma; Cherin et al., 2019). Fossils of these ungulates have been found in all the Palearctic of Eurasia, from the Iberian Peninsula to China (Dong, 2008; Garrido, 2008), and from northern India to, possibly, the British Isles (Pilgrim, 1937; Breda et al., 2010). Since the establishment of the genus by Rüttimeyer (1877–1878), a large number of remains was attributed to *Leptobos* and several species were erected. According to the most recent review, *Leptobos* includes the species: *Leptobos brevicornis* (Asia), *Leptobos crassus* (Asia), *Leptobos falconeri* (Asia), *Leptobos*

* Corresponding author.

E-mail address: leonardo.sorbelli@icp.cat (L. Sorbelli).

stenometopon (Europe), *Leptobos elatus* (Europe), *Leptobos merlai* (Europe), *Leptobos furtivus* (Europe), *Leptobos etruscus* (Europe), and *Leptobos vallisarni* (Eurasia) (Cherin et al., 2019).

Masini (1989) and Masini et al. (2013) divided the European species of *Leptobos* into two groups or lineages, the first including *L. stenometopon*, *L. elatus*, *L. merlai*, and *L. furtivus*; the second *L. etruscus* and *L. vallisarni*. Duvernois (1990, 1992), on the basis of horn and tooth morphologies, established two subgenera for the aforementioned groups: *Leptobos* (*Leptobos*) and *Leptobos* (*Smer-tiobos*), respectively, adding to the latter the species *Leptobos bravardi*. These two subgenera, however, suffer from nomenclatural inconsistencies (see Croitor and Popescu, 2011; Cherin et al., 2019), thus this subdivision is not commonly used in literature (Masini et al., 2013). The Asian group includes the species *L. falconeri* (type species), *L. brevicornis* (which embraces also *L. amplifrontalis* and *L. laochihensis*), and *L. crassus* (Mead et al., 2014). Over the years, several authors tried to find relationships between the Asian and European forms (Dong, 2008). However, up to date, it is still not clear if these groups are actually related or if, for instance, the Asian taxa are part of a third, distinct, clade (Mead et al., 2014). This incapability of linking the European and Asian groups might find a solution in the species *L. vallisarni*, which is the only occurring at the geographical extremes of the continents (Zheng et al., 1985; Tong et al., 2016). The existence of advanced *Leptobos* forms in the Early Pleistocene of eastern Asia, along with the fact that the earliest *Bison sensu lato* (s.l.) species are known from India and China roughly in the same timespan, led most authors to suggest that *Bison* could have originated in Asia, emerging from a derivate stock of *Leptobos* (Sala, 1986; Masini, 1989; Duvernois, 1990; Martínez-Navarro et al., 2007; Sorbelli et al., 2021a among others).

1.2. Earliest Eurasian bison in the paleontological literature, a review

The earliest forms of *Bison* most probably emerged in the Eastern Palearctic and, as soon as they reached Europe at the end of the Early Pleistocene, started to replace *Leptobos* in all the large herbivore guilds. Indeed, a possible co-existence between *Bison* and *Leptobos* is reported only in few late Villafranchian European localities of south-eastern Europe (Duvernois, 1990; Agadzhanian et al., 2017; Kostopoulos et al., 2018; Lopatin et al., 2019). In Asia, on the contrary, *Bison* and *Leptobos* seem to have shared the same geographic areas for a prolonged time, possibly for almost two million years (Tong et al., 2016). This long overlap could be explained (i) by the large size of suitable habitats in Asia, which may have triggered niche partitioning among these bovines in a context of wide trophic availability, and/or (ii) by bias in the taxonomic identification and/or stratigraphic range of fossils.

The first occurrence of *Bison* s.l. is represented by the scanty remains of *Bison* (*Eobison*) *sivalensis* and *B. (Eobison) palaeosinensis* from India and China, respectively. Flerov (1972) referred to the newly erected subgenus *Eobison* these two Asian species, as well as *B. (Eobison) tamanensis* from Eastern Europe. The author, however, did not deepen the diagnosis of the subgenus, which is currently flawed by several issues. *Bison* (*Eobison*) *georgicus* from Dmanisi (Georgia) is putatively the earliest *Bison* s.l. approaching Europe at ca. 1.77 Ma (Burchak-Abramovich and Vekua, 1994; Bukhsianidze, 2005). From the late Villafranchian on, a large number of localities in Mediterranean and Eastern Europe are characterized by the presence of these mid-sized bison-like bovines (Fig. 1), still commonly grouped in the subgenus *Eobison* (Masini et al., 2013; Sorbelli et al., 2021a). After 1.2 Ma (i.e., at the beginning of the Epivillafranchian stage), with the onset of new climatic conditions in the context of the Early-Middle Pleistocene Transition (EMPT; Head and Gibbard, 2005; Clark et al., 2006), *Eobison* was replaced

by the larger-sized *Bison sensu stricto* (s.s.) (i.e., *B. schoetensacki*, *B. menneri*, and *B. priscus*, in chronological order of appearance), which rapidly colonized most of the Holarctic (Kahlke, 1999; Sorbelli et al., 2021a).

In the time interval between the age of the Dmanisi fauna and the beginning of the Epivillafranchian, crucial information on the evolution of early bison can be sought, but, unfortunately, paleontological records are scarce. Here, we describe the rich sample from Pietrafitta (central Italy), which can shed new light on this intriguing topic. In a preliminary analysis, this sample was attributed to *Leptobos* aff. *vallisarni* based on cranial similarities with the holotype of *L. vallisarni* from the Upper Valdarno (Italy; Masini, 1989). Later on, this attribution was confirmed by Gentili and Masini (2005), although not supported by quantitative comparative analysis. Nevertheless, the authors noticed that the material from Pietrafitta was characterized by some features more advanced than in *L. vallisarni*, hence the choice of open nomenclature. Building on that insight, this paper presents the first detailed description of the Pietrafitta record, in the context of the arrival of the first bison in Europe and the replacement of *Leptobos*.

2. Geological setting

The Tavernelle-Pietrafitta Basin is located in the upper valley of the Nestore River. During the early stages of the Pleistocene, after an intense phase of tectonic activity, the Tavernelle-Pietrafitta Basin became part of a lateral branch of the main Tiberino Basin and started to be characterized, alternatively, by lacustrine/palustrine and alluvial plain conditions (Conti and Esu, 1981; Cherin et al., 2012; Pazzaglia et al., 2013). The lignite deposition was a result of the elevation of the delta of the Nestore paleo-river causing the formation of several small basins filled with stagnant water (Gentili et al., 1996). At the end of the Pleistocene, new tectonic events occurred causing an uplift of the area and the desiccation of the basin, which subsequently underwent an erosive phase (Ambrosetti et al., 1989). The site of Pietrafitta (42°59'33"N 12°12'42"E) is located close to the homonymous village in the municipality of Piegara. The lignite seam had a thickness comprised between 5 and 8.5 m and was exploited industrially for almost half a century. Lignite was intercalated with thin layers of organic clay yielding freshwater mollusks and oligohaline ostracods (Gliozzi et al., 1997). Facies analysis suggests that the lignite was deposited in a swampy area located on the edge of a lake (Conti and Girotti, 1977; Ambrosetti et al., 1992, 1995; Martinetto et al., 2014). This hypothesis is furtherly confirmed by paleobotanical studies, which report the presence of a large water body surrounded by broad-leaved deciduous forests in a humid climatic context. The plant assemblage of Pietrafitta is dominated by aquatic genera such as *Azolla*, *Najas*, *Nymphaea*, and *Potamogeton* (Martinetto et al., 2014). Palynological data show a variation in the forest composition surrounding the swamp, due to a progressive harshening of the climatic conditions. In particular, moving along the stratigraphic succession from bottom to top, the disappearance of *Taxodium*-type and its replacement by "Quercetum" taxa is observed, followed by the spread of herbaceous plants and *Pinus* in the upper layers (Lona and Bertoldi, 1972; Kottek et al., 2006; Martinetto et al., 2017). The depositional and environmental conditions of the swamp allowed the preservation of one of the richest continental vertebrate samples in the Italian Early Pleistocene, including some thousand specimens belonging to almost 40 taxa of freshwater fishes, anurans, reptiles, birds, and mammals (see revised faunal lists in Martinetto et al., 2014 and Sorbelli et al., 2021b). The vertebrate assemblage is referred to the Farneta Faunal Unit (FU; approx. 1.6–1.4 Ma) of the late Villafranchian ELMA, corresponding to late MNQ 18 in the Guérin's mammal

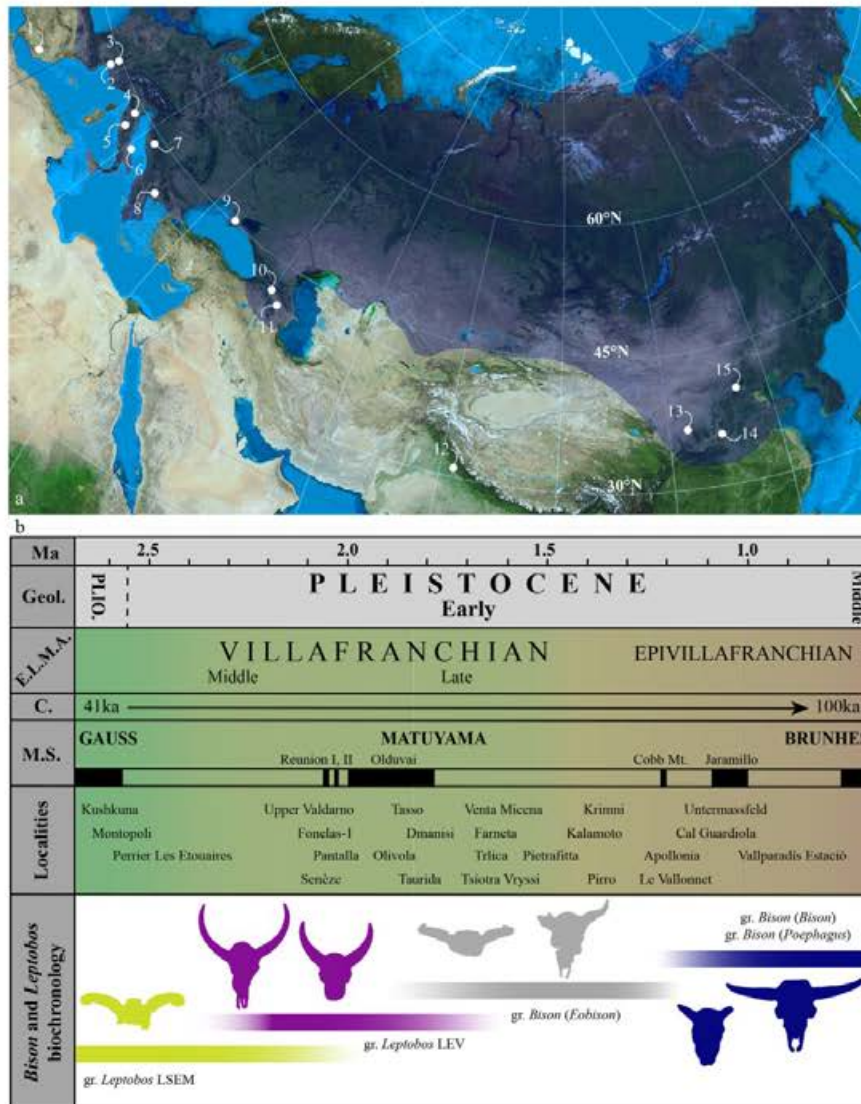


Fig. 1. a. Major Eurasian sites with the occurrence of primitive *Bison*: 1, Venta Micena (Spain); 2, Sainzelles (France); 3, Maar du Riege (France); 4, Salita di Oriolo (Italy); 5, Central Italy (Upper Valdarno, Pietrafitta, Capena); 6, Pirro Nord (Italy); 7, Trlica (Montenegro); 8, Mygdonia Basin (Greece); 9, Taurida Cave (Ukraine); 10, Dmanisi (Georgia); 11, Kushkuna (Azerbaijan); 12, Upper Siwaliks (Pakistan); 13, North-West China (Bajiazui, Huiduipo, Zhangjiapo, Yangguo, Genjiagou, Gonghe); 14, South Shanxi area (Yushe, Linyi, Pinglu, Mianchi; China); 15, Nihewan Basin area (Jiajiashan, Chifeng, Xiashagou, Shanshenmiaozui, Cenjiawan; China). Shaded blue area: putative geographic distribution of *B. prisus* during the Pleistocene (taken from Kahlke, 1999). b, Time scale showing the chronological/biochronological distribution of the studied taxa in Europe and the most important Plio-Pleistocene sites of Europe and Western Asia mentioned in the text. Abbreviations: Ma, mega annum; Geol., geochronology; ELMA, European Land Mammal Age; C, glacial/interglacial cyclicality; MS, magnetostratigraphy. (For interpretation of the references to colour in this figure legend, the reader is referred to the Web version of this article.)

biochronology scheme (Guérin, 1982, 2007; Torre et al., 1992; Gliozzi et al., 1997; Gentili et al., 2000; Rook and Martínez-Navarro, 2010). The taphonomic evidence and the presence of numerous skeletons of large mammals found in their original anatomical position or slightly scattered, suggest a low degree of post-mortem displacement (Ambrosetti et al., 1992).

3. Materials and methods

More than 400 remains of a large bovid have been recovered from the lignite deposits of Pietrafitta (Table S1). Most of the material comes from the “Miniera Vecchia” and few from “Poderetto” and “Poderone” excavations (Gentili et al., 1996). The studied sample is stored in the “Museo Paleontologico Luigi Boldrini” at

Pietrafitta except for a metacarpal (IGF 1011), a cast of the original fossil which is lost, housed in the IGF (see abbreviations below). The fossils present different state of preservation and colours, suggesting that the bones underwent different taphonomic processes. Most of the specimens share the same kind of preservation with dark grey to dark brown colour, mildly to strongly deformed volumes, and slightly to strongly cracked surfaces testifying a certain degree of subaerial exposure before final burial. Few of the cranial and postcranial remains are characterized by dark greyish colour and are less deformed or cracked.

In this review of the primitive forms of *Bison* we attempt to use the largest comparative sample available, including both the putative ancestors and descendants of this group (i.e., *Leptobos* and *Bison* s.s.). However, due to the difficulties in studying the original

material, lack of data in the literature, debated taxonomy, or scanty fossil record, we kept out from the discussion some samples, e.g., *Leptobos* spp. from China and *L. furtivus* and *L. bravardi* from Europe. The two *Leptobos* groups considered in this work are thus, the one including *L. stenometopon*, *L. elatus*, and *L. merlai* (gr. LSEM hereinafter) and the one including *L. etruscus* and *L. vallisarni* (gr. LEV hereinafter). A large number of *Leptobos* specimens reported by Masini (1989) from unknown localities of the Upper Valdarno and referred to *L. etruscus*, *L. cf. etruscus*, or *L. cf. vallisarni* were not considered due to their undefined stratigraphic provenience and uncertain taxonomy. The genera *Bos*, *Bison*, *Poephagus* (as well as other bovines) are often grouped within *Bos* based on molecular evidence (Groves and Grubb, 2011; Hassanin, 2014; Castelló, 2016 among others). In order to keep consistency with decades of paleontological studies, we follow the nomenclature by Kostopoulos et al. (2018) which retain *Bison* (including both extinct and extant species) as a separate genus. In this context, *Bison* s.l. is used to indicate members of the three subgenera *Bison* (*Bison*), *Bison* (*Poephagus*), and *Bison* (*Eobison*). The marked sexual dimorphism in large bovids is well known and has been matter of study both on extant and extinct taxa (e.g., Drees, 2005; Polák and Frynta, 2010; Grange et al., 2018; Sorbelli et al., 2021a). Grange et al. (2018) suggested that in order to obtain more reliable results, the studied sample should belong only to one sex (i.e., only female or male individuals). However, if this methodology is practical when dealing with very large samples coming from the same locality (e.g., most of Late Pleistocene or Holocene records), this discrimination becomes less feasible when dealing with fragmentary and scanty samples, as in our case. For this reason, we preferred to keep our records intact, including both male and female specimens in the analyses, though with a special attention on sex-dependent morphometric features.

The fossil material directly studied by us includes the following records (for the institutional abbreviations see below): *Leptobos* spp. from Villarroya (Spain), Upper Valdarno, Pantalla, and Umbria undetermined locality (Italy), housed in the ICP, IGF, NHMB, and SABAP UMB; *B. (E.) degiulii* from Pirro Nord (Italy), housed in the DST and PF; *B. (E.) degiulii* from Mygdonia Basin (Greece) housed in the LGPUT and NHCK; *B. (E.) cf. degiulii* from Capena (Italy) and *B. (B.) cf. schoetensacki* from Cava Redicicoli (Italy) housed in the MUST; *B. (E.) sp.* from Mugello (Italy) housed in the MGCB; *B. (E.) cf. georgicus* from Salita di Oriolo (Italy) housed in the MCSNF; *B. (B.) schoetensacki* from Isernia La Pineta (Italy), Cesi (Italy), and Vallparadis Section (Spain) housed in the MPPPL, MuPA, and ICP, respectively; *B. (B.) priscus* from Siberia (Russia), housed in the Yakutia AS. The digital material studied by us includes the 3D models of *B. (E.) georgicus* from Dmanisi (Georgia) housed in the GNM; *B. (B.) bonasus* from Białowieża (Poland) housed in the MRI PAS; *B. (B.) latifrons* from several North American sites housed in the IMNH. Other comparative data were retrieved from the literature. Juvenile specimens are not included in the study. The measurements of the fossils were taken with digital and analogic

callipers and recorded at the nearest 0.1 mm. The measurements on the digital 3D models were taken with the aid of the software MeshLab (Cignoni et al., 2008). Statistical analyses were performed with PAST v.4 (Hammer et al., 2001). The anatomical terminology used in this paper are from (Heintz, 1970), Sala (1986), Masini (1989), Kostopoulos et al. (2018), and Sorbelli et al. (2021a) with minor changes. Linear measurements follow Masini (1989) and Sorbelli et al. (2021a) with minor changes, and are explained in Table S2 and shown in Fig. S1.

The shape and size of horn-core bases were defined by bivariate plot comparing the anteroposterior and dorsoventral diameters (HDV vs HAP). The shape and size of the intertemporal bridge and frontal bones were analysed with bivariate plots featuring IBH vs IBW and FWmin vs FLmin, respectively. Log₁₀ diagrams of teeth (Simpson, 1941) were constructed based on the average values of eight selected variables of *Leptobos* and *Bison* samples from various Eurasian sites. The record of *B. (B.) priscus* from Krasny Yar, R–W was used as a standard of comparison ($y = 0$; data taken from Vasiliev, 2008). To assess the stoutness of limb bones, we used bivariate plots featuring Lmax vs DEW/Lmax % for the metapodials and astragali and Lmax vs PEW/Lmax % for the radii. Principal component analyses (PCAs) were performed based on metapodials and cranial remains to estimate the differences between *Leptobos* and *Bison* species. These analyses rely on seven Mosimann Log-Shape variables for the metapodials and six for the crania (Table 1), obtained by log-transforming the ratio between each measurement and the geometric mean of the measurements for each specimen (Jungers et al., 1995). Histograms were employed to determine the length of metatarsals and radii relatively to the metacarpals, featuring the average values of LmaxMT/LmaxMC %-100 and LmaxRAD/LmaxMC %-100, respectively. The robusticity index of metacarpals was defined by the ratio DEW/Lmax %. Body mass estimations were obtained as the average of three estimations based on metatarsal linear measurements (PEW, PET, and DEW) following Scott (1983), taken in consideration only complete specimens.

Institutional abbreviations—DGPU, Department of Geology, Panjab University, Chandigarh, (India); DST, Dipartimento di Scienze della Terra, Università di Firenze (Italy); GIN RAS, Geological Institute of Russian Academy of Sciences, Moscow (Russia); ICP, Institut Català de Paleontologia Miquel Crusafont, Sabadell (Spain); IGF, Museo di Storia Naturale, Sezione di Geologia e Paleontologia, Università di Firenze (Italy); IGPB, Museo di Scienze della Terra, Università degli Studi di Bari "Aldo Moro" (Italy); IMNH, Idaho Museum of Natural History, Pocatello (USA); LGPUT, Museum of Geology, Palaeontology and Palaeoanthropology of the Aristotle University of Thessaloniki (Greece); MAEGR, Museo Arqueológico y Etnológico de Granada (Spain); MCSNF, Museo Civico delle Scienze Naturali di Faenza (Italy); GNM, S. Janashia Georgian National Museum, Tbilisi (Georgia); MPLB, Museo Paleontologico "Luigi Boldrini" di Pietrafitta, Piegara (Italy); MPPPL, Museo di Paleontologia e Preistoria "Piero Leonardi", Università di Ferrara (Italy);

Table 1

Shape variables used for the principal component analysis. Abbreviations: ms, Mosimann shape variable; GM, Geometric Mean. Abbreviations of measurements as in Fig. S1 and Table S2.

Selected Mosimann shape variables for cranium	Fig. 7	Selected Mosimann shape variables for metapodials	Fig. 9
msIBW = Log (IBW/GM)	1a	msLmax = Log (Lmax/GM)	1 b
msCW = Log (CW/GM)	2a	msPEW = Log (PEW/GM)	2 b
msFMW = Log (FMW/GM)	3a	msPET = Log (PET/GM)	3 b
msMW = Log (MW/GM)	4a	msDW = Log (DW/GM)	4 b
msOSHmax = Log (OSHmax/GM)	5a	msDT = Log (DT/GM)	5 b
msPPW = Log (PPW/GM)	6a	msDEW = Log (DEW/GM)	6 b
		msDETM = Log (DETM/GM)	7 b

MGCB, Museo di Geologia e Paleontologia “Giovanni Capellini”, Università di Bologna (Italy); MR PAR, Mammal Research Institute, Polish Academy of Sciences (Poland); MuPA, Museo Paleontologico Archeologico di Serravalle di Chienti (Italy); MUST, Museo Universitario di Scienze della Terra, Sapienza Università di Roma (Italy); NHCK, Natural History Collection of Kalamoto, Kalindoia (Greece); NHMB, Natural History Museum of Basel (Switzerland); PF, PaleoFactory Lab, Dipartimento di Scienze della Terra, Sapienza Università di Roma (Italy); PIN, Orlov Paleontological Museum, Moscow (Russia); SABAP UMB, Soprintendenza Archeologia Belle Arti e Paesaggio dell’Umbria, Perugia (Italy); Yakutia AS, Academy of Sciences Republik of Sakha, Yakutsk (Russia); ZIN RAS, Zoological Institute of Russian Academy of Sciences, St. Petersburg (Russia).

4. Results

Class Mammalia Linnaeus, 1758
 Order Artiodactyla Owen, 1848
 Family Bovidae Gray, 1821
 Subfamily Bovinae Gray, 1821
 Genus *Bison* Hamilton Smith, 1827
 Subgenus *Eobison* Flerov, 1972.

Emended diagnosis—Small to mid-sized *Bison* with small horns (present in both males and females) and slender limbs. Cranium with relatively deep and high temporal fossae; lower than in *Leptobos* but higher than in *Bison* (*Bison*). The fossae extend far behind the horn-cores, along the lateral sides of the postcornual part of the cranium (not so much as in *Leptobos*). As a result, the occipital squama is separated from the frontal by an abrupt constriction, giving to it a trapezoidal to semi-circular or bell shape with a wide base and a narrow top. Nuchal crest outline, in dorsal view, undulated or semicircular, never squared or straight. Supraoccipital portion of the cranium quite reduced; intertemporal bridge almost completely fused with the nuchal crest. Orbits protruding anterolaterally, weakly tubular, without thickened edges. Postorbital notch variable depending on the sex but, generally, stronger than in *Leptobos* and weaker than in *Bison* (*Bison*). Frontals short; their length (distance from the edge of nuchal crest to Nasion) is shorter than the width of frontals between postorbital notches. Frontals slightly convex or concave and pneumatized at the horn-core bases; elevated above the occipital area. Horn-core pedicles shorter than in *Leptobos*. Horn-cores short and stout, emerging posterolaterally (the angle between the sagittal axis and the midline of the horn-core is comprised between 50° and 75°); horn-cores bending posteriorly and ventrally at the base, then laterally and markedly dorsally at the tip; in some cases, there can be a slight anticlockwise torsion of the right horn-core (i.e., clockwise torsion of the left horn-core); horn-cores dorsoventrally compressed at the base; section oval in the first two third, tending to get circular toward the tips; absence of keels; posteroventral surface strongly furrowed. Premaxillary bone ends before the nasals. Nasals elongated, ending at the level of the anterior margin of the orbit or slightly behind. Mandible with relatively straight corpus and short symphysis. Angle between ramus and corpus around 90° or slightly obtuse. Coronoid process projects backwards, often exceeding the level of processus condyloideus. Teeth are generally smaller than in *Bison* (*Bison*). Neural processes of the thoracic vertebrae well developed but less than in *Bison* (*Bison*). Limbs relatively slender and short. Metapodials stouter than in *Leptobos* but slenderer than in *Bison* (*Bison*). Metatarsal less than 20% longer than metacarpal. Radius generally shorter than in *Bison* (*Bison*) but longer than in *Leptobos*; more than 30% but less than 50% longer than metacarpal.

Bison (*Eobison*) *degiulii* Masini et al., 2013

(Figs. 2–5; Figs. S2–S6) **Diagnosis**—Mid- to large-sized *B.* (*Eobison*). Frontals slightly convex or concave between the horn-

cores with a small crest running along the suture line in the posterior portion. Very short and stout horn-cores. Postcornual portion of the cranium moderately developed. Temporal fossae wide and stretched posteriorly. Nuchal crest outline in dorsal view, arched, feebly undulated. Occipital squama trapezoidal or bell shaped.

Referred specimens—The Pietrafitta record includes 97 cranial (Figs. 2–4) and 358 postcranial remains (Fig. 5 and Figs. S2–S6). See Table S2 for the complete list.

4.1. Description

4.1.1. Cranial material

Five incomplete crania were unearthed from Pietrafitta, all affected by taphonomic deformation. The most complete crania are SABAP UMB 19. 2.1178 and SABAP UMB 19. 2.1179, both flattened in dorsoventral direction. The former preserves most of the frontals, nasals, and the left horn-core whereas the latter is represented by the occipital and basioccipital areas and the horn-cores. In both specimens four of the upper molars (left and right M2s and M3s) and three not identified upper premolars are still embedded in the cranium or matrix. SABAP UMB 19. 2.1178 is associated with its two hemimandibles. The ossified sutures and the stage of wear of teeth (where present) suggest that all the five crania belong to adult individuals. The small size of the horn-cores and the reduced tuberosities of the basioccipital indicate that SABAP UMB 19. 2.1178 was probably a female whereas SABAP UMB 19. 2.1179 is characterized by larger horn-cores and a massive basioccipital, indicating it is a male. The horn-cores are located rather close to the orbits but far from each other and emerge posterolaterally (i.e., the angle between the sagittal axis and the midline of the horn-core is around 65°). Compared to the overall cranium size, the horn-cores are small and stout whereas the pedicles are relatively long. The horn-cores are thicker at the pedicle contact and taper abruptly. Their section at the base is ovoidal with the major axis developing in anteroposterior direction, then it tends to become circular toward the tips. The horn-cores weakly curve ventrally in the first third, then bend laterally and dorsally, then posteriorly and somewhat medially (especially in SABAP UMB 20. 1.6803). The ventral surface is deeply grooved whereas the dorsal one is less furrowed. The grooves tend to disappear toward the apex. In some specimens (i.e., SABAP UMB 21. 1.1323, SABAP UMB 20. 2.7345) the dorsal side of the tips is marked by deep irregular furrows that run parallel to the major axis of the horn-core. In all the specimens the tips are marked by numerous small nutrient foramina. In the broken specimen SABAP UMB 21. 1.1179 it is possible to observe that the most basal part of the horn-core is strongly pneumatized. The horns and pedicles are elevated above the frontals, even if the compression does not permit to assess the degree of elevation. In SABAP UMB 19. 2.1178 the frontal area is quite wide and, although strongly deformed, it is possible to observe a slight concavity in the central part, between the pedicles. A small crest runs in the middle of this depression, following the interfrontal suture. This suture is very clear as well as the Bregma. The supraorbital foramina are far from each other, positioned just behind the orbits, in narrow but elongated grooves. These grooves are anteriorly converging and end at the level of the posterior margin of the orbits. The postorbital constriction is strongly convex. One orbit is preserved in SABAP UMB 19. 2.1178. Although the deformation altered the outline of the orbit, a certain tubular shape can be still recognized. The nasal bone wedges into the frontals with an acute angle, posteriorly to the anterior margin of the orbits. The nasals anterior end is bifurcated. The maxilla thins towards its anterior end expanding below the premaxilla, which prolongs anteriorly with a shovel-like knot in the anterior edge. The contact between maxilla and premaxilla ends above the alveolar level. The posterior part of the premaxilla tapers



Fig. 2. Cranial remains of *Bison (Eobison) degiulii* from Pietrafitta. a, Cranium SABAP UMB 19. 2.1178 in dorsal view; b Cranium SABAP UMB 19. 2.1179 in posterior (b1) and ventral (b2) views; c, Atlas SABAP UMB 21. 4.1314 in anterior (c1), posterior (c2), dorsal (c3), and ventral (c4) views; d, Occipital and basioccipital fragments SABAP UMB 21. 4.1177 in posterior (d1) and ventral (d2) views; e, Occipital and basioccipital fragments SABAP UMB 19. 2.1179 in posterior (e1) and ventral (e2) views. Scale bar: 100 mm.

rapidly and abruptly ends before the nasals. The postcornual portion of the neurocranium is relatively reduced in both SABAP_UMB 19.2.1178 and SABAP_UMB 19.2.1179. The intertemporal bridge (=chignon, *sensu* Duvemois, 1990) is fused with the nuchal crest which is characterized by a vaulted dorsal outline, and slightly undulated edges. The occipital squama is preserved in SABAP UMB 19. 2.1179 and SABAP UMB 21. 2.1177; it is large and has a semi-circular outline, marked by a narrow top and a wide base. The two temporal fossae indent behind the horns, nonetheless their posterior ends are well separated by the dorsal margin of the squama. The jugular processes are hooked, bending inward and projecting below the ventral margin of the condyles. The bulging and robust mastoid processes are separated from the jugular processes by a shallow groove. The condyles are large and sub-triangular with the pointed end located ventrally. The position and number of the foramina on the occipital squama are variable (e.g., a single foramen is visible dorsally to the right condyle of SABAP UMB 21. 2.1177). The basioccipital has a wedged shape formed by the two pairs of tuberosities. Overall, it is short and broad. The posterior tuberosities are triangular and wide and separated by a shallow depression. A faint, small crest starts between the anterior bases of these tuberosities, follows the median axis of the basioccipital, and reaches the anterior tuberosities. The latter are elongated but much

smaller than the posterior ones, and are divided by a deep V-shaped furrow. Anteriorly to the anterior tuberosities there is a secondary crest, which is the prolongation of the one mentioned above. A small foramen is located on the posterior margin of this crest, just at the anterior limit of the tuberosities. SABAP UMB 19. 2.1179, SABAP UMB 21. 2.1177, and SABAP UMB 20. 1.6803 differs for having: larger posterior tuberosities divided by a narrower depression; wider and shorter anterior tuberosities; less developed crest in the valley between the anterior and posterior tuberosities; more developed crest anteriorly to the anterior tuberosities; and an overall larger size. In SABAP_UMB 20.1.6802 the basioccipital still articulates with a portion of the basisphenoid and the pterygoid processes. The basisphenoid is strongly bent upward. A small canal is present on both sides of the basioccipital, just above the posterior tuberosities.

The most complete hemimandibles (SABAP UMB 130074 and SABAP UMB 130075) associated to SABAP UMB 19. 2.1178 are in good state of preservation except for some parts of the rami. The angle formed by the ramus and the corpus is slightly obtuse. The symphysis is relatively short with a bulge on the ventral edge and a rugose surface. In dorsal view, the symphyseal area is slightly inflated as well as the molar portion of the corpus. SABAP UMB 21. 1. 1298 is the only mandible preserving the processus condyloideus.



Fig. 3. Cranial remains of *Bison (Eobison) degiulii* from Pietrafitta. a, Basioccipital SABAP UMB 20. 1.6802/4 in ventral (a1) and lateral (a2) views; b, Basioccipital SABAP UMB 20. 1.6803/2 in ventral (b1) and lateral (b2) views; c, Horn-core tip SABAP UMB 21. 4.1323; d, Left horn-core SABAP UMB 19. 2.1179/1 in posterior (d1), dorsal (d2), and ventral (d3) views; e, Left horn-core SABAP UMB 21. 4.1179 in posteroventral view; f, Nasal fragments SABAP UMB 20. 1.6802/3 in dorsal view; g, Right horn-core SABAP UMB 19. 2.1179/2 in anterior view; h, Right premaxilla SABAP_UMB 20.1.6802/2 in lateral view; i, Left horn-core SABAP UMB 20. 1.6803/1 in posterior view; j, Left horn-core SABAP UMB 20. 1.6802/5 in anterior view; k, Right (?) horn-core tip SABAP_UMB 20.1.7345 in posterior (k1) and dorsal (k2) views. Scale bar: 50 mm.

The condyle is stout and depressed in the middle. The coronoid process is quite elongated and projects backwards, ending posteriorly to the processus condyloideus.

4.1.2. Dentognathic material

The studied specimens include 30 isolated teeth and 70 associated to mandibles.

The upper teeth are quadrangular in occlusal shape (especially the 4th premolar and the molars) with a wide base and high crown. In the P2, the parastyle and paracone are shifted mesially and the paracone fold is quite deep. The metastyle is poorly separated from the labial wall of the tooth. The enamel central cavity has a complex outline, being divided into three islets in SABAP UMB 20. 1.7361. The P3 is characterized by a well-developed metastyle in all the specimens, protruding distally. The parastyle is relatively reduced. The paracone is shifted toward the metastyle, oblique in labial view. The enamel central cavity is simple in most of the specimens except for SABAP UMB 20. 1.7358 which shows a more complex outline. The P4 is the largest and stoutest premolar and has a squared occlusal outline. It shows various degree of molarization. The metastyle is slightly more pronounced than the parastyle, the former protrudes distolabially whereas the latter mesiolabially. The paracone is not particularly protruding, its fold is slightly shifted toward the metastyle and it is divided from the styles by two pronounced furrows. The outline of the central cavity is U-shaped with a more complex distal wall, often featuring a small fold. SABAP UMB 20. 1.6804/8, SABAP UMB 20. 1.6804/7, and SABAP UMB 21. 4.1230 (the first two belonging to the same individual) show the most incipient molarization with a faint hypocone developing

distolingually and the presence, in the latter two specimens, of a small enamel islet distally to the central cavity. SABAP UMB 21. 4.1230 is the most peculiar P4, characterized also by a secondary style lingually to the metastyle. The upper molars show a high degree of hypsodonty with strong pillars and almost parallel margins, slightly diverging occlusally. In all the upper molars the distal lobe is slightly shifted labially. In M1 and M3 the mesial lobe is buccolingually more developed than the distal one whereas, in M2, the two lobes are generally of the same size. The styles are strong and labially projected, marked by a small constriction at the contact with the main body of the tooth forming ribbon-like structures. In M1 and M2 the parastyle is slightly larger than the mesostyle and metastyle which are, more or less, of the same size. The metastyle is strongly projected distally in M3, creating, thus, a vertical, shallow furrow that delimitates its distal contact with the main body of the lobe. In all upper molars the paracone and metacone are less prominent than the styles. In occlusal view, the entostyle shows a subcircular (e.g., SABAP UMB 20. 1.6804/5) to relatively complex outline (e.g., SABAP UMB 20. 1.7346/1), with a prevalence of the former morphology (60% of the observable entostyles). The cement is always present in upper molars, especially on the lingual side; in some specimens it is scarce (e.g., SABAP UMB 20. 1.6806), but in few teeth is present in both the labial and lingual sides (e.g., SABAP UMB 20. 1.7346/1). The cement, in the lingual side, penetrates deeply between the entostyle and the two lobes. The outline of the central cavities has an irregular crescent-moon shape, sometimes characterized by the so-called "bubaline fold" (*sensu* Merla, 1949). This fold is always present in the distal wall of the distal cavity, in some cases in both the cavities (e.g., SABAP UMB 20. 1.6804/3,



Fig. 4. Dentognathic remains of *Bison (Eobison) degiullii* from Pietrafitta. a, Right M3 SABAP UMB 20. 1.7346/1 in occlusal (a1), labial (a2), and lingual (a3) views; b, Right M3 SABAP UMB 20. 1.6804/2 in occlusal view; c, Right M2 SABAP UMB 20. 1.7348 in occlusal (c1) and labial (c2) views; d, Right M2 SABAP UMB 21. 4.1325 in occlusal view; e, Left M1 SABAP UMB 20. 1.6804/5 in occlusal (e1) and lingual (e2) views; f, Right M1 SABAP UMB 20. 1.7350 in occlusal view; g, Right P4 SABAP UMB 21 0.4.1230 in occlusal (g1) and labial (g2) views; h, Right P4 SABAP UMB 20. 1.6804/7 in occlusal view; i, Left P3 SABAP UMB 20. 1.6802/14 in occlusal (i1) and labial (i2) views; j, Left P2 SABAP UMB 20. 1.7361 in occlusal (j1) and labial (j2) views; k, Right m3 SABAP UMB 20. 1.1227 in occlusal (k1), labial (k2), and lingual (k3) views; l, Left m2 SABAP UMB 20. 1.7365 in occlusal (l1) and labial (l2) views; m, Left m1 SABAP UMB 20. 1.1228 in occlusal (m1) and labial (m2) views; n, Right hemimandible with p4-m1 SABAP UMB 21. 4.1235 in occlusal (n1) and lingual (n2) views; o, Right hemimandible with p2-p4 SABAP UMB 21. 4.1236 in labial (o1) and occlusal (o2) views; p, Fragment of right mandibular ramus SABAP UMB 21. 4.1298 in lateral view; q, Right hemimandible with p2-m3 SABAP UMB 130074 in occlusal (q1) and lingual (q2) views; r, Right hemimandible with p2-m3 SABAP UMB 20. 1.7341 in occlusal (r1) and labial (r2) views; s, Left hemimandible with p2-m3 SABAP UMB 20. 1.7342 in occlusal (s1) and labial (s2) views. Scale bars: 30 mm (top) and 50 mm (bottom).

SABAP_UMB 20. 1.7348) although is always more complex in the distal one. The double “bubaline fold” is the rarest to find (25% of the sample). No enamel islets were found between the two lobes.

The lower teeth are mesiodistally elongated with high crowns.

The p3 is quite similar to the p4, differing in the less developed paraconid and the more joined entoconid/entostylid, a deeper distal valley developed mesially, and a less globular metaconid. The p4 is narrow and, in most of the specimens, relatively shortened.



Fig. 5. Metapodials of *Bison* (*Eobison*) *degiulii* from Pietrafitta. a, Left metacarpal SABAP UMB 20. 1.7325 in anterior (a1) and proximal (a2) views; b, Right metacarpal SABAP UMB 130038 in anterior (b1) and proximal (b2) views; c, Right metacarpal SABAP UMB 22. 4.247/8 in anterior (c1) and proximal (c2) views; d, Left metacarpal SABAP UMB 20. 1.7324 in anterior (d1) and proximal (d2) views; e, Right metatarsal SABAP UMB 20. 1.7330 in anterior (e1) and proximal (e2) views; f, Right metatarsal SABAP UMB 20. 1.7331 in anterior (f1) and proximal (f2) views; g, Left metatarsal in anterior (g1) and proximal (g2) views; h, Right metatarsal SABAP_UMB 20.1.7332 in anterior (h1) and proximal (h2) views. Scale bars: 50 mm.

The parastylid is sharp and projects mesiolingually, divided from the paraconid by a shallow and short groove that ends well before the neck (1st valley, *sensu* Heintz, 1970). In some specimens this

groove is quite reduced (e.g., SABAP UMB 20. 1.7342). The paraconid is perpendicular to the mesiodistal axis of the tooth except for SABAP UMB 21. 1.1236 in which it is directed distally. The 2nd valley separating the paraconid from the metaconid, is deep and wide (but less in some specimens, e.g., SABAP UMB 20. 1.7340/3). The protoconid is quite developed, especially lingually, creating a small stylid-like bulge in the 2nd valley, mesially to the metaconid (stronger in 50% of the specimens analysed). The metaconid itself is a robust pillar and projects lingually (e.g., SABAP UMB 20. 1.7342) or distally with a thinner outline (e.g., SABAP UMB 21. 1.1236) with a prevalence of the latter morphology (more than 60% of the specimens). Toward the cervix the metaconid is mesiodistally enlarged and shows a flat lingual surface. The 3rd valley, due to the constriction of the metaconid, is quite deep but ends well before the neck of the tooth. The entoconid and entostylid are almost completely fused, separated by a faint 4th valley which is more or less developed depending on the specimen but tends to disappear rapidly with the wear of the tooth (still well visible in SABAP UMB 21. 1.1236). In the eldest individuals, due to the wear of the tooth, the metaconid and entoconid are fused. The labial valley separating the protoconid from the hypoconid is deep and short, ending before the base of the tooth. The molars have large and sharp metastyle projecting mesiolabially (especially m2 and m3). The protoconid is more developed mesiodistally than the hypoconid. The ectostylid is narrow and located in the mid-point between the two lobes, slightly shifted toward the mesial one. In m2 and m3 the ectostylid has an elliptical shape in occlusal view whereas it has a more complex outline in m1. Labially the molars are flattened, the protoconid and hypoconid are lingually separated by an open valley. The hypoconid size varies depending on the specimen from mesiodistally elongated (e.g., SABAP UMB 20. 1.7340/5) to short and robust (e.g., SABAP UMB 20. 1.7341/6). All molars are characterized by a thick layer of cement on both sides.

4.1.3. Metapodials

Eight metacarpals are known from the lignite of Pietrafitta. Four specimens (SABAP UMB 20. 1.7324, SABAP UMB 20. 1.7325, SABAP UMB 130038, IGF 1011) are almost complete and little deformed. There are no significant differences in the shape of the proximal facets neither in the trochlear surfaces of the analysed specimens. Two metacarpals belong to the same individual (SABAP UMB 22. 4.247), being part of an almost complete skeleton. Generally, all specimens are characterized by a relatively slender built; the two epiphyses have roughly the same width and are much wider than the diaphysis. Seen from above, the proximal outline of the bone is D-shaped; the anterior margin has subrounded edge whereas the posterior one is markedly straight. The proximal articular surface is composed by two facets. The lateral one for the unciform is triangular and smaller than the medial for the trapezoid-magnum which is sub-quadrangular with rounded anterior margin. The former is separated from the latter by a small crest perpendicular to the mediolateral axis of the articulation. The lateral facet is anterolaterally marked by a small notch. The proximal foramen is visible only in SABAP UMB 20. 1.7324 and is located in a deep and narrow groove, at the posterior end of the crest that divides the two facets. A foramen is present distally to the proximal end, in the middle of the posterior side of the epiphysis. The anterior margin of the proximal epiphysis is marked by a large, protruding tuberosity. The diaphysis has hourglass-shaped medial and lateral margins, the minimum width of the shaft is located slightly above mid length. The anterior vascular groove is narrow and shallow, deeper in the distal portion. The ovoidal foramen is located just above the distal end of the vascular groove. In few specimens the distal groove is partially or totally occluded by a bone growth (possibly due to the old age of the individuals, e.g., in SABAP UMB 130038 and SABAP

UMB 22. 4.247/8). The contact area between the diaphysis and the distal epiphysis is marked by an evident tubercle (in both medial and lateral sides), so that the maximum distal width between these tubercles is almost the same as that across the trochleae (larger in 38% of the specimens). A slight mediolateral constriction is present between these tubercles and the distal articulation surface of the corresponding trochlea. The intertrochlear margins converge distally. The distal intercondylar crests are generally sub-parallel. Two deep depressions are present proximally to either side of each trochlear crest, on the anterior side of the epiphysis. The two outer depressions are larger and deeper than the inner ones. The same four pits are present on the posterior side of the bone, proximally to the crests. The lateral and medial trochlear pits are deep and marked by radial rugosities. The lateral abaxial hemicondyle is slightly to strongly anteroposteriorly thinner than the medial one but is laterally more protruding.

Twelve metatarsals were recovered from Pietrafitta, of which six are well preserved. These bones are hourglass shaped with a slender and long shaft and a stout distal end. The proximal epiphysis hosts two major articulation surfaces (anterolateral and anteromedial facets for the articulation with the cubonavicular and cuneiform respectively) and two secondary ones (posterolateral and posteromedial facets for the accommodation of the two cubonavicular posterior facets). The two primary facets converge anteriorly, separated by a well-developed ridge, proximally protruding in the anterior portion. The anteromedial articular facet is ovoidal, having the major axis oblique respect to the sagittal plane. The anteromedial margin is proximally concave and irregular whereas the posterolateral is flattened. The lateral facet is slightly smaller and less inclined with smoother outline. The angle between the two facets is variable between 40° and 45°. The posterolateral articular facet is small and leaf shaped with a very narrow anteroposterior diameter. The posteromedial facet has a subrounded outline and lies attached to the posteromedial margin of the medial primary facet. The proximal portion of the diaphysis is delimited by three crests that follow the main axis of the bone. The posterior surface of the diaphysis is slightly concave to flat in its proximal half, where two faint and shallow longitudinal grooves are present. Toward the distal portion, the posterior side of the shaft flattens and is marked by an ovoidal foramen. The anterior vascular groove is deep, wide and reaches the intercondylar fissure. The anterior foramen is located in the distal portion of the groove, proximally to the contact with the epiphysis. The epitrochlear tubercles at the contact between the diaphysis and the distal epiphysis are well developed, thus, the width at the level of the tubercles is about the same as that between the outer trochlear margins or even larger (e.g., SABAP UMB 20. 1.7328 and SABAP UMB 20. 1.7330). This character is more common in metatarsals than in metacarpals (featured in almost 50% of metatarsals). The distal epiphysis slightly bends posteriorly. The two trochlear ridges are subparallel relative to the medial and lateral margins of the distal end and converge anteriorly. The lateral and medial trochlear pits are deep and proximally surrounded by radial rugosities.

4.2. Comparisons and taxonomic assignment of the Pietrafitta sample

Although the Pietrafitta specimens are characterized by different taphonomic features, on the whole the record is homogeneous, both morphologically and metrically (Figs. 2–9; Tables 2–4; Figs. S2–S6; Tables S3 and S5, S7–S9, S11, S13–S16, S18, S20, S22, S24, S28). The hypothesis that the bovid sample is roughly isochronous is supported by the overall uniformity of the faunal and floral assemblages along the Pietrafitta stratigraphic succession and by the high sedimentation rate estimated for this

kind of brown coal deposits (Cameron et al., 1989; Martinetto et al., 2014).

The general morphology of the cranial and postcranial remains from Pietrafitta is typical of bovines, and in particular of leptobovines and bison. Most of the systematics of these bovids has been historically based on skulls and metapodials but, as suggested by recent studies (e.g., Sorbelli et al., 2021a), other postcranial bones might provide useful taxonomic information.

The Pietrafitta specimens are different from the members of the earliest *Leptobos* species (gr. LSEM) in several cranial features including: shorter braincase (postcornual area), quite reduced intertemporal bridge, shorter and stouter horn-cores, nasal ending at the orbit level, premaxilla not in contact with the nasal, and abundant cement in the upper molars (Figs. 6 and 7; Table 5). Equally, the larger size and robusticity of all the postcranials clearly separate the Pietrafitta bovid from the LSEM leptobovines (Table 6; Tables S10, S12, S19, S23, S25, S26). At the same time, the increased stoutness and larger limb size of the late representatives of *Leptobos* (gr. LEV) make a comparative distinction from the Pietrafitta bovid more difficult. Indeed, the studied postcranial remains share several morphometric features with this group, and especially with *L. vallisarni* from Italy (see section 5.2; Figs. 8 and 9). In spite of that, taking the cranium into consideration, the differences from *Leptobos* gr. LEV are much more evident. The wider occipital, the anteroposterior compression of the intertemporal bridge, the longer nasals, and the shorter premaxillae clearly differentiate the Pietrafitta bovine from *L. etruscus*. Most interestingly, the double bending of the horn-cores, their wide angle of projection from the frontals, and their short and bulk built are characters that separate the Pietrafitta bovine from both *L. etruscus* and *L. vallisarni*.

It is clear that some of the aforementioned features can be interpreted as apomorphies, approaching the Pietrafitta bovine to *Bison* s.l. Nonetheless, the studied sample still retains several features that are generally considered primitive in the evolution of *Bison*, including: small and short horn-cores, weakly tubular orbits, concave frontals, trapezoidal occipital squama, strong indentation of the temporal fossae behind the horn-cores, and relatively short and slender limb bones.

On the whole, the Pietrafitta sample shows numerous similarities with the primitive bison forms attributed to the subgenus *Eobison*. In order to identify the samples at species level, within this subgenus, we provide below detailed comparisons of its most complete and diagnostic elements with several *Leptobos* and *Bison* s.l. species (Figs. 6–11; Tables 5 and 6).

4.2.1. Horn-cores

The best-preserved horn-core (right core of SABAP UMB 19. 2.1179) is plotted in the bivariate diagram that compares the anteroposterior (HAP) and dorsoventral (HDV) diameters of the core bases between various samples of the leptobovine and bison groups (Fig. 6a). All early *Bison*, on average, display smaller horns compared to the priscoid group of *B. schoetensacki* and *B. priscus*, with some specimens (e.g., Kalamoto and Dmanisi samples) showing even smaller sizes than *Leptobos*. Most of *Eobison*, *Leptobos* gr. LSEM, and some *B. schoetensacki* specimens are characterized by HAP values considerably higher than HDV ones. These dorsoventrally compressed cores are clearly different from the more cylindrical ones of *Leptobos* gr. LEV and Late Pleistocene-Holocene *Bison*. The Pietrafitta specimen falls within the variability of *Eobison*, in the area occupied by the Salita di Oriolo, Capena, and Dmanisi samples (Fig. 6a). The position of the horn-cores in relation to the frontals can give some taxonomic hints (McDonald, 1981). The angle formed by the midline of the core at the base and the sagittal line is wider in *Bison* s.l. and *Leptobos* gr. LSEM than in *Leptobos* gr. LEV (Fig. 6b). In particular, the horns of

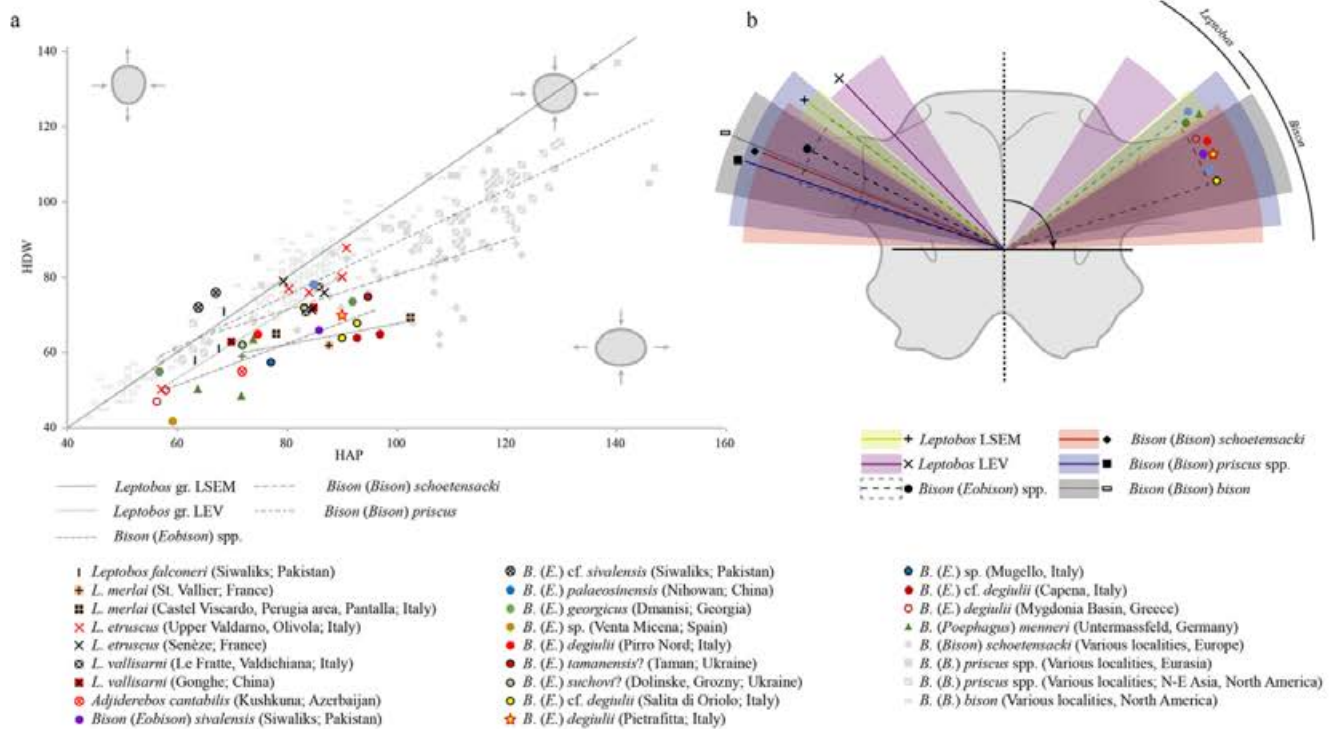


Fig. 6. Horn-core morphology in several species of *Leptobos* and *Bison* s.l. a, Biplot of the horn-core section at the base. Measurement abbreviations are explained in Table S2 and shown in Fig. S1. Measurements are in mm. b, Diagram of the angle between the sagittal axis of the cranium and the horn-core midline.

B. priscus, *B. schoetensacki*, and *B. bison* are directed more laterally, forming wide angles, whereas *Leptobos* gr. LSEM, *B. menneri*, and *Eobison* show cores shifted backwards and, in *Leptobos* gr. LEV, even more posteriorly. The two specimens from Pietrafitta exhibit approximated angles of 65° and 70° fitting with the variability of *Bison*, and more specifically of *B. (Eobison)*.

4.2.2. Intertemporal bridge and frontals

The anteroposterior compression of the intertemporal bridge represents an important trend in the evolution of *Leptobos* and *Bison* (Pilgrim, 1947; Masini, 1989; Duvernois, 1990; Cherin et al., 2019). The primitive forms of *Leptobos* are characterized by a well-developed postcornual portion of the neurocranium with a high and narrow intertemporal bridge, posteriorly elongated. Conversely, in later forms (i.e., *Leptobos* gr. LEV), the bridge tends to shorten anteroposteriorly and widen, due to the anterodorsal shifting of the occipital squama and the squeezing outward of the temporal fossae. In *Bison*, the occipital squama is even more advanced and the intertemporal bridge disappears, fusing with the nuchal crest. Following Cherin et al. (2019), in Fig. 7a we show the progressive change in the proportions of the intertemporal bridge from high and narrow in *Leptobos* to short and wide in *Bison*. This latter condition, in which the bridge is fused with the nuchal crest, is present in the Pietrafitta bovid. Nonetheless, in this form, it is still present a strong indentation of the temporal fossae behind the horn pedicles and, consequently, a constriction of the upper occipital squama; a character which is present in later species of *Leptobos* (i.e., *L. vallisarni*) and in *Eobison* (Flerov, 1979; Toniato et al., 2017; Kostopoulos et al., 2018 among others).

Another evolutionary trend of *Leptobos* and *Bison* is the widening of the frontals and the reduction of their relative length. The biplot in Fig. 7b clearly shows that the earliest representatives

of *Leptobos* and *Bison* (gr. LSEM and *Eobison* respectively) have more elongated and narrower frontals compared with their respective descendants (gr. LEV and *B. priscus*). The Pietrafitta specimen SABAP UMB 19. 2.1178 falls close to the *Eobison* samples from Dmanisi, Capena, and Pirro Nord (Fig. 7b).

4.2.3. Occipital and basioccipital

In order to assess the most diagnostic morphometric traits of the occipital and basioccipital in *Leptobos* and *Bison*, a PCA was performed on 41 crania, using six adjusted variables (Fig. 7d; Table S6). According to the results, the first two PCs explain the 79% of the total variance. PC1 (67.9% of variance) is influenced by the distance between the posterior ends of the temporal fossae (IBW positive), by the width of the foramen magnum and of the basioccipital posterior tuberosities (FMW and PPW both negative), and by the shape of the occipital squama (OSHmin negative, MW positive). This component divides the specimens having wide intertemporal bridge and dorsoventrally compressed occipital squama (x positive) from those with narrow intertemporal bridge, high and narrow occipital squama, and wider foramen magnum and basioccipital (x negative). PC2 (11.8% of variance) is dominated by the width of the foramen magnum (FMW negative), the distance between the posterior ends of the temporal fossae (IBW negative), and by the size of the occipital squama and basioccipital tuberosities (MW, OSHmin and PPW positive). Thus, this component helps distinguishing the specimens with more developed occipital squama and basioccipital (y positive) from those with larger foramen magnum and wider intertemporal bridge (y negative). The Pietrafitta specimen SABAP UMB 19. 2.1179 is found in the top right area, close to the centre of the diagram, fitting with the variability of *Bison* s.l. (Fig. 7d). The bi-condylar width (CW) appears to be the less influencing variable in both PC1 and PC2.

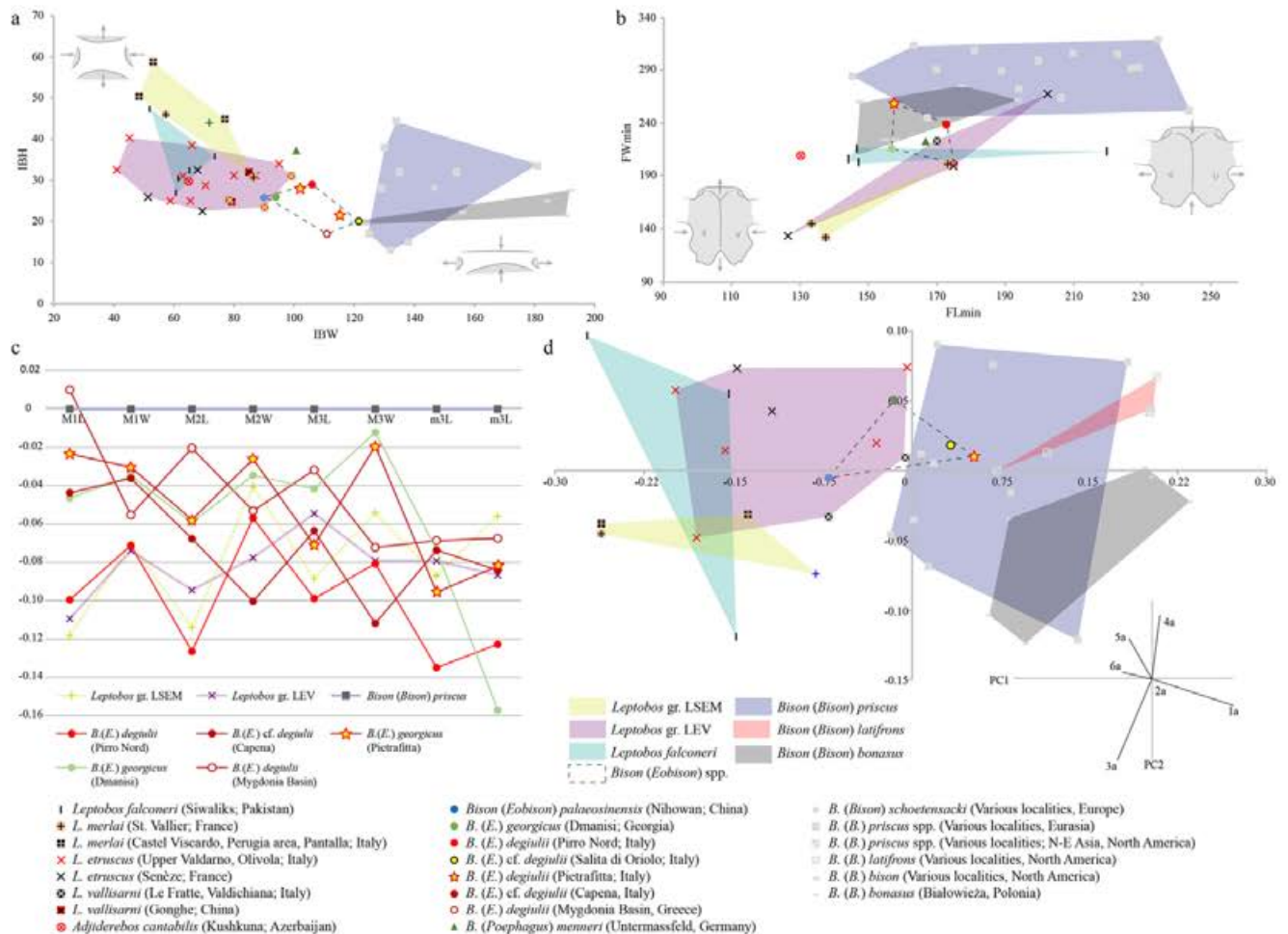


Fig. 7. Biometric comparisons of cranial and dental variables in several species of *Leptobos* and *Bison* s.l. a, Biplot of the intertemporal bridge shape. b, Biplot of the frontal shape. Measurement abbreviations are explained in Table S2 and shown in Fig. S1. Measurements are in mm. c, \log_{10} ratio of upper molars and third lower molar; d, Principal component analysis of six selected variables of the occipital and basioccipital areas.

4.2.4. Teeth

The comparative study of teeth revealed that the Pietrafitta bovine was characterized by a mixture of plesiomorphic and apomorphic characters and a wide morphological variability. The degree of hypsodonty in bovines tends to increase from the middle Villafranchian on, reaching the highest levels in Late Pleistocene and Holocene forms of *Bison* (Asperen van and Kahlke, 2017). The high and columnar teeth of the Pietrafitta bovine are different from those of early *Leptobos*, characterized by more brachydont dentition. On the contrary, the distinction with *Leptobos* gr. LEV is less marked due to their higher hypsodonty (Merla, 1949; Masini, 1989; Duvernois, 1990). The amount of cement in the upper molars is another character that may bear diagnostic value, as it is quite scarce or absent in *Leptobos* and more commonly found in *Bison*. All upper teeth from Pietrafitta present abundant cement, especially within the folds of the lingual side. The mesiodistal constriction of the lingual cones of upper molars has been considered as plesiomorphic in *Leptobos* (Cherin et al., 2019). As a matter of fact, this character is recognizable – albeit variably – in all analysed *Leptobos* and some *Eobison* samples (e.g., Pirro, Mygdonia Basin), whereas is less common in more derived species such as *B. schoetensacki* and *B. priscus*. The Pietrafitta sample shows mesiodistal constriction of the lingual cones in all upper teeth, with various degree of

development. The presence of a bubaline fold in the upper molars, sometimes considered as a primitive feature (e.g., Cherin et al., 2019), is not a reliable source of taxonomic information, being variably expressed within Bovinae and quite common in *Bison* s.l. (Merla, 1949; McDonald, 1981; Asperen van and Kahlke, 2017; Sorbelli et al., 2021a). The p4 has been regarded as one of the most diagnostic anatomical elements of *Eobison*. For instance, a large metaconid with cylindrical shape and lingual projection was considered a distinctive trait in the first description of the *B. (E.) degiulii* type material by Masini (1989). The latter author, however, suggests that the morphology of the p4 in this species may show a certain variability, confirmed by our personal analysis of the unpublished material from Pirro Nord (IGF collections). The Pietrafitta record shows a wide spectrum of morphologies of the p4 metaconid, from bulky and lingually projected (e.g., SABAP UMB 20.17341) to thin and distally projected (e.g., SABAP UMB 130074), with a prevalence of the former condition (Fig. 4). Raw measurements (Table S4) and \log_{10} ratio plot (Fig. 7c) show that the dimensions of the teeth from Pietrafitta are similar to those from Dmanisi and Capena, with short and relatively wide molars, amongst the largest within the *Eobison* group.

On the whole, the teeth from Pietrafitta are characterized by bison-like morphology, with some noteworthy exceptions.

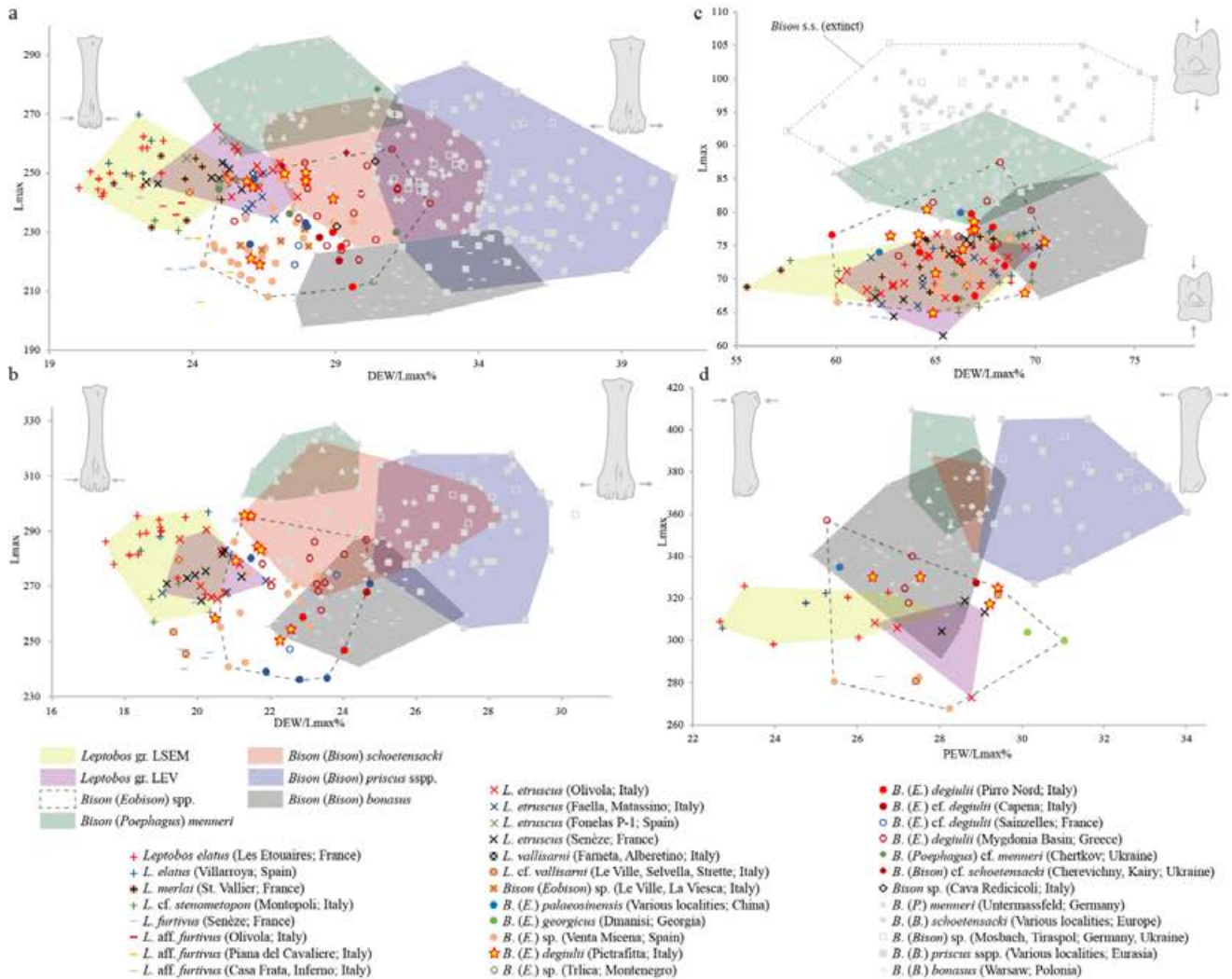


Fig. 8. Bivariate plots of postcranial stoutness in several species of *Leptobos* and *Bison* s.l. a. Metacarpals; b. Metatarsals; c. Astragali; d. Radii. Measurement abbreviations are explained in Table S2 and shown in Fig. S1. Measurements of Lmax are in mm.

Although over the decades several authors have defined diagnostic characters in the teeth of *Leptobos* and *Bison* (e.g., Masini, 1989; Duvernois, 1990; Cherin et al., 2019), we collided with the evidence that dental morphology is highly variable in these taxa. Skinner and Kaisen (1947: 140) exhaustively commented on this issue in their monography on extinct and extant bison: “The pronounced similarity in *Bison* teeth has defied the present attempt to establish useful characters that would permit specific or even subgeneric separations based on tooth characters alone. Large population samples suggest tendencies but show no clear-cut differences. Isolated examples of various *Bison* species appear to have tooth characters that would aid in making specific determinations. These characters, however, soon intergrade when a large population sample is examined”. Other authors remarked furtherly the wide spectrum of variability in bovines’ dental traits when dealing with large samples: “Many students who dealt with very voluminous collections of bovines hold rather sceptical view on the subject, especially concerning isolated teeth” (Sher, 1997: 114). The Pietrafitta sample reinforces this vision, allowing only trends to be recognized, not defined diagnostic characters. For these reasons, we advocate a cautious approach in using isolated teeth for

taxonomic purposes in bovines, especially when small samples are available and/or the putative presence of more than one taxon is inferred.

4.2.5. Metapodials

Metapodials (Table 6; Table S26) are the most frequently used postcranial bones in the taxonomy of Bovinae thanks to their abundance in the fossil record and distinct features (Schertz, 1936; Sher, 1997; Maniakas and Kostopoulos, 2017; Sorbelli et al., 2021a). Recent studies, however, recommend a prudent approach due to the considerable degree of intraspecific variability of these elements, which might be partially caused by ecophenotypic changes (Maniakas and Kostopoulos, 2017; Sorbelli et al., 2021a). The morphology of metapodials of *Leptobos* and *Bison* is quite variable. Over the years, several scholars tried to define morphological characters that could help in differentiating the various species belonging to these two genera (e.g., Masini, 1989; Duvernois, 1990) as it has been done, for example, for *Bos* vs *Bison* (e.g., Brugal, 1983; Sala, 1986; Gee, 1993; Sorbelli et al., 2021a). However, our comprehensive analysis of numerous samples of *Leptobos* and *Bison* shows that, although there might be some features that could

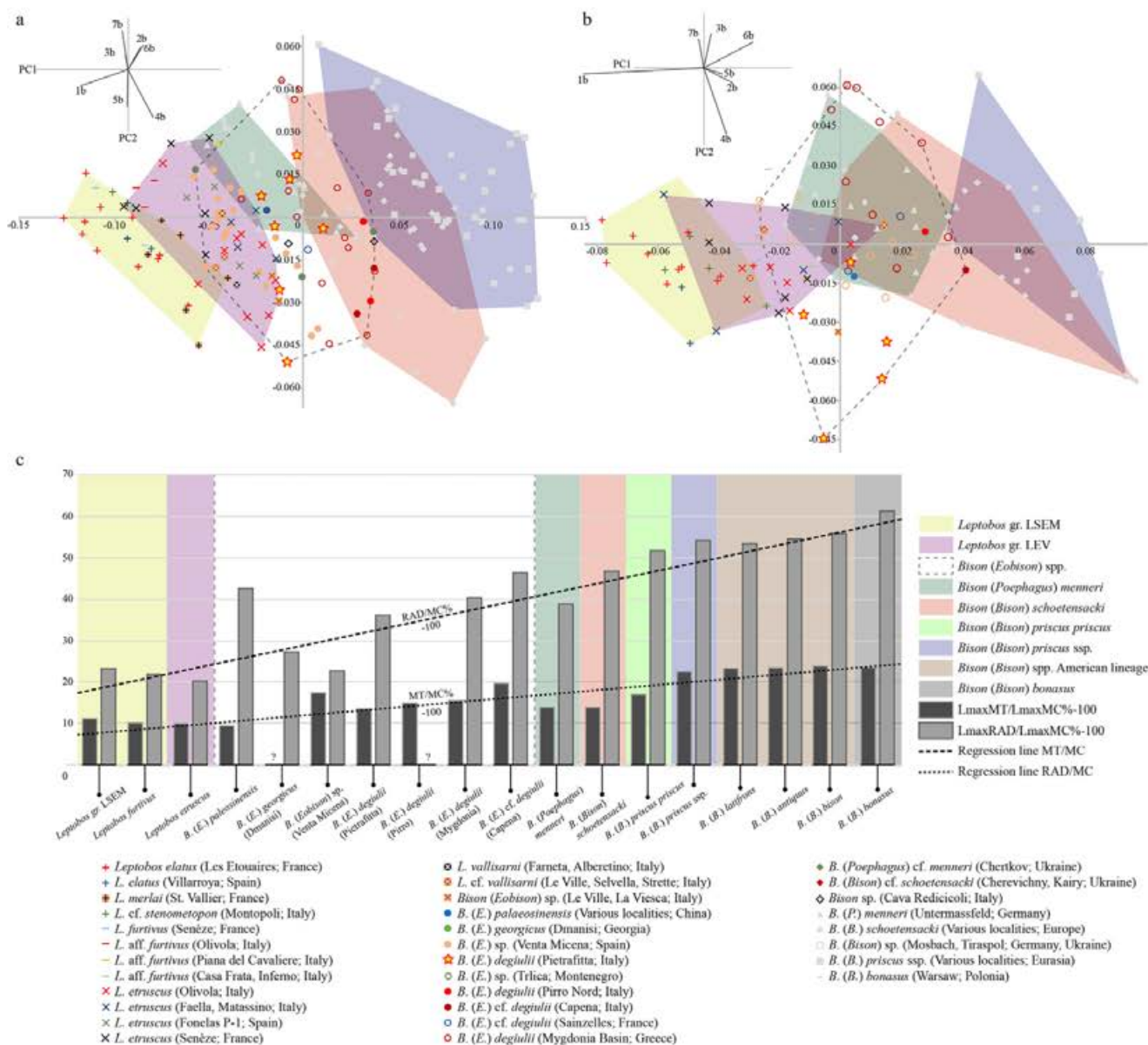


Fig. 9. Comparisons of limb bone dimensions and proportions in several species of *Leptobos* and *Bison* s.l. a–b, Bivariate plots of the first two principal component (PC) scores resulting from PCA of metacarpals (a) and metatarsals (b), based on seven selected variables presented in Table 1; c, Histogram representing the ratio between the lengths of respectively metatarsal (MT) and radius (RAD) to metacarpal (MC).

describe general trends, straightforward morphological differences between the two groups are difficult to be found. On the other hand, metapodial proportions proved to be more solid and useful for taxonomic purposes, especially when dealing with large samples. Comparisons based on Lmax and DEW are widely used to assess the metapodial robusticity, which tends to increase on average from *Leptobos* to *Bison* (Sher, 1997; Kostopoulos et al., 2018; Bukhsianidze, 2020; Sorbelli et al., 2021a). The metacarpal biplot Lmax vs DEW/Lmax% (Fig. 8a) shows the presence of various morphotypes: the left part of the diagram is occupied by the slenderest forms such as *Leptobos* (especially the species of the gr. LSEM); the upper part is occupied by the large-sized and long-legged *B. menneri*; on the right, the more robust species such as *B. schoetensacki* and *B. priscus*, can be found. The Pietrafitta sample

is located in the middle of the diagram, within the variability range of late Villafranchian *Bison*. It is noticeable the partial overlap of the Pietrafitta sample with the most robust specimens of *L. etruscus* and *L. cf. vallisarni* from the Valdarno historical collections. Two specimens (SABAP UMB 130038 and SABAP UMB 20. 1.7325) are very short and slender, fitting well with *B. (Eobison)* sp. from Venta Micena (Spain), one metacarpal of *B. (E.) palaeosinensis*, and some of the metacarpals from the Upper Valdarno (Le Ville, La Viesca) referred to *L. cf. vallisarni*. Four specimens display larger and stouter built, fitting better with *B. (E.) degiulii* from the Mygdonia Basin and *B. (E.) georgicus* from Dmanisi, overlapping with the slenderest specimens of *B. schoetensacki* from various sites of Europe. The two associated metacarpals belonging to the only articulated skeleton from Pietrafitta (SABAP UMB 22. 4.247/7 and SABAP UMB 22. 4.247/

Table 2

Measurements (mm) of the crania of *Bison (Eobison) degiulii* from Pietrafitta. Estimated measurements are in italics. Abbreviations as in Fig. S1 and Table S2.

Measurements	SABAP UMB 19. 2.1178	SABAP UMB 19. 2.1179	SABAP UMB 20. 1.6803	SABAP UMB 20. 1.6802	SABAP UMB 21. 4.1177
HS	65	75	–	–	–
IBW	<i>102.0</i>	<i>115.0</i>	–	–	–
IBH	28.0	22.0	–	–	–
CW	–	116.0	–	–	101.0
FMH	–	36.0	–	–	35.0
FMW	–	34.0	–	–	39.9
MW	–	202.0	–	–	217.4
OSHmin	–	<i>90.0</i>	–	–	–
OSHmax	–	<i>130.0</i>	–	–	–
PW	<i>146.0</i>	–	–	–	–
BAW	<i>90.0</i>	–	–	–	–
HLmax	–	–	<i>340.0</i>	<i>310.0</i>	–
HAP	–	<i>90.0</i>	–	–	–
HVD	–	<i>70.0</i>	<i>77.0</i>	–	–
HLmin	<i>206.0</i>	<i>226.0</i>	<i>223.0</i>	<i>215.0</i>	–
HBWmax	<i>326.0</i>	<i>335.0</i>	–	–	–
HBWmin	<i>250.0</i>	<i>270.0</i>	–	–	–
FFW	<i>144.0</i>	–	–	–	–
HOD	<i>77.0</i>	–	–	–	–
FWmin	<i>259.0</i>	–	–	–	–
FFLmin	<i>231.0</i>	–	–	–	–
FLmax	<i>157.0</i>	–	–	–	–
FLmin	<i>157.0</i>	–	–	–	–
PPW	58.0	67.0	69.0	59.0	66.0
APW	33.0	33.0	38.0	34.0	36.0

Table 3

Measurements (mm) of the metacarpals of *Bison (Eobison) degiulii* from Pietrafitta. Estimated measurements are in italics. Abbreviations as in Fig. S1 and Table S2.

ID Specimen	Side	Lmax	Lf	PEW	PET	DW	DT	DDW	DEW	DETm	DETI	PFWm	PFWI	ABETm	ABETI	AETm	AETI
SABAP UMB 20. 1.7324	L	249.6	239.1	74.2	51.1	42.5	31.6	67.2	68.0	39.4	38.8	43.1	29.3	30.8	28.0	37.3	36.8
SABAP UMB 20. 1.7325	L	220.8	211.6	59.7	<i>40.8</i>	36.7	24.9	58.2	57.5	33.3	32.9	35.1	21.9	26.6	23.4	31.0	31.0
SABAP UMB 22. 4.247/7	L	<i>245.0</i>	–	66.4	45.4	42.5	30.0	61.8	64.0	35.7	35.7	–	–	27.6	26.1	33.8	33.1
SABAP UMB 20. 1.7329/1	R	<i>250.2</i>	–	–	–	<i>50.0</i>	–	<i>70.0</i>	<i>69.0</i>	<i>38.0</i>	–	–	–	<i>30.8</i>	<i>28.5</i>	<i>35.9</i>	<i>36.5</i>
SABAP UMB 22. 4.247/8	R	249.0	240.4	66.4	42.8	44.9	31.0	60.1	64.0	35.7	37.5	37.8	26.3	–	–	–	–
SABAP UMB 20. 1.7326	R	247.3	238.0	73.1	43.5	44.6	30.5	66.7	69.2	39.2	38.6	37.0	33.0	28.6	27.3	36.5	35.6
SABAP UMB 130038	R	218.9	–	60.2	38.9	37.0	26.0	57.8	57.7	33.5	33.3	34.7	24.9	25.8	24.8	31.0	30.8
ICF 1011	R	241.0	230.0	69.9	44.4	40.5	30.5	65.2	69.8	39.5	39.4	39.5	28.6	31.6	31.1	37.9	37.3

Table 4

Measurements (mm) of the metatarsals of *Bison (Eobison) degiulii* from Pietrafitta. Estimated measurements are in italics. Abbreviations as in Fig. S1 and Table S2.

ID Specimen	Side	Lmax	Lf	PEW	PET	DW	DT	DDW	DEW	DETm	DETI	PFOm	PFOI	ABETm	ABETI	AETm	AETI
SABAP UMB 20. 1.7330	R	258.2	248.2	47.8	48.2	34.8	33.3	54.2	52.9	33.8	33.0	33.9	31.8	24.9	24.1	29.8	31.2
SABAP UMB 20. 1.7331	R	284.3	270.5	58.8	55.0	36.9	36.0	63.0	61.5	37.6	35.0	36.6	34.0	28.5	23.0	33.5	33.3
SABAP UMB 20. 1.7332	R	295.3	283.9	64.5	56.8	42.8	36.9	–	63.3	38.5	36.9	40.1	–	28.4	27.1	33.3	34.7
SABAP UMB 20. 1.7333	L	254.3	–	–	–	37.0	–	56.8	57.4	33.5	35.0	43.7	–	25.1	26.7	32.7	30.6
SABAP UMB 20. 1.7335	R	288.0	–	–	–	–	–	–	–	40.0	37.6	–	–	28.7	28	36.2	36.4
SABAP UMB 20. 1.7336	R	296.0	–	–	–	–	–	62.3	63.0	38.5	37.4	41.4	37.6	29.2	26.7	33.9	35.6
SABAP UMB 20. 1.7338	R	–	–	–	–	–	–	63.3	65.6	41.2	40.0	–	–	30.6	29.3	36.1	37.9
SABAP UMB 20. 1.7328	R	250.3	–	53.2	–	34.5	35.7	57.1	55.7	34.3	33.8	–	–	26.1	25.9	30.8	31.7
SABAP UMB 20. 1.7327	R	–	–	–	–	–	–	66.0	71.3	39.1	39.0	–	–	31.5	28.5	36.8	37.9
SABAP UMB 130037	L	283.0	–	58.2	35.9	36.6	36.5	62.2	61.5	38.7	36.6	40.0	35.9	29.4	25.7	32.7	34.5
SABAP UMB 22. 4.247/15	R	278.9	–	59.5	54.8	38.2	40.6	59.7	58.7	35.5	35.1	39.5	39.8	26.3	25.4	31.6	33.9

8), fall at the left border of the *Eobison* group and overlap with the largest *L. etruscus*. The same plot built for the metatarsals reveals a similar pattern (Fig. 8b). The largest and stoutest sample, on the right, is mainly composed by the prisoid forms (*B. schoetensacki* and *B. prisus*). The upper part is occupied by the tallest specimens (i.e., *B. menneri* and some *B. schoetensacki* individuals), whereas the bottom left is occupied by *Leptobos*, characterized by slenderer and shorter metatarsals. Again, *Eobison* is found in the middle. The Pietrafitta record falls at the left border of the *Eobison* range, partially overlapping with *Leptobos*.

In order to increase taxonomic resolution, we performed a

principal component analysis of seven adjusted variables, on both metacarpals and metatarsals (Fig. 9). The two principal components (PC1 and PC2) explain a significant amount of the variance, expressing 80% and 66% of the total variance for metacarpals and metatarsals, respectively. The metacarpal analysis shows that PC1 (71% variance) is negatively influenced by Lmax, PET, and DET, whereas positively by PEW, DW, and DEW. These results separate the longer and thicker metacarpals (x negative) from the shorter and wider ones (x positive). PC2 (9% variance) is mainly dominated by Lmax, DW, and DT for negative values, whereas on the positive axis by PEW, PET, DEW, and DET, so that this axis separates longer

Table 5
Comparative cranial measurements (mm) of selected *Leptobos* and *Bison* s.l. samples. Abbreviations of taxa: LSEM, *Leptobos* gr. *sternomicroton-elatis-miriani*; LE, *Leptobos elatus*; LV, *Leptobos vellianii*; AC, *Adjiderbos cantabrigis*; EP, *Bison (Eobison) polioestensis*; ECDm, *Bison (Eobison) georgicus* from Dmanisi; EDPT, *Bison (Eobison) degiulii* from Pietrafitta; EDPr, *Bison (Eobison) degiulii* from Pietrafitta; EDKm, *Bison (Eobison) degiulii* from Kalamoto; EcdSO, *Bison (Eobison) cf. degiulii* from Salita di Oriolo; BM, *Bison (Peoplugus) menneri*; BS, *Bison (Bison) schweinschaeferi*; BP, *Bison (Bison) priscus* ssp. Estimated measurements are in Fig. 51 and Table S2. Data taken from: ^aMasini (1988); ^bDubrovko and Burchakov (1988); ^cFelhard de Chantoin and Piveteau (1930); ^dBukhtsuaidze (2005); ^ethis work; ^fKostopoulos et al. (2018); ^gBukhtsuaidze (2020); ^hSala (1986); ⁱYafossi et al. (1999); ^jPreat et al. (2003); ^kVercoerens and Guerin (2010); ^lVastanos et al. (2012).

Meas.	Scale	LSEM ^a	LE ^b	LV ^c	AC ^d	EP ^e	ECDm ^f	EDPT ^g	EDKm ^g	EcdSO ^g	BM ^h	BS ^h	BP ^h
IBW	Mean (N)	61.5 (5)	66.2 (13)	86.4 (5)	65.0 (1)	92.0 (2)	94.0 (1)	108.5 (2)	111.0 (1)	122.0 (1)	100.8 (1)	146.0 (1)	172.7 (25)
	Min-Max	48.4–77.0	41.0–95.0	78.5–99.0	–	90.0–94.0	–	102.0–115.0	–	–	–	–	125–230
IBH	Mean (N)	48.8 (5)	30.6 (13)	27.3 (5)	30.0 (1)	25.8 (1)	26.0 (1)	25.0 (2)	17.0 (1)	20.0 (1)	37.0 (1)	28.0 (1)	60.3 (16)
	Min-Max	44.0–59.0	22.5–40.0	23.4–32	–	–	–	22–28	–	–	–	–	13.0–147.0
CW	Mean (N)	92.4 (3)	89.5 (11)	93.8 (4)	106.0 (1)	100.3 (2)	99.8 (1)	101.3–115.5	–	118.0 (1)	110.2 (1)	136.7 (11)	135.3 (39)
	Min-Max	84.5–103.0	56.5–101.0	88.3–97.0	–	100.0–100.5	–	35.5 (2)	–	–	–	129.0–145.0	107.5–156.0
FMH	Mean (N)	35.5 (4)	35.8 (10)	36.6 (3)	–	42.5 (1)	30.0 (1)	35.0 (2)	–	46.0 (1)	–	40.3 (11)	44.0 (37)
	Min-Max	30.3–41.4	32.0–41.0	31.9–40.0	–	–	–	35.0–36.0	–	–	–	30.0–52.0	33.6–53.0
FMW	Mean (N)	42.9 (4)	36.4 (10)	38.2 (3)	–	42.8 (1)	33.0 (1)	37.0 (2)	–	43.0 (1)	40.7 (1)	44.0 (11)	41.9 (37)
	Min-Max	37.5–46.7	28.9–39.4	35.1–42.1	–	–	–	34.0–39.9	–	–	–	36.0–52.0	19.6–59.0
MW	Mean (N)	162.7 (4)	193.5 (8)	177.96 (5)	220.0 (1)	217.0 (2)	200.0 (1)	209.7 (2)	204.0 (1)	246.0 (1)	–	269.1 (7)	274.4 (35)
	Min-Max	131.9–200.0	155.3–220	145–200.8	–	210.0–224.0	–	202.0–217.4	–	–	–	208.0–322.0	218.0–350.0
OSHmin	Mean (N)	101.9 (4)	90.9 (12)	92.1 (2)	–	94.8 (1)	100.0 (1)	90.0 (1)	–	120.0 (1)	97.4 (1)	104.0 (8)	122.8 (30)
	Min-Max	96.8–106.8	75.4–103.0	91.2–93.0	–	–	–	–	–	–	–	72.0–130.0	93.0–151.0
OSHmax	Mean (N)	134.5 (4)	128.0 (8)	108.5 (4)	102.0 (1)	131.5 (2)	134.0 (1)	130.0 (1)	–	143.0 (1)	131.7 (1)	136.0 (8)	160.9 (31)
	Min-Max	125.8–141.0	115.6–141.0	85.0–130.5	–	129.0–134.0	–	–	–	–	–	120.0–164.0	132.6–188.0
PW	Mean (N)	125.3 (5)	144.4 (11)	155.5 (2)	–	208.0 (1)	143.0 (1)	146.0 (1)	–	205.0 (1)	–	233.0 (1)	239.4 (16)
	Min-Max	94.0–161.0	85.5–220.0	151.0–160.0	–	–	–	–	–	–	–	–	205.0–259.0
BAW	Mean (N)	86.5 (5)	87.1 (10)	70.4 (4)	–	55.3 (2)	63.0 (1)	90.0 (1)	48.0 (1)	–	47.6 (1)	74.0 (1)	98.6 (17)
	Min-Max	80.0–99.0	61.0–101.6	53.0–78.0	–	50.0–60.5	–	–	–	–	–	–	69.0–149.0
HLmax	Mean (N)	435.0 (1)	440.0–540	322.0 (3)	280.0 (1)	450.0 (1)	344.0 (1)	325.0 (2)	–	–	–	–	440.6 (9)
	Min-Max	–	–	270.0–360.0	–	–	–	310.0–340.0	–	–	–	–	310.0–420.0
HAP	Mean (N)	79.3 (3)	82.2 (4)	80.3 (3)	65.0 (1)	85.0 (1)	92.1 (1)	90.0 (1)	58.0 (1)	106.0 (1)	67.8 (1)	105.1 (8)	110.2 (10)
	Min-Max	72.0–87.8	79.5–84.5	70.0–86.0	–	–	–	–	–	–	–	91.0–116.0	74.5–140.0
HDV	Mean (N)	62.0 (3)	75.9 (4)	70.8 (3)	85.0 (1)	78.2 (1)	73.6 (1)	73.5 (2)	60.0 (1)	80.0 (1)	49.4 (1)	75.1 (8)	108.2 (10)
	Min-Max	59.0–65.0	71.5–79.0	63.0–77.5	–	–	–	70.0–77.0	–	–	–	58.0–87.0	77.5–136.5
HLmin	Mean (N)	245.0 (1)	374.3 (3)	275.5 (3)	173.0 (1)	210.0 (2)	245.0 (1)	217.5 (4)	–	–	159.9 (1)	276.0 (10)	395.1 (8)
	Min-Max	–	343.0–400.0	250.0–296.5	–	200.0–220.0	–	206.0–226.0	–	–	–	235.0–325.0	255.0–505.0
HBWmax	Mean (N)	238.5 (2)	306.3 (3)	303.3 (1)	–	317.0 (1)	294.3 (1)	330.5 (2)	245.0 (1)	–	–	314.1 (10)	–
	Min-Max	232.0–245.0	283.0–320.0	–	–	–	–	326.0–335.0	–	–	–	280.0–350.0	–
HBWmin	Mean (N)	135.5 (2)	268.0 (3)	202.0 (1)	–	247.5 (2)	195.0 (1)	260.0 (2)	153.0 (1)	310.0 (1)	–	–	314.4 (6)
	Min-Max	118.0–153.0	224.0–350.0	–	–	220.0–275.0	–	250.0–270.0	–	–	–	–	236.5–390.0
FFW	Mean (N)	102.4 (6)	105.7 (8)	126.9 (3)	–	152.0 (2)	127.4 (1)	144.0 (1)	134.3 (1)	132.0 (1)	142.1 (1)	–	195.8 (15)
	Min-Max	84.0–123.0	77.0–159.0	107.6–144.0	–	143.0–161.0	–	–	–	–	–	–	180.5–217.0
ROD	Mean (N)	93.8 (2)	102.8 (2)	92.0 (1)	75.0 (1)	–	72.0 (1)	77.0 (1)	65.0 (1)	90.0 (1)	–	–	97.1 (18)
	Min-Max	85.0–102.5	95.0–110.5	–	–	–	–	–	–	–	–	–	73.0–111.0
PWmin	Mean (N)	159.2 (5)	205.3 (7)	249.5 (3)	210.0 (1)	237.0 (1)	241.8 (1)	259.0 (1)	239.5 (1)	244.0 (1)	223.5 (1)	290.9 (11)	296.6 (37)
	Min-Max	132.0–201.0	133.7–267.4	223.4–280.0	–	–	–	–	–	–	–	255.0–335.0	232.0–344.0
FFLmin	Mean (N)	134.3 (3)	150.2 (8)	166.0 (1)	–	150.0 (1)	154.5 (1)	231.0 (1)	182.9 (1)	–	–	–	208.4 (15)
	Min-Max	105.0–153.0	132.1–174.4	–	–	–	–	–	–	–	–	–	167.0–249.0
FLmax	Mean (N)	234.1 (2)	226.2 (3)	–	–	–	223.0 (1)	247.0 (1)	230.0 (1)	225.0 (1)	214.4 (1)	–	274.6 (16)
	Min-Max	231.2–237.0	196–282	–	–	–	–	–	–	–	–	–	233.0–303.0
FLmin	Mean (N)	148.0 (3)	160.9 (4)	157.7 (3)	130.0 (1)	–	147.5 (1)	157.0 (1)	194.0 (1)	159.0 (1)	166.8 (1)	–	196.0 (12)
	Min-Max	133.0–173.5	126.4–202	–	–	–	–	–	–	–	–	–	145.4–244.0
PPW	Mean (N)	58.3 (6)	64.5 (7)	65.5 (5)	–	65.5 (1)	61.8 (1)	63.8 (5)	–	–	–	–	73.8 (20)
	Min-Max	50.3–63.0	49.7–76.3	62.0–69.5	–	–	–	58.0–68.9	–	–	–	–	55.5–90.0
APW	Mean (N)	29.7 (6)	39.8 (6)	34.9 (5)	–	42.5 (1)	33.6 (1)	34.68 (5)	–	–	–	–	46.8 (17)
	Min-Max	24.8–36.6	35.0–55.5	29.0–43.6	–	–	–	33.0–38.0	–	–	–	–	32.0–56.6

Table 6
Comparative measurements (mm) of the metacarpal in selected *Leptobos* and *Bison* s.l. samples. Abbreviations as in Fig. S1 and Table S2. Data taken from: ^aMaxini (1989); ^bPodings (2011); ^cGarnido (2008); ^dJong et al. (2016); ^eBubstianidae (2005); ^fthis work; ^gManiakas and Kostopoulos (2017); ^hKostopoulos et al. (2018); ⁱSher (1997); ^jBrugal (1995); ^kMovable (1992); ^lBrugal and Fosse (2005); ^mSchertz (1936); ⁿSala (1986); ^oSorbelli et al. (2021a); ^pRueda et al. (2010); ^qVercoutère and Gaudin (2010); ^rPrat et al. (2003); ^sDrees (2005); ^tCastanos et al. (2012); ^uEmpel and Boskosz (1963).

Taxon	Site	Statistics	Lmax	PEW	PET	DW	DT	DEW	DEIm
<i>Leptobos elonus</i> ^{ab}	Les Étrouaires, Villarroya (France, Spain)	Mean (N)	253.6 (25)	57.5 (32)	37.8 (27)	33.9 (20)	26.1 (18)	55.1 (23)	34.5 (23)
		Min-Max	242.2–270.0	52.0–64.7	32.1–42.9	29.6–39.4	22.0–30.0	49.1–63.6	31.5–36.9
		SD	8.1	3.7	2.9	3.0	2.2	3.8	1.6
<i>Leptobos merliar</i> ^{ab}	St. Vallier (France)	Mean (N)	245.5 (8)	58.2 (13)	39.2 (14)	36.8 (7)	27.1 (7)	57.5 (14)	33.8 (13)
		Min-Max	231.6–255.8	51.1–62.5	34.5–46.4	32.5–40.0	23.4–29.1	51.9–62.9	30.3–37.4
		SD	9.2	3.9	3.6	3.0	2.1	3.7	2.1
<i>Leptobos etruscus</i> ^{ac}	Sensize, Faella, Marassino, Olivola, Fontelas-1 (France, Italy, Spain)	Mean (N)	248.3 (32)	58.1 (40)	45 (40)	39.3 (37)	28.5 (37)	62.6 (49)	35.7 (43)
		Min-Max	234.5–265.5	36.2–67.9	36.7–65.6	31.8–43.7	25.0–31.5	50.4–68.6	32.0–41.1
		SD	6.9	9.5	9.2	3.0	1.6	3.9	1.7
<i>B. (Eobison) polioossinensis</i> ^d	Nihowan Basin (China)	Mean (N)	234.8 (4)	68.4 (4)	40.4 (3)	39.4 (1)	30.6 (1)	63.5 (4)	34.6 (3)
		Min-Max	226.0–248.1	60.0–73.8	35.0–47.5	–	–	58.8–65.2	34.2–34.9
		SD	9.4	6.1	6.4	–	–	3.1	0.4
<i>B. (Eobison) georgicus</i> ^d	Dmanisi (Georgia)	Mean (N)	237.0 (3)	66.9 (4)	42.4 (4)	39.9 (3)	29.2 (3)	65.3 (4)	35.4 (4)
		Min-Max	230.0–244.7	62.8–70.8	37.7–45.2	34.3–44.6	25.8–31.1	61.0–71.6	33.2–37.8
		SD	7.3	3.6	3.3	5.2	3.0	4.5	2.0
<i>B. (Eobison) sp.</i> ^e	Venta Micena (Spain)	Mean (N)	225.6 (30)	58.5 (43)	36.6 (44)	35.3 (31)	26.9 (30)	60.1 (36)	33.0 (35)
		Min-Max	208.2–248.7	52.3–69.5	32.8–46.5	31.4–44.2	24.1–32.1	53.5–69.1	30–36.3
		SD	10.2	4.6	3.4	3.7	2.1	4.7	1.6
<i>B. (Eobison) degliati</i> ^f	Pietrafitta (Italy)	Mean (N)	240.0 (8)	67.1 (7)	43.8 (7)	42.3 (8)	29.5 (7)	65.0 (8)	36.8 (8)
		Min-Max	218.9–250.2	59.7–74.2	38.9–51.1	36.7–50.0	24.9–32.9	57.5–70	33.3–39.5
		SD	12.8	5.7	3.9	4.4	2.9	5.2	2.6
<i>B. (Eobison) degliati</i> ^g	Pirro Nord (Italy)	Mean (N)	222.2 (3)	62.1 (4)	38.7 (4)	38.5 (3)	27.4 (3)	64.8 (4)	33.1 (5)
		Min-Max	211.5–230.0	58.0–69.5	35.5–41.7	29.8–46.2	25–30.1	62.0–66.4	29.3–37.3
		SD	9.6	5.3	3.2	8.3	2.6	1.9	3.2
<i>B. (Eobison) degliati</i> ^h	Mygdonia Basin (Greece)	Mean (N)	238.5 (19)	67.4 (24)	40.1 (24)	42.4 (23)	29.4 (23)	70.3 (22)	39.3 (22)
		Min-Max	220.7–258.1	57.7–78.3	32.9–48.4	31.8–51.2	23.5–35.2	59.5–88.8	34.4–48.2
		SD	10.6	4.9	3.0	5.1	2.9	6.7	3.0
<i>B. (Eobison) cf. degliati</i> ^f	Capena (Italy)	Mean (N)	222.5 (2)	68.4 (2)	43.1 (2)	44.4 (2)	29.7 (1)	64.6 (2)	35.4 (2)
		Min-Max	220.0–225.0	68.1–68.7	42.0–44.0	44.3–44.4	–	64.1–65.0	34.1–36.7
		SD	3.5	0.4	1.4	0.1	–	0.6	1.8
<i>B. (Phephagus) memmeri</i> ^{ia}	Untermaßfeld (Germany)	Mean (N)	276.4 (37)	77.0 (50)	46.5 (48)	44.8 (43)	32.8 (40)	75.6 (41)	38.2 (38)
		Min-Max	255.8–296.0	64.4–91.4	39.3–52.6	35.3–57.7	27.8–39.0	65.4–86.0	29.5–47.3
		SD	10.2	5.6	3.2	4.7	3.0	6.3	5.8
<i>B. (Bison) schoentensacki</i> ^{fg,kl,m,n,o,p}	Dürfort, Le Vallonnet, Le Vassiré, Mauet, Süssenborn, Cesi, Vallparadis, Cromer Forest-bed (France, Germany, Italy, UK)	Mean (N)	252.2 (54)	78.4 (68)	46.8 (61)	49.3 (49)	33.9 (51)	76.9 (67)	42.1 (54)
		Min-Max	225.0–277.0	46.9–93.0	37.6–56.0	36.3–64.0	27.9–46.6	65.9–88.5	35.3–52.4
		SD	12.8	7.0	3.6	5.7	3.9	6.0	3.3
<i>B. (Bison) cf. schoentensacki</i> ^{qm}	Mosbach (Germany)	Mean (N)	256.0 (22)	84.5 (18)	48.9 (19)	49.9 (4)	32.6 (4)	82.9 (19)	42.8 (4)
		Min-Max	241.1–277.8	72.0–97.3	43.4–56.4	43.3–55.1	30.2–35.1	73.0–97.1	40.1–46.0
		SD	11.3	6.9	3.3	5.2	2.5	6.3	2.5
<i>B. (Bison) priscus priscus</i> ^{qa}	Chatillon-Saint-Jean, Romain-La-Roche, Taubach (France, Germany)	Mean (N)	254.5 (40)	87.9 (39)	53.1 (38)	55.7 (38)	36.3 (38)	87.9 (23)	46.1 (40)
		Min-Max	232.0–286.5	71.4–102.0	44.0–63.0	42.3–63.0	30.6–42.5	75.5–98.1	37.0–51.5
		SD	13.0	8.1	5.2	6.1	3.6	6.9	3.1
<i>B. (Bison) priscus</i> ^{ra,sa,t,u,v}	Habarra, Roter Berg, Cava Fló, North Sea, Kiputz IX, Joint Mitnor Cave (France, Germany, Italy, North Sea, Spain, UK)	Mean (N)	234.5 (58)	81.5 (66)	48.2 (31)	50.3 (40)	33.4 (29)	84.7 (56)	42.6 (50)
		Min-Max	216.8–260.0	60.0–96.5	42.5–56.0	39.5–59.0	28.8–40.0	70.5–101.5	31.1–53.0
		SD	10.0	7.1	3.5	5.9	2.8	7.1	5.8
<i>B. (Bison) bonasus</i> ^a	Białowieża (Poland)	Mean (N)	213.9 (32)	73.5 (31)	45.7 (30)	42.9 (31)	27.1 (32)	69.9 (32)	39.7 (30)
		Min-Max	202.0–231.0	64.0–88.0	39.0–54.0	35.0–55.0	23.0–32.0	61.0–80.0	30.0–46.0
		SD	7.6	6.6	3.8	5.7	2.5	5.5	3.3

metacarpals with larger diaphysis (y negative) from shorter ones with larger epiphyses (y positive). The PCA diagram, although not resolving the overlapping issues between groups, helps us in distinguishing the three major morphotypes without the influence of size effect: the *Leptobos* morphotype with slender diaphysis and deep and narrow epiphyses; the “true bison” morphotype (including *B. schoetensacki*, *B. priscus*, and *B. bonasus*) with robust built and wide diaphysis and epiphyses; the *Eobison* morphotype (including also *B. menneri*) with intermediate features between the two former groups. The Pietrafitta specimens fall within this last group.

In the metatarsal analysis (Fig. 9b; Table S27), PC1 (48% variance) is mainly influenced by Lmax for the positive values and by DEW, PEW, DW, DT for the negative ones, thus dividing the long and slender metatarsals (x positive) from the stouter ones with wider shaft and distal end (x negative). PC2 (18% variance) is determined, positively, by the size of the distal epiphysis (DET and DEW) and the anteroposterior diameter of the proximal end (PET), whereas negatively by the width of the diaphysis (DW), which influences way more than the other variables (PEW, Lmax, and DT). PC2 allows to distinguish the metatarsals with thick ends (y positive) from the ones with wide shafts (y negative). The Pietrafitta specimens, characterized by very thick and wide diaphysis, lie along the negative PC2 axis, occupying an empty space, and partially overlapping the *Eobison* record.

Both the PCAs show that the Pietrafitta sample is characterized by metapodials with intermediate proportions between *Leptobos* and *Bison* s.s., fitting with the known *Eobison* variability. It is worth mentioning that some isolated bones from the late Villafranchian of central Italy referred to *L. etruscus* and *L. cf. vallisarni* (Masini, 1989), display proportions similar to some *Eobison* specimens. It has to be considered, in fact, that the first *Bison* and last *Leptobos* likely coexisted in Europe during this period. Thus, it is possible that some of these isolated remains could have been erroneously attributed to *Leptobos* and, instead, pertain to *Bison*.

4.2.6. Radii, astragali, and other postcranials

Among the other postcranial bones, the radii are the most helpful. As already shown by Sorbelli et al. (2021a), their size and built can provide interesting information for taxonomy. The biplot that compares the length and slenderness degree of this bone shows a clear increase in stoutness and size from *Leptobos* to *Bison* (Fig. 8d; Table S12). The Pietrafitta specimens plot in the space occupied by the early *Bison* samples from Pirro Nord, Capena, and the Mygdonia Basin at the upper border of the *Leptobos* cloud. Other postcranials such as calcanei and cubonavicular are not particularly significant due to their considerable dimensional homogeneity between the last *Leptobos* and early *Bison* (Tables S21 and S25). Conversely, it is worth noting that the astragali allow a certain separation between “true” *Bison* and *Eobison*-*Leptobos* based on total length and, secondarily, stoutness (Fig. 8d; Table S23). The low number of complete humeri, femurs, and tibiae does not allow us to perform dimensional comparisons. In spite of that, the average measurements of these elements in the Pietrafitta sample (and in other roughly coeval samples) are always intermediate between those available for *Leptobos* and *Bison* s.s. (Tables S10, S17, S19). As mentioned above for metapodials, we further underline that also for other postcranial elements, a prudent attitude toward the use of morphological characters in taxonomic attributions is strongly recommended, especially when dealing with isolated remains.

4.2.7. Limb proportions and concluding remarks

Interesting results can also be obtained from the dimensional comparison between different bones. The analysis of the ratio

between the metatarsal and metacarpal lengths shows that the latter bone is relatively longer in most primitive forms than in the priscoid group (Fig. 9c). Indeed, in *Leptobos* and most *Eobison*, including the Pietrafitta sample, the metatarsals are less than 15% longer than the metacarpals, whereas in Late Pleistocene *Bison* from Eurasia and North America (including the living species *B. bonasus* and *B. bison*), it is more than 20% longer (Fig. 9c). On the contrary, the ratio between radius and metacarpal lengths shows that the Pietrafitta bovine and other records of *Eobison* share with *Bison* s.s. a relatively elongated radius compared to the metacarpal (Fig. 9c). This analysis reveals that in all late Villafranchian *Bison* the radius length exceeds by more than 30% the metacarpal length, with the exception of the samples from Dmanisi and Venta Micena (Fig. 9c). Interestingly, the earliest members of *Bison* s.s. (i.e., *B. menneri*, *B. schoetensacki*, *B. p. priscus*) differ significantly from their later relatives (i.e., *B. p. mediator*, *B. antiquus*, *B. latifrons*, *B. bison*, *B. bonasus*) in having longer metacarpals compared to both metatarsals and radii.

Considering all the above pieces of evidence, the bovid sample from Pietrafitta can be confidently referred to the subgenus *Eobison*. More specifically, most cranial and limb bone morphological and biometric characters are consistent with those described in *B. (E.) degiulii*, a well-known species from the late Villafranchian of Southern Europe (Italy and Greece) (Fig. 10). Another species with similar morphology is *B. (E.) georgicus* from Georgia. However, it is represented by a rather scarce sample, which needs to be enriched by new discoveries in order to clarify its taxonomic status (see Discussion).

5. Discussion

5.1. *Leptobos*: state of the art

During the twentieth century, several diagnoses of *Leptobos* have been proposed (Pilgrim, 1939; Merla, 1949; Masini, 1989; Duvernois, 1990). Unfortunately, this multiplicity of interpretations has led to a rather vague definition of this genus. Nevertheless, some distinctive characters of *Leptobos* are accepted by the different authors, including: horn-core bases located not far from the orbits, emerging posterolaterally, slightly to strongly compressed dorsoventrally; horn-cores furrowed in the first half, without evident keel; female hornless; premaxilla in contact with nasal; presence of ethmoidal fenestrae; temporal fossae well developed in the postcornual portion of the cranium; sub-triangular basioccipital; occipital squama from semi-circular to bell-shaped; presence of a more or less developed intertemporal bridge; slender limbs; small size (Figs. 11 and 12). Below we provide a review of *Leptobos* records in the European Villafranchian.

The first group of species (here called gr. LSEM), generally considered more primitive, includes *L. stenometopon*, *L. elatus*, *L. merlai*, and the poorly-known *L. furtivus*. *Leptobos stenometopon* (Fig. 13b) is a small-to mid-sized species described on the basis of a horned calvarium from the Late Pliocene of Dusino (Italy; Rüttimeyer, 1867). The taxonomy of this species has been debated over the last decades, being considered either a younger synonym of *L. elatus* (Duvernois and Guérin, 1989; Duvernois, 1990, 1992) or a valid species (Masini, 1989; Geraads, 1992; Rodrigo, 2011; Masini et al., 2013; Cherin et al., 2019). It is also reported - as *L. cf. stenometopon* - from the Plio-Pleistocene transition in Montopoli (Italy) and from some sites of uncertain age in the Upper Valdarno (Merla, 1949; Masini, 1989). *Leptobos elatus* is a species described by Depéret (1884) on cranial material from the latest Pliocene of Perrier-Les Étouaires (France). Unfortunately, the type material is no longer available (Viret, 1954; Masini, 1989) and the neo-diagnosis given by Duvernois (1990, 1992) was based only on



Fig. 10. Morphological comparison between *Bison* (*Eobison*) specimens from the Mediterranean area, studied in this work. a, *B. (E.) degiulii* from Pietrafitta, SABAP UMB 19. 2.1178 in dorsal view; b, *B. (E.) degiulii* from Pietrafitta, SABAP UMB 21. 4.1177 in posterior view; c, *B. (E.) degiulii* from Pietrafitta, SABAP UMB 19. 2.1179 in posterior (c1) and ventral (c2) views; d, *B. (E.) cf. degiulii* from Capena, MUST (ex MPUR) s.n., in dorsal (d1), posterior (d2), and ventral (d3) views; e, *B. (E.) cf. degiulii* from Salita di Oriolo, MCSNF s.n., in dorsal (e1), posterior (e2), right lateral (e3), and ventral (e4) views; f, *B. (E.) degiulii* holotype from Piarro Nord, IGPB s.n., in dorsal (f1), posterior (f2), right lateral (f3), and ventral (f4) views; g, *B. (E.) degiulii* from Kalamoto-2, NHCK KLT-638, in dorsal (g1), posterior (g2), left lateral (g3), and ventral (g4) views; h, *B. (Eobison)* sp. from Mugello, MGCB s.n., in anterior (h1) and dorsal (h2) views. Scale bar: 100 mm.

dental and postcranial remains and on the original descriptions by Depéret (1884). The synonymy between *L. elatus* and *L. stenometopon* proposed by Duvernois and Guérin (1989) and Duvernois (1990) has been questioned by other authors (e.g., Masini et al., 2013; Cherin et al., 2019) due to some flaws in the taxonomic status of *L. elatus* and to significant differences between the material from the type localities of the two species. Other remains attributed to *L. elatus* are from the sites of Rocaneyra (France; dated to the Plio-Pleistocene boundary), Villarroya (Spain; ca. 2.15 Ma), and Tegelen (The Netherlands; ca. 2.0 Ma) (Schreuder, 1946; Viret, 1954; Masini, 1989; Duvernois, 1990; Rodrigo, 2011). *Leptobos merlai* (Fig. 13c) is a mid to large-sized species from the middle Villafranchian of France (type locality: Saint Vallier) and

Italy. First referred to *L. elatus* (Viret, 1949) then to *L. stenometopon* (Viret, 1954), De Giuli, 1986 recognized diagnostic differences between the remains from Dusino and those from Saint Vallier and erected the species *L. merlai* to accommodate the latter. Later, Duvernois and Guérin (1989) and Duvernois (1990, 1992) similarly to what was done for *L. stenometopon*, proposed *L. merlai* as a subspecies of *L. elatus*. Finally, in their description of the material from Pantalla (ca. 2.0 Ma) and other Italian sites, Cherin et al. (2019) supported the validity of *L. merlai* as a distinct species (and questioned the validity of *L. elatus* itself, being based on scanty material). *Leptobos furtivus* is considered the smallest and actually rarest species of this genus in Europe. It was first described by Duvernois and Guérin (1989) on the basis of few teeth, some postcranials, and

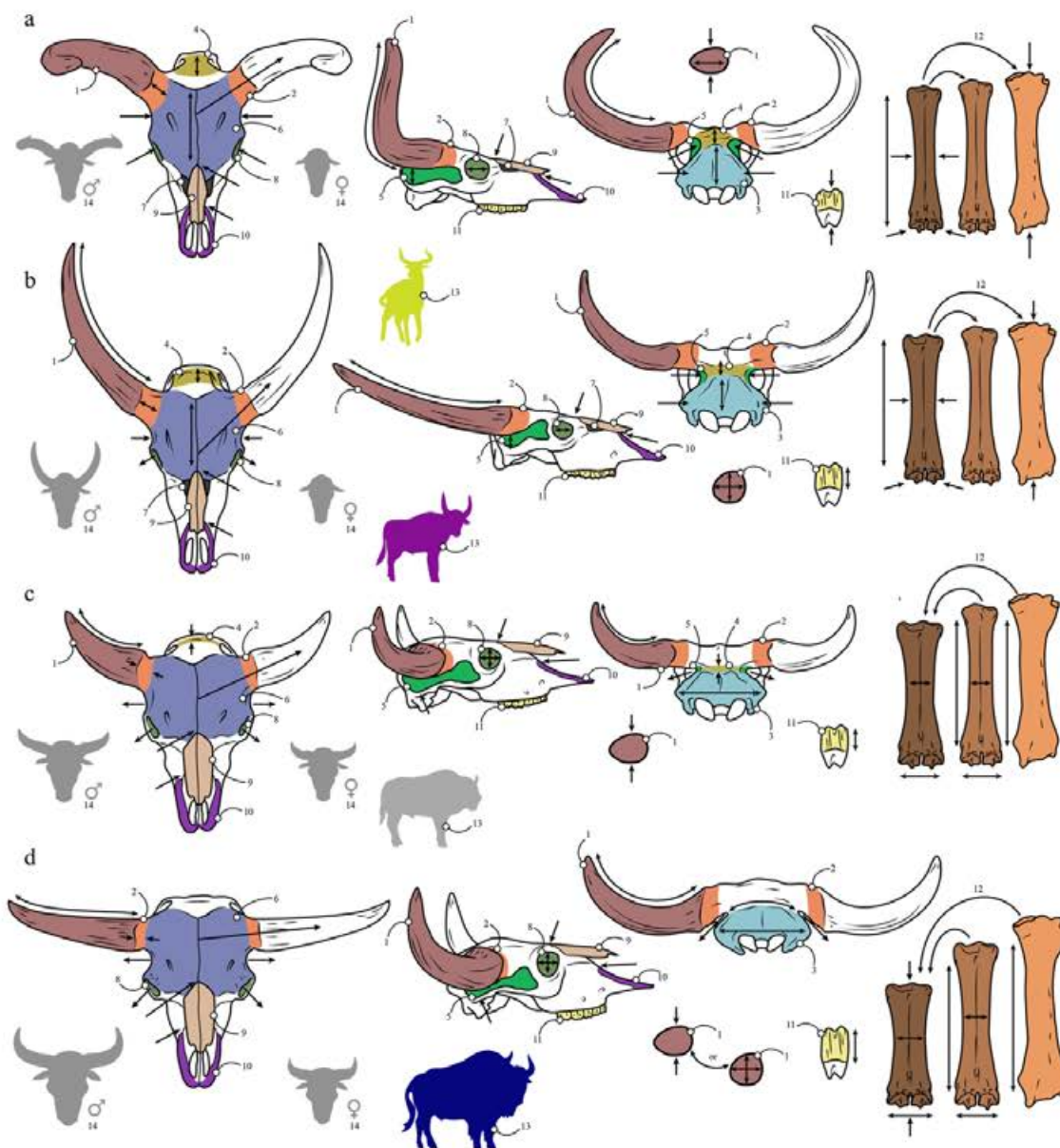


Fig. 11. Graphical representation of the morphological characters that define the four main groups of *Leptobos* and *Bison* presented in Table 7 a, *Leptobos* gr. LSEM; b, *Leptobos* gr. LEV; c, *B.* (*Eobison*); d, *B.* (*Bison*). The arrows mark the evolutionary trends of the considered characters. Legend (same numbers as in Table 7): 1, horn-core shape; 2, horn-core position; 3, occipital squama; 4, intertemporal bridge; 5, temporal fossae; 6, frontals; 7, ethmoidal fenestrae; 8, orbits; 9, frontals; 10, premaxillae; 11, teeth; 12, limbs; 13, body size; 14, sexual dimorphism.

an isolated horn-core from the middle Villafranchian of Senèze (France), where also the larger *L. etruscus* is recorded. Isolated remains from the late Villafranchian of Italy are also referred to *L. furtivus* (Masini, 1989; Duvernois, 1990). An incomplete cranium and some postcranials from Piana del Cavaliere (Italy) may be attributed to the same or a similar species (*L. aff. furtivus* in Masini, 1989; Gentili and Masini, 2005; Fabbi et al., 2021). In spite of the above records, *L. furtivus* remains a little-known species and conclusions on its own validity can only be granted by future discoveries (Cherin et al., 2019).

The second group of species (gr. LEV in this manuscript) includes *L. etruscus*, *L. vallisarni*, and the poorly-known *L. bravardi*. *Leptobos etruscus* (Fig. 13e) - erected by Falconer (1868) based on the rich

collection from the Upper Valdarno - is the best-known species of the genus, occurring in most Europe during the first stages of the late Villafranchian. Fossils of *L. etruscus* have been found in several sites of Spain, France, Italy, Greece, Romania, and possibly the United Kingdom (Merla, 1949; Masini, 1989; Duvernois, 1990; Garrido, 2008; Breda et al., 2010; Croitor and Popescu, 2011; Kostopoulos, 2022 and references therein). This species has been considered closely related with *L. vallisarni* based on numerous craniodental similarities (Masini, 1989), to the point that Duvernois (1990) interpreted *L. vallisarni* as a junior synonym of *L. etruscus*. *Leptobos vallisarni* (Fig. 13f) - described by Merla (1949) based on a partial cranium from the late Villafranchian of the Upper Valdarno - is characterized by some apomorphic cranial features shared with

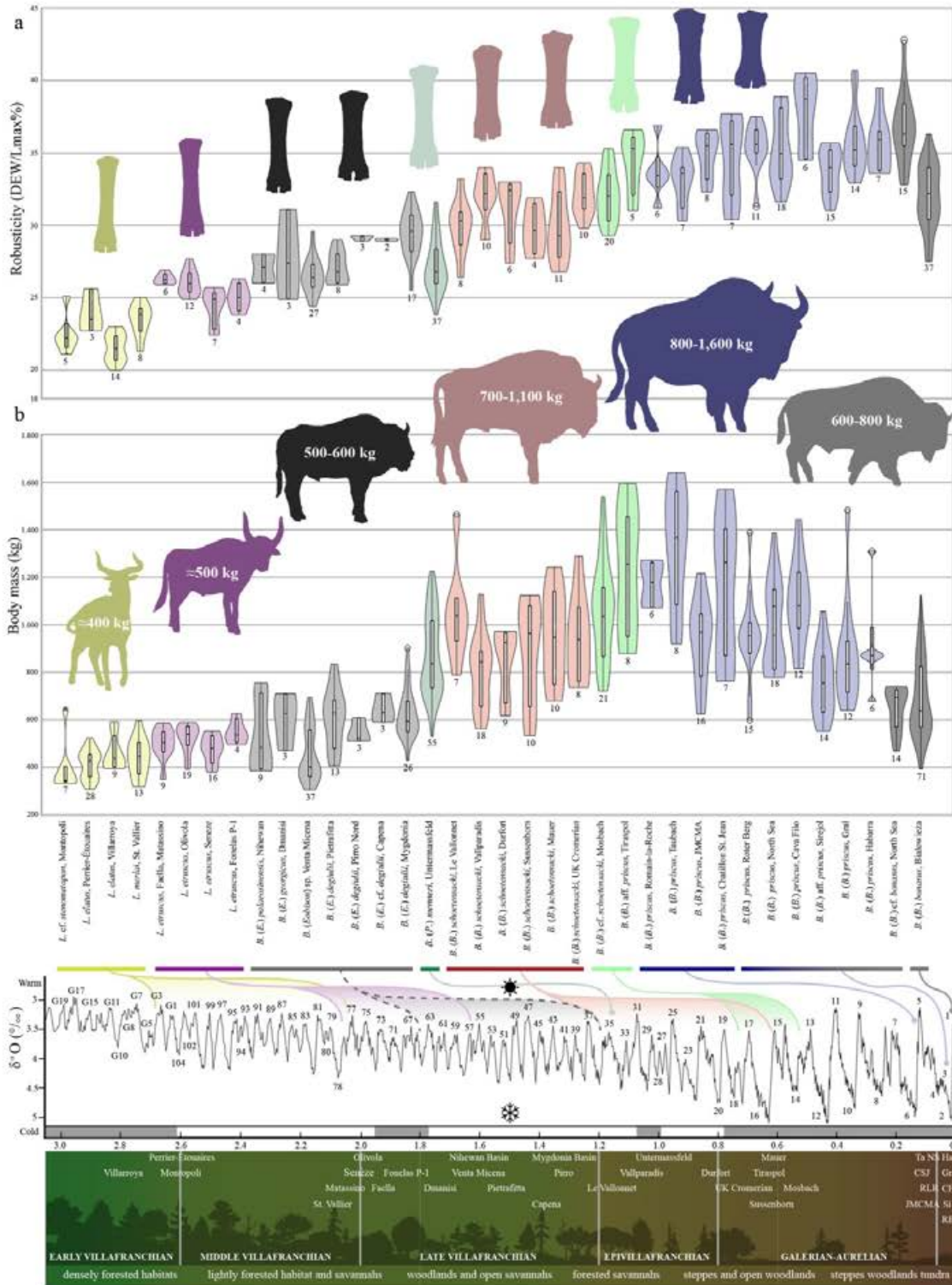


Fig. 12. Evolutionary trends in *Leptobos* and *Bison* over the last 3 Ma, a, Stoutness violin plot of metacarpals; b, Body mass estimation violin plot. The numbers at the base of the plots indicate the number of specimens for each sample. At the bottom, the age of the samples is shown on a chronological and paleoclimatological diagram of LR04 Benthic Stack (Lisiecki and Raymo, 2005); each paleontological locality is associated with the predominant paleoenvironment in Western Palearctic in the considered timespan. European Land Mammal Ages are indicated at the bottom. Abbreviations: Ta, Taubach; CSJ, Chatillon St. Jean; RLR, Romain-la-Roche; JMCMA, Joint Mitnor Cave Mammal Assemblage sites; Ha, Habarra; Gr, Gral; CF, Cava Filo; Si, Sirejol; RB, Roter Berg.

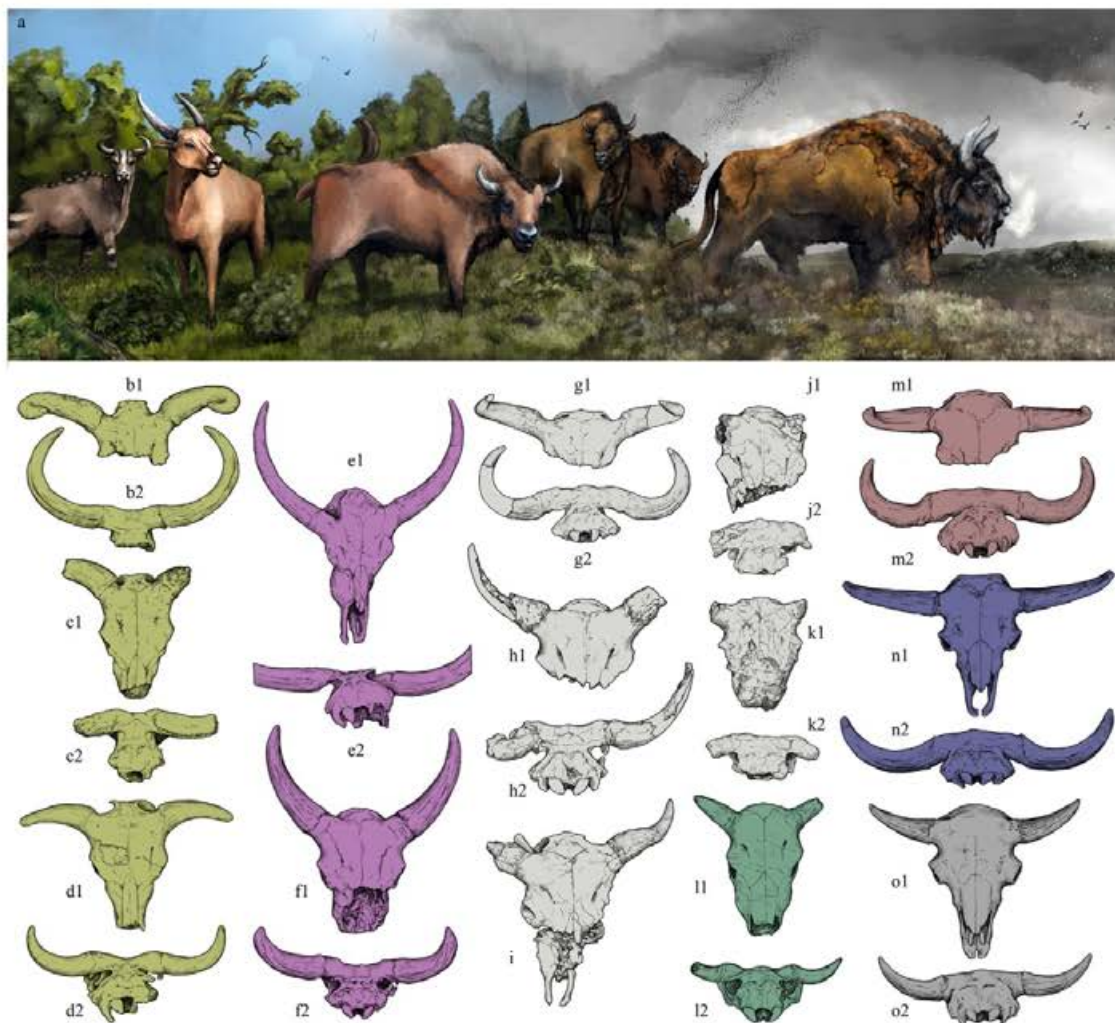


Fig. 13. Comparisons of Bovinae considered in this review. a, Life reconstructions of *Leptobos* and *Bison* species from the Late Pliocene (left) to Late Pleistocene (right). From left to right: *Leptobos* gr. LSEM, *Leptobos* gr. LEV, *Bison* (*Eobison*) *degiulii*, *Bison* (*Poephagus*) *menneri*, *Bison* (*Bison*) *schoetensacki*, *Bison* (*Bison*) *priscus*. b–o, Morphological comparison between crania of several species of Bovinae mentioned in this work: b, *L. stenometopon* from Dusino in dorsal (b1) and posterior (b2) views; c, *L. merlai* from St. Vallier in dorsal (c1) and posterior (c2) views; d, *A. cantabilis* from Kushkuna in dorsal (d1) and posterior (d2) views; e, *L. etruscus* from Upper Valdarno in dorsal (e1) and posterior (e2) views; f, *L. vallisarni* from Le Fratte (Upper Valdarno) in dorsal (f1) and posterior (f2) views; g, *B. (E.) palaeosinensis* from Nihowan in dorsal (g1) and posterior (g2) views; h, *B. (E.) georgicus* from Dmanisi in dorsal (h1) and posterior (h2) views; i, *B. (E.) degiulii* from Pietrafitta in dorsal view; j, *B. (E.) degiulii* from Pirro Nord in dorsal (j1) and posterior (j2) views; k, *B. (E.) degiulii* from Kalamoto-2 in dorsal (k1) and posterior (k2) views; l, *B. (P.) menneri* from Untermassfeld in dorsal (l1) and posterior (l2) views; m, *B. (B.) schoetensacki* from Mauer in dorsal (m1) and posterior (m2) views; n, *B. (B.) priscus* from Po River in dorsal (n1) and posterior (n2) views; o, *B. (B.) bonasus* from Białowieża in dorsal (o1) and posterior (o2) views. Specimens not in scale. Artworks by LS.

the earliest bison. Unfortunately, very little is known on the postcranial anatomy of *L. vallisarni* due to absence of sites where associated cranial and postcranial remains were found. Several isolated metapodials from central Italy were tentatively referred to this species by Masini (1989); however, due to the unclear stratigraphic context (e.g., Upper Valdarno indeterminate localities) and their affinities with the roughly coeval *L. etruscus* and *Eobison* spp., we advocate a prudent approach to their attribution. Two almost complete skulls from the Gonghe Basin (China) were attributed to *L. vallisarni* (Zheng et al., 1985), unfortunately not associated with postcranial bones, again. *Leptobos bravardi* is a mid to large-sized species described by Duvernois (1990) from Perrier-Les Étouaires, where also *L. elatus* is reported. The same author referred to this species also some of the remains from Villarroya (Spain), where, again, the co-occurrence of *L. elatus* is hypothesized. The validity of *L. bravardi* has been questioned by Rodrigo (2011) who attributed

the variability recognized in the Spanish and French samples to sexual dimorphism. The fragmented neurocranium of *L. bravardi* from Perrier-Les Étouaires (Duvernois, 1990) was referred to *L. elatus* by Masini (1989).

5.2. *Leptobos*: comments on the European taxa

The crania of LSEM are easily distinguishable from those of LEV and *Bison* s.l. thanks to the peculiar morphology of the cornual and postcornual areas (Fig. 11a). The double curvature of the horns (anteroposterior and dorsoventral) differentiates these species from *L. etruscus* and *L. vallisarni*. The large size and slenderness of the horns distinguish them from primitive bison, whereas the dorsoventrally compression of the core bases (Fig. 6a) and the strong core curvature distinguish them from *Bison* s.s. The divergence angle between the horn-core axis and the sagittal axis is

higher in LSEM than in LEV and fits with the variability of *Bison* s.l. (Fig. 6b). The temporal fossae of LSEM are wide and deep, especially in the posterior portion, causing a constriction of the dorsal part in the occipital squama (Fig. 11a). In addition, the ventral portion of the latter is wider due to massive mastoid processes, resulting in a bell shape of the squama itself (Cherin et al., 2019). These *Leptobos* species, due to the posterior elongation of the temporal fossae, display a distinctly high and narrow intertemporal bridge, which clearly separates the nuchal crest from the frontals (Fig. 11a). This feature, as mentioned above, tends to be reduced as a consequence of the progressive shortening of the postcranial portion of the neurocranium in the evolution of *Leptobos* and *Bison*, and disappears in the most derived forms fusing with the nuchal crest (Fig. 7a). LSEM is also distinguished by markedly narrow and elongated frontals (Fig. 7b). Our analyses point out that, on the whole, the cranial morphology of *L. stenometopon*, *L. elatus*, and *L. merlai* is similar to a degree that makes it difficult their distinction at species rank (see PCA in Fig. 7d). The horn-core morphology is very useful also for the taxonomic recognition of LEV. In these species, the horn-core base section is almost perfectly circular (Fig. 6a), and the horn-cores emerge in a more posterior direction than the other bovines considered thus the angle between the middle line of the horn and the sagittal plane is quite reduced (Fig. 6b). Moreover, the horn-cores are characterized by simple curvature describing a half-moon shape and lie parallel to the frontal plane, clearly different from both LSEM and *Bison* s.l. (Fig. 11b). In addition, in LEV the intertemporal bridge is much lower and wider than in LSEM; this character is quite evident in *L. vallisarni*, in which the shape of the intertemporal bridge is similar to what is observed in early *Bison* (Fig. 7a). The occipital squama of LEV is semicircular due to the increasing distance between the posterior edges of the temporal fossae and the shortening of the intertemporal bridge (Fig. 11b). Finally, there is a trend in the widening of the frontals and a general increase of stoutness and size of the cranium from LSEM to LEV as shown by our biometric data and analyses (Figs. 7 and 11; Table 5). Other cranial characters (apart from the teeth) are similar between the two *Leptobos* groups (e.g., presence of ethmoidal fenestrae, premaxillae in touch with the nasals, absence of horns in females). The teeth of *Leptobos* are characterized by strong polymorphism, and a relative homogeneity in size (Fig. 7c). Nonetheless, some characters can be useful to discriminate the two groups, given that sufficiently large samples are available. These characters include the hypsodonty degree, molarization of P4, amount of enamel folds in the central cavities, and cement abundance (see Duvernois, 1990; Cherin et al., 2019).

The postcranials of LSEM show small size and overall light built compared with those of LEV and *Bison* s.l. Body mass estimations based on metacarpals give an average value slightly higher than 400 kg for LSEM, that is, the smallest in the studied sample (Fig. 12b). In our analyses, the metapodials and radii are characterized by narrow epiphyses and relatively elongated and slender diaphysis (Figs. 8 and 9; Table 6; Table S12). Comparing the lengths of different long bones, it emerges that the radius is relatively shorter than the metacarpal, while the latter is relatively longer than the metatarsal (Fig. 9c). The humeri, astragali, and calcanei are among the slenderest of all the studied records (Tables S10, S23, S25). Again, the samples referred to gr. LSEM do not present clear-cut biometric differences in the postcranials, except for the metacarpal sample from Saint Vallier (*L. merlai*), which appears slightly stouter than the others (Fig. 8a). The homogeneity in long bone size and proportions between *L. stenometopon*, *L. elatus*, and *L. merlai* might suggest that they actually represent a single species. From this perspective, the small differences in stoutness between the various records might be correlative with local

ecomorphotypes rather than interspecific variation.

On the contrary, LEV features larger and stouter bodies compared with early *Leptobos*, and more similar to *Eobison* (Tables S10, S12, S17, S19, S21, S23, S25, S26). The average body mass of LEV is about 500 kg (Fig. 12b). The radius is characterized by gracile structure and small size (Fig. 8c). The metacarpals are long and slender, but still stouter than those of LSEM (Figs. 8a, 9a and 11a). Nonetheless, the low mean value for the length ratio RAD/MC% indicates that the radii are relatively shorter than the forelimb, i.e., the same as in LSEM (Fig. 9c). The low values of the ratio MT/MC% clearly separate *L. etruscus* from *Bison* s.l. (Fig. 9c). The astragali are small compared with those of *Bison* s.l. and overlap in size those of LSEM (Fig. 8d). The lack of postcranial material undoubtedly referable to *L. vallisarni* makes difficult the comparison between this species and its relatives. In fact, our biometric analyses of metapodials show a significant overlapping of the remains putatively attributed to *L. vallisarni* and those of earliest *Bison*. This issue suggests that isolated bones might have been misinterpreted and their attributions must be taken cautiously (e.g., sample from Le Ville in the Upper Valdarno, which probably belongs to a primitive form of bison).

5.3. *Eobison* and other "transitional" forms: state of the art

Several species have been included into *Eobison* since the establishment of this subgenus by Flerov (1972). Unfortunately, over the decades, *Eobison* has become a wastebasket taxon for all bison-like bovid remains found in the Eurasian Villafranchian, hampering its clear definition. The diagnosis provided by Flerov (1979) is rather insufficient, also due to the scarce fossil record available at that time. For this reason, we propose the emended diagnosis of the subgenus in Section 4 and a resume of its main features compared with its closest relatives (Table 7; Fig. 11c).

Up to date, the oldest bison fossils belong to *B. (E.) sivalensis*. This species was erected by Lydekker (1878) on the basis of a partial skull from the Upper Siwaliks (Pakistan); later, Pilgrim (1939) published the diagnosis based on the same cranial material. Since then, few more cranial elements from the Indian Plio-Pleistocene were tentatively attributed to *B. sivalensis*, all chronologically constrained between 3.3 and 2.6 Ma, making thus, this species the first representative of the *Bison* s.l. clade (Khan et al., 2010, 2011). In spite of that, since the holotype skull has apparently been lost (Olsen, 1990) and additional material is too fragmentary for clear attributions, there are no remains that can undoubtedly represent *B. (E.) sivalensis*. Olsen (1990) and Bukhsianidze (2020) even questioned referral of the type material to the genus *Bison* based on a number of morphological characters.

Bison (E.) palaeosinensis (Fig. 13g) is a small-sized primitive bison occurring in China shortly after *B. (E.) sivalensis*. The taxonomic status of this species has been debated for a long time. *Bison (E.) palaeosinensis* was erected by Teilhard de Chardin and Piveteau (1930) on the basis of three partial skulls - a male (cranium A), a female (cranium B), and a third without sex attribution - and some limb bones from the Nihowan (=Nihewan) Basin. The authors described the characters of this species as "intermediate" between *Leptobos* and *Bison*, sharing more similarities with the latter. Two other incomplete skulls from Yushe and Jinyuan cave in Dalian were referred to this taxon (Teilhard de Chardin and Trassaert, 1938; Jin et al., 2021). Skinner and Kaisen (1947) designated the cranium A as lectotype, evidencing the similarities between cranium B and the holotype of *B. (E.) sivalensis*, thus not excluding a synonymy between the two species. McDonald (1981) attributed the cranium A to *B. priscus* and the cranium B to *B. (E.) sivalensis*, hence invalidating the species. Tong et al. (2016) redefined the taxon and described a large number of dentognathic and postcranial remains

Table 7
Summary list of morphological characters that define the four main groups of *Leptobos* and *Bison* studied in this work.

	<i>Leptobos</i> gr. LSEM	<i>Leptobos</i> gr. LEV	<i>Bison</i> (<i>Eobison</i>)	<i>Bison</i> (<i>Bison</i>)
1. Horn-core shape	Long with double bending and strong torsion. Markedly compressed dorsoventrally at the base.	Long with single bending and feeble torsion. Circular section at the base.	Short and stout with double bending and feeble torsion. Dorsoventrally compressed at the base.	From short and stout to very long. Single or double bending with feeble torsion. Circular to dorsoventrally compressed at the base.
2. Horn-core position	Emerging more laterally than posteriorly (i.e., forming a wide angle with the sagittal axis). Pedicle long.	Emerging more posteriorly than laterally (i.e., forming a small angle with the sagittal axis). Pedicle long.	Emerging more laterally than posteriorly (i.e., forming a wide angle with the sagittal axis). Pedicle long to short.	Emerging laterally (i.e., forming a very wide angle with the sagittal axis). Pedicle short.
3. Occipital squama	Small. Bell shaped, wide base and narrow top.	Trapezoidal to semicircular shaped, wide base and narrow top.	Trapezoidal to bell shaped, wide base and narrow top.	Trapezoidal to square shaped, wide base and top. Dorsoventrally compressed.
4. Intertemporal bridge	Well developed. High and narrow.	Poorly developed. Short and wide.	Poorly developed to absent.	Absent.
5. Temporal fossae	High, developing posteriorly. The distance between the two posterior ends is short.	High, developing posteriorly. The distance between the two posterior ends is relatively short.	Relatively low, developing posteriorly. The distance between the two posterior ends is relatively long.	High, developing posteriorly. The distance between the two posterior ends is very long.
6. Frontals	Relatively small, long and narrow. Concave, poorly pneumatized at the horn-core bases.	Relatively large, long and narrow. Concave, poorly pneumatized at the horn-core bases.	Relatively large, short and wide. Concave to slightly convex, poorly pneumatized at the horn-core bases.	Large, very short and wide. Concave to convex, strongly pneumatized at the horn-core bases.
7. Ethmoidal fenestrae	Present.	Present.	Absent.	Absent.
8. Orbits	Not tubular nor protruding.	Slightly protruding, not tubular.	Protruding and slightly tubular.	Extremely protruding and tubular.
9. Nasals	Ending anteriorly to the anterior margin of the orbits.	Ending anteriorly to the anterior margin of the orbits.	Ending at the anterior margin of the orbits or slightly posteriorly.	Ending posteriorly the anterior margin of the orbits.
10. Premaxillae	In contact with the nasals.	In contact with the nasals.	Not in contact with the nasals.	Not in contact with the nasals.
11. Teeth	Low degree of hypsodonty.	Medium degree of hypsodonty.	Medium degree of hypsodonty.	High degree of hypsodonty.
12. Limbs	Very slender. Radius short. Metatarsals slightly longer than metacarpals.	Slender. Radius relatively short. Metatarsals slightly longer than metacarpals.	Relatively robust. Radius relatively short. Metatarsals relatively longer than metacarpals.	Relatively to extremely robust. Radius long. Metatarsals from relatively to extremely longer than metacarpals.
13. Body size	Small.	Medium.	Medium to large.	Large to very large.
14. Sexual dimorphism	Female hornless. Size difference between male and females reduced.	Female hornless. Size difference between males and females reduced.	Female horned. Size difference between male and females accentuated.	Female horned. Size difference between male and females extremely accentuated.

from the site of Shanshenmiaozui in the Nihowan Basin. These authors also remarked that the cranium B shared some important similarities with *Leptobos*. Up to date, this taxon represents the best-known species of *Eobison* in Asia.

Bison (*E.*) *georgicus* (Fig. 13h) is a mid-sized, primitive species, originally defined by Burchak-Abramovich and Vekua, 1994 as *Dmanisibos georgicus*, based on material (including a fragmented and reconstructed cranium) from the renowned late Villafranchian site of Dmanisi. Bukhsianidze (2005) revised the material and included it into *Bison* (*Eobison*). The limb bone sample (in particular metapodials) is heterogeneous, showing the presence of two different morphotypes, possibly referable to another taxon, suggesting that *Eobison* from Dmanisi could have been sympatric with a more primitive bovid, possibly *Leptobos*, as hypothesized in other regions of Eurasia (Tong et al., 2016; Kostopoulos et al., 2018; Sorbelli et al., 2021a).

Bison (*E.*) *degiulii* (Fig. 13i, j, k) is, up to date, the best-known species of early *Bison*. It was described informally by Masini (1989) in his PhD dissertation and, later, validated by Masini et al. (2013), based on material from Pirro Nord (latest Villafranchian). The holotype is a partial cranium, associated with several post-cranials. An almost complete skeleton from Capena was also referred to this species (Masini, 1989; Masini et al., 2013). Masini (1989) and Sorbelli et al. (2021a) attributed several large bovid remains from Sainzelles (France) to *Eobison* cf. *degiulii*. Kostopoulos et al. (2018) described the rich record from Mygdonia as *B.* (*Bison*) cf. *degiulii*, choosing the open nomenclature due to the lack of clear-cut diagnostic characters in this Greek sample, which seems to display a large number of derived features. The authors, indeed, stressed that the morphological features of this species can be

considered closer to *B.* (*Bison*) than to *B.* (*Eobison*), in agreement with Bukhsianidze (2005), referring this species to the former subgenus. The timespan covered by the aforementioned sites is comprised between 1.7 and 1.2 Ma, thus suggesting that primitive bison, at least in the Mediterranean area, survived until the beginning of the Epivillafranchian and, potentially, co-existed with the larger and more derivate "priscoid" forms of *Bison* s.s., such as *B.* (*B.*) *schoetensacki*, whose first occurrence is at ca. 1.2 Ma (Kostopoulos et al., 2018; Sorbelli et al., 2021a).

Bison (*E.*) *tamanensis* was first mentioned, without a diagnosis, by Verestchagin (1959) on scanty cranial material from Tzimbali in the Taman Peninsula (Russia). Later on, the species was validated as member of *Eobison* by Flerov (1979) who gave a diagnosis and designated a lectotype (a partial calvarium). In more recent years, a better-preserved skull was found in Semibalki (Taman Peninsula) and attributed to *B.* cf. *tamanensis* (Baigusheva, 2000). Isolated metapodials and a fragment of horn-core from the three Ukrainian sites of Kairy, Chortkiv, and Cherevychnyy were also referred to this species (David and Svistun, 1981). At present, our knowledge of *B.* (*E.*) *tamanensis* is poor and the taxonomic validity of this species is still discussed (*species inquirenda* in Kostopoulos et al., 2018).

The species *Eobison suchovi* was erected by Alekseeva (1967) based on a single horn-core and few postcranial bones from Dolinskoye (Ukraine). Due to the quite scanty record, the taxonomic validity of this species has been questioned and it has been often synonymized with *B. tamanensis* (Flerov, 1975; Gromov and Baranova, 1981; Croitor, 2016).

Adjiderebos cantabilis (Fig. 13d) was described by Dubrovo and Burchak-Abramovich (1984) on the basis of a nearly complete skull from the middle-late Villafranchian of Kushkuna (Azerbaijan);

Bukhsianidze and Koiava, 2018; Krijgsman et al., 2019). Bukhsianidze (2005) suggested that this species might belong to an early form of *Eobison*. No postcranials are known to date. From older layers of the same locality, scanty remains of another bovid were described by Burchak-Abramovich et al. (1980) and referred to *Protobison kushkunensis*. This latter taxon, dated to the late early Villafranchian, could be the first “bisontine” form outside Asia (Bukhsianidze and Koiava, 2018). The type material of this species although poorly preserved, share some plesiomorphic characters with LSEM (Bukhsianidze, 2005).

Probison dehmi is a small bovid from the Tatrot of the Upper Siwaliks (Pakistan) described by Shani and Khan (1968). The holotype is a badly preserved partial cranium with one horn-core, showing common traits with the Asian *Leptobos falconeri* and *B. (E.) sivalensis* (Shani and Khan, 1968; Khan et al., 2010).

Over the decades, several other samples of bison-like bovids were described from late Villafranchian sites of Europe and referred to as “early *Bison*” or “*Eobison*”, but without a specific attribution. The largest of these samples is from Venta Micena. This site, dated between 1.6 and 1.5 Ma (Palmqvist et al., 2022), yielded a large number of bovid taxa (Moyà Solà, 1987). This last author recognized, in the larger-sized form, some bison-like characters and attributed the remains to *Bison* sp. Later on, the study of a partial juvenile calvarium confirmed that a relatively small and primitive bison was present in Venta Micena during the late Villafranchian (Martínez-Navarro et al., 2011). The postcranial bones from the site are slightly stouter compared with those of *Leptobos* but shorter and more gracile than those of *Bison* s.s., resembling those of *Eobison* although characterized by relatively smaller size (Masini, 1989; Sorbelli et al., 2021a).

A well-preserved neurocranium with both horn-cores from Salita di Oriolo (Italy) was referred to *Bison (Eobison) sp.* by Toniato et al. (2017) due to primitive characters in the occipital and temporal. To *Bison (Eobison) sp.* were attributed other scanty records from the Italian Peninsula, including an isolated horn-core from Mugello and few postcranial bones from Cava Redicicoli (Italy) (Masini, 1989; Caloi and Palombo, 1995). Cregut-Bonnoure and Dimitrijevic (2006) referred to an undefined primitive bison several fragmentary remains from the lower layers of Trlica cave (Montenegro). A skull fragment from the Early Pleistocene of Maar du Riege (France) may belong to the same group (Ambert et al., 1996). Finally, from the late Villafranchian site of Taurida cave (Crimea, Ukraine), the putative co-occurrence of *Leptobos* and *Eobison* is reported (Lopatin et al., 2019), but no further information of the fossils is available. Due to the scarcity of data, the last three records are not further discussed and were not included in our comparisons.

5.4. *Eobison* and other “transitional” forms: comments

5.4.1. Dmanisi

The Dmanisi bovid has been considered the first bison reaching Europe in the first part of the late Villafranchian. The few remains attributed to *B. (E.) georgicus* include a neurocranium and some postcranials, although more elements are pending to be published (Bukhsianidze, 2020). The neurocranium (GNM D354) is broken at the level of the orbits, posteriorly to the nasals. The occipital and basioccipital regions are well preserved on the whole. The right horn-core and the base of the left are present, although the reconstruction of their original orientation is not trustworthy (Bukhsianidze, pers. comm.). In agreement with Bukhsianidze (2005), the neurocranium from Dmanisi shows many features supporting its attribution to *Eobison*, including: trapezoidal occipital squama, high temporal fossae strongly indenting within the postcornual area, weakly tubular orbits, arched nuchal crest in

dorsal view, long pedicles and posterolaterally directed horns (angle of 55° with the sagittal axis). Our biometric comparisons of cranial districts reveal that the Dmanisi bovid is well-fitting with the variability of *Bison* s.l., and in particular with the most primitive forms (Figs. 7 and 8). The postcranial elements evidence a certain heterogeneity, which might suggest the presence of two different taxa in Dmanisi (Kostopoulos et al., 2018; Sorbelli et al., 2021a), as advocated in Taurida cave (Lopatin et al., 2019) and Tsiotra Vryssi (Kostopoulos et al., 2018). The three most complete metacarpals from Dmanisi have been re-measured and the analyses show that two of them (GNMD2812 and GNM D3426) have proportions compatible with *Eobison* and one (GNM D2288) features slenderer proportions, fitting with the variability of the largest *Leptobos* (Fig. 8a). The two complete radii from Dmanisi (GNM D2165 and GNM D2962) have short and stout appearance, recalling robust forms of *Eobison* and differing from the smaller radii of *Leptobos* spp. and Venta Micena *Bison* (Fig. 8d). In our opinion, on the basis of their proportions at least the two stouter metacarpals and the radii can be confidently referred to *Eobison* and not to *Leptobos*. The same goes for the cranium GNM D354, which shows *Eobison* features. The more pronounced concavity of the forehead and the stronger constriction of the upper occipital squama, are traits that distinguish the Dmanisi specimen from the younger remains of *B. (E.) degiulii* from Pirro Nord and Kalamoto (Figs. 6, 7 and 11; Table 5). However, as far as our current knowledge is concerned, it is not possible to attest if these differences can be due to inter or intra-specific variability (e.g., sexual dimorphism, which we know to play an important role in determining the cranial morphology in bison). Pending new discoveries, we consider *B. (E.) georgicus* as a distinct taxon. Although we cannot exclude the presence of both *Leptobos* and *Eobison* in Dmanisi, new fossils and more evidence are needed to attest the coexistence of these two genera in the Georgian site. It is worth remembering that, in southwestern Europe, in the interval corresponding to the age of the Dmanisi assemblage (ca. 1.8 Ma; early late Villafranchian), *Leptobos* was the only bovine present. It will be replaced by *Eobison* only after ca. 1.6 Ma (latest Villafranchian).

5.4.2. Venta Micena

Venta Micena yielded one of the richest records of late Villafranchian *Bison*. Our analyses of metapodials show that this bovine was relatively small and had quite short metacarpals (few specimens exceed 230 mm in length) and elongated metatarsals (most of the specimens exceed 260 mm in length), which is a common feature of *Bison* species (Fig. 8a). The robusticity biplots and PCAs show that the metapodial record from Venta Micena falls within the variability of *Eobison*, mostly in the area occupied by the smallest and slenderest specimens. As stated by other authors (Moyà-Solà, 1987; Palmqvist et al., 2022), the wide biometric variability of the sample is the result of marked sexual dimorphism (Sorbelli et al., 2021a). The overall small size of the specimens from Venta Micena (estimated average body mass of 440 kg; Fig. 12b) might be related to the fact that most fossils are part of a biogenic concentration interpreted as a *Pachyrocota brevisrostris* den (Arribas and Palmqvist, 1998; Palmqvist et al., 2022). It has been hypothesized that this fossil assemblage is strongly biased in favour of females and young individuals, characterized by small sizes and, thus, more commonly hunted by predators like hyaenas (Arribas and Palmqvist, 1998). On the other hand, the three complete radii from the site display oddly primitive proportions with reduced lengths (Figs. 8d and 9c); indeed, the value for RAD/MC% is similar to those found in *Leptobos*. Nonetheless, the lack of an abundant sample of complete radii might affect these results, as does the aforementioned sex ratio bias in metacarpals. The juvenile cranium of *Bison* sp. MAEGR VM 8000 described by Martínez-Navarro et al.

(2011) is strongly damaged and quite uninformative. Even so, the estimated diameters of the horn-core bases are within the variability of *Eobison* (Fig. 6a). Its reduced size is most probably due to the early ontogenetic stage. Waiting for a comprehensive reappraisal of the Venta Micena sample, we agree with previous scholars in referring it to the subgenus *Eobison* without further conclusions on its specific attribution. The possible co-occurrence between *Leptobos* and *Bison* in Venta Micena (Sorbelli et al., 2021a) might be suggested by the presence of two metacarpals and one metatarsal with a slightly elongated morphology, fitting with the variability of gr. LEV. However, in both biplots and PCAs, the larger *Leptobos* and *Eobison* are similar to each other, making it difficult to differentiate them in the overlapping areas (Fig. 8a-b, 9a-b).

5.4.3. Pirro Nord and Mygdonia Basin

The vertebrate assemblage from the karstic site of Pirro Nord is dated, on a biochronological basis, to 1.6–1.3 Ma, although some authors lean towards the upper part of this interval (ca. 1.4–1.3 Ma; Arzarello et al., 2015 and references within). The holotype of *B. (E.) degiulii* (IGPB s.n., temporarily hosted in DST), a partial cranium of an elder individual, is broken just anteriorly to the orbits. Only horn-core pedicles are partially preserved. It clearly shows bison-like features such as enlarged occipital, laterally placed horn-cores, and protruding orbits. In the first descriptions by De Giuli et al., 1986 and Masini (1989), the authors emphasized the primitive aspect of the cranium, fitting with the original definition of *Eobison* by Flerov (1979). On the contrary, Bukhsianidze (2005) and Kostopoulos et al. (2018) suggested that the Pirro Nord bovine already shows a derived morphology, referable to “true” *Bison*. In fact, the deep and narrow temporal fossae and doomed frontals are apomorphic characters observed in the Pirro Nord cranium. Nonetheless, the section of the horn-core base and shape of the occipital squama, the size of the teeth, and the proportions of the limb bones are still primitive (Figs. 10 and 12; Table 5). The intertemporal bridge biplot (Fig. 7a) shows that the Pirro Nord specimen exhibits a marked dorsal constriction of the occipital squama, resembling the *Eobison* remains from Dmanisi and Pietrafitta and *L. vallisarni* from the Upper Valdarno. The biplots on frontal and horn-core dimensions highlight the same similarities (Figs. 7 and 8). Teeth from Pirro Nord are characterized by quite small size (Fig. 7c). Their morphology is variable, as already mentioned by Masini (1989). The Pirro Nord bovine displays, on average, more robust metacarpals than the slightly older primitive bison from the Iberian and Italian Peninsulas (Figs. 8a and 11a). The metatarsals, on the contrary, are less stout and fit better with the smaller specimens of *Eobison* (Fig. 8b). These discrepancies in metapodial proportions, however, might be caused by the strong sexual dimorphism of these bovids, thus to a possible sex bias in the Pirro Nord record. The length ratio between metatarsal and metacarpal points out that the former is less than 15% longer than the latter, fitting with the variability of *Eobison* and some *Bison* s.s. species (Fig. 9c). Taking into consideration that the younger age estimations for the Pirro Nord assemblage are around 1.3 Ma, it is possible that this record represents one of the last and most derived forms of *Eobison*, roughly coeval with the stout *B. (E.) cf. degiulii* from Apollonia. The latter locality lies in the Mygdonia Basin as well as the sites of Tsiotra Vryssi, Krimni, and Kalamoto-2, with an overall age spanning from 1.78 to 1.2 Ma (Kostopoulos et al., 2018; Konidaris et al., 2021). Among the most interesting remains of *B. (E.) cf. degiulii* from this area, a fragmentary cranium and several complete limb bones including metapodials and radii stand out. The cranium (NHCK KLT-638; Fig. 10f) from Kalamoto-2, lacks the horn-cores and most of the splanchnocranium, being broken at the level of the P3. Most of its features, including the morphology of the orbits, occipital, and

frontals, are similar to those of the holotype of *B. (E.) degiulii* from Pirro Nord (Kostopoulos et al., 2018). The horn-core bases from Mygdonia sites are among the smallest and dorsoventrally compressed among those examined, fitting with other *Eobison* samples and with *B. menneri* (Fig. 6a). The intertemporal bridge is not preserved; however, the occipital squama shows a constriction in its upper section due to the posterior elongation of the temporal fossae, as in all *Eobison*. The robusticity biplot performed on the metapodials shows that, compared with the other records of *Eobison*, the Mygdonia sample (especially the Apollonia specimens), is characterized by marked stoutness, which causes a partial overlap with the records of *B. schoetensacki* (Fig. 8a). In spite of that, PCAs confirm that the Mygdonia bovine clearly falls within the variability of early bison (Fig. 9a). In the metrical analysis, the four complete radii from Apollonia fall at the upper limit of the *Eobison* range, reinforcing the idea that this record can be referred to a short-legged, but still relatively slender form of *Bison*, different from the larger and stouter *B. schoetensacki* and *B. priscus* from the Epivillafranchian onwards. This is also supported by length ratios between metacarpals, metatarsals, and radii (Fig. 9c; Table 6; Tables S12 and S26).

In sum, the records of *B. (E.) degiulii* from Pirro Nord and the Mygdonia Basin clearly represent a derived stage of this group, marked by a greater expression of bisontine characters and larger body size (i.e., estimated body mass of ca. 600 kg, on average; Fig. 12b). In particular, the metacarpals from Apollonia (ca. 1.2 Ma) are the most robust among all primitive bison, setting a turning point, at the late Villafranchian-Epivillafranchian transition, towards increased forelimb stoutness. This might be related to an aridification of the habitat, already inferred for the locality (Maniakas and Kostopoulos, 2017; Kostopoulos et al., 2018). Based on our review, we agree with Bukhsianidze (2005) and Kostopoulos et al. (2018) that *B. (E.) degiulii* is not completely fitting with the original diagnosis of *Eobison* by Flerov (1979). However, we have provided compelling evidence that this species is markedly different from *Bison* s.s. and conforms to our emended diagnosis of the subgenus.

5.4.4. Capena, Salita di Oriolo, and other Italian sites

The bovid skeleton (MUST (ex MPUR) s.n.) recovered from Capena (late Early Pleistocene) in 1970, has been recently restored allowing its study in this paper (Fig. 10d1-3). Masini (1989), in his preliminary description of the material, recognized clear bisontine features and attributes this specimen to the newly erected species *B. (E.) degiulii* due to some primitive traits of the appendicular skeleton. The skeleton is almost complete and in good state of preservation, although the skull is severely cracked and deformed. In spite of that, the horn-cores are almost intact; they are large-sized and emerge laterally, dorsoventrally flattened at the base, and with single curvature (directed downward at the base then upward at the tips). The biplot in Fig. 6a shows that this specimen has the most compressed and large horns in the *Eobison* group (although dorsoventral compression might be slightly exaggerated by taphonomic deformation). The postcornual portion is shortened and the occipital region is wide and flattened (Fig. 10d2). The left premaxilla is partially intact, and its posterior margin does not reach the nasal; the latter has a bifid anterior edge (Fig. 10d1). The rest of the cranium is severely damaged thus providing poor information. Teeth do not differ significantly from those of other bovids. The bubaline fold is present in all upper molars, which present faint constriction of the lingual lobes. The cement is abundant, especially on the labial side, concentrated in the recess between the protocone and metacone. The entostyle of the upper molars has a relatively simple outline. The p4 is characterized by a large and cylindrical metaconid. In the Log₁₀ diagrams, dental

dimensions follow the general trend of *Eobison*. Based on the size of the appendicular skeleton, the Capena bovine stands out for being particularly large (estimated body mass of about 600 kg; Fig. 12b). The metapodials and radii are among the stoutest and largest in *Eobison*, always placed in the upper range of variability of this group in both biplots and PCAs, very close to *Bison* s.s. (Figs. 8 and 9). Moreover, the metatarsal and radius are elongated with respect to the metacarpal, recalling the typical condition of more derived species of *Bison*. Consequently, the size and proportions of this skeleton may lead to the question of whether it belongs to a relatively large and derived species of *Eobison*, such as the specimens from Pirro Nord and Apollonia, or to a small-sized form of true *Bison* (e.g., female of *B. schoetensacki*). The lack of any other fossil from Capena does not help dispel this doubt. Even if we are more inclined to agree with Masini (1989) and Masini et al. (2013) in referring this specimen to *B. (E.) degiulii*, here we prefer cautiously to use the open nomenclature *B. (E.) cf. degiulii*.

The calvarium of *Eobison* (MCSNF s.n.) from the "Sabbie Gialle" formation of Salita di Oriolo (Fig. 10c), dated to the late Early Pleistocene (Toniato et al., 2017), was found associated with a fragment of mandible, some upper teeth, and a cervical vertebra. The fossil is strongly weathered but not fractured or deformed except for the left jugular process and some portions of the occipital which are missing (Fig. 10c1-4). The dorsal edge of the right orbit is still preserved as well as the basioccipital region. The horn-cores are virtually intact. The occipital is characterized by a large but narrow squama with a marked bell-shape. The intertemporal bridge is wide and anteroposteriorly compressed. The frontals are wide and slightly inflated between the horn-core bases; as a result, the forehead is concave except for a small crest running along the interfrontal suture. The orbits are weakly tubular. The pedicles are relatively long. The horn-cores are massive and relatively short, without an evident keel; they emerge in posterolateral direction (ca. 72° with the sagittal axis; Fig. 6b), bend laterally after the first third, and point posteriorly toward the tips; in posterior view, they are directed downward and then curve markedly upward. The horn-core base is wide, with strong dorsoventral compression (Fig. 6a). The teeth are heavily worn. This affects also their morphology, making their description difficult (e.g., the metaconid, entoconid, and entostylid of p4 are fused). However, it is possible to recognize constricted lingual lobes in the upper molars and a bubaline fold in the P4. To sum up, the general morphology of the material from Salita di Oriolo is primitive (see, in particular, the strong constriction of the upper occipital squama, the high intertemporal fossae, the concave frontals, and the overall small size). Similarities with *B. (E.) degiulii*, *B. (E.) palaeosinensis*, and *B. (E.) georgicus*, especially in the occipital region, are striking (Figs. 10 and 12; Table 5). In our PCA of neurocranial variables, the Salita di Oriolo specimen falls within the range of variation of *Bison* s.l. (Fig. 7d), but it stands out as one of the smallest known crania of *Eobison* (Fig. 10). Based on this evidence, we support the attribution of the Salita di Oriolo sample to a primitive form of *Bison*, with strong affinities with *B. (E.) degiulii*. The age of the fossils is debated (Toniato et al., 2017). Considering the similarities between the bovine material and *B. (E.) degiulii*, we tend to consider the "Sabbie Gialle" formation of late Villafranchian age, that is, slightly older than previously estimated (ca. 1.0 Ma; Toniato et al., 2017).

An isolated right horn-core (MGCB s.n.) from Mugello, although damaged and badly restored, appears to preserve its original morphology. It is relatively short and has a wide base. In dorsal view, it slightly curves posteriorly, then anteriorly, then again posteriorly toward the tip. In anterior view, it bends downward and then markedly upward. The base is dorsoventrally compressed. Furrows are mainly concentrated on the posteroverventral portion. The shape and size (Fig. 6a) are well fitting with the variability of

primitive bison, as already suggested by Masini (1989). For these reasons, we confirm referral of this specimen to *B. (Eobison)* sp. This specimen might be the same coming from the lignite mine of Lumena (Mugello) and referred to *Leptobos* sp. by Merla (1949).

From Cava Redicicoli, dated around 0.8 Ma, the co-occurrence of the large *B. schoetensacki* and the smaller *B. (Eobison)* cf. *degiulii* is reported, due to the presence of few metapodials of different sizes (Caloi and Palombo, 1995; Masini et al., 2013). The two complete metacarpals, however, show a feeble discrepancy in size and proportions that might be explainable by sexual dimorphism. In the PCA (Fig. 8a), they fall within the variability of larger *Eobison* and smaller *B. schoetensacki*. Even if the Cava Redicicoli sample is surely referable to *Bison* s.l., and most probably to a single species, further studies are needed to assess their specific taxonomy.

Several metapodials from the Upper Valdarno area were ascribed to *L. cf. vallisarni* and *L. cf. etruscus* by Masini (1989) due to their large size and relatively stout appearance. Our comprehensive comparative analysis reveals that some of these fossils might be attributed to *Eobison*. Of the four metacarpals from Le Ville previously referred to *L. cf. vallisarni*, two (IGF 3279, IGF 2374) show different preservation and are characterized by shorter diaphysis and stouter structure, fitting better with the variability shown by the *Eobison* group. The same goes for the metacarpal IGF VA661 from La Viesca (Figs. 8a and 9a). For these three specimens we propose a new identification under *B. (Eobison)* sp.

5.4.5. Eastern Europe and Asia

The (lost) holotype of *B. (E.) sivalensis* is a partial skull missing the horn-cores and part of the splanchnocranium. In our revision of the species original definition, we found an incongruence in the horn-core description by Lydekker (1878). The author states: "The horn-cores are compressed antero-posteriorly; their anterior surface is flat from above downwards and concave from within outwards; their posterior surface is convex in both directions" (Lydekker, 1878: 23). However, in the drawing of the specimen (Lydekker, 1878: pl. XV) the figured section of the horn is clearly dorsoventrally compressed and, in the measurements given by the same author (Lydekker, 1878: 125–138), the anteroposterior diameter is 3.4 inches (=86.4 mm) whereas the transverse (dorsoventral?) diameter is 2.6 inches (=66 mm), suggesting, again, a dorsoventral compression of the horn-core. This issue led to a series of misleading conceptions of this species. For example, Khan et al. (2010) attributed to *B. (E.) cf. sivalensis* two complete horn-cores from Late Pliocene deposits of the Tatrot formation, distinguishing from *L. etruscus* for their anteroposterior compression, absence of torsion, and shorter length. Taking into consideration that the latter two characters are not diagnostic in differentiating this sample from *L. etruscus* (the length of the horn-cores actually fit with the variability of *L. etruscus*, which in addition, shows only a feeble torsion), and, if it is true that the holotype of *B. (E.) sivalensis* had dorsoventrally compressed horn-core bases, then these horn-cores from the Tatrot more resemble the sub-cylindrical sections typical of *L. etruscus* and *Bison* s.s. (Fig. 6a). Based on literature data and available figures, the shape of the occipital area of *B. (E.) sivalensis*, with its markedly indenting temporal fossae, recalls the typical condition of primitive bison. Olsen (1990) and Bukhsianidze (2020), following the idea of Lydekker (1878), suggested that this species could belong to a different *Bison* subgenus and attributed it to cf. *Poepagus*, in light of similarities with the wild yak. Although we agree that several aspects (e.g., morphology, chronological and geographical ranges) may lead to the same conclusion, the lack of available material does not allow us to infer further on the taxonomy of this form.

Bison (E.) palaeosinensis is considered one of the most primitive forms of bison, unfortunately suffering from a confused taxonomic

definition, only partially solved by the emended diagnosis recently given by Tong et al. (2016). One of the main concerns lies in the differences between the two most complete syntypic specimens, cranium A and cranium B, originally attributed to a male and female, respectively (Teilhard de Chardin and Piveteau, 1930). We were not able to study directly the type material, but the measurements and figures available in the literature clearly show that cranium B is actually different from cranium A, somewhat resembling *L. vallisarni* in various traits of the horn-cores and occipital. However, we still know too little about the intraspecific variability of primitive bison to rule out that the differences between the two crania may actually be due to sexual dimorphism (Tong et al., 2016). The idea by McDonald (1981) that cranium A belongs to a small form of *B. priscus* is debatable due to the clearly primitive features of the occipital squama and temporal fossae, as well as its age. Some similarities especially in the shape and orientation of the horn-cores, can be observed between cranium B and the holotype of *B. (E.) sivalensis* figured by Lydekker (1878). However, the unavailability of the type material of the latter species imposes caution in taxonomic conclusions. Biometric comparisons support affinities of both cranium A and cranium B with other records of *Eobison* (Table 5). The same goes for cranial morphology, which shows an array of primitive characters including flattened to concave frontals marked by a sagittal crest along the suture, long pedicles, short postcornual section, high temporal fossae. Moreover, cranium A shares with *L. vallisarni* and *Eobison* the intertemporal bridge proportions (Fig. 7a), again disproving its possible inclusion in *B. priscus*. The postcranials referred to *B. (E.) palaeosinensis* are characterized by a relatively slender built and small size, fitting with the largest *Leptobos* specimens and most *Eobison* (Figs. 6 and 7; Table 6; Tables S12, S19, S23, S25, S26).

The holotype of *B. (E.) tamanensis* is a portion of left horn-core still attached to fragments of occipital, temporal, and frontal bones (ZIN RAS 26010). Although the postorbital constriction is visible, it seems to be less developed than in most primitive forms of *Bison*. The temporal fossa is slightly indenting the occipital area, ending not far from the horn-core base, which has a relatively short pedicle. The horn-core is dorsoventrally flattened and has a faint keel on the posterior side. As shown in the biplot in Fig. 6a, the specimen is quite large compared to other records of *Eobison*, falling not far from the area occupied by *B. schoetensacki* from Süssenborn and Mauer. David and Svistun (1981) assigned to this species three isolated metacarpals from different Ukrainian localities (Cherevichny, Chertkov, and Kairy) but, as already suggested by Sher (1997), there is strong heterogeneity in the sample and their attribution to *B. (E.) tamanensis* is mainly based on the Pre-Tiraspolian age of the deposits in which they were found. Croitor (2010) referred the metacarpals from Kairy and Chertkov to *B. cf. menneri* and the one from Cherevichny to *Eobison* sp. The robusticity biplot (Fig. 8a) shows that the Chertkov specimen is, in fact, similar to the largest *B. menneri* individuals, whereas the Kairy one fits better with the variability of *B. schoetensacki*, and the slenderest specimen from Cherevichny falls in the overlapping range between *Eobison* and *B. menneri*. Therefore, as for the first two specimens, we agree with the identification by Croitor (2010), while we prefer to attribute the metacarpal from Kairy to *B. cf. schoetensacki* due to its robustness. The poor preservation of the holotype of *B. (E.) tamanensis* prevents to define clear-cut diagnostic characters for this species which, however, seems to be overall similar to *B. schoetensacki*. The presence of a more complete cranium from Semibalki attributed to *B. (E.) cf. tamanensis* (Baigusheva, 2000) could help in assessing the validity of this taxon. Kostopoulos et al. (2018) noticed some similarities between the cranium from Semibalki and that of *B. schoetensacki* suggesting, again, a possible synonymy between the two species. If confirmed, this may

reinforce the idea that large and stout prisicoid *Bison* had already arrived at the gates of Europe at the end of the Villafranchian and reached the Mediterranean area during the Epivillafranchian (e.g., Le Vallonnet and Vallparadis Section; Sorbelli et al., 2021a).

Bison (E.) suchovi is the less known species of *Eobison*. The holotype, described by Alekseeva (1967), is a distal fragment of juvenile female horn-core from Dolinskoye (GIN RAS 391–2) characterized by stout built and subtriangular section with flattened base. This scanty material does not allow to assess the validity of this species. Croitor (2010) suggested that the alleged differences between this horn-core and the holotype of *B. (E.) tamanensis* are due to sexual dimorphism, hence considering *B. (E.) suchovi* as a junior synonym of *B. (E.) tamanensis*. Sher (1997) stated that the metapodials from Dolinskoye are similar to those from Süssenborn, Mauer, and Mosbach, which, at least for the first two localities, belong to *B. schoetensacki* (Sorbelli et al., 2021a). Based on these pieces of evidence, *B. (E.) suchovi* is an invalid species in our opinion.

The almost complete cranium of *Adjiderebos cantabilis* (PIN 3723–1) from Kushkuna is one of the best preserved and yet under-considered specimens of Villafranchian large bovid in Eurasia. The cranium misses a portion of the occipital area and fragments of the splanchnocranium, but is in a very good state of preservation on the whole. The first descriptions of this outstanding fossil were given by Dubrovo and Burchak-Abramovich, 1984, 1986, who erected this new genus of bovine evidencing its similarities with *Bison* and *Leptobos*. In fact, this cranium shows several features shared with these two genera, but also some autapomorphies including: zygomatic arc elevated over the mandibular articulation and unciform rims at the external borders of the occipital condyles (Dubrovo and Burchak-Abramovich, 1986; Bukhsianidze, 2005). Both these characters, however, can be found in other genera of bovines. The zygomatic elevation at the mandibular articulation is clearly visible in some specimens of *Leptobos*, *Bos*, and *Bison* s.l. (e.g., the female *L. etruscus* NHMB VA605 from the Upper Valdarno and the holotype of *B. (E.) degiulii*) and the hooked process of the occipital condyles is well known in *Bison* s.s. (McDonald, 1981: 187, pl. 26). Our morphometric analyses show that the horn-core bases share the same proportions with the smallest *Eobison* specimens whereas the postcornual constriction is quite developed with a marked posterior indentation of the temporal fossae, which resembles the condition found in the most primitive *Leptobos* forms (Fig. 7a). In addition, the frontals are extremely narrow (Fig. 7b). The well-developed intertemporal bridge, the premaxilla in contact with the nasal, and the presence of ethmoidal fenestrae are all leptobovine features. On the other side, the nasals ending posteriorly to the anterior border of the orbits and the wide angle of horn-core insertion are bisontine features. On the whole, the characters that would distinguish *Adjiderebos* from *Leptobos* and *Eobison* seem to be not diagnostic, thus, most probably, this taxon actually belongs to one of these two genera. A direct revision of the Kushkuna material, paired with a phylogenetic study of these clades, are requested in order to clarify the taxonomic position of this extremely interesting “transitional” form between *Leptobos* and *Eobison*.

The holotype of *Probison dehmi* is a fragmented cranium from the Tatrot stage of the Upper Siwaliks (DGPU B/7), dated to the Late Pliocene (Shani and Khan, 1968). The cranium is severely damaged and badly restored. Nevertheless, it shows interesting characters in common with gr. LSEM including: long frontals, shallow and high temporal fossae, strong constriction of the upper occipital squama, developed mastoid processes, premaxilla in contact with nasal, presence of ethmoidal vacuity. Shani and Khan (1968) stated that the only complete horn-core is anteroposteriorly compressed; in fact, observing the holotype pictures, it is clear that the horn-core is

markedly compressed in dorsoventral direction. It shows a peculiar orientation, bending downward and forward. According to Bukhsianidze (2005), it is most probable that the horn-core was mounted on reverse (the base is completely hidden by plaster). This hypothesis is supported by the fact that the well-marked ribs and furrows visible on the convex surface of the horn-core, are normally present on the ventral side and not on the dorsal. If the horn-core was actually mounted incorrectly, it would originally emerge posterolaterally, then bend upward and forward with a strong posterior twist as in gr. LSEM lineage. A revision and new restoration of the material is required to assess the validity of this taxon or the possible incorporation of *P. dehmi* into *Leptobos*.

5.5. Comments on the evolutionary trends in limb proportions and body mass

Several studies on the morpho-functional adaptations of bovid limb bones in response to climate/environmental changes over the Pleistocene, have been published in the last decades (Scott, 1985; Plummer and Bishop, 1994; Klein et al., 2010; Scott and Barr, 2014; Maniakas and Kostopoulos, 2017; Etienne et al., 2021; among others). The comprehensive study by Scott (1979) on the proportions of bovid limbs showed that long-legged small-sized taxa typical of open habitats rely on their cursorial skills to outrun the predators, whereas in other taxa, passive defence strategies based on large body size and/or gregarious behaviour are preferred. Consequently, small-sized cursorial forms underwent to an elongation of the distal limb elements, while similar evolutionary changes are not expected in large bovines living in the same open environments (Scott, 1979, 1985). On the contrary, in these forms, a marked increase in limb width against length is observed, most probably as an allometric response to heavier bodies (Biewener, 2005; Etienne et al., 2021). This is indirectly confirmed by regression equations for body mass prediction that, if performed on the length of distal bones, overestimate the mass of small bovines of open/arid habitats (i.e., Antilopini, Alcelaphini) and largely underestimate the mass of larger bovines, whereas the epiphysis measurements give much more reliable estimations (Scott, 1983). In addition, it has been proved that bovines exceeding 300 kg in body mass are characterized by an allometric pattern of the anterior zygopodium and autopodium (Scott, 1985; Etienne et al., 2021), in the fact that this section underwent to a stronger increase of size and robusticity, compared to the other forelimb sections, as a response to heavier mass and subsequent change in posture. In their analysis of several samples of *Bison* from the Pleistocene of Europe, Sorbelli et al. (2021a) suggested that the robusticity of metacarpals in bison is inversely related to the amount of tree cover in the environment.

The present study, including data from numerous species of *Leptobos* and *Bison* covering a wide chronological range, supports the above observations and gives further hints on the morphological response of these bovines to environmental changes over the last 2 Ma in Western Palearctic. *Leptobos* (especially LSEM) is considered as typical of relatively closed environments (Rook and Martínez-Navarro, 2010). In fact, it is inferred that one of the main causes of the extinction of these forms was the progressive contraction of wooded areas started at the end of the Pliocene and specially during the late Villafranchian (Head and Gibbard, 2005, 2015; Maslin and Brierley, 2015). *Bison*, due to its capability to adapt to a wider spectrum of environments, occupied the new available niches, in particular after the onset of new asymmetric glacial/interglacial cycles and the increase of seasonality during the EMPT (Maslin and Brierley, 2015). Our results show a clear trend towards an increased robusticity of metapodials from the Pliocene onwards (Fig. 12a). The violin plot of body mass estimations (Fig. 12b)

highlights a constant increase of average weight starting from the Late Pliocene and reaching a peak during the late Middle Pleistocene, before recording an opposite trend in the Late Pleistocene and Holocene (see also Maniakas and Kostopoulos, 2017). Similarly, the biplot of radius robusticity (Fig. 8d) and the RAD/MC% histogram (Fig. 9c) show that *Leptobos* and *Bison* underwent to a clear increase in size and stoutness of the anterior zygopodium correlated with larger body masses (Fig. 12b).

It is even possible to observe the same parallel trends within *Leptobos* and *Bison* at smaller scale. In *Leptobos*, there is a transition from the slender and short metapodials of LSEM to the stouter and longer ones of LEV, paired with an increase of radius size, body mass, and hypsodonty, following the first contraction of forested environments at the middle-late Villafranchian transition (Rook and Martínez-Navarro, 2010; Madurell-Malapeira et al., 2014). In *Bison*, due to their long history, wide geographic distribution, and abundant fossil record, the situation is much more complex. The primitive *Eobison*, roughly coeval to the last *Leptobos*, features increased body mass and robusticity, characterized by larger and heavier heads and limbs, although not yet displaying the massive appearance of later forms. Their limb structure shows a wide spectrum of variability (e.g., slender morphology from Pietrafitta, stouter from Apollonia), which could reflect either separate taxa or ecophenotypic variations. It is clear, however, that close to the beginning of the Epivillafranchian, their size and stoutness started to increase, especially in the most arid environments such as those of Pirro Nord and Apollonia. An even wider variability is present in *Bison* s.s. due to the extremely widespread geographic distribution of these derived forms. It is true indeed, that if both *Leptobos* and *Eobison* are mainly (if not exclusively) found between the 45th and 35th parallels, later forms of *Bison* (i.e., priscoïd group) populated all the Palearctic, from Siberia to the Mediterranean area (Fig. 1a) (Kahlke, 1999). This wide distribution led to the evolution of several morphotypes adapted to the dominant habitats and climatic conditions, in a timespan that covers more than 1 Ma. The very slender *B. menneri* and the stouter *B. schoetensacki* were the most common forms in Europe during the Early-Middle Pleistocene boundary (Sala, 1986; Moullé, 1992; Brugal, 1995; Sher, 1997; Sorbelli et al., 2021a). Although characterized by large size and priscoïd characters, they still featured slender built compared with the extremely stout *B. priscus*. As already pointed out by Sher (1997) and Sorbelli et al. (2021a), the common misconception that *B. schoetensacki* was a small-sized forest-adapted form, is disproved by the records from Le Vallonnet and Vallparadis Section, which show that these animals were adapted to a wider spectrum of habitats and very large body mass, even reaching 1000 kg (Fig. 12b). The first occurrence of *B. priscus* is still debated. Between 0.9 and 0.5 Ma, bison with priscoïd morphologies started to appear in fossil records such as those from the Kuznetsk Basin, Tiraspol, and Mosbach, which are, however, still pending a clear taxonomic status (Freudenberg, 1914; Sher, 1997; Foronova, 2001; Sorbelli et al., 2021a). In the late Middle Pleistocene, giant and massive forms such as *B. p. gigas* and *B. p. priscus* from Riverenert, Châtillon-Saint-Jean, Romain-La-Roche, and Taubach, are recorded (body mass reaching 1600 kg; Fig. 12b) (Mourer-Chauviré, 1972; Flerov, 1977a, 1977b; Vercoutère and Guérin, 2010). Some of these animals, however, were still characterized by relatively elongated metacarpals (Fig. 12a). From the Late Pleistocene on, the body mass and metapodial length of *B. priscus* (often referred to the subspecies *B. p. mediator*, *B. p. minor* or *B. p. deminutus*; van der Vlerk, 1942; Brugal, 1999; Kahlke, 1999) started to decrease. In agreement with the aforementioned model by Sorbelli et al. (2021a), the slenderer forms of *Bison* s.s. (e.g., the long-legged *B. menneri* from Untermaassfeld or the samples of *B. schoetensacki* from Le Vallonnet and Mauer) are found in more humid, heterogeneous habitats (i.e., mosaic of forested and open

patches), while the samples of *B. schoetensacki* from more arid sites such as Süssenborn, Durfort, and Vallparadis Section exhibit stouter proportions (Fig. 12a). Similarly, the tallest and slenderest specimens of *B. priscus* are those from Taubach, a site characterized by fully developed interglacial conditions with warm and forested environment (Kahlke, 1977), whereas the stouter members of this species inhabited open, steppe/prairie-like habitats during the last glacial both in Eurasia and North America (Fig. 12a). The common misconception that the smallest and stoutest forms of *B. priscus* living during MIS 3 and MIS 2 (*B. p. mediator sensu Flerov, 1979*) were typical of forested areas, was already questioned with reason by Sala (1986), Guérin and Valli (2000), and Castaños et al. (2012). These authors emphasized how this form is always associated with horses and reindeer (e.g., in Kiputz IX), suggesting that the typical habitat of this subspecies was the cold steppe of the last glaciation tundra. Our robusticity analysis confirms this idea, evidencing that *B. p. mediator* was well adapted to open environments thanks to its robust and stout limbs (Fig. 12a). This correlation is maintained also in Pleistocene *Eobison* from the Mediterranean area and in Holocene species. *Bison (E.) degiulii* from Pietrafitta lived in the surroundings of a humid and wooded habitat (see Section 2) and featured slender metapodials (slightly stouter than those of *L. etruscus*); conversely, members of the same species from Pirro Nord and Apollonia, adapted to drier or rocky environments, bear more robust limbs, similar to those shown by the stouter *B. schoetensacki* (Maniakas and Kostopoulos, 2017; Blain et al., 2019). The extant subspecies *B. bison bison* populates the open grasslands of North America and is characterized by the shortest metacarpals among living bison, whereas the taller and slenderer woodland bison *B. bison athabascae* and European wisent *B. bonasus* prefer sub-hygic and mixed habitats (McDonald, 1981; Stephenson, 2001).

These multiple pieces of evidence are further supported by the dietary habits inferred for extinct and extant taxa by Asperen van and Kahlke (2017). Based on tooth wear analysis, these authors showed that the extremely tall *Bison* from Taubach and Untermassfeld, as well as *B. b. athabascae* are better defined as browser-mixed feeders, whereas the stouter *Bison* from Süssenborn and extant *B. bonasus* display more grazer signatures. The North American plain bison *B. b. bison*, namely a species with extremely short metacarpals, shows typical dental wear features of an open habitat grazer.

It has been already remarked by several scholars that the mean body size of *Bison*, except for few exceptions, decreased after the last interglacial in the Holarctic region (Vasiliev, 2008; Saarinen et al., 2016; Maniakas and Kostopoulos, 2017). Our body mass estimations computed on a large sample of *Leptobos* and *Bison* confirm this statement, showing a clear trend toward gigantism from *Leptobos* to *Eobison* and to *Bison* s.s. and an opposite trend from the Late Pleistocene on (Fig. 12b). In particular, during the latest Middle Pleistocene (e.g., MIS 6–MIS 5e), the largest forms are recorded (e.g., samples from Châtillon-Saint-Jean, Romain-La-Roche, and Taubach). The main driving factors of increasing body size throughout the Early-Middle Pleistocene, are still matter of debate. Maniakas and Kostopoulos (2017) observed that bison specimens from Joint Mitnor Cave mammal assemblage (UK) were significantly smaller than the roughly isochronous ones from Taubach (ca. 0.12 Ma). This apparently contrasts with the Bergmann's rule, which expects a positive correlation between body size and latitude. Meiri et al. (2007) pointed out that in taxa with wide geographical ranges (such as *Bison*), body size can be influenced by a complex array of factors, including not only ecogeographical rules but also - often predominantly - food availability and interspecific competition. During the MIS 5e interglacial, the presence of numerous geothermal springs at Taubach would have favoured the

development of a humid dense forest with a large amount of food (Asperen van and Kahlke, 2017), while the paleoenvironmental conditions of the British islands would have been harsher. Therefore, the Taubach bison may have reached gigantic size thanks to extremely favourable trophic conditions, while the Joint Mitnor Cave bison may have kept smaller dimensions due to the combination of severe environmental context and geographic isolation. A recent study on *B. priscus* inhabiting the Yukon territory in the last 0.05 Ma demonstrated that they experienced body mass increase and population growth during warmer periods and opposite trends in harsher phases (Kelly et al., 2021). In their comprehensive analysis of *Bison* s.s. records from the Middle-Late Pleistocene of Germany and UK, Saarinen et al. (2016) showed that populations living in open arid landscapes had smaller body size than those living in wooded humid landscapes. The same pattern was found in other large herbivores such as caballine horses, in which body mass increased in relatively closed, highly productive environments as a result of the combined effect of resource availability, habitat partitioning, inter- and intraspecific competition, and herd density (Asperen van, 2010; Saarinen et al., 2021).

Our study provides further evidence to support the above inferences. The progressive harshening of climate during the Last Glacial Maximum did not allow the development of very large body size in *Bison*, which in most Late Pleistocene sites (e.g., Roter Berg, Habarra, Gral), are characterized by mean body mass lower than 1000 kg, in contrast with the considerably heavier weights reached during MIS 5e and previous interglacial stages (e.g., Romain-La-Roche, Taubach) (Fig. 12b). Going further back in time, the Pietrafitta sample fits perfectly into this model. The primitive bison from this locality was characterized by relatively slender limbs but large body on the whole (i.e., slightly heavier than 600 kg; Fig. 12b). Slender limbs and large body size can be related with a warm climate environment rich in forested patches, as suggested by palaeobotanical and paleoherpetological evidence (Martinetto et al., 2014; Sorbelli et al., 2021b). The excellent ecological suitability would have allowed the Pietrafitta bison to develop larger dimensions than, for example, the almost contemporary Venta Micena bison, which lived in a more arid environment and with greater competition in the herbivore guild.

6. Conclusions

Pietrafitta (ca. 1.5 Ma) is one of the key sites of the European late Villafranchian thanks to the extremely rich paleozoological and paleobotanical evidence (Martinetto et al., 2014; Sorbelli et al., 2021b). The abundant large-sized bovid record from Pietrafitta, which was preliminarily believed to represent an advanced form of *Leptobos* (Masini, 1989; Gentili and Masini, 2005), is here referred to *B. (E.) degiulii* based on a combination of characters found in several skeletal districts (e.g., cranium and metapodials). *Bison (E.) degiulii* represents one of the earliest representatives of its genus that appeared in Western Palearctic.

The study of the Pietrafitta material triggered the reappraisal of all available records of Villafranchian *Leptobos* and *Bison*, with a focus on the subgenus *Eobison*. Our revision of the taxonomy and variability of this group of early bison has resulted in the emended diagnosis provided in this paper, which has served as a basis for the summary of comparative characters in Table 7 and Fig. 11. As far as the available data are concerned, we think that among all the species of *Eobison* described so far, only three can be considered valid, namely *B. (E.) palaeosinensis*, *B. (E.) georgicus*, and *B. (E.) degiulii*. Among these, the best-known species - also thanks to the very rich sample from Pietrafitta - is *B. (E.) degiulii*, which occurred in Mediterranean Europe during the latest Villafranchian. Additional fossils would be desirable to enrich our knowledge of *B. (E.)*

palaeosinensis and *B. (E.) georgicus* which, thanks to their older age and geographical distribution, could clarify further aspects on the evolutionary transition between *Leptobos* and *Bison*.

In agreement with previous works, our study also confirms the validity of limb bone dimensions and proportions as (1) reliable taxonomic tools, (2) proxies for the estimation of body mass, and (3) predictors of paleoenvironmental preferences in bovines. Thanks to these data, we suggest that European *Leptobos* and *Bison* responded to the progressive Pleistocene climatic deterioration through changes in limb proportions and average body mass. In particular, the contraction of forested habitats and the spread of open environments under colder and more arid climate, led to an increase in metapodial stoutness and in body size, and to higher hypsodonty associated with grazing-based diet. This trend can be traced along the transition from *Leptobos* to *Bison*, but also on a smaller scale, within the two groups.

Despite the average tendency to increase in size, a more detailed analysis of the *Bison* s.l. record in the interval 1.8–0.01 Ma (Fig. 12) shows that there have been fluctuations. In our opinion, it is probable that these may be attributable to punctual habitat changes and/or shifts between glacial and interglacial stages, but often the paleoenvironmental data and dating available for the various paleontological sites do not have sufficient resolution to verify this hypothesis. It should not be forgotten that these phenomena of variation in body size and proportions were determined by a complex combination of factors, including ecogeographical patterns (e.g., Cope-Depéret and Bergmann's rules), resource availability, intraspecific competition, and predatory pressure.

Author contributions

LS, M.C and J.M.-M conceived the research and wrote the paper; LS, performed the analyses; LS, M.C, D.S.K., R.F., B.M., V.P., M.P.V., B.A., S.V.B. and J.M.-M. collected the data, revised all the manuscript versions and made improvements in the manuscript.

Declaration of competing interest

The authors declare that they have no known competing financial interests or personal relationships that could have appeared to influence the work reported in this paper.

Data availability

Data will be made available on request.

Acknowledgments

This work is funded by the Agencia Estatal de Investigación European Regional Development Fund of the European Union (CGL2016-76431-P and CGL2017-82654-P, AEI/FEDER-UE) and the Generalitat de Catalunya (CERCA Programme). LS is supported by the FI AGAUR fellowship (ref. 2020 FL_B2 00189) funded by the Secretaria d'Universitats i Recerca de la Generalitat de Catalunya and the European Social Fund. The present manuscript has been prepared during a Visiting Professor fellowship at the Earth Sciences Department of the University of Florence awarded to JM-M in May–June 2021. The present manuscript is part of the PhD thesis of LS within the Geology PhD program of the Universitat Autònoma de Barcelona.

We would like to thank Paola Romi (Soprintendenza Archeologia Belle Arti e Paesaggio dell'Umbria) for the possibility to study the Pietrafitta bovid collection at the MPLB and for her kindness and availability; Elisabetta Cioppi and Luca Bellucci for the possibility to study the Valdarno bovid collections at the IGF; Lorenzo

Rook for the possibility to study the Pirro Nord bovid collection at the DST; Maia Bukhsianidze for sending to us the 3D model and pictures of *B. (E.) georgicus* holotype and for precious information about the Dmanisi bovid; Marco Sami for having sent to us measurements and pictures of the Salita di Oriolo bovid; Michela Contessi for having sent to us pictures of the Mugello bovid; Roman Croitor for having sent to us measurements of some East European *B. (B.) priscus*; Omar Cirilli for the help in the bibliographic and data collection at the DST; Dawid Adam Iurino for the useful discussions about the methodological approach; Grant Zazula and Elizabeth Hall for having sent to us some comparative *B. (B.) bison* pictures; and Elpiniki Maria Parparousi, for the digital data elaboration. Raffaele Sardella thanks "Fabbrica Conservazione e Restauro SCPL" for the restoration work of the Capena skeleton housed at MUST, supported by Polo Museale of Sapienza University of Rome. We thank Marzia Breda and an anonymous reviewer who helped to significantly improve the manuscript.

Appendix A. Supplementary data

Supplementary data to this article can be found online at <https://doi.org/10.1016/j.quascirev.2022.107923>.

References

- Agadzhanian, A.K., Vislobokova, I.A., Shunkov, M.V., Ulyanov, V.A., 2017. Pleistocene mammal fauna of the Trlica locality, Montenegro. *Fossil Imprint* 73 (1–2), 93–114.
- Alekseeva, L.L., 1967. To the history of subfamily Bovinae during the Pleistocene in the European USSR. In: *Paleontologiya, Geologiya i Poleznye Iskopaemye Moldavii Vyp. 2*. Shtiintsa, Kishinev, pp. 123–127 (in Russian).
- Ambrosetti, P., Cattuto, C., Gregori, L., 1989. Geomorfologia e neotettonica nel bacino di Taverne/Pietrafitta (Umbria). *Il Quat.* 2, 57–64.
- Ambert, P., Brugal, J.P., Houles, N., 1996. Le maar du Riège (Hérault, France): géologie, paléontologie, perspectives de recherches. *C. R. Acad. Sci. Sér. IIa* 322, 125–132.
- Ambrosetti, P., Argenti, P., Basile, G., Gentili, S., Ikome, F.E., 1992. The pleistocene fossil vertebrata of the Pietrafitta basin (Umbria, Italy): preliminary taphonomic analyses. In: *Taphonomy: Processes and Products*. European Paleontological Association Workshop, Strasbourg, pp. 20–21.
- Ambrosetti, P., Basile, G., Capasso Barato, L., Carboni, M.G., Di Stefano, G., Esu, D., Gliozzi, E., Petronio, C., Sardella, R., Squazzini, E., 1995. Il Pleistocene inferiore nel ramo Sud-Occidentale del Bacino Tiberino (Umbria): aspetti litostatigrafici e biostratigrafici. *Il Quat.* 8 (1), 19–36.
- Anfossi, G., Rossi, M., Santi, G., 1999. Osteologia e morfologia di resti di *Bison* delle provincie di Pavia e di Como (Lombardia). *Atti Soc. it. Sci. Nat. Museo civ. Stor. Nat. Milano* 140, 237–278.
- Arribas, A., Palmqvist, P., 1998. Taphonomy and palaeoecology of an assemblage of large mammals: hyaenid activity in the lower Pleistocene site at Venta Micena (Orce, Guadix-Baza Basin, Granada, Spain). *Geobios* 31, 3–47.
- Arzarello, M., Peretto, C., Moncel, M.H., 2015. The Pirro Nord site (apricena, fg, southern Italy) in the context of the first European peopling: convergences and divergences. *Quat. Int.* 389, 255–263.
- Asperen E.N., van, 2010. Ecomorphological adaptations to climate and substrate in late Middle Pleistocene caballid horses. *Palaeoecol. Palaeoecol.* 297, 584–596.
- Asperen van, E.N., Kahlke, R.D., 2017. Dietary traits of the late early Pleistocene *Bison menneri* (Bovidae, Mammalia) from its type site Untermaßfeld (Central Germany) and the problem of Pleistocene 'wood bison'. *Quat. Sci. Rev.* 177, 299–313.
- Baigúsheva, V.S., 2000. New data on Tamaran faunal assemblage from the excavation site near Semibalki village (Azov Area). *Historical-Archaeological in Azov and Lower Don in 1998*, 16, 27–57.
- Biewener, A.A., 2005. Biomechanical consequences of scaling. *J. Exp. Biol.* 208 (9), 1665–1676.
- Blain, H.A., Fagoaga, A., Ruiz-Sánchez, F.J., Bisbal-Chinesta, J.F., Delfino, M., 2019. Latest Villafranchian climate and landscape reconstructions at Pirro Nord (southern Italy). *Geology* 47 (9), 829–832.
- Breda, M., Collinge, S.E., Parfitt, S.A., Lister, A.M., 2010. Metric analysis of ungulate mammals in the early Middle Pleistocene of Britain, in relation to taxonomy and biostratigraphy: I: rhinocerotidae and Bovidae. *Quat. Int.* 228, 136–156.
- Brugal, J.-P., 1983. Applications des Analyses Multidimensionnelles à l'Étude du Squelette des Membres des Grands Bovidés Pleistocènes. *Grotte de Lunel-Viel, Hérault*.
- Brugal, J.-P., 1995. Le bison (Bovidae, Artiodactyla) du Pleistocène moyen ancien de Durfort (gard, France). *Bull. Mus. Natl. Hist. Nat.* 16C 2–4 349–381.
- Brugal, J.-P., 1999. Étude de populations de grands Bovidés européens: intérêt pour la connaissance des comportements humains au Paléolithique. In: Brugal, J.P.,

- David, F., Enloe, J.G., Jaubert, J. (Eds.), Le Bison: gibier et moyen de subsistance des hommes du Paléolithique aux Paléindiens des Grandes Plaines. APDCA, Antibes, pp. 85–104.
- Brugal, J.-P., Fosse, P., 2005. Les grands bovidés (*Bison cf. schoetensacki*) du site Pléistocène moyen de la Vayssière (Aveyron, France). In: Crégut-Bonnoure, E. (Ed.), Les ongulés holarctiques du Pliocène et du Pléistocène. Quaternaire, Hors série 2, 75–80.
- Bukhsianidze, M., 2005. The fossil Bovidae of Dmanisi. Ph.D. Dissertation, Università degli Studi di Ferrara.
- Bukhsianidze, M., Koiava, K., 2018. Synopsis of the terrestrial vertebrate faunas from the middle kura basin (eastern Georgia and western Azerbaijan, south caucasus). Acta Palaontol. Pol. 63 (3), 441–461.
- Bukhsianidze, M., 2020. New results on bovids from the early pleistocene site of Untermaassfeld. In: Kahlke, R.D. (Ed.), Das Pleistozän von Untermaassfeld bei Meiningen (Thüringen). Teil 4. Habelt-Verlag, Bonn, pp. 1169–1195.
- Burchak-Abramovich, N.I., Gadzhiev, D.D., Vekua, A.K., 1980. Concerning ancestral form of bisons from the akchagyl of southern caucasus. Bull. Georgian Natl. Acad. Sci. 97 (2), 48–488 (in Russian).
- Burchak-Abramovich, N.I., Vekua, A.K., 1994. On a new pleistocene bovine from eastern Georgia. Teriologii Paleoteriologija 253–261 (in Russian).
- Caloi, L., Palombo, M.R., 1995. The Early Galerian Fauna of Redicicoli. XIV INQUA Congress, Berlin.
- Cameron, C.C., Esterle, J.S., Palmer, C.A., 1989. The geology, botany and chemistry of selected peat-forming environments from temperate and tropical latitudes. Int. J. Coal Geol. 12 (1–4), 105–156.
- Castañón, J., Castañón, P., Murelaga, X., Alonso-Olazabal, A., 2012. Kiputz IX: un conjunto singular de bisonte estepario (*Bison priscus* Bojanus, 1827) del Pleistoceno Superior de la Península Ibérica. Ameghiniana 49 (2), 247–261.
- Castelló, J., 2016. Bovids of the World: Antelopes, Gazelles, Cattle, Goats, Sheep, and Relatives. Princeton University Press, Princeton, p. 664.
- Cherin, M., Bizzarri, R., Buratti, N., Caponi, T., Grossi, F., Kotsakis, T., Pandolfi, L., Pazzaglia, F., Barchi, M.R., 2012. Multidisciplinary study of a new Quaternary mammal-bearing site from Ellera di Corciano (central Umbria, Italy): preliminary data. Rend. Onl. Soc. Geol. Ital. 21, 1075–1077.
- Cherin, M., D'Allestro, V., Masini, F., 2019. New bovid remains from the early pleistocene of Umbria (Italy) and a reappraisal of *Leptobos merlai*. J. Mamm. Evol. 26, 201–224.
- Cignoni, P., Callieri, M., Corsini, M., Dellepiane, M., Ganovelli, F., Ranzuglia, G., 2008. Meshlab: an open-source mesh processing tool. In: Eurographics Italian Chapter Conference, pp. 129–136, 2008.
- Clark, P.U., Archer, D., Pollard, D., Blum, J.D., Rial, J.A., Brovkin, V., Mix, A.C., Piasias, N.G., Roy, M., 2006. The middle Pleistocene transition: characteristics, mechanisms, and implications for long-term changes in atmospheric pCO₂. Quat. Sci. Rev. 25, 3150–3184.
- Conti, M.A., Esu, D., 1981. Considerazioni sul significato paleoclimatico e geodinamico di una serie lacustre pleistocenica inferiore presso Tavernelle (Perugia, Umbria). Geogr. Fis. Din. Quaternaria 4, 3–10.
- Conti, M.A., Girotti, O., 1977. Il villafranchiano nel "lago Tiberino", ramo sud-occidentale: schema stratigrafico e tettonico. Geol. Romana 16, 67–80.
- Crégut-Bonnoure, E., Dimitrijevic, V., 2006. *Megalovis balcanicus* sp. nov. and *Soergelia intermedia* sp. nov. (Mammalia, Bovidae, Caprinae), new Ovivovini from the Early Pleistocene of Europe. Rev. de Paléobiologie 25 (2), 723–773.
- Croitor, R., 2010. Critical remarks on genus *Bison* (Bovidae, Mammalia) from pleistocene of moldova. Revista Archeologica 5, 172–188 (in Russian).
- Croitor, R., 2016. Genus *Bison* (Bovidae, Mammalia) in early pleistocene of moldova. In: Coropceanu, E. (Ed.), Materialele Conferinței Științifice Naționale Cu Participare Internațională "Mediul și Dezvoltare Durabilă", Ediția a III-A, pp. 14–20. Chișinău.
- Croitor, R., Popescu, A., 2011. Large-sized ruminants from the early pleistocene of leu (oltenia, Romania) with remarks on biogeographical aspects of the "Pachyrocota event. Neues Jahrb. für Geol. Paläontol. - Abh. 261 (3), 353–371.
- David, A.I., Svistun, V.I., 1981. Bison remains from upper Pliocene and lower pleistocene deposits of moldova and south Ukraine. In: Biostratigraphy of Anthropogene and Neogene of South-West of USSR. Shtiintsa, Kishinev, pp. 3–15 (in Russian).
- De Giuli, C., 1986. Late villafranchian faunas in Italy: the selvella local fauna in southern Chiana Valley - Umbria. Palaeontogr. Ital. 74, 11–50.
- De Giuli, C., Masini, F., Torre, D., 1986. The latest villafranchian faunas in Italy: the Pirro Nord fauna (Apricena, Gargano). Palaeontogr. Ital. 74, 51–62.
- Depéret, C., 1884. Nouvelles études sur les ruminants pliocènes et quaternaires d'Auvergne. Bull. Soc. Geol. Fr. 22, 247–284.
- Dong, W., 2008. Nouveau matériel de *Leptobos (Smertiobos) crassus* (Artiodactyla, Mammalia) du Pléistocène inférieur à Renzidong (Chine de l'Est). Geobios 41, 355–364.
- Drees, M., 2005. Sexual dimorphism in pleistocene *Bison priscus* (Mammalia, Bovidae) with a discussion on the position of *Bison schoetensacki*. Senckenberg. Lethaea 85 (1), 153–157.
- Dubrovo, I.A., Burchak-Abramovich, N.I., 1984. A new Pliocene bovid genus, *Adjiderebov* gen. Nov., from transcaucasia. Dokl. Akad. Nauk SSSR 276 (3), 717–720.
- Dubrovo, I.A., Burchak-Abramovich, N.I., 1986. New data on the evolution of Bovine of the tribe Bovini. Quartarpalaontologie 6, 13–21.
- Duvernois, M.P., 1990. Les *Leptobos* (Mammalia, Artiodactyla) du Villafranchien d'Europe occidentale. Doc. Lab. Geol. Fac. Sci. Lyon 113, 1–213.
- Duvernois, M.P., 1992. Mise au point sur le genre *Leptobos* (Mammalia, Artiodactyla, Bovidae): implications biostratigraphiques et phylogénétiques. Geobios 25, 155–166.
- Duvernois, M.P., Guérin, C., 1989. Les Bovidae (Mammalia, Artiodactyla) du Villafranchien supérieur d'Europe occidentale. Geobios 22, 339–379.
- Empel, W., Roskosz, T., 1963. Bisoniana X. Das Skelett der Gliedmassen des Wisents. *Bison bonasus* (Linnaeus, 1758): *Bisoniana X. Kościc koczyn zubra*, *Bison bonasus* (Linnaeus, 1758). Acta Theriol. 7 (13), 259–300.
- Etienne, C., Filippo, A., Cornette, R., Houssaye, A., 2021. Effect of mass and habitat on the shape of limb long bones: a morpho-functional investigation on Bovidae (Mammalia: cetartiodactyla). J. Anat. 238 (4), 886–904.
- Fabbi, S., Romano, M., Strani, F., Sardella, R., Bellucci, L., 2021. The Pleistocene vertebrate fauna of the Oricola-Carsoli intermontane Basin (Latium-Abruzzi, Italy): state of the art and historical review. Boll. Soc. Pal. Ital. 60, 255–268.
- Falconer, H., 1868. In: Murchison, I.R.J. (Ed.), Paleontological Memoirs and Notes, vol. II, p. 590. London.
- Flerov, C.C., 1972. The most ancient Bisons and the history of genus *Bison*. In: Teriologiya, vol. 1. Nauka, Novosibirsk, pp. 81–86 (in Russian).
- Flerov, K.K., 1975. Die Bison-reste aus den travertinen von Weimar-ehringendorf. Abh. Zentr. Geol. Inst. 23, 171–199.
- Flerov, K.K., 1977a. Gigantic bisons of Asia. J. Palaeontol. Soc. India 20, 77–80.
- Flerov, K.K., 1977b. Die fossilen Bisonreste von Taubach und ihre Stellung in der Entwicklungsgeschichte der Gattung *Bison* in Europa. In: Kahlke, R.-D. (Ed.), Das Pleistozän von Untermaassfeld bei Meiningen (Thüringen), Teil 1. Quartarpalaontologie 2, pp. 179–208.
- Flerov, K.K., 1979. Morphology, systematic, evolution, ecology. In: Sokolov, E.V. (Ed.), European Bison. Nauka, Moscow, pp. 9–127 (in Russian).
- Foronova, I.V., 2001. In: Kanygin, A.V. (Ed.), Quaternary Mammals of the South-East of Western Siberia (Kuznetsk Basin). Phylogeny, Biostatigraphy, and Paleocology. Publishing house of SB RAS, Branch "GEO", p. 234 p. (in Russian).
- Freudentberg, W., 1914. Die saugetierte des alteren Quartas von Mitteleuropa. Geol. Paleont. Abh 12, 455–670.
- Garrido, G., 2008. Primera cita de *Leptobos etruscus* (Falconer, 1868) (Bovidae, Artiodactyla, Mammalia) en la Península Ibérica (Fonelas P-1, Cuenca de Guadix, Granada). Cuadernos del Museo Geominero 10, 489–516.
- Gentili, S., Abbazzi, L., Masini, F., Ambrosetti, P., Argenti, P., Torre, D., 1996. Voles from the early pleistocene of Pietrafitta (central Italy, Perugia). Acta Zool. Cracov. 3, 185–199.
- Gentili, S., Barili, A., Ambrosetti, P., 2000. Un museo per i fossili di Pietrafitta. Nuova Museologia 2, 16–17.
- Gentili, S., Masini, F., 2005. An outline of Italian *Leptobos* and a first sight on *Leptobos aff. vallisarni* from Pietrafitta (early pleistocene, Perugia). In: Crégut-Bonnoure, E. (Ed.), Les ongulés holarctiques du Pliocène et du Pléistocène. Quaternaire, Hors série 2, 81–89.
- Gliozzi, E., Abbazzi, L., Argenti, P., Azzaroli, A., Caloi, L., Barbato, L.C., Di Stefano, G., Esu, D., Ficarelli, G., Girotti, O., Kotsakis, T., 1997. Biochronology of selected mammals, molluscs and ostracods from the Middle Pliocene to the Late Pleistocene in Italy. The state of the art. Riv. Ital. Paleontol. Stratigr. 103, 369–388.
- Gee, H., 1993. The distinction between postcranial bones of *Bos primigenius* Bojanus, 1827 and *Bison priscus* Bojanus, 1827 from the British Pleistocene and the taxonomic status of *Bos* and *Bison*. J. Quat. Sci. 8, 79–92.
- Geraads, D., 1992. Phylogenetic analysis of the tribe bovine (Mammalia: Artiodactyla). Zool. J. Linn. Soc. 104, 193–207.
- Grange, T., Brugal, J.P., Flori, L., Gautier, M., Uzunidis, A., Geigl, E.M., 2018. The evolution and population diversity of bison in pleistocene and holocene Eurasia: sex matters. Diversity 10 (3), 65.
- Gromov, I.M., Baranova, G.I. (Eds.), 1981. Catalogue of Mammals of the USSR (Pliocene-Recent). Nauka, Leningrad, p. 456 (in Russian).
- Groves, C., Grubb, P., 2011. Ungulate Taxonomy. The John Hopkins University Press, Baltimore, p. 309.
- Guérin, C., 1982. Première biozonation du Pléistocène européen, principal résultat biostratigraphique de l'étude des Rhinocerotidae (Mammalia, Perissodactyla) du Miocène terminal au Pléistocène supérieur d'Europe occidentale. Geobios 15 (4), 593–598.
- Guérin, C., Valli, A.M., 2000. Le gisement pléistocène supérieur de la grotte de Jaurens à Nespoules, Corrèze, France: les Bovidae (Mammalia, Artiodactyla). Publications du musée des Confluences 1 (1), 7–39.
- Guérin, C., 2007. Biozonation continentale du Plio-Pléistocène d'Europe et d'Asie occidentale par les mammifères: état de la question et incidence sur les limites Tertiaire/Quaternaire et Plio/Pléistocène. Quaternaire. Revue de l'Association française pour l'étude du Quaternaire 23–33.
- Hammer, Ø., Harper, D.A., Ryan, P.D., 2001. PAST: paleontological statistics software package for education and data analysis. Paleontol. Electron. 4, 1–9.
- Hassanin, A., 2014. Systematic and evolution of bovine. In: Melletti, M., Burton, J. (Eds.), Ecology, Evolution and Behavior of Wild Cattle: Implications for Conservation. Cambridge University Press, Cambridge, pp. 7–20.
- Head, M.J., Gibbard, P.L., 2005. Early-Middle Pleistocene transitions: an overview and recommendation for the defining boundary. Geol. Soc. London Special Publications 247, 1–18.
- Head, M.J., Gibbard, P.L., 2015. Early-Middle Pleistocene transitions: linking terrestrial and marine realms. Quat. Int. 389, 7–46.
- Heintz, É., 1970. Les cervidés Villafranchiens de France et d'Espagne. Paris, Abbreviated: Mém. Mus. Natl. Hist. Nat., Sér. C Géol. 22, 206–p.
- Jin, C., Wang, Y., Liu, J., Ge, J., Zhao, B., Liu, J., Zhang, H., Shao, Q., Gao, C., Zhao, K., Sun, B., 2021. Late cenozoic mammalian faunal evolution at the jinyuan cave site of luotuo hill, dalian, northeast China. Quat. Int. 577, 15–28.
- Jungers, W.L., Falsetti, A.B., Wall, C.E., 1995. Shape, relative size, and size-

- adjustments in morphometrics. *Am. J. Phys. Anthropol.* 38, 137–161.
- Das Pleistozän von Taubach bei Weimar. In: Kahlke, H.-D. (Ed.), *Quartarpalaentologie* 2, 1–509.
- Kahlke, R.D., 1999. The History of the Origin, Evolution and Dispersal of the Late Pleistocene *Mammuthus-Coelodonta* Faunal Complex in Eurasia (Large Mammals). Fenske Companies, Rapid City, p. 218 (1999).
- Kelly, A., Miller, K., Joshua, H., DeSantis, L., Wooller, M., Zazula, G., 2021. Niche Stability through Environmental Change: A Late Pleistocene Chronology of *Bison Priscus* Paleocology from Yukon Territory, Canada. SVP 2021 Annual Meeting. 2021 Program and Abstract Book, p. 157.
- Khan, M.A., Kostopoulos, D.S., Akhtar, D.S., Nazir, M., 2010. Bison remains from the upper Siwaliks of Pakistan. *Neues Jahrbuch Geol. Palaontol. Abhand.* 258, 121–128.
- Khan, M.A., Nasim, S., Ikram, T., Ghafoor, A., Akhtar, M., 2011. Dental remains of early bison from the Tatrot formation of the upper Siwaliks, Pakistan. *J. Anim. Plant Sci.* 21 (4), 862–867.
- Klein, R.G., Francis, R.G., Steele, T.E., 2010. Morphometric identification of bovid metapodials to genus and implications for taxon-free habitat reconstruction. *J. Archaeol. Sci.* 37, 389–401.
- Konidaris, G.E., Kostopoulos, D.S., Maron, M., Schaller, M., Ehlers, T.A., Aidona, E., Marini, M., Tourloukis, V., Muttoni, G., Koufos, G.D., Harvati, K., 2021. Dating of the lower pleistocene vertebrate site of Tsotra Vryssi (Mygdonia Basin, Greece): biochronology, magnetostratigraphy, and cosmogenic radionuclides. *Quat. J.* 1, 1.
- Kostopoulos, D.S., 2022. In: Vlachos, E. (Ed.), *Fossil Vertebrates of Greece*, 2. Springer, Cham, pp. 113–203.
- Kostopoulos, D.S., Maniakas, I., Tsoukalas, E., 2018. Early bison remains from Mygdonia Basin (northern Greece). *Geodiversitas* 40, 283–319.
- Kottek, M., Grieser, J., Beck, C., Rudolf, B., Rubel, F., 2006. World map of the Köppen-Geiger climate classification updated. *Meteorol. Z.* 15, 259–263.
- Krijgsman, W., Tesakov, A., Yanina, T., Lazarev, S., Danukalova, G., Van Baak, C.G., Agustí, J., Alçiçek, M.C., Aliyeva, E., Bista, D., Bruch, A., 2019. Quaternary time scales for the Pontocaspian domain: interbasinal connectivity and faunal evolution. *Earth Sci. Rev.* 188, 1–40.
- Lydekker, R., 1878. Crania of ruminants from the Indian tertiaries. *Pal. Indica* 10 (1), 88–171.
- Lopatin, A.V., Vislobokova, I.A., Lavrov, A.V., Startsev, D.B., Gimranov, D.O., Zelenkov, N.V., Maschenko, E.N., Sotnikova, M.V., Tarasenko, K.K., Titov, V.V., 2019. The Taurida cave, a new locality of early pleistocene vertebrates in Crimea. *Dokl. Biol. Sci.* 485 (1), 40–43.
- Lisiecki, L.E., Raymo, M.E., 2005. A Pliocene–Pleistocene stack of 57 globally distributed benthic $\delta^{18}O$ records. *Paleoceanography* 20 (1), PA1003.
- Lona, F., Bertoldi, R., 1972. La storia del Plio-Pleistocene Italiano in alcune sequenze vegetazione-ali lacustri e marine. *Atti Accad. Naz. Lincei Cl. Sci. Fis. Mat. Natur. Memorie Serie 8* (11), 1–47.
- Madurell-Malapeira, J., Ros-Montoya, S., Espigares, M.P., Alba, D.M., Aurell-Garrido, J., 2014. Villafranchian large mammals from the Iberian Peninsula: paleobiogeography, paleoecology and dispersal events. *J. Iber. Geol.* 40, 167–178.
- Maniakas, I., Kostopoulos, D.S., 2017. Morphometric-palaeoecological discrimination between *Bison* populations of the western Palaeartic. *Geobios* 50, 155–171.
- Martinetto, E., Bertini, A., Basilici, G., Baldanza, A., Bizzarri, R., Cherin, M., Gentili, S., Pontini, M.R., 2014. The plant record of the Dunarobba and Pietrafitta sites in the Plio-Pleistocene palaeoenvironmental context of Central Italy. *Alp. Mediterr. Quat.* 27, 29–72.
- Martinetto, E., Momohara, A., Bizzarri, R., Baldanza, A., Delfino, M., Esu, D., Sardella, R., 2017. Late persistence and deterministic extinction of “humid thermophilous plant taxa of East Asian affinity” (HUTEA) in southern Europe. *Palaeoecol. Palaoclimatol. Palaeoecol.* 467, 211–231.
- Martínez-Navarro, B., Pérez-Claros, J.A., Palombo, M.R., Rook, L., Palmqvist, P., 2007. The Olduvai buffalo *Pelorovis* and the origin of *Bos*. *Quat. Res.* 68, 220–226.
- Martínez-Navarro, B., Ros-Montoya, S., Espigares, M.P., Palmqvist, P., 2011. Presence of the Asian origin bovine, *hemibos* sp. aff. *Hemibos gracilis* and *Bison* sp. at the early pleistocene site of Venta Micena (Orce, Spain). *Quat. Int.* 243, 54–60.
- Masini, F., 1989. I Bovini Villafranchiani dell'Italia. Ph.D. Dissertation, Università di Modena-Bologna-Firenze-Roma.
- Masini, F., Palombo, M.R., Rozzi, R., 2013. A reappraisal of the early to middle pleistocene Italian Bovidae. *Quat. Int.* 288, 45–62.
- Maslin, M.A., Brierley, C.M., 2015. The role of orbital forcing in the early middle pleistocene transition. *Quat. Int.* 389, 47–55.
- McDonald, J.N., 1981. North American Bison: Their Classification and Evolution. University of California Press, Berkeley, p. 316.
- Mead, J.I., Jin, C., Wei, G., Sun, C., Wang, Y., Swift, S.L., Zheng, L., 2014. New data on *Leptobos crassus* (Artiodactyla, Bovidae) from renzidong cave, early pleistocene (nihewanian) of anhui, China, and an overview of the genus. *Quat. Int.* 354, 139–146.
- Meiri, S., Yom-Tov, Y., Geffen, E., 2007. What determines conformity to Bergmann's rule? *Global Ecol. Biogeogr.* 16 (6), 788–794.
- Merla, G., 1949. I *Leptobos* rütimeyeri. *Palaentogr. Ital.* 46, 41–155.
- Moullé, P.E., 1992. Les grands mammifères du Pléistocène inférieur de la grotte du Vallonnet (Roquebrune-Cap-Martin, Alpes-Maritimes). Étude paléontologique des Carnivores, Equidés, Suidés et Bovidés. Ph.D. Dissertation, Muséum national d'Histoire naturelle, Paris.
- Mourer-Chauviré, C., 1972. Étude de nouveaux restes de vertébrés provenant de la carrière Fournier à Châtillon-Saint-Jean. III. Artiodactyles, chevaux, oiseaux. *Quaternaire* 9, 271–305.
- Moya-Solà, S., 1987. Los bóvidos (Artiodactyla, Mammalia) del yacimiento del Pleistoceno inferior de Venta Micena (Orce, Granada, España). *Paleontol. Evol. Mem. Esp.* 1, 181–236.
- Olsen, S.J., 1990. Fossil ancestry of the yak, its cultural significance and domestication in Tibet. *Proc. Acad. Nat. Sci.* 73–100. Philadelphia.
- Palmqvist, P., Espigares, M.P., Pérez-Claros, J.A., Figueirido, B., Guerra-Merchán, A., Ros-Montoya, S., Rodríguez-Gómez, G., García-Aguilar, J.M., Granados, A., Martínez-Navarro, B., 2022. Déjà vu: a reappraisal of the taphonomy of quarry VM4 of the early pleistocene site of Venta Micena (baza basin, SE Spain). *Sci. Rep.* 12 (1), 1–16.
- Pazzaglia, F., Barchi, M.R., Buratti, N., Cherin, M., Pandolfi, L., Ricci, M., 2013. Pleistocene calcareous tufa from the Ellera basin (Umbria, central Italy) as a key for an integrated paleoenvironmental and tectonic reconstruction. *Quat. Int.* 292, 59–70.
- Pilgrim, G.E., 1937. Siwalik antelopes and oxen in the American Museum of natural history. *Bull. Am. Mus. Nat. Hist.* 72, 7.
- Pilgrim, G.E., 1939. The fossil Bovidae of India. *Mem. Geol. Surv. India, Pal. Indica*, n.s. 26 (1), 356.
- Pilgrim, G.E., 1947. The evolution of the buffaloes, oxen, sheep and goats. *Zool. J. Linn. Soc.* 41 (279), 272–286.
- Plummer, T.W., Bishop, L.C., 1994. Hominid paleoecology at Olduvai Gorge, Tanzania as indicated by antelope remains. *J. Hum. Evol.* 27, 47–75.
- Polák, J., Frynta, D., 2010. Patterns of sexual size dimorphism in cattle breeds support Rensch's rule. *Evol. Ecol.* 24 (5), 1255–1266.
- Prat, F., Delpéch, F., Cancel, N., Guadelli, J.L., Slott-Møller, R., 2003. Le Bison des steppes, *Bison priscus* Bojanus, 1827, de la grotte d'Hararra à Arudy (Pyrénées-Atlantiques). *PALEO. Revue d'archéologie préhistorique* 15, 1–102.
- Rodrigo, M.A., 2011. Los Bóvidos Villafranchienses de La Puebla de Valverde y Villarroja: sistemática, filogenia y paleobiología. Ph.D. Dissertation, Universidad de Zaragoza.
- Rook, L., Martínez-Navarro, B., 2010. Villafranchian: the long story of a Plio-Pleistocene European large mammal biochronologic unit. *Quat. Int.* 219 (1–2), 134–144.
- Rütimeyer, L., 1867. Versuch einer natürlichen Geschichte des Rindes. *Neuen Denkschr. Allgem. Schweiz. Ges. Naturwiss.* II 22.
- Saareinen, J., Eronen, J., Fortelius, M., Seppä, H., Lister, A.M., 2016. Patterns of diet and body mass of large ungulates from the Pleistocene of Western Europe, and their relation to vegetation. *Palaentol. Electron.* 19 (3), 1–58.
- Saareinen, J., Cirilli, O., Strani, F., Meshida, K., Bernor, R.L., 2021. Testing equid body mass estimate equations on modern zebras—with implications to understanding the relationship of body size, diet, and habitats of *Equus* in the pleistocene of Europe. *Front. Ecol. Evol.* 9, 90.
- Sala, B., 1986. *Bison schoetensacki* Freud, from Isernia la Pineta (early Mid-Pleistocene – Italy) and revision of the European species of bison. *Palaentogr. Ital.* 74, 113–170.
- Schertz, E., 1936. Zur Unterscheidung von *Bison priscus* Boj. und *Bos primigenius* Boj. an Metapodien und Astragalus, nebst Bemerkungen über einige diluviale Fundstellen. *Seckenbergiana* 18, 37–71.
- Schreuder, A., 1946. The Tegelen fauna, with a description of new remains of its rare components (*Leptobos*, *Archidiskodon meridionalis*, *Macaca*, *Sus strozzi*). *Arch. Neerl. Zool.* 7 (1), 153–204.
- Scott, K.M., 1979. Adaptation and Allometry in Bovid Postcranial Proportions. Ph.D. Dissertation, Yale University, New Haven.
- Scott, K.M., 1983. Prediction of body weight of fossil Artiodactyla. *Zool. J. Linn. Soc.* 77 (3), 199–215.
- Scott, K.M., 1985. Allometric trends and locomotor adaptations in the Bovidae. *Bull. Am. Mus. Nat. Hist.* 197, 197–288.
- Scott, R.S., Barr, W.A., 2014. Ecomorphology and phylogenetic risk: implications for habitat reconstruction using fossil bovids. *J. Hum. Evol.* 73, 47–57.
- Shani, M.R., Khan, E., 1968. *Proboscidea* n. g. n. sp., a recent find of the Upper Siwalik bovid. *Mittl. Bayer. Staatssamm. Palaontol. Hist. Geol.* 8, 247–251.
- Sher, A.V., 1997. An early quaternary *Bison* population from untermaßfeld: *Bison merner* sp. nov. In: Kahlke, R.D. (Ed.), *Das Pleistozän von Untermaßfeld bei Meiningen* (Thüringen). Teil 2. Habelt-Verlag, Bonn, pp. 101–180.
- Simpson, G.G., 1941. Large pleistocene felines of North America. *Am. Mus. Novit.* 1136, 1–27.
- Skinner, M.R., Kaisen, O.C., 1947. The fossil *Bison* of Alaska and preliminary revision of the genus. *Bull. Am. Mus. Nat. Hist.* 89, 123–256.
- Sorbelli, L., Alba, D.M., Cherin, M., Moullé, P.E., Brugal, J.P., Madurell-Malapeira, J., 2021a. A review on *Bison schoetensacki* and its closest relatives through the early-Middle Pleistocene transition: insights from the Vallparadis Section (NE Iberian Peninsula) and other European localities. *Quat. Sci. Rev.* 261, 106933.
- Sorbelli, L., Villa, A., Gentili, S., Cherin, M., Carnevale, G., Tschopp, E., Delfino, M., 2021b. The early pleistocene ectothermic vertebrates of Pietrafitta (Italy) and the last western European occurrence of *latonia meyer*, 1843. *C. R. Palevol.* 20 (26), 555–583.
- Stephenson, R.O., 2001. Wood bison in late Holocene Alaska and adjacent Canada: paleontological, archaeological and historical records. In: SC Gerlach and MS Murray. *Wildlife and People in Northern North America. Essays in Honor of R. Dale Guthrie*. British Archaeological Reports, International Series, p. 944.
- Teilhard de Chardin, P., Piveteau, J., 1930. Les mammifères fossiles de Nihowan (Chine). *Ann. Paleontol.* 19, 1–134.
- Teilhard de Chardin, P., Trassaert, M., 1938. Caviconia of south-south-eastern shansi. *Pal. Sin. New Ser. C* 6, 1–106.

L. Sorbelli, M. Cherin, D.S. Kostopoulos et al.

Quaternary Science Reviews 301 (2023) 107923

- Tong, H.W., Chen, X., Zhang, B., 2016. New fossils of *Bison palaeosinensis* (Artiodactyla, Mammalia) from the steppe mammoth site of early pleistocene in Nihewan Basin, China. *Quat. Int.* 445, 450–468.
- Toniato, G., Marabini, S., Sala, B., Vai, G.B., 2017. Revised bison skull from the Salita di Oriolo quarry near Faenza, "sabbie gialle". Pleistocene, Northern Apennines. *Alp. Mediterr. Quat.* 30 (1), 11–23.
- Torre, D., Ficcarelli, G., Masini, F., Rook, L., Sala, B., 1992. Mammal dispersal events in the early pleistocene of western Europe. *Cour. Forsch. Inst. Senckenberg* 153, 51–58.
- Vasiliev, S.K., 2008. Late Pleistocene bison (*Bison p. priscus* Bojanus, 1827) from the southeastern part of western Siberia. *Archaeol. Ethnol. Anthropol. Eurasia* 34, 34–56.
- Vercoutère, C., Guérin, C., 2010. les Bovidae (Mammalia, Artiodactyla) du Pléistocène moyen final de l'Aven de Romain-La-Roche (Doubs, France). *Rev. Paleobiol.* 9, 655–696.
- Verestchagin, N.K., 1959. The Mammals of the Caucasus. A History of the Fauna. Academia Nauk, Leningrad (Translated from Russian. Israel Program for Scientific Translations, Jerusalem, 1967.
- Viret, J., 1949. La vie dans la moyenne vallée du Rhône au début des temps quaternaires (Essai d'écologie de la faune des mammifères fossiles de Saint-Vallier). *Bull. Mens. Soc. Linn. Lyon* 18, 20–24.
- Viret, J., 1954. Le loess à banc durcis de Saint-Vallier (Drôme) et sa faune de mammifères villafranchiens. Avec une analyse granulométrique. *Nouv. Arch. Mus. Hist. Nat. Lyon* 4, 1–200.
- Vlerk, I.M. van der, 1942. Kwartaire Bovidae van Nederland. De schedels en hoornpitten, welke zich bevinden in het Rijksmuseum van Geologie te Leiden. *Leidse Geol. Meded.* 13 (1), 1–28.
- Zheng, S.H., Wu, W.Y., Li, Y., Wang, G.D., 1985. Late cenozoic mammalian faunas of guide and Gonghe basins, qinghai province. *Vert. PalAs.* 23, 89–134 (in Chinese).



Chapter 5.



The results of this chapter were published as:

Sorbelli, L., Alba, D.M., Cherin, M., Moullé, P.É., Brugal, J.P. and Madurell-Malapeira, J., 2021. A review on *Bison schoetensacki* and its closest relatives through the early-Middle Pleistocene transition: Insights from the Vallparadís Section (NE Iberian Peninsula) and other European localities. *Quaternary Science Reviews*, 261: 106933.

DOI: <https://doi.org/10.1016/j.quascirev.2021.106933>

Original paper presented in **chapter 5**. Supplementary material presented in **chapter S3**.

In this work, Leonardo Sorbelli contributed in:

- (I) Original conceptualization of the paper.
- (II) Direct observation and study of the fossil material.
- (III) Formal analysis of the data.
- (IV) Interpretation and discussion of the results.
- (V) Writing of the original draft.
- (VI) Review and editing of the final draft.
- (VII) Funding acquisition.



A review on *Bison schoetensacki* and its closest relatives through the early-Middle Pleistocene transition: Insights from the Vallparadís Section (NE Iberian Peninsula) and other European localities

Leonardo Sorbelli ^a, David M. Alba ^a, Marco Cherin ^b, Pierre-Élie Moullé ^c, Jean-Philip Brugal ^d, Joan Madurell-Malapeira ^{a,*}

^a Institut Català de Paleontologia Miquel Crusafont, Universitat Autònoma de Barcelona, Edifici ICTA-ICP, c/ Columnes s/n, Campus de la UAB, 08193, Cerdanyola del Vallès, Barcelona, Spain

^b Dipartimento di Fisica e Geologia, Università degli Studi di Perugia, Via A. Pascoli, 06123, Perugia, Italy

^c Musée de Préhistoire Régionale de Menton, 06500, Menton, France

^d Aix-Marseille Université, CNRS, Minist. Culture, UMR 7269 Lampea, MMSH, 13094, Aix-en-Provence, Cedex 2, France

ARTICLE INFO

Article history:

Received 4 December 2020

Received in revised form

17 March 2021

Accepted 2 April 2021

Available online xxx

Handling Editor: Danielle Schreve

Keywords:

Bison

Bovidae

Early-Middle Pleistocene transition

Epivillafranchian

Europe

Quaternary

ABSTRACT

The evolutionary history of *Bison* is a matter of debate due to the scarcity of fossil remains from the earliest members of this clade and the close morphological similarities among species. To clarify the taxonomic status of the earliest stouter bison and their relationships to their putative ancestor, *Leptobos*, as well as other primitive forms traditionally referred to subgenus *Bison* (*Eobison*), we carry out a complete revision of the available European fossil record, with a focus on the forms occurring during the Early-Middle Pleistocene Transition. Emphasis is put on the description of the unpublished *Bison* remains from the Vallparadís Composite Section (VCS), including the sites of Cal Guardiola and Vallparadís Estació (Terrassa, NE Iberian Peninsula). VCS fossiliferous layers yielded one of the richest faunal assemblages from the European latest Early Pleistocene and one of the few European fossil sites covering almost entirely the Early-Middle Pleistocene Transition (1.2–0.6 Ma). The collection comprises thousands of ungulates remains, especially abundant fossils of a large *Bison* species. The morphology of the postcranial sample from VCS fits that of *Bison* (*Bison*) *schoetensacki*, i.e., the earliest stout bison (*Bison* s.s.) recorded in Europe. We studied more than 200 cranial and postcranial elements with a focus on the metapodial remains. Comparisons were performed with all the available fossil record of Pleistocene Eurasian fossil *Bison* species. We confirm the taxonomic validity of *B. schoetensacki* and recognize distinct ecomorphotypes of European bison between the late Early Pleistocene and the beginning of the Holocene based on the size and proportions of the metapodials. Although the appendicular skeleton shows reliable characters for the diagnosis of different species, the great morphological homogeneity recognized within the genus requires a cautious approach in systematic studies based on postcranial material.

© 2021 Elsevier Ltd. All rights reserved.

1. Introduction

The genus *Bison* Hamilton Smith, 1827 includes two extant species, the North American bison (*Bison bison*) and the European bison or wisent (*Bison bonasus*). Additional extinct species are distinguished, but the evolutionary history of this group is still unclear, mainly due to the difficulty in distinguishing early *Bison* remains from those of its putative ancestor. Nowadays, it is

commonly accepted that *Bison* originated during the Early Pleistocene from a species of mid-sized bovid *Leptobos* (e.g., Pilgrim, 1947; Brugal, 1985; Masini, 1989; Bukhsianidze, 2005; Martínez-Navarro et al., 2007). During the last century, a large amount of *Bison* remains has been discovered from many European Quaternary sites and several species, or sub-species, of this genus, or subgenus, have been described fueling the debate regarding the evolutionary history of this group of Bovini (Masini, 1989; Sher, 1997; Bukhsianidze, 2005; Maniakas and Kostopoulos, 2017a; Kostopoulos et al., 2018) (Fig. 1).

* Corresponding author.

E-mail address: joan.madurell@icp.cat (J. Madurell-Malapeira).

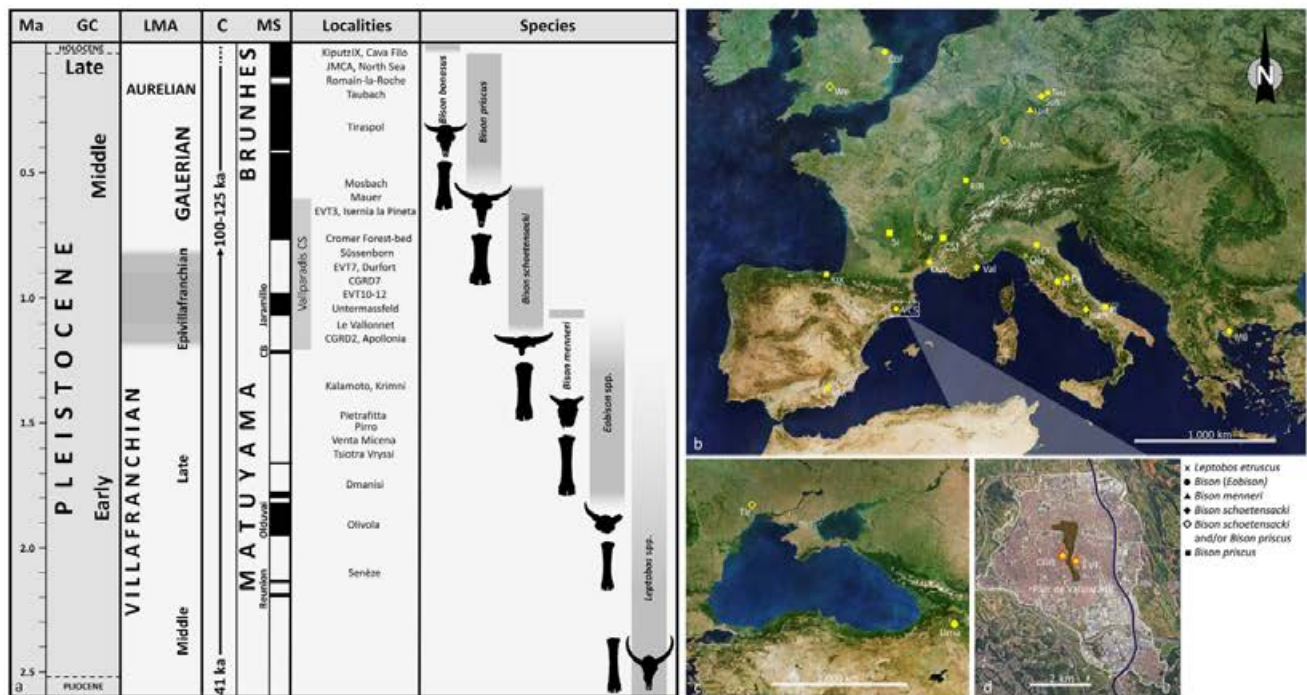


Fig. 1. a, Quaternary time scale showing the chronological/biochronological distribution of the studied taxa in Europe and the most important Early-Middle Pleistocene sites mentioned in the text. b, Map of Europe with the location of some of the sites mentioned in the text. c, Focus on the Black Sea area. d, Geographic location of the studied sites of Cal Guardiola and Vallparadis Estació in the town of Terrassa (Iberian Peninsula). Abbreviations: Ma, million years ago; GC, geochronology; LMA, Land Mammal Age; C, glacial/interglacial cyclicity; MS, magnetostratigraphy; CF, Cava Filo (Italy); CBF, Cromer Forest-Bed sites (United Kingdom); Ce, Cesi (Italy); CSL, Châtillon-Saint-Jean (France); Dma, Dmanisi (Georgia); Dur, Dürfort (France); Ise, Isernia La Pineta (Italy); KIX, Kiputz IX (Spain); Mau, Mauer (Germany); MB, Mygdonia Basin sites (Greece); Mos, Mosbach (Germany); Olv, Olivola (Italy); Pf, Pietrafitta (Italy); Pir, Pirro (Italy); RIR, Romain-la-Roche (France); Se, Senèze (France); Si, Siréjol cave (France); Sus, Süssenborn (Germany); Tau, Taubach (Germany); Tir, Tiraspol (Ukraine); Unt, Untermassfeld (Germany); Val, Le Vallonnet (France); VCS, Vallparadis Composite Section (Spain); VM, Venta Micena (Spain); We, Westbury (United Kingdom).

1.1. The European record of *Leptobos*

The genus *Leptobos* includes medium-sized slender bovids from the whole Villafranchian Land Mammal Age (sensu Rook and Martínez-Navarro, 2010), being constantly present in the faunal assemblages from the Late Pliocene to most of the Early Pleistocene across Eurasia (from Iberia to northern China). According to the most recent review (Cherin et al., 2019), this genus includes the following species: *Leptobos brevicornis* and *Leptobos crassus* (China), *Leptobos falconeri* (Pakistan), *Leptobos stenometopon* and *Leptobos merlai* (France and Italy), *Leptobos furtivus* (France and, possibly, Italy), *Leptobos etruscus* (France, Italy, and Spain), and *Leptobos vallisarni* (Italy and China). According to Masini et al. (2013), *Leptobos* species from Europe can be divided into two groups or lineages: one includes *L. stenometopon*, *L. merlai*, and *L. furtivus*; and the other includes *L. etruscus* and *L. vallisarni*. The latter group comprises the younger, larger and more derived *Leptobos* species, which have been considered—not without controversy (Bukhsianidze, 2005)—as possible ancestors of bison (Masini, 1989). The dispersal of bison from Asia marks the last occurrences of *Leptobos* in Europe, even if the coexistence between early *Bison* and *Leptobos* seems documented in some late Villafranchian Chinese, Greek-Balkan and Eastern Europe localities (Duvernois, 1990; Tong et al., 2016; Agadzhanian et al., 2017; Kostopoulos et al., 2018; Lopatin et al., 2019).

1.2. Earliest Asian and European bison

The earliest occurrences of *Bison* date to the Late Pliocene–Early

Pleistocene of Southeast Asia (Tong et al., 2016). The poorly-known *Bison (Eobison) sivalensis* from India (3.4–2.6 Ma) and *Bison (Eobison) palaeosinensis* from China (ca. 2.6 Ma) share some features with the most derived *Leptobos* species and differ in size and cranial morphology from “true” bison of subgenus *Bison* s.s. (Flerov, 1972; Tong et al., 2016). In some areas of Asia, these primitive bison might have been partially coeval and even co-occurring for some time with *Leptobos*, which eventually went extinct by the end of the Villafranchian (Tong et al., 2016).

Flerov (1972) erected the subgenus *Eobison* to include the two aforementioned primitive Asian species as well as the poorly-known *Bison (Eobison) tamanensis* from Europe, first described by Verestchagin (1959). Later on, *Eobison* has been widely used, either as a subgenus (Masini et al., 2013) or as a separate genus (Geraads, 1992), to allocate all the Early Pleistocene small-sized bison remains from Europe. However, this taxonomic arrangement has been recently questioned (Bukhsianidze, 2005; Kostopoulos et al., 2018), by showing that *Eobison* is a weakly defined taxon and that some forms previously included in this subgenus should be transferred to *Bison (Bison)* (e.g., *Bison degiulii*).

The earliest record of *Bison* in Europe is represented by *B. (Eobison) georgicus* from Dmanisi (Georgia; 1.76 Ma; Burchak-Abramovich and Vekua, 1994; Bukhsianidze, 2005). Other species from Eastern Europe include the above-mentioned *B. tamanensis*, from the Epivillafranchian (ca. 1 Ma) of the Azov Sea area, and whose taxonomic status is uncertain (being considered a species inquirenda by Kostopoulos et al., 2018), as well as *Bison suchovi* from the late Villafranchian of Dolinskoye (Ukraine; Alekseeva, 1967, 1977), whose taxonomic validity has similarly been

questioned (Sher, 1997).

The earliest records of the genus *Bison* from Europe include: *Bison* sp. from Venta Micena (Spain; ca. 1.5 Ma; Moyà-Solà, 1987; Martínez-Navarro et al., 2011); *B. (Eobison)* sp. from Le Riège (France; ca. 1.4 Ma; Ambert et al., 1996); *B. (Eobison) degiulii* from Pirro Nord and Capena (Italy; ca. 1.6–1.2 Ma; Masini, 1989; Masini et al., 2013); and *Bison* cf. *degiulii* from the Mygdonia Basin (Greece; ca. 1.7–1.2 Ma; Kostopoulos et al., 2018). By the end of the Early Pleistocene, the first “true” large bison appear, being represented by the long-legged *Bison (B.) menneri* from Untermassfeld (Germany; 1.05 Ma; MIS31; Sher, 1997; Bukhsianidze, 2020)—recently included in the subgenus *Bison (Poephagus)* by Bukhsianidze (2020)—and the relatively stouter woodland wisent *B. (B.) schoetensacki* from Le Vallonnet (France; ca. 1.2 Ma; Moullé, 1992), Durfort (France; ca. 1.0; Brugal, 1995), Mauer (Germany; ca. 0.6 Ma; Freudenberg, 1914), Süssenborn (Germany; ca. 0.6 Ma; Flerov 1969) and Isernia La Pineta (Italy; ca. 0.58 Ma; Sala, 1986; Peretto et al., 2015). *Bison menneri* and *Bison schoetensacki* are characterized by derived cranial features, large body size, relatively long limbs, and short and swollen horn-cores. During this same period, *Bison* cf. *menneri* and *Bison (Bison) voigtstedtensis* have been respectively recorded from Gran Dolina TD8 and Sima del Elefante TE9c (Spain; ca. 1.1–0.75 Ma; Huguet et al., 2017; Van der Made et al., 2017). The taxonomic status of *B. voigtstedtensis*, originally described on the basis of cranial material from Voigtstedt (Germany; ca. 0.7 Ma), has been debated, being considered a subspecies of *Bison (Bison) schoetensacki* by some authors (e.g., Fischer, 1965; Sala, 1986; Brugal, 1995; van Asperen and Kahlke, 2017), and a distinct species by others (e.g., Flerov, 1979; Van der Made et al., 2017).

Only by the mid-Middle Pleistocene, the well-known steppe bison, *Bison (Bison) priscus*, with the two subspecies *B. priscus priscus* and *B. priscus mediator*, appears in eastern Eurasia (Kahlke, 1999). This massive species exhibits stouter limbs, larger head, and longer horns than earlier bison, but is overall very polymorphic throughout its chronostratigraphic and geographic range (Kahlke, 1999). The steppe bison dispersed across the whole Holarctic, reaching North America through Beringia and giving rise to the American bison lineages in the Late Pleistocene, as demonstrated by fossil and molecular evidence (Shapiro et al., 2004; Froese et al., 2017). In turn, the extant European wisent *Bison (B.) bonasus* appears during the Late Pleistocene as a possible relative of the steppe bison (Soubrier et al., 2016) or, with more uncertainty, to the woodland wisent, with probable introgression from the auroch (*Bos primigenius*), as testified by recent molecular studies (e.g., Palacio et al., 2017; Grange et al., 2018).

2. The Vallparadís Composite Section

The Vallparadís Composite Section (VCS) includes the paleontological open-air sites of Cal Guardiola (CGR) and Vallparadís Estació (EVT), located in the Vallès-Penedès Basin (NE Iberian Peninsula; Madurell-Malapeira et al., 2010, 2017; Fig. 1). During the excavations carried out between 1997 and 2008, more than 30 000 remains of vertebrates from the late Early to Middle Pleistocene sequences were recovered from CGR and EVT. The two sites are characterized by a depositional setting influenced by the dynamics of an alluvial fan system and the geometry of the Miocene paleo-relief. The excavated sediments consist of debris-flows and mud-flows resulting from alluvial fan system dynamics with influence of close colluvial processes.

Biochronological, magnetostratigraphic, and U-series-ESR data indicate that the VCS ranges from before the Jaramillo paleomagnetic subchron (ca. 1.1–1.0 Ma) to the early Middle Pleistocene (ca.

0.6 Ma; Madurell-Malapeira et al., 2010, 2012, 2014, 2017; Minwer-Barakat et al., 2011). The timespan embraced by the VCS can be divided into four different time intervals (Madurell-Malapeira et al., 2010, 2014, 2017; Minwer-Barakat et al., 2011): (1) pre-Jaramillo (layers CGRD1 to CGRD3); (2) Jaramillo subchron interval (layers EVT9 to EVT12); (3) post-Jaramillo, Matuyama (layers EVT4 to EVT7 and CGRD4 to CGRD8); and (4) early Middle Pleistocene interval (layers EVT2 and EVT3).

The timespan comprised between 1.25 and 0.6 Ma was marked by the onset of new asymmetric glacial/interglacial cycles that affected climate (decrease in temperatures and humidity coupled with seasonality with longer and harsher winters) as well as vegetation structure (long alternations between steppe and deciduous forests) in Europe—the so-called ‘Early-Middle Pleistocene Transition’ (EMPT; Head and Gibbard, 2005; Clark et al., 2006). In the older part of the VCS (ca. 1.1 Ma) the pollen and wood analyzed from CGRD2 suggest a warm-temperate and humid paleoenvironment, indicating the presence of a river or river-marsh ecosystem with a variety of plant groups, from aquatic macrophytes to deciduous trees and grasses. The abundance of hippo remains in this layer is consistent with the inferred fluvial/lacustrine main depositional environment, and the high diversity of large-sized ungulates such as deer, horses, and bison suggest the existence of a wide spectrum of different environments in the surroundings, including woodlands and more open and dry areas (Mijarra et al., 2007). Meso- and microwear analyses performed on a large sample of ungulate teeth from VCS indicate that, since 0.9 Ma (MIS22), the paleoenvironments experienced a substantial change, from the predominance of open dry grasslands with a certain seasonality (Layer EVT12, ca. 1.0 Ma; MIS31) to more humid woodlands with, possibly, an even more marked seasonality (Layers EVT7 and CGRD7; ca. 0.86 Ma; MIS21), in agreement with data from other Southern European coeval sites (Strani et al., 2019).

3. Materials and methods

The VCS bovid sample analyzed herein is housed in the Institut Català de Paleontologia Miquel Crusafont (ICP), Sabadell, Spain. The complete list of specimens is reported Table S1. The stratigraphic provenance of the bovid material is unbalanced: 135 specimens come from CGRD7 and EVT7 (0.86–0.78 Ma); 70 from EVT10 and EVT12 (1.07–0.99 Ma); 14 from CGRD2, CGRD3, and CGRD4 (1.1–1.0 Ma); and 4 from EVT3 (<0.6 Ma). The descriptions of dental and postcranial features follow the nomenclature used by Masini (1989), Sala (1986), Sher (1997), and Maniakas and Kostopoulos (2017a). Measurement abbreviations are explained in Table 1 and shown in Fig. 2. Measurements are partially modified from Brugal (1985), Masini (1989) and Maniakas and Kostopoulos (2017a). All measurements were taken with a digital caliper to the nearest 0.1 mm. Juvenile specimens are not included in the analyses.

Throughout this work we use *Bison* s.l. for all members of the genus *Bison*, and *Bison* s.s. for species referred to the subgenus *Bison (Bison)*, i.e., excluding those commonly attributed to *Bison (Eobison)*.

Comparative material of *Leptobos* spp. from Upper Valdarno and Olivola (Tuscany, Italy), *Leptobos* aff. *vallisarni* from Pietrafitta (Umbria, Italy) and *Bison schoetensacki* (Isernia La Pineta, Italy) studied by us is housed, respectively, in the IGF, MPLB, and MPPPL—see institutional abbreviations below. Other comparative data were taken from the literature.

Z-scores were used to compare dental measurements of the described specimens with those from other samples. Box plots of the ratio (%) between tooth width and length (W/L%) and bivariate plots of L vs W were employed to assess the size and proportions of

Table 1
Abbreviations of the measurements taken and shown in Fig. 2.

Abbreviation	Measurement taken
ABETl	Abaxial emicondyle thickness (lateral emicondyle)
ABETm	Abaxial emicondyle thickness (medial emicondyle)
AETm	Axial emicondyle thickness (medial emicondyle)
AL	Articular surface length
AT	Articular surface thickness
BLm	Calcaneum minimum length (medial view)
BLp	Calcaneum body length (posterior view)
CBHmin	Calcaneum body minimum height
CBWmin	Calcaneum body minimum width
CH	Centrum height
CL	Centrum length
CW	Centrum width
DDT	Distal diaphysis thickness
DDW	Distal diaphysis width
DEAAW	Distal epiphysis astragalus articulation width
DEAT	Distal end articular thickness
DEATmin	Distal end articular thickness (without the distal end of ulna)
DEAW	Distal end articular width
DET	Distal end thickness
DETI	Distal end thickness (lateral trochlear crest)
DETM	Distal end thickness (medial trochlear crest)
DEW	Distal end width
DT	Diaphysis thickness (midshaft)
DTmin	Diaphysis minimum thickness
DW	Diaphysis width (midshaft)
DWmin	Diaphysis minimum width
GL	Glenoid cavity length
GPL	Glenoid process length
GW	Glenoid cavity width
Hmax	Maximum height
HST	Height at sustentaculum tali level
HTC	Height of tuber calcanei
L	Length
Ll	Lateral length
Lmax	Maximum length
Lmin	Minimum length
MFL	Malleolar facet length
MPW	Malleolar facet width
NCFL	Cubonavicular articular facet length
NSL	Neural spine length
NSW	Neural spine width
OL	Olecranon length
OTmin	Olecranon minimum thickness
OW	Olecranon fossa width
PEAT	Proximal end articular thickness
PEATI	Lateral facet articular thickness (proximal end)
PEAW	Proximal end articular width
PET	Proximal end thickness
PEW	Proximal end width
PFOl	Metatarsal proximal articular facet oblique diameter (lateral facet)
PFOm	Metatarsal proximal articular facet oblique diameter (medial facet)
PFWl	Metacarpal proximal articular facet width (lateral facet)
PFWm	Metacarpal proximal articular facet width (medial facet)
SCW	Spinal canal width
SOL	Oblique length of the sole
STT	Sustentaculum tali thickness
T	Thickness
TCH	Trochlea crest height
THl	Lateral trochlear height
THm	Medial trochlear height
TI	Lateral thickness
TTl	Trochlea thickness (lateral epicondyle)
TTm	Trochlea thickness (medial epicondyle)
TTW	Intertrochlear width
TWl	Trochlear lateral articulation width
TWm	Trochlear medial articulation width
Wmax	Maximum width
Wmin	Minimum width
WTC	Width of tuber calcanei

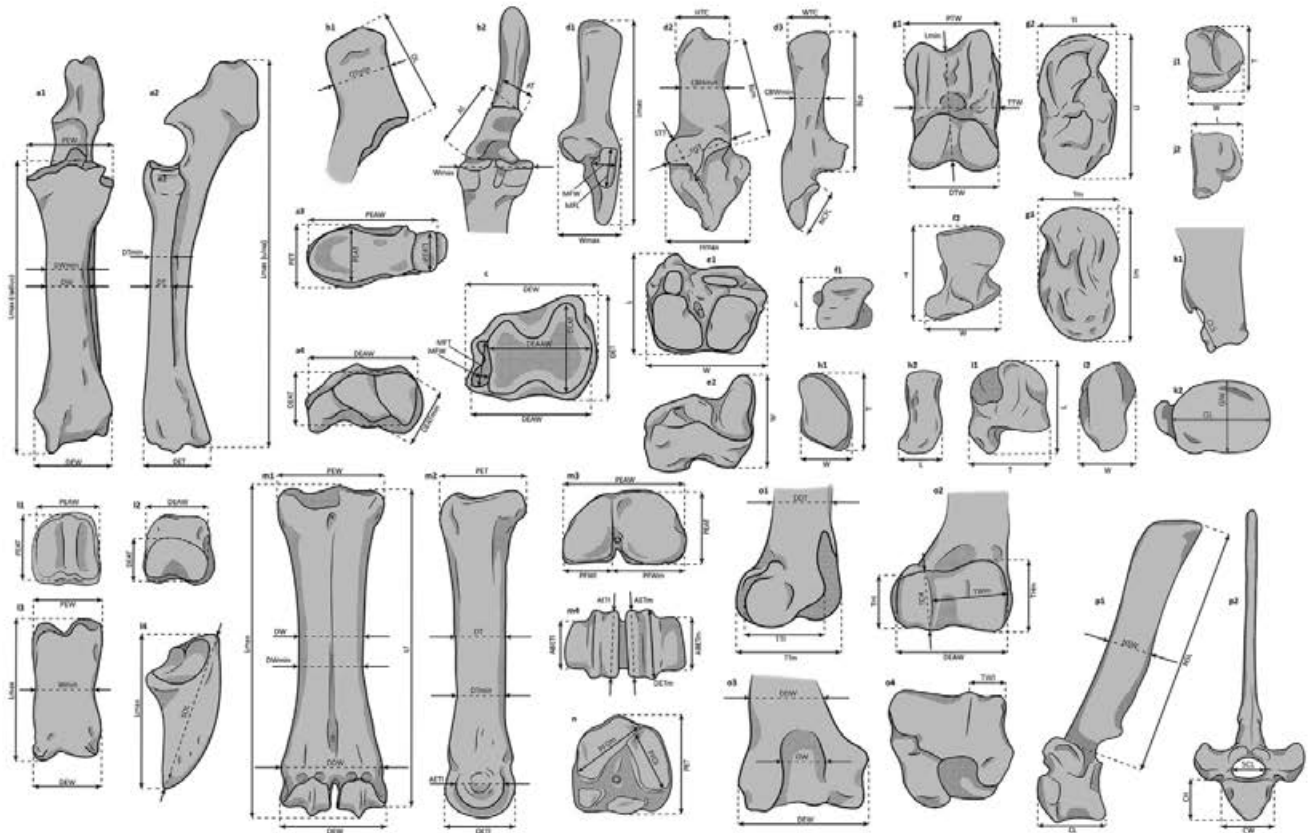


Fig. 2. Some of the measurements taken on postcranial bones in this work: a, radioulna in anterior (1), lateral (2) proximal (3) and distal (4) views; b, ulna in lateral (1) and anterior (2) views; c, tibia in distal view; d, calcaneum in anterior (1), medial (2) and posterior (3) views; e, cubonavicular in distal (1) and anterior (2) views; f, semilunar in proximal (1) and anterior (2) views; g, astragalus in anterior (1), lateral (2) and medial (3) views; h, cuneiform in distal (1) and medial (2) views; i, pyramidal in lateral (1) and proximal (2) views; j, unciform in proximal (1) and lateral (2) views; k, scapula in lateral (1) and distal (2) views; l, phalanx in proximal (1), distal (2) and anterior (3) views; m, metacarpal in anterior (1), posterior (2), proximal (3) and distal (4) views; n, metatarsal in proximal view; o, humerus in lateral (1), posterior (2), anterior (3) and distal (4) views; p, thoracic vertebra in anterior (1) and lateral (2) views. Abbreviations as in Table 1.

the molars among the different *Bison* s.l. populations. Two shape indices were computed for the humerus to distinguish *Bison* from *Bos* and *Leptobos*: Stampfli's trochlea index (Stampfli, 1963), computed as the ratio (%) between DEAW and TWI; and Lehmann trochlear index (Martin, 1987), computed as the ratio (%) between THl and THm (all measurement abbreviations are explained in Table 1). To distinguish *Bison* from *Bos* metapodials we used an index expressed as the ratio (%) between DEW and DDW (Delpech, 1972). A shape index for the metacarpals was computed as the ratio (%) between PFWl and PFWm. To quantify the magnitude of sexual dimorphism in metacarpals we applied, to the samples in which putative males and females were recognized, the equation given by Schertz (1936b): $(x_1 - x_2)/x_1 * 100$, where x_1 and x_2 are the average male and female value, respectively, for the selected variable. To identify sources of significant biometric differences within the VCS sample, we performed (1) univariate ANOVA on eight variables (raw values of Lmax, PEW, PET, DW, DT, DEW, DT) for metacarpals and metatarsals from the two main chronologies of VCS (1.07–0.99 Ma and 0.86–0.78 Ma) and (2) a MANOVA on the complete metapodials (metacarpals and metatarsals analyzed separately) based on five variables (raw values of Lmax, PEW, DW, DEW, DEW/Lmax%). Moreover, biometric differences in teeth were assessed by means of an ANOVA based on the W/L% ratio of M2 and M3 (the scarcity of specimens from different layers prevented us to perform the same analysis on other teeth). Significance level set at

0.05. To assess the stoutness of metapodials, bivariate plots of Lmax vs DEW/Lmax % were employed. Log₁₀ ratio diagrams (Simpson, 1941) were constructed based on the average values of seven selected variables of *Bison* samples from various Eurasian sites. The extant *Bison bonasus* was used as a standard of comparison ($y = 0$; data taken from Reshetov and Sukhanov, 1979). Principal component analyses (PCAs) were performed based on metacarpal and metatarsal bones separately to explore the main morphological differences among different extinct *Bison* forms and series. Two sets of variables were used. The first approach relies on seven Mosimann shape variables (Table 2) obtained by log-transforming the ratio between each measurement and the geometric mean of the seven measurements for each specimen (Jungers et al., 1995). The second approach considers eight variables calculated following Scott and Barr (2014), i.e., adjusting each measurement as the log transformed ratio between the measurement and Scott's (2004) metapodial global size variable (MGSV). $MGSW = ((PEW * PET * DW * DT * ABETI * AETm * DEW * (DETm * DETI))^{1/2})^{1/9}$. For consistency, a second multivariate approach was used with the computation of a MANOVA on seven raw variables (Lmax, PEW, PET, DW, DT, DEW, DET). Significance level was set at 0.05.

Statistical computations were made with PAST v. 3 (Hammer et al., 2001).

Institutional abbreviations: AUTH, Aristotle University of Thessaloniki, Greece; GNM, Georgina National Museum, Tbilisi

Table 2

Shape variables used for the principal component analysis. Abbreviations: DETI, distal epiphysis thickness (lateral trochlear crest); DETm, distal epiphysis thickness (medial trochlear crest); DEW, distal epiphysis width; DT, diaphysis thickness (midshaft); DW, diaphysis width (midshaft); Lmax, maximum length; MGSV, metapodial global size variable (for the equation see Section 3); ms, Mosimann shape variable; PET, proximal epiphysis thickness; PEW, proximal epiphysis width; re, relative.

Selected Mosimann shape variables	Fig. 10a	Relative dimension variables, after Scott and Barr (2014)	Fig. 10b
msLmax = Log(Lmax/GM)	1a	reLmax = Log(Lmax/MGSV)	1 b
msPET = Log(PET/GM)	2a	reDW = Log(DW/MGSV)	2 b
msPEW = Log(PEW/GM)	3a	reDT = Log(DT/MGSV)	3 b
msDT = Log(DT/GM)	4a	reDETI = Log(DETI/MGSV)	4 b
msDW = Log(DW/GM)	5a	reDETm = Log(DETm/MGSV)	5 b
msDETm = Log(DETm/GM)	6a	reDEW = Log(DEW/MGSV)	6 b
msDEW = Log(DEW/GM)	7a	rePEW = Log(PEW/MGSV)	7 b
		rePET = Log(PET/MGSV)	8 b

(Georgia); HLMD Hessisches Landesmuseum, Darmstadt (Germany); ICP, Institut Català de Paleontologia Miquel Crusafont, Sabadell (Spain); IGF, Museo di Storia Naturale, Sezione di Geologia e Paleontologia, Università di Firenze (Italy); IPHES, Institut Català de Paleocologia Humana i Evolució Social, Tarragona (Spain); IQW, Senckenberg Research Station of Quaternary Palaeontology, Weimar (Germany); IVPP, Institute of Vertebrate Paleontology and Paleoanthropology, Beijing (China); MCM, Musée Cuvier de Montbéliard (France); MNHN, Muséum national d'Histoire naturelle, Paris (France); MPLB: Museo Paleontologico Luigi Boldrini" di Pietrafitta (Italy); MPPPL, Museo di Paleontologia e Preistoria Piero Leonardi, University of Ferrara (Italy); MPRM, Musée de Préhistoire Régionale, Menton (France); MuPA, Museo Archeologico e Paleontologico, Serravalle del Chienti (Italy); NAS, National Alliance of Shidlovskiy "Ice Age Period" "Ice Age Museum", Moscow (Russia); UNIFE, Prehistoric Sciences section of the Department of Humanistic Studies, University of Ferrara (Italy).

4. Systematic paleontology

Order Artiodactyla Owen, 1841
 Family Bovidae Gray, 1821
 Subfamily Bovinae Gray, 1821
 Genus *Bison* Hamilton Smith, 1827
 Subgenus *Bison* Hamilton Smith, 1827
Bison (Bison) schoetensacki Freudenberg, 1914
 (Figs. 3–8; Figs. S1–3)

4.1. Referred specimens

The VCS sample includes a total of 90 cranial (Figs. 3–4) and 130 postcranial (Figs. 4–8; Figs. S1–3) remains. See Table S1 for details.

4.2. Descriptions

4.2.1. Horn cores

Description—Only a well-preserved apical portion of a horn core (IPS92970; Fig. 4c) and several fragments of a basal part of a second horn (IPS92971) were recovered from EVT7 and EVT10, respectively. In IPS92970 the tip curves markedly upward, the section is subcircular, slightly dorso-ventrally compressed in the basal portion. In dorsal view, the horn core is slightly curved backward along the longitudinal axis. The longitudinal grooves along the surface are quite shallow and more pronounced on the ventral side in the proximal portion. Narrower, shorter, and shallower furrows are present on the dorsal portion of the tip. IPS92971 is severely fragmented. The estimated large diameter and the presence of sinuses on the internal side of some fragments suggest that the remains represent the basal portion of the horn core. Relatively deep furrows are present on the external ventral surface. No further

characters are recognizable.

Remarks and comparisons—Bovine horn cores are very variable, also within *Bison*. Early bison species (e.g., *B. menneri*) are characterized by short horns that emerge backward (i.e., inserted caudally) and commonly taper abruptly, whereas the more derived species (e.g., *B. priscus*) have longer, laterally inserted, and more gently tapering horn cores (Sala, 1986). *Bison schoetensacki* shows an intermediate morphology. Even if these features are relatively stable, it must be taken into account that the size, shape, and position of horn cores in *Bison* spp. are strongly influenced by sexual dimorphism and ontogenetic stage. This may cause erroneous taxonomic attributions of fossils, especially based on small samples. The horn cores from VCS are too fragmentary to substantiate a determination to species rank, mainly because their basal portion is not preserved. However, the two available specimens (especially IPS92970) exhibit some features (ventral furrows in the middle portion of the horn core, smaller dorsal furrows on the tip, dorso-ventral compression of the horn core, and backward bending of the tip) that have previously been described by Sala (1986) and Brugal (1995) for *B. schoetensacki*. However, at the state of the art, we cannot exclude that similar characters were also present in some species of *Bison* (*Eobison*), for which the morphology of the horn cores is still largely unknown.

4.2.2. Dentognathic remains

The studied specimens include a large number of isolated teeth, a few fragmentary mandibles, and a maxillary fragment (Figs. 3 and 4; Table 3). Almost all the specimens come from layer EVT7. The cheek teeth are typically bovine in overall morphology, mesiodistally elongate, moderately hypsodont, and have well-developed styles/stylids.

Description of the upper dentition—The P2 is mesially tapering and narrow relatively to length. The parastyle is pointed, the paracone rib is relatively marked, and the metastyle is faint (Fig. 3f). The P3 is mesiodistally elongate (Fig. 3g) whereas the P4 has a square occlusal contour (Fig. 3h). In the P3 and P4, the parastyle and metastyle are similar in size and somewhat protruding on the labial side (more markedly in the P4). The paracone rib is not particularly protruding. A small fold can be observed in the inner recess on the lingual margin of the P3. In the M1 the mesial lobe is slightly narrower buccolingually than the distal one, whereas in the M2 the two lobes are similar in width, and in the M3 the distal lobe is markedly narrower. The cement is visible in most of the molars, concentrated on the lingual walls and less abundant on the buccal side (e.g., IPS93005). The styles are strong and prominent, with the parastyle and metastyle being the equally developed. The mesostyle, which is somewhat distally oriented, is generally the most developed. In the M3, the metastyle protrudes distally. The entostyle is relatively high and cylindrical in lingual view, and in most cases shows an ovoid occlusal section (only in a few specimens it has an irregular occlusal outline). In most specimens, the cement

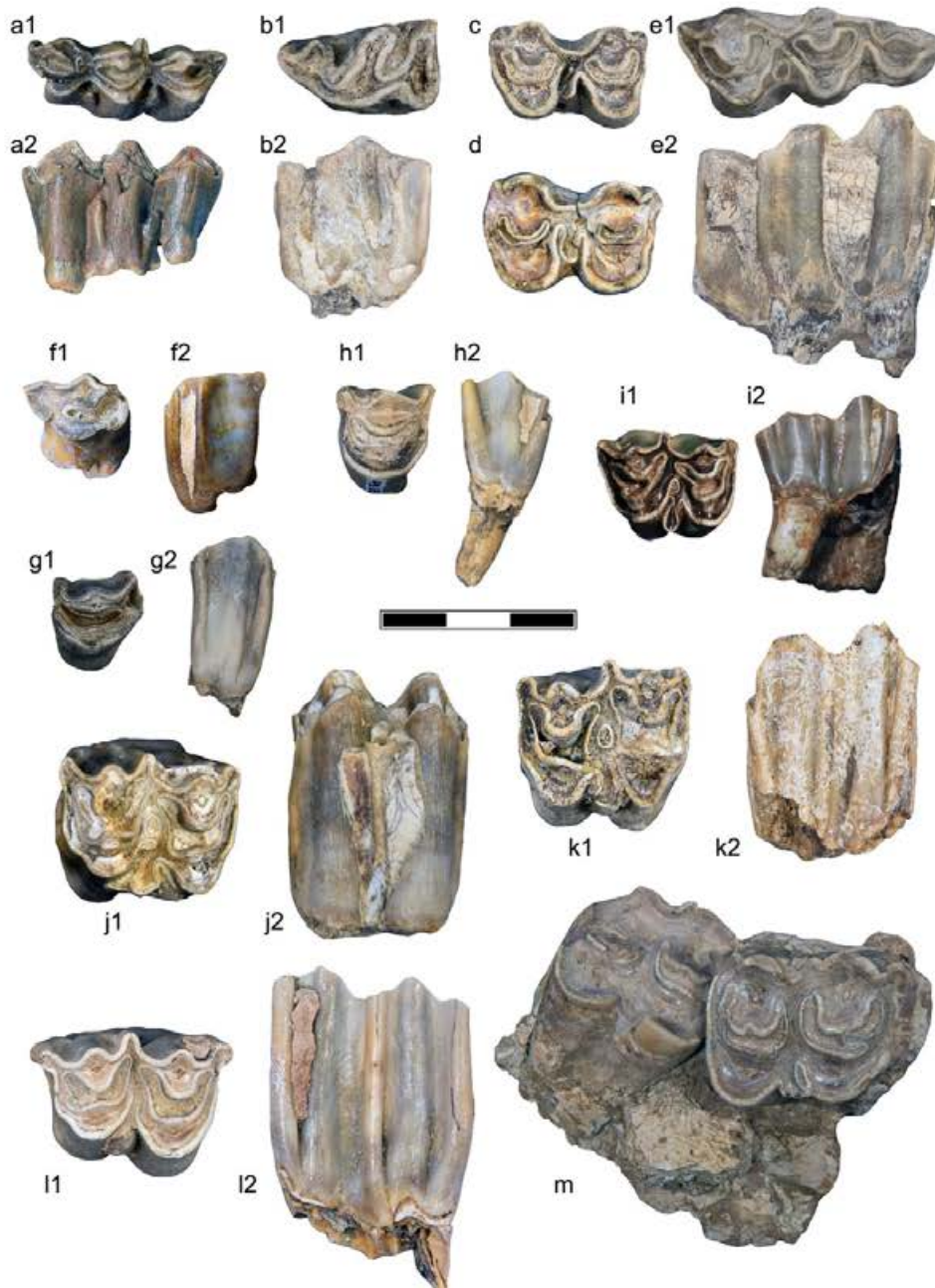


Fig. 3. Dentognathic remains of *Bison schoetensacki* from the Vallparadis Composite Section: a, left dp4 IPS93008 in occlusal (1) and lingual (2) views; b, left p4 IPS93015 in occlusal (1) and lingual (2) views; c, right m1 IPS93027 in occlusal view; d, left m2 IPS93044 in occlusal view; e, left m3 IPS92989 in occlusal (1) and buccal (2) views; f, left P2 IPS92986 in occlusal (1) and buccal (2) views; g, left P3 IPS92998 in occlusal (1) and buccal (2) views; h, right P4 IPS13557 in occlusal (1) and buccal (2) views; i, left M1 IPS93029 in occlusal (1) and buccal (2) views; j, left M2 IPS93005 in occlusal (1) and lingual (2) views; k, right M2 IPS93032 in occlusal (1) and lingual (2) views; l, right M3 IPS20182 in occlusal (1) and lingual (2) views; m, left maxillary fragment with M2–M3 IPS92993 in occlusal view. Scale bar: 30 mm.

penetrates deeply between the entostyle and the two lobes, isolating the entostyle from the protocone and the metaconule. In some specimens, the central cavities have a simple crescent-shaped enamel outline, while in other cases the enamel shows a fold in the middle of the distal wall of the central cavities. This “bubaline fold” (after Masini, 1989), if present, is deeper in the distal central cavity. A small enamel islet is present between the two lobes in several specimens (e.g., IPS93032, IPS93018).

Description of the lower dentition—Only two p4 are preserved in

the entire sample. The parastylid is large and relatively sharp, curved toward the lingual margin. The lingual wall has three vertical grooves of varying depth. The entoconid is well developed and slightly curved distally. The distal margin of the tooth is flat. The molars have cement both lingually and buccally. Like in the upper molars, the cement is concentrated on the lingual inner walls between the protoconid and hypoconid. On the buccal wall, cement is absent in most specimens. The stylids are very prominent; the parastylid and entostylid (especially in the m1 and m2) are similar

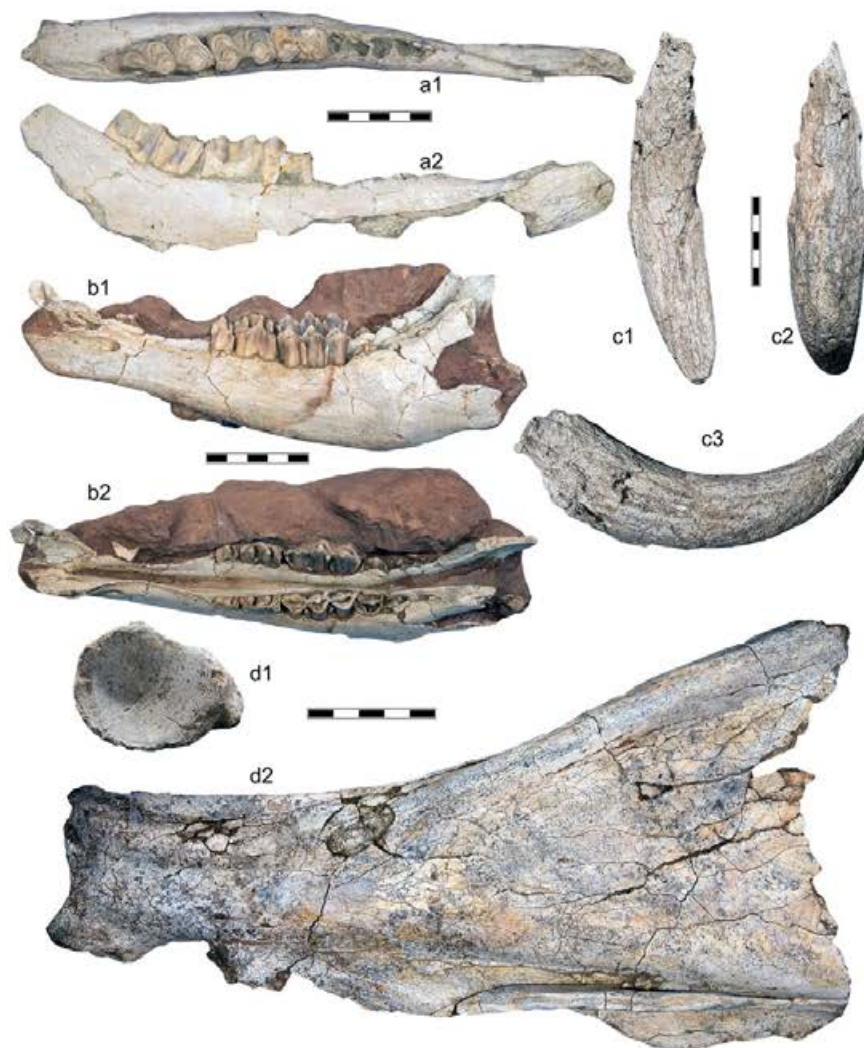


Fig. 4. Craniodental and postcranial remains of *Bison schoetensacki* from the Vallparadis Composite Section: a, left hemimandible with m1–m3 IPS92973 in occlusal (1) and lingual (2) views; b, juvenile mandible with dp2–dp4 IPS92968 in left lateral (1) and occlusal (2) views; c, horn core IPS92970 in dorsal (1), ventral (2), and anterior/posterior (undetermined laterality) (3) views; d, right scapula IPS107637 in distal (1) and lateral (2) views. Scale bars: 50 mm.

in size; in the m3, the parastyloid is prominent (mesially projecting). The m3 ectostylid, located between the protoconid and the hypoconid, is slightly mesiodistally flattened, with an ovoid occlusal outline; in some teeth, the ectostylid is located on the distal portion of the protoconid, whereas in others it is more shifted distally, between the two lobes. The recess filled by the enamel between the entostylid and protoconid is deeper and generally narrower than that of the hypoconid internal flange. In the less worn m1 and m2, the entostylid and the parastyloid are slightly bent distally. In the m3, the labial recess between the hypoconulid and the hypoconid is deep and narrow.

Remarks and comparisons—82 out of 86 dental remains from the VCS were unearthed from layer EVT7, dated to ca. 0.86 Ma. The teeth are relatively homogeneous both in size and shape. This is also confirmed by the one-way ANOVA results performed on the W/L% ratio of M2 and M3 from the two main VCS chronologies, that are, syn-Jaramillo (EVT10 and EVT12) and post-Jaramillo (CGRD7 and EVT7) (Table 4). Generally, their morphology is typically “bisontine”, with a square and buccolingually wide occlusal contour, especially the upper teeth. Decades ago, bison tooth size and

shape were considered taxonomically relevant (e.g., Merla, 1949; Flerov, 1969; Sala, 1986). However, based on our experience, we concur with Sher (1997) that tooth morphology is strongly influenced by the degree of wear and, hence, is not particularly diagnostic, especially when working with small samples. Nevertheless, some characters such as enamel penetration in the inner lingual wall of the upper molars, entostyle development, and tooth size overall can give some taxonomic hints. The presence of a “bubaline fold” in the upper molars from the VCS is variable, as in other bovines (e.g., it is absent in *Proamphibos*, but variably developed in *Leptobos*, and subject to individual variation in *Bos* and *Syncerus*; Merla, 1949), and thus of little taxonomic value. The VCS upper molars are distinctly swollen just above the cervix, as often in *Bison*, but unlike in *Bos* (where this feature is almost entirely absent; Sala, 1986). However, a less-developed swelling is present in some *Leptobos* specimens from Upper Valdarno and Olivola, thus only unequivocally distinguishing *Bos* from *Leptobos* and *Bison*. In contrast, cement is commonly present on the lingual side of the teeth from the VCS (especially in old individuals), and even on the buccal side in some specimens, whereas in *Leptobos* cement is

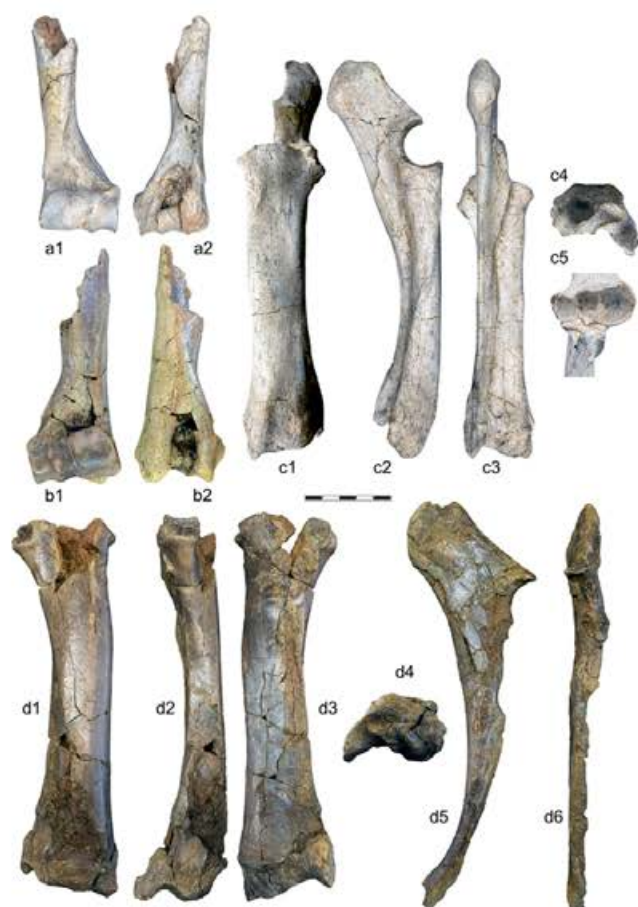


Fig. 5. Forelimb remains of *Bison schoetensacki* from the Vallparadis Composite Section: a, distal fragment of left humerus IPS107620 in anterior (1) and posterior (2) views; b, distal fragment of right humerus IPS50672 in anterior (1) and posterior (2) views; c, left radioulna IPS107617 in anterior (1), medial (2), posterior (3), distal (4), and proximal (5) views; d, right radius IPS39893 in anterior (1), lateral (2), posterior (3), and distal (4) views and associated right ulna in anterior (5) and lateral (6) views. Scale bar: 100 mm.

almost entirely absent (Masini, 1989; Demirel and Mayda, 2014). The abundance of cement is very variable among European *Bison* populations (Sher, 1997)—e.g., it is lacking in *B. priscus* from Taubach but present in *B. menneri* from Untermassfeld. The presence of an enamel islet in the upper molars between the protocone and the hypocone distinguishes *B. (Eobison) spp.*, *B. menneri* and *B. schoetensacki* from *B. priscus* and *Bos primigenius*, where it is rare (Prat, 1968; Sala, 1986) although these islets are relatively common in recent *B. bonasus* populations. The VCS sample displays this character in almost all the teeth with a medium-advanced wear stage, fitting the morphology of *B. schoetensacki* from Isernia and other European sites (Sala, 1986).

Average values of tooth length and width for the analyzed *Bison* samples (Table S2) show that there is a general overlap between all the considered species. The L vs W diagram and the box-plots of the ratio W/L% of m3, M1, M2, and M3 (Fig. S1) help us to compare the size and proportions of *Bison* s.l. teeth. The extremely massive *B. priscus* from Taubach features large teeth (especially m3) (Fig. S1a–d) but with low values of W/L%, i.e., teeth are narrow as compared with total length (Fig. S1e–h). *Bison* cf. *priscus* from Westbury shows long and very wide teeth (Fig. S1a–d). The *B. schoetensacki* specimens from Le Vallonnet, Cromer Forest-bed and

the few remains from Durfort are characterized by general smaller size (especially the M1s from Durfort; Fig. S1b), but higher values of W/L%, i.e., relatively more squared teeth (Fig. S1e–h). The Isernia m3s and M3s are quite stout and relatively large (Fig. S1a, d, e, h), whereas the Süssenborn specimens are elongated with very low values of W/L%, similar to those of *B. menneri* from Untermassfeld and *B. priscus* from Taubach (Fig. S1a–h). The *B. menneri* remains display a high degree of variation but, generally, are among the narrowest teeth analyzed (Fig. S1). The bovid from Mygdonia basin also shows high variation (see, for instance, the M1 biplot and box plot; Fig. S1b, f), overlapping with almost every other sample. The *B. (Eobison)* teeth from Pirro are among the shortest and stoutest (Fig. S1). The teeth from VCS appear short and relatively wide, compared with the other samples examined, showing proportions similar to those of *B. schoetensacki* from Le Vallonnet, Cromer forest-bed, and Durfort (Fig. S1). On the other hand, the VCS teeth differ from those from Isernia and Süssenborn, which feature larger size and more elongated proportions. Some specimens from VCS (e.g., the single M3 from EVT3; IPS93023) display a quite short and stout morphology, similar to that shown by the older remains of *B. (Eobison) degiulii* from the Italian Peninsula. The z-scores computed for the VCS sample (Table S3) show negative values in most instances for the length of the upper molars and the m3 compared with the other *Bison* populations, being similar to the specimens from Venta Micena, Mygdonia basin, and Le Vallonnet. On the contrary, for the width, z-scores are positive in most cases, showing that the VCS sample has relatively wide molars, also compared with the large form of *B. priscus* from Taubach (Table S3; Fig. S1).

4.2.3. Vertebrae

Description—An axis (IPS114551), another cervical vertebra (IPS107615), and four fragmentary thoracic vertebrae (IPS92954, IPS92955, IPS92956, IPS118117) were recovered from VCS (Fig. S2; Table S4). The axis is quite high and elongate, and displays a low spinous process directed dorsally. The transverse foramina are small and located on the posterior portion of the lateral expansions. The neural canal is teardrop-shaped in anterior view. The lateral expansions of the anterior articulation are quite prominent and have a circular anterior outline. The anterior part of the neural process and the transverse processes are broken.

The cervical vertebra IPS107615 is short and massive, with subcircular neural canal, and robust pre- and postzygapophyses. Most of the spinous and transverse process and part of the vertebral body are missing. Its general morphology indicates that it could be one of the last cervical vertebrae due to the anteriorly prominent prezygapophysis, the enlarged postzygapophysis, the position of the transverse process (directed anteroposteriorly to dorsoventrally) and the reduced posterior tuberculum of the ventral crest.

The thoracic vertebrae display smaller bodies with subcircular anterior and posterior rib facets. The neural canal is large and slightly compressed dorso-ventrally. The left transverse process is broken in IPS92954, and both transverse processes are missing in IPS92956 and IPS92954. In IPS92956, the foramina on the left side are absent, but there is a narrow, deep groove between the transverse process and the posterior rib facet. The spinous process is inclined posteriorly; in IPS92954, it is almost complete (about 400 mm high).

Remarks and comparisons—The five vertebrae from VCS have the typical morphology of large bovids. It is noteworthy that the extremely long spinous process of the thoracic vertebra IPS92954 exceeds the height recorded for any species of *Leptobos* and *Bos*. According to Sher (1997), the tallest spinous process recorded for *B. menneri* is ca. 360 mm, whereas in some specimens of *B. priscus* from Siberia it exceeds 600 mm. Apart from this character, no other vertebral features are helpful in distinguishing *Bison* from either



Fig. 6. Metapodials of *Bison schoetensacki* from the Vallparadis Composite Section: a, left metacarpal IPS14917 (male) in anterior (1), proximal (2), distal (3) and posterior (4) views; b, left metacarpal IPS107635 (male) in anterior (1), proximal (2), distal (3) and posterior (4) views; c, left metacarpal IPS92910 (female) in anterior (1), proximal (2), distal (3) and posterior (4) views; d right metatarsal IPS92934 (male) in anterior (1), proximal (2), distal (3) and posterior (4) views; e, right metatarsal IPS107634 (male) in anterior (1), proximal (2), distal (3) and posterior (4) views; f, right metatarsal IPS92932 (female) in anterior (1), proximal (2), distal (3) and posterior (4) views. Scale bar: 100 mm.

Leptobos or *Bos*.

4.2.4. Scapula

Description—See Fig. 4d and Table S5. IPS107637 is almost complete, although slightly fragmentary and lacking the distal margin, while IPS92922 only preserves the glenoid cavity and a proximal portion of the blade. The glenoid cavity is subovoid, with its major axis oriented anteroposteriorly. The lateral margin of the cavity is slightly concave in distal view. The acromion, partially preserved in both specimens, is not particularly pointed. The spine, almost complete in IPS107637, is relatively sharp in the proximal half and constituted by a flat surface in the distal half (about 80 mm of width), which displays a small, shallow groove that runs along the lateral surface up to the distal margin. The incisura scapulae is straight and relatively deep. The supraglenoid tubercle (only preserved in IPS92922) is large, displays a rough surface, and slopes dorsally from the edge of the glenoid. There is a narrow groove on the medial surface of the collum scapulae between the glenoid cavity and the supraglenoid tubercle. The infraglenoid tubercle is developed posteroventrally and located on the medial side of the bone, just above the glenoid margin.

Remarks and comparisons—The two scapulae from VCS closely resemble each other in size and shape, and fit well with the morphology of large Bovids, especially *Bison* (e.g., glenoid cavity more rounded in *Bos*). The dimensions of the glenoid cavity in the VCS specimens fall within the variation ranges of the smallest species of *Bison* (i.e., *B. menneri* and *B. bonasus*; Table S6).

4.2.5. Humerus

Description—Six humeri from the VCS are available (Fig. 5a and

b; Table S7). They only preserve the distal epiphysis and, in some cases, part of the diaphysis. The distal epiphysis is massive and has the typical bovid morphology, with a large trochlea divided by a crest shifted toward the lateral margin. The medial margin of the trochlea is proximodistally higher than the lateral, thus the trochlea in anterior view tapers lateralward. The large groove and the crest that separate the two epitrochleae are located slightly lateral to the distal articulation midline. On the lateral margin of the trochlea, a large and bulging trochlear crest is present. The coronoid fossa is a mediolaterally wide. The olecranon fossa is deep, relatively narrow, and medially and laterally delimited by strong crests that slightly converge distally. On the lateral surface of the shaft, at the contact between the diaphysis and distal epiphysis there is a rough half-moon-shaped ridge. The lateral trochlear pit (which is absent on the medial side) is large and deep.

Remarks and comparisons—The VCS humeri are morphologically homogeneous, except for the differences in overall size and robusticity, which are attributable to sexual dimorphism. The presumably male specimens IPS50672 and IPS114549 display a larger distal epiphysis than the rest of the sample, which are likely female. The humerus of *Bison* s.s. generally resembles that of *Leptobos* and *B. (Eobison)*, except for the larger distal ends of the former and some small differences in the trochlear elements (see below). The distal epiphysis of the VCS humeri falls within the size variation of *Bison*, in particular *B. schoetensacki* and *B. menneri*, being slightly smaller compared to *B. priscus* (Table S8). Several studies have attempted to find diagnostic characters in the humerus, focusing on the distal epiphysis, to distinguish *Bison* from other large bovids such as *Bos*. The humeri of *Bos* and *Bison* are markedly polymorphic (Martin, 1987; Sher, 1997), but according to Martin (1987) the two genera



Fig. 7. Hindlimb remains of *Bison schoetensacki* from the Vallparadis Composite Section: a, right tibia IPS107618 in posterior (1), medial (2), lateral (3), distal (4) and anterior (5) views; b, left tibia IPS92942 in posterior (1), medial (2), lateral (3), distal (4) and anterior (5) views. Scale bar: 100 mm.

differ in the proportions between the medial and lateral epitrochleae (affected by the position of the trochlear crest), the shape of the trochlear crest, and the shape of the olecranon fossa. In particular, *Bison* has parallel trochlear margins and a smoother outline of the trochlear crest, whereas *Bos* has a higher crest, a deeper trochlear groove, and generally irregular dorsal and ventral edges of the trochlea (Stampfli, 1963; Sala, 1986). However, we concur with Sher (1997) that this last difference is not reliable. The VCS specimens show a wide range of variation in this character (e.g., sharp in IPS50672 and smooth in IPS107620), indicating it has no diagnostic value. The proportions between the lateral and medial epitrochleae, as measured by Stampfli's trochlea-index (Stampfli, 1963), is extremely variable in the VCS sample and the analyzed comparative sample (including *Leptobos*, *Eobison*, *Bison*, and *Bos*), indicates great overlapping (Table S9). The lateral tapering of the trochlea has been proposed as a diagnostic character, as measured by the Lehmann trochlear index (Table S10), although it is proved similarly undiagnostic (Sher, 1997). In the VCS sample, this index has the widest range of variation among the analyzed samples (ranging between 62.9 and 76.5), although on average it most closely resembles the values displayed by the smallest taxa (*Eobison* and *B. menneri*; Table S10).

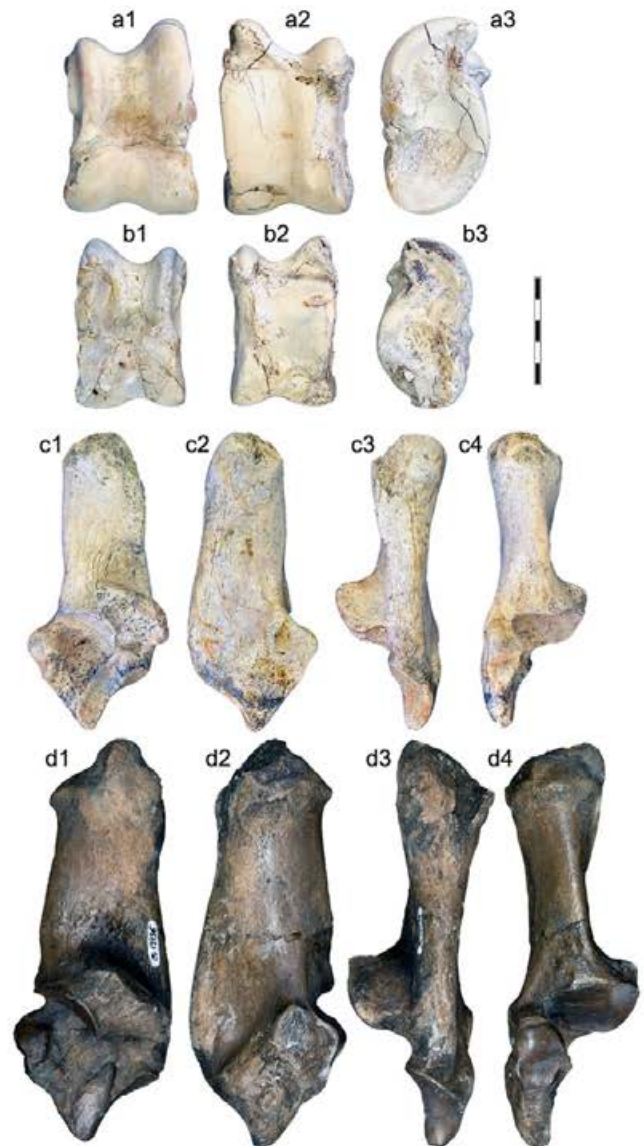


Fig. 8. Tarsals of *Bison schoetensacki* from the Vallparadis Composite Section. a, left astragalus IPS92953 (male) in anterior (1), posterior (2), and lateral (3) views; b, right astragalus IPS92952 (female) in anterior (1), posterior (2), and lateral (3) views; c, right calcaneum IPS92945 (female) in medial (1), lateral (2), posterior (3), and anterior (4) views; d, right calcaneum IPS13936 (male) in medial (1), lateral (2), posterior (3), and anterior (4) views. Scale bar: 50 mm.

4.2.6. Radius

Description—Radii are among the most common and best-preserved long bones found in VCS (Fig. 5c and d and Table S11). The ulna is fused with the radius in all studied specimens except IPS39893 and IPS92916. The lateral tuberosity of the radius, which has an antero-posterior diameter roughly similar to the proximodistal one, forms an obtuse angle with the distal epiphysis. The dorsomedial and medial portions of the proximal epiphysis form a clearly protruding shelf with a square proximal outline. The posterior contour of the proximal articulation is slightly undulated, forming an obtuse angle with the lateral edge. The outline of the lateral glenoid cavity is dorsally convex, being more or less deep depending on the specimen (e.g., gentle and shallow dorsal convexity in IPS13570, deep and almost angular in IPS48775). Distal to

Table 3
Measurements (mm) of the teeth of *Bison schoetensacki* from Vallaradís Estació (EVT) and Cal Guardiola (CGR) layers. Abbreviations: L, length; W, width.

ID Specimen	Layer	Tooth	L	W
IPS92968	EVT12	dp2	11.4	7.1
IPS92968	EVT12	dp3	19.6	10.3
IPS14965	CGRD7	dp4	29.4	16.0
IPS92968	EVT12	dp4	32.5	14.1
IPS92997	EVT7	dp4	25.0	12.8
IPS93008	EVT7	dp4	31.0	14.3
IPS92977	EVT7	dp4	20.3	13.2
IPS93015	EVT7	p4	20.5	12.4
IPS93045	EVT7	p4	17.4	11.7
IPS93056	EVT7	p4	19.4	11.3
IPS93027	EVT7	m1	24.8	15.7
IPS93042	EVT7	m1	24.6	17.0
IPS92973	EVT7	m1	25.0	16.5
IPS92977	EVT7	m1	23.9	15.1
IPS93009	EVT7	m2	25.3	16.1
IPS93014	EVT7	m2	24.0	17.2
IPS93019	EVT7	m2	26.2	18.4
IPS93030	EVT7	m2	24.8	17.1
IPS93044	EVT7	m2	27.7	18.7
IPS92973	EVT7	m2	24.7	18.6
IPS92977	EVT7	m2	28.5	17.6
IPS92990	EVT7	m2	26.8	24.5
IPS93043	EVT7	m3	41.9	17.6
IPS92977	EVT7	m3	38.2	16.3
IPS92973	EVT7	m3	41.7	18.4
IPS92987	EVT7	m3	46.5	18.4
IPS92989	EVT7	m3	40.3	16.7
IPS92986	EVT7	P2	16.3	13.0
IPS92996	EVT10	P3	19.4	16.2
IPS92998	EVT7	P3	13.8	19.9
IPS13557	CGRD7	P4	14.7	19.2
IPS92995	EVT10	P4	15.6	21.8
IPS93013	EVT3	P4	19.5	21.4
IPS93020	EVT7	P4	15.8	21.7
IPS92992	EVT10	M1	25.2	25.6
IPS93016	EVT6	M1	27.2	24.2
IPS93017	EVT6	M1	24.7	25.9
IPS93029	EVT7	M1	21.9	26.8
IPS93036	EVT7	M1	21.0	23.8
IPS93047	EVT7	M1	20.6	23.4
IPS92988	EVT7	M2	25.8	25.3
IPS92991	EVT10	M2	28.1	28.8
IPS92994	EVT10	M2	26.9	27.6
IPS93005	EVT7	M2	27.6	28.2
IPS93003	EVT7	M2	24.9	25.1
IPS93022	EVT7	M2	29.3	21.2
IPS93032	EVT7	M2	28.3	27.3
IPS93034	EVT7	M2	23.3	23.7
IPS93038	EVT7	M2	25.7	26.1
IPS20182	CGRD7	M3	30.6	26.0
IPS92993	EVT10	M3	30.4	27.6
IPS92994	EVT10	M3	31.0	27.5
IPS93007	EVT7	M3	27.3	24.7
IPS93011	EVT7	M3	28.0	24.3
IPS93018	EVT7	M3	27.8	26.0
IPS93021	EVT7	M3	29.1	25.7
IPS93023	EVT7	M3	23.5	25.0
IPS93028	EVT7	M3	32.3	24.5
IPS93033	EVT7	M3	27.0	26.5

the lateral glenoid cavity, on the lateral part of the posterior portion, there is a wide depression of variable depth and, medially, a rough area. The notch between the two proximal glenoid cavities is wide and shallow (V-shaped in IPS48775). When preserved, the articular surface for the ulna is well visible in the middle of the proximal diaphysis of the radius, being wide and rough. On the anterior surface of the distal epiphysis there is a grooved area for the tensor tendon, parallel to the diaphysis and delimited medially and laterally by blunt crests. The distal epiphysis is inclined posteriorly and shows a circular pit at the mediolateral end, surrounded

by radial rugosities. The fissure marking the contact between radius and ulna in the distal diaphysis is well visible (e.g., in IPS107628 and IPS92919). The articular surfaces for the scaphoid and semilunar are particularly deep in the anterior portion, edged posteriorly by two pits. Between the ulnar articular surface and the pointed styloid process there is a wide and deep notch. On the medial side of the distal end there is a small bulge for the metacarpal carpal ligament, more developed in the largest specimens (IPS92916, IPS39893, and IPS92918) than in the rest of the sample.

Remarks and comparisons—The radii from the VCS show the typical morphology of *Bison*. They can be distinguished from the ones of *Bos* based on several characters, including: the poorly developed lateral tuberosity of the proximal epiphysis, the wide and shallow notch between the two proximal glenoid facets with a smooth posterior outline, and a fissure marking the contact between ulna and radius (Brugal, 1983; Sala, 1986; Gee, 1993; Sher, 1997). These characters are also present in *Leptobos* spp. (Masini, 1989) which nevertheless show smaller and slenderer radii. The VCS radii display stout proportions as showed by the diagram of stoutness (built as the ratio between proximal epiphysis width and total bone length VS the total length; Fig. 9c), especially when compared with *Leptobos* and *Eobison*. The VCS radii are similar in size to those of *B. menneri* and *B. schoetensacki*. The aforementioned index of stoutness indicates that VCS specimens overlap with those of *B. schoetensacki*, being slenderer than those of *B. priscus* (which is characterized by a very stout radius, i.e., wide diaphysis and epiphyses) but slightly more robust than those of *B. menneri* (which displays similarly long radii but with lower width values; Table S12).

4.2.7. Ulna

Description—Three almost complete ulnae are available from EVT and CGR (IPS39893, IPS107616, IPS107617; Fig. 5c and d; Table S13), all of them paired with the corresponding radii. The olecranon process is large and square, gently inclined posteriorly with respect to the long axis of the bone. The medial and lateral surfaces of the olecranon are slightly concave. The ulnar shaft is posteriorly concave. The medial articular facet for the radius is subrectangular and concave. The radius lateral articulation is lateromedially wide, divided into two facets by a small crest, one distal to the other. The proximal facet is subtriangular and almost flat, while the distal facet is subcircular and concave. The semilunar notch is large and has a small pointed tip at the distal margin which reaches the medial articulation facet for the radius.

Remarks and comparisons—There are no substantial differences between the VCS ulnae and those of *Bos* and *Bison* (Table S14). Even if some authors noted some minor differences between these genera (Bibikova, 1958; Gee, 1993; Brown and Gustafson, 2000), the only clear difference relates to the articulation between the radius and the ulna (Gee, 1993; Sher, 1997): in *Bison*, the lateral articulation with the radius is wide and does not intrude into the posteroproximal part of the radius, whereas in *Bos* this facet is shaped as an elongated triangle that deeply intrudes into the radius. The VCS sample displays the former condition, although with some degree of variation, as already noticed in *Bison* spp. by Sher (1997).

4.2.8. Carpal bones

Only very few carpal bones are available from the VCS collection (Fig. S3; Table S15), mostly from layer EVT10 (IPS92960, IPS92961, IPS92962, IPS92963). Morphological description and comparisons of large bovid carpal bones are often neglected in literature (Sher, 1997); moreover, the few studies performed are sometimes contradictory and do not agree on the measurements to be taken (Bibikova, 1958; Stampfli, 1963; Sala, 1986; Sher, 1997). For these reasons, only a short description and comparison are presented for

Table 4

Univariate and multivariate analyses of variance of M2 and M3, metacarpals, and metatarsals from the two main VCS chronologies: 1.07–0.99 Ma (EVT10–12) and 0.86–0.78 (CGRD7–EVT7) (only complete metapodials included). Values with $p < 0.05$ are in bold. Abbreviations: DET, distal epiphysis thickness (maximum); DEW, distal epiphysis width; DT, diaphysis thickness (midshaft); DW, diaphysis width (midshaft); F, F statistic; L, length; Lmax, maximum length; p, significance; PET, proximal epiphysis thickness; PEW, proximal epiphysis width; W, width.

Molars ANOVA		
Variable	F	p
M2: W/L%	0.5891	0.4719
M3: W/L%	0.05129	0.8273
Metacarpals ANOVA		
Variable	F	p
Lmax	18.55	0.00259
PEW	0.03753	0.849
PET	0.1259	0.728
DW	2.737	0.1263
DT	1.765	0.2109
DEW	2.107	0.19
DET	1.017	0.3467
DEW/Lmax%	0.04082	0.8456
Metacarpals MANOVA		
	F	p
	4.009	0.1412
Metatarsals ANOVA		
Variable	F	p
Lmax	0.06263	0.8107
PEW	1.466	0.2513
PET	3.524	0.08726
DW	0.004166	0.9497
DT	0.898	0.3637
DEW	5.131	0.0641
DET	3.995	0.1021
DEW/Lmax%	7.579	0.03316
Metatarsals MANOVA		
	F	p
	2.049	0.3597

these anatomical elements. The lack of *Leptobos* material precludes comparisons with this genus, while no differences in size or shape were found among *Bison* species.

Pyramidal (carpi ulnare)—The laterally S-shaped morphology of the pyramidal, with an elongated distal portion, is typical of *Bos* and *Bison*. According to Sala (1986), the proximal margin of the facet for the unciform in *Bison* has a smaller radius of curvature as compared with *Bos* (Stampfli, 1963; Sala, 1986). This is disproved by the two pyramidal bones from the VCS, which display a quite wide radius of curvature, as well as by the pyramidal of *B. menneri* figured by Sher (1997), who emphasized the high degree of variation in the population from Untermassfeld.

Semilunar (carpi intermedium)—The only specimen recovered from VCS is partially broken. Its morphology does not differ from that of *Bison* and *Bos*. Sala (1986) evidenced some differences regarding the proximal and distal facets, which are hard to recognize in our sample due to the fragmentary state of the fossil. The comparison of IPS92961 with the *Bos* and *Bison* spp. semilunars figured by Sala (1986: Figs. 11 and 12) does not highlight appreciable differences, although the VCS single specimen more closely resembles the *B. schoetensacki* sample from Isernia.

Unciform (os carpale IV)—According to Sher (1997), this bone is extremely variable in size within a single population of *Bison*. This is confirmed by the two specimens from VCS, which are similar in shape, but differ in size (IPS92962 is about 25% larger than IPS92964). This variation might be due to sexual dimorphism. Their morphology fits well with that described for *Bison* (Sala, 1986), being quite different from the one of *Bos* (i.e., the more rounded shape of the axial edge in the proximal articular facet of *Bison*).

Capitatotrapezoid (os carpale II + III)—The poor state of preservation of the single available capitatotrapezoid does not allow a detailed description or comparisons.

4.2.9. Metacarpal

Description—All the VCS metacarpals are stout (Fig. 6a–c; Table 5). The proximal and distal epiphyses have almost the same width. Four specimens (of which two complete: IPS107626, IPS92910 from EVT12) are slenderer than the remaining ones, most probably due to sexual dimorphism (see Section 6.3.). The proximal articular surface displays a D-shaped outline in proximal view. The lateral articular facet is triangular and located on a lower plane than the medial articular facet, being separated from it by a high crest oriented anteroposteriorly. In some specimens the lateral facet is characterized by a small depression on the anterior margin (e.g., IPS92907, IPS92909, IPS92908). The medial facet is larger and subsquare. Its medial outline varies from subcircular to square. The synovial fossette is a variably developed irregular pit located in the middle of the medial facet (not visible or very small in IPS92912, IP92911, and IPS14985). The proximal epiphysis is marked by a bulging ridge that follows the articular surface, interrupted in the posterior margin by a U-shaped small notch that corresponds to the proximal nutrient foramen, which is located at the posterior margin of the crest that separates the two proximal facets. On the lateral margin of the ridge cited above, there is a subrectangular facet for the fifth metacarpal. The posteroproximal nutrient foramen is teardrop-shaped and located in the middle of a deep rough depression. This depression does not extend onto the posterior portion of the diaphysis, which is almost flat. In anterior view, the

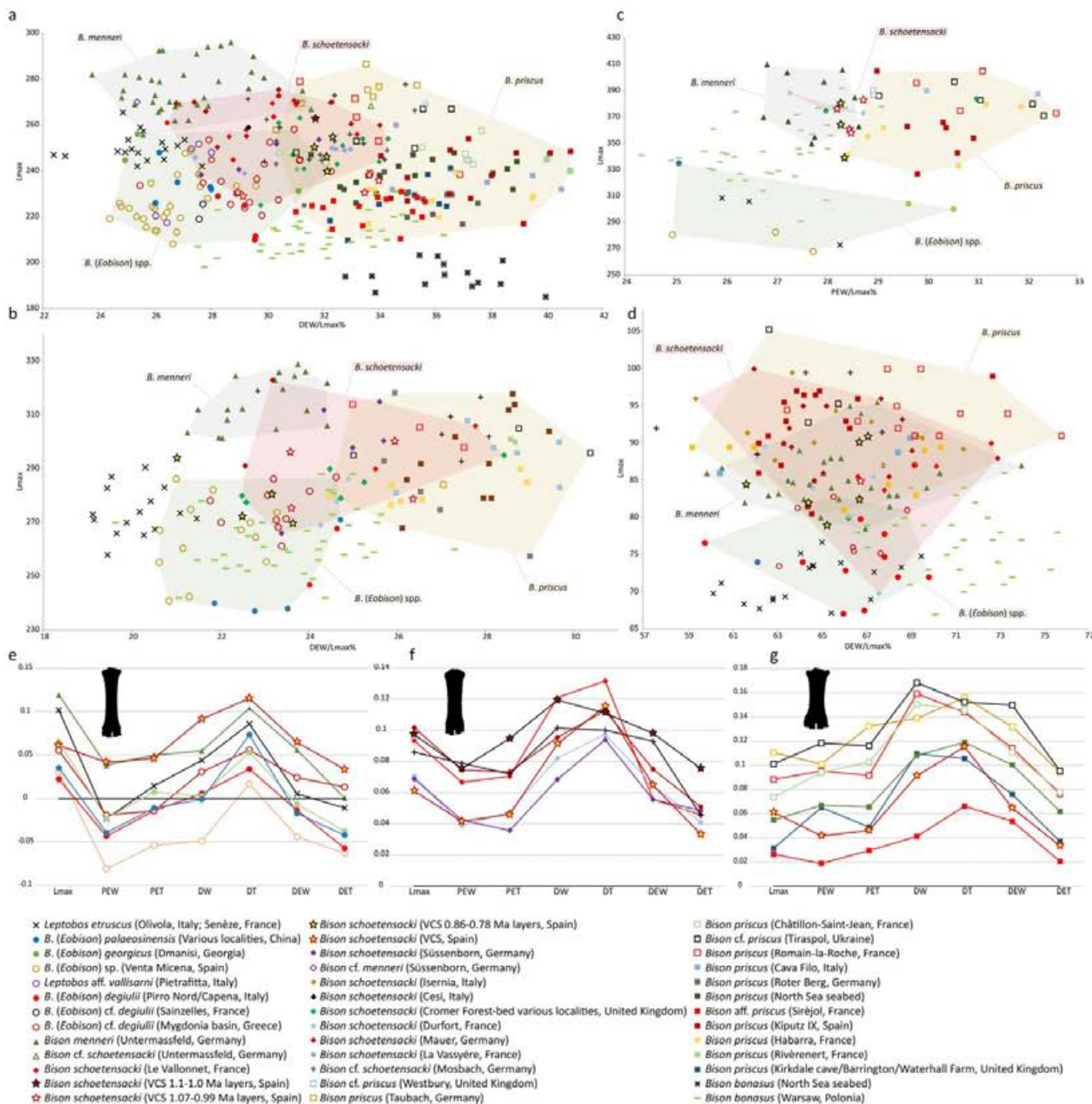


Fig. 9. a–d, Bivariate plots of maximum length (Lmax) vs distal end width (DEW)/maximum length (Lmax) % to evaluate stoutness of metacarpals (a), metatarsals (b), radii (c), and astragali (d) in several *Leptobos* and *Bison* s.l. species. e, Log₁₀ ratio diagrams of seven selected metacarpal variables, in which the VCS bison is compared with *Leptobos etruscus*, *B. (Eobison) spp.*, and *B. menneri* (1), *B. schoetensacki* from several sites (2), and *B. priscus* from several sites (3).

diaphysis is generally wide and hourglass-shaped, with the narrowest mediolateral diameter located in the distal half of the diaphysis. The vascular groove on the distal portion of the diaphysis shows a great variation, from narrow and shallow to wide and deep; its deepest part is located just proximally to the distal epiphysis, and the groove always stops distally to the midshaft. The distal anterior foramen is always present, although variable in size, located within the vascular groove just above the distal end of the groove itself. The distal portion of the diaphysis displays marked epitrochlear tubercles (sensu Sher, 1997), so that the maximum

width between them almost equals that measured across the trochleae. There is a constriction between each tubercle and the distal end of the corresponding trochlea. The intertrochlear margins tend to converge distally. The distal trochlear crests (intercondylar crests) are subparallel to distally convergent. Two deep depressions are present proximally to either side of each trochlear crest. The two outer depressions are larger and deeper than the inner ones. The lateral and medial trochlear pits are deep and marked by radial rugosities.

Remarks and comparisons—The metacarpals from VCS are

Table 5

Measurements (mm) and descriptive statistics of the metacarpals of *Bison schoetensacki* from Vallparadis Estació (EVT) and Cal Guardiola (CGR) layers. Abbreviations: ABETl, abaxial emicondyle thickness (lateral emicondyle); ABETm, abaxial emicondyle thickness (medial emicondyle); AETl, axial emicondyle thickness (lateral emicondyle); AETm, axial emicondyle thickness (medial emicondyle); DETl, distal epiphysis thickness (lateral trochlear crest); DETm, distal epiphysis thickness (medial trochlear crest); DEW, distal epiphysis width; DDW, distal diaphysis width (above the epiphysis); DT, diaphysis thickness (midshaft); DW, diaphysis width (midshaft); F, female; L, left; Lf, functional length; Lmax, maximum length; M, male; PET, proximal epiphysis thickness; PEW, proximal epiphysis width; PFWl, proximal articular facet width (lateral facet); PFWm, proximal articular facet width (medial facet); R, right.

ID Specimen	Layer	Side	Sex	Lmax	Lf	PEW	PET	DW	DT	DDW	DEW	DETm	DETl	PFWl	PFWm	ABETm	ABETl	AETm	AETl
IPS796	CGRD7	R	M			75.0		50.4	34.6					43.5	29.7				
IPS13547	CGRD7	R	M	254.7	243.9	81.3	47.6	52.9	33.6	78.6	82.4	43.7	43.8	43.3	35.9	32.8	30.1	39.8	38.5
IPS13911	CGRD2	L	M					53.9	36.6										
IPS13928	CGRD7	R	M	250.2	239.4	79.3	47.0	49.55	30.0	72.6	79.3	45.9	43.6	45.9	32.6	36.7	33.8	39.9	39.4
IPS14102	CGRD7	R	F			70.6	42.1							39.0	27.3				
IPS14702	CGRD7	L	F?			73.5	42.2							40.4	29.5				
IPS14815	CGRD7	L	M	242.5		77.0	46.3	51.8	34.6			37.5		44.4	28.0				
IPS14917	CGRD2	L	M	262.7	251	83.9	51.5	52	33.4	78.5	83.4	45.4	41.4	49.7	31.2	33.1	29.9	40.7	40.3
IPS14985	CGRD7	R	M			83.0	50.2							46.1	31.4				
IPS15002	CGRD7	R	M			79.0	46.9	46.5	46.6					44.2	30.8				
IPS92905	CGRD7	R	M											46.2					
IPS92907	EVT10	L	M	230.3	220.9	83.2	47.0	50.2	33.4	75.2	77.1	41.7	41.7	46.2	28.7	31.6	30.5	37.5	37.0
IPS92909	EVT12	R	M			85.1	49.0	48.7	33.4	74.0				45.2	31.2				
IPS92910	EVT12	L	F	230.5	223.6	67.7	41.3	38.42	29.9	62.8	66.7	36.5	36.5	37	24.1		25.7		
IPS92911	EVT7	R	M	246	232.4	78.2	45.3	50.3	33	74.4	79.1			44.3	34.1	29.6	28.4		
IPS92912	EVT7	R	M	239.5	230.4	77.3	45.5	49.3	32.5	74.6	77.0	41.2	41.6	43.1	32.1	32.9	30.7	39.6	38.0
IPS92913	EVT12	L	M			75.8	45.6							42.9	31.5				
IPS107626	EVT12	L	F	228.9		69.5	44.5	36.3	27.9		66.8	35.3	35.0			29.2	26.3	32.3	32.8
IPS107635	EVT12	L	M	238.0	224.01	78.3	45.8	50.4	32.9	75.8	80.1	42.5	41.9	42.1	34.2	32.5	29.9	40.8	39.9
IPS107636	EVT12	R	M	235.7	224.7	79.0	45.0	50.7	33.5	75.6	80.2	42.4	42.6	42.2	31.9	32.2	30.6	40.5	39.0
	Mean			241.7	232.3	77.6	46.1	48.8	33.7	74.2	77.2	41.2	40.9	38.6	39.2	31.6	28.8	37.9	38.4
	Minimum			228.9	220.9	67.7	41.3	36.3	27.9	62.8	66.7	35.3	35	32.7	29	25	20.8	29.5	32.8
	Maximum			262.7	251	85.1	51.5	53.9	46.6	78.6	83.4	45.9	43.8	42.6	43.1	36.7	33.8	40.8	40.3
	SD			10.8	10.4	5.0	2.7	5.0	4.14	4.4	5.9	3.7	3.1	4.2	5.8	3.1	3.5	4.1	2.5
	N			11	9	18	17	15	15	10	10	10	9	7	5	10	11	9	8

characterized by similar morphologies with some exceptions. Two specimens (IPS107626 and IPS92910) from EVT12 are particularly slender, with narrower diaphysis and epiphyses than most of the sample, although two proximal epiphyses (IPS14102 and IPS14702) from CGR7 show similar dimensions. This is most likely attributable to sexual dimorphism, which is quite common in bovines and normally implies that females have slenderer metapodials than males (Sher, 1997; Brugal and Fosse, 2005; Kostopoulos et al., 2018). The one-way ANOVA test, performed on 8 eight selected variables of the specimens coming from the two main VCS chronologies of VCS (EVT10-EVT12 and CGRD7-EVT7) shows that, except for the maximum length, no significant differences were found (Table 4). It is noteworthy that one of the specimens (IPS14917) from layer CGRD2 displays a pathological bone outgrowth (of unknown etiology) along the medial margin of the distal shaft, which reaches the epiphysis and expands in a large and thick bone outgrowth on the posterior portion of the diaphysis. A similar malformation is also present in one intermediate phalanx (IPS16778) from the same layer and given their corresponding size it might belong to the same individual. A MANOVA between the two main subsamples from VCS (i.e., specimens divided by stratigraphic provenance), performed on five variables, does not evidence significant differences between the two groups (Table 4). The aforementioned metacarpal IPS14917 was not included in the ANOVA and MANOVA because it is the only metacarpal from the pre-Jaramillo layers. Nonetheless, the "stoutness" diagram and the PCA clearly show the overall similarity between this specimen and the rest of the sample (particularly the specimens from EVT7-CGRD7; see below).

Given their abundance in the fossil record and distinctive features, metacarpals are the most diagnostic postcranial bones for bovines and thus those most frequently used for taxonomic purposes in the literature (Table S16). *Bison* s.l. is readily distinguished from *Bos* based on the diaphysis distal end (contact between the diaphysis and distal epiphysis; Schertz, 1936a, 1936b; Lehman,

1949; Bibikova, 1958; Stampfli, 1963; Ayrolles, 1973; Brugal, 1983, 1985, 1995; Sala, 1986; Gee, 1993; Sher, 1997). Our analysis performed on several samples of Pleistocene large bovines shows that the ratio between DDW and DEW (Delpech, 1972) is a very useful tool to distinguish *Bos* and *Bison/Leptobos*, with the former showing significantly lower values (Table S17). In *Bison*, this area has marked tubercles, so that the width of the bone is roughly equal to, and sometimes even greater, than maximum distal width; on the contrary, in *Bos* the epitrochlear inflation is less pronounced and the distal end gently curves, following the distal margins of the hourglass-shaped diaphysis being quite medio-laterally thinner than the distal epiphysis width. According to our observations, the *Bison*-like distal inflation is also present in the *Leptobos* sample. Despite some minor individual variation, the specimens from VCS resemble the condition of the *Bison/Leptobos* group. According to many authors (e.g., Schertz 1936a, b; Bibikova, 1958), the medial facet of the proximal articular surface would be quadrangular in *Bos*, and more rounded and medio-laterally developed in *Bison*. However, this feature is very variable (Sher, 1997), as shown by the VCS sample, where it ranges from rounded (e.g., IPS13928, IPS13547) to square (e.g., IPS14072, IPS92913). Nevertheless, the ratio between the diameters of the lateral and medial facets distinguishes *Bison* from *Leptobos*, with the latter displaying a relatively wider lateral facet. The *Bison* sample from VCS overlaps the mean values of the *Bison* s.l. group (Table S18).

The VCS metacarpals, despite some variation, are quite heavily built, especially the male specimens. They are more robust than those of *B. menneri*, and longer and stouter than those of *Leptobos* or *B. (Eobison)* spp., but less massive than those of *B. priscus*, and most similar to those of *B. schoetensacki* (Table S16). Our "stoutness" diagram (Fig. 9a) indicates that, despite some overlap, the VCS metacarpals (especially the specimens coming from EVT7, CGRD2, and CGRD7) fall within the variation range of *B. schoetensacki* from various localities (Süssenborn, Mauer, Mosbach, Le Vallonnet,

Durfort, and Cromer Forest-bed) although some large specimens (IPS107636, IPS107635, and IPS92907) also resemble those of female *B. priscus*. The curves established by the Log_{10} ratio diagrams (Fig. 9e–g) confirm these results, as the VCS bison is characterized by a trend that closely resembles *B. schoetensacki* samples.

The PCAs highlight the considerable overlap between different *Bison* samples. In the first PCA (Fig. 10a, Table S19), PC1 (60% variance) is mostly driven by L_{max} (negative scores) and, to a lesser extent, $mv\text{DW}$, $mv\text{DEW}$ and $mv\text{PEW}$ (negative scores), separating slender with relatively elongated metacarpals, toward the negative values, from stout and short metacarpals at the opposite portion of the diagram, characterized by robust structures. *Bison priscus* and *B. schoetensacki* display the most positive scores, whereas *Leptobos* and *B. (Eobison) spp.* show the most negative values. PC2 (14% variance) is mostly driven by $mv\text{DT}$ and $mv\text{DW}$ (negative scores) and by $mv\text{PET}$, $mv\text{PEW}$, $mv\text{DET}$ and $mv\text{DEW}$ (positive scores); thus, the specimens with wide and thick shaft have negative values, while the ones with a narrow diaphysis but robust epiphyses are characterized by positive values. The VCS sample (positive, for PC1 and negative for PC2, in all the male specimens except for IPS14917 and IPS13928 which have positive PC2 values) is characterized by stout metacarpals with a massive distal epiphysis and relatively large diaphysis. The specimens overlap with the *B. schoetensacki* in both PCs. The two VCS female specimens are located at the edges of the *B. schoetensacki* convex hull, close to the Durfort and Süßenborn female specimens and overlapping with the *Eobison* group.

The second PCA (Fig. 10b, Table S20), based on Scott and Barr's (2014) method, shows no substantial differences relatively to the

first PCA. PC1 (58% variance) is affected principally by reL_{max} and $re\text{DW}$, and separates long metacarpals with a relatively narrow diaphysis (positive scores) from shorter but stouter metacarpals (negative scores). PC2 (14% variance) is mostly influenced by reL_{max} and the stoutness of the shaft ($re\text{DW}$ and $re\text{DT}$) regarding positive scores, while it is negatively affected by the dimensions of the proximal epiphysis ($re\text{PET}$ and $re\text{PEW}$), thus segregating long metacarpals with a wide diaphysis (positive scores) from short metacarpals with a massive proximal epiphysis (negative scores). The VCS specimens display negative scores for both PCs, except for the single female specimen (IPS107626, which displays a positive for PC1), and cluster with the *B. schoetensacki* and *B. priscus* scatter of points. The only exception is IPS13928, which is characterized by an extremely stout distal epiphysis and hence overlaps with the lower range of *B. priscus* from UK for PC2. The main convex hull of VCS is bordered below by the single metacarpal from Süßenborn and above by the remains from Le Vallonnet and Mauer/Mosbach. The MANOVA performed among the VCS sample, other species of *Bison* s.l., and *Leptobos etruscus* shows that the Iberian sample is characterized by significant differences from all the others, with the exception of those attributed to *B. schoetensacki* (Table S21).

4.2.10. Tibia

Description—A partial tibia (IPS107618) lacking the proximal epiphysis is the most complete specimen from the VCS, whereas the rest of the sample is composed of distal fragments (Fig. 8; Table S22). The medial malleolus is variably developed (from poorly marked in IPS92943 to strongly developed in IPS92942). It extends

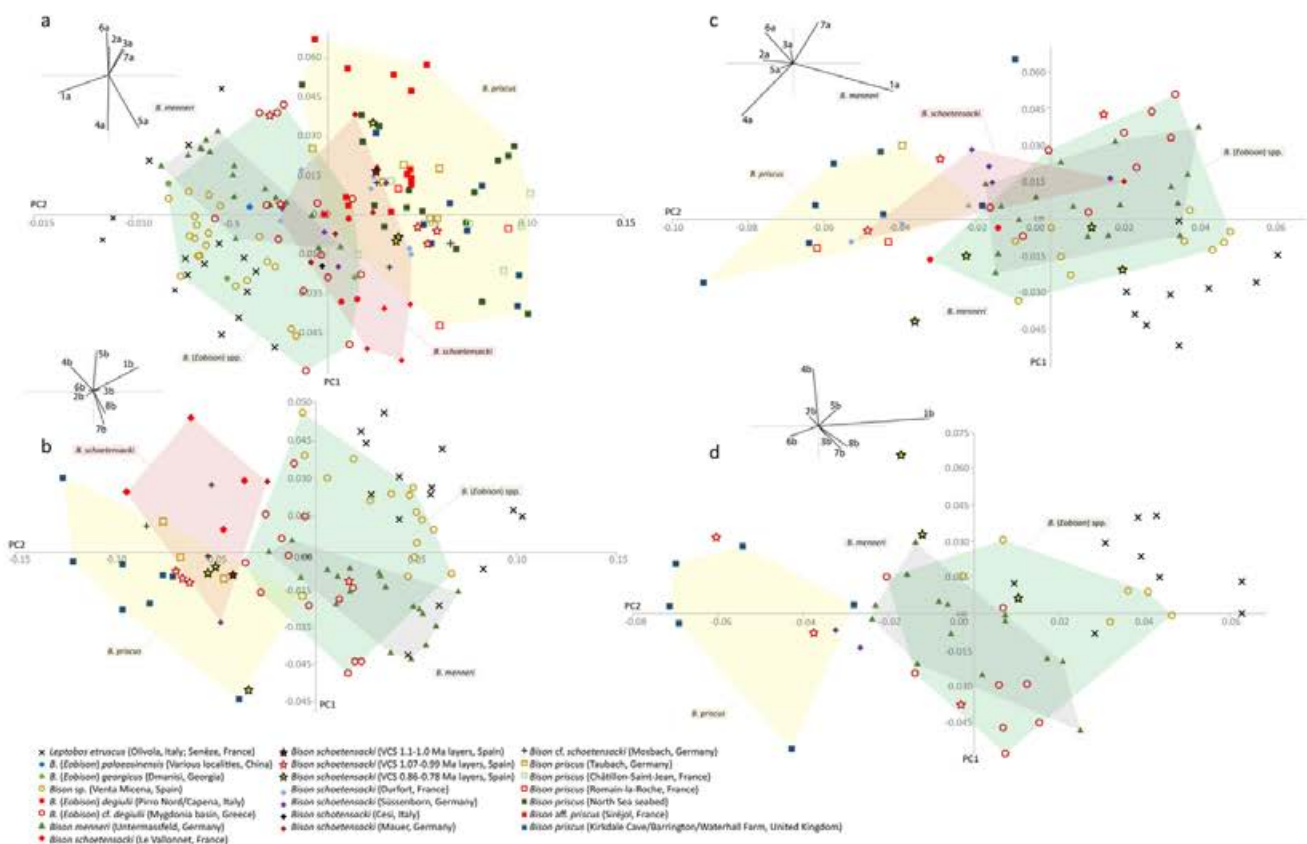


Fig. 10. Bivariate plots of the first two principal component (PC) scores resulting from principal components analyses of metacarpal (a) and metatarsal (b) variables, based on the seven variables used in this study (1), as well as in those used by Scott and Barr (2004) (2). Significant PCs with variance and coefficient of variables are in Tables S19, S20, S30, S31. Abbreviations as in Table 2.

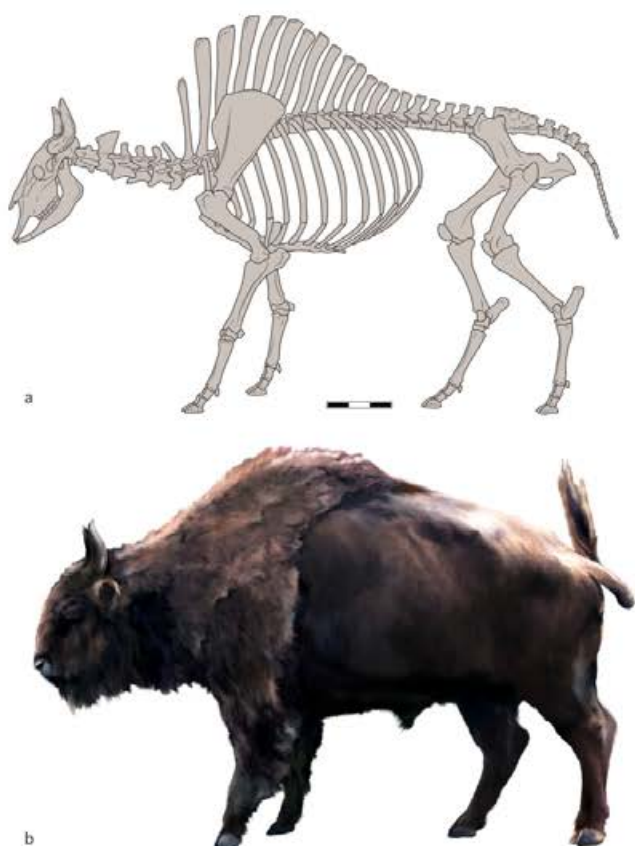


Fig. 11. Reconstruction of the skeleton (a) and external appearance (b) of an adult male of *Bison schoetensacki* based on the remains recovered from VCS and other European sites. Scale bar: 300 mm.

distally below the trapezoidal process, separating the two articular grooves. The area immediately anterior to the medial malleolus is characterized by a raised tubercle. The anterior malleolar facet is inclined anteriorly. The posterior surface of the distal diaphysis is slightly convex. Between the medial malleolus and the subtriangular process separating the two articular grooves, there is a shallow furrow that extends up to the shaft ending distally to the midshaft (in IPS92942, this furrow is deeper than in the others and delimited by two crests, the medial one being sharper). The lateral margins of the two malleolar facets are concave dorsally and separated by a deep U-shaped notch. The lateral articular groove is anteroposteriorly longer but mediolaterally narrower than the mesial one. The anterior margin of the lateral articular groove is pointed and more anteriorly protruding than the mesial groove. Conversely, the posterior margins of the two grooves lie almost at the same level. The posteromedial corner of the medial groove forms a right angle. In all the specimens but IPS92943, on the posterior margin of the medial malleolus there is a marked step. The lateral malleolus is more developed than the medial and hosts the anterior and posterior malleolar facets. The subcircular anterior facet is small and slightly concave, while the subtriangular posterior facet is larger and more concave than the anterior one.

Remarks and comparisons—The VCS tibiae attest to marked sexual dimorphism, with male specimens (IPS107618, IPS92942, IPS114546) being larger and more robust than female ones (IPS92940, IPS92943). Gee (1993) recognized several diagnostic criteria between the tibiae of *Bos* from *Bison*. However, we found that the most reliable lies in the two facets for the malleolus

(Brugal, 1985; Sala, 1986; Sher, 1997). In *Bos*, the facets are often confluent, and the anterior one is quite smaller and flatter than the posterior one. The VCS tibiae depart from this morphology and more closely resemble *Bison*, where the two facets are well separated by a marked notch and the anterior facet is concave to some extent. The size of the distal epiphysis in the VCS sample fits within the variation of *Bison* spp. (Table S23).

4.2.11. Astragalus

Description—See Fig. 7a and b and Table S24. The bone is large and stout, and the mediolateral diameter is always larger than half of the maximum proximodistal length. The proximal lateral trochlea is wider and higher than the medial one. The intertrochlear notch is narrow and smooth, and ends distally in a deep and rough fossa. The distal trochleae are more similar to each other than the proximal ones, although the lateral one is slightly wider. The distal intertrochlear notch is wider and shallower compared to the proximal one. There is a small tubercle between the proximal and distal trochleae along the medial margin of the bone. Most of the posterior surface of the talus is occupied by the wide and subrectangular calcaneal articular facet. This facet is delimited dorsally by a transversal groove. The posterior margin of the calcaneal facet is separated from the distal trochlea and the central tarsal facet by a deep and narrow L-shaped groove. The angle between the two segments of this groove is slightly higher than 90°. The cubonavicular facet is located at the distomedial corner of the calcaneal facet and is delimited laterally by a step, which is less marked in IPS92952 and IPS92951 than in the remaining specimens.

Remarks and comparisons—The VCS astragali are homogenous in size and shape, with the only exception of IPS92951, which is slightly smaller and slenderer than the others. The astragalus exhibits several diagnostic features that distinguish *Bison* from *Bos* (Schertz, 1936a; Bibikova, 1958; Stampfli, 1963; Brugal, 1985; Sala, 1986; Gee, 1993; Sher, 1997). On the posterior side, the groove that separates the calcaneal facet from the central tarsal facet is less accentuated in *Bos* than in *Bison* (Schertz, 1936a) and the L-shaped angle described by this groove is almost right in *Bos* and obtuse in *Bison* (Brugal, 1985; Sala, 1986). These characters, even if somewhat variable in both *Bos* and *Bison*, can help discriminating them based on large samples. All the VCS specimens display a deep and obtuse groove, thus more closely resembling *Bison*. Furthermore, according to Bibikova (1958), *Bos* would also differ from *Bison* in having a longer and thinner prolongation of the calcaneal facet on the lateral side of the astragalus. However, this feature is highly variable in the VCS sample, with some specimens (e.g., IP92953) displaying the supposedly *Bos*-like condition and others (e.g., IPS92949) being instead *Bison*-like. Gee (1993) evidenced that in *Bos* the posterior lateral margin of the astragalus is curved, whereas it is straight in *Bison*. We found that this character is generally reliable, as further shown by the VCS astragalus sample, which shows very straight margins.

Leptobos and *B. (Eobison)* somewhat differ from *Bison* s.s. in the ratio between the width of the distal trochlea and the total length of the astragalus (Fig. 9), with the former taxa having smaller and thinner bones. However, the ranges given by the DEW/Lmax of all the species referred to *Bison* s.l. overlap widely, making this feature not particularly diagnostic, especially for isolated remains. Within *Bison* s.s., *B. priscus* has larger (both longer and wider) astragali compared to *B. menneri* and *B. schoetensacki*, but there are not many evidence of differences in stoutness (Fig. 9d; Table S25).

4.2.12. Calcaneum

Description—See Fig. 8c and d and Table S26. The calcaneum body displays an hourglass-shaped anterior contour, with a constriction just above the sustentaculum tali and a massive tuber

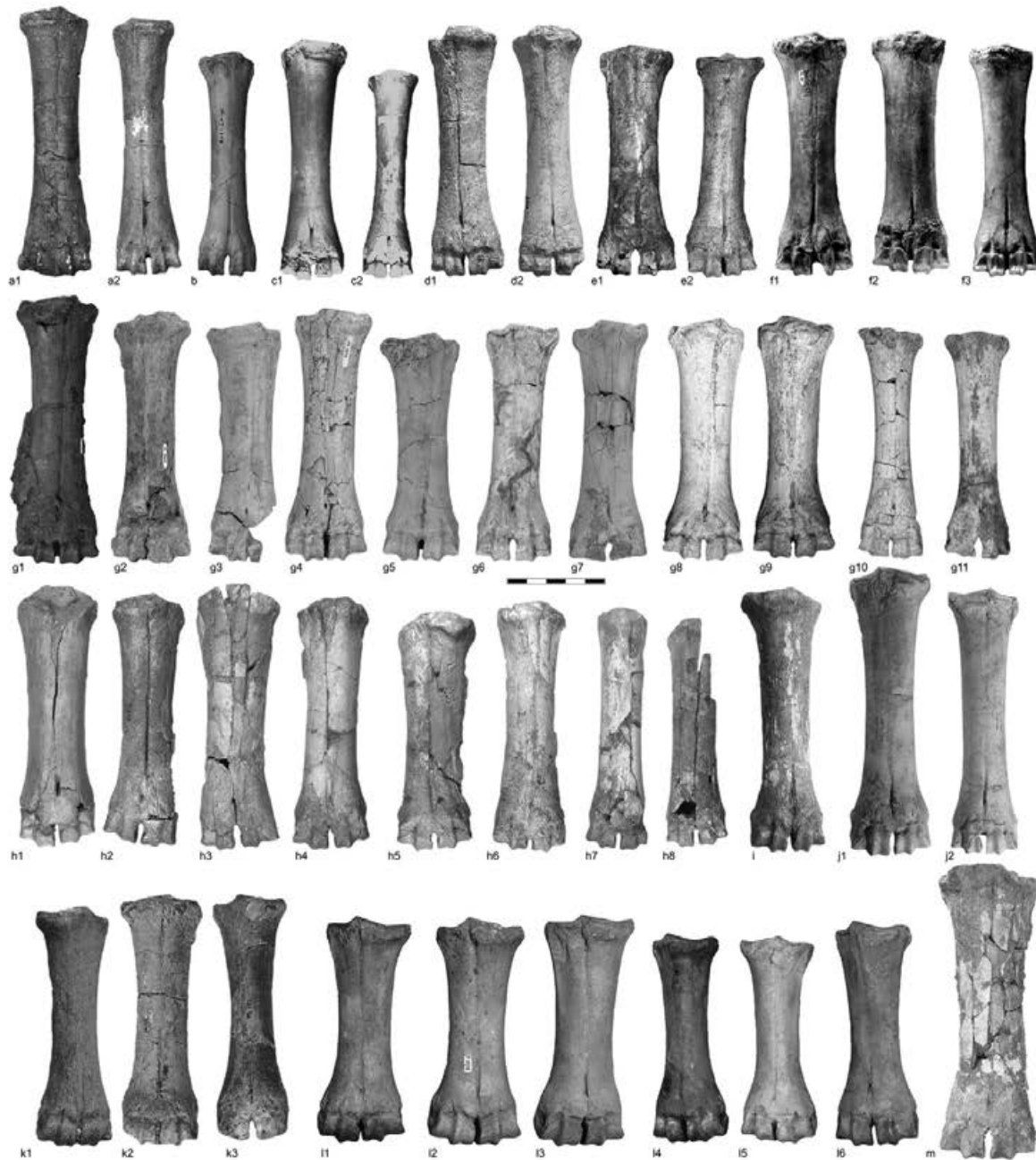


Fig. 12. Comparison of metacarpals among *Leptobos* and *Bison* s.l. species. a, *Leptobos etruscus* male IGF 2452 (1) and female IGF 2471 (2) from Olivola (Italy); b, *Bison (Eobison) palaeosinensis* IVPP V 22655 from Shanshenmiaozui (China; taken from [Tong et al., 2016](#)); c, *Bison (Eobison)* sp., male IPHES VM 83.C-3.G-85 (1) and female IPHES VM 83.C-3.G-711 (2) from Venta Micena (Spain; taken from [Moya-Solà, 1987](#)); d, *Bison (Eobison) georgicus* males GNM D2812 (1) and GNM D2288 (2) from Dmanisi (Georgia; taken from [Bukhsianidze, 2005](#)); e, *Bison (Eobison)* cf. *degiulii* male AUTH KLT-646 (1) and female AUTH APL-373 (2) from Mygdonia Basin (Greece; taken from [Kostopoulos et al., 2018](#)); f, *Bison schoetensacki* males MNHN DUR-105 (1), MNHN DUR-107 (2) and female MNHN DUR-106 (3) from Durfort (France); g, *Bison schoetensacki* males IPS14917 (1), IPS13928 (2), IPS14815 (3), IPS13547 (4), IPS92907 (5), IPS92912 (6), IPS92911 (7), IPS107635 (8), IPS107636 (9) and females IPS107626 (10), IPS107626 (11) from VCS (Spain); h, *Bison schoetensacki* males MPRM A8 B1 3748 (1), MPRM A7 AH14 8424 (2), MPRM E7 C 242 (3), MPRM C6 359 (4), MPRM C4 CE13 209 (5), MPRM C6 200 (6) and females MPRM A8 B2 326 (7); MPRM B9 BJ7 346 (8) from Le Vallonnet (France); i, *Bison schoetensacki* HLMD-Mau-401 from Mauer (Germany; kindly provided by Marisa Blume and Oliver Sandrock); j, *Bison menneri* male IQW 1980/15235 (1) and female IQW 1980/16658 (2) from Untermassfeld (Germany; taken from [Sher, 1997](#)); k, *Bison schoetensacki* HLMD-Mb-433 (1), HLMD-Mb-435 (2) HLMD-Mb-785 (3) from Mosbach (Germany; kindly provided by Marisa Blume and Oliver Sandrock); l, *Bison priscus* males NAS F-3072 (1), NAS F-1155 (2), NAS F-1275 (3) and females NAS F-1353 (4), NAS F-1339 (5), NAS F-1348 (6) from Siberia (Russia; taken from [Kirilova et al., 2015](#)); m, *Bison priscus*: MCM BOV 1520 M 13–34 Ro 87 from Romain-la-Roche (France; kindly provided by Lionel Cavin and Corinne Charvet). Scale bar: 100 mm.

calcanei (particularly developed in IPS13936, IP92946, and IPS92948). The anterior and posterior edges of the tuber are slightly convergent toward the proximal end which, in medial view, has subrounded margin. The angle between the calcaneum body and the sustentaculum tali is almost right. The cubonavicular facet is elongate and shows a sinuous concavity (oriented posteromedially in the proximal half and posteriorly in the distal). The anterior and posterior margins of the calcaneum are convergent towards the tuber calcanei. The medial surface of the anterior process bears a large tuberosity, edged posteriorly by a shallow depression. Posterior to the sustentaculum tali, there is a very small crest (not visible, probably due by taphonomic damage, in IPS92945). In distal view, the astragalus facet has a subsquare shape. This articulation expands also on the antero-medial side of the sustentaculum tali and has a semicircular outline. This articulation forms a right angle with the curved cubonavicular facet. This facet is delimited on the medial margin of the postero-medial sustentaculum tali by a subtriangular rough area. The facet for the malleolus is concave, in anterior view is proximodistally elongated and has a subrectangular shape. The anterior process is pointed and projects distally.

Remarks and comparisons—The VCS calcanei come from EVT7, apart from IPS13936, which comes from CGR-D2. The EVT specimens are morphologically quite homogeneous, except minor differences in the development of the tuber calcanei, probably related to sexual dimorphism or age. In contrast, IPS13936 is much larger. Previous studies tried to find diagnostic features in the calcaneum, especially based on the relative size of the central tarsal and astragalus articular facets (Bibikova, 1958; Stampfli, 1963; Sala, 1986). However, the size of these facets is extremely variable even within a single bovine population (Sher, 1997) and thus lacks any taxonomic value. The average dimensions of the VCS calcanei resemble those of *Bison* spp. (Table S27). Like other postcranial elements, the calcaneum of *Bison* s.s. is generally larger than in the most primitive species. However, it has to be noted that the calcaneum of female specimens of *B. priscus* and *B. schoetensacki* is much smaller than that of the males, being similar to that of small-sized species of *Leptobos* and *B. (Eobison)*.

4.2.13. Other tarsal bones

See Fig. S3 and Table S15. As for the carpal bones, very few tarsal bones were recovered from the VCS (one cuneiform and two cubonaviculars). The lack of comparative samples and the scarcity of the material do not allow us to perform proper comparison with other bovid populations.

Cuneiform—The only cuneiform (IPS92965) recovered from VCS comes from EVT10. It is complete, although slightly damaged, and resembles in size and shape those of *Bison* and *Bos* (Sala, 1986: Figs 32 and 33).

Central tarsal bone—The two specimens from EVT10 are quite similar to each other. IPS92957 is slightly fragmented in some portions of the proximal and distal surfaces, whereas IPS92958 is complete. The articular facets for the astragalus are ovoid, with the medial facet being slightly larger than the lateral. Overall, their morphology is typical of *Bison* and *Bos*. The comparison with the material of *B. schoetensacki* from Isernia shows that the VCS specimens are quite similar to those from the Italian site.

4.2.14. Metatarsals

Description—The metatarsals are less abundant and morphologically more homogeneous than the metacarpals in the VCS collection (Fig. 6d–f; Table 6). Half of the specimens are lacking the distal epiphysis and most of them are damaged, but four specimens (IPS92934, IPS92931, IPS107634, and IPS92932) are very well preserved.

The medial articular facet is posteriorly concave and shows an irregular pit joined to the posterior margin. The lateral facet is higher and relatively flat. They are separated by a well-developed ridge. Three specimens (IPS92932, IP92933, and IPS92934) show a small bulge in the middle of the medial margin, posteriorly to the medial facet (particularly developed in IPS92932). The posterior articular facet is small, anteroposteriorly short, strongly inclined toward the lateral margin, and of variable maximum length. A secondary facet for the articulation with the second metatarsal is present at the posteromedial corner of the proximal epiphysis. There is a small crest along the posterolateral corner of the articular surface. Two specimens (IPS92932 and especially IPS92932) have a markedly slenderer diaphysis than the rest of the sample. A very small and narrow proximal foramen is still visible only in IPS92931, IPS92936, IPS92937, IPS92938, and IPS107634. The anterior side of the bone is characterized by the well-marked and deep vascular groove. In their distal portion, the edges of the groove are shaped as sharp ridges. There is a secondary, shallower groove located on the dorsolateral aspect of the proximal portion of the shaft in most of the specimens (although it is very faint in IPS92932 and IPS92932). An elliptical distal foramen is present in all the specimens. In the distal epiphysis, the margins of the intertrochlear space are subparallel to distally convergent. As in the metacarpals, the epitrochlear tubercles are well developed, so that the width at the level of the tubercles is about the same as that measured between the outer trochlear margins. The only notable feature in the posterior side of the proximal epiphysis is the pointed medial corner. Distally next to it, IPS92930 and IPS92932 show a small circular facet, which is also present (although less marked) in IPS107634, corresponding to the posterior articular facet for the second metatarsal. The large proximal foramen is located inside a deep subcircular depression distal to the posterior margin of the proximal epiphysis. The proximal diaphysis is delimited by two crests, the medial being usually stronger than the lateral, which do not extend beyond the proximal third of the shaft. The posterior surface of the diaphysis is slightly concave to flat in its proximal half, where two very shallow longitudinal grooves are present. These two grooves disappear toward the distal portion, which is completely flat. The distal foramen is distinct and elliptical. As in the metacarpals, on the anterior side, proximally to each trochlear crest, two depressions develop, with the outer one being larger and deeper than the inner. The distal epiphysis is slightly curved posteriorly. The lateral and medial trochlear pits are deep and proximally surrounded by radial rugosities. The two trochlear ridges are subparallel relative to the medial and lateral margins of the distal end and converge anteriorly.

Remarks and comparisons—As for the metacarpals, the metatarsals have often been considered diagnostic for large bovids in the literature (Table S28). In the proximal articular surface, the angle between the lateral and medial facets is lower in *Bos* (13–22°) than in *Bison* (22–40°; Schertz 1936a; Sala, 1986; Sher, 1997), even if the measurement can be somewhat biased depending on the methods (Sher, 1997). The VCS sample most closely resembles *Bison* in this regard (20–30°). The anterior contact between the two proximal facets is different in *Bos* and *Bison* (Brugal, 1985; Gee, 1993). In *Bos* there is no contact between these two facets, often divided by a narrow channel. In *Bison*, the facets are confluent forming, in most of the cases, a small but sharp ridge (Gee, 1993). In the VCS metatarsals, the two facets are in contact and a clear ridge is present in all the specimens. Nevertheless, the major difference in metatarsal morphology between *Bos* and *Bison* lies at the distal half of the bone. As for the metacarpals, the VCS metatarsals display the typical morphology of *Bison* s.l., where the contact between the diaphysis and the distal epiphysis is medio-laterally inflated (Sala, 1986; Sher, 1997)—so that medio-lateral width at this level is

Table 6

Measurements and descriptive statistics of the metatarsals of *Bison schoetensacki* from Vallparadís Estació (EVT) and Cal Guardiola (CGR) layers. Abbreviations: ABETl, abaxial emicondyle thickness (lateral emicondyle); ABETm, abaxial emicondyle thickness (medial emicondyle); AETl, axial emicondyle thickness (lateral emicondyle); AETm, axial emicondyle thickness (medial emicondyle); DETl, distal epiphysis thickness (lateral trochlear crest); DETm, distal epiphysis thickness (medial trochlear crest); DEW, distal epiphysis width; DDW, distal diaphysis width (above the epiphysis); DT, diaphysis thickness (midshaft); DW, diaphysis width (midshaft); F, female; L, left; Lf, functional length; Lmax, maximum length; M, male; PET, proximal epiphysis thickness; PEW, proximal epiphysis width; PFOl, proximal articular facet oblique diameter (medial facet); PFOm, proximal articular facet oblique diameter (lateral facet); R, right.

ID Specimen	Layer	Side	Sex	Lmax	Lf	PEW	PET	DW	DT	DDW	DEW	DETm	DETI	PFOm	PFOl	ABETm	ABETl	AETm	AETl
IPS92906	EVT7	L	F			54.5	56.5	37.5	42.0					46.5					
IPS92930	CGRD7	R	F	280.5	265.6	58.1	53.2	36.6	34.8	59.0	65.0			37.4	37.6				
IPS92931	EVT7	L	F	269.7	253.0	57.0	56.8	39.4	40.3	62.5	63.8	34.5	35.1	39.3	41.1	25.5			
IPS92932	EVT12	R	F	275.2	258.6	57.3	57.5	34.0	37.9	65.3	65.0	41.4	38.7	40.0	36.9	26.5	25.8	32.2	33.7
IPS92933	EVT7	L	M?			62.6	61.6	42.8	44.3					33.5	52.5	30.7	28.5	35.8	37.3
IPS92934	EVT7	R	M?	296.2	275.3	63.8	59.2	42.2	43.0	72.1	69.9	41.9	41	45.5	43.0				
IPS92935	EVT7	R	M?			63.7	62.0	42.0	40.5					44.5	42.8	31.5	28.9	35.0	40.2
IPS92936	EVT7	L	F					40.3	39.5										
IPS92937	EVT12	R	M	300.2	287.4	68.3	66.0	45.5	45	76.5	78	43.6	41.1	46.0	53.3				
IPS92938	EVT10	L	F			61.0	60.0							41.3	42.0	34.4	32.1	39.1	40.4
IPS92939	EVT7	R	F			59.0	55.5	39.9	40.5					37.5	40.0				
IPS107634	EVT12	R	M	279.0	258.3	60.4	60.0	39.5	42.4	70.7	73.6	42.5	41.9	44.0	40.2				
IPS114552	EVT7	L	F	272.3	268.3	53.0	52.7	36.9	34.2	60.9	61.3	39.5	37.0	37.0	39.0	31.9	30.2	38.7	39.6
IPS114553	EVT7	R	F	293.8	287.4	57.0	55.9	37.7	37.7	63.3	61.8	38.9		44	36.4	30.2	27.7	33.0	32.0
	Mean			283.4	269.2	59.7	58.2	39.6	40.2	65.8	67.3	40.3	39.1	41.3	42.1	30.1	28.8	35.6	37.2
	Minimum			269.7	253.0	53.0	52.7	34.0	34.2	55.0	61.3	34.5	35.1	33.5	36.4	25.5	25.8	32.2	32.0
	Maximum			300.2	287.4	68.3	66.0	45.5	45.0	76.5	78.0	43.6	41.9	46.5	53.3	34.4	32.1	39.1	40.4
	SD			11.7	13.1	4.2	3.7	3.1	3.3	6.9	6	3.1	2.7	4.2	5.5	3.1	2.2	2.9	3.6
	N			8	8	13	13	13	13	8	8	7	6	13	12	7	6	6	6

similar or even larger than that between the trochlear margins—whereas in *Bos* the medial and lateral margins of the distal end are strongly divergent (Table S29).

Bison can readily be distinguished from *Leptobos* given based on the possession of larger and stouter metatarsals, but given the considerable variation within *Bison* s.l. it is difficult to find reliable differences among different species (Table S28). The “stoutness” diagram (Fig. 9b) shows that *B. priscus* and *B. schoetensacki* have generally heavily-built metatarsals with wider ends compared to other samples, despite considerable variation; in contrast, *B. menneri* has much slenderer metatarsals, while those of *B. (Eobison)* spp. are both smaller and slenderer. Most of the VCS sample displays an intermediate size and slender built, except for two specimens (IPS107634 and IPS92937 from EVT12) that are particularly large and massive, and a quite slender specimen (IPS114553 from EVT7). The ANOVA shows that, although there are some differences between syn-Jaramillo (EVT10 and EVT12) and post-Jaramillo (CGRD7 and EVT7) subsamples, these are not significant for seven out of the eight analyzed variables (Table 4). The “stoutness” diagram and PCAs further confirm that, despite the rather homogeneous morphology of the whole sample, a change from stouter to slenderer metatarsals can be recognized from EVT10-EVT12 to CGRD7-EVT7. The MANOVA on five variables confirms that the relative proportions of the VCS metatarsal sample are not characterized by significant differences (Table 4).

As for the metacarpals, the PCAs enable the distinction of various groups of *Bison* s.l. despite considerable overlap. In the first PCA (Fig. 10c, Table S30), based on seven shape variables, PC1 (40% variance), positive scores are mainly influenced by msLmax and, to a lesser extent, msDET, whereas negative scores are mostly driven by msDW, msPEW, and msDEW. In turn, PC2 (21% variance) is mainly determined by msDEW and msDET (positive scores) and msDW, and to a lesser extent Lmax (negative scores). The VCS sample is rather scattered in the diagram. The most massive specimens (IPS107634 and IPS92937), characterized by a relatively stout appearance (short and wide bones), overlap with the bulk *B. priscus* from UK and Taubach (negative PC1 scores). The VCS slender specimens (possibly females) overlap with the more gracile *B. (Eobison)* group and *B. menneri*, which feature positive PC1 values

due to their relatively long and narrow diaphysis.

In the second PCA (Fig. 10d, Table S31), PC1 (39% variance) is almost totally influenced positively by reMLmax, separating long metatarsals (positive scores) from short ones (negative scores). PC2 (25% variance), on the contrary, separates metatarsals with more massive diaphysis (high positive values of reDT and reDW) from those with a stouter distal epiphysis. The VCS metacarpals partially overlap with *B. menneri* from Untermassfeld, *B. (Eobison)* cf. *degiulii* from the Mygdonia Basin, and *B. priscus* from UK, highlighting the high variation of these bones in the VCS sample. The meager comparative data for *B. schoetensacki* do not allow us to further assess the variation of this species. The MANOVA indicates that our sample differs significantly only from the extremely slender samples from Venta Micena and Untermassfeld (Table S32). This result obtained for the metatarsals highlight less differences between taxa than the same analyses carried out on metacarpals (see Section 4.2.9), pointing out that the bison hindlimbs are more variable.

4.2.15. Phalanges

Proximal phalanges—The proximal phalanges are overall well preserved and morphologically very similar (Fig. S4; Table S33). The abaxial and interdigital margins are parallel so that the width of the phalanx is similar throughout its length. The abaxial tuberosity is more developed than the interdigital one; in IPS14977 and IPS92925, the former constitutes a large bulging prominence. Between these tuberosities and the two small sesamoid facets, there are two tubercles separated by a depression of variable depth. A depression, developed mediolaterally, is present in the proximal part of the phalanx, between the posterior tuberosities and the proximal end. In the proximal articulation, the interdigital glenoid cavity is higher and narrower than the abaxial one. The abaxial sesamoid facet is larger and flatter than the interdigital one.

Intermediate phalanges—See Fig. S4 and Table S33. The shaft of the phalanx is stout and massive. The interdigital surface is concave, while the abaxial is convex. In the proximal articulation, the abaxial glenoid cavity is slightly larger than the interdigital, and both are inclined dorsally and interdigitally. Below the articular surface there is a small depression. The outline of the distal articular trochlea is triangular, with the abaxial lobe larger than the

interdigital; the groove that divides the two lobes is inclined dorsally and interdigitally.

Distal phalanges—See Figure S4 and Table S33. In dorsal view, the abaxial margin is convex and the interdigital is almost straight. Proximally, the two glenoid cavities are similar in size and inclined dorsally and interdigitally, aligned obliquely relative to the sagittal plane. Posteriorly to them, a small subtriangular, interdigitally-oriented sesamoid facet is visible. Below the sesamoid facet, there is a deep oblique groove, delimited by a small crest. The abaxial surface is convex while the interdigital one is slightly concave.

Remarks and comparison (phalanges)—The phalanges of *Leptobos*, *Bison* and *Bos* are quite similar and no morphological differences were found. Discriminating between forelimb and hindlimb phalanges, also taking in account the sexual dimorphism in bovids, is not easy. Generally, the forelimb proximal phalanges are shorter and more compact than the hindlimb ones (Revilliod et Dottrens, 1946), which are longer and relatively slenderer (Sala, 1986), shorter and wider according to Sher (1997). The intermediate phalanges are slightly longer but considerably wider in the forelimbs than in the hindlimbs (Sala, 1986; Sher, 1997). According to Sala (1986) the forelimb distal phalanges are shorter and broader compared to the hindlimb ones, whereas Sher (1997) stated that, on the contrary, the forelimb distal phalanges are longer than the hindlimb ones. The fact that in most cases the phalanges are found isolated make this discrimination difficult, which is further aggravated by the fact that phalangeal measurements are seldom published and not all the authors agree in how to distinguish the manual and pedal phalanges (e.g. Sala, 1986; Sher, 1997). Regarding the sample from VCS, the lack of comparative measurements, the scarcity of the material, and the lack of associated specimens make it impossible to reliably discriminate between fore and hind phalanges or between male and female specimens.

5. Results

5.1. The VCS sample: taxonomy and morphological variation

Based on the qualitative and quantitative comparisons reported above, it is possible to confidently refer all described remains from the VCS to the same species (Table 4). The analyses performed on the metapodials suggest that two morphotypes are recognizable, characterized by slightly different proportions probably due to ecophenotypic variation (see Section 6.1.). The study performed on the 220 remains allow us to refer the large bovid from VCS to the genus *Bison*. Moreover, the large size and the stout morphology of the limb bones support their assignment to subgenus *Bison*, which includes the largest species of the genus. Some features, such as the relatively slender limbs, most closely resemble the early members of this subgenus, namely *B. menneri* and *B. schoetensacki*, which are first recorded during the Epivillafranchian. The VCS bison differs from the roughly coeval *B. menneri* in the markedly stouter limb bones, as well as the shorter and wider metapodials (in particular, the metacarpals). The steppe bison *B. priscus* is characterized by even more robust proportions (Fig. 9). The partial overlap in metapodial dimensions between the larger and stouter specimens from the VCS and the smaller and slenderer specimens of *B. priscus* probably reflects sexual size dimorphism in the two samples, with male individuals from VCS displaying a similar size to female individuals of *B. priscus*.

In sum, the morphological characters of the VCS bison allow the referral of this sample to *Bison schoetensacki*, which was the most common bison species in Europe during the Middle Pleistocene, although it originated during the latest Early Pleistocene (Flerov, 1975; 1979). The chronostratigraphic distribution of *B. schoetensacki* might span from ca. 1.1 to 0.5 Ma (Grange et al., 2018). *Bison*

schoetensacki has been regarded as an early member of the lineage that ultimately led to the steppe bison and extant European wisent (Palacio et al., 2017), but this needs to be clarified further. Although *B. schoetensacki* is quite common in the European fossil record, only a few localities have yielded a large number of fossils, hindering a more detailed assessment of its phylogenetic relationships.

The VCS sample is the largest collection of *B. schoetensacki*, together with that from Isernia, thus substantially improving our knowledge on the anatomy of this species and allowing us to provide the reconstruction depicted in Fig. 11. Moreover, almost all the fossils from VCS were recovered from layers dated between 1.1 and 0.86 Ma, thus offering a broader chronological perspective on the morphology of this species, which was likely influenced by major paleoenvironmental changes in the study area (see Section 6.1.).

5.2. The *Leptobos etruscus*–*Leptobos vallisarni* lineage

Bison probably evolved in Asia from a derived species of *Leptobos* (Pilgrim, 1947; Tong et al., 2016). Among the described species of the latter genus, *L. etruscus* from the Late Villafranchian of Europe is the largest and one of the most derived, showing some cranial features that closely resemble those of *Bison* s.l. (Masini, 1989; Bukhsianidze, 2005; Masini et al., 2013). The postcranial skeleton of *L. etruscus* is well known thanks to the large collections from Senèze (France), Olivola and Upper Valdarno (Italy). Its metapodials are particularly slender (length reaching 26.5 mm and epiphysis width not exceeding 70 mm; Table S16), being similar in size to those of *B. (Eobison)* (Fig. 10). Other postcranial bones (e.g., radii, astragali) are overall smaller and slenderer than those of *Bison* s.l. (Fig. 10).

Leptobos vallisarni, which is up to date the only *Leptobos* species reported both in Europe and Asia, is characterized by even more derived features (Masini, 1989). This large-sized species was described by Merla (1949) on the basis of a partial cranium from the Early Pleistocene of the Upper Valdarno, but two almost complete skulls from the Gonghe Basin (central China) testify to the wide geographic distribution of this taxon (Zheng et al., 1985). Unfortunately, the postcranial skeleton of *L. vallisarni* is poorly known. The very rich sample from the late Villafranchian of Pietrafitta (central Italy), which is attributed to *L. aff. vallisarni* (Masini, 1989; Gentili and Masini, 2005) and also includes a large number of metapodials, displays a derived cranial morphology that resembles that of *Bison* s.l.—thereby rendering the attribution to *Leptobos* unreliable. A few metapodials from the Upper Valdarno, housed in the Natural History Museum of the University of Florence, have been attributed to this species (Masini, 1989; Masini et al., 2013), but our analysis of the collection suggests that they might have been mixed with material of other *Leptobos* species. For this reason, we refrain from making further assumptions about the limb proportions of *L. vallisarni* until a complete revision of the European *Leptobos* spp. postcranial collections is undertaken.

5.3. Early bison species

The early occurrences of *Bison* s.l. correspond to *B. (E.) palaeosinensis* and *B. (E.) sivalensis* from Asia. While many authors agree on an Asian origin of *Bison* s.l. (e.g., Flerov, 1972; Sala, 1986; Sher, 1997), there is still no consensus on the chronology. The earliest known remains are referred to *B. (E.) cf. sivalensis* from the Upper Siwaliks (northern Pakistan), dated to 3.3–2.6 Ma (Khan et al., 2010). These fossils mostly consist of cranial material, and therefore we did not include them in our comparative analyses. However, the remains attributed to *B. (E.) sivalensis*, apart from the lost

holotype cranium, are too fragmentary to confirm that they belong to a single species, particularly in the light of their unclear stratigraphic provenance (Kostopoulos et al., 2018).

In turn, *B. (E.) palaeosinensis* is a small-sized and primitive species from the Early-Middle Villafranchian of Asia, whose taxonomic status has been much debated (Teilhard de Chardin and Piveteau, 1930; Skinner and Kaiser, 1947; Tong et al., 2016). The three incomplete crania and several postcranial bones of this species come from different sites of Yushe and Nihowan Basins (China). Our analyses reveal that the metacarpals were short and relatively slender, falling within the *B. (Eobison)* range (Fig. 9). One metacarpal from Nihowan (NIH113; Masini, 1989) displays a slender morphology that fits with *L. etruscus* (Fig. 9), whereas the remaining metacarpals are most similar to those of *Bison* sp. from Venta Micena and *B. (Eobison) degiulii* from the Italian Peninsula (Fig. 9). The metatarsals, radii and astragali are small and slender, largely overlapping with *Leptobos* but not with *Bison* s.s.

The earliest record of *Bison* s.l. from Europe corresponds to the small and primitive species *B. (Eobison) georgicus*. The remains of this species come from the Late Villafranchian site of Dmanisi (Georgia; ca. 1.77 Ma) and consist of a single neurocranium with horn cores and several postcranial bones (Bukhsianidze, 2005). Our analyses show that two metacarpals (GNM D2288, GNM D2812) display slender proportions similar to those of *L. etruscus*, whereas another (GNM D3426) is clearly stouter and matches instead the variation of *B. (Eobison)* spp. and also overlaps to some extent with *B. schoetensacki* (Fig. 10). The slender specimens are about 8% longer, but more than 12% narrower distally, than the stouter ones. Given that, often, female *Bison* metacarpals are shorter and narrower than those of males (Schertz, 1936a), the aforementioned differences might simply be explained by sexual dimorphism. On the other hand, two complete radii from Dmanisi (GNM D2962, GNM D2165) do not display the elongated and slender morphology of *L. etruscus* but closely resemble that of *Bison* s.l. Taking into account the age of the site, Dmanisi might record the co-occurrence of the last *Leptobos* and earliest of *Bison* s.l. with transitional characters, as already suggested by Kostopoulos et al. (2018), but additional fossils would be required to adequately test such a possibility.

A large bovid from Venta Micena (southern Spain; ca. 1.6 Ma) was attributed to *Bison* sp. due to its clearly "bisontine" size and proportions (Moyà Solà, 1987). The metapodials are shorter than those of *L. etruscus* but slenderer than those of late forms of *Bison* s.s., resembling the samples of the *B. (E.) degiulii* and *B. (E.) palaeosinensis* (Fig. 9). In metacarpal proportions (Fig. 9a), two specimens (VM-9033 and VM-925) at the upper range of the Venta Micena sample overlap with those of *L. etruscus* from Olivola and Senèze. The rest of the Spanish sample is otherwise quite homogeneous, albeit clearly showing differences attributable to sexual dimorphism in the size and robusticity of the metacarpals. The metatarsals similarly plot with the smaller and slenderer forms (i.e., *Leptobos* and *Eobison*; Fig. 9b). The PCAs, irrespective of the variables used, indicate that the metapodials of the Venta Micena bovid are intermediate between *Leptobos* and *Bison* s.s., partially overlapping with the former (Fig. 10). The three most complete radii from Venta Micena are quite short and slender, being the smallest ones in our comparative sample (Fig. 9c). The identification of the bovid postcranials from Venta Micena is further complicated by the attribution of cranial remains to both *Bison* sp. and *Hemibos* aff. *gracilis*, of Asian origin (see Martínez-Navarro et al., 2011). A revision of the cranial and postcranial bovid material from Venta Micena is pending, but our morphometric analyses indicate that the metapodials fit well with the morphology of *B. (Eobison)* (Figs. 9 and 10). On geographic and chronological grounds, the Venta Micena sample might be referable to *B. (E.) degiulii*, but more in-

depth analyses would be required to confirm such an attribution.

Current knowledge of *B. (E.) degiulii* is limited. The type material includes the partial cranium of an elder individual (holotype) and six metapodials (five metacarpals and one metatarsal) from the latest Villafranchian of Pirro Nord (southern Italy; ca. 1.6–1.4 Ma; Masini, 1989). Masini (1989) also attributed to this species one metacarpal and one metatarsal from Capena (central Italy, Late Villafranchian) and three metacarpals from Sainzelles (southern France, Late Villafranchian, Brugal, 1995). As noted above, the metacarpals of *B. (E.) degiulii* are quite similar to those from Venta Micena, albeit they are slightly shorter and stouter (Fig. 9). The bovid sample from the Mygdonia Basin (Greece), mainly including metapodial remains and a few cranial elements from Kalamoto, Tsiotra Vryssi, Krimni, and Apollonia (dated to between 1.7 and 1.2 Ma), was attributed to *B. (E.) cf. degiulii* by Kostopoulos et al. (2018). The marked morphological variation among metapodials was interpreted as the result of an increasing size and stoutness trend in relation to progressive climate deterioration throughout the Late Villafranchian (Kostopoulos et al., 2018). Several metacarpals from the younger locality of Apollonia (ca. 1.2–1.1 Ma) resemble male specimens of *B. schoetensacki* in size and robusticity, but most of the sample displays the typical proportions of *B. (Eobison)*, and only two (AUTH APL-677, AUTH KRM) are slightly slenderer and more *Leptobos*-like (Fig. 9). The PCAs performed Maniakas and Kostopoulos (2017a) and Kostopoulos et al. (2018) showed considerable overlap among *Bison* s.l. species, only distinguishing "slender" from "stout" forms. They revealed proportion similarities between the Mygdonia bovid remains and those of *B. menneri* from Untermassfeld, as well as between the latter and *Bison* sp. from Venta Micena. These similarities are also evident from our "stoutness" and Log₁₀ ratio diagrams (Fig. 9), which show that *B. menneri* and *B. (Eobison)* spp. mostly differ in size but not in proportions. Kostopoulos et al. (2018) questioned the inclusion of *B. degiulii* into subgenus *Eobison* based on some derived characters of the holotype and the cranium KLT-638 from Kalamoto. If the whole sample from the Mygdonia basin belongs to a single species (Kostopoulos et al., 2018), the postcranial remains further display a mosaic of derived and primitive features, because some metacarpals from Apollonia (AUTH APL-745, AUTH APL-414, AUTH APL-578, AUTH APL-446, and AUTH APL-95) resemble in robusticity the male specimens of *B. schoetensacki* from Mosbach, Durfort, Cromer Forest-bed, and VCS (Fig. 9). Nevertheless, our PCAs, ANOVAs and Log₁₀ ratio diagrams confirm that, despite some overlap, the Mygdonia sample is distinct from "priscoid" forms and show that, on average, the Greek metacarpals are characterized by relatively shorter and slenderer proportions (Fig. 9e–g, Fig. 10a and b, Table S21). Such results suggest that the assignment to *B. (E.) cf. degiulii* by Kostopoulos et al. (2018) is well supported, at least until a more detailed revision of this species is undertaken.

Two additional species of *B. (Eobison)* are poorly known. *Bison (E.) tamanensis* from the Taman Peninsula and *B. (Eobison) suchovi* from central Ukraine, erected without a diagnosis by Verestchagin (1959) and Alekseeva (1967), respectively. Both these late Early Pleistocene Eastern European species have a debated taxonomic history and are described on quite scanty fossil material (see Croitor, 2010; Kostopoulos et al., 2018 and references therein). In the light of these issues the taxonomic status of this species cannot be properly assessed and is not discussed in this paper.

Unlike the above, *B. menneri* is a well-known species from the German site of Untermassfeld (ca. 1.0 Ma; MIS31), being considered one of the earliest members of *Bison* s.s. (Sher, 1997). Bukhsianidze (2020) recently referred this species to the subgenus *Bison (Poephagus)* based on purported closer cranial similarities with extant yaks. The postcranial morphology of *B. menneri* has adequately been characterized (the holotype itself, IQW, 1982/17948, is a male

metacarpal; Sher, 1997). The species is described as a long-legged bovid with tall appearance, as well as a relatively small head and short horns (Sher, 1997; van Asperen and Kahlke, 2017; Bukhsianidze, 2020). Among large bovids, *B. menneri* has the longest and most slender metacarpals, and displays a mixture of *Bison*-like and, to a lesser extent, *Bos*-like features in the limb bones (Sher, 1997; Bukhsianidze, 2020). The extremely elongated metapodials are similar in proportions to those of *Leptobos* and *B. (Eobison)* (Fig. 9a and b), with considerable overlap with the latter in our PCAs (Fig. 10). Nevertheless, Sher (1997) ruled out the possibility that the Untermassfeld bovid could represent a boreal variant of a Mediterranean/Asian *Eobison* species, due to its large size and metapodial built. The most complete skull displays some primitive characters for the bison lineage, such as not very tubular orbits, elongated postcornual portion of the cranium, and horn cores very backwardly orientated. According to Bukhsianidze (2020) these elements are shared with the yak lineage (subgenus *Poephagus*). From the site of Untermassfeld, a juvenile skull and a single metacarpal (IQW 1983/19 253 (Mei. 18 773)) are not referable to the aforementioned species (Bukhsianidze, 2020); indeed, IQW 1983/19 253 (Mei. 18 773) resembles in stoutness the more “priscoid” form *B. schoetensacki* (Fig. 9), although the scanty remains do not enable a specific attribution. *Bison menneri* has also been reported from the North Sea seabed “Het Gat” site (Mol et al., 2003) and, tentatively (*B. cf. menneri*), from layer TE9c of Sima del Elefante (Spain) (Huguet et al., 2017) and from Cimichioi-III and Hadjimus (Moldova) (Croitor, 2016).

The three species from east Europe and Asia: *Adjiderebos cantabilis*, *Protobison kushkunensis* and *Probison dehmi* (Dubrovo and Burchak-Abramovich, 1986; Burchak-Abramovich, Gadzhiev and Vekua, 1980; Shani and Khan, 1968) are known for isolated cranial remains. Their affinities and relationships with *Bison* s.l. group are still matter of debate, although their transitional morphology from *Leptobos* to *Bison* could shed lights on the first forms of primitive bison.

5.4. Other samples of *Bison schoetensacki*

5.4.1. Le Vallonnet

The bison remains from Le Vallonnet (southeastern France, ca. 1.2–1.1 Ma), which is one of the few European localities that record the earliest Epivillafranchian (de Lumley et al., 1988; Moullé, 1992; Moullé et al., 2006; Michel et al., 2017), were attributed to *B. schoetensacki* by Moullé (1992). The metapodials from Le Vallonnet are characterized by large size and quite slender proportions, resembling material of *B. schoetensacki* from the type locality of Mauer, and partially overlapping with the specimens from Mosbach and Durfort (Fig. 9). Sexual dimorphism is particularly pronounced in the Le Vallonnet metacarpal sample, with the putative female specimens (MPRM A8 B2 326 and MPRM B9 BJ7 346) being located on the left portion of the stoutness diagram due to their slenderer morphology (Fig. 9a). Both the Le Vallonnet and the Mauer samples partially overlap with that of *B. menneri* from Untermassfeld, which they resemble in the elongated diaphysis and relatively narrow distal epiphysis, despite the larger diaphysis (Fig. 9a). Other postcranial bones from Le Vallonnet, such as astragali and humeri, are within the size range of *Bison* s.s., even though the astragali are slightly stouter than in other samples of *B. schoetensacki* (Fig. 9d). The two complete metatarsals (MPRM B6278(G) and MPRM E7C186(D)) from Le Vallonnet most likely belong to large males, due to their heavily-built morphology. Indeed, B6278(G) is one of the largest specimens in the entire sample of *B. schoetensacki* and falls within the range of “priscoid” forms (Fig. 9b). Based on the Log₁₀ ratio diagrams, PCAs, and

pairwise comparison, the sample of metacarpals from Le Vallonnet is similar to those of *B. schoetensacki*, except for some diaphyseal measurements that appear relatively wider and thicker (Figs. 9 and 10). Overall, the Le Vallonnet sample fits well with the variation of *B. schoetensacki*, and in particular with the large morphotype represented by the Mauer sample, thereby confirming the presence of this species before the Jaramillo subchron. Together with the specimens described here from roughly coeval VCS layers (CGRD2), they represent the first occurrences of *B. schoetensacki*, conclusively indicating that *Bison* s.s. was recorded in Europe since the Villafranchian-Epivillafranchian boundary.

5.4.2. Durfort and La Vassière

The bison sample from Durfort (southwestern France; ca. 1.0–0.5 Ma) was referred to *B. schoetensacki* on the basis of cranial (horn cores) and metapodial features (Brugal, 1995). The metapodials are morphologically intermediate between those of *B. menneri* and *B. priscus*, and resemble the earlier fossils of *B. schoetensacki* from Le Vallonnet at a slightly smaller size (particularly the metacarpals; Fig. 9). The “stoutness” and Log₁₀ diagrams and both PCAs (Figs. 9 and 10) indicate that the Durfort sample fits with the variation of *B. schoetensacki*, resembling the stout forms from Mosbach and the VCS—as the male specimens (MNHN 010 D, MNHN 107 G, MNHN 105 G, MNHN 104 G) approach the “priscoid” scatter, and the putative female specimens (MNHN 106 G, MNHN 108 G) overlap with *B. (Eobison)* (Figs. 9a and 10a–b). The analysis of metatarsals (Figs. 9b and 10c–d) shows the same pattern, with the material from Durfort being intermediate between the “priscoid” and slenderer forms. Our results confirm the attribution of the Durfort sample to *B. schoetensacki*, being characterized by slightly stouter metapodial proportions than the material from Le Vallonnet and Mauer, and most similar to the VCS bovid (Figs. 9 and 10). From the Early Pleistocene site of La Vassière (southern France; ca. 0.6) several remains of a large bovid were recovered. The fossils were attributed to *Bison cf. schoetensacki* (Brugal and Fosse, 2003). The general morphology and proportions of the only complete metacarpal fit perfectly with the variation of *B. schoetensacki* (Fig. 9).

5.4.3. Mauer and Mosbach

Bison schoetensacki was originally described by Freudenberg (1914) on the basis of remains from Mauer (Germany; Middle Pleistocene, ca. 0.4 Ma). The holotype is a partial cranial vault (which was lost during World War II; Sala, 1986), but Freudenberg (1914) also referred to the same species other cranial and few postcranial remains from Mauer and Cromer Forest-bed, and to *B. cf. schoetensacki* an almost complete skull from Mosbach. Multiple studies on this species have not entirely clarified its diagnostic features (e.g., Hilzheimer, 1918; Schertz, 1936a, b; Skinner and Kaisen, 1946; Flerov, 1969; Sala, 1986; Sher, 1997; Drees, 2005). Sala (1986) described the cranial anatomy of *B. schoetensacki* based on the remains from Mauer and Isernia (Italy; Middle Pleistocene, ca. 0.55 Ma), but for the postcranium only summarized the most important differences between *Bos* and *Bison*. In contrast, Sher (1997) focused on metapodial proportions and rejected the common misconception that *B. schoetensacki* was a small-sized *Bison* (Sher, 1997), improving the original description given by Freudenberg (1914), in which only the relative slenderness of the limbs and the small horn cores were stressed.

During the last century, the material from Mauer and Mosbach was scattered across more than five different institutions. We managed to measure some of the specimens, while for others we relied on the few published measurements (Freudenberg, 1914; Schertz, 1936a, b; Sher, 1997). However, it should be taken into

account that the collections from Mauer/Mosbach might mix two different species, *B. schoetensacki* and *B. priscus* (Schertz, 1936a, b; Sher, 1997). Their stratigraphic context is not clear, especially for Mosbach in which two different levels with different ages and faunas are recognized (Breda and Marchetti, 2005), and both sites include layers dated to 0.6–0.5 Ma (Wagner et al., 2010; Kahlke et al., 2011), close to MIS11–9 (0.4–0.3 Ma), when the first occurrence of the large and stout *B. priscus* is recorded (Kahlke, 1999). According to Schertz (1936b) and Sher (1997), most of the material from Mosbach and some specimens from Mauer would indeed belong to *B. priscus*. This idea derives from the assumption that *B. priscus* has long metacarpals, whereas, in fact, the various well-known populations of *B. priscus* from Eurasia (except the gigantic ones from Taubach, Romain la Roche and, possibly, Tiraspol) are characterized by very short and extremely stout metacarpals (e.g., North Sea, Krasny Yar, Roter Berg, Chumysh, Kiputz IX, among others)—a misconception already remarked by Van der Made et al. (2017). Furthermore, Sher (1997) did not consider the samples from Le Vallonnet and Durfort, which based on both morphology and chronology undoubtedly belong to *B. schoetensacki* even if they fall within the variation of most of the specimens that he attributed to *B. priscus*. The “stoutness” biplot, show that all the metacarpals from Mauer indeed share the same diagram area with other populations of *B. schoetensacki*, being, altogether with Le Vallonnet sample, among the slenderest ones, whereas the metacarpals from Mosbach are characterized by a more pronounced stoutness (Fig. 9). Moreover, based on the specimens morphologically closer to *B. schoetensacki*, our Log₁₀ diagrams indicate that the Mauer sample fits with the characters of *B. schoetensacki* and that the Mosbach specimens feature slightly stouter metacarpals than that from Mauer and other *B. schoetensacki* populations (Fig. 9). The more massive, *B. priscus*-like proportions of the Mosbach material further agrees with the derived and “priscoid” cranial features displayed by some cranial remains from this locality (Sala, 1986). In the two PCAs (Fig. 10), the Mauer/Mosbach metacarpals cluster in the area occupied by the species *B. schoetensacki* and *B. priscus*, with the Mauer specimens being recognizable by their slenderer proportions. Overall, our results confirm that the *Bison* sample from Mosbach display an increased robusticity, suggesting the presence of very large *B. priscus*-like morphologies in the German site. For this reason, we prefer to use open nomenclature when assigning Mosbach remains to *B. cf. schoetensacki*.

In turn, the few analyzed metatarsals from Mauer and Mosbach are quite heterogeneous. In the “stoutness” diagrams (Fig. 9), all the Mosbach metatarsals are long and stout, resembling those of *B. priscus*. In turn, one of the two metatarsals from Mauer (DMSTD in Schertz, 1936b) fits with the variation of *B. schoetensacki*, whereas the other (MAU402) displays an extremely slender structure, similar to that of *B. menneri*.

A complete revision of the cranial and postcranial material from Mauer and Mosbach would be required: (1) to clarify the diagnosis of *B. schoetensacki* (especially based on the sample from Mauer, which is the type locality) and (2) to confirm the possible first co-occurrence with larger “priscoid” forms (in the case of the larger specimens from Mosbach). An earlier co-occurrence of *B. schoetensacki* and *B. priscus* at Mosbach cannot be ruled out, as it is consistent with our results, which indicate relatively stout metacarpal proportions with a wide variation in the sample (Fig. 9). Moreover, it has to be considered that, even if most of the Mosbach material comes from the upper layers (Mosbach 2) roughly coeval to Mauer and Isernia, its lowermost sediments are dated to around 1.0 Ma (Koenigswald and Tobien, 1987). Unfortunately, the stratigraphic provenance of the remains was not recorded. Nonetheless, we disagree with Schertz (1936b) and Sher (1997) and state-consider that the entire sample from Mauer and, possibly, some of

the Mosbach specimens, are attributable to *B. schoetensacki* instead of *B. priscus*.

5.4.4. Süssenborn

Flerov (1969) referred the large bovid remains from Süssenborn (Germany; Middle Pleistocene, ca. 0.6 Ma) to two subspecies of *B. schoetensacki* (*B. schoetensacki schoetensacki* and *B. schoetensacki lagenocornis*) based on cranial characters without any reference to the metapodials. *Bison schoetensacki lagenocornis* was subsequently synonymized with the nominotypical onesubspecies by Sala (1986), who found that the roughly coeval *B. schoetensacki* from Isernia displayed a range of cranial morphologies that encompassed the differences between the two purported subspecies, which were reinterpreted as resulting from sexual dimorphism.

Sher (1997) concluded that the metacarpals from Süssenborn are quite heterogeneous and probably referable to more than a single species. Indeed, our results (Fig. 9) indicate that three out of five metacarpals fall in the range of *B. schoetensacki* from Mosbach, whereas one fits within *B. menneri* from Untermassfeld, and the remaining one more closely resembles *Bison* sp. from Venta Micena. However, Sher’s (1997) interpretation was based again on a misinterpretation of the size and proportions of *B. priscus* forelimbs. The “stoutness” diagram and both the PCAs (Fig. 9) shows that the three stoutest metacarpals from Süssenborn (IQW, 1965/2330, IQW, 1965/2325, IQW, 1965/2319), referred to *B. priscus* by Sher (1997), fit well within the variation of male specimens of *B. schoetensacki* from Le Vallonnet, Durfort, and the VCS, while the smallest specimen from Süssenborn (IQW, 1965/2331) is also very close to female specimens of *B. schoetensacki* from the same sites. The only exception is represented by the metacarpal IQW 1965/2333, here attributed to *B. cf. menneri*, which probably comes from earlier deposits than the rest of the assemblage due to the different type of preservation from most Süssenborn fossils and its extremely elongate and slender morphology. In turn, the metatarsals from Süssenborn fit quite well with the available sample of *B. schoetensacki* in the “stoutness” and the PCAs (Figs. 9b and 10c–d). In summary, the bulk of metapodials from Süssenborn can be confidently referred to a stout form of *B. schoetensacki*, very similar to those from the VCS and Durfort.

5.4.5. Isernia and cCesi

The site of Isernia La Pineta (southern Italy; 0.58 Ma; Coltorti et al., 2005; Peretto et al., 2015) has yielded a rich sample of *B. schoetensacki* cranial and postcranial remains (Sala, 1986), although no complete long bones are preserved due to carcass exploitation by hominins (Sala, 1983). The distal epiphysis of some metapodials (e.g., IS.F.1979.t.3q(1) and IS.I.q.73.t.3(1)) has large mediolateral and anteroposterior diameters, resembling the proportions of heavily-built forms of *B. schoetensacki*. On the other hand, complete astragali and calcanei fit well with those of *Bison* s.s. and are overall larger than those of earlier populations of *B. schoetensacki* from Durfort and the VCS (Tables S25, S27). We therefore conclude that the rich sample from Isernia attests to the presence of a stout form of *B. schoetensacki* in Italy during the earliest Middle Pleistocene, exhibiting some postcranial features akin to the “priscoid” forms. Among the few remains of *Bison* from the early Middle Pleistocene site of Cesi (central Italy; Ficarelli et al., 1997) the most informative is a complete metacarpal. The size and proportions fit with the ones observed in the *B. schoetensacki* sample in both the stoutness diagram and the PCA (Fig. 9), confirming that in the early Middle Pleistocene this species was already populating the Italian Peninsula.

5.4.6. Cromer Forest-bed, Boxgrove, and wWestbury

The bovinds from various sites of the Cromer Forest-bed

Formation (eastern UK), Boxgrove and Westbury (western UK) collectively encompassing the whole early Middle Pleistocene (ca. 0.7–0.4 Ma; Breda et al., 2010), have been described by several authors (Freudenberg, 1914; Sala, 1986; Breda et al., 2010). Two horn cores (M/6559 and M/1426) from an unknown locality were attributed to *B. schoetensacki* (Freudenberg, 1914; Flerov, 1969; Sala, 1986), and according to the latest review (Breda et al., 2010) multiple bovids would be recorded by teeth and a few postcranial remains in the Forest-bed Formation: *B. cf. schoetensacki*, *B. priscus*, and *cf. Bos primigenius*.

The “stoutness” diagram (Fig. 9a) indicates that the metapodials from most of these sites (Boxgrove, Trimmingham, Sidestrang, Ostend, and Palling) fit with the general proportions of stouter *B. schoetensacki* from Süssenborn, Durfort, Mosbach, and the VCS, whereas the three metacarpals from the yellow breccia of Westbury-sub-Mendip are stouter and more closely resemble *B. priscus*, as already suggested by Breda et al. (2010).

The only available complete radius, which comes from Pakefield, fits with the variation of both *B. schoetensacki* and *B. menneri*, while the one from the younger site of Boxgrove falls far from these taxa and more closely resembles in length and stoutness those of *B. priscus* (Fig. 9a). The two radii from Westbury also overlap the borders of the “priscoid” variation (Fig. 9c). We therefore conclude that the material from the Cromer Forest-bed Formation most likely probably belongs to *B. schoetensacki*, whereas the assignment of the small sample from Boxgrove is more debatable, being attributed here to *Bison* sp. Finally, the Westbury sample is referred to *B. cf. priscus* due to the stoutness of both radii and metapodials.

5.4.7. Châtillon-Saint-Jean and Siréjol cave

Mourer-Chauvire (1972) described a large number of bovid remains from the late Middle Pleistocene site of Châtillon-Saint-Jean (France). The author referred to *B. schoetensacki* the smaller and slender postcranial specimens and to *B. priscus* the larger and stouter ones. Our morphometric analyses on the metacarpals question these attributions. On the whole, the Châtillon-Saint-Jean assemblage is characterized by the presence of a large bison featuring quite large metacarpals (Fig. 9) and long and very wide diaphysis (Fig. 10) fitting with the variation of *B. priscus*. The presence of two morphologically distinct groups is here interpreted as the result of intraspecific differences (i.e., sexual dimorphism) in the same sample of *B. priscus* (Fig. 9, Table S34), confirming the interpretation of Brugal (1985). The size and stoutness of the Châtillon-Saint-Jean bison metacarpals resemble those recorded for the very large-sized *B. priscus* from Romain-la-Roche, referred to *B. priscus priscus* together with the Taubach sample (Flerov, 1976; Vercoutère and Guérin, 2010), and for the bison from Tiraspol, referred to *B. schoetensacki* by Flerov (1972), and then to *B. aff. priscus* by Sher (1997).

The sample from the Late Pleistocene cave of Siréjol (France), attributed to *B. schoetensacki* (Guérin and Philippe, 1971), then reported to *B. priscus* nov. ssp. (Brugal, 1985, 1999) is characterized by relatively short and robust metacarpals. The “stoutness” and Log10 ratio diagrams (Fig. 9) as well as the PCA (Fig. 10) show that the distal and proximal epiphysis width is larger (relative to total length) than in *B. schoetensacki*, fitting with the variation of *B. priscus*. Nonetheless, the bison from Siréjol is distinguishable from latest Pleistocene *B. priscus* based on the significantly narrower metacarpal diaphysis compared with the distal and proximal epiphysis (especially the specimens n°100 000 + 658, n°100 000 + 664, n°100 000 + 665, n°100 000 + 667, n°100 000 + 668; Figs. 9 and 10). This latter difference is particularly interesting in the light of recent molecular studies (Palacio et al., 2017; Grange et al., 2018), which recognize the Siréjol

specimens as genetically distinct from *B. priscus* and close to the extant *B. bonasus*. Further discoveries from the same site and/or coeval sites are needed to investigate the intriguing presence of another bison species in the European Late Pleistocene, hitherto only suggested by molecular data.

6. Discussion

6.1. Metapodials variation within *Bison schoetensacki*

The metacarpal IPS14917 from CGRD2 (ca. 1.1 Ma) is quite long and slightly slenderer than the rest of the sample, which comes from younger layers (ca. 1.0–0.86 Ma). The “stoutness” diagram and Log₁₀ ratio diagrams (Fig. 9a–e) show that IPS14917 fits with the size and proportions of *B. schoetensacki* from the type locality of the species, Mauer, and the pre-Jaramillo cave site of Le Vallonnet (ca. 1.2 Ma). The Mauer fauna is characterized by taxa typical of forest environments (Soergel, 1914; Breda and Marchetti, 2005; Kahlke et al., 2013), and the palynological study performed on the fossiliferous layers of Le Vallonnet suggest that the site might have been a tree refugia in a period of relatively dry and cold phase. The stout metapodials from EVT10–EVT12 exhibit more “priscoid” proportions, similar to (but overall smaller than) the metapodials of the steppe-adapted Late Pleistocene *B. priscus mediator*. From EVT12, two slenderer metacarpals were also recovered, interpreted as the only female metacarpals of the collection. The EVT7–CGRD7 metacarpals are characterized by less stout limb proportions, similar to the remains from the sites of Durfort, Süssenborn, and Cromer Forest-bed, all sites featuring a mixture of open and forested landscapes (Brugal, 1995; Stuart and Lister, 2001; van Asperen and Kahlke et al., 2011).

The lowermost layers of VCS (CGRD2–CGRD4) span from 1.1 to 1.0 Ma (Madurell-Malapeira et al., 2010). Paleobotanical data indicate that the VCS pre-Jaramillo period was characterized by a relatively warm-temperate and humid paleoenvironment with a mixture of habitats dominated by wooden landscapes, as suggested by the abundance of arboreal taxa (Mijarra et al., 2007). This fits with the aforementioned paleoenvironmental reconstructions of the nearly coeval and geographically close site of Le Vallonnet and of the younger site of Mauer. The dental wear pattern of the large herbivore remains from the VCS syn-Jaramillo layers (1.0–0.99 Ma; EVT10–EVT12) points to a generally abrasive diet, suggesting an environment with a significant predominance of open dry grasslands (Strani et al., 2019). This might explain the stouter and “priscoid” metapodials unearthed from these layers. The same study, performed on the post-Jaramillo layers of VCS dated to 0.86–0.78 Ma (EVT7–CGRD7), suggests an increase of average humidity and a relative expansion of forested habitats, in accordance with the study of the micromammal fauna (Lozano-Fernandez et al., 2015; Strani et al., 2019). This fits with the Durfort, Cromer Forest-bed, and Süssenborn inferred paleoenvironments mentioned above. In sum, the metapodial proportions of the VCS *Bison* sample, though characterized by an overall homogeneous morphology, show a certain degree of variation when sub-samples from different stratigraphic contexts are compared. This variation shows a remarkable correlation with the dominant paleoenvironment conditions reconstructed along the composite section, with an increase of limbs stoutness corresponding to more arid conditions and slenderness to more humid ones, also tracing the trend observed in other *B. schoetensacki* samples. A similar interpretation has been even anticipated by Flerov (1979), who stated that the slenderer and taller forms of *Bison* are better adapted to closed and forested environments as opposite to the stouter ones, which are more suited to open and arid conditions. This idea is further confirmed by the extremely slender *B. menneri* from Untermassfeld

and the massive but very tall *B. priscus priscus* from Taubach and Romain-la-Roche, all sites characterized by a mixture of closed and open habitats (Sher, 1997; Argant, 2010; van Asperen and Kahlke et al., 2011). On the contrary, *B. priscus mediator*, featuring the typical "priscoid" proportions with short and large metapodials, was one of the most representative taxa of the so-called Mammoth Steppe fauna during the Late Pleistocene (Kahlke, 1999).

6.2. The metapodial morphology of *Bison schoetensacki*

Our comparative analysis indicates that the metacarpals are the most useful postcranial skeletal elements for distinguishing the different species of *Bison* s.l. Most of the metacarpals attributable to *B. schoetensacki* are characterized by the following features (ranges based on all the samples attributed to *B. schoetensacki* in Table S16): total length between 225 and 270 mm, ratio of distal width to total length between 27 and 34%, ratio of midshaft width to total length between 16 and 21%, and ratio of proximal width to total length between 28 and 36%. In early Middle Pleistocene sites with uncertain chronology and potentially redeposited/mixed material, such as Mauer, Mosbach, and Süssenborn, some metacarpals fall outside the aforementioned variation ranges and are not considered in this discussion. With the exception of these remains and the clearly different *B. menneri* from Untermassfeld, all the remaining bison samples from Epivillafranchian-early Middle Pleistocene European sites are distinguishable from earlier and later samples, and are here referred to *B. schoetensacki*.

Our morphometric data show some morphometric variation among samples from different localities, especially for the metacarpals (Fig. 9). This variation is probably due to ecophenotypic changes in limb robusticity and size through time and space in a single wide-ranging and long-lasting species (see Section 6.1.). However, excluding these small intraspecific differences, our results show that all the putative *B. schoetensacki* samples display no significant differences. After 0.5 Ma, with the first occurrence of the massive *B. priscus*, it is virtually impossible to discern female *B. priscus* from male *B. schoetensacki* individuals based on postcranial material. This may lead to possibly erroneous taxonomic attributions in sites where the two species purportedly co-occur, particularly in the Middle and Late Pleistocene (e.g., Chatillon-Saint-Jean and Sirejol cave; Mourer-Chauvire, 1972), but determined as male and female of *B. priscus* (Brugal, 1999; Grange et al., 2018). This is also relevant in the light of molecular studies (Palacio et al., 2017; Grange et al., 2018; Vershinina et al., 2019) indicating the presence of various Late Pleistocene *Bison* lineages in Eurasia, which are not easily distinguishable on morphometric grounds.

6.3. Sexual dimorphism

Fifteen complete metacarpals from the sites of Mauer, Le Vallonnet, Durfort, EVT12 of VCS, Trimmingham, and Süssenborn are slenderer and overall smaller than the rest of the sample attributed to *B. schoetensacki*, with values of DEW/Lmax% less than 30 (Figs. 9 and 10). These metacarpals are here attributed to females, indicating a significant degree of sexual dimorphism, as it is frequently observed in large bovids like bison. To quantify the magnitude of these differences and to assess if it is similar to those recorded for extant species, we applied the equations by Schertz (1936a) (see Section 3) to all the available samples in which putative males and females were recognized (*B. schoetensacki* from VCS layer EVT12, Durfort, and Süssenborn; *B. menneri* from Untermassfeld; *B. priscus* from Châtillon-Saint-Jean, North Sea, and Krasny Yar; extant *B. bonasus*, and *B. bison*; Table S34). The results obtained for all analyzed EVT12 show that the sample has similar values to those of

the extant and fossil *Bison* species (except for an unusual high value for DW).

In most of the studied localities, including VCS, males represent the majority of the metacarpal record (e.g., 75% in VCS, 53% in Le Vallonnet, 67% in Durfort, 81% in Taubach, 56% in North Sea), apparently in contrast with what is observed in extant gregarious large mammals, in which female individuals are normally more abundant (Gower et al., 2019). This imbalance in the frequency of sex distribution has been reported for several fossil collections of large mammals, including carnivores such as *Ursus*, and female-herd-based herbivores such as *Mammuthus* and *Bison* (Pečnerová et al., 2017; Gower et al., 2019). This might be explained by (1) bias in the fossil collection (e.g., focused on larger remains, especially in historical times), (2) taphonomic reasons (e.g., greater resistance of larger and more massive skeletal remains against destructive taphonomic agents), (3) different behaviors between the two sexes (i.e., segregation of males), and/or (4) seasonality factor for the bone accumulation. Gower et al. (2019) genetically sexed both cranial and postcranial bones belonging to 186 fossil individuals of *Bison* spp. from several Holarctic sites and found that the sample was composed by ca. 75% of males, a percentage very similar to that estimated for the VCS sample.

6.4. Final remarks on the postcranial differences among *Leptobos* and *Bison*

Metatarsals are less diagnostic due to their greater variation, but their distal end is nevertheless useful to distinguish large and stout *Bison* s.s. from the slenderer *Leptobos* and *B. (Eobison)*. Of the most common variables used in the literature, only a few are useful to discriminate among *Bison* species (Fig. 10), particularly metapodial total length, robustness of diaphysis and distal epiphysis width (Scott and Barr, 2014), despite some overlap. These differences in the proportions of metapodials, and the appendicular skeleton in general, are often linked to ecophenotypic variation in bovids, and must be therefore taken with caution when making taxonomic attributions or inferring phylogenetic relationships (Brugal, 1999; Scott and Barr, 2014).

The astragalus is also often used as a diagnostic element for large bovids. The geometric morphometric analysis of astragali performed by Maniakas and Kostopoulos (2017b) on a large sample of *Bison* suggests that the shape of this bone is strongly (but not only) related to habitat preferences. Although there are some differences between the *Bos* and *Leptobos/Bison*, the astragalus is not diagnostic enough for reliable taxonomic distinction between *Leptobos* and *Bison*. Size and proportions of the talus may help in distinguishing large and stout *Bison* s.s. from small and slender *Leptobos* and *B. (Eobison)*, but the overlap between the ranges of variation is significant. In our opinion, the radius is one of the more useful long bones to distinguish *Leptobos* and *Bison*, and also different species of *Bison* s.l. In particular, *B. menneri* and *B. (Eobison)* have significantly slenderer radii than *B. priscus*, while *B. schoetensacki* is characterized by intermediate proportions (Fig. 9). Finally, phalanges, carpals, and tarsals (other than the astragalus) can only give some hints on the overall size and built, but are too homogeneous among large bovids to have any taxonomic value. Similarly, humeri and tibiae are taxonomically uninformative within the *Leptobos/Bison* group.

Postcranial differences between *Leptobos* and *Bison* almost exclusively relate to dimensions and proportions. Some of these morphometric differences are also reflected in the identification of distinct groups within *Bison* s.l., which in some cases correspond to specific taxa. In particular, our results allow us to clearly distinguish among *B. (Eobison)* (Dmanisi, Venta Micena, Pirro Nord, Capena,

Mygdonia Basin), *B. menneri* (Untermassfeld), *B. schoetensacki*, and early *B. priscus*. In turn, the last two species are very polymorphic, which results in the identification of local samples with peculiar postcranial proportions and/or dimensions, e.g., *B. schoetensacki* “slender” (CGRD2 of VCS, Mauer, Le Vallonnet) and “stout” (EVT7, EVT 10, EVT 12, and CGRD7 of VCS, Durfort, Süßenborn, Cromer Forest-bed, possibly Isernia and Mosbach) forms; *B. p. priscus* (Taubach, Romain-la-Roche, Tiraspol, Châtillon-Saint-Jean) and *B. p. mediator* (North Sea, Habarra, Kiputz IX and others) subspecies. At least for the case of *B. schoetensacki* (a deeper look into *B. priscus* is out of the scope of this manuscript) these differences might be related to ecophenotypic changes related to paleoenvironmental conditions (Section 6.1). At the state of the art, we are unable to establish, at least for *B. schoetensacki*, whether these differences can be the result of ecophenotypic variation within the same species, or whether they can correspond to different taxa or different stages within a single evolutionary lineage. From the late Middle Pleistocene onwards, the second hypothesis could find indirect support in the recognition of different haplotypes in the ancient DNA of European bison (Palacio et al., 2017), which to date do not correspond to species defined on a morphological basis. Regarding *B. priscus*, the two putative subspecies *B. p. priscus* and *B. p. mediator* — which, until now, had been distinguished on the basis of cranial features and size — display substantial differences in proportions also in the metapodials (especially the metacarpals; Grange et al., 2018, Fig. 9).

7. Conclusions

The described bison sample from the VCS is attributed to *B. schoetensacki*. The records of this species in the lower layers of CGR and the roughly coeval site of Le Vallonnet in France represent the first occurrences of *Bison* s.s. in Europe, dating to the beginning of the Epivillafranchian (ca. 1.2–1.1 Ma). *Bison schoetensacki* can therefore be considered a biochronological marker for the beginning of this biochron (Kahlke, 2007; Bellucci et al., 2015), in association with the first occurrence of *Megaloceros savini* (see Madurell-Malapeira et al., 2019) and the reappearance of *Sus strozzi* in Europe after the latest Villafranchian “suid gap” (Cherin et al., 2020). According to our results, *B. schoetensacki* was widely distributed across Eastern and Central Europe (from UK to Italy, and from Iberia to Germany) between 1.2 and 0.6–0.5 Ma, representing the most common large bovid during the Epivillafranchian and early Middle Pleistocene. In the absence of sufficiently complete cranial remains, the morphometric analysis on postcranial bones (especially metapodials) represents the most powerful tool for diagnosing Pleistocene bovine taxa. In particular, metapodial proportions enable a reliable distinction among the genera *Leptobos*, *Bison*, and *Bos*, as well as among different *Bison* species. For the two most polymorphic and geographically widespread species, namely *B. schoetensacki* and *B. priscus*, it is even possible to distinguish several morphotypes, whose biological meaning (local ecophenotypic variation vs taxonomic differences) should be subject to further research. The relatively wide range of morphometric variation exhibited by the VCS sample of *B. schoetensacki* may be related to ecophenotypic changes and/or local adaptations in response to environmental changes that affected the VCS area during the Epivillafranchian (Strani et al., 2019). In particular, these changes may be related to the important ecological transitions that occurred during the EMPT. Moreover, the increased size and robusticity observed in the long bones from the VCS intermediate

layers (EVT10 and EVT12) represent the earliest record of “priscoid” characters in *Bison* s.s. at ca. 1.0 Ma.

Author contributions

L.S., D.M.A., M.C. and J.M.-M conceived the research and wrote the paper; L.S., D.M.A., M.C. and J.M.-M performed the analyses; L.S., D.M.A., M.C., J.P.B., P.E.M. and J.M.-M. revised all the manuscript versions and made improvements in the manuscript.

Declaration of competing interest

The authors declare that they have no known competing financial interests or personal relationships that could have appeared to influence the work reported in this paper.

Acknowledgments

This work is funded by the Agencia Estatal de Investigación—European Regional Development Fund of the European Union (CGL2016-76431-P and CGL2017-82654-P, AEI/FEDER-UE) and the Generalitat de Catalunya (CERCA Programme). LS is supported by the FI AGAUR fellowship (ref. 2020 FL_B1 00131) funded by the Secretaria d'Universitats i Recerca de la Generalitat de Catalunya and the European Social Fund. D.M.A. and J.M.M. are members of consolidated research group 2017 SGR 116 (AGAUR, Generalitat de Catalunya). We would like to thank Marzia Breda for sending us measurements of the UK bovids; Marisa Blume and Oliver Sandrock for measurements of the bovids from Mosbach and Mauer; Lionel Cavin and Corinne Charvet for sending us measurements of the bovids from Romain-la-Roche; Paola Romi (Soprintendenza Archeologia Belle Arti e Paesaggio dell'Umbria) for the possibility to study the Pietrafitta bovid collection at the MPLB; Benedetto Sala and Claudio Berto for the possibility to study the Isernia bovid collection at the UNIFE and MPPPL; Alessandro Blassetti for the possibility to study the Cesi bovid collection at the MuPA; Elisabetta Cioppi and Luca Bellucci for the possibility to study the Valdarno bovid collection at the IGF. Comments by Marzia Breda and an anonymous reviewer helped to significantly improve the manuscript.

Appendix A. Supplementary data

Supplementary data to this article can be found online at <https://doi.org/10.1016/j.quascirev.2021.106933>.

References

- Agadzhanian, A.K., Vislobokova, I.A., Shunkov, M.V., Ulyanov, V.A., 2017. Pleistocene mammal fauna of the Trlica locality, Montenegro. *Fossil Imprint* 73, 93–114.
- Alekseeva, L.I., 1967. To the history of subfamily Bovinae during the Pleistocene in the European USSR. In: *Paleontologiya, geologiya i poleznye iskopaemye Moldavii Vyp. 2*. Shtiintsa, Kishinev, pp. 123–127 (in Russian).
- Alekseeva, L.I., 1977. Theriofauna of the early anthropogene of eastern Europe. *Trudy Geol. Inst. Akad. Nauk SSSR* 300, 1–214 (in Russian).
- Ambert, P., Brugal, J.P., Houles, N., 1996. Le maar du Riege (Hérault, France): géologie, paléontologie, perspectives de recherches. *C. R. Acad. Sc. Paris* 322, 125–132.
- Argant, J., 2010. Palynologie des coprolithes d'hyène de Romain-la-Roche (Doubs, France): apport paléoenvironnemental. *Rev. Paléobiol.* 29, 473–476.
- Asperen van, E.N., Kahlke, R.D., 2017. Dietary traits of the late early Pleistocene *Bison menneri* (Bovidae, Mammalia) from its type site Untermassfeld (Central Germany) and the problem of Pleistocene ‘wood bison’. *Quat. Sci. Rev.* 177, 299–313.
- Ayrolles, P., 1973. Essai de distinction des genres *Bos* et *Bison* d'après deux métacarpes. *Etudes préhistoriques* 7, 13–15.

- Bellucci, L., Sardella, R., Rook, L., 2015. Large mammal biochronology framework in Europe at Jaramillo: the Epivillafranchian as a formal biochron. *Quat. Int.* 389, 84–89.
- Bibikova, V.I., 1958. Some distinguishing features in the bones of the genera *Bison* and *Bos*. *Bull. Mosk. Obschtschestva Isp. Privoda NS Otdel Biol.* 63, 23–35.
- Breda, M., Collinge, S.E., Parfitt, S.A., Lister, A.M., 2010. Metric analysis of ungulate mammals in the early Middle Pleistocene of Britain, in relation to taxonomy and biostatigraphy: I: rhinocerotidae and Bovidae. *Quat. Bar Int.* 228, 136–156.
- Brugal, J.P., -1983. Application des analyses multidimensionnelles à l'étude systématique du squelette des membres des Grands Bovidés Pléistocènes (Grottes de Lunel-Viel, Hérault): Perspectives évolutives. Ph.D. Dissertation, Université Aix-Marseille II.
- Brugal, J.P., 1985. Le *Bos primigenius* Boj., 1827 du Pléistocène moyen des grottes de Lunel-Viel (Hérault). *Bull. Mus. Anthr. Préh.* Monaco 28, pp. 7–62.
- Brugal, J.-P., 1995. Le bison (Bovidae, Artiodactyla) du Pléistocène moyen ancien de Durfort (gard, France). *Bull. Mus. Natl. Hist. Nat.* 16C (2–4), 349–381.
- Brugal, J.P., 1999. Etude des populations de grands Bovidés européens: intérêt pour la connaissance des comportements humains au Paléolithique. In: Brugal, J.P., David, F., Enloe, J.G., Jaubert, J. (Eds.), *Le Bison: gibier et moyen de subsistance des hommes du Paléolithique aux Paléindiens des Grandes Plaines*, Ed. APDCA, Antibes, pp. 85–104.
- Brugal, J.P., Fosse, P., 2005. Les grands bovidés (*Bison cf. schoetensacki*) du site pléistocène moyen de La Vayssière (Aveyron, France). In: Crégut-Bonnoure, E. (Ed.), *Les Ongulés Holarctiques du Pliocène et du Pléistocène Quaternaire H.S.*, vol. 2, pp. 75–80.
- Bukhsianidze, M., 2005. Ph.D. Dissertation The Fossil Bovidae of Dmanisi. Università degli Studi di Ferrara.
- Bukhsianidze, M., 2020. New results on bovids from the early pleistocene site of Untermaßfeld. In: Kahlke, R.D. (Ed.), *Das Pleistozän von Untermaßfeld bei Meiningen (Thüringen)*. Teil 4. Habelt-Verlag, Bonn, pp. 1169–1195.
- Burchak-Abramovich, N.I., Gadzhiev, D.V., Vekua, A.K., 1994. On a new pleistocene bovine from eastern Georgia. *Teriologii Paleoteriologija* 253–261 (in Russian).
- Cherin, M., D'Allestro, V., Masini, F., 2019. New bovid remains from the early pleistocene of Umbria (Italy) and a reappraisal of *Leptobos merlai*. *J. Mamm. Evol.* 26, 201–224.
- Cherin, M., Alba, D.M., Crotti, M., Menconero, S., Moullé, P.É., Sorbelli, L., Madurell-Malapeira, J., 2020. The post-jaramillo persistence of *Sus strozzi* (suidae, mammalia) in Europe: new evidence from the Vallparadis section (NE Iberian Peninsula) and other coeval sites. *Quat. Sci. Rev.* 233, 106–234.
- Clark, P.U., Archer, D., Pollard, D., Blum, J.D., Rial, J.A., Brovkin, V., Mix, A.C., Pisias, N.G., Roy, M., 2006. The middle Pleistocene transition: characteristics, mechanisms, and implications for long-term changes in atmospheric pCO₂. *Quat. Sci. Rev.* 25, 3150–3184.
- Coltorti, M., Feraud, G., Marzoli, A., Peretto, C., Ton-That, T., Voinchet, P., Bahain, J.J., Minelli, A., Hohenstein, U.T., 2005. New 40Ar/39Ar, stratigraphic and palaeoclimatic data on the Isernia La Pineta lower palaeolithic site, Molise, Italy. *Quat. Int.* 131, 11–22.
- Croitor, R., 2010. Critical remarks on genus *Bison* (Bovidae, mammalia) from pleistocene of moldova. *Rev. Archeol.* 5, 172–188 (in Russian).
- Croitor, R., 2016. Genus *Bison* (Bovidae, mammalia) in early pleistocene of moldova. In: Coropceanu, E. (Ed.), *Materialele Conferinței tiințifi Ce Naționale Cu Participare Internațională "Mediul și Dezvoltare Durabilă"*, Ediția a III-A. Chișinău, pp. 14–20.
- Delpéch, F., 1972. Fouilles de sauvetage dans le gisement magdalénien de Fongaban. Commune de Saint-Emilion (Gironde), 3ème partie: la Faune. *L'Anthropologie* 76, 615–629.
- Demirel, F.A., Mayda, S., 2014. A new early Pleistocene mammalian fauna from Burdur Basin, SW Turkey. *Russ. J. Theriol.* 13, 55–63.
- Drees, M., 2005. Sexual dimorphism in pleistocene *Bison priscus* (mammalia, Bovidae) with a discussion on the position of *Bison schoetensacki*. *Senck. Leth.* 85, 153–157.
- Duvernois, M.P., 1990. Les *Leptobos* (Mammalia, Artiodactyla) du Villafranchien d'Europe occidentale. *Doc. Lab. Geol.*, Lyon 113, 1–213.
- Ficcarelli, G., Abbazzi, L., Albanelli, A., Bertini, A., Coltorti, M., Magnatti, M., Masini, F., Mazza, P., Mezzabotta, C., Napoleone, G., Rook, L., 1997. Cesi, an early middle pleistocene site in the colliorino basin (Umbro-Marchean apennine), central Italy. *J. Quat. Sci.* 12, 507–518.
- Fischer, K.H., 1965. Bisonreste (*Bison schoetensacki voigtstedtensis* ssp. n.) aus den altpleistozänen Tonen von Voigtstedt in Thüringen. *Paläontol. Abh. A Paläozool.* 2, 364–377.
- Flerow, K.K., 1969. Die Bison-Reste aus den Kiesen von Süßenborn bei Weimar. *Paläontol. Abh.* 3, 489–520.
- Flerow, C.C., 1972. The most ancient Bisons and the history of genus *Bison*. In: *Teriologiya*, vol. 1. Nauka, Novosibirsk, pp. 81–86 (in Russian).
- Flerow, K.K., 1979. Morphology, systematic, evolution, ecology. In: Sokolov, E.V. (Ed.), *European Bison*. Nauka, Moscow, pp. 9–127 (in Russian).
- Flerow, K.K., 1975. Die Bison-reste aus den travertinen von Weimar-ehringendorf. *Abh. Zentr. Geol. Inst.* 23, 171–199.
- Freudenberg, W., 1914. Die Säugetiere des älteren Quartärs von Mitteleuropa. *Geol. Paleont. Abh. NF* 12, 533–549.
- Froese, D., Stiller, M., Heintzman, P.D., Reyes, A.V., Zazula, G.D., Soares, A.E., Meyer, M., Hall, E., Jensen, B.J., Arnold, L.J., MacPhee, R.D., 2017. Fossil and genomic evidence constrains the timing of bison arrival in North America. *Proc. Natl. Acad. Sci. USA* 114, 3457–3462.
- Gee, H., 1993. The distinction between postcranial bones of *Bos primigenius* Bojanus, 1827 and *Bison priscus* Bojanus, 1827 from the British Pleistocene and the taxonomic status of *Bos* and *Bison*. *J. Quat. Sci.* 8, 79–92.
- Gentili, S., Masini, F., 2005. An outline of Italian *Leptobos* and a first sight on *Leptobos aff. vallisami* from Pietrafitta (early pleistocene, Perugia). *Quaternarie Hors Series* 2, 81–89.
- Geraads, D., 1992. Phylogenetic analysis of the tribe Bovini (mammalia: Artiodactyla). *Zool. J. Linn. Soc.* 104, 193–207.
- Gower, G., Fenderson, L.E., Salis, A.T., Helgen, K.M., van Loenen, A.L., Heiniger, H., Hofman-Kaminska, E., Kowalczyk, R., Mitchell, K.J., Llamas, B., Cooper, A., 2019. Widespread male sex bias in mammal fossil and museum collections. *Proc. Natl. Acad. Sci. USA* 116, 19019–19024.
- Grange, T., Brugal, J.P., Flori, L., Gautier, M., Uzunidis, A., Geigl, E.M., 2018. The evolution and population diversity of bison in Pleistocene and Holocene Eurasia: sex matters. *Divers* 10, 65.
- Hammer, Ø., Harper, D.A., Ryan, P.D., 2001. PAST: paleontological statistics software package for education and data analysis. *Paleontol. Electron* 4, 1–9.
- Head, M.J., Gibbard, P.L., 2005. Early-Middle Pleistocene transitions: an overview and recommendation for the defining boundary. *Geol. Soc. London Special Publications* 247, 1–18.
- Hilzheimer, M., 1918. Dritter Beitrag zur Kenntnis der Bisonten. *Arch. Naturg* 84, 41–87.
- Huguet, R., Vallverdú, J., Rodríguez-Álvarez, X.P., Terradillos-Bernal, M., Bargalló, A., Lombera-Hermida, A.D., Menéndez, L., Modesto-Mata, M., Van der Made, J., Soto, M., Blain, H.A., 2017. Level TE9c of Sima del Elefante (Sierra de Atapuerca, Spain): a comprehensive approach. *Quat. Bar Int.* 433, 278–295.
- Jungers, W.L., Falsetti, A.B., Wall, C.E., 1995. Shape, relative size, and size-adjustments in morphometrics. *Yrbk. Phys. Anthropol* 38, 137–161.
- Kahlke, R.D., 1999. The History of the Origin, Evolution and Dispersal of the Late Pleistocene Mammuthus-Coelodonta Faunal Complex in Eurasia (Large Mammals). Fenske Companies, Rapid City.
- Kahlke, R.-D., 2007. Late Early Pleistocene European large mammals and the concept of an Epivillafranchian biochron. In: Kahlke, R.-D., Maul, L.C., Mazza, P. (Eds.), *Late Neogene and Quaternary Biodiversity and Evolution: Regional Developments and Interregional Correlations*. Volume II. Proceedings of the 18th International Senckenberg Conference (VI International Palaeontological Colloquium in Weimar), vol. 259. Cour. Forsch.-inst. Senck, pp. 265–278.
- Kahlke, R.D., García, N., Kostopoulos, D.S., Lacombat, F., Lister, A.M., Mazza, P.P., Spassov, N., Titov, V.V., 2011. Western Palaearctic palaeoenvironmental conditions during the Early and early Middle Pleistocene inferred from large mammal communities, and implications for hominin dispersal in Europe. *Quat. Sci. Rev.* 30, 1368–1395.
- Khan, M.A., Kostopoulos, D.S., Akhtar, D.S., Nazir, M., 2010. Bison remains from the upper Siwaliks of Pakistan. *Neues Jahrbuch Geol. Palaontol. Abhand.* 258, 121–128.
- Kostopoulos, D.S., Maniakas, I., Tsoukala, E., 2018. Early bison remains from Mygdonia basin (northern Greece). *Geodiversitas* 40, 283–319.
- Lehman, U., 1949. Der Ur in diluvium Deutschlands und seine verbreitung. *Neues Jb. Miner. Abh.* 90, 163–266.
- Lopatín, A.V., Vislobokova, I.A., Lavrov, A.V., Startsev, D.B., Gimranov, D.O., Zelenkov, N.V., Maschenko, E.N., Sotnikova, M.V., Tarasenko, K.K., Titov, V.V., 2019. The taurida cave, a new locality of early pleistocene vertebrates in crimea. *Dokl. Biol. Sci.* 485, 40–43.
- Lumley, H., de Kahlke, H.D., Moigne, A.M., Moullé, P.É., 1988. Les faunes de grands mammifères de la grotte du Vallonet. *L'Anthropologie* 92, 465–495.
- Madurell-Malapeira, J., Minwer-Barakat, R., Alba, D.M., Garcés, M., Gómez, M., Aurell-Garrido, J., Ros-Montoya, S., Moyà-Solà, S., Berástegui, X., 2010. The Vallparadis section (Terrassa, Iberian Peninsula) and the latest villafranchian faunas of Europe. *Quat. Sci. Rev.* 29, 3972–3982.
- Madurell-Malapeira, J., Alba, D.M., Minwer-Barakat, R., Aurell-Garrido, J., Moyà-Solà, S., 2012. Early human dispersals into the Iberian Peninsula: a comment on Martínez et al. (2010) and García et al. (2011). *J. Hum. Evol.* 62, 169–173.
- Madurell-Malapeira, J., Ros-Montoya, S., Espigares, M.P., Alba, D.M., Aurell-Garrido, J., 2014. Villafranchian large mammals from the Iberian Peninsula: paleobiogeography, paleoecology and dispersal events. *J. Iber. Geol.* 40, 167–178.
- Madurell-Malapeira, J., Alba, D.M., Espigares, M.P., Vinuesa, V., Palmqvist, P., Martínez-Navarro, B., Moyà-Solà, S., 2017. Were large carnivores and great climatic shifts limiting factors for hominin dispersals? Evidence of the activity of *Pachycrocuta brevirostris* during the Mid-Pleistocene Revolution in the Vallparadis Section (Valles-Penedès Basin, Iberian Peninsula). *Quat. Int.* 431, 42–52.
- Madurell-Malapeira, J., Sorbelli, L., Bartolini Lucenti, S., Ruff, I., Prat-Vericat, M., Ros-Montoya, S., Espigares, M.P., Martínez-Navarro, B., 2019. The Iberian latest Early Pleistocene: glacial pulses, large carnivores and hominins. In: Martínez-Navarro, B., Palmqvist, P., Espigares, M.P., Ros-Montoya, S. (Eds.), *Libro de Resúmenes XXXV Jornadas de la Sociedad Española de Paleontología*, pp. 155–159.
- Maniakas, I., Kostopoulos, D.S., 2017a. Morphometric-paleoecological discrimination between *Bison* populations of the western Palaearctic. *Geobios* 50, 155–171.
- Maniakas, I., Kostopoulos, D.S., 2017b. Assessing astragalar morphology and biomechanics in western Palaearctic *Bison* populations with geometric morphometrics. *C. R. Palevol* 16, 783–794.
- Martin, T., 1987. Artunterschiede an den Langknochen großer Artiodactyla des Jungpleistozäns Mitteleuropas. *Cour. Forsch.-inst. Senckenbergiana* 96, 1–121.
- Martínez-Navarro, B., Pérez-Claros, J.A., Palombo, M.R., Rook, L., Palmqvist, P., 2007. The Olduvai buffalo *Pelorovis* and the origin of *Bos*. *Quat. Res.* 68, 220–226.

- Martínez-Navarro, B., Ros-Montoya, S., Espigares, M.P., Palmqvist, P., 2011. Presence of the asian origin Bovini, *Hemibos* sp. aff. *Hemibos gracilis* and *Bison* sp., at the early pleistocene site of Venta Micena (orce, Spain). *Quat. Int.* 243, 54–60.
- Masini, F., 1989. I Bovini Villafranchiani dell'Italia. Ph.D. Dissertation. Università di Modena-Bologna-Firenze-Roma.
- Masini, F., Palombo, M.R., Rozzi, R., 2013. A reappraisal of the early to middle pleistocene Italian Bovidae. *Quat. Bar Int.* 288, 45–62.
- Merla, G., 1949. I Leptobos Rütim. italiani. *Palaeontogr. Ital.* 46, 41–155.
- Michel, V., Shen, C.-C., Woodhead, J., Hu, H.-M., Wu, C.-C., Moullé, P.-É., Khatib, S., Cauché, D., Moncel, M.-H., Valensi, P., Chou, Y.-M., Gallet, S., Echassoux, A., Orange, F., de Lumley, H., 2017. New dating evidence of the early presence of hominins in Southern Europe. *Sci. Rep.* 7, 10074.
- Mijarra, J.M.P., Burjachs, F., Manzanque, F.G., Morla, C., 2007. A palaeoecological interpretation of the lower–middle Pleistocene Cal Guardiola site (Terrassa, Barcelona, NE Spain) from the comparative study of wood and pollen samples. *Rev. Palaeobot. Palynol.* 146, 247–264.
- Minwer-Barakat, R., Madurell-Malapeira, J., Alba, D.M., Aurell-Garrido, J., De Esteban-Trivigno, S., Moyà-Solà, S., 2011. Pleistocene rodents from the Torrent de Vallparadis section (Terrassa, northeastern Spain) and biochronological implications. *J. Vertebr. Paleontol.* 31, 849–865.
- Mol, D., Post, K., Reumer, J.W.F., de Vos, J., Laban, C., 2003. Het Gat: preliminary note on a Bavelian fauna from the North Sea with possibly two mammoth species. *Deinsea* 9, 253–266.
- Moullé, P.E., 1992. Les grands mammifères du Pléistocène inférieur de la grotte du Vallonnet (Roquebrune-Cap-Martin, Alpes-Maritimes). Étude paléontologique des Carnivores, Equidés, Suidés et Bovidés. Ph.D. Dissertation. Muséum national d'Histoire naturelle, Paris.
- Moullé, P.E., Lacombat, Echassoux, A., 2006. Apport des grands mammifères de la grotte du Vallonnet (Roquebrune-Cap-Martin, Alpes-Maritimes, France) à la connaissance du cadre biochronologique de la seconde moitié du Pléistocène inférieur d'Europe. *L'Anthropologie* 110, 837–849.
- Mourer-Chauvire, C., 1972. Etude de nouveaux restes de vertébrés provenant de la carrière Fournier à Châtillon-Saint-Jean. III. Artiodactyles, chevaux, oiseaux. *Quaternaire* 9, 271–305.
- Moyà-Solà, S., 1987. Los bóvidos (Artiodactyla, Mammalia) del yacimiento del Pleistoceno inferior de Venta Micena (Orca, Granada, Espana). *Paleontol. Evol. Mem. Esp.* 1, 181–236.
- Palacio, P., Berthonaud, V., Guérin, C., Lambourdière, J., Maksud, F., Philippe, M., Plaire, D., Stafford, T., Marsolier-Kergoat, M.C., Elalouf, J.M., 2017. Genome data on the extinct *Bison schoetensacki* establish it as a sister species of the extant European bison (*Bison bonasus*). *BMC Evol. Biol.* 17, 48.
- Pečnerová, P., Díez-del-Molino, D., Dussex, N., Feuerborn, T., von Seth, J., van der Plicht, J., Nikolskiy, P., Tikhonov, A., Vartanyan, S., Dalén, L., 2017. Genome-based sexing provides clues about behavior and social structure in the woolly mammoth. *Curr. Biol.* 27, 3505–3510.
- Peretto, C., Arnaud, J., Moggi-Cecchi, J., Manzi, G., Nomade, S., Pereira, A., Falguères, C., Bahain, J.J., Grimaud-Hervé, D., Berto, C., Sala, B., Lembo, G., Muttillo, B., Gallotti, R., Thun Hohenstein, U., Vaccaro, C., Coltorti, M., Arzarello, M., 2015. A human deciduous tooth and new $^{40}\text{Ar}/^{39}\text{Ar}$ dating results from the Middle Pleistocene archaeological site of Isernia La Pineta, Southern Italy. *PLoS One* 10 e0140091.
- Pilgrim, G.E., 1947. The evolution of the buffaloes, oxen, sheep and goats. *Zool. J. Linn. Soc. Lond.* 41, 272–286.
- Prat, F., 1968. Observations sur quelques ossements découverts dans la Basse Terrasse de l'Oise à Moru (Rhuis, Oise). In: *La Préhistoire, Problèmes et Tendances*. CNRS, Paris, pp. 337–348.
- Revilliod, P., Dottrens, E., 1946. La faune néolithique de la couche profonde de St-Aubin. Etude préliminaire des phalanges osseuses de *Bos taurus domesticus*. *Revue Suisse de Zoologie* Genève 53, 739–774.
- Rook, L., Martínez-Navarro, B., 2010. Villafranchian: the long story of a Plio-Pleistocene European large mammal biochronologic unit. *Quat. Int.* 219, 134–144.
- Sala, B., 1986. *Bison schoetensacki* freud. From Isernia La Pineta (early middle-pleistocene – Italy) and revision of the European species of bison. *Palaeontogr. Ital.* 74, 113–170.
- Schertz, E., 1936a. Zur Unterscheidung von *Bison priscus* Boj. und *Bos primigenius* Boj. an Metapodien und Astragalus, nebst Bemerkungen über einige diluviale Fundstellen. *Seckenbergiana* 18, 37–71.
- Schertz, E., 1936b. Der Geschlechts-Unterschied an Metapodien von *Bison*. *Senckenbergiana* 18, 357–381.
- Scott, R.S., Barr, W.A., 2014. Ecomorphology and phylogenetic risk: implications for habitat reconstruction using fossil bovids. *J. Hum. Evol.* 73, 47–57.
- Shapiro, B., Drummond, A.J., Rambaut, A., Wilson, M.C., Matheus, P.E., Sher, A.V., Pybus, O.G., Gilbert, M.T.P., Barnes, I., Binladen, J., Willerslev, E., 2004. Rise and fall of the Beringian steppe bison. *Science* 306, 1561–1565.
- Sher, A.V., 1997. An Early Quaternary *Bison* population from Untermaßfeld: *Bison menneri* sp. nov. In: Kahlke, R.D. (Ed.), *Das Pleistozän von Untermaßfeld bei Meiningen* (Thüringen). Teil 2. Habelt-Verlag, Bonn, pp. 101–180.
- Simpson, G.G., 1941. Large pleistocene felines of North America. *Am. Mus. Novit.* 1136, 1–27.
- Skinner, M.R., Kaisen, O.C., 1946. The fossil *Bison* of Alaska and preliminary revision of the genus. *Bull. Am. Mus. Nat. Hist.* 89, 123–256.
- Soubrier, J., Gower, G., Chen, K., Richards, S.M., Llamas, B., Mitchell, K.J., Ho, S.Y., Kosintsev, P., Lee, M.S., Baryshnikov, G., Bollongino, R., 2016. Early cave art and ancient DNA record the origin of European bison. *Nat. Commun.* 7, 13158.
- Stampfli, H.R., 1963. Wisent, *Bison bonasus* (Linné) 1758, Ur, *Bos primigenius* Bojanus, 1827, und *Hausrind Bos taurus* (Linné) 1758. In: Boessneck, J., Jéquier, J.-P., Stampfli, H.R. (Eds.), *Burgäschisee-Süd, Teil 3: Die Tierreste, 2. Acta Bernensia, Beiträge zur prähistorischen, klassischen und jüngeren Archäologie II*. Verlag Stämpfli & Cie, Bern, pp. 117–196.
- Strani, F., DeMiguel, D., Alba, D.M., Moyà-Solà, S., Bellucci, L., Sardella, R., Madurell-Malapeira, J., 2019. The effects of the “0.9 Ma event” on the Mediterranean ecosystems during the Early-Middle Pleistocene transition as revealed by dental wear patterns of fossil ungulates. *Quat. Sci. Rev.* 210, 80–89.
- Stuart, A.J., Lister, A.M., 2001. The mammalian faunas of Pakefield/Kessingland and Corton, Suffolk, UK: evidence for a new temperate episode in the British early Middle Pleistocene. *Quat. Sci. Rev.* 20, 1677–1692.
- Teilhard de Chardin, P., Piveteau, J., 1930. Les mammifères fossiles de Nihowan (Chine). *Ann. Paleontol.* 19, 1–134.
- Tong, H.W., Chen, X., Zhang, B., 2016. New fossils of *Bison palaeosinensis* (Artiodactyla, mammalia) from the steppe mammoth site of early pleistocene in nihewan basin, China. *Quat. Bar Int.* 445, 450–468.
- Van der Made, J., Rosell, J., Blasco, R., 2017. Faunas from Atapuerca at the Early–Middle Pleistocene limit: the ungulates from level TD8 in the context of climatic change. *Quat. Bar Int.* 433, 296–346.
- Verestchagin, N.K., 1959. *The Mammals of the Caucasus. A History of the Fauna*. Academia Nauk, Leningrad (Translated from Russian; Israel Program for Scientific Translations, Jerusalem 1967).
- Vershinina, A.O., Kapp, J.D., Soares, A.E.R., Heintzman, P.D., Lowson, C., Cassatt-Johnstone, M., Shidlovskiy, F.K., Kirillova, I.V., Shapiro, B., 2019. Ancient DNA analysis of a Holocene bison from the Rauchua River, Northwestern Chukotka, and the existence of a deeply divergent mitochondrial clade. *Zool. J.* 98, 1091–1099.
- Von Koenigswald, W., Tobien, H., 1987. Bemerkungen zur Altersstellung der pleistozänen Mosbach-Sande bei Wiesbaden. *Geologisches Jahrbuch Hessen* 115, 227–237.
- Wagner, G.A., Krbetschek, M., Degering, D., Bahain, J.J., Shao, Q., Falguères, C., Voinchet, P., Dolo, J.M., Garcia, T., Rightmire, G.P., 2010. Radiometric dating of the type-site for *Homo heidelbergensis* at Mauer, Germany. *Proc. Natl. Acad. Sci. USA* 107, 19726–19730.
- Zheng, S.H., Wu, W.Y., Li, Y., Wang, G.D., 1985. Late cenozoic mammalian faunas of guide and Gonghe basins, qinghai province. *Vert. PalAs* 23, 89–134 (in Chinese).



Chapter 6.



6.1. The ‘suid gap’ debate and the persistence of *S. strozzi* in the Epivillafranchian

Sus strozzi is a continuous presence in the middle and late Villafranchian faunal assemblages of the Western Palearctic, appearing in all the major paleontological localities dated between 2.5 and 1.8 Ma (Cherin et al., 2018; chapters 3, S1) (Fig. 10). After 1.8 Ma, a strong reduction, if not complete absence, of suids is evident in the fossil records of Europe. This ‘suid gap’ could be already noticed in the taxon range charts of Van der Made and Moyà Solà (1989) and Van der Made (1990, 1997) but remained relatively unrecognized until Martínez-Navarro et al. (2015) defined this bias in the fossil record and ignited the debate between supporters and opposers of this gap theory. Van der Made et al. (2017), in particular, strongly disagree with Martínez-Navarro and colleagues, stating that there are localities which: “cover the whole range from the well-known records of *Sus strozzi* from the Upper Valdarno (Olduvai subchron) till Untermassfeld and Vallonnet (Jaramillo subchron)” (Van der Made et al., 2017: 307). The first authors provided a list of sites, dated between 1.8 and 1.2 (MN18-19), that yielded suid remains, de facto invalidating the ‘suid gap’ of Martínez-Navarro et al. (2015). In order to clarify this matter, firstly we have to define the gap itself. As Martínez-Navarro et al. (2015: 132) suggested, the gap could be considered as: “The consistent absence of suids from any of the rich large mammal assemblages unearthed from the Late Villafranchian sites of Europe with chronologies between 1.8 and 1.2 Ma”. This statement limits the lack of suid fossil record exclusively to the rich, large, and well-known localities of the considered timespan. Nonetheless the authors provided, in the abstract of the same work, another interpretation which describes the gap as: “no pig record in the biochronological range comprised between the post Tasso Faunal Unit, which marks the base of the Late Villafranchian (1.8 Ma), and their arrival in Western Europe at layer TE9 from Sima del Elefante, Atapuerca, Northern Spain (1.2 Ma)” (Martínez-Navarro et al., 2015: 131). In this trenchant definition the authors included all the sites of the latest Villafranchian, providing a stronger statement that exclude whatsoever presence of this group in Europe between 1.8 and 1.2 Ma. In my opinion, the first interpretation is preferable to the second due to its broader and less strict definition. Keeping this in mind and considering also the fact that the absence of a taxon in a fossil record is not the evidence of its absence from the original faunal assemblage, we can approach the ‘suid gap’ debate.

Van der Made et al. (2017) affirmed that there is a constant presence of suids in Europe from the Pliocene to the Holocene, without a major bias in the fossil record, and inferred that the scantier remains of the gap might be interpreted as a mere lack of documentation. As suggested in chapter S1, this explanation appears to be too simplistic and unsatisfactory. The authors provided a list of latest Villafranchian localities in which putative remains of suids were unearthed including: Selvella, Mugello and Pirro Nord from the Italian Peninsula, Ceyssaguet and Peyrolles from

France, and Atapuerca TE9 from the Iberian Peninsula, to which few other reports are added (Martínez-Navarro, 2015; Iannucci et al., 2020a; chapter S1). I believe that these records, when compared with other major assemblages from Europe of similar age, confirm, in fact, the ‘suid gap’ theory (Fig. 10).

The attribution of the fossil from Pirro Nord, referred to *Sus* sp. by De Giuli et al., (1986), is quite doubtful. Freudenthal (1971) provided a list of the taxa recorded from the site, citing but not describing the suid remains. The presence of *Sus* in the Pirro Nord assemblage was kept in the work of De Giuli et al (1986) but, neither this time, the authors presented whatsoever identification of the anatomical elements attributed to this animal. To complicate the matter, the collection of Pirro is scattered between several institutions in the Italian territory and the exact location of the discussed fossil is not available. At the present state, the identity, and the whereabouts, of these putative remains are unknown. Few teeth of *Sus strozzii* from Mugello basin were cited by Azzaroli (1954). These fossils came from the locality Pulicciano altogether with remains of *Mammuthus meridionalis*. The Mugello basin sites are commonly referred to the late Villafranchian, however, on the whole, they possibly span from middle Villafranchian to Galerian (Abbazzi et al., 1995). The presence of *M. meridionalis* and *S. strozzii* alone in Pulicciano does not help in defining the depositional age of the locality which, therefore, could be previous or subsequent to the ‘suid gap’. Ellera historical collection, recently reappraised in the work of Pazzaglia et al. (2013), includes an isolated suid molar referred to *Sus* cf. *S. strozzii*. The estimated age of the locality (Tasso-Farneta FUs, ca. 1.8-1.6 Ma), however is debatable (Martínez-Navarro et al., 2015). The Selvella *Sus* sp. specimen was briefly described by De Giuli (1986: 13) who wrote: “a diaphysis of a humerus can be assigned to this genus because of its strong curvature”. This sample, although very scanty, is the only described pig remain from the Italian peninsula which it is reliably dated to the ‘suid gap’.

Among the French localities with putative fossil suids, the most interesting is the volcanic lake site of Ceysaguet. These dentognathic remains were never described but are often cited in literature (Tsoukala and Guérin, 2016; Van der Made et al., 2017) and used as comparative sample by Guérin and Faure (1997) and Vaquero et al. (2018) who assigned them to *S. scrofa* and *S. strozzii* respectively. In the absence of any other data, I believe that, due to the presence of various Villafranchian taxa in Ceysaguet (Argant and Bonifay, 2010), the attribution to *S. strozzii* seems to be more parsimonious. It is however remarkable that, among the studies focusing on the fauna of Ceysaguet, there is not a single mention of suids remains (e.g., Croitor and Bonifay, 2001; Argant and Bonifay, 2010; Mourer-Chauviré and Bonifay, 2018 and references therein). In addition to that, the correlation between the absolute dating of the site and the biochronological information given by the fauna is strongly contradicting. The basalt on which the fossiliferous layers deposited were dated by K/Ar in 1985 by the University of Clermont-Ferrand but the

results were never published. Moreover, the scholars provided different age estimations (e.g., 1.3 Ma in Kaiser and Croitor, 2004 and 1.4 Ma in Mourer-Chauviré and Bonifay, 2018). Finally, the long faunal list is particularly heterogeneous with the presence of several taxa which range spans from the middle Villafranchian (e.g., *Eucladoceros ctenoides* and *Pseudodama rhenana*) to the Galerian (*Lynx lynx* and *Palaeoloxodon antiquus*) (Argant and Bonifay, 2010; Tsoukala and Bonifay, 2004; Mourer-Chauviré and Bonifay, 2018). The putative co-existence of these taxa in Ceysaguet would surely advocates the presence of more than one depositional event, possibility that is still not faced by any of the paper mentioning the locality. In the absence of a well-defined suid material and considering the evident issue with the chronology of the site, this record cannot be considered reliable until further studies are performed. The Peyrolles suid sample was cited by Van der Made et al. (2017) as hosted in the NHM but the authors did not provide further data on that. No other mention of suids from this French assemblage are available, which according to the latest review includes *Eucladoceros* sp, *Pseudodama* (= *Metacervoceros*) *perolensis*, *Stephanorhinus etruscus* and *Leptobos* sp. (Valli et al., 2006). The Peyrolles site was biochronologically dated to MNQ19, around 1.5-1.4 Ma, by Valli et al. (2006) and to MIS 32-30 by Brugal et al. (2020). In spite of that, the presence of two middle Villafranchian cervids suggests an older age for Peyrolles than the one conjectured by previous studies which should be reappraised.

The older levels of the Atapuerca cave complex (Iberian Peninsula) yield few suid remains briefly discussed in chapter S1. Without further stress the taxonomic attribution debate, it interesting to linger on the age of these remains which spans from ca. 1.3-1.1 Ma (Sima del Elefante TE9) to ca. 0.8 Ma (Gran Dolina TD8) including the fossils of Gran Dolina TD3-TD4+TD5? dated to ca. 1.0 Ma (Van der Made, 1999; Rodríguez et al., 2011; Van der Made et al., 2017). Of these sample the only that could fit with the 'suid gap' is the one from TE9 which, in its older estimation, includes the latest stages of the bias. No other Suidae remains are reported from the Iberian Peninsula before the Epivillafranchian transition (chapter S1).

The Greek area has always been a reservoir for suid remains during the Plio-Pleistocene (Kostopoulos and Sylvestrou, 2022 and references therein) and could be the only European region in which a reliable presence of this group during the 'suid gap' is confirmed. Kostopoulos et al. (2022) referred to *S. cf. strozzii* few dentognathic remains from two of the three sites of Krimni, biochronologically dated to ca. 1.5 Ma. Despite the scantiness of the sample, the presence of suids in a Greek locality, just in the middle of the 'suid gap', challenges its validity. The authors believe that the *Sus* from Krimni testify the presence of a refugia for this group in Southern Balkans during a period of demographic decrease in Europe. The absence of pigs from the chronologically nearby faunas of Tsiotra Vryssi and Apollonia 1 could be mere accidental or/and related to environmental reasons (Kostopoulos et al., 2022). East European sample of *S. strozzii*, possibly dated to the 'suid gap' comes from the site of Dunaalmás in Hungary,

recently described by Iannucci et al. (2020b). Nonetheless, the estimated age of the locality spans from 2.0 to 1.5 Ma, hence possibly precedent to the gap. The Tegelen historical collection includes some remains undisputedly referable to *S. strozzi* (Richarz 1921; Schreuder, 1946). Although the age of the site is not well-constrained and still debated (Hoek van den and de Vos, 2006; Westerhoff et al., 2020), most of the authors assign the main fauna to the middle to late Villafranchian boundary (ca. 2.1-1.8 ma), thus preceding the gap (Spaan, 1992; Van den Hoek and de Vos, 2006; Villa et al., 2018 and references therein). Up to date, the only site of Western Palearctic dated to the ‘suid gap’ period and from which considerable pigs remains were recovered is the site of ‘Ubeidiya (Palestine; Geraads et al., 1986).

Although these aforementioned samples could be considered proofs against the ‘suid gap’ theory, if correlated with the richest European sites of this period, and with older and younger localities, the results are quite the opposite. The chronological range covered by the ‘suid gap’ (1.8–1.2 Ma) includes several sites that, for number and quality of the remains and for biochronological meaning, are among of the most studied of the whole Pleistocene. In these localities is constantly registered the absence of suids, which, on the other hand, are always present in the major fossil associations coming from pre and post ‘suid gap’ periods. This, allied with the extremely opportunistic behaviour and high reproductive rates of suids (Martínez-Navarro et al., 2015) suggest that this bias is hardly justifiable with preservation issues (i.e., taphonomic destruction of the remains). The sites of Venta Micena 3-4, Barranco León 5, Fuente Nueva 3, in the Guadix-Baza basin stand out as the richest and most important sites of the Iberian Peninsula dated between 1.8 and 1.2 Ma (Martínez-Navarro et al., 1997; Toro-Moyano et al., 2013; Sánchez-Bandera et al., 2020; Luzón et al., 2021; Saarinen et al., 2021 among others). The heated debate about putative human presence in these sites which might represent the first *Homo* dispersal in Western Europe, strongly focused the efforts of palaeontologists on new findings and studies in this area. For this reason, since the 80’, dozens of systematic excavations were carried out (Saarinen et al., 2021 and references therein). These decades of fieldworks unearthed thousands of fossils which provided a deep knowledge on the Iberian faunal assemblages of the latest Villafranchian. It is indeed quite impressive that no pig remains were recognized among the 27,000 large mammal fossils recollected from the Orce complex (Martínez-Navarro et al., 2015). On the other hand, the Iberian Peninsula provided some important samples of suids coming from the periods before and after the ‘suid gap’, including the site of Fonelas P-1 (ca. 2.0), Cal Guardiola (ca. 1.2–0.8 Ma) and Vallparadís Estació (ca. 1.0–0.6 Ma) (Arribas and Garrido, 2008; Madurell-Malapeira et al., 2014; chapters 3, S1). The Italian peninsula, as for the Iberian one, is characterized by a hiatus of suid sample. In particular, the rich faunal assemblage of Pietrafitta (Central Italy) consists of 10 different species of large mammals (for a total of ca. 40 vertebrate taxa) with more than 5,000 remains including isolated bones and partially articulated skeletons (Sorbelli et al., 2021 and references therein). The multiple studies carried out on the

mammal sample of this late Villafranchian site evidenced the total absence of suid remains (Azzaroli and Mazza, 1993; Mazza et al., 1993; Gentili et al., 1996; Zucchetta et al., 2003; Sorbelli et al., 2021 among others). The palaeoenvironmental reconstruction of Pietrafitta suggest the presence of a humid and forested landscape on the edge of a lake during a relatively warm period (see chapter 4 and references therein). This habitat would have been suitable for humid-specialized suids such as *S. strozzi* (Azzaroli, 1954; Faure and Guérin 1984). The absence of this clade in Pietrafitta is, therefore, a remarkable anomaly. In addition to the Umbrian locality, other large and well-known collections from the 1.8–1.2 timespan do not have traces of this group, including: Farneta, Monte Peglia, Monte Argentario, Capena, Ellera “Ex-Quasar” (Petronio 1979; Rook and Martínez-Navarro, 2010; Cherin et al., 2012; Siori et al., 2014; Petronio et al., 2020). Although debatably (see above), Pirro Nord and Selvella are the only major localities of the Italian Peninsula in which suid remains were found. On the other hand, the pre and post ‘suid gap’ periods are rich of well-preserved *Sus* fossils including the samples of: Upper Valdarno (ca. 2.0 Ma), Olivola (ca. 2.0 Ma), Pantalla (ca. 2.0 Ma), Frantoio (ca. 1.0 Ma), Slivia (ca. 0.8 Ma) and some scantier reports from Castagnone, Pagliare di Sassa, and Madonna della Strada, all dated to the Epivillafranchian-Galerian (Cherin et al., 2018; chapter S1 and references therein). The Mygdonia basin complex (Greece) includes the sites of Kalamoto, Krimni, Tsiotra Vryssi and Apollonia which cover all the ‘suid gap’ chronological range (Kostopoulos et al., 2018; Kostopoulos and Sylvestrou, 2022). As aforementioned, the only locality of the complex which yielded suid remains is Krimni. This record, however, is quite scarce (two isolated molars of which one went destroyed) and wedged between sites which did not provide any suid remains in spite of the abundance of fossils collected during the years (Kostopoulos, 1997; Tsoukala and Chatzopoulou, 2005; Konidaris et al., 2015). As for the other areas discussed here, the pre ‘suid gap’ period in Greece is well documented by the sites of Gerakarou 1 and Vassiloudi (ca. 2.0–1.8 Ma) which provided a good amount of *Sus strozzi* remains (Koufos 1986; Kostopoulos and Athanassiou 2005). Among the most important sites of the Balkan area, stands out the long stratigraphic section of Trlica (Montenegro). In spite of the abundant fossil record unearthed, no suids were recognized in either of the two faunal assemblages: TRL11–10 (late Villafranchian) and TRL6–5 (Epivillafranchian) (Vislobokova and Agadjanyan, 2016). Dmanisi (Georgia) is the most famous and studied site of Caucasian Early Pleistocene. The presence of the oldest record of *Homo* at the borders of Europe started up a series of systematic excavations which collected thousands of fossils remains, referable to the late Villafranchian (Bartolini-Lucenti et al., 2022 and references therein). The complete absence of suid traces from the rich Dmanisi record is another proof of ‘suid gap’ legitimacy.




All these evidences provided suggest that most of the European territory seem to been affected by a steep decrease in the abundance of suid fossils in the 1.8–1.2 Ma timespan (Fig. 10). This loss it is not easily explainable

without advocating a substantial shrinking of the Suidae population during the latest Villafranchian. Central and Northern Europe are unfortunately lacking of a sufficient number of fossiliferous localities that could shed light on the distribution of suids at the higher latitudes of the continent during the late Villafranchian. The explanations of this bioevent are still obscure. Although it is true that the whole Villafranchian is characterized by a shift toward drier and colder climates, this process became stronger only at the Epivillafranchian passage with the EMPT (ca. 1.2 Ma) (see chapter 1). For this reason, the environmental changes, on its own, seems to be not enough to explain this suid demographic loss, which started during the late Villafranchian and finished just by the onset of the climate crisis peak. This is furtherly corroborated by the extremely plasticity of suids which allow them to populate a wide array of habitats from the savannahs of Africa to the tropical forests of South East Asia, from the temperate woodlands of Europe to the tundra of Siberia (Martínez-Navarro et al., 2015 and reference therein). Equally, the competition with other large herbivores or the overhunting by carnivores alone, seem to be not sufficient as justification for this strong demographic reduction. It is indeed plausible that there is not a single triggering event for this bioevent, rather a concurrence of several causes which led to the shrinking in the population of the late Villafranchian suids in Europe. Further studies are required in order to define the possible causes for this (in)famous gap.

Given all these evidences, the ‘suid gap’ of the late Villafranchian could be determined as a timespan, comprised between 1.8 and 1.2 Ma, in which the suids, represented exclusively by the species *S. strozzi*, are not common in Europe, missing from all the major localities of the continent with the exception of few, scanty remains in peripheral areas of the Mediterranean area (e.g., Greece, Levantine area) or in isolated enclaves which could have been acted as a refugia in a period of demographic decline. At the beginning of Epivillafranchian, *S. strozzi*, or a variant of this species (see Iannucci, 2022) was able to recover completely and repopulate most of Europe until its final extinction concurrently with the passage to Galerian LMA.

Next page. Fig. 10. Selected Early Pleistocene Western Palearctic localities showing the records of *Sus strozzi* and *Sus scrofa* and the hypothetical refugia for suids during the late Villafranchian ‘suid gap’. The asterisk marks the absence of *Sus* in the locality. 1, Dmanisi*; 2, ‘Ubeidiyah; 3, Taurida cave; 4, Tzimal; 5, Gerakarou 1; 6, Vasiloudi; 7, Krimni 3; 8, Apollonia 1*; 9, Tsiotra Vryssi; 10, Kalamoto 2*; 11, Trlica 10-11*; 12, Dunaalmás; 13, Slivia; 14, Frantoio (Arda); 15, Olivola; 16, Mugello; 17, Poggio Rosso; 18, Upper Valdarno; 19, Selvella; 20, Farneta*; 21, Monte Argentario*; 22, Pietrafitta*; 23, Pantalla; 24, Monte Peglia*; 25, Pirro Nord*?; 26, Untermassfeld; 27, Süssenborn; 28, Mauer; 29, Tegelen; 30, West Runton; 31, Pakefield; 32, Le Vallonnet; 33, Saint Vallier; 34, Senèze; 35, Sainzelles*; 36, Ceyssaguet*?; 37, Peyrolles*?; 38, Cal Guardiola; 39, Vallparadís Estació; 40, Sima del Elefante TE9c; 41, Gran Dolina TD8; 42, Venta Micena*; 43, Barranco León 5*; 44, Fuente Nueva 3*; 45, Fonelas P1.



Ma	2.2 2.0 1.8 1.6 1.4 1.2 1.0 0.8 0.6									
GEO-CHRON.	P L E I S T O C E N E									
	Early					Middle				
ELMA	V I L L A F R A N C H I A N					E P I V I L L A F R A N C H I A N			G A L .	
	middle					late				
LOCALITIES	Fonelas 1	Poggio Rosso	Venta Micena*	Sainzelles*	Ceyssaguet*?	Untermassfeld	West Runton			
	Senèze	Upper Valdarno	Dunaalmás	Selvella	Krimni	Kalamoto*	Apollonia*	Cal Guardiola	Gran Dolina TD8	Mauer
			Dmanisi*	Trlica 10-11*	Pietrafitta*	Mugello	Pirro Nord*?	Vallparadís Estació		
	St. Vallier	Pantalla	Vasiloudi	Taurida*	Tsiotra Vryssi*	Mt. Argentario*	Le Vallonnet	Slivia	Süssenborn	
			Olivola	Peyrolles	'Ubeidiya	Barranco León*	S. del Elefante 9	Frantoio (Arda)		
			Gerakarou	Tegelen	Farneta*	Mt. Peghia*	Fuente Nueva*	Gran Dolina TD6-8	Tsimbal	Pakefield
SUS BIOCHRON. IN EUROPE	 <i>Sus strozzi</i>		'Suid gap'				 <i>Sus strozzi</i>		 <i>Sus scrofa</i>	

6.2. The early bison, *Bison* (*Eobison*), their origin and dispersal in Europe

The arrival of the first forms of *Bison* in Europe is a pivotal event for the faunal assemblages of the European Early Pleistocene. Unfortunately, the tempo and mode of this dispersal has been never clarified, hampered by the scanty fossil remains of this group. During the last decades, however, the discovery of new Villafranchian and Epivillafranchian localities, which provide abundant records referred to these large bovids, ignites the interest on their first steps in the Western Palearctic. The late Villafranchian localities of Dmanisi, Mygdonia basin, Pietrafitta and Venta Micena yielded extremely informative samples representing the earliest stages of *Bison* dispersal in Europe (chapter 4) (Fig. 11).

More than 100 years ago the pioneering works by Lydekker (1878, 1898), and, later of Teilhard de Chardin and Piveteau (1930), already recognized the presence of bison-like bovids from the Plio-Pleistocene of Asia. These forms, sharing a series of characters which are considered primitives in the evolution of *Bison* (see chapter 4), were grouped in the subgenus *Eobison* by Flerov (1972). From the second half of 20th century, several species of early bison were erected and lumped into *Eobison* which, unfortunately, became a ‘wastebasket’ taxon, eventually generating a distorted definition of the subgenus (chapter 4). Only in the last decades, the aforementioned discoveries shed new lights on the European evolutionary history of this group, making thus possible the reappraisal of this obscure and yet important clade. The works of Masini (1989); Sher (1997), Bukhsianidze (2005), Croitor (2010), Maniakas and Kostopoulos (2017) and Kostopoulos et al. (2018) are the most recent studies which embrace the systematics and evolution of late Villafranchian *Bison* (*Eobison*). In spite these works, the oversplitting trend affecting this clade persisted and, at the current state of the art, *Eobison* includes between 5 and 6 species, co-occurred in a timespan of less than 1.0 Ma. The study provided in chapter 4 of this thesis dissertation tried to detangle the most impelling taxonomic issues, disposing of those species defined on the basis of extremely scanty material, and defining the status and chrono-spatial range of the whole subgenus.

The origin of *Eobison* has been localized in the Asian subcontinent due to the presence of primitive forms this group, namely *B. (E.) sivalensis* and *B. (E.) palaeosinensis*, in the Early Pleistocene of India-Pakistan and China respectively (Tong et al., 2016 and references therein). Although the study performed in this thesis was not focused on the Asian *Eobison*, a reappraise of the group could not be performed without including the very first precursors of the whole genus (Flerov, 1979). It is commonly accepted that these forms were the earliest members of *Bison* s.l., however, the scanty and often inaccessible material (i.e., the lost holotype of *E. sivalensis*) paired with the unclear chronology of many of the oldest remains attributed to these taxa, severely complicate the verification of this long-

lasting hypothesis. In spite of that, at least for *E. palaeosinensis*, thanks also to a richer record compared with its Indian relative, was possible to attest its validity as one of the most primitive and oldest species of *Bison* and to confirm its taxonomic position as type species of the subgenus. On the other hand, the similarities between the yak (*Poephagus*) and the holotype of *E. sivalensis* pointed out by various authors in the past (i.e., Olsen, 1990; Bukhsianidze, 2020) are addressing to other directions for this species. Unfortunately, the unknown whereabouts of the holotype and the extremely doubtful attribution of isolated bones to this species, does not help in clarifying its systematics. Although some authors suggested the presence *E. sivalensis* before 2.5 Ma (e.g., Khan et al., 2010; Khan et al., 2011), the aforementioned issues prevent to confirm these assumptions (see chapter 4). A badly preserved neurocranium from Pakistan, preliminary described and referred by Akhtar (1992) to this species, is still pending of revision in order to validate its taxonomic attribution. The oldest attested records of *Bison* s.l. (i.e., *E. palaeosinensis*), thus, come from the Haiyan formation (Yushe basin) and Nihewan (Nihewan basin), dated between 2.5 and 1.8 Ma (Fig. 10), well-fitting with the chronology of the first Western Palearctic *Bison* findings (Teilhard de Chardin and Piveteau, 1930; Teilhard de Chardin and Trassaert, 1938; Tedford et al., 1991; Farjand et al., 2022).

The long-lasting theory that sees *Leptobos* and early *Bison* as part of the same monophyletic group due to their shared morphological characters, is a pivotal point for understanding the evolutionary history of both taxa (Pilgrim, 1947; Merla, 1949; McDonald, 1981; Sher, 1997 among others). *Leptobos* represents one of the first large bovines dispersing in Eurasia with at least three different lineages which, although having been debated for almost a century, are still missing of a solid phylogenetic framework (Pilgrim, 1937; Merla, 1947; Masini, 1989; Duvernois, 1990; Cherin et al., 2019b; chapter 4 and references therein). With the exception of the studies of Geraads (1992) and Bibi (2009) -which, however, focused on much larger groups (i.e., the whole Bovini and Bovinae, respectively)- the evolutionary history of *Leptobos* and its relationships with *Bison* have never been reconstructed by specific phylogenetic analyses. Chapter 4, although not providing any phylogenetic study, contributes to the debate with some interesting pieces of evidence including:

- I. The numerous synapomorphies shared by *L. stenometopon*, *L. elatus*, and *Leptobos merlai* (LSEM group) strongly suggest that these species might be part of the same monophyletic clade, or might be even included into a single species. Their differences in cranial features and metapodial robusticity might be related to ecomorphological variation and/or sexual dimorphism.
- II. *Leptobos etruscus* and *L. vallisarni* (LEV group) show striking similarities between each other, as already evidenced by other authors (e.g., Duvernois, 1990; Geerads, 1992). Despite that, some cranial elements (i.e., horns and intertemporal bridge) are still useful to discriminate the two species.

- III. The purported similarities between *Leptobos* and *Bison* are indeed well-supported by the statistical analyses performed in this work. An evident trend toward larger heads with broader frontals, massive horns and shorter neurocranium, increased size and robusticity of the appendicular skeleton characterize the evolutionary transition from the former to the latter genus.
- IV. The presence of some Plio-Pleistocene large bovids in western Asia with “transitional” characters and questionable taxonomy (e.g., *Adjiderebos cantabilis*, *Protobison kushkunensis*) supports the legitimacy of a *Leptobos* ancestry of *Bison*. The reappraisal of these Asian records is required to clarify their relationships with these genera.
- V. The earliest records of *Bison* in Asia and the widespread presence of *Leptobos* in China and India since the Pliocene, coupled with the evidence that continental Asia has been the centre of origin of many other mammal clades (‘megacerines’ deer, *Pachycrocuta*, and *Canis (Xenocyon)* among others), suggest that an Asian origin for both *Leptobos* and *Bison* is most likely.
- VI. The compelling differences between the three groups of *Leptobos*, namely LSEM, LEV, and the Asian lineage, and the discrepancies affecting the diagnosis of the genus, strongly challenge the monophyly of the group. This issue is a major topic for understanding the true origin of *Bison* that requires further studies.

The arrival of *Eobison* at the gates of Europe is first recorded at ca. 1.77 Ma in Dmanisi (Georgia) with the species *B. (E.) georgicus*. Later on, these primitive bison dispersed in the whole Mediterranean area as testified by the late Villafranchian samples from Mygdonia basin, Pietrafitta, Pirro Nord, Sainzelles, and Venta Micena, with at least one species, *B. (E.) degiulii* (Fig. 11). The total absence of this group in Central and NW Europe could be an environmental indicator and/or a bias related to the scantiness of late Villafranchian fossiliferous localities in those regions (see chapter 1).

Masini (1989) in his phylogenetic reconstruction of *Leptobos-Eobison*, rightfully separated LSEM and LEV, however, he groups the latter with the Asian lineage. The author, although supporting the *Leptobos* origin for *Bison*, did not provide any hints on the possible ancestor of *Eobison* within the two lineages. Masini (1989), Gentili and Masini (2005), and Masini et al. (2013) referred the bison sample to Pietrafitta to *L. vallisarni* and date the arrival of *Bison* s.l. in Europe at the post-Olduvai/pre-Jaramillo interval (Venta Micena and Pirro Nord). The recent work by Kostopoulos et al. (2018) and the study performed in this thesis proved that *Eobison* was present also in Greece at ca. 1.6 Ma as well as in the Italian Peninsula, in Pietrafitta, slightly later (chapter 4).

Sher (1997), although focusing on the first description of the long-legged Epivillafranchian *B. menneri* (see below), gave a rapid excursus on the most primitive forms of bison and their dispersal. According to the author, *Eobison* populated Europe at the same time as the first “true” *Bison*, geographically relegated in the western and eastern parts of the continent, respectively. If it is true that the obscure species *B. tamanensis* (*Eobison* for Flerov, 1979) represents an early member of *B. schoetensacki* and not a particularly large and stout *Eobison* (Kostopoulos et al., 2018), Sher’s hypothesis would be confirmed. Pending a reappraisal of the *B. tamanensis* record I tend to agree with Sher. In addition to that, the same author evidences the existence of a possible speciation area for bovines in the Caucasus. This statement is indeed plausible, given the abundance of unique bovid genera discovered in this region (Vekua, 1972; Burchak-Abramovich et al., 1980; Dubrovo and Burchak-Abramovich, 1986 among others). Nonetheless, I am very critic with the oversplitting trend shown by many authors who worked on Caucasus bovids in the last century, which might have inflated this presumed high diversity (chapters 1 and 4).

Bukhsianidze (2005), for the first time, attributed the species *Dmanisibos georgicus* to the subgenus *Eobison*. The author also proposes that *Eobison* might have originated from a stock including the LSEM group and other leptobovine bovids of Caucasus (i.e., *P. kushkunensis*) and India (i.e., *P. dehmi*). The author considered that these latter middle Villafranchian leptobovines (including also *L. elatus*) already show bisontine characters and can be included in *Bison* as the earliest members of the genus. Therefore, the origin of *Bison* would have occurred in Europe, most probably branching from *L. stenometopon*. Later, *Bison* would have reached the Caucasus and Eastern Asia and, from there, dispersed in all Eurasia (Bukhsianidze, 2005). Although some of these inferences are worth of further investigations, this hypothesis seems to be, overall, groundless due to the evident cranial differences between LSEM and *Bison* s.l. (chapter 4). In spite of that, the author rightfully remarks the importance of some “forgotten” taxa coming from the Plio-Pleistocene of Caucasus which might represent crucial steps in the evolutionary history of *Leptobos* and *Bison*. In addition to that, Bukhsianidze (2005) suggests that *B. (E.) degiulii*, on the basis of the characters shown by the cranium from Pirro Nord, already belongs to the group of “true” bison. However, as already demonstrated by Masini et al. (2013) and in chapter 4 of this thesis, *B. (E.) degiulii* features some plesiomorphies (i.e., constriction of the upper occipital crest, small-sized dentition, orbits not extremely protruding nor tubular, reduced frontals) which are much more closely related to primitive bison. Its inclusion into *Eobison* is furtherly confirmed by the large sample from the Mygdonia basin described by Kostopoulos et al. (2018) and partially reappraised in chapter 4. Although showing a stouter built, the limbs of Mygdonia sample are different from those of the larger and more derived Epivillafranchian *Bison* from Le Vallonnet and Cal Guardiola (Fig. 12) (Moullé, 1992; chapter 5). Nonetheless, the Pirro Nord and Apollonia *E. degiulii* samples are characterized by slightly more derived traits

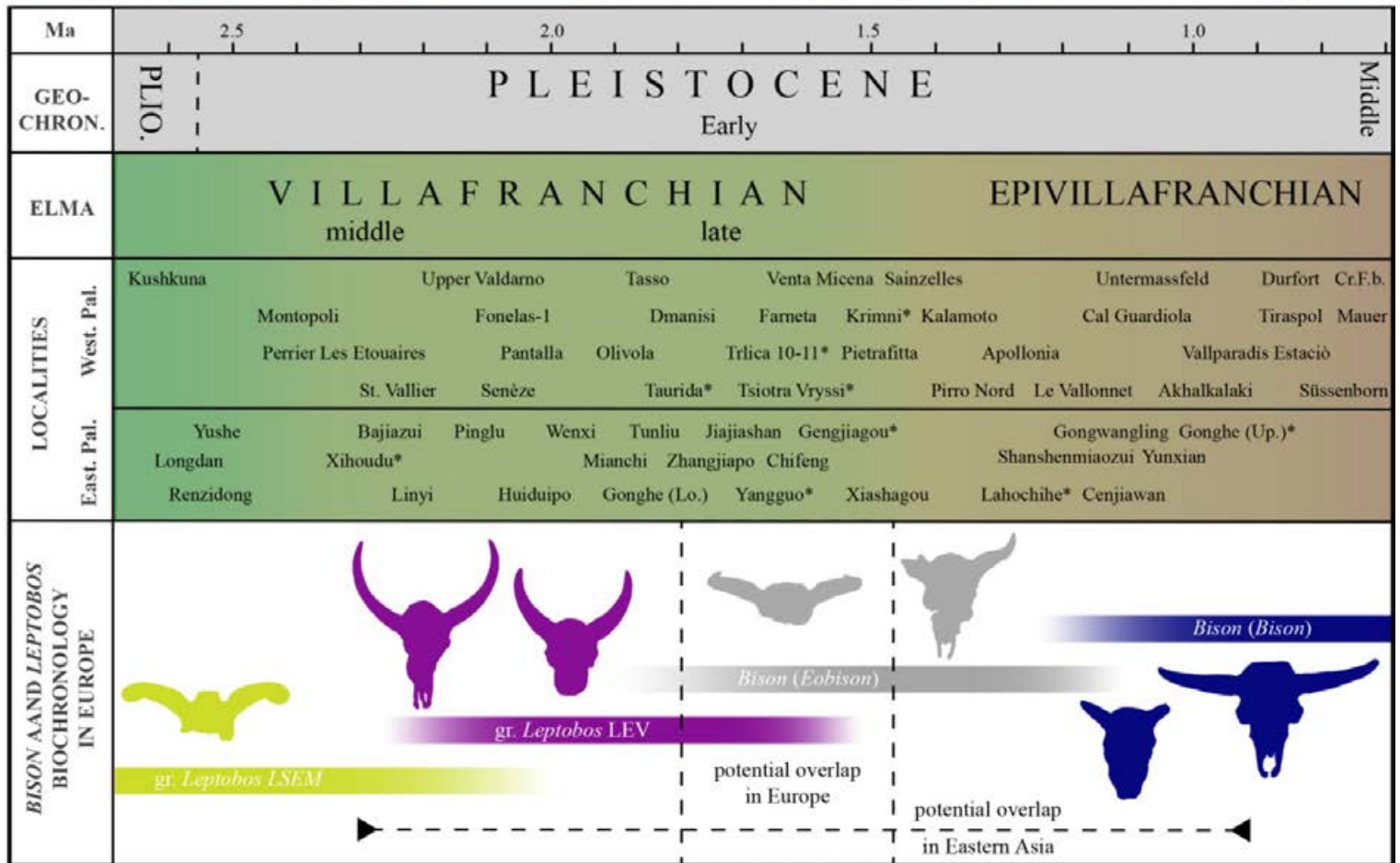
compared with those featured in the Pietrafitta, Venta Micena, and Dmanisi samples (Fig. 12). These peculiar aspects might be related either to sexual dimorphism and ontogeny (the Pirro cranium belongs to an old male individual), chronology (Pirro Nord and Apollonia are dated to the final stages of the late Villafranchian and represent the last occurrences of the subgenus), or ecomorphological variation (Pirro Nord and Apollonia hosted relatively dry and open habitats) (chapter 4 and references therein).

Croitor (2010) suggested that the earliest *Bison* s.l. entering Europe can be divided in two groups, the ‘boreal’ and the ‘southern’ lineages. The first includes the large and long-legged *B. (E.) palaeosinensis*, *B. menneri*, and *Bison* sp. from Tiraspol, whereas the second is composed by smaller and shorter-legged species such as *B. (E.) sivalensis*, *B. (E.) georgicus*, *B. (E.) tamanensis*, and *B. (E.) degiulii*. The author implies also that the latter species was endemic of the Italian Peninsula and, thus, potentially subjected to parallel/insular evolution. According to Croitor, these two lineages evolved independently, separated by the Alpine-Himalayan Mountain chains acting as natural barriers. Slender cursorial forms would have spread in the boreal open environments and stouter bison in the forested temperate habitats in southern regions. These hypotheses, however, are disputed by multiple evidence including: the presence of relatively long-legged *Bison* from the Mediterranean area (e.g., Le Vallonnet, Cal Guardiola), the discovery of *B. (E.) degiulii* outside Italy (i.e., in Mygdonia basin), the abundant forested habitats of Central Europe (e.g., Untermassfeld), the common misconception that long-legged *Bison* are associated to open environments (see chapters 4 and 5). It is indeed plausible that Early Pleistocene *Bison*, as it has been for their younger relatives (i.e., *B. priscus* subspecies), were capable to move across Europe, adapting to the glacial pulses which already started to characterize the Northern Hemisphere during the late Villafranchian (see chapter 1). Kostopoulos et al. (2018) agreed with Bukhsianidze (2005) in evidencing that *E. degiulii* is too “advanced” for being placed in *Eobison*. Nonetheless, as stated above, the evident differences with the slightly younger samples from Le Vallonnet and Vallparadís composite section (chapter 5), paired with the new findings in Pietrafitta (chapter 4), strongly support the inclusion of all these late Villafranchian forms into *Eobison*.

The late Villafranchian arrival of *Eobison* is a major bioevent for the whole European faunal assemblages. This primitive bison clade dispersed in a relatively short time span (Fig. 11), given that there is only a 0.2 Ma gap between the arrival of *Eobison* in Eastern Europe (Dmanisi; ca. 1.8 Ma) and in Southwestern Europe (Venta Micena; ca. 1.6 Ma). Its co-existence with the latest *Leptobos* is not reliably tested yet, although some records from SE Europe (i.e., Balkans and Greece) might be further investigated on this regard (Kostopoulos et al., 2018 and references therein). Given the evidence provided by the fossil record, the most parsimonious hypothesis is an Asian or Ponto-Caucasian origin of *Eobison* between the late Pliocene and earliest Pleistocene (Fig. 11). *Eobison* records are common

in all the Mediterranean area, and some doubtful remains come from Eastern Europe (Fig. 11). The subgenus was replaced by the earliest “true” *Bison* ca. 1.2 Ma, that is, at the Villafranchian/Epivillafranchian transition (Fig. 13). The last occurrence of *Eobison* is recorded in Apollonia (ca. 1.2 Ma) where these forms reached their largest sizes and stoutest proportions, comparable to those of some *B. schoetensacki* individuals (chapter 5).

Next page. Fig. 11. Early Pleistocene Northern Hemisphere localities showing the most significant records of *Leptobos* and *Bison* s.l. and potential dispersal routes from the two possible centres of origin. The asterisk marks the putative co-occurrence of the two genera in the locality. The blue shaded area represents the putative geographical distribution of *Bison priscus* during the Pleistocene (taken from Kahlke, 1999). 1, Nihewan Basin, (Xiashagou, Shanshenmiaozui, Cenjiawan); 2, Jiajiashan; 3, Chifeng; 4, Renzidong; 5, Eastern Shanxi (Tunliu: *Leptobos*; Yushe: *Eobison*); 6, South Shanxi (Wenxi: *Leptobos*; Linyi, Mianchi, Pinglu: *Eobison*; Xihoudu*); 7, Xi’An area (Gongwangling: *Leptobos*; Huiduipo, Zhangjiapo: *Eobison*; Lahochihe*, Yangguo*); 8, Gengjiagou*; 9, Bajazui; 10, Longdan; 11, Gonghe (Lower unit: *Leptobos*; Upper unit*); 12, Upper Siwaliks; 13, Kushkuna; 14, South Georgia (Dmanisi, Akhalkalaki); 15, Taurida Cave*; 16, Tiraspol; 17, Northern Greece (Gerakarou, Vasiloudi: *Leptobos*; Apollonia 1, Kalamoto: *Eobison*; Krimni 3*, Tsiotra Vryssi*, Kalamoto); 18, Trlica*; 19, Slivia (Italy); 20, Salita di Oriolo; 21, Central Italy (Upper Valdarno, Olivola, Farneta: *Leptobos*; Pietrafitta, Capena: *Eobison*); 22, Pirro Nord; 23, Central Germany (Untermassfeld, Mauer); 24, Süssenborn (Germany); 25, Tegelen; 26, Cromer forest-bed; 27, Le Vallonnet; 28, South-East France (Perrier Les Étouaires, Saint Vallier; Seneze: *Leptobos*; Sainzelles: *Eobison*); 29, Maar du Riège; 30, Durfort; 31, Eastern Spain (Cal Guardiola, Vallparadís Estació); 32, Southern Spain (Fonelas P-1: *Leptobos*; Venta Micena: *Eobison*).



6.3. The role of *Bison s.s.* as a marker of the Epivillafranchian and the *B. schoetensacki*

issues

Until the end of the last century, the most common hypothesis proposed a late dispersal of bison in Europe at the beginning of the Middle Pleistocene (Flerov, 1979; McDonald, 1981; Sala, 1986 among others). Only in the last decades, new Epivillafranchian sites evidenced that large and derived forms of this group were already populating the European continent before the Jaramillo subchron (ca. 1.0 Ma). The sites of Le Vallonnet (France), Untermassfeld (Germany), and Cal Guardiola and Vallparadís Estació (Spain) yielded clear evidence that these massive bovids were present in the continent well before the onset of the Middle Pleistocene (chapter 5). The first “true” bison in Europe are commonly referred to the two species *B. schoetensacki* and *B. menneri* (Sher, 1997; Maniakas and Kostopoulos, 2018; chapter 5).

Bison menneri is an oddly slender-legged species of large bison erected on the basis of the rich sample from Untermassfeld, originally referred to *Bison s.s.* (Sher, 1997) and recently included in the subgenus *Poephagus* (Bukhsianidze, 2020). The systematic debate regarding *B. menneri* and its allocation within *Poephagus* will be discussed in the next section. In spite of these disputes, since its discovery, *B. menneri* has been considered a major biochronological marker of the Epivillafranchian due to its presence in one of the most representative and rich localities of this biochron (e.g., Kahlke, 2007; Bellucci et al., 2015). Nonetheless, the distribution of this bovid seems to be geographically and chronologically relegated to the type locality of Untermassfeld and few other sites of Central Europe, although the scantiness of the remains from these latter sites, in fact, does not provide reliable taxonomic data (chapter 5 and references therein). The absence of *B. menneri* from other territories of Central and Northern Europe (e.g., British Islands) would make this species a peculiar form of the Untermassfeld region. Alternatively, this punctual distribution might be an artifact due to the lack of other high-latitude Epivillafranchian sites in Europe. On the other hand, the presence of another Epivillafranchian large and derived bison in Southern Europe, namely *B. schoetensacki*, might have hindered the dispersal of *B. menneri* at lower latitudes. The study performed in this thesis unequivocally supports the presence of *B. schoetensacki* in Mediterranean Europe already at the beginning of the Epivillafranchian. The usefulness of *B. menneri* in biochronological studies is mined by its absence in Southern Europe and its uncertain presence in post-Jaramillo mammal assemblages of Central and Northern Europe. Until new discoveries allow to improve our knowledge on the chronospatial distribution of this species, its value as a biochronological marker of the Epivillafranchian remains debatable (contra Bellucci et al., 2015).

Bison schoetensacki is a taxon with a long history. Erected by Freudenberg (1914) on the basis of the sample from the German site of Mauer, this species is well known from the latest stages of the Epivillafranchian and the whole Galerian (e.g., Durfort, Süssenborn, Isernia la Pineta), although quite rare before 0.8 Ma (Flerov, 1969; Sala, 1986; Brugal, 1995; Breda et al., 2010). The discovery of this bison in Le Vallonnet cave (Moullé, 1992) and in the lowermost levels of the Vallparadís composite section sets its first occurrence in Europe between 1.2 and 1.0 Ma (chapter 5). From 0.9-0.8 Ma on, *B. schoetensacki* became extremely common in all Europe, populating an area that spans from the British Isles to the Italian Peninsula (chapter 5). This wide geographical distribution in almost half million years of chronological range led to the evolution of several ecomorphotypes adapting to the climate and environmental changes during the EMPT (chapter 5). It is indeed true that during the last century, some species (or subspecies) related to *B. schoetensacki* were erected, including: *B. voigtstedtensis*, *B. s. lagenocornis*, *B. s. schoetensacki* (Flerov, 1979). These taxa, although still recognized by few scholars (e.g., Van der Made et al., 2017), are not often used in modern literature and, sometimes, even considered expressions of secondary sexual characters in the cranium (see Sala, 1986). I tend to agree with the more parsimonious opinion of the latter author in including all the aforementioned taxa within the variability of *B. schoetensacki*. In addition to that, the study performed in this thesis (chapter 5) shows how the postcranial bones of *Bison* constrained between 1.2. and 0.6 Ma fit with the variability expected for a single species. During the last stages of the Galerian, ca. 0.6-0.5 Ma, larger and more derived *Bison* appeared in some areas of Europe, including the gigantic forms from Mosbach (Fig. 12) and Tiraspol (Germany and Ukraine, respectively) (Flerov and David, 1971; Flerov, 1976). Albeit the taxonomy of these precursors of the “prisoid” group is still unsettled (see Sher, 1997 and chapter 5), their arrival is a strong indicator of the first faunal changes of the late Galerian which ultimately led to the Mammoth-*Coelodonta* complex of the late Middle Pleistocene (sensu Kahlke, 1999).

The origins of *B. schoetensacki* are still obscure and seldom faced by modern scholars. Flerov (1979) proposed that this species originated from *B. voigtstedtensis* (= *B. schoetensacki voigtstedtensis*) which, in turn, emerged from the East European species *B. (Eobison) tamanensis* from the Taman Peninsula (easternmost Russia). This last species, however, is poorly characterized due to the scanty remains on which the diagnosis was based. In addition to that, the few fossils attributed to this form present strong resemblances with the most primitive forms of *B. schoetensacki* (Kostopoulos, 2018; chapter 4). In spite of that, the presence of the first *Bison* s.s. at the eastern borders of Europe by the Villafranchian/Epivillafranchian boundary is a probable scenario, also taking into account the dispersal of these forms in Southwestern Europe soon after (chapter 5). McDonald (1981) proposed that *B. schoetensacki* originated in Eurasia from a stock of *B. priscus*. This hypothesis has been already criticized by Sala

(1986) who, rightfully, remarks that the occurrence of *B. schoetensacki* widely precedes that of *B. priscus*. The latter author links the origin of *B. schoetensacki* to the *Eobison* group (including the Pirro Nord and Venta Micena bovids and also *B. tamanensis*, in his views). This idea, partially shared with that of Flerov (1979), seems to be the most plausible, according to the currently available knowledge. The presence of a stout form of *Eobison* from the Mygdonia basin is an indicator that, at the very end of the Villafranchian, bison of Europe started to develop large size and robust built, strongly resembling those of the smallest *B. schoetensacki* from Durfort and Vallparadís Estació (chapter 5, Fig. 12). Although I do not believe in a direct ancestor-descendant relationship between *E. degiulii* and *B. schoetensacki*, I support the hypothesis that the origin of the latter genus is nested within *Eobison*. Again, the most likely centre of origin of *B. schoetensacki* is continental Asia or the Caucasus.

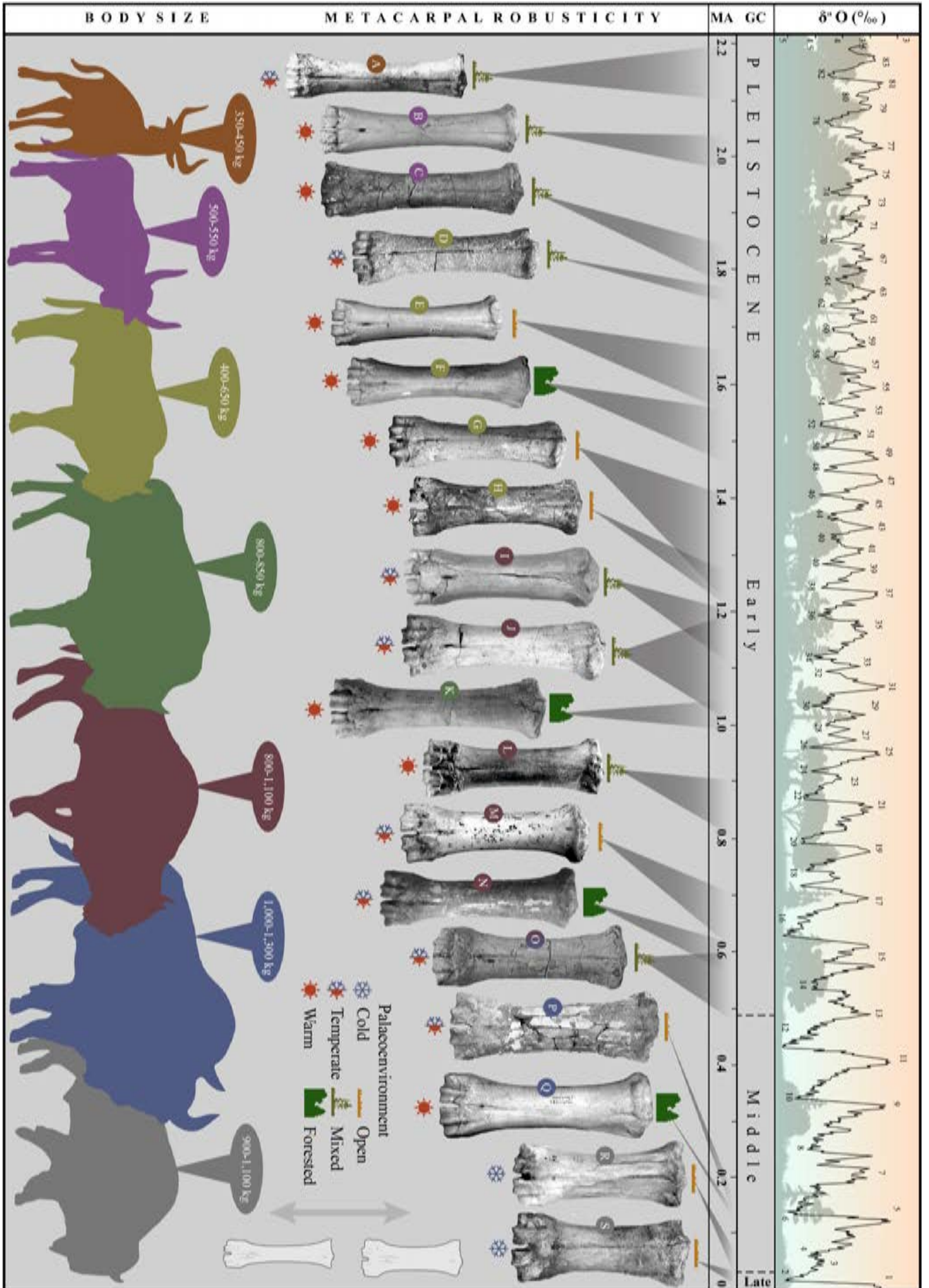
The latter territory is characterized by the presence of an extremely stout form of *Bison* in the site of Akhalkalaki (Georgia), which resembles *B. priscus* of the last Glacial. Nonetheless, the site was dated to the Epivillafranchian at ca. 1.0-0.8 Ma (Tappen et al., 2002), thus almost half a million year before the appearance of *B. priscus*. Indeed, the size and proportions of the Akhalkalaki bovid limbs are not fitting with the variability of any Epivillafranchian bison (see diagrams in Bukhsianidze, 2020: fig. 11). It is possible that in Georgia, a form of *Eobison* which had its ancestor in SE Europe (e.g., Mygdonia basin) survived in the Epivillafranchian, evolving an extremely stout appearance, adapting to the opening of the environments and the harshening of the climate that characterized that interval (see chapter 4). Its relationship with the coeval, slenderer *B. schoetensacki* it is not easily recognizable. Few metacarpals from Vallparadís composite section and Cromer forest-bed, referred to the latter species, are identical to those from Akhalkalaki, complicating furtherly the identification of this very stout form on the one hand, and the definition of the variability of *B. schoetensacki* on the other. All these inferences should be tested in a detailed analysis of the sample from the Georgian locality which, up to date, has never been fully described and does not include any cranial elements (Vekua, 1987). I find the Akhalkalaki bison the most staggering oddity in the evolution of this clade. Its own presence and its similarities with few other specimens from other samples furtherly complicate an already entangled systematic framework.

A crucial point in the evolution of “true” *Bison* is the putative late extinction of *B. schoetensacki*, a view which has persisting in the modern literature even more than the “small *B. schoetensacki*” misconception (see chapters 4 and 5). Guérin and Philippe (1971) report the presence of this species in Siréjol cave (France) at ca. 0.36 ka. The analysis performed in this thesis (chapter 5), however, demonstrates that the postcranial remains of this bovid are more similar to those commonly referred to the steppe wisent *B. priscus*. Brugal (1999) already evidenced the differences between *B. schoetensacki* and the bovid from Siréjol, attributing the latter to *Bison priscus* nov. ssp. Recent molecular

analysis performed on the bison from the cave, showed that it was genetically different from *B. priscus*, being more related with the extant European wisent *B. bonasus* (Palacio et al., 2018). In agreement with the original assignment of the sample to *B. schoetensacki*, the paper by Palacio et al. (2018) suggests that *B. schoetensacki* is the sister taxon of *B. bonasus*. The presence of a second species of *Bison* in the Late Pleistocene, namely CladeX or Bb1 (Soubrier et al., 2016; Grange et al., 2018), morphologically similar to *B. priscus* but genetically distinguishable, is widely demonstrated by several molecular studies (see chapter 1). It is erroneous, however, referring this species to the Epivillafranchian-Galerian *B. schoetensacki* on the basis of old taxonomic attribution (Grange et al., 2018; chapter 5). This incapability of recognizing phenotypical traits useful to distinguish these taxa is an issue which often adds up to misinterpretations of sexual dimorphism. Especially in the past, various authors were wrong in attributing males and females of the same taxon to two different species. A major example is the late Middle Pleistocene site of Chatillon-Saint-Jean in which Mourer-Chauvire (1972) recognizes both *B. schoetensacki* and *B. priscus* instead of males and females of the same species, most likely *B. priscus* (chapter 5). It is however evident that *B. schoetensacki*, during the second half of the Galerian, was already showing prisicoid features as testified by the massive forms of Isernia la Pineta and Mosbach 2 (Sala, 1986). After 0.5 Ma, when the first *B. priscus* entered Europe, the distinction between the two species becomes difficult (chapter 5). The widely demonstrated capability of interbreeding between different species of *Bison* furtherly entangles the situation, leading to not exclude the presence of multiple hybrid populations starting from ca. 0.5 Ma. Although not clear, the extinction of *B. schoetensacki* is almost certainly happened between 0.5 and 0.4 Ma and it is quite unlikely that this species represents the CladeX or *Bison* Bb1 which roamed the Western Palearctic during the Late Pleistocene. This latter species has still to be morphologically defined but a preliminary analysis of the metapodials evidences that these elements could bear some subtle distinguishing features (chapter 5). The study of cranial remains is required in order to clarify this issue.

In chapter 5 I tried to detangle the complex taxonomic definition of *B. schoetensacki* focusing on the diagnostic traits of limb bones. Although I concede that most of the considerations of this chapter are still valid, since its writing -more than two years ago- I have changed my mind on some others. The recent finding of few undescribed remains from the Jaramillo layers (ca. 1.0 Ma) of Vallparadís Estació in the collections of the ICP, gave me a better idea of the actual variability of *Bison* size and slenderness. A horn tip (still without ID number) from EVT12 (MIS31; ca. 1.0 Ma) is one of the few cranial elements (aside from teeth) which were preserved from the Vallparadís composite section. Its enormous size and stout built is well fitting with the variability of the massive *B. schoetensacki* males from Isernia la Pineta. If compared with the female horn-core IPS92970 of the EVT7 layer (ca. 0.86 Ma), which have a more gracile structure, the difference in size and built is quite impressive. Sher (1997: 172) states: “While Freudenberg emphasized

its smaller horns and more slender legs versus *B. priscus*, Schertz believed that Mauer bison (*B. schoetensacki*) was the smallest form among all the fossil *Bison* species. The latter has given rise to a long-living myth that *B. schoetensacki* was not only short-horned, but small-sized in general, which is evidently not true.” and I could not agree more. The misconception that *B. schoetensacki* was a small form is widely disproved by many evidence (e.g., chapter 4 and 5) but still quite common in literature. From the same layer of Vallparadís Estació (EVT12) as the aforementioned horn-core tip, a very large metacarpal (EVT-22688, unpublished) was also collected, comparable in size with those of the gigantic *B. priscus* from Taubach and standing out as one of the largest metacarpals of *B. schoetensacki* ever recorded. The comparison with the other Vallparadís specimens highlights that, at 1.0 Ma, in NE Iberian Peninsula, there were both tall and short forms of *Bison*, one resembling the Mauer type material (large and long) and one more priscoid in its built (similar to the Akhalkalaki form). Although these differences appear to fit with the overall variation of a single species, finding the two opposite morphotypes in the same layers rings some alarm bells. A deeper analysis of variability in extant *Bison* or in well-sampled extinct bison records (i.e., some Late Pleistocene *B. priscus* ones) is required to confirm if this discrepancy is explainable by sexual dimorphism and/or ontogenetic changes or it has some taxonomic meaning. I still believe that the variation due to sexual dimorphism, ontogeny, and ecophenotypic adaptations in *Bison* is often underacknowledged. On the other hand, the presence of a “hidden” species of *Bison* coeval with *B. priscus* and only identifiable on the basis of molecular characters (see above) compels a more cautious approach in grouping different morphotypes in one species. The most interesting fact, however, is that some specimens coming from the older layers of the Vallparadís composite section -CGR2 and EVT10 (ca. 1.2-1.0 Ma)- are perfectly fitting with the variability expressed by the type material of Mauer, confirming that this species was already well distributed in Europe at the beginning of the Epivillafranchian. Therefore, the Vallparadís composite section is added to Le Vallonnet and Untermassfeld as the first localities which register the arrival of large-sized “trues” bison species in Western Palearctic.



Previous page. Fig. 12. Evolutionary trends of metacarpal robusticity in selected *Leptobos* and *Bison* samples from various Western Palearctic localities over the last 2 Ma, correlated with: average body-mass estimated for each studied group, inferred paleoenvironmental condition of each site, paleoclimatological diagram of LR04 Benthic Stack (Lisiecki and Raymo, 2005). A, *Leptobos merlai* from Saint Vallier; B, *Leptobos etruscus* from Fonelas P 1; C, *Leptobos etruscus* from Olivola; D, *Bison (Eobison) georgicus* from Dmanisi; E, *Bison (Eobison) sp.* from Venta Micena; F, *Bison (Eobison) degiulii* from Pietrafitta; G, *Bison (Eobison) degiulii* from Pirro Nord; H, *Bison (Eobison) degiulii* from Mygdonia Basin; I, *Bison (Bison) schoetensacki* from Le Vallonnet; J, *Bison (Bison) schoetensacki* from Vallparadis composite section; K, *Bison (Bison) menneri* from Untermassfeld; M, *Bison (Bison) schoetensacki* from Durfort; M, *Bison (Bison) schoetensacki* from Süssenborn; N, *Bison (Bison) schoetensacki* from Mauer; O, *Bison (Bison) cf. schoetensacki* from Mosbach; P, *Bison (Bison) priscus priscus* from Romain-la-Roche; Q, *Bison (Bison) priscus priscus* from Taubach; R, *Bison (Bison) priscus mediator* from Habarra; S, *Bison (Bison) priscus mediator* from Cava Filo. Data taken from chapter 4.

6.4. Systematics of *Bison menneri*

Bison menneri is the most recently described species of *Bison* from Eurasia. It was first erected by Sher (1997) based on a rich collection of more than 1,000 remains from the Epivillafranchian of Untermassfeld. The systematics of this bovid was reappraised with the description of further material by Bukhsianidze (2020), who referred the species to the subgenus *Poephagus*, that is, the group including the extant yak and its extinct relatives. Although being among the best-known Early Pleistocene bovids from the anatomical point of view, and despite being considered a marker taxon of the Epivillafranchian for long time (e.g., Kahlke et al., 2011; Bellucci et al., 2015; but see the previous section), the systematics of *B. (P.) menneri* needs some clarifications. Before entering the core of the discussion, however, it is worth to mention that the phylogenetic affinity between “true” bison (subgenus *Bison*) and yak (subgenus *Poephagus*) is widely demonstrated (e.g., Li et al., 2007; Zeyland et al., 2012; Soubrier et al., 2016) and that their extant representatives share a large number of synapomorphies (Olsen, 1990), hence it is legit to presume that also the primitive members of these clades might share some similarities. For instance, it is very likely that they might exhibit a marked sexual dimorphism, as in extant forms.

The attribution to *Poephagus* was proposed by Bukhsianidze (2020) on the basis of some characters of the metapodials and the cranium IQW 2003/28 250 (Mei. 27 412) which was left undescribed in the previous work of Sher (1997). According to Bukhsianidze (2020: 1187), this almost complete specimen (paratype of the species) is referable to a male individual due to: “the dorso-ventrally compressed horn-core bases and remarkably vaulted nasals”. However, there are several aspects that challenge this attribution, starting from the two putative male characters. Although less accentuated in females, the dorsoventral compression of the horn-core bases is a typical

feature of all Early-Middle Pleistocene *Bison* species (Sala, 1986; chapter 4). The vaulted nasals might be, according to the same Bukshianidze (2020: 1187), a unique character of this form and not strictly related to sexual dimorphism. It is noteworthy that vaulted nasals (which increase the nasal cavity volume) is also present in Middle-Late Pleistocene forms of *B. priscus* of Siberia (Kahlke, 1999) and observed in many females of *B. bison* (see pictures in Allen, 1876). If these male characters are debatable, on the other hand, the cranium from Untermassfeld shows a remarkable list of characters which are clearly pointing toward an opposite interpretation. All the following female traits are recognized in the specimen IQW 2003/28 250 (Mei. 27 412): overall gracile morphology, elongated rostrum, narrow frontals, small horns emerging posteriorly with no burr at the bases, unobliterated sutures, low degree of pneumatization of the skull roof, unprotruding orbits without thickened edges, reduced posterior tuberosities of the basioccipital (Skinner and Kaisen, 1947; Sala, 1986; chapter 4). On the basis of that, I strongly believe that the paratype of *B. menneri* belongs to a female individual. This attribution becomes pivotal when we deal with the taxonomy of the whole Untermassfeld sample.

Bukshianidze (2020: 1187) summarizes the features shared by *B. menneri* and *Poephagus*, however, the comparison with a larger sample of *Leptobos* and *Bison* (especially in light of sexual dimorphism) evidences that these traits appear quite common within the leptobovine-bisontine groups:

- I. “Elongation of frontals and shortening of parietals”. Elongated frontals are commonly observed in both *Leptobos* and *Eobison* (chapter 4), being one of the diagnostic traits for the latter in distinguishing it from the subgenus *Bison*. This feature is also typical of females of *Bison* s.s. (both extinct and extant) (McDonald, 1981). The analysis of a large *Leptobos* and *Bison* sample in chapter 4 shows that the frontals of *B. menneri* perfectly fit with the variability of *Bison* s.l.
- II. “Position of orbits behind M3”. This character is considered a diagnostic trait of *Poephagus* by Bukshianidze (2020: 1185) and is included in the emended diagnosis of *B. menneri*. Nonetheless in the subadult skull IQW 1993/24 343 (Mei. 23 872), figured by Bukshianidze (2020: fig. 8) and referred to the same species, the anterior margin of the orbit is at the level of M3-M2 contact. Moreover, the cranium NHCK KLT-638 of *B. (E.) cf. degiulii* from the Mygdonia basin (most probably a female) the orbit are behind M3, as in the paratype of *B. menneri*.
- III. “Caudal insertion of horn-cores, backward direction of horn-cores and their downward bending in the beginning”. These traits are quite common in female individuals of *Bison* s.l. (see pictures in Skinner and Kaisen, 1947). Most of the *Eobison* crania studied in chapter 4 are characterized by various degrees of the aforementioned traits.

- IV. “Thin and arched nuchal crests”. This character that defines the shape of the occipital squama is quite variable in *Bison* s.l. (chapter 4). However, the Untermassfeld squama is perfectly fitting within the variability of both *Poephagus* and *Bison*.
- V. “Low degree and even pneumatization of the braincase roof”. The low pneumatization of the braincase is a typical feature of *Eobison* and is present also in females of *Bison* s.s. (Sala, 1986; McDonald, 1981). McDonald (1981) suggests that short-horned bison species have a higher degree of cranial roof vaulting (given by a strong, uneven pneumatization of the frontals), in order to better cope with the head-butting. Head-butting is an activity performed exclusively by males; thus, the females of these species show flattened and less pneumatized frontals (McDonald, 1981).
- VI. “Long and wide nasals”. All species of *Bison* s.l. are characterized by wide and long nasals which reach the level of the anterior margin of the orbit or slightly behind (Sala, 1986; chapter 4).

It is therefore evident that most, if not all, the characters which allow us to refer *B. menneri* to *Poephagus* are equally valid for the attribution of the German sample to *Bison* s.l., as originally suggested by Sher (1997). To these, the shape of the lacrimal bone and the nasal process of the premaxilla are added, as they both are *Bison*-like (Bukshianidze, 2020). Among the characters pairing *B. menneri* with *Bison* s.l. and passed unnoticed by Bukshianidze (2020) there are: the torsion of the horns in *Poephagus* which is strongly heteronymous, whereas in many *Bison* species as in the *B. menneri* paratype is less accentuated; the presence of a “folded” maxillary segment dividing the premaxilla from the nasal (sensu Olsen, 1990), which is autapomorphic in *Poephagus* and seems to be not present in IQW 2003/28 250 (Mei. 27 412).

In addition to that, Bukshianidze (2020: 1187) recognizes in *B. menneri* a series of putative pedomorphic characters, including: “upward rising and backward directed horn-core pedicles, caudo-laterally directed short and gracile horn cores, unobliterated sutures, hiatus between nasal, frontal and lacrimal, more open angle between basisphenoid and praesphenoid”. The last character, however, is shared with bison and not with yak and most of the other traits are, as aforementioned, well documented in the females of derivate *Bison* or in primitive species of the same clade. According to the author, the presence of these neotenic features in *Poephagus* from Untermassfeld suggests that the most primitive forms of yak were characterized by pedomorphism as it has been hypothesized for bison (Flerov, 1979; Sala, 1986). Therefore, Bukshianidze (2020) justifies the presence of *Bison*-like and non-*Poephagus*-like traits in the Untermassfeld cranium as pedomorphic and overlooks those characters which actually indicate a possible attribution to a female individual of bison. I fully agree with the aforementioned authors stating that females of *Bison*, *Poephagus*, and *Leptobos* feature neotenic traits, however this should not be used as a taxonomic

lock pick in a circular argument. Among the pedomorphies displayed by IQW 2003/28 250 (Mei. 27 412) the hiatus between nasal, frontal, and lacrimal is surely the most intriguing. This feature seems to represent the ethmoidal fenestra which is a diagnostic trait of *Leptobos* and not present in *Bison* neither in *Poephagus* (Masini, 1989; Duvernois, 1990; chapter 4). Therefore, it might be an ancestral trait (possible neoteny) retained by the Untermassfeld cranium, furtherly confirming its attribution to a female. The presence of other four partial crania of juvenile individuals in Untermassfeld furtherly complicates the debate. Bukshianidze (2020) suggests that the subadult specimens IQW 1980/17 380 (Mei. 16 902) and IQW 2003/27 716 (Mei. 27 221) belong to another species of bovine due to the reduced horn pedicle and large size (horns and frontals) in the former and the anterior margin of the orbits at the level of M2 in the latter. However, as noticed above, the anteriorly shifted orbit is present in another skull referred to *B. menneri* by the author and the size of horns, pedicles, and frontals could be related to ontogeny and sexual dimorphism, contra Bukshianidze (2020).

Bukshianidze (2020) affirms that the morphology of *B. menneri* metapodials, especially in the distal end, is one of the traits that enforce its attribution to *Poephagus*. The author rightfully states that the Untermassfeld metapodials are similar to those of both *Poephagus* and *Bison* and different from those of *Bos*. It is indeed true that the distal ends of metapodials of yak and bison (including their relative *Leptobos*) show an analogous morphology. Therefore, although it is correct to exclude the attribution to *Bos* due to the well-distinguishable metapodial distal ends (see Sala, 1986; Sher, 1997; chapter 5), it is biased to affirm that the morphology of metapodials contributes to refer the Untermassfeld sample to *Poephagus* instead of *Bison*. On the other hand, the proportions of these bones are quite useful in distinguishing yak and bison due to the extremely stouter built of the former. The structure of *Poephagus* metapodials evolved to sustain the animal in a dry rocky environment such as the Himalayan mountains, where the wild yak can be found today (Olsen, 1990; Vasiliev, 2021). For this reason, their built is exceptionally robust, even more than that of Late Pleistocene steppe bison (see chapter 5). On the contrary, the bovid from Untermassfeld is characterized by much slenderer limbs featuring the longest metapodials among all bovines, both extant and extinct (see Maniakas and Kostopoulos, 2018 and chapters 4, 5). Although it is clear that the habitats of *B. menneri* and the extant yak is a strong driving factor for the evolution of their metapodial structure (see chapters 4 and 5), the similarity between them, claimed by Bukshianidze (2020), is quite debatable and, in my opinion, not sufficient in lumping *B. menneri* in *Poephagus*. The presence in Untermassfeld of an isolated metacarpal with a more robust built fitting with the variability of *B. schoetensacki* (see chapter 5) challenges the presence of a single large bovid species in the site. In spite of that, this specimen could represent an abnormally stout individual of *B. menneri* recorded in the extremely abundant bison sample unearthed from this locality.

Finally, both the chronological and geographical ranges of *Poephagus* is another argument against the inclusion of *B. menneri* within this clade. The records of fossil yak from Eurasia are extremely rare and all limited to the latest stages of the Pleistocene and the Holocene of Asia (i.e., China, eastern Russia, Pakistan) (Olsen, 1990; Kahlke, 1999; Bukshianidze, 2020; Vasiliev, 2021 and references therein). The attribution to *Poephagus* would make *B. menneri* the oldest and most western yak recorded up to date. This interpretation thus would suggest that yak evolved first in Central Europe, then reached Asia during the Middle-Late Pleistocene; alternatively, it might have originated in Asia during the Early Pleistocene and then dispersed in Europe before the Jaramillo subchron. These two hypotheses, however, should contemplate the existence of primitive forms of yak in the western part of Asia or eastern Europe in the timespan comprised between the Early and Late Pleistocene. At the current state of the art, there is no other remains of *Poephagus* outside western Asia apart from the Untermassfeld ones. In addition to that, the strongly contrasting molecular studies does not allow to set a precise date for the divergence of yak from bison which oscillates between 2.1 and 0.3 Ma (Li et al. 2006; Zeyland et al. 2012; Massilani et al., 2013; Bai, 2015 among others). According to our present knowledge, the most parsimonious interpretation is that *Poephagus* is an eastern Asian taxon with a relatively recent history, which, starting from the Holocene, saw a progressive shrinking of its distribution and ended relegated into the Himalayan region. All the fossil record, with the exception of *B. menneri*, suggests that this genus never reached the Western Palearctic.

These multiple lines of evidence advocate another accommodation for the Untermassfeld bovid, in one of the groups belonging to the leptobovine-bisontine lineages. The primitive traits shown by the cranium and metapodials of this slender form indicate a relationship with the less derived species of *Bison*, grouped in the subgenus *Eobison* (chapter 4). If it is true that the large size of this animal is an oddity for this early *Bison* (Sher, 1997), it is equally evident that *B. menneri* and *Eobison* spp. share a considerable series of synapomorphies (e.g., slender limbs, small horns, narrow skull). On the other hand, some of these traits might be purely linked to the female sex of the most complete cranium from Untermassfeld, hence potentially misleading the attribution. It is indeed possible that, due to the suggested paedomorphic (= primitive) traits shown by the female specimen IQW 2003/28 250 (Mei. 27 412), the characters allyng this species with the more derived *Bison* s.s. could remain unknown. At the state of the art, the lack of other adult skulls of *B. menneri* prevents the evaluation of the sexual dimorphism in this taxon, which however, is expected to be similar to that observed in its relatives. Although, this issue does not allow to properly assign *B. menneri* to neither the two subgenera of *Bison* recognized in this work, I tend to agree with the original vision of Sher (1997) who considered the Untermassfeld bovid as part of the “true” *Bison* group.





Chapter 7.

7. Conclusions

This thesis aimed to reconstruct the taxonomy, paleobiology, distribution, and chronological ranges of *Bison* and *Sus* species in Western Palearctic during the latest stages of the Early Pleistocene (Fig. 13). These two iconic genera include some of the most successful large mammals in the last 2.0 Ma, able to colonize most of Eurasia and North America, and still persisting in many modern faunal assemblages. Due to their almost constant presence and abundance in the fossil record of Europe, their value as biochronological tools is undisputed. Their debated systematics and evolutionary history have been at the centre of many studies for more than one century and, still nowadays, there is poor consensus among scholars. The new paleontological and molecular findings and the reappraisal of old collections carried out in the last decades ignited the controversies and discussions about *Sus* and *Bison* and their role in the paleontological studies of European Quaternary.

The EMPT, started between 1.4 and 1.2 Ma, is a crucial period for the history of the biosphere. The Northern Hemisphere, and in particular Europe, were affected by a major climatic shift which led to stronger glacial-interglacial pulses and overall drier and cooler conditions. This change had strong repercussions on European environments which were characterized by a general shrinking of the forested habitats and the widespread diffusion of open landscapes (Fig. 1). The mammal communities of the latest Early Pleistocene were, therefore, subject to a strong pressure derived by the onset of these new conditions. As the Villafranchian large mammals of Europe started to disappear, new groups, originated in the eastern territories of Eurasia, found the suitable conditions for their dispersal toward the west, rapidly becoming part of the faunal assemblages (Fig. 3). By the beginning of the Middle Pleistocene (ca. 0.8 Ma), these new elements had almost completely replaced their Villafranchian counterparts and the Galerian biochron settled. This period of transition, roughly constrained between 1.2 and 0.8 Ma, in which both old taxa and newcomers coexisted, has been named Epivillafranchian (Fig. 13).

In this framework, the three main chapters of this thesis were developed with the final aim of understanding the pathway taken by two of the most important biochronological markers of this period, namely *Sus* and *Bison*. Here a resume of the three chapters included in this thesis and their results, is provided:

- (I) Chapters 3 and S1 focused on the reappraisal of *Sus* record of Europe. The rich suid collection from the Vallparadís composite section (Spain) accounted as case study. Our analysis showed that, contrarily to what was believed by most of the scholars until now, the European dispersal of *S. scrofa* did not occur before the onset of the Middle Pleistocene. The Vallparadís sample, as well as all other Epivillafranchian European records, are confidently referred to the well-known species *S. strozzi*. This species is thus added

to the list of those taxa which survived the first stages of EMPT, thus characterizing the transitional faunas of the Epivillafranchian (Fig. 13). On the other hand, the arrival of *S. scrofa* and the extinction of the verrucosic group in Europe could be considered one of the most important bioevents at the beginning of the Galerian. The so-called ‘suid gap’ -i.e., the strong demographic contraction of suids of Europe at the end of the Villafranchian- is here somewhat confirmed. The almost total absence of suid remains from the major fossiliferous localities dated between ca. 1.8 and 1.2 Ma is a strong indicator of their scarcity also from the paleocommunities of Western Palearctic during the last phases of the Villafranchian. Scanty, and sometimes dubious, remains from peripheral or isolated areas of Europe testify the persistence of these ungulates in the continent despite the major collapse of their populations (Fig. 10).

- (II) Chapter 4 focused on the reappraisal of *Eobison* record of Europe. The rich bovid collection from Pietrafitta (Italy) accounted as case study. Our work evidenced that this sample previously attributed to *Leptobos*, actually belongs to an early member of *Bison* s.l. These late Villafranchian forms are commonly grouped in the subgenus *Eobison*, characterized by primitive cranial features and slenderer body structures compared with their larger successor (*Bison* s.s.). The analysis of the Pietrafitta bovid, here attributed to *B. (E.) degiulii*, compelled the revision of the confused hypodigm of the subgenus, which revealed to be affected by an overabundance of species. At least three species of *Eobison*, namely *B.(E.) palaeosinensis*, *B. (E.) georgicus*, *B. (E.) degiulii*, were considered valid. The study of the cranial and postcranial skeleton of the available *Eobison* record from Eurasia evidenced a series of evolutionary trends within the *Leptobos-Bison* group. In particular, the limb proportions and body size followed a clear trend toward an increased stoutness and gigantism in both lineages. The robustness of metapodials is here positively related with the presence of open habitats (Fig. 12).
- (III) Chapter 5 focused on the reappraisal of *B. schoetensacki* record of Europe. The rich bovid collection from the Vallparadís composite section (Spain) accounted as case study. Our study remarked that the first *Bison* s.s. dispersed in Europe already at the beginning of the Epivillafranchian. By 1.2-1.1 Ma, large and derived forms, referrable to the species *B. (B.) schoetensacki*, replaced *Eobison* and populated Mediterranean Europe, whereas the extremely tall and slender *B. (B.) menneri* colonized Central-North Europe. Therefore, the dispersal of *Bison* s.s. in Western Palearctic is an important bioevent which marks the beginning of the Epivillafranchian (Fig. 13). These newcomers flourished later, with the onset of the Galerian (ca. 0.8 Ma), colonizing all the European continent. Our analyses of metapodials suggest the presence of various ecomorphotypes of *Bison*, most probably belonging to one taxon, namely *B.*

schoetensacki (Fig. 12). During the Epivillafranchian and Galerian, this species adapted to the everchanging environments given by the rather unstable climatic conditions of this biochron, developing a relatively wide range of body sizes and proportions.

This thesis attempted to improve the present knowledge about the suids and bovids of Europe during the last phases of the Early Pleistocene, and their coping with the major climatic changes that affected the continent between 1.4 and 0.4 Ma. These results are, however, only the start of the works that should be done on the extremely complex and entangled evolutionary history of these groups. As mentioned in the previous chapter, since the first studies performed for this thesis, several new discoveries came to my knowledge, broadening the spectrum of possibilities toward new problems and, hopefully, new solutions. For this reason, I consider this thesis, and the works included within, only the ‘tip of the iceberg’ of a larger project, aimed to reconstruct the environments and faunal assemblages which succeeded during the EMPT. The reappraisal of long-forgotten historical collections and the finding of new localities joined with the inclusion of other groups of large mammals and the use of powerful molecular techniques are the tools required in the next future, in order to shed new light on the major faunal turnovers over the Quaternary.

Next page. Fig. 13. Approximated occurrences of the most important large mammal taxa in Europe during the latest stages of Early Pleistocene, correlated with geochronology, LR04 Benthic Stack (Lisiecki and Raymo, 2005) and the Land Mammal Ages scheme discussed in this work. White stars indicate that the taxon is a Villafranchian species persisting during the Epivillafranchian; black stars indicate that the taxon is a Galerian precursor in the Epivillafranchian.

Chapter 8.



8. References

- Abbazzi, L., 2004. Remarks on the validity of the generic name *Praemegaceros* Portis 1920, and an overview on *Praemegaceros* species in Italy. *Rendiconti Lincei*. 15(2): 115–132.
- Abbazzi, L. and Azzaroli, A., 1995. Occurrence of palmated *Cervus elaphus* from Italian Late Pleistocene localities. *Rendiconti Lincei*. 6(3): 189–206.
- Abbazzi, L., Benvenuti, M., Rook, L. and Masini, F., 1995. Biochronology of the Mugello intermontane basin (northern Apennines, Italy). *Il Quaternario*, 8(1): 5–10.
- Adams, N.F., Candy, I. and Schreve, D.C., 2022. An Early Pleistocene hippopotamus from Westbury Cave, Somerset, England: support for a previously unrecognized temperate interval in the British Quaternary record. *Journal of Quaternary Science*, 37(1): 28–41.
- Agustí, J., Arbiol, S. and Martín Suárez, E., 1987. Roedores y lagomorfos (Mammalia) del Pleistoceno inferior de Venta Micena (depresión de Guadix Baza, Granada). *Paleontologia i Evolució, Memòria Especial* 1: 95-107.
- Agustí, J., Cabrera, L., Garcés, M., Krijgsman, W., Oms, O., Parés, JM. 2001. A calibrated mammal scale for the Neogene of Western Europe. State of the art. *Earth-Science Reviews*, 52: 247–260.
- Akhtar, M., 1992. Taxonomy and Distribution of the Siwalik Bovids. PhD dissertation, University of the Punjab, Lahore, Pakistan: 372 p.
- Ambrosetti, P., Azzaroli, A., Bonadonna, F.P., Follieri, M., 1972. A scheme of Pleistocene chronology for the Tyrrhenian side of Central Italy. *Bollettino della Società Geologica Italiana*, 91: 169–184.
- Antón, M., 2013. Sabertooth. Indiana University Press, Bloomington: 245 p.
- Ao, H., Rohling, E.J., Stringer, C., Roberts, A.P., Dekkers, M.J., Dupont-Nivet, G., Yu, J., Liu, Q., Zhang, P., Liu, Z. and Ma, X., 2020. Two-stage mid-Brunhes climate transition and mid-Pleistocene human diversification. *Earth-Science Reviews*, 210: 103354.
- Argant, J. and Bonifay, M.F., 2011. Les coprolithes de hyène (*Pachycrocuta brevirostris*) de la couche 2 du site villafranchien de Ceyssegues (Lavoûte-sur-Loire, Haute-Loire, France): analyse pollinique et indications paléoenvironnementales. *Quaternaire - Revue de l'Association française pour l'étude du Quaternaire*, 22(1): 3–11.
- Arribas A., Garrido, G., 2008. Un nuevo jabalí del género *Potamochoerus* (Suidae, Artiodactyla, Mammalia) en el Plioceno superior terminal euroasiático (Fonelas P-1, Cuenca de Guadix, Granada). In: A. Arribas (Ed.), *Vertebrados del Plioceno*

superior terminal en el suroeste de Europa: Fonelas P-1 y el Proyecto Fonelas. Cuadernos del Museo Geominero, n° 10. Instituto Geológico y Minero de España, Madrid: 337–364.

Arzarello, M., Marcolini, F., Pavia, G., Pavia, M., Petronio, C., Petrucci, M., Rook, L. and Sardella, R., 2007. Evidence of earliest human occurrence in Europe: the site of Pirro Nord (Southern Italy). *Naturwissenschaften*, 94(2): 107–112.

Asperen van, E.N. and Kahlke, R.D., 2015. Dietary variation and overlap in Central and Northwest European *Stephanorhinus kirchbergensis* and *S. hemitoechus* (Rhinocerotidae, Mammalia) influenced by habitat diversity: “You’ll have to take pot luck!” (proverb). *Quaternary Science Reviews*, 107: 47–61.

Azzaroli, A., 1954. Revisione della fauna dei terreni fluvio-lacustri del Valdarno Superiore, V. Filogenesi e biologia di *Sus strozzii* e di *Sus minor* *Palaeontographia Italica*, 48: 41–76.

Azzaroli, A., 1977. The villafranchian stage in Italy and the Plio–Pleistocene boundary. *Giornale di Geologia*, 41: 61–79.

Azzaroli, A., 1983. Quaternary mammals and the end-villafranchian dispersal event— a turning point in the history of Eurasia. *Palaeogeography, Palaeoclimatology, Palaeoecology*, 44: 117–139.

Azzaroli, A., 1992. The cervid genus *Pseudodama* ng in the Villafranchian of Tuscany. *Palaeontographia Italica*, 79: 1–41.

Azzaroli, A., and Mazza, P., 1993. Large early Pleistocene deer from Pietrafitta lignite mine, Central Italy. *Palaeontographia Italica*, 80: 1–24.

Azzaroli, A., De Giuli, C., Ficarelli, G., Torre, D., 1988. Late Pliocene to early mid- Pleistocene mammals in Eurasia: faunal succession and dispersal events. *Palaeogeography, Palaeoclimatology, Palaeoecology*, 66: 77–100.

Bai, J.L., 2015. Phylotaxonomic position of Tianzhu white yak (*Poephagus grunniens*) based on nucleotide sequences of multiple subunits of cytochrome c oxidase. *Journal of Applied Animal Research*, 43(4): 431–438.

Barnosky, A.D., Koch, P.L., Feranec, R.S., Wing, S.L. and Shabel, A.B., 2004. Assessing the causes of late Pleistocene extinctions on the continents. *Science*, 306(5693): 70–75.

Barrios-Garcia, M.N. and Ballari, S.A., 2012. Impact of wild boar (*Sus scrofa*) in its introduced and native range: a review. *Biological Invasions*, 14(11): 2283–2300.

Barth, A.M., Clark, P.U., Bill, N.S., He, F. and Pisias, N.G., 2018. Climate proxies of sea-surface temperature, carbon isotopes, and dust flux for the last 800kyr and the Mid-Brunhes Transition, PANGAEA. Supplement to: Barth et al. (2018): Climate evolution across the Mid-Brunhes Transition. *Climate of the Past*, 14(12): 2071-2087.

- Bartoli, G., Sarnthein, M., Weinelt, M., Erlenkeuser, H., Garbe-Schönberg, D. and Lea, D.W., 2005. Final closure of Panama and the onset of northern hemisphere glaciation. *Earth and Planetary Science Letters*, 237(1-2): 33–44.
- Bartoli, G., Hönisch, B. and Zeebe, R.E., 2011. Atmospheric CO₂ decline during the Pliocene intensification of Northern Hemisphere glaciations. *Paleoceanography*, 26(4): 4213.
- Bartolini-Lucenti, S., Madurell-Malapeira, J., Martínez-Navarro, B., Cirilli, O., Pandolfi, L., Rook, L., Bushkianidze, M. and Lordkipanidze, D., 2022. A comparative study of the Early Pleistocene carnivore guild from Dmanisi (Georgia). *Journal of Human Evolution*, 162: 103108.
- Bellucci, L., Sardella, R. and Rook, L., 2015. Large mammal biochronology framework in Europe at Jaramillo: the Epivillafranchian as a formal biochron. *Quaternary International*, 389: 84–89.
- Berdondini, E., 1992. Suids of the early Villafranchian of Villafranca d’Asti and China. *Rendiconti Lincei*, 3(2): 109–124.
- Berger, W.H. and Jansen, E., 1994. Mid-Pleistocene climate shift-the Nansen connection. *Washington DC American Geophysical Union Geophysical Monograph Series*, 85: 295–311.
- Berggren, W.A. and Van Couvering, J.A., 2011. The late Neogene: biostratigraphy, geochronology, and paleoclimatology of the last 15 million years in marine and continental sequences. *Palaeogeography, Palaeoclimatology, Palaeoecology*, 16: 1–216.
- Bertini, A., 2010. Pliocene to Pleistocene palynoflora and vegetation in Italy: state of the art. *Quaternary International*, 225(1): 5–24.
- Bibi, F., 2007. Origin, paleoecology, and paleobiogeography of early Bovini. *Palaeogeography, Palaeoclimatology, Palaeoecology*, 248(1-2): 60–72.
- Bibi, F., 2009. *Evolution, systematics, and paleoecology of Bovinae (Mammalia: Artiodactyla) from the Late Miocene to the recent*. PhD dissertation, Yale University, New Haven: 469 p.
- Bibi, F., 2013. A multi-calibrated mitochondrial phylogeny of extant Bovidae (Artiodactyla, Ruminantia) and the importance of the fossil record to systematics. *BMC evolutionary biology*, 13(1): 1–15.
- Bibi, F., Bukhsianidze, M., Gentry, A.W., Geraads, D., Kostopoulos, D.S. and Vrba E.S., 2009. The fossil record and evolution of Bovidae: state of the field. *Palaeontologia Electronica*, 12(3): 1–11.
- Bon, M., Piccoli, G., Sala, B., 1992. La fauna pleistocenica della Breccia di Slivia (Carso Triestino) nella collezione del Museo Civico di Storia Naturale di Trieste. *Atti del Museo Civico di Storia Naturale di Trieste*, 44: 33–51.

- Bona, F. and Sala, B., 2016. Villafranchian-Galerian mammal faunas transition in South-western Europe. The case of the late early Pleistocene mammal fauna of the Frantoio locality, Arda River (Castell'Arquato, Piacenza, northern Italy). *Geobios*, 49(5): 329–347.
- Bourdier, F., 1958. *Le bassin du Rhône au Quaternaire, géologie et préhistoire*. PhD dissertation, Faculté des Sciences de l'Université de Paris : 364 p.
- Bourdier, F., 1961. Le Bassin du Rhone au Quaternaire. In: *Géologie et Préhistoire*, Tome 1. CNRS, Paris
- Bout, P., 1960. *Le Villafranchien du Velay et du bassin hydrographique moyen et supérieur de l'Allier*. Imprimerie Jeanne d'Arc, Le Puy-en-Velay: 344 p.
- Breda, M., 2008. Palaeoecology and palaeoethology of the Plio-Pleistocene genus cervalces (Cervidae, Mammalia) in Eurasia. *Journal of Vertebrate Paleontology*, 28(3): 886–899.
- Breda, M. and Marchetti, M., 2005. Systematical and biochronological review of Plio-Pleistocene Alceini (Cervidae; Mammalia) from Eurasia. *Quaternary Science Reviews*, 24(5-6): 775–805.
- Breda, M. and Lister, A.M., 2013. *Dama roberti*, a new species of deer from the early Middle Pleistocene of Europe, and the origins of modern fallow deer. *Quaternary Science Reviews*, 69: 155–167.
- Breda, M., Collinge, S.E., Parfitt, S.A. and Lister, A.M., 2010. Metric analysis of ungulate mammals in the early Middle Pleistocene of Britain, in relation to taxonomy and biostratigraphy: I: Rhinocerotidae and Bovidae. *Quaternary International*, 228(1-2): 136–156.
- Breda, M., Peretto, C. and Thun Hohenstein, U., 2015. The deer from the early Middle Pleistocene site of Isernia la Pineta (Molise, Italy): revised identifications and new remains from the last 15 years of excavation. *Geological Journal*, 50(3): 290–305.
- Breda, M., Kahlke, R.D. and Lister, A.M., 2020. New results on cervids from the Early Pleistocene site of Untermassfeld. In: Kahlke R.D. (Ed.), *The Pleistocene of Untermassfeld near Meiningen (Thüringen, Germany)*, 4. Römisch-Germanisches Zentralmuseum, Mainz: 1197–1249.
- Brugal, J.-P., 1995. Le bison (Bovidae, Artiodactyla) du Pléistocène moyen ancien de Durfort (gard, France). *Bulletin du Museum national d'Histoire naturelle*, 16C: 349–381.
- Brugal, J.P., 1999. Etude des populations de grands Bovidés européens: intérêt pour la connaissance des comportements humains au Paléolithique. In: Brugal, J.P., David, F., Enloe, J.G., Jaubert, J. (Eds.), *Le Bison: gibier et moyen desubsistance des hommes du Paléolithique aux Paléoindiens des Grandes Plaines*, Ed. APDCA, Antibes: 85–104.

Brugal, J.P., Argant, A., Boudadi-Maligne, M., Crégut-Bonnoure, E., Croitor, R., Fernandez, P., Fourvel, J.B., Fosse, P., Guadelli, J.L., Labe, B. and Magniez, P., 2020. Pleistocene herbivores and carnivores from France: An updated overview of the literature, sites and taxonomy. *Annales de Paléontologie*, 106 (2), 102384.

Bukhsianidze, M., 2005. *The fossil Bovidae of Dmanisi*. PhD dissertation, Università degli Studi di Ferrara: 192 p.

Bukhsianidze, M., 2020. New Results on Bovids from the Early Pleistocene site of Untermassfeld. In: Kahlke R.D. (Ed.), *The Pleistocene of Untermassfeld near Meiningen (Thüringen, Germany)*, 4. Römisch-Germanisches Zentralmuseum, Mainz: 1169–1195.

Burchak-Abramovich, N.I., Gadzhiev, D.V., and Vekua, A.K. 1980. Concerning ancestral form of bisons from the Akchagyl of South Caucasus Soobšeniâ Akademii Nauk Gruzinskoj SSR 97 (2): 485–488.

Caloi, L. and Palombo, M.R., 1996. Latest Early Pleistocene mammal faunas of Italy, biochronological problems. *II Quaternario* 8: 391–402.

Candy, I. and McClymont, E.L., 2013. Interglacial intensity in the North Atlantic over the last 800 000 years: investigating the complexity of the mid-Brunhes Event. *Journal of Quaternary Science*, 28(4): 343–348.

Candy, I., Schreve, D.C., Sherriff, J. and Tye, G.J., 2014. Marine Isotope Stage 11: Palaeoclimates, palaeoenvironments and its role as an analogue for the current interglacial. *Earth-Science Reviews*, 128: 18–51.

Capraro, L., Asioli, A., Backman, J., Bertoldi, R., Channell, J.E.T., Massari, F. and Rio, D., 2005. Climatic patterns revealed by pollen and oxygen isotope records across the Matuyama-Brunhes Boundary in the central Mediterranean (southern Italy). *Geological Society, London, Special Publications*, 247(1): 159–182.

Chalk, T.B., Hain, M.P., Foster, G.L., Rohling, E.J., Sexton, P.F., Badger, M.P., Cherry, S.G., Hasenfratz, A.P., Haug, G.H., Jaccard, S.L. and Martínez-García, A., 2017. Causes of ice age intensification across the Mid-Pleistocene Transition. *Proceedings of the National Academy of Sciences*, 114 (50): 13114–13119.

Cherin, M., Bizzarri, R., Buratti, N., Caponi, T., Grossi, F., Kotsakis, T., Pandolfi, L., Pazzaglia, F. and Barchi, M.R., 2012. Multidisciplinary study of a new Quaternary mammal-bearing site from Ellera di Corciano (central Umbria, Italy): preliminary data. *Rendiconti Online della Società Geologica Italiana*, 21: 1075–1077.

Cherin, M., Iurino, D.A., Sardella, R. and Rook, L., 2014. *Acinonyx pardinensis* (Carnivora, Felidae) from the Early Pleistocene of Pantalla (Italy): predatory behavior and ecological role of the giant Plio–Pleistocene cheetah. *Quaternary Science Reviews*, 87: 82–97.

Cherin, M., Sorbelli, L., Crotti, M., Iurino, D.A., Sardella, R. and Souron, A., 2018. New material of *Sus strozzi* (Suidae, Mammalia) from the Early Pleistocene of Italy and a phylogenetic analysis of suines. *Quaternary Science Reviews*, 194: 94–115.

- Cherin, M., Azzarà, B., Breda, M., Brobia Ansoleaga, A., Buzi, C., Pandolfi L. and Pazzaglia, F., 2019a. Large mammal remains from the Early Pleistocene site of Podere San Lorenzo (Perugia, central Italy). *Rivista Italiana di Paleontologia e Stratigrafia*, 125: 489–515.
- Cherin, M., D'Allestro, V. and Masini, F., 2019b. New bovid remains from the Early Pleistocene of Umbria (Italy) and a reappraisal of *Leptobos merlai*. *Journal of Mammalian Evolution*, 26(2): 201–224.
- Cherin, M., Breda, M., Esattore, B., Hart, V., Turek, J., Porciello, F., Angeli, G., Holpin, S. and Iurino, D.A., 2022. A Pleistocene Fight Club revealed by the palaeobiological study of the *Dama*-like deer record from Pantalla (Italy). *Scientific reports*, 12(1): 1–12.
- Cignoni, P., Callieri, M., Corsini, M., Dellepiane, M., Ganovelli, F., Ranzuglia, G., 2008. Meshlab: an open-source mesh processing tool. In: *Eurographics Italian Chapter Conference*: 129–136.
- Cirilli, O., Saarinen, J., Pandolfi, L., Rook, L. and Bernor, R.L., 2021. An updated review on *Equus stenonis* (Mammalia, Perissodactyla): New implications for the European early Pleistocene *Equus* taxonomy and paleoecology, and remarks on the Old World *Equus* evolution. *Quaternary Science Reviews*, 269: 107155.
- Cirilli, O., Machado, H., Arroyo-Cabrales, J., Barrón-Ortiz, C.I., Davis, E., Jass, C.N., Jukar, A.M., Landry, Z., Marín-Leyva, A.H., Pandolfi, L. and Pushkina, D., 2022. Evolution of the Family Equidae, Subfamily Equinae, in North, Central and South America, Eurasia and Africa during the Plio-Pleistocene. *Biology*, 11(9): 1258.
- Clark, P.U., Archer, D., Pollard, D., Blum, J.D., Rial, J.A., Brovkin, V., Mix, A.C., Pisias, N.G. and Roy, M., 2006. The middle Pleistocene transition: characteristics, mechanisms, and implications for long-term changes in atmospheric pCO₂. *Quaternary Science Reviews*, 25(23–24): 3150–3184.
- Cooke, H.B.S., 1978. Suid evolution and correlation of African hominid localities: an alternative taxonomy. *Science*, 201(4354): 460–463.
- Croitor, R. and Bonifay, M.F., 2001. Étude préliminaire des cerfs du gisement Pléistocène inférieur de Ceysaguet (Haute-Loire). *PALEO Revue d'archéologie préhistorique*, 13: 129–144.
- Croitor, R., 2006a. Early Pleistocene small-sized deer of Europe. *Hellenic Journal of Geosciences*, 41(1): 89–117.
- Croitor, R., 2006b. Taxonomy and systematics of large-sized deer of the genus *Praemegaceros* Portis, 1920 (Cervidae, Mammalia). *Courier-Forschungsinstitut Senckenberg*, 256: 91–116.
- Croitor, R., 2010. Critical remarks on genus *Bison* (Bovidae, Mammalia) from Pleistocene of moldova. *Revista Archeologica*, 5: 172–188.

- Cronin, T.M., Dwyer, G.S., Caverly, E.K., Farmer, J., DeNinno, L.H., Rodriguez-Lazaro, J. and Gemery, L., 2017. Enhanced Arctic amplification began at the Mid-Brunhes Event~ 400,000 years ago. *Scientific Reports*, 7(1): 1–7.
- Crucifix, M., 2012. Oscillators and relaxation phenomena in Pleistocene climate theory. *Philosophical Transactions of the Royal Society A: Mathematical, Physical and Engineering Sciences*, 370 (1962): 1140–1165.
- Crucifix, M., 2013. Why could ice ages be unpredictable?. *Climate of the Past*, 9(5), 2253–2267.
- De Giuli, C., 1986. Late Villafranchian faunas of Italy: the Selvella local fauna in the southern Chiana Valley-Umbria. *Palaeontographia Italica*, 74: 11–50.
- De Giuli, C., Masini, F. and Torre, D., 1986. The latest villafranchian faunas in Italy: the Pirro Nord fauna (Apricena, Gargano). *Palaeontographia Italica*, 74: 51–62.
- De La Vega, E., Chalk, T.B., Wilson, P.A., Bysani, R.P. and Foster, G.L., 2020. Atmospheric CO₂ during the Mid-Piacenzian Warm Period and the M2 glaciation. *Scientific Reports*, 10(1): 1–8.
- De Lumley, H.D., Kahlke, H.D., Moigne, A.M. and Moulle, P.E., 1988. Les faunes de grands mammifères de la grotte du Vallonnet, Roquebrune-Cap-Martin, Alpes-Maritimes. *L'Anthropologie*, 92(2): 465–496.
- De Soler, B.G., Vall-Llosera, G.C., van der Made, J., Oms, O., Agustí, J., Sala, R., Blain, H.A., Burjachs, F., Claude, J., Catalán, S.G. and Riba, D., 2012. A new key locality for the Pliocene vertebrate record of Europe: the Camp dels Ninots maar (NE Spain). *Geologica Acta*, 10(1): 1–17.
- Ditlevsen, P.D. and Ashwin, P., 2018. Complex climate response to astronomical forcing: The middle-Pleistocene transition in glacial cycles and changes in frequency locking. *Frontiers in Physics*: 62.
- Dowsett, H.J., Foley, K.M., Stoll, D.K., Chandler, M.A., Sohl, L.E., Bentsen, M., Otto-Bliesner, B.L., Bragg, F.J., Chan, W.L., Contoux, C. and Dolan, A.M., 2013. Sea surface temperature of the mid-Piacenzian ocean: a data-model comparison. *Scientific reports*, 3(1): 1–8.
- Dubrovo, I.A. and Burchak-Abramovich, N.I., 1983: A New Pliocene Bovid Genus, *Adjiderebos* gen. nov., from Transcaucasia. *Proceedings of the USSR Academy of Sciences*, 276(3), 717–720.
- Dubrovo, I.A. and Burchak-Abramovich, N.I. 1986. New data on the evolution of Bovine of the tribe Bovini. *Quartärpalaontologie*, 6: 13–21.
- Ducrocq, S., 2019. *Pakkokuhyus* and *Progenitohyus* (Artiodactyla, Mammalia) from the Eocene of Southeast Asia are not Helohyidae: paleobiogeographical implications. *PalZ*, 93(1): 105–113.

- Duvernois, M.P., 1990. Les *Leptobos* (Mammalia, Artiodactyla) du Villafranchien d'Europe occidentale. Systématique, évolution, biostratigraphie, paléoécologie. *Travaux et Documents des Laboratoires de Géologie de Lyon*, 113(1): 3–213.
- Elderfield, H., Ferretti, P., Greaves, M., Crowhurst, S., McCave, I.N., Hodell, D. and Piotrowski, A.M., 2012. Evolution of ocean temperature and ice volume through the mid-Pleistocene climate transition. *Science*, 337(6095): 704–709.
- Etourneau, J., Schneider, R., Blanz, T. and Martinez, P., 2010. Intensification of the Walker and Hadley atmospheric circulations during the Pliocene–Pleistocene climate transition. *Earth and Planetary Science Letters*, 297(1-2): 103–110.
- Farjand, A., Zhang, Z., Kaakinen, A., Bi, S., Gibbard, P.L. and Lihua, W., 2022. Rediscovery and stratigraphic calibration of the classic Nihewan Fauna, Hebei Province, China. *Quaternary International*. In press.
- Faure, M. and Guérin, C., 1984. *Sus strozzi* et *Sus scrofa*, deux mammifères artiodactyles, marqueurs des paléoenvironnements. *Palaeogeography, Palaeoclimatology, Palaeoecology*, 48(2-4): 215–228.
- Ferring, R., Oms, O., Agustí, J., Berna, F., Nioradze, M., Shelia, T., Tappen, M., Vekua, A., Zhvania, D. and Lordkipanidze, D., 2011. Earliest human occupations at Dmanisi (Georgian Caucasus) dated to 1.85–1.78 Ma. *Proceedings of the National Academy of Sciences*, 108(26): 10432–10436.
- Flerov, C.C., 1969. Die Bison-Reste aus den Kiesen von Süßenborn bei Weimar. *Paläontologische Abhandlungen*, 3: 489–520.
- Flerov, C.C., 1972. The most ancient bison and the history of genus *Bison*. In: *Teriologiya vol. 1*. Nauka, Novosibirsk: 81–86.
- Flerov, C.C., 1976. Die fossilen Bison-Reste von Taubach und ihre Stellung in der Entwicklungsgeschichte der Gattung *Bison* in Europa. *Quartärpaläontologie 2*: 179–208.
- Flerov, C.C., 1979. Systematics and evolution. In: Sokolov, E.V. (Ed.), *European Bison*. Nauka, Moscow: 9–127.
- Flerov, C.C. and David, A.I., 1971. Genus *Bison* H. Smith, 1827. In: Nikiforova, K.V. (Ed.), *Pleistocene of Tiraspol*. Shtiința, Kishinev: 156–165.
- Frantz, L., Meijaard, E., Gongora, J., Haile, J., Groenen, M.A. and Larson, G., 2016. The evolution of Suidae. *Annual Review of Animal Biosciences*, 4(1): 61–85.
- Freudenthal, M., 1914. Freudenthal, W., 1914. Die saugetierte des alteren Quartas von Mitteleuropa. *Geologische und Palaeontologische Abhandlungen, Neue Folge*, 12: 455–671.
- Freudenthal, M., 1971. Neogene vertebrates from the Gargano Peninsula, Italy. *Scripta Geologica*, 3: 1–10.

- Froese, D., Stiller, M., Heintzman, P.D., Reyes, A.V., Zazula, G.D., Soares, A.E., Meyer, M., Hall, E., Jensen, B.J., Arnold, L.J. and MacPhee, R.D., 2017. Fossil and genomic evidence constrains the timing of bison arrival in North America. *Proceedings of the National Academy of Sciences*, 114(13): 3457–3462.
- Fujita, M., Kawamura, Y., and Murase, N., 2000. Middle Pleistocene wild boar remains from NT Cave, Niimi, Okayama Prefecture, west Japan. *Journal of Geosciences*, 43: 57–95.
- Gatesy, J., Milinkovitch, M., Waddell, V. and Stanhope, M., 1999. Stability of cladistic relationships between Cetacea and higher-level artiodactyl taxa. *Systematic Biology*, 48(1): 6–20.
- Geisler, J.H. and Uhen, M.D., 2003. Morphological support for a close relationship between hippos and whales. *Journal of Vertebrate Paleontology*, 23(4): 991–996.
- Geisler, J.H., Theodor, J.M., Uhen, M.D. and Foss, S.E., 2007. Phylogenetic relationships of cetaceans to terrestrial artiodactyls. In: Prothero, D.R., Foss, S.E. (Eds.) *The evolution of artiodactyls*. Johns Hopkins University Press, Baltimore: 19–31.
- Gentili, S. and Masini, F., 2005. An outline of Italian *Leptobos* and a first sight on *Leptobos* aff. *vallisarni* from Pietrafitta (early pleistocene, Perugia). In: Crégut- Bonnoure, E. (Ed.), *Les ongulés holarctiques du Pliocène et du Pléistocène. Quaternaire, Hors-série 2*, 81–89.
- Gentili, S., Abbazzi, L., Masini, F., Ambrosetti, P., Argenti, P., and Torre, D., 1996. Voles from the Early Pleistocene of Pietrafitta (central Italy, Perugia). *Acta zoologica cracoviense*, 39 (1): 185–199.
- Gentry, A.W. and Gentry, A., 1978a. Fossil Bovidae (Mammalia) of Olduvai Gorge, Tanzania, part I. *Bulletin of the British Museum (Natural History) (Geology)* 29: 289–446.
- Gentry, A.W. and Gentry, A., 1978b. Fossil Bovidae (Mammalia) of Olduvai Gorge, Tanzania, part II. *Bulletin of the British Museum (Natural History) (Geology)*, 30: 1–83.
- Geraads, D., 1992. Phylogenetic analysis of the tribe Bovini (Mammalia: Artiodactyla). *Zoological Journal of the Linnean Society*, 104(3): 193–207.
- Geraads, D., 2004. New skulls of *Kolpochoerus phacochoeroides* (Suidae: Mammalia) from the Late Pliocene of Ah1 a1 Oughlam, Morocco. *Palaeontologia Africana*, 40: 69–83.
- Geraads, D., Guérin, C. and Faure, M., 1986. Les suidés du Pléistocène ancien d'Oubeidiyeh (Israël). *Mémoires et Travaux du Centre de Recherches français de Jérusalem*, 5: 93–105.

- Ghassemi-Khademi, T., Madjdzadeh, S.M., Khosravi, R. and Asadi, A., 2021. The Phylogenetic Relationships within the Tribe Bovini (Bovidae: Bovinae) Using Mitochondrial Genome. *Journal of Genetic Resources*, 7(1): 15–28.
- Gibbard, P. and Cohen, K.M., 2008. Global chronostratigraphical correlation table for the last 2.7 million years. *Episodes Journal of International Geoscience*, 31(2): 243–247.
- Gliozzi, E., Abbazzi, L., Argenti, P., Azzaroli, A., Caloi, L., Capasso Barbato, L., Di Stefano, G., Esu, D., Ficcarelli, G., Girotti, O., Kotsakis, T., Masini, F., Mazza, P., Mezzabotta, C., Palombo, M.R., Petronio, C., Rook, L., Sala, B., Sardella, R., Zanalda, E., Torre, D., 1997. Biochronology of selected mammals, molluscs and ostracods from the middle Pliocene to the late Pleistocene in Italy. *The state of the art. Rivista Italiana di Paleontologia e Stratigrafia*, 103: 369–388.
- Goloboff, P.A. and Catalano, S.A., 2016. TNT version 1.5, including a full implementation of phylogenetic morphometrics. *Cladistics*, 32(3): 221–238.
- Gongora, J., Cuddahee, R.E., Nascimento, F.F.D., Palgrave, C.J., Lowden, S., Ho, S.Y., Simond, D., Damayanti, C.S., White, D.J., Tay, W.T. and Randi, E., 2011. Rethinking the evolution of extant sub-Saharan African suids (Suidae, Artiodactyla). *Zoologica Scripta*, 40(4): 327–335.
- Gongora, J., Groves, C., Meijaard, E., Melletti, M. and Meijaard, E., 2017. Evolutionary relationships and taxonomy of suidae and tayassuidae. In Melletti, M., and Meijaard, E. (Eds.) *Ecology, Conservation and Management of Wild Pigs and Peccaries*. Cambridge University Press, Cambridge: 1–19.
- González-Sampériz, P., Leroy, S.A., Carrión, J.S., Fernández, S., García-Antón, M., Gil-García, M.J., Uzquiano, P., Valero-Garcés, B. and Figueiral, I., 2010. Steppes, savannahs, forests and phytodiversity reservoirs during the Pleistocene in the Iberian Peninsula. *Review of Palaeobotany and Palynology*, 162(3): 427–457.
- Gradstein, F.M., Ogg, J.G., Schmitz, M. and Ogg, G., 2012. *The geologic time scale 2012*. Elsevier.
- Grange, T., Brugal, J.P., Flori, L., Gautier, M., Uzunidis, A. and Geigl, E.M., 2018. The evolution and population diversity of bison in pleistocene and holocene Eurasia: Sex matters. *Diversity*, 10(3): 65.
- Graur, D. and Higgins, D.G., 1994. Molecular evidence for the inclusion of cetaceans within the order Artiodactyla. *Molecular Biology and Evolution*, 11(3): 357–364.
- Gromolard, C., 1980. Revision du type de l'espèce *Parabos? boodon* (Gervais)(Mammalia, Artiodactyla, Bovidae) du gisement Neogene d'Alcoy (Espagne). *Publications de la Société Linnéenne de Lyon*, 49(9): 525–533.
- Groves, C.P., 1981a. Ancestors for the pigs: taxonomy and phylogeny of the genus *Sus*. *Technical Bulletin N°3 of the Department of Prehistory*. Research School of Pacific Studies Canberra. Australian National University Press, Canberra: 96 p.

- Groves, C.P., 1981b. Systematic relationships in the bovini (Artiodactyla, Bovidae). *Journal of Zoological Systematics and Evolutionary Research*, 19(4): 264–278.
- Groves, C.P. and Grubb, P., 1993. The suborder Suiformes. In: Oliver, W. (Ed.), *Pigs, Peccaries, and Hippos: Status Survey and Conservation Action Plan*. IUCN, Gland: 1–4.
- Groves, C.P. and Grubb, P., 2011. *Ungulate Taxonomy*. Johns Hopkins University Press, Baltimore: 309 p.
- Guérin, C., 1980. Les rhinoceros (Mammalia, Perissodactyla) du Miocene terminal au Pleistocene superieur en Europe occidentale: comparaison avec les especes actuelles. *Documents du Laboratoire de Géologie de la Faculté des Sciences de Lyon*, 79: 1–1182.
- Guérin, C., 1982. Première biozonation du Pléistocène européen, principal résultat biostratigraphique de l'étude des Rhinocerotidae (Mammalia, Perissodactyla) du Miocène terminal au Pléistocène supérieur d'Europe occidentale. *Geobios*, 15(4): 593–598.
- Guérin, C., 1990. Biozones or mammal units? Methods and limits in biochronology. In: Lindsay, E.H., Fahlbush, V., Mein, P. (Eds.), *European Neogene Mammalian Chronology*. NATO ASI Series a Life Sciences, 180. Plenum Press, New York: 119–130.
- Guérin, C., 2007. Biozonation continentale du Plio-Pléistocène d'Europe et d'Asie occidentale par les mammifères: état de la question et incidence sur les limites Tertiaire/Quaternaire et Plio/Pléistocène. *Quaternaire - Revue de l'Association française pour l'étude du Quaternaire*, 18(1) : 23–33.
- Guérin, C. and Philippe, M., 1971. Les gisements de vertébrés pléistocènes du Causse de Martel. *Bulletin de la Société Historique Archéologique*, 93: 31–46.
- Guérin, C. and Faure, M., 1997. The wild boar (*Sus scrofa priscus*) from the post-Villafranchian Lower Pleistocene of Untermassfeld. In: Kahlke R.D. (Ed.) *Das Pleistozän von Untermassfeld bei Meiningen (Thüringen)*, 1. Römisch-Germanisches Zentralmuseum, Mainz: 375–383.
- Gunther, K.A. and Haroldson, M.A., 2020. Potential for recreational restrictions to reduce grizzly bear–caused human injuries. *Ursus*, 2020(31–6): 1–17.
- Hardjasasmita, H.S. and Hardjasasmita, H.S., 1987. Taxonomy and phylogeny of the Suidae (Mammalia) in Indonesia. *Scripta Geologica*, 85: 1–68.
- Harris, J.M. and White, T.D., 1979. *Evolution of the Plio-Pleistocene African Suidae*. *Transactions of the American Philosophical Society*, 69(2): 1–128.

- Harris, J.M. and Liu, L.P., 2007. Superfamily Suoidea (pp.). In: Prothero, D.R. and Foss, S.E. (Eds.), *The Evolution of Artiodactyls*. Johns Hopkins University Press, Baltimore: 130–150.
- Hassanin, A. and Douzery, E.J., 2003. Molecular and morphological phylogenies of Ruminantia and the alternative position of the Moschidae. *Systematic biology*, 52(2): 206–228.
- Hassanin, A. and Ropiquet, A., 2004. Molecular phylogeny of the tribe Bovini (Bovidae, Bovinae) and the taxonomic status of the Kouprey, *Bos sauveli* Urbain 1937. *Molecular phylogenetics and evolution*, 33(3): 896–90.
- Hassanin, A., Delsuc, F., Ropiquet, A., Hammer, C., Van Vuuren, B.J., Matthee, C., Ruiz-Garcia, M., Catzeflis, F., Areskoug, V., Nguyen, T.T. and Couloux, A., 2012. Pattern and timing of diversification of Cetartiodactyla (Mammalia, Laurasiatheria), as revealed by a comprehensive analysis of mitochondrial genomes. *Comptes rendus biologiques*, 335(1): 32–50.
- Hassanin, A., Houck, M.L., Tshikung, D., Kadjo, B., Davis, H. and Ropiquet, A., 2018. Multi-locus phylogeny of the tribe Tragelaphini (Mammalia, Bovidae) and species delimitation in bushbuck: evidence for chromosomal speciation mediated by interspecific hybridization. *Molecular phylogenetics and evolution*, 129: 96–105.
- Haug, G.H., Ganopolski, A., Sigman, D.M., Rosell-Mele, A., Swann, G.E., Tiedemann, R., Jaccard, S.L., Bollmann, J., Maslin, M.A., Leng, M.J. and Eglinton, G., 2005. North Pacific seasonality and the glaciation of North America 2.7 million years ago. *Nature*, 433(7028): 821–825.
- Hayashi, T., Yamanaka, T., Hikasa, Y., Sato, M., Kuwahara, Y. and Ohno, M., 2020. Latest Pliocene Northern Hemisphere glaciation amplified by intensified Atlantic meridional overturning circulation. *Communications Earth & Environment*, 1(1): 1–10.
- Hays, J.D., Imbrie, J. and Shackleton, N.J., 1976. Variations in the Earth's Orbit: Pacemaker of the Ice Ages: For 500,000 years, major climatic changes have followed variations in obliquity and precession. *Science*, 194(4270), 1121–1132.
- Head, M.J. and Gibbard, P.L., 2005. Early-Middle Pleistocene transitions: an overview and recommendation for the defining boundary. *Geological Society, London, Special Publications*, 247(1): 1–18.
- Head, M.J. and Gibbard, P.L., 2015. Early–Middle Pleistocene transitions: linking terrestrial and marine realms. *Quaternary International*, 389: 7–46.
- Head, M.J., Pillans, B. and Farquhar, S.A., 2008. The Early–Middle Pleistocene Transition: characterization and proposed guide for the defining boundary. *Episodes Journal of International Geoscience*, 31(2) : 255–259.
- Heintz, E., 1968. Principaux résultats systématiques et biostratigraphiques de l'étude des Cervidés villafranchiens de France et d'Espagne. *Comptes Rendus de l'Académie de Sciences de Paris*, 266 : 2184–2186.

- Heintz, E., 1970. Les cervidés Villafranchiens de France et d'Espagne. *Mémoires du Muséum national d'Histoire Naturelle de Paris*, C 22: 1–206.
- Heintz, E., Guérin, C., Martin, R. and Prat, F., 1974. Principaux gisements villafranchiens de France: listes fauniques et biostratigraphie. *Mémoires du Bureau pour la Recherche Géologique et Minière (France)*, 78: 131–135.
- Hemmer and Kahlke, 2022. New results on felids from the Early Pleistocene site of Untermassfeld. In: Kahlke R.D. (Ed.), *The Pleistocene of Untermassfeld near Meiningen (Thüringen, Germany)*, 4. Römisch-Germanischen Zentralmuseums: 1465–1566.
- Hürzeler, J. 1982. Sur le suidé du lignite de Montebamboli (prov. Grosseto, Italie). *Comptes Rendus de l'Académie des Sciences de Paris, Série 2*, 295: 697–701.
- Huybers, P., 2006. Early Pleistocene glacial cycles and the integrated summer insolation forcing. *Science*, 313(5786): 508–511.
- Iannucci A., 2022. New results on suids from the Early Pleistocene site of Untermassfeld. In: Kahlke R.D. (Ed.) *The Pleistocene of Untermassfeld near Meiningen (Thüringen, Germany)*, 5. Römisch-Germanischen Zentralmuseums, Mainz: 40, 5.
- Iannucci, A., Cherin, M., Sorbelli, L. and Sardella, R., 2021b. Suidae transition at the Miocene-Pliocene boundary: a reassessment of the taxonomy and chronology of *Propotamochoerus provincialis*. *Journal of Mammalian Evolution*, 28(2): 323–335.
- Iannucci, A., Mecozzi, B., Sardella, R. and Iurino, D.A., 2021a. The extinction of the giant hyena *Pachycrocuta brevirostris* and a reappraisal of the Epivillafranchian and Galerian Hyaenidae in Europe: Faunal turnover during the Early–Middle Pleistocene Transition. *Quaternary Science Reviews*, 272: 107240.
- Iannucci A., Bellucci L., Conti J., Mazzini I., Mecozzi B., Sardella R. and Iurino D.A., 2022. Neurocranial anatomy of *Sus arvernensis* (Suidae, Mammalia) from Colleparado (Early Villafranchian; central Italy): taxonomic and biochronological implications. *Historical Biology*, 34: 108–120.
- Imbrie, J., Boyle, E.A., Clemens, S.C., Duffy, A., Howard, W.R., Kukla, G., Kutzbach, J., Martinson, D.G., McIntyre, A., Mix, A.C. and Molfino, B., 1992. On the structure and origin of major glaciation cycles 1. Linear responses to Milankovitch forcing. *Paleoceanography*, 7(6): 701–738.
- Irwin, D.M. and Árnason, Ú., 1994. Cytochrome b gene of marine mammals: phylogeny and evolution. *Journal of Mammalian Evolution*, 2(1): 37–55.
- IUCN. 2022. The IUCN Red List of Threatened Species. Version 2022-1 <https://www.iucnredlist.org>. Accessed on December 2022.

- Iurino, D.A., Mecozzi, B., Iannucci, A., Moscarella, A., Strani, F., Bona, F., Gaeta, M. and Sardella, R., 2022. A Middle Pleistocene wolf from central Italy provides insights on the first occurrence of *Canis lupus* in Europe. *Scientific Reports*, 12(1): 1–13.
- Janis, C. M., and K. M. Scott. 1988. The phylogeny of the Ruminantia (Artiodactyla, Mammalia). *In*: M. J. Benton (Ed.), *The Phylogeny and Classification of Tetrapods; Volume 2, Mammals*. Academic Press for the Systematics Association, London-New York: 273–282.
- Jansen, J.H.F., Kuijpers, A. and Troelstra, S.R., 1986. A mid-Brunhes climatic event: long-term changes in global atmosphere and ocean circulation. *Science*, 232(4750): 619–622.
- Jiménez-Moreno, G., Fauquette, S. and Suc, J.P., 2010. Miocene to Pliocene vegetation reconstruction and climate estimates in the Iberian Peninsula from pollen data. *Review of Palaeobotany and Palynology*, 162(3): 403–415.
- Jiménez-Moreno, G., Burjachs, F., Expósito, I., Oms, O., Carrancho, Á., Villalain, J.J., Agustí, J., Campeny, G., de Soler, B.G. and van der Made, J., 2013. Late Pliocene vegetation and orbital-scale climate changes from the western Mediterranean area. *Global and Planetary change*, 108: 15–28.
- Jungers, W.L., Falsetti, A.B. and Wall, C.E., 1995. Shape, relative size, and size- adjustments in morphometrics. *American Journal of Physical Anthropology*, 38: 137–161.
- Kahlke, R.D., 1999. The History of the Origin, Evolution and Dispersal of the Late Pleistocene *Mammuthus-Coelodonta* Faunal Complex in Eurasia (large mammals). Fenske Companies, Rapid City (1999), 218 p.
- Kahlke, R.D., 2001a. *Das Pleistozän von Untermassfeld bei Meiningen (Thüringen)*, 1. Römisch-Germanisches Zentralmuseum, Mainz: 699–1030.
- Kahlke, R.D., 2001b. Schädelreste von Hippopotamus aus dem Unterpleistozän von Untermaßfeld. *In*: Kahlke R.D. (Ed.), *Das Pleistozän von Untermaßfeld bei Meiningen (Thüringen)*, 2. Römisch-Germanisches Zentralmuseum, Mainz: 483–500.
- Kahlke, R.D., 2006. Untermassfeld - a late Early Pleistocene (Epivillafranchian) fossil site near Meiningen (Thuringia, Germany) and its position in the development of the European mammal fauna. *British Archaeological Reports, International Series*, 1578: 1–144.
- Kahlke R.D., 2007. Late Early Pleistocene European large mammals and the concept of an Epivillafranchian biochron. *Courier Forschungsinstitut Senckenberg*, 259: 265–278.
- Kahlke, R.D. and Lacombat, F., 2008. The earliest immigration of woolly rhinoceros (*Coelodonta tologojensis*, Rhinocerotidae, Mammalia) into Europe and its adaptive evolution in Palaeartic cold stage mammal faunas. *Quaternary Science Reviews*, 27(21–22): 1951–1961.

- Kahlke, R.D., García, N., Kostopoulos, D.S., Lacomat, F., Lister, A.M., Mazza, P.P., Spassov, N. and Titov, V.V., 2011. Western Palaeartic palaeoenvironmental conditions during the Early and early Middle Pleistocene inferred from large mammal communities, and implications for hominin dispersal in Europe. *Quaternary Science Reviews*, 30(11–12): 1368–1395.
- Kaiser, T.M. and Croitor, R., 2004. Ecological interpretations of early Pleistocene deer (Mammalia, Cervidae) from Ceyssaguet (Haute-Loire, France). *Geodiversitas*, 26(4): 661–674.
- Kerley, G.I., Kowalczyk, R. and Cromsigt, J.P., 2012. Conservation implications of the refugee species concept and the European bison: king of the forest or refugee in a marginal habitat?. *Ecography*, 35(6): 519–529.
- Khan, M.A., Kostopoulos, D.S., Akhtar, D.S. and Nazir, M., 2010. *Bison* remains from the upper Siwaliks of Pakistan. *Neues Jahrbuch für Geologie und Paläontologie Abhandlungen*. 258: 121–128.
- Khan, M.A., Nasim, S., Ikram, T., Ghafoor, A. and Akhtar, M., 2011. Dental remains of early bison from the Tatrot formation of the upper Siwaliks, Pakistan. *Journal of Animal and Plant Sciences*, 21 (4): 862–867.
- Koenigswald, W.V., Schwermann, A.H., Keiter, M. and Menger, F., 2019. First evidence of Pleistocene *Bubalus murrensis* in France and the stratigraphic occurrences of *Bubalus* in Europe. *Quaternary International*, 522: 85–93.
- Konidaris, G.E., 2022. Guilds of large carnivorans during the Pleistocene of Europe: a community structure analysis based on foraging strategies. *Lethaia*, 55(2): 1–18.
- Kostopoulos, D.S. and Athanassiou, A., 2005. In the shadow of bovids: suids, cervids and giraffids from the Plio-Pleistocene of Greece. In: Crégut- Bonnoure, E. (Ed.), *Les ongulés holarctiques du Pliocène et du Pléistocène. Quaternaire, Hors-série 2*, 179–190.
- Kostopoulos, D.S., 1997. The Plio-Pleistocene artiodactyls (Vertebrata, Mammalia) of Macedonia 1. The fossiliferous site “Apollonia-1”, Mygdonia basin of Greece. *Geodiversitas*, 19(4): 845–875.
- Kostopoulos, D.S. and Koufos, G.D., 2006. *Pheraios chryssomallos*, gen. et sp. nov. (Mammalia, Bovidae, Tragelaphini), from the Late Miocene of Thessaly (Greece): Implications for tragelaphin biogeography. *Journal of Vertebrate Paleontology*, 26(2): 436–445.
- Kostopoulos, D.S. and Sylvestrou, I., 2022. The Fossil Record of Suoids (Mammalia: Artiodactyla: Suoidae) in Greece. In: Vlachos, E. (Ed.), *Fossil Vertebrates of Greece Vol. 2*. Springer, Cham: 249–269.
- Kostopoulos, D.S., Spassov, N. and Kovachev, D., 2001. Contribution to the study of *Microstonyx*: evidence from Bulgaria and the SE European populations. *Geodiversitas*, 23(3): 411–437.

- Kostopoulos, D.S., Maniakas, I. and Tsoukala, E., 2018. Early bison remains from Mygdonia Basin (Northern Greece). *Geodiversitas*, 40(3): 283–319.
- Kostopoulos, D.S., Konidaris, G.E., Amanatidou, M., Chitoglou, K., Fragkioudakis, E., Gerakakis, N., Giannakou, V., Gkeme, A., Kalaitzi, C., Tsakalidis, C. and Tsatsalis, V., 2022. The new fossil site Krimni-3 in Mygdonia Basin and the first evidence of a giant ostrich in the Early Pleistocene of Greece. *PalZ*: 1–15.
- Koufos, G.D., 1986. The presence of *Sus strozzii* in the Villafranchian (Villanyian) of Macedonia (Greece). *Paläontologische Zeitschrift*, 60(3): 341–351.
- Koufos, G.D., 2001. The Villafranchian mammalian fauna and biochronology of Greece. *Bollettino della Società Paleontologica Italiana* 40: 217–223.
- Koufos, G.D., 2022. The fossil record of hyaenids (Mammalia: Carnivora: Hyaenidae) in Greece *In*: Vlachos, E. (Ed.), *Fossil Vertebrates of Greece Vol. 2*. Springer, Cham: 555–576.
- Koufos, G.D., Konidaris, G.E. and Harvati, K., 2018. Revisiting *Ursus etruscus* (Carnivora, Mammalia) from the Early Pleistocene of Greece with description of new material. *Quaternary International*, 497: 222–239.
- Kurten B. 1968. *Pleistocene Mammals of Europe*. Aldine, Chicago: 317 p.
- Lacombat, F., 2005. Les rhinocéros fossiles des sites préhistoriques de l'Europe méditerranéenne et du Massif Central. *Paléontologie et implications biochronologiques BAR International Series*, 1419: 1–175.
- Lang, N. and Wolff, E.W., 2011. Interglacial and glacial variability from the last 800 ka in marine, ice and terrestrial archives. *Climate of the Past*, 7(2): 361–380.
- Larramendi, A., Zhang, H., Palombo, M.R. and Ferretti, M.P., 2020. The evolution of *Palaeoloxodon* skull structure: Disentangling phylogenetic, sexually dimorphic, ontogenetic, and allometric morphological signals. *Quaternary Science Reviews*, 229: 106090.
- Leonardi, G. and Petronio, C. 1976. The fallow deer of European Pleistocene. *Geologica Romana* 15: 1–67.
- Li, Q., Li, Y., Zhao, X., Liu, Z., Xu, Y., Song, D., Qu, X., Li, N. and Xie, Z., 2007. Study on the origin and taxonomic status of yak (*Poephagus*) using cytochrome b gene of mitochondrial DNA. *Frontiers of Agriculture in China*, 1(3): 329–333.
- Lindsay, E.H., 1990. The setting. *In*: Lindsay, E.H., Fahlbush, V., Mein, P. (Eds.), *European Neogene Mammalian Chronology*. Springer, New York: 1–14.
- Lisiecki, L.E. and Raymo, M.E., 2007. Plio–Pleistocene climate evolution: trends and transitions in glacial cycle dynamics. *Quaternary Science Reviews*, 26(1–2): 56–69.

- Liu L.P. 2001. Eocene suoids (Artiodactyla, Mammalia) from Bose and Yongle basins, China, and the classification and evolution of the Paleogene suoids. *Vertebrata Palasiatica*, 39: 115–128
- Lunt, D.J., Valdes, P.J., Haywood, A. and Rutt, I.C., 2008. Closure of the Panama Seaway during the Pliocene: implications for climate and Northern Hemisphere glaciation. *Climate Dynamics*, 30(1): 1–18.
- Luzón, C., Yravedra, J., Courtenay, L.A., Saarinen, J., Blain, H.A., DeMiguel, D., Viranta, S., Azanza, B., Rodríguez-Alba, J.J., Herranz-Rodrigo, D. and Serrano-Ramos, A., 2021. Taphonomic and spatial analyses from the Early Pleistocene site of Venta Micena 4 (Orce, Guadix-Baza Basin, southern Spain). *Scientific reports*, 11(1): 1–17.
- Lydekker R., 1878. Crania of ruminants from the Indian Tertiaries. *Paleontologia Indica* 10 (1): 88–171.
- Lydekker, R. 1898. Wild oxen, sheep and goats of all lands, living and extinct. Rowland Ward Limited, London, United Kingdom: 318 p.
- Maasch, K.A., 1988. Statistical detection of the mid-Pleistocene transition. *Climate dynamics*, 2(3): 133–143.
- MacEachern, S., McEwan, J. and Goddard, M., 2009. Phylogenetic reconstruction and the identification of ancient polymorphism in the Bovini tribe (Bovidae, Bovinae). *BMC genomics*, 10(1): 1–17.
- Madurell-Malapeira, J., Minwer-Barakat, R., Alba, D.M., Garcés, M., Gómez, M., Aurell-Garrido, J., Ros-Montoya, S., Moyà-Solà, S. and Berástegui, X., 2010. The Vallparadís section (Terrassa, Iberian Peninsula) and the latest Villafranchian faunas of Europe. *Quaternary Science Reviews*, 29(27-28): 3972–3982.
- Madurell-Malapeira, J., Ros-Montoya, S., Espigares, M.P., Alba, D.M. and Aurell-Garrido, J., 2014. Villafranchian large mammals from the Iberian Peninsula: paleobiogeography, paleoecology and dispersal events. *Journal of Iberian Geology*, 40(1): 167–178.
- Madurell-Malapeira, J., Alba, D.M., Espigares, M.P., Vinuesa, V., Palmqvist, P., Martínez-Navarro, B. and Moyà-Solà, S., 2017. Were large carnivorans and great climatic shifts limiting factors for hominin dispersals? Evidence of the activity of *Pachycrocuta brevirostris* during the Mid-Pleistocene Revolution in the Vallparadís Section (Vallès-Penedès Basin, Iberian Peninsula). *Quaternary International*, 431: 42–52.
- Madurell-Malapeira, J., Bartolini-Lucenti, S., Prat-Vericat, M., Sorbelli, L., Blasetti, A., Ferretti, M.P., Goro, A. and Cherin, M., 2022. Jaramillo-aged carnivorans from Collecorti (Colfiorito Basin, Italy). *Historical Biology*, 34(10): 1928–1940.
- Magri, D., Di Rita, F., Aranbarri, J., Fletcher, W. and González-Sampériz, P., 2017. Quaternary disappearance of tree taxa from Southern Europe: Timing and trends. *Quaternary Science Reviews*, 163: 23–55.

- Maniakas, I., Kostopoulos, D.S., 2017. Morphometric-palaeoecological discrimination between Bison populations of the western Palaearctic. *Geobios* 50: 155–171.
- Marcot, J.D. 2007. Molecular phylogeny of terrestrial artiodactyls, *In*: Prothero, D.R. and Foss, S.E. (Eds.), *The Evolution of Artiodactyls*. Johns Hopkins University Press, Baltimore: 4–18.
- Marino, M., Maiorano, P., Lirer, F. and Pelosi, N., 2009. Response of calcareous nannofossil assemblages to paleoenvironmental changes through the mid-Pleistocene revolution at Site 1090 (Southern Ocean). *Palaeogeography, Palaeoclimatology, Palaeoecology*, 280(3–4): 333–349.
- Marra, F., Pandolfi, L., Petronio, C., Di Stefano, G., Gaeta, M. and Salari, L., 2014. Reassessing the sedimentary deposits and vertebrate assemblages from Ponte Galeria area (Rome, central Italy): an archive for the Middle Pleistocene faunas of Europe. *Earth-Science Reviews*, 139: 104–122.
- Marsolier-Kergoat, M.C., Palacio, P., Berthonaud, V., Maksud, F., Stafford, T., Bégouën, R. and Elalouf, J.M., 2015. Hunting the extinct steppe bison (*Bison priscus*) mitochondrial genome in the Trois-Freres Paleolithic Painted Cave. *PLoS One*, 10(6): 0128267.
- Martin T (1987) Artunterschiede an den Langknochen großer Artiodactyla des Jungpleistozäns Mitteleuropas. *Courier Forschungsinstitut Senckenberg* 96: 1–121.
- Martinetto, E., Momohara, A., Bizzarri, R., Baldanza, A., Delfino, M., Esu, D. and Sardella, R., 2017. Late persistence and deterministic extinction of “humid thermophilous plant taxa of East Asian affinity”(HUTEA) in southern Europe. *Palaeogeography, Palaeoclimatology, Palaeoecology*, 467: 211–231.
- Martínez-Navarro, B., Pérez-Claros, J.A., Palombo, M.R., Rook, L. and Palmqvist, P., 2007. The Olduvai buffalo *Pelorovis* and the origin of *Bos*. *Quaternary research*, 68(2): 220–226.
- Martínez-Navarro, B. 2010a. Early Pleistocene faunas of Eurasia and hominin dispersals. *In*: Fleagle, J.G., Shea, J.J., Grine, F.E., Baden, A.L. and Leakey, R.E. (Eds), *Out of Africa I. The First Hominin Colonization of Eurasia*. Springer, Dordrecht: 207–224.
- Martínez-Navarro, B., Rook, L., Papini, M. and Libsekal, Y., 2010b. A new species of bull from the Early Pleistocene paleoanthropological site of Buia (Eritrea): parallelism on the dispersal of the genus *Bos* and the Acheulian culture. *Quaternary International*, 212(2): 169–175.
- Martínez-Navarro, B., Ros-Montoya, S., Espigares, M.P. and Palmqvist, P., 2011. Presence of the Asian origin Bovini, *Hemibos* sp. aff. *Hemibos gracilis* and *Bison* sp., at the early Pleistocene site of Venta Micena (Orce, Spain). *Quaternary International*, 243(1): 54–60.

- Martínez-Navarro, B., Madurell-Malapeira, J., Ros-Montoya, S., Espigares, M.P., Medin, T., Hortola, P. and Palmqvist, P., 2015. The Epivillafranchian and the arrival of pigs into Europe. *Quaternary International*, 389: 131–138.
- Martino, R. and Pandolfi, L., 2022. The Quaternary *Hippopotamus* records from Italy. *Historical Biology*, 34(7): 1146–1156.
- Masini, F., 1989. *I bovini villafranchiani dell'Italia*. PhD Dissertation, Università di Modena-Bologna-Firenze-Roma: 374 p.
- Masini, F. and Sala, B., 2007. Large-and small-mammal distribution patterns and chronostratigraphic boundaries from the Late Pliocene to the Middle Pleistocene of the Italian peninsula. *Quaternary International*, 160(1): 43–56.
- Masini, F., Palombo, M.R. and Rozzi, R., 2013. A reappraisal of the early to middle pleistocene Italian bovidae. *Quaternary International*, 288: 45–62.
- Maslin, M.A. and Brierley, C.M., 2015. The role of orbital forcing in the Early Middle Pleistocene Transition. *Quaternary International*, 389: 47–55.
- Maslin, M.A. and Ridgwell, A.J., 2005. Mid-Pleistocene revolution and the 'eccentricity myth'. *Geological Society, London, Special Publications*, 247(1): 19–34.
- Maslin, M.A., Li, X.S., Loutre, M.F. and Berger, A., 1998. The contribution of orbital forcing to the progressive intensification of Northern Hemisphere glaciation. *Quaternary Science Reviews*, 17(4–5): 411–426.
- Massilani, D., Guimaraes, S., Brugal, J.P., Bennett, E.A., Tokarska, M., Arbogast, R.M., Baryshnikov, G., Boeskorov, G., Castel, J.C., Davydov, S. and Madelaine, S., 2016. Past climate changes, population dynamics and the origin of *Bison* in Europe. *BMC biology*, 14(1): 1–17.
- Mazza, P. and Rustioni, M., 1997. Neotype and phylogeny of the suid "*Eumaichoerus etruscus*" (Michelotti) from Montebamboli (Grosseto, southern Tuscany). *Paleontologia i evolució*, (30): 5–18.
- Mazza, P., Sala, B., Fortelius, M., 1993. A small latest Villafranchian (late Early Pleistocene) rhinoceros from Pietrafitta (Perugia, Umbria, Central Italy), with notes on the Pirro and Westerhoven rhinoceroses. *Palaeontographia Italica*, 80: 25–50.
- McClymont, E.L., Sostdian, S.M., Rosell-Melé, A. and Rosenthal, Y., 2013. Pleistocene sea-surface temperature evolution: Early cooling, delayed glacial intensification, and implications for the mid-Pleistocene climate transition. *Earth-Science Reviews*, 123: 173–193.
- McDonald, J. N., 1981. *North American Bison: their Classification and Evolution*. University of California Press, Berkeley: 316 p.

- McKenzie, S., Sorbelli, L., Cherin, M., Almécija, S., Pina, M., Abella, J., Luján, À.H., DeMiguel, D. and Alba, D.M., 2022. Earliest Vallesian suid remains from Creu de Conill 20 (Vallès-Penedès Basin, NE Iberian Peninsula). *Journal of Mammalian Evolution*: 1–58.
- Mein, P., 1975. Resultats du groupe de travail des vertébrés. Working Groups. In: Senes, J. (Ed.), *Report on Activity of the R.C.M.N.S. Regional Committee on Mediterranean Neogene Stratigraphy*, Bratislava: 78–81.
- Mein, P., 1990. Updating the MN zones. In: Lindsay, H., Fahlbusch, W., Mein, P. (Eds.), *European Neogene Mammalian Chronology*. NATO ASI Series a Life Sciences, 180. Plenum Press, New York: 73–90.
- Melis, C., Selva, N., Teurlings, I., Skarpe, C., Linnell, J.D. and Andersen, R., 2007. Soil and vegetation nutrient response to bison carcasses in Białowieża Primeval Forest, Poland. *Ecological Research*, 22(5): 807–813.
- Meredith, R.W., Janečka, J.E., Gatesy, J., Ryder, O.A., Fisher, C.A., Teeling, E.C., Goodbla, A., Eizirik, E., Simão, T.L., Stadler, T. and Rabosky, D.L., 2011. Impacts of the Cretaceous Terrestrial Revolution and KPg extinction on mammal diversification. *Science*, 334(6055): 521–524.
- Merla, G., 1949. I *Leptobos* Rütim. italiani. *Palaeontographia Italica*, 46: 41–155.
- Métais, G., and Vislobokova, I., 2007. Basal ruminants. In: Prothero, D.R. and Foss, S.E. (Eds.), *The Evolution of Artiodactyls*. Johns Hopkins University Press, Baltimore: 189–212.
- Michaux, J., Aguilar, J.P., Calvet, M., Duvernois, M.P. and Sudre, J., 1991. *Alephis tignerese* nov. sp., un bovidé nouveau du Pliocène du Roussillon (France). *Geobios*, 24(6): 735–745.
- Michel, V., Shen, C.C., Woodhead, J., Hu, H.M., Wu, C.C., Moullé, P.É., Khatib, S., Cauche, D., Moncel, M.H., Valensi, P. and Chou, Y.M., 2017. New dating evidence of the early presence of hominins in Southern Europe. *Scientific reports*, 7(1): 1–8.
- Moigne, A.M., Palombo, M.R., Belda, V., Heriech-Briki, D., Kacimi, S., Lacombat, F., de Lumley, M.A., Moutoussamy, J., Rivals, F., Quilès, J. and Testu, A., 2006. Les faunes de grands mammifères de la Caune de l'Arago (Tautavel) dans le cadre biochronologique des faunes du Pléistocène moyen italien. *L'anthropologie*, 110(5): 788–831.
- Montgelard, C., Catzeflis, F.M. and Douzery, E., 1997. Phylogenetic relationships of artiodactyls and cetaceans as deduced from the comparison of cytochrome b and 12S rRNA mitochondrial sequences. *Molecular Biology and Evolution*, 14(5): 550–559.
- Montoya, P., Ginsburg, L., Alberdi, M.T., Van der Made, J., Morales, J. and Soria, M.D., 2006. Fossil large mammals from the early Pliocene locality of Alcoy (Spain) and their importance in biostratigraphy. *Geodiversitas*, 28(1): 137–173.

- Moullé, P.-É., 1992. Les grands mammifères du Pléistocène inférieur de la grotte du Vallonet (Roquebrune-Cap-Martin, Alpes-Maritimes). Étude paléontologique des Carnivores, Equidé, Suidéet Bovidés. PhD dissertation. Muséum National d'Histoire Naturelle, Paris: 338 p.
- Moullé, P.E., Lacombat, F. and Echassoux, A., 2006. Apport des grands mammifères de la grotte du Vallonet (Roquebrune-Cap-Martin, Alpes-Maritimes, France) à la connaissance du cadre biochronologique de la seconde moitié du Pléistocène inférieur d'Europe. *L'anthropologie*, 110(5): 837–849.
- Mourer-Chauvire, C., 1972. Etude de nouveaux restes de vertébrés provenant de la carrière Fournier à Châtillon-Saint-Jean. III. Artiodactyles, chevaux, oiseaux. *Quaternaire - Revue de l'Association française pour l'étude du Quaternaire*, 29, 9(4): 271–305.
- Mourer-Chauviré, C. and Bonifay, M.F., 2018. The birds from the Early Pleistocene of Ceysseguyet (Lavoûte-sur-Loire, Haute-Loire, France): description of a new species of the genus *aquila*. *Quaternaire - Revue de l'Association française pour l'étude du Quaternaire*, 29(3): 183–194.
- Moyà-Solà, S. 1983. Los Boselaphini (Bovidae Mammalia) del Neogeno de la Península Ibérica. *Publicaciones de Geología, Universidad Autònoma de Barcelona*, 18:1–236.
- Mudelsee, M. and Raymo, M.E., 2005. Slow dynamics of the Northern Hemisphere glaciation. *Paleoceanography*, 20(4): PA4022.
- Muttoni, G., Scardia, G. and Kent, D.V., 2013. A critique of evidence for human occupation of Europe older than the Jaramillo subchron (~ 1 Ma): comment on The oldest human fossil in Europe from Orce (Spain) by Toro-Moyano et al. (2013). *Journal of Human Evolution*, 65 (6): 746–749
- Muttoni, G., Scardia, G. and Kent, D.V., 2018. Early hominins in Europe: The Galerian migration hypothesis. *Quaternary Science Reviews*, 180: 1–29.
- Nikaido, M., Rooney, A.P. and Okada, N., 1999. Phylogenetic relationships among cetartiodactyls based on insertions of short and long interspersed elements: hippopotamuses are the closest extant relatives of whales. *Proceedings of the National Academy of Sciences*, 96(18): 10261–10266.
- Nomade, S., Pastre, J.F., Guillou, H., Faure, M., Guérin, C., Delson, E., Debard, E., Voinchet, P. and Messenger, E., 2014. ⁴⁰Ar/³⁹Ar constraints on some French landmark Late Pliocene to Early Pleistocene large mammalian paleofaunas: Paleoenvironmental and paleoecological implications. *Quaternary Geochronology*, 21: 2–15.
- Olsen, S.J., 1990. Fossil ancestry of the yak, its cultural significance and domestication in Tibet. *Proceedings of the National Academy of Sciences*, 142: 73–100.

- Orliac, M.J., and O’Leary, M.A., 2014. Comparative anatomy of the petrosal bone of dichobunoids, early members of Artiodactylamorpha (Mammalia). *Journal of Mammalian Evolution* 21: 299–320.
- Orliac, M.J., Pierre-Olivier, A. and Ducrocq, S., 2010. Phylogenetic relationships of the Suidae (Mammalia, Cetartiodactyla): new insights on the relationships within Suoidea. *Zoologica Scripta*, 39(4): 315–330.
- Palacio, P., Berthonaud, V., Guérin, C., Lambourdière, J., Maksud, F., Philippe, M., Plaire, D., Stafford, T., Marsolier-Kergoat, M.C. and Elalouf, J.M., 2017. Genome data on the extinct *Bison schoetensacki* establish it as a sister species of the extant European bison (*Bison bonasus*). *BMC Evolutionary Biology*, 17(1): 48.
- Palombo, M.R., 2004. Biochronology of Plio-Pleistocene mammalian faunas on the Italian Peninsula: Knowledge, problems and perspectives. *Alpine and Mediterranean Quaternary*, 17(2/2): 565–582.
- Palombo, M.R., 2014. Deconstructing mammal dispersals and faunal dynamics in SW Europe during the Quaternary. *Quaternary Science Reviews*, 96, 50–71.
- Palombo, M.R., 2016. Large mammals faunal dynamics in Southwestern Europe during the late Early Pleistocene: Implications for the biochronological assessment and correlation of mammalian faunas. *Alpine and Mediterranean Quaternary*, 29(2): 143–168.
- Palombo, M.R., 2018. Twenty years later: Reflections on the Aurelian European Land Mammal Age. *Alpine and Mediterranean Quaternary*, 31: 177–180.
- Palombo, M.R. and Mussi, M., 2006. Large mammal guilds at the time of the first human colonization of Europe: the case of the Italian Pleistocene record. *Quaternary International*, 149(1), 94–103.
- Palombo, M.R., Sardella, R. and Novelli, M., 2008. Carnivora dispersal in Western Mediterranean during the last 2.6 Ma. *Quaternary International*, 179(1): 176–189.
- Pandolfi, L. and Erten, H., 2017. *Stephanorhinus hundsheimensis* (Mammalia, Rhinocerotidae) from the late early Pleistocene deposits of the Denizli Basin (Anatolia, Turkey). *Geobios*, 50(1): 65–73.
- Pandolfi, L., Cerdeño, E., Codrea, V. and Kotsakis, T., 2017. Biogeography and chronology of the Eurasian extinct rhinoceros *Stephanorhinus etruscus* (Mammalia, Rhinocerotidae). *Comptes Rendus Palevol*, 16(7): 762–773.
- Pareto, L., 1865. Note sur les subdivisions que l’on pourrait établir dans les terrains tertiaires de l’Apennin septentrional. *Bulletin de la Société Géologique de France* 22: 210–277.

- Pazzaglia, F., Barchi, M.R., Buratti, N., Cherin, M., Pandolfi, L. and Ricci, M., 2013. Pleistocene calcareous tufa from the Ellera basin (Umbria, central Italy) as a key for an integrated paleoenvironmental and tectonic reconstruction. *Quaternary International*, 292: 59–70.
- Peretto, C., Amore, F., Antoniazzi, A., Bahain, J.J., Cattani, L., Esposito, P., Falgures, C., Gagnepain, J., Hedley, I., Laurent, M. and Lebreton, V., 1998. L'industrie lithique de Ca' Belvedere di Monte Poggiolo: stratigraphie, matière première, typologie, remontages et traces d'utilisation. *L'Anthropologie*, 140: 343–465.
- Petronio, C., 1979. *Dama nesti eurygonos* Azz. di Capena (Roma). *Geologica Romana*, 18: 105–125.
- Petronio, C. and Sardella, R., 1999. Biochronology of the Pleistocene mammal fauna from Ponte Galeria (Rome) and remarks on the Middle Galerian faunas. *Rivista Italiana di Paleontologia e Stratigrafia*, 105(1), 155–164.
- Petronio, C., Bellucci, L., Martiinetto, E., Pandolfi, L. and Salari, L., 2011. Biochronology and palaeoenvironmental changes from the Middle Pliocene to the Late Pleistocene in Central Italy. *Geodiversitas*, 33(3): 485–517.
- Petronio, C., Angelone, C., Atzori, P., Famiani, F., Kotsakis, T. and Salari, L., 2020. Review and new data of the fossil remains from Monte Peglia (late Early Pleistocene, central Italy). *Rivista Italiana di Paleontologia e Stratigrafia*, 126(3): 791–819.
- Pfeiffer, T. 2002. The first complete skeleton of *Megaloceros verticornis* (Dawkins, 1868) Cervidae, Mammalia, from Bilshausen (Lower Saxony, Germany): description and phylogenetic implications. *Mitteilungen aus dem Museum für Naturkunde Berlin (Geowissenschaftliche Reihe)*, 5: 289–308.
- Pickford, M. 1986. A revision of the Miocene Suidae and Tayassuidae (Artiodactyla, Mammalia) of Africa. *Tertiary Research Special Papers*, 7: 1–83.
- Pickford, M. 1988. Revision of the Miocene Suidae of the Indian Subcontinent. *Münchener Geowissenschaftliche Abhandlungen*, 12: 1–91.
- Pickford, M., 2006. Synopsis of the biochronology of African Neogene and Quaternary Suiformes. *Transactions of the Royal Society of South Africa*, 61(2): 51–62.
- Pickford, M., 2012. Ancestors of Broom's pigs. *Transactions of the Royal Society of South Africa*, 67(1): 17–35.
- Pickford, M., 2015. Late Miocene Suidae from Eurasia: the *Hippopotamodon* and *Microstonyx* problem revisited. *Münchener Geowissenschaftliche Abhandlungen Reihe A: Geologie und Paläontologie*, 42:1–126.
- Pickford, M. and Obada, T., 2016. Pliocene suids from Musaitu and Dermenji, Moldova: implications for understanding the origin of African *Kolpochoerus* van Hoepen & van Hoepen, 1932. *Geodiversitas*, 38(1): 99–134.

- Pilgrim, G.E. 1937. Siwalik antelopes and oxen in the American Museum of Natural History. *Bulletin of the American Museum of Natural History* 72: 729–874.
- Pilgrim, G.E. 1939. The fossil Bovidae of India. *Memories of the Geological Survey of India, Palaeontologia Indica, New Series*, 26: 1–356.
- Pilgrim, G.E., 1947. The evolution of the buffaloes, oxen, sheep and goats. *Zoological Journal of the Linnean Society*, 41(279): 272–286.
- Postigo Mijarra, J.M., Barrón, E., Gómez Manzaneque, F. and Morla, C., 2009. Floristic changes in the Iberian Peninsula and Balearic Islands (south-west Europe) during the Cenozoic. *Journal of Biogeography*, 36(11): 2025–2043.
- Prat-Vericat, M., Marciszak, A., Rufí, I., Sorbelli, L., Llenas, M., Lucenti, S.B. and Madurell-Malapeira, J., 2022. Middle Pleistocene Steppe Lion Remains from Grotte de la Carrière (Têt Valley, Eastern Pyrenees). *Journal of Mammalian Evolution*, 29: 547–569.
- Prothero D.R., 2016. *The Princeton field guide to prehistoric mammals*. Princeton Field Guides. Princeton University Press, New Jersey: 240 p.
- Prothero, D.R., Domning, D., Fordyce, R.E., Foss, S., Janis, C., Lucas, S., Marriott, K.L., Metais, G., Naish, D., Padian, K. and Rössner, G., 2022. On the unnecessary and misleading taxon “Cetartiodactyla”. *Journal of Mammalian Evolution*, 29(1): 93–97.
- R Core Team, 2019. R: A Language and Environment for Statistical Computing. R Foundation for Statistical Computing, Vienna, Austria. <https://www.R-project.org>.
- Remondino, F. and El-Hakim, S., 2006. Image-based 3D modelling: a review. *The photogrammetric record*, 21(115): 269–291.
- Reshetov, V. and Sukhanov, V.B., 1979. Postcranial skeleton. European bison—Morphology, systematics, evolution, ecology. In: Sokolov, E.V. (Ed.), *European Bison*. Nauka, Moscow: 142–195.
- Richarz, S., 1921. Neue Wirbeltierfunde in den Tonen von Tegelen bei Venlo. *Centralblatt für Mineralogie Geologie und Paläontologie*, 21: 664–669.
- Risch, D.R., Ringma, J. and Price, M.R., 2021. The global impact of wild pigs (*Sus scrofa*) on terrestrial biodiversity. *Scientific reports*, 11(1): 1–10.
- Ritz, L.R., Glowatzki-Mullis, M.L., MacHugh, D.E. and Gaillard, C., 2000. Phylogenetic analysis of the tribe Bovini using microsatellites. *Animal genetics*, 31(3): 178–185.

Rodríguez, J., Burjachs, F., Cuenca-Bescós, G., García, N., Van der Made, J., González, A.P., Blain, H.A., Expósito, I., López-García, J.M., Antón, M.G. and Allué, E., 2011. One million years of cultural evolution in a stable environment at Atapuerca (Burgos, Spain). *Quaternary Science Reviews*, 30(11–12): 1396–1412.

Rodriguez-Gomez, G., Palmqvist, P., Ros-Montoya, S., Espigares, M.P. and Martinez-Navarro, B., 2017. Resource availability and competition intensity in the carnivore guild of the Early Pleistocene site of Venta Micena (Orce, Baza Basin, SE Spain). *Quaternary Science Reviews*, 164: 154–167.

Rook, L. and Martínez-Navarro, B., 2010. Villafranchian: the long story of a Plio-Pleistocene European large mammal biochronologic unit. *Quaternary International*, 219(1–2): 134–144.

Ros-Montoya, S., Palombo, M.R., Espigares, M.P., Palmqvist, P. and Martínez-Navarro, B., 2018. The mammoth from the archaeo-paleontological site of Huéscar-1: A tile in the puzzling question of the replacement of *Mammuthus meridionalis* by *Mammuthus trogontherii* in the late Early Pleistocene of Europe. *Quaternary Science Reviews*, 197: 336–351.

Rozzi, R., Winkler, D.E., De Vos, J., Schulz, E. and Palombo, M.R., 2013. The enigmatic bovid *Duboisia santeng* (Dubois, 1891) from the Early–Middle Pleistocene of Java: A multiproxy approach to its paleoecology. *Palaeogeography, Palaeoclimatology, Palaeoecology*, 377: 73–85.

Ruddiman, W.F., Raymo, M. and McIntyre, A., 1986. Matuyama 41,000-year cycles: North Atlantic Ocean and northern hemisphere ice sheets. *Earth and Planetary Science Letters*, 80(1–2): 117–129.

Rufi, I., Drucker, D.G., Bocherens, H., Lloveras, L., Madurell-Malapeira, J., Maroto, J., Soler, J. and Soler, N., 2020. Revision of the occurrence of muskox (*Ovibos moschatus* Zimmermann 1780) from the Gravettian of Arbreda Cave (Serinyà, northeastern Iberian Peninsula): new insights for the study of Iberian cold-adapted faunas. *Boreas*, 49(4): 858–872.

Saarinen, J., Oksanen, O., Žliobaitė, I., Fortelius, M., DeMiguel, D., Azanza, B., Bocherens, H., Luzón, C., Solano-García, J., Yravedra, J. and Courtenay, L.A., 2021. Pliocene to Middle Pleistocene climate history in the Guadix-Baza Basin, and the environmental conditions of early Homo dispersal in Europe. *Quaternary Science Reviews*, 268: 107132.

Sala, B., 1986. *Bison schoetensacki* Freud. from Isernia la Pineta (early Mid-Pleistocene, Italy) and revision of the European species of bison. *Palaeontographia Italica*, 74: 113–170.

Sanchez-Bandera, C., Oms, O., Blain, H.A., Lozano-Fernandez, I., Bisbal-Chinesta, J.F., Agustí, J., Saarinen, J., Fortelius, M., Tilton, S., Serrano-Ramos, A. and Luzon, C., 2020. New stratigraphically constrained palaeoenvironmental reconstructions for the first human settlement in Western Europe: The Early Pleistocene herpetofaunal assemblages from Barranco León and Fuente Nueva 3 (Granada, SE Spain). *Quaternary Science Reviews*, 243: 106466.

- Sardella, R., Palombo, M.R., 2007. The Pliocene-Pleistocene boundary: which significance for the so called “wolf event”? Evidences from western Europe. *Quaternaire* 18: 65–71.
- Schertz, E., 1936. Der Geschlechts-Unterschied an Metapodien von Bison. *Senckenbergiana* 18, 357–381.
- Schreuder, A., 1946. The Tegelen fauna, with a description of new remains of its rare components (*Leptobos*, *Archidiskodon meridionalis*, *Macaca*, *Sus strozzi*). *Archives Néerlandaises de Zoologie*, 7(1): 153–204.
- Scott, K.M., 1983. Prediction of body weight of fossil Artiodactyla. *Zoological Journal of Linnean Society*, 77 (3), 199–215.
- Scott, R.S., 2004. The comparative paleoecology of Late Miocene Eurasian hominoids. PhD. Dissertation. The University of Texas at Austin.
- Scott, R.S., Barr, W.A., 2014. Ecomorphology and phylogenetic risk: implications for habitat reconstruction using fossil bovids. *Journall of Human Evolution*: 73, 47–57.
- Shani, M. R. and Khan, E., 1968. *Probison dehmi* n. g. n. sp., a recent find of the Upper Siwalik bovid. *Mitteilungen der Bayerischen Staatssammlung für Paläontologie und Histor. Geologie*, 8, 247–251.
- Sher, A.V., 1997. An Early Quaternary *Bison* population from Untermaßfeld: *Bison menneri* sp. nov. In: Kahlke, R.D. (Ed.), *Das Pleistozän von Untermaßfeld bei Meiningen (Thüringen)*, 2. Römisch-Germanisches Zentralmuseum, Mainz: 101–180.
- Simpson, G.G., 1941. Large pleistocene felines of North America. *American museum novitates*, 1136: 1–27.
- Siori, M.S., Boero, A., Carnevale, G., Colombero, S., Delfino, M., Sardella, R. and Pavia, M., 2014. New data on Early Pleistocene vertebrates from Monte Argentario (Central Italy). Paleocological and biochronological implications. *Geobios*, 47(6): 403–418.
- Sipko, T.P., 2009. European bison in Russia—past, present and future. *European Bison Conservation Newsletter*, 2: 148–159.
- Sirakov, N., Guadelli, J.L., Ivanova, S., Sirakova, S., Boudadi-Maligne, M., Dimitrova, I., Ph, F., Ferrier, C., Guadelli, A., Iordanova, D. and Iordanova, N., 2010. An ancient continuous human presence in the Balkans and the beginnings of human settlement in western Eurasia: A Lower Pleistocene example of the Lower Palaeolithic levels in Kozarnika cave (North-western Bulgaria). *Quaternary International*, 223: 94–106.
- Skinner, M.F. and Kaisen O.C., 1947. The Fossil *Bison* of Alaska and Preliminary Revision of the Genus. *Bulletin of the American Museum of Natural History*, 89(12): 7–256.

- Sokolov, J.J. 1953. *Natural Classification of Bovidae. Trudy Zoologicheskogo Instituta, Akademiya Nauk SSSR*, 14: 1–295.
- Sorbelli, L., Villa, A., Gentili, S., Cherin, M., Carnevale, G., Tschopp, E. and Delfino, M., 2021. The Early Pleistocene ectothermic vertebrates of Pietrafitta (Italy) and the last Western European occurrence of *Latonia* Meyer, 1843. *Comptes Rendus Palevol*, 20(26): 555–583.
- Sotnikova, M.V. and Foronova, I.V., 2014. First Asian record of *Panthera (leo) fossilis* (Mammalia, Carnivora, Felidae) in the early Pleistocene of western Siberia, Russia. *Integrative Zoology*, 9(4): 517–530.
- Soubrier, J., Gower, G., Chen, K., Richards, S.M., Llamas, B., Mitchell, K.J., Ho, S.Y., Kosintsev, P., Lee, M.S., Baryshnikov, G., Bollongino, R., 2016. Early cave art and ancient DNA record the origin of European bison. *Nature Communications* 7: 13158.
- Souron, A., Boisserie, J.R. and White, T.D., 2013. A new species of the suid genus *Kolpochoerus* from Ethiopia. *Acta Palaeontologica Polonica*, 60(1): 79–96.
- Spaan, A., 1992. A revision of the deer from Tegelen (province of Limburg, The Netherlands). *Scripta Geologica*, 98: 1–85.
- Spassov, N., 2003. The Plio-Pleistocene vertebrate fauna in South-Eastern Europe and megafaunal migratory waves from the east of Europe. *Revue de Paléobiologie*, 22 (1): 197–229.
- Spaulding, M., O'Leary, M.A. and Gatesy, J., 2009. Relationships of Cetacea (Artiodactyla) among mammals: increased taxon sampling alters interpretations of key fossils and character evolution. *Plos one*, 4(9): e7062.
- Stampfli, H.R., 1963. Wisent, *Bison bonasus* (Linné, 1758), Ur, *Bos primigenius* Bojanus, 1827, und Hausrind, *Bos taurus* Linné, 1758. *Seeburg Burgäschisee-Süd*, 3: 117–206.
- Stewart, J.R. and Lister, A.M., 2001. Cryptic northern refugia and the origins of the modern biota. *Trends in Ecology & Evolution*, 16(11): 608–613.
- STG, Stratigraphic Table of Germany 2002. German Stratigraphic Commission. GeoForschungsZentrum, Potsdam.
- Swofford, D.L., 2002. *PAUP*. Phylogenetic Analysis Using Parsimony (*and Other Methods)*, Version 4. Sinauer Associates, Sunderland: 142 p.
- Szymanek, M. and Julien, M.A., 2018. Early and Middle Pleistocene climate-environment conditions in Central Europe and the hominin settlement record. *Quaternary Science Reviews*, 198: 56–75.

- Tachikawa, K., Rapuc, W., Vidal, L., Dubois-Dauphin, Q., Westerhold, T., Guihou, A., Bickert, T., Pérez-Asensio, J.N., Deschamps, P. and Skonieczny, C., 2021. Eastern Atlantic deep-water circulation and carbon storage inferred from neodymium and carbon isotopic compositions over the past 1.1 million years. *Quaternary Science Reviews*, 252: 106752.
- Tappen, M., Adler, D.S., Ferring, C.R., Gabunia, M., Vekua, A. and Swisher III, C.C., 2002. Akhalkalaki: the taphonomy of an Early Pleistocene locality in the Republic of Georgia. *Journal of Archaeological Science*, 29(12): 1367–1391.
- Tedford, R.H., Flynn, L.J., Zhanxiang, Q., Opdyke, N.D. and Downs, W.R., 1991. Yushe Basin, China; Paleomagnetically calibrated mammalian biostratigraphic standard from the late Neogene of eastern Asia. *Journal of Vertebrate Paleontology*, 11(4): 519–526.
- Teilhard de Chardin, P., and Piveteau, J., 1930. Les mammifères fossiles de Nihowan (Chine). *Annales de Paléontologie*, 19: 1–154.
- Teilhard de Chardin, P., Trassaert, M., 1938. Caviconia of south-eastern shansi. *Palaeontologia Sinica. New series C*, 6, 1–106.
- Terhune, C.E., Curran, S., Croitor, R., Drăgușin, V., Gaudin, T., Petculescu, A., Robinson, C., Robu, M. and Werdelin, L., 2020. Early Pleistocene fauna of the Olteț River Valley of Romania: Biochronological and biogeographic implications. *Quaternary International*, 553: 14–33.
- Thenius, E. (1970). Zur Evolution und Verbreitungsgeschichte der Suidae. *Zeitschrift für Säugetierkunde*, 35: 321–342.
- Theodor, J.M., Erfurt, J., and Métais, G., 2007. The earliest artiodactyls. In: Prothero, D.R., and Foss, S.E. (Eds.), *The Evolution of Artiodactyla*: John Hopkins University Press, Baltimore: 32–58.
- Tiedemann, R., Sarnthein, M. and Shackleton, N.J., 1994. Astronomic timescale for the Pliocene Atlantic $\delta^{18}\text{O}$ and dust flux records of Ocean Drilling Program Site 659. *Paleoceanography*, 9(4): 619–638.
- Tong, H.W., Chen, X., Zhang, B., 2016. New fossils of *Bison palaeosinensis* (Artiodactyla, Mammalia) from the steppe mammoth site of early pleistocene in Nihewan Basin, China. *Quaternary International*, 445: 450–468.
- Toro-Moyano, I., Martínez-Navarro, B., Agustí, J., Souday, C., de Castro, J.M.B., Martínón-Torres, M., Fajardo, B., Duval, M., Falguères, C., Oms, O. and Parés, J.M., 2013. The oldest human fossil in Europe, from Orce (Spain). *Journal of Human Evolution*, 65(1): 1–9.
- Tsoukala, E. and Bonifay, M.F., 2004. The early Pleistocene carnivores (Mammalia) from Ceysaguet (Haute-Loire). *Paléo (Les Eyzies de Tayac-Sireuil)*, (16): 193–242.

- Tsoukala, E. and Guérin, C., 2016. The Rhinocerotidae and Suidae of the Middle Pleistocene from Petralona Cave (Macedonia, Greece). *Acta Zoologica Bulgarica*, 68(2): 243–264.
- Tsoukala, E. and Chatzopoulou, K., 2005. A new Early Pleistocene (latest Villafranchian) site with mammals in Kalamotó (Mygdonia Basin, Macedonia, Greece)—preliminary report. *Mitteilungen der Kommission für Quartärforschung der Österreichischen Akademie Wissen*, 14: 213–233.
- Valli, A.M., Caron, J.B., Debard, E., Guérin, C., Pastre, J.F. and Argant, J., 2006. Le gisement paléontologique villafranchien terminal de Peyrolles (Issoire, Puy-de-Dôme, France): résultats de nouvelles prospections. *Geodiversitas*, 28(2): 297–317.
- Vallverdu, J., Saladie, P., Rosas, A., Huguet, R., Cáceres, I., Mosquera, M., Garcia-Tabernero, A., Estalrich, A., Lozano-Fernández, I., Pineda-Alcalá, A. and Carrancho, Á., 2014. Age and date for early arrival of the Acheulian in Europe (Barranc de la Boella, la Canonja, Spain). *PloS one*, 9(7): 103634.
- Van den Hoek, O., L.W. and de Vos, J., 2006. A century of research on the classical locality of Tegelen (province of Limburg, The Netherlands). *Courier Forschungsinstitut Senckenberg*, 256: 291–304.
- Van der Made, J., 1996. Listriodontinae (Suidae, Mammalia), their evolution, systematics and distribution in time and space. *Contributions to Tertiary and Quaternary Geology*, 33: 3–254.
- Van der Made, J., 1997. Los suoides de la Península Ibérica. In: Calvo, J.P., Morales, J., (Eds) *Avances en el conocimiento del Terciario Ibérico*, Madrid: 109–112.
- Van der Made, J., 1998. Biometrical trends in the Tetraconodontinae, a subfamily of pigs. *Earth and Environmental Science Transactions of The Royal Society of Edinburgh*, 89(3): 199–225.
- Van der Made, J., 1999. Ungulates from Atapuerca TD6. *Journal of Human Evolution*, 37(3–4): 389–413.
- Van der Made, J., 2013. First description of the large mammals from the locality of Penal, and updated faunal lists for the Atapuerca ungulates—*Equus altidens*, *Bison* and human dispersal into Western Europe. *Quaternary International*, 295: 36–47.
- Van der Made, J. and Moyà-Solà, S., 1989. European Suinae (Artiodactyla) from the late Miocene onwards. *Bollettino della Società Paleontologica Italiana*, 28(2–3): 329–339.
- Van der Made, J. and Hussain, T. S. 1992. Sanitheres from the Miocene Manchar Formation of Sind, Pakistan and remarks on sanithere taxonomy and stratigraphy. *Proceedings of the Koninklijke Nederlandse Akademie van Wetenschappen*, 95: 81–95.

- Van der Made, J., Morales, J. and Montoya, P., 2006. Late Miocene turnover in the Spanish mammal record in relation to palaeoclimate and the Messinian Salinity Crisis. *Palaeogeography, Palaeoclimatology, Palaeoecology*, 238(1-4): 228–246.
- Van der Made, J., Rosell, J. and Blasco, R., 2017. Faunas from Atapuerca at the Early–Middle Pleistocene limit: The ungulates from level TD8 in the context of climatic change. *Quaternary International*, 433: 296–346.
- Van Vuure, C. 2005. *Retracing the Aurochs: History, Morphology and Ecology of an Extinct Wild Ox*. Pensoft Publishers, Sofia: 431 p.
- Vangengeim, E.A., 2010. Evolution of views on Quaternary stratigraphic scales worked out in the Geological Institute, Russian Academy of Sciences. *Stratigraphy and Geological Correlation*, 18: 674–684.
- Vaquero, M., Van der Made, J., Blain, H.A., Ibáñez, N., López-García, J.M., Rivals, F., Alonso, S., Ameijenda, A., Bennàsar, M., Fernández-García, M. and de Lombera-Hermida, A., 2018. Fauna, environment and human presence during MIS5 in the North of Spain: The new site of Valdavara 3. *Comptes Rendus Palevol*, 17(8): 557–593.
- Vasiliev, S.K., 2008. Late Pleistocene bison (*Bison p. priscus* Bojanis, 1827) from the southeastern part of western Siberia. *Archaeology, Ethnology and Anthropology of Eurasia*, 34(2): 34–56.
- Vasiliev, S.K., Remains of the Baikal yak (*Poehpagus mutus baikalensis* N. Verestchagin, 1954) from Late Pleistocene localities of Southern Siberia. *Proceedings of the Zoological Institute RAS*, 325(4): 384–408.
- Vekua A. K., 1972: *Kvabebi fauna of Akchagylian vertebrates*. Nauka, Moscow: 351 p.
- Vekua, A., 1987. The Lower Pleistocene mammalian fauna of Akhalkalaki (Southern Georgia, USSR). *Palaeontographia Italica* 74: 63–96.
- Velitzelos, D., Bouchal, J.M. and Denk, T., 2014. Review of the Cenozoic floras and vegetation of Greece. *Review of Palaeobotany and Palynology*, 204: 56–117.
- Verkaar, E.L., Nijman, I.J., Beeke, M., Hanekamp, E. and Lenstra, J.A., 2004. Maternal and paternal lineages in cross-breeding bovine species. Has wisent a hybrid origin? *Molecular biology and evolution*, 21(7): 1165–1170.
- Villa, A., Blain, H.A., van den Hoek Ostende, L.W. and Delfino, M., 2018. Fossil amphibians and reptiles from Tegelen (Province of Limburg) and the early Pleistocene palaeoclimate of The Netherlands. *Quaternary Science Reviews*, 187: 203–219.
- Vislobokova, I.A. and Agadjanyan, A.K., 2016. New data on age of the Pleistocene fauna from the Trlica locality (Montenegro, Central Balkans) and its correlation with other faunas of Europe. *Stratigraphy and Geological Correlation*, 24(2): 188–202.

- Von den Driesch, A., 1976. *A guide to the measurement of animal bones from archaeological sites (Vol. 1)*. Peabody Museum of Archaeology and Ethnology Press, Cambridge: 136 p.
- Vrba, E.S., 1987. A revision of the Bovini (Bovidae) and a preliminary revised checklist of Bovidae from Makapansgat. *Palaeontologia africana*, 26(4): 33–46.
- Wang, K., Lenstra, J.A., Liu, L., Hu, Q., Ma, T., Qiu, Q. and Liu, J., 2018. Incomplete lineage sorting rather than hybridization explains the inconsistent phylogeny of the wisent. *Communications biology*: 1(1): 1–9.
- Westerhoff, W.E., Donders, T.H., Alexandre, N.T. and Busschers, F.S., 2020. Early Pleistocene Tiglian sites in the Netherlands: A revised view on the significance for quaternary stratigraphy. *Quaternary Science Reviews*: 242: 106417.
- White, T.D. and Harris, J.M., 1977. Suid evolution and correlation of African hominid localities. *Science*, 198(4312): 13–21.
- Zeyland, J., Wolko, Ł., Lipiński, D., Woźniak, A., Nowak, A., Szalata, M., Bocianowski, J. and Słomski, R., 2012. Tracking of wisent–bison–yak mitochondrial evolution. *Journal of applied genetics*, 53(3): 317–322.
- Zhou, X., Xu, S., Yang, Y., Zhou, K. and Yang, G., 2011. Phylogenomic analyses and improved resolution of Cetartiodactyla. *Molecular Phylogenetics and Evolution*, 61(2): 255–264.
- Zong G F, 1984. Fossils of *Bos primigenius* from Apa Tibetan Autonomous Prefecture, Sichuan. *Vertebrata Palasiatica*, 25(1): 69–76.
- Zucchetta, G., Gentili, S., and Pavia, M., 2003. A new early Pleistocene bird association from Pietrafitta (Perugia, Central Italy). *Rivista Italiana di Paleontologia e Stratigrafia*, 109(3): 527–538.
- Zurano, J.P., Magalhães, F.M., Asato, A.E., Silva, G., Bidau, C.J., Mesquita, D.O. and Costa, G.C., 2019. Cetartiodactyla: updating a time-calibrated molecular phylogeny. *Molecular phylogenetics and evolution*, 133: 256–262.

SUPPLEMENTARY SECTION

Chapter S1

Original paper and supplementary material:

Cherin, M., Alba, D.M., Crotti, M., Menconero, S., Moullé, P.É., Sorbelli, L. and Madurell-Malapeira, J., 2020. The post-Jaramillo persistence of *Sus strozzi* (Suidae, Mammalia) in Europe: new evidence from the Vallparadís Section (NE Iberian Peninsula) and other coeval sites. *Quaternary Science Reviews*, 233: 106234.

DOI: <https://doi.org/10.1016/j.quascirev.2020.106234>



The post-Jaramillo persistence of *Sus strozzi* (Suidae, Mammalia) in Europe: New evidence from the Vallparadís Section (NE Iberian Peninsula) and other coeval sites

Marco Cherin ^{a, *}, David M. Alba ^b, Marco Crotti ^c, Sofia Menconero ^d, Pierre-Élie Moullé ^e, Leonardo Sorbelli ^b, Joan Madurell-Malapeira ^b

^a Dipartimento di Fisica e Geologia, Università degli Studi di Perugia, Via A. Pascoli, 06123, Perugia, Italy

^b Institut Català de Paleontologia Miquel Crusafont, Universitat Autònoma de Barcelona, Edifici ICTA-ICP, c/ Columnes s/n, Campus de la UAB, 08193, Cerdanyola del Vallès, Barcelona, Spain

^c Institute of Biodiversity, Animal Health and Comparative Medicine, University of Glasgow, G12 8QQ, Glasgow, UK

^d Dipartimento di Storia, Disegno e Restauro dell'Architettura, Sapienza Università di Roma, P.le A. Moro 5, 00185, Roma, Italy

^e Musée de Préhistoire Régionale de Menton, 06500, Menton, France

ARTICLE INFO

Article history:

Received 25 October 2019

Received in revised form

30 January 2020

Accepted 15 February 2020

Available online xxx

Keywords:

Dispersal

Early-Middle Pleistocene transition

Epivillafranchian

Europe

Quaternary

Suidae

Systematics

ABSTRACT

The Vallparadís composite section (VCS) includes the nearby paleontological sites of Cal Guardiola and Vallparadís Estació (Vallès-Penedès Basin, northeastern Iberian Peninsula). The section spans from before the Jaramillo subchron to the early Middle Pleistocene (ca. 1.2–0.6 Ma). In this study, we describe the suid record from VCS and we review those from several other European sites, in order to refine the taxonomic identity and chronostratigraphic range of Quaternary suids in Europe. The VCS sample includes a nearly complete skull, several teeth, and postcranial elements, and stands out as the richest European suid collection from the latest Early Pleistocene. Suid remains have been unearthed from both Cal Guardiola and Vallparadís Estació layers, whose age spans from the Jaramillo subchron (ca. 1.07–0.99 Ma; MIS31) to post-Jaramillo time (ca. 0.86 Ma; MIS21). Several craniomandibular and dental morphological features support an attribution to *Sus strozzi*. These features include a low and very deep preorbital fossa, a narrow nuchal crest, a well-developed longitudinal swelling in the middle of the mandibular corpus, the presence of styles/stylids in the upper/lower premolars, and especially the “verrucosic” morphology of the lower canine. The attribution to *S. strozzi* is also sustained by a cladistic analysis. These results provide interesting clues on the chronological occurrence of Quaternary suids. *Sus strozzi* is relatively common in Europe during the middle and early late Villafranchian (ca. 2.5–1.8 Ma), but it almost completely disappears during the latest Villafranchian (ca. 1.8–1.2 Ma). During and slightly after the Epivillafranchian (ca. 1.2–0.8 Ma), *S. strozzi* reappears in Europe although with relatively small samples, at VCS and several other sites including Untermassfeld (Germany; ca. 1.0 Ma), Le Vallonnet (France; ca. 1.2–1.1 Ma), Taman Peninsula (Russia; ca. 1.1–0.8 Ma), Arda River (Italy; ca. 0.99 Ma), and Slivia (Italy; ca. 0.8 Ma), among others. Consequently, in contrast to previous knowledge, we conclude that (1) *S. strozzi* survived in Europe (or returned there with a second dispersal event from Asia during the Epivillafranchian) at least until the end of the Early Pleistocene and (2) the arrival of *Sus scrofa* into that continent is not older than the Early-Middle Pleistocene boundary.

Crown Copyright © 2020 Published by Elsevier Ltd. All rights reserved.

1. Introduction

At the beginning of the Quaternary, suids are represented in

Europe by a single species of the subfamily Suidae, namely *Sus strozzi*. This large-sized species is overall morphologically similar and phylogenetically related to extant and extinct suines occurring in Island South East Asia (ISEA) (Azzaroli, 1954; Cherin et al., 2018). The most primitive species of this clade—as well as the earliest member of the genus *Sus*—is *Sus arvernensis*, occurring during the Pliocene (Ruscinian and early Villafranchian Land Mammal Ages;

* Corresponding author.

E-mail address: marco.cherin@unipg.it (M. Cherin).

LMAs) from Europe to China (Cherin et al., 2018). Living representatives of the clade such as *Sus verrucosus* or *Sus celebensis*, are sometimes known as “warty pigs”, due the presence of facial warts of different shapes, particularly developed in males (Groves and Grubb, 1993). One of the main skeletal synapomorphies of this clade of suines is the “verrucosic” morphology of the male lower canine—i.e., the tooth cross-section is shaped like an isosceles triangle, with the distal side being the shortest (Stehlin, 1899–1900; see Section 5.1).

Sus strozzi replaces *S. arvernensis* at the beginning of the Early Pleistocene, i.e., at the early-middle Villafranchian transition (ca. 2.6 Ma). The former species is recorded in nearly 30 sites in Europe from the Iberian Peninsula to Azerbaijan, and in Israel (Cherin et al., 2018 and references therein). The ages of these localities span the whole Gelasian, i.e., the middle and early late Villafranchian, before the Olduvai subchron (ca. 1.8 Ma). The only geologically younger exceptions are (1) some dentognathic remains from ‘Ubeidiya, Israel, approximately dated to 1.6–1.3 Ma (Geraads et al., 1986; Martínez-Navarro et al., 2009, 2012); (2) the scanty record from the Ellera basin, Italy (Pazzaglia et al., 2013), whose alleged age of 1.6–1.5 Ma is doubtful (Martínez-Navarro et al., 2015); and (3) undescribed remains of *Sus* sp. reported—but never described—in the faunal list of Pirro Nord (latest Villafranchian of southern Italy; Freudenthal, 1971; De Giuli et al., 1986). Besides the above poor and/or doubtful records, no occurrences of *S. strozzi*, nor any other species of Suidae, are confirmed to date in Europe during the latest Villafranchian (ca. 1.8–1.2 Ma). According to Martínez-Navarro et al. (2015), this “suid gap” cannot be explained by taphonomic causes. As a matter of fact, suids are opportunistic feeders with r-selection-like life history profile, which allows them to display high dispersal rates in very different environments and, in turn, corresponds to a relatively high preservation rate. In addition, suid remains have never been found even at latest Villafranchian sites that yielded hundreds to thousands of vertebrate fossils, such as Dmanisi (Georgia), Pietrafitta (Italy), Venta Micena, Fuente Nueva-3, or Barranco León (Spain). This evidence makes unlikely that the gap is the result of low sampling effort (Martínez-Navarro et al., 2015).

After the “suid gap”, *Sus* reappears in the European record during the Epivillafranchian (ca. 1.2–0.8 Ma), that is, the intermediate biochron between the Villafranchian and Galerian (Kahlke et al., 2011; Madurell-Malapeira et al., 2014, 2017; Bellucci et al., 2015). To date, it has been widely accepted that the recolonization of Europe by suines was due to the wild boar, *Sus scrofa*, which would have replaced the extinct *S. strozzi* (Kahlke et al., 2011; Martínez-Navarro et al., 2015). Indeed, the arrival of *S. scrofa* in Europe has been considered as a biochronological marker for the beginning of the Epivillafranchian (Bellucci et al., 2015; Martínez-Navarro et al., 2015). In some cases, these alleged early wild boar records have been attributed to the subspecies *S. scrofa priscus*—e.g., see Guérin and Faure (1997) for the Epivillafranchian site of Untermassfeld, Germany. This taxon was established as a distinct species, *Sus priscus*, by Goldfuss (1823) based on a single edentulous maxillary fragment from Heinrichshöhle Cave at Sundwig, Germany, whose earliest layers are not older than 250 ka (Riechelmann et al., 2014). de Serres, 1835 considered it as a valid species, to which he referred the well-preserved mid-Middle Pleistocene material from Lunel-Viel, France. However, the taxon was later interpreted as a subspecies of *S. scrofa* by Hünermann (1969), further including as a junior synonym *S. scrofa mosbachensis*, which had initially been established by Kütze (1933) for the Middle Pleistocene material from Mosbach and Mauer, Germany (Kuss, 1961; Guérin and Faure, 1997). Being almost entirely based on size differences, we consider that the taxonomic validity of *S. scrofa priscus* is doubtful (see Section 4.5 for a discussion on the

reliability of tooth dimensions as diagnostic characters in suines).

One of the main incentives to undertake the present study was the publication of a nearly complete mandible of *S. strozzi* from the site of Frantoio, Arda River, Italy (Bona and Sala, 2016). Being dated to ca. 0.99 Ma, this record represents the last occurrence of *S. strozzi* and an evidence of the survival of this species after the latest Villafranchian “suid gap” (Cherin et al., 2018). Starting from this evidence, we have undertaken a comprehensive review of the Epivillafranchian and early Galerian European suine record, in order to ascertain the taxonomic attribution of the available remains and hence clarify the chronostratigraphic distribution of *S. strozzi* and *S. scrofa*. With this aim in mind, here we describe the unpublished material from the Vallparadís composite section (VCS; Iberian Peninsula), which represents the richest *Sus* sample for the considered time span, and we further review the suine records from other late Early Pleistocene European key sites such as Untermassfeld (Germany), Le Vallonnet (France), and Slivia (Italy).

1.1. Geographical and geological framework

The VCS includes two different paleontological sites, Cal Guardiola (CGR) and Vallparadís Estació (EVT), respectively located in the western and eastern banks of the Torrent de Vallparadís, in the center of the town of Terrassa (Madurell-Malapeira et al., 2010, 2014, 2017). The studied area belongs to the Vallès-Penedès Basin, a NE-SW graben parallel to the Catalan margin (Cabrera and Calvet, 1996). The deposits of the VCS correspond to the Pleistocene alluvial fan system of Terrassa that overlies a marked Mio-Pliocene paleorelief. The CGR sediments, unearthed during construction works in 1997, consist of a 7 m-thick unit of massive decimetric to centimetric conglomerates and gravels in a matrix-supported fabric. The seven layers recognized in the outcrop are about 1 m thick and yield fossil remains of vertebrates and plants. The richest paleontological layers correspond to the units CGRD7 and CGRD2 (Madurell-Malapeira et al., 2010, 2017). The EVT site, also discovered during construction works from 2005 to 2008, is a 14 m-thick sedimentary sequence, which is mainly composed by conglomerates and mudstones separated by an erosive angular unconformity. The lower unit (layers EVT6 to EVT12; Madurell-Malapeira et al., 2014) is made up of clast-supported, polymictic, and poorly-sorted conglomerate layers with a thickness of about 1 m. The upper unit (layers EVT1 to EVT5) starts with poorly-sorted conglomerates that show an erosive lower contact. This bed is 1 m thick, its fabric is clast-supported, and laterally passes into mudstones. Massive brownish mudstones with paleosols, root-marks, and freshwater gastropods crop out at the top of the upper unit.

1.2. Chronology

On the basis of magnetostratigraphic and biostratigraphic data, the VCS spans from before the Jaramillo paleomagnetic subchron (ca. 1.2–1.1 Ma) to the early Middle Pleistocene (0.6 Ma; Madurell-Malapeira et al., 2010, 2014, 2017; Minwer-Barakat et al., 2011). This time span can be divided into four intervals: R1, pre-Jaramillo times (layers CGRD1 to CGRD3), with a reversed paleomagnetic polarity; N1, the Jaramillo subchron (bottom of layer EVT8, and layers EVT9 to EVT12), with a normal polarity; R2, post-Jaramillo, Matuyama times, with a reversed polarity (bottom of layer EVT3, layers EVT4 to EVT7 and the top of layer EVT8 and layers CGRD4 to CGRD8); N2, early Middle Pleistocene times (layers EVT2 and EVT3), with a normal polarity that corresponds to the beginning of the Brunhes chron (Madurell-Malapeira et al., 2010, 2014, 2017; Minwer-Barakat et al., 2011).

The specimens studied in this paper come from layer EVT12

correlated with the Jaramillo subchron (1.07–0.99Ma; MIS31) and layers EVT7 and CGRD7 correlated with the post-Jaramillo interval of the Matuyama chron (0.99–0.78Ma). An absolute dating of 0.858 ± 0.087 Ma was obtained for EVT7 based on the ESR method (Duval et al., 2015), which probably corresponds to the interglacial stage MIS21.

2. Materials and methods

2.1. Materials

The new *Sus* material from VCS is housed at the Institut Català de Paleontologia Miquel Crusafont and is listed in Table 1. The craniomandibular and dental specimens were compared to the available material of *S. strozzii* from different European sites, recently reviewed by Cherin et al. (2018).

Dental terminology used in this study is after Van der Made (1996). Morphometric measurements of the VCS specimens were recorded to the nearest 0.1 mm with a digital caliper, mainly following Von den Driesch (1976) and Cherin et al. (2018). Comparative measurements of m3 (maximum length and width), which are widely used in the literature for systematic purposes, are from Cherin et al. (2018) for *S. strozzii* and *S. arvernensis*, and from Hünemann (1975, 1977, 1978), Albarella et al. (2009), and Lister et al. (2010) for fossil and extant *S. scrofa*. Labial, lingual, and distal lengths of lower canines were taken near the alveolus for teeth inserted in the mandible and at the level of wider section (roughly corresponding to half length) for isolated teeth. To compare lower canine morphology and proportions, we only considered adult male individuals. We did not include isolated teeth for which a reasonably certain sex determination was not possible. Comparative measurements (labial, lingual, and distal length) of lower canines of extant and extinct suines were taken from specimens stored in HHNM, IGF, IQW, ISEM, MCSNT, MZUF,

NHM, NHM:MZ, and NRM (see abbreviations below). Additional measurements were taken from Hünemann (1977, 1978), Fistani (1996), Titov (2000), Fujita et al. (2000), and Bona and Sala (2016), or kindly provided by colleagues from several European institutions (see Acknowledgments). The final dataset is composed of a total of 120 specimens of different *Sus* species (Appendix 3).

In order to assess the level of morphological divergence between “scrofic” and “verrucosic” canines, the distal/labial and lingual/labial ratios were compared between canine types with an analysis of variance (ANOVA) in the R statistical environment (R Core Team, 2019). Furthermore, we conducted a principal component analysis (PCA) with the function *prcomp* in R on the Mosimann shape variables, i.e., the three canine sizes (lengths of labial, lingual, and distal sides) standardized by their geometric mean, so as to identify the major axes of phenotypic variation. Whenever possible, the three lengths were averaged between the left and right canines.

2.2. Photogrammetry

A 3D model of the VCS cranium IPS107041a (Appendix 1) was obtained through the Structure-from-Motion photogrammetric technique (Remondino and El-Hakim, 2006), starting from a set of 221 digital images. The acquisition was made with a Nikon D750 DSLR camera with a focal length of 62 mm, without having a photo-set designed for the specific specimen. This led to several problems during the elaboration. The problems encountered in the acquisition phase are related to the positioning of the cranium in the various rotations. In small-scale photogrammetry operations, it is common practice to place the object on a neutral background and rotate it gradually until it is photographed at 360°. Sometimes the morphology of the fossil does not allow to place it in all the positions necessary to have a good coverage for the alignment of the frames. In this specific case, the cranium was entirely photographed, as it does not present any missing portions, but the

Table 1
List of fossil material of *Sus strozzii* from VCS. EVT, Vallparadís Estació; CGR, Cal Guardiola.

ID	Layer	Anatomical element	Preserved parts	Side
n/a	EVT7	Tooth fragment	Not identifiable	–
IPS107041a	EVT7	Cranium	Almost complete	–
IPS107041b	EVT7	Hemimandible with c1-m3	Almost complete	Right
IPS107041c	EVT7	Hemimandible with c1-m3	Almost complete	Left
IPS107042	EVT7	C1	Complete crown	Left
IPS107043	EVT7	I2	Crown and partial root	Right
IPS107044a	EVT12	dI2	Almost complete	Right
IPS107044b	EVT12	C1	Fragmented crown	Left
IPS107045	EVT7	Lower tooth fragment	Crown fragment	–
IPS107046	EVT7	Tooth fragment	Not identifiable	–
IPS107047	EVT7	c1	Crown (fragmented)	Left
IPS107049	EVT7	m3	Crown (fragmented mesially) and partial root	Left
IPS107050	EVT7	m3	Crown (mesial part) and root fragments	Right
IPS107051a-b	EVT12	P4-M1	Crown (P4 complete, M1 fragmented)	Left
IPS107052	EVT7	m3	Crown and partial root	Left
IPS107053	EVT7	Tooth fragment	Not identifiable	–
IPS107054	EVT7	c1	Crown (very fragmented)	Left?
IPS107055	EVT12	Maxillary fragment with dp3-dp4	Complete crowns	Right
IPS107056	EVT7	M1	Crown (fragmented mesiolabially)	Right
IPS107057	EVT12	Maxillary fragment with C1-M2	Complete crowns	Right
IPS107058	EVT7	M3	Crown and root fragment	Right
IPS107061	EVT7	Humerus	Fragmented shaft	–
IPS107062	EVT7	Astragalus	Almost complete	Left
IPS107063	EVT7	Astragalus	Complete	Right
IPS107064	EVT7	Scapula	Partially preserved	Left
IPS107065	EVT7	Bone fragments	Not identifiable	–
IPS107066	EVT7	Tibia	Proximal part fragmented	Right
IPS13818	CGRD7	c1	Fragmented crown	?
IPS14972	CGRD7	Astragalus	Complete	Left
IPS20134	CGRD7	P4	Crown and partial root	–

overlap between adjacent frames was enough to allow the automatic alignment of the images by the software Agisoft Photoscan v. 1.2.6.

The software enabled the automatic alignment of a few photos at a time, corresponding to the single set acquired for each movement (rotation) of the object. The cranium was subjected to six rotations in total (Fig. 1a), and an average of 40 shots were taken for each rotation, i.e., for each set of photos. The method was to process one set at a time until it reached the dense point cloud; the dense clouds were then gradually oriented and merged together. The software failed to align the six clouds automatically, as there was not enough overlap between the parts. For this reason, the alignment was done manually, finding common points (at least three for every two contiguous sets) on the surface of the cranium (Fig. 1b). To make the relative orientation of the sets more "solid", we tried to take the homologous points as scattered as possible on the surface, avoiding close and aligned points.

The final point cloud also had noise problems due to the low level of illumination of the photos. To overcome this problem, the point cloud was imported into Geomagic Design X where it was cleaned by filtering outliers, i.e., those points that statistically deviate from the ideal surface represented discontinuously by the

points of the cloud. Finally, CloudCompare v. 2.10.2 was used to create the polygonal surface (Fig. 1c), which was then reimported into Photoscan for the application of photorealistic texture (Fig. 1d).

2.3. Phylogenetic analysis

A cladistic phylogenetic analysis was carried out by means of the data matrix published by Cherin et al. (2018). The phylogenetic reconstruction was performed in PAUP*4.0 (Swofford, 2002), under parsimony using heuristic searches with tree bisection reconnection branch-swapping algorithm and ACCTRAN optimization. All characters were treated as unordered and unweighted. Branch support was calculated with 100,000 bootstrap replicates with random stepwise addition, and with Bremer index using the bremer.run script in TNT 1.5 (Goloboff and Catalano, 2016). With respect to the original analysis by Cherin et al. (2018), we decided to exclude the Chinese species *Sus lydekkeri*. This is because only a single complete skull of the latter species (NNMO HY13-58.1-2 from Yangshuizhan in Nihewan Basin, China; Liu et al., 2017) is known to date, and the hypodigm of the species is heterogeneous and needs a revision. With the inclusion of the VCS suine and the exclusion of *S. lydekkeri*, we obtained a data matrix with 19

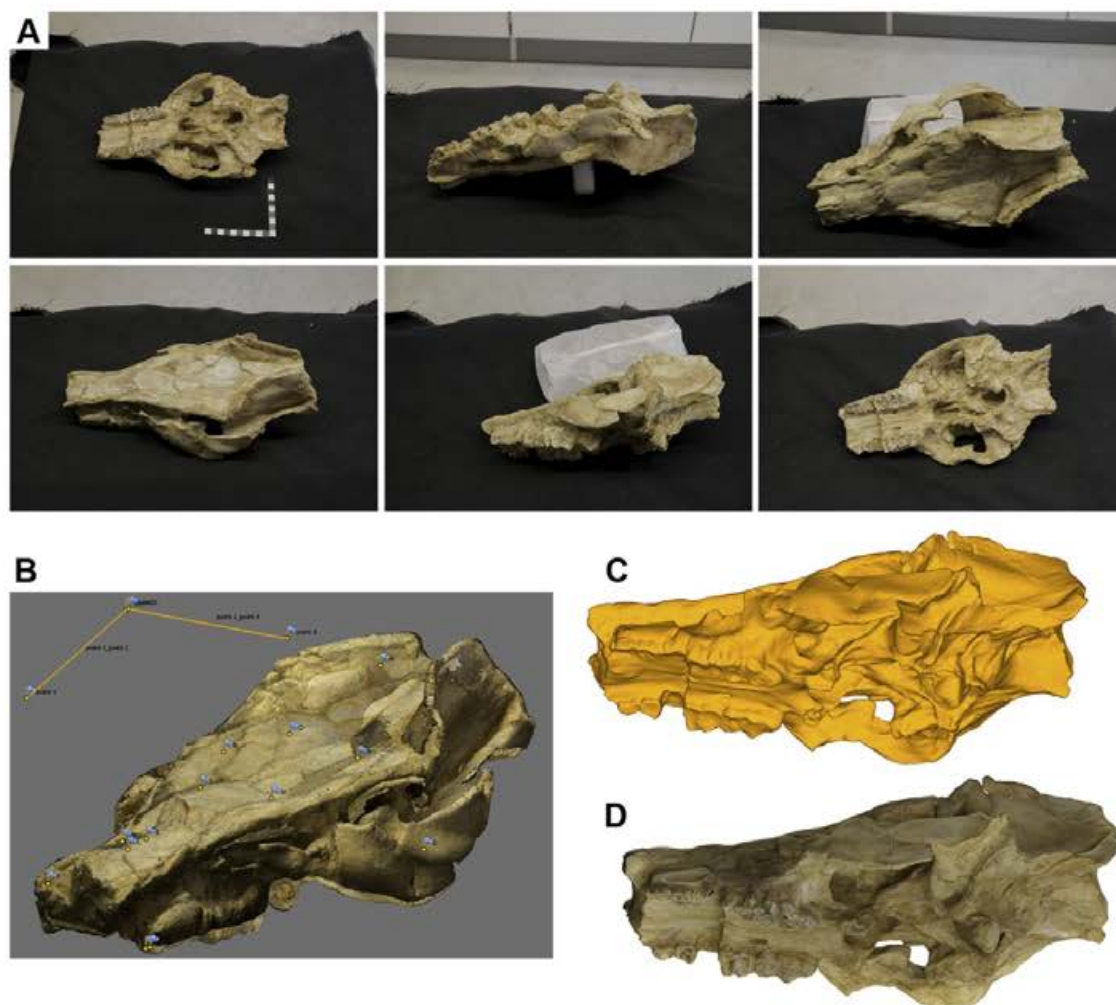


Fig. 1. Photogrammetry workflow. A, First shot for every position of the cranium; B, Homologous points between the six point clouds; C, Polygonal surface after the noise correction; D, Final model with texture (see Appendix 1).

operational taxonomic units and 52 craniomandibular and dental characters (Appendix 2).

Institutional abbreviations – HHM: Hungarian Natural History Museum, Budapest (Hungary); IGF: Museo di Storia Naturale, Sezione di Geologia e Paleontologia, Università di Firenze (Italy); IPS: Institut Català de Paleontologia Miquel Crusafont (Spain); IQW: Research Station of Quaternary Palaeontology, Senckenberg Research Institute (Germany); ISEM: Institut des Sciences de l'Évolution de Montpellier (France); IVPP: Institute of Vertebrate Paleontology and Paleoanthropology, Beijing (China); MCCA: Museo "G. Cortesi" di Castell'Arquato (Italy); MCSNT: Museo Civico di Storia Naturale di Trieste (Italy); MPRM: Musée de Préhistoire Régionale, Menton (France); MZUF: Museo di Storia Naturale, Sezione di Zoologia "La Specola", Università di Firenze (Italy); NHM: Natural History Museum, London (UK); NHM:MZ: Natural History Museum Mainz (Germany); NNMO: Nihewan National Nature Reserve Management Office, Hebei Province (China); NRM: Naturhistoriska Riksmuseet Stockholm (Sweden); SMNS: Staatliches Museum für Naturkunde Stuttgart (Germany).

3. Systematic paleontology

Order Cetartiodactyla Montgelard et al., 1997.

Family Suidae Gray, 1821.

Subfamily Suinae Gray, 1821.

Genus *Sus* Linnaeus, 1758.

Sus strozzii Forsyth-Major, 1881

(Figs. 2–4, Tables 2–4)

Type material: The lectotype IGF 424 was selected by Azzaroli (1954) because Forsyth-Major (1881) did not designate a holotype. It consists of an adult male partial skeleton including the cranium with mandible, 4 cervical, 14 thoracic, and 2 lumbar vertebrae, some fragmented ribs, both scapulae, and the proximal part of the left humerus.

Diagnosis: Large-sized suine with relatively narrow parietal region; gently undulating dorsal cranial profile in lateral view, with slight ventral concavity in the middle part; widely diverging and pneumatized zygomatic arches tending to be broader in the middle than at the rear (more gracile in females); laterally expanded nasals separated by a bony prominence; anteroposteriorly elongated and rugose supracanine flange in males (shaped as gracile and low crests in females); labial longitudinal thickening of the mandibular corpus (more gracile in females), with major lateral convexity in the middle; thick enamel in cheek teeth; verrucosic lower canines; elongated m3 with single cuspid (hypopreconulid) between the first and second lobes and well-developed talonid composed by four main distal cuspids arranged in a cross (Cherin et al., 2018).

Type locality: Upper Valdarno Basin, Tuscany (Italy).

Age and geographical distribution: Early Pleistocene of Europe and western Asia, from Spain to Azerbaijan. Biochronology: middle–early late Villafranchian (ca. 2.5–1.8 Ma) plus Epivillafranchian (ca. 1.2–0.8 Ma); no confirmed records from the latest Villafranchian (ca. 1.8–1.2 Ma) are known to date.

New material: The new material from VCS is listed in Table 1. It includes an almost complete cranium (IPS107041a) with associated mandible (IPS107041b and IPS107041c), two maxillary fragments

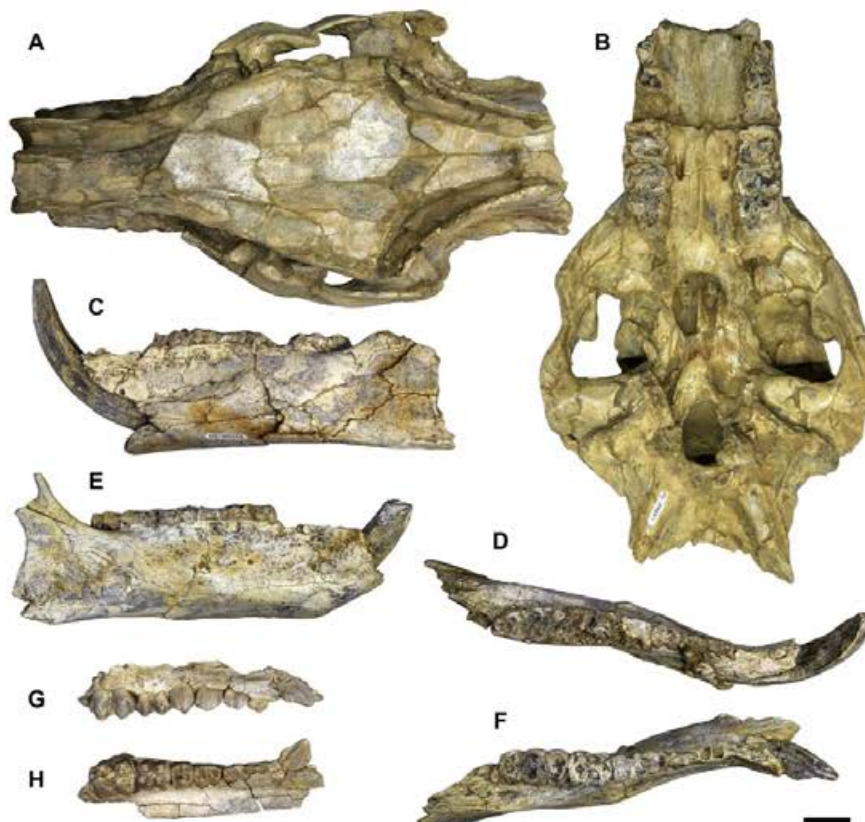


Fig. 2. *Sus strozzii* from the Vallparadis composite section (Iberian Peninsula). A–B, Cranium IPS107041a in dorsal (A) and ventral (B) views; C–D, Left hemimandible IPS107041c in labial (C) and occlusal (D) views; E–F, Right hemimandible IPS107041b in labial (E) and occlusal (F) views; G–H, Right maxilla IPS107057 in labial (G) and occlusal (H) views. Scale bar: 30 mm.

6

M. Cherin et al. / Quaternary Science Reviews 233 (2020) 106234

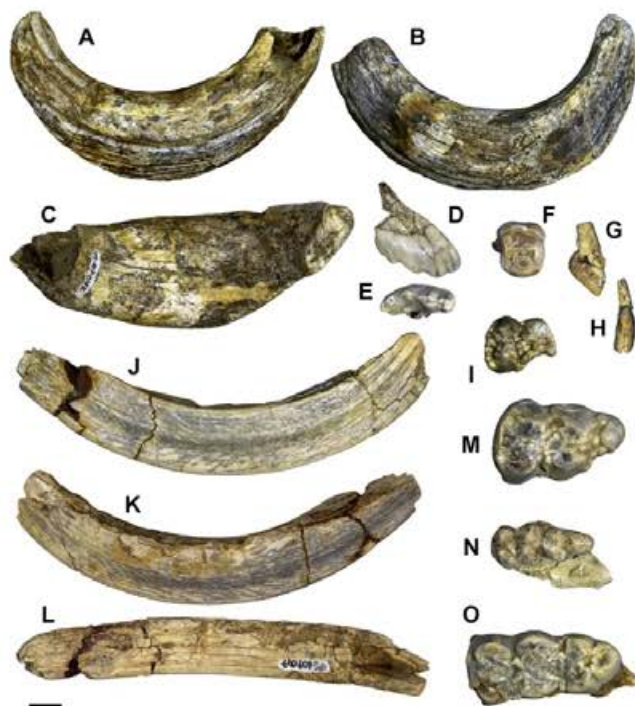


Fig. 3. *Sus strozzi* from the Vallparadis composite section (Iberian Peninsula). A-C, Right C1 IPS107042 in mesial (A), distal (B), and dorsal (C) views; D-E, Right I2 IPS107043 in labial (D) and occlusal (E) views; F, Left P4 IPS20134 in occlusal view; G-H, Right dI2 IPS107044a in labial (G) and distal (H) views; I, Right M1 IPS107056 in occlusal view; J-L, Left c1 IPS107047 in labial (J), lingual (K), and distal (L) views; M, Right M3 IPS107058 in occlusal view; N, Right maxillary fragment with DP3-dP4 IPS107055 in occlusal view; O, Left m3 IPS107052 in occlusal view. Scale bar: 10 mm.

with teeth (IPS107055 and IPS107057), several isolated upper and lower teeth, and some postcranial bones.

4. Results

4.1. Description

4.1.1. Cranium

IPS107041a (Fig. 2; 3D model in Appendix 1) is an almost complete cranium missing the anterior half of the muzzle (it is broken just anteriorly to the P3) and the right M1. Diagenetic deformation acted mainly in dorsoventral direction. The dorsal part of the cranium collapsed ventrally, especially in the frontoparietal area, with the orbits being displaced ventrally with respect to their original position. On the opposite side, the occipital squama is rotated anterodorsally, so that the occipital condyles and the foramen magnum are found in a ventral position at the base of the neurocranium. Conversely, the temporal fossae, temporal ridges, and zygomatic arches seem quite undeformed, like the muzzle, with the exception of a slight dorsal displacement of its anterior portion, resulting in a sharp longitudinal step between M1 and M2.

In dorsal view, the deformation of the specimen does not allow a detailed description. The frontal area gently enlarges from the frontonasal suture (marked by a longitudinal elevated fractured crest) to the orbital processes of the frontals. Unfortunately, the supraorbital sulci and foramina have been obliterated by diagenesis. Posteriorly, the neurocranium becomes much narrower, with the postorbital constriction being about as wide as the preserved part of the muzzle. The frontoparietal sutures are visible as two almost straight lines running obliquely from just behind the orbital

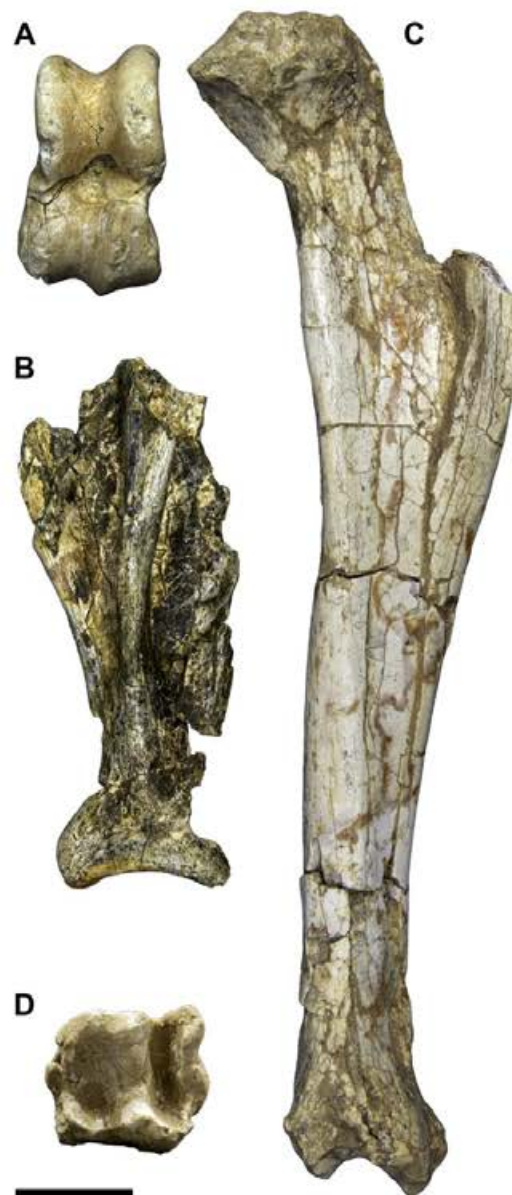


Fig. 4. *Sus strozzi* from the Vallparadis composite section (Iberian Peninsula). A, Left astragalus IPS14972 in dorsal view; B, Left scapula IPS107064 in dorsal view; C-D, Right tibia IPS107066 in medial (C) and distal (D) views. Scale bar: 30 mm.

processes to the straight interparietal suture, thus forming a Y shape. The posterior portion of the temporal ridges (i.e., their connection with the nuchal crests) is damaged. The right zygomatic arch is bent medially in the median part due to diagenesis; the left one is less deformed and appears strong and robust, especially in the anterior portion.

In lateral view, the robustness of the zygomatic arch can be appreciated also in dorsoventral direction, especially on the left side. The frontal process of the zygomatic is particularly well developed. Despite the dorsoventral deformation of the neurocranium, it is worth noting the development of the preorbital fossa, which is very elongated and deep, but relatively low. The infraorbital foramina are obliterated.

In ventral view, the preserved part of the palate is relatively wide and with subparallel lateral margins. Two wide and deep

Table 2Measurements (in mm) of *Sus strozzi* from the VCS; cranium and mandible. Values in italics are estimated.

Measurement	IPS107041a		IPS107057
	Left	Right	Right
CRANIUM			
Basicranial axis: Basion - Hormion	46.5		
Upper neurocranium length: Akrokranium - Supraorbitale	170		
Parietal length: Akrokranium - Bregma	73		
Frontal length: Bregma - Nasion	96.0		
Basion - Staphylion	80		
Entorbitale - Infraorbitale	87.5		
Height of the lacrimal	16.5		
Ectorbitale - Entorbitale	31		
Max mastoid breadth: Otion - Otion	138.3		
Max breadth occipital condyles	57.6		
Max breadth at the base of paraoccipital processes	104.4		
Max breadth foramen magnum	19.0		
Max breadth of the squamous part of the occipital bone	92		
Min breadth of the squamous part of the occipital bone	59.4		
Min breadth of the parietal: min breadth between temporal lines	57.0		
Max frontal breadth: Ectorbitale - Ectorbitale	124.0		
Min breadth between supraorbital foramina	48.8		
Zygomatic breadth	173.5		
Max palatal breadth	82.4		
Length of premolar row			52.8
Length of molar row	79.7	77	
MANDIBLE			
	IPS107041b	IPS107041c	
	Right	Left	
Distance between distal border of c1 and distal border of m3	158.2	156.5	
Height of mandibular corpus at the mesial border of p2	60	59.0	
Height of mandibular corpus at the mesial border of m1	59.1	60.1	
Height of mandibular corpus at the distal border of m3	60.3	54.4	
Length of c1-p1 diastema	7.6	7.2	
Length of p1-p2 diastema	15.0	14.7	
Length of cheek tooth row (p1 included)	148.2	145.6	
Length of cheek tooth row (p1 excluded)	123.4	122	
Length of molar row	80.1	79.5	
Length of premolar row (p1 included)	71.3	67.7	
Length of premolar row (p1 excluded)	45.1	43	

palatine foramina open at the level of the contact between M2 and M3, in a lateral position. The median palatine suture is well visible and has the shape of a sharp crest in the area included between the last two molars. The transverse palatine suture is instead indistinct. The posterior margin of the palatines is relatively narrow and with a marked U-shaped concavity. No nasal spine is visible in its middle part. Laterally, the pyramidal processes of the palatines are very strong and rounded, and are connected posteriorly to poorly-preserved, subtriangular pterygoid processes. The visible portions of the choanae are narrow and elongated, separated medially by a sharp vomer. The sphenoid bone significantly enlarges anteroposteriorly, being as wide as the palatines in the anterior part (pterygoid processes of the sphenoid) and much wider in the posterior part, where it connects to the squamosal bones. In its median portion, the basilar tubercle appears as a bulky subtriangular prominence, which was pushed forward by the deformation of the occipital region. The tympanic bullae are not preserved, nor are the jugular processes. Observed from the ventral side, the zygomatic arches open gently in the anterior part (i.e., their anterior margin forms an obtuse angle with the lateral margin of the maxilla) and they diverge laterally towards the posterior part. The glenoid fossae are oriented obliquely with respect to the sagittal axis, but this morphology might result from deformation. They are delimited posteriorly by well-developed, crest-like, and obliquely oriented retroarticular processes.

In posteroventral view, although damaged and ventrally oriented by deformation, the occipital squama shows a triangular shape, pointing ventrally toward the foramen magnum. The latter is

deformed and has acquired an ellipsoidal outline, delimited by relatively small occipital condyles. The depth of the occipital fossa is likely exaggerated by diagenetic processes. The nuchal crests are massive and diverge dorsolaterally. The external occipital protuberance is missing. The posterior portions of the squamosal bones are wide and flat and delimited posteroventrally by crest-like mastoid processes. The occipitosquamosal sutures are visible as subvertical lines slightly diverging ventrolaterally. On the right side, a large blade-like posterodorsal process of the zygomatic arch is well preserved and delimits dorsolaterally the external auditory meatus.

4.1.2. Mandible

The right and left hemimandibles (IPS107041b and IPS107041c, respectively; Fig. 2) were found in close proximity to the cranium IPS107041a and most likely belong to the same adult male individual. Both miss the rostral portion (symphyseal area and lower incisors) and most of the ramus. Lower canines and postcanine teeth are preserved, with the exception of the right p1 and p2. A long diastema is present between p1 and p2, while the diastema between c1 and p1 is extremely short, so that these two teeth are almost in contact.

In occlusal view, the corpus appears massive, especially in the molar area. It shows a longitudinal swelling running along the corpus, with a major convexity in the median part, between m1 and m2. The corpus enlarges in a triangular and concave area distolabially to m3. The edge of the corpus in the area of the diastema between p1 and p2 is sharp like a crest.

Table 3

Measurements (in mm) of *Sus strozzi* from the VCS; teeth, L, length; LLD, labiolingual diameter of the tooth measured at right angle to the base line; Lla, labial length; Lli, lingual length; Ldi, distal length; Lt, length of the talon/talonid; MMD, mesiodistal diameter of the tooth measured at right angle to the base line; W, width; Wd, distal width; Wm, mesial width; Wt, width of the talon/talonid. Values in italics are estimated.

ID	Tooth	Side	LLD	MMD	Lla	Lli	Ldi	L	W	Wm	Wd	Lt	Wt	
IPS107041	P3	Left						13.7	12.04					
	P3	Right						14.1						
	P4	Left						12.9	15.75					
	P4	Right						12.8	14.61					
	M1	Left						16.5		18	20.0			
	M1	Right												
	M2	Left						23.2		23.1	22.8			
	M2	Right						24.2		22.5	23.9			
	M3	Left						38.2		24.1	12.4	25.8	22.4	
IPS107057	M3	Right						37.9		24.7	12.9	25.1	22.4	
	P1	Right						11.4	4.93					
	P2	Right						13.7	9.96					
	P3	Right						14.4	13.01					
	P4	Right						12.4	15.66					
	M1	Right						19.5		16.1	17.0			
IPS107043	I2	Right	7.5	17.7				26.0		21.2	21.0			
	IPS107042	C1			22.2	20.0	30.5							
IPS107044	I1	Left	5.6	10.7										
	C1	Left			15.2	14.5	21.9							
IPS20134	P4	Left						12.6	14.51					
IPS107051	P4	Left						11.3	12.72					
	M1	Left								15.0				
IPS107056	M1	Right						19.9		15.9				
IPS107058	M3	Right						37.8		23.4	12.3	22.9	21.0	
IPS107055	dP3	Right						14.0		6.7	9.5			
	dP4	Right						15.0		11.9	12.2			
IPS107041b	c1	Right			20.0	19.7	17.8							
	p1	Right						10.3	6.34					
	p2	Right						13.5	6.60					
	p3	Right						13.9	9.22					
	p4	Right						15.1		9.7	11.6			
	m1	Right						16.8		12.6	13.5			
	m2	Right						24.5		16.3				
	m3	Right						40				15.3	27.3	18.6
	IPS107041c	c1	Left			18.9	18.7	17.1						
p1		Left						8.7	5					
p2		Left						13	6.8					
p3		Left						14.5	9.43					
p4		Left						14.6		9.7	11.8			
m1		Left						15.2		12.5	14.2			
m2		Left						22.1		16.8	18.6			
m3		Left						41.5		19.7	16.7	27.3	18.9	
IPS13818		c1	Right			20.2	22.2	18.2						
	IPS107047	c1			18.9	20.6	16.0							
IPS107054	c1	Left			19.8	21.0	17.4							
IPS107052	m3	Left						41.8		19.4	16.3	28.9	18.2	
IPS107049	m3	Left						41.3		18.1	14.5	26.9	18.1	
IPS107050	m3	Right								17.8			17.5	

In lateral view, the dorsal and ventral margins of the corpus are subparallel. The anteroventral margin of the corpus forms an evident mental prominence, that is, an obtuse angle with the ventral margin, roughly in correspondence of half-length of the p1–p2 diastema. A subcircular mental foramen is visible on each hemimandible at about the same level. Two smaller foramina are present on each hemimandible in a more posterior position (one below the mesial part of p3 and one below the distal margin of p4 on the left side; one below the mesial margin and one below the distal margin of p4 on the right side). The surface just below the premolars is slightly concave and rugose. Posteriorly, the extramolar ridge below the molars is nearly indistinct.

In medial view, the mandibular foramen extends anteriorly up to the contact between m1 and m2.

4.1.3. Upper teeth

Upper incisors are not preserved in the cranium IPS107041a or

in the right maxillary fragment IPS107057. The isolated right I2 IPS107043 (Fig. 3) preserves the complete crown and almost half of the root. The crown is very little worn. It is considerably elongated mesiodistally and laterally flattened. In occlusal view, the mesial half is wider than the distal. Two adjacent main cusps are visible in the mesial part of the tooth, the precone and paracone. Distally to the latter, the postcrista develops along the labial margin of the tooth and is divided into three undulated parts in labial view. In the distolingual part of the tooth, three small tubercles develop close to the cervix, that is, the mesiolingual, the lingual, and the distolingual cingula. Between these cingula and the postcrista, the crown is visibly concave, forming a deep basal fossa.

Two male upper canines (IPS107042, right, and IPS107044b, left) are present (Fig. 3). IPS107044b is smaller than IPS107042 and is damaged along the mesial portion, so the description is mainly based on the latter. The upper canine is a large open-rooted tooth curved dorsally. It shows a variable section, which is subtriangular

Table 4Measurements (in mm) of *Sus strozii* from the VCS: postcranial bones. Values in italics are estimated.

Measurement	IPS14972	IPS107062	IPS107063
ASTRAGALUS			
	Left	Left	Right
Anteroposterior diameter from the anterior border of the trochlea to the posterior border of the facet for calcaneum	30.3	26.7	
Lateral length	53.3	52.0	
Medial length	50.8	46.5	48.4
Proximal mediolateral diameter	26.5	24.4	
Distal mediolateral diameter	32.3	29.1	32.0
IPS107064			
SCAPULA			
	Left		
Greatest length of glenoid process	40.8		
Smallest length of the collum scapulae	27		
IPS107066			
TIBIA			
	Left		
Mediolateral diameter of the shaft (minimum)	27.4		
Anteroposterior diameter of the shaft (minimum)	20.8		
Mediolateral diameter of the distal epiphysis	37.6		
Anteroposterior diameter of the distal epiphysis	33.2		

at the base, elliptical (with a long axis oriented mesiodistally) in the middle part, and again subtriangular near the tip. The mesiodistally enlargement in the middle part is particularly evident in dorsal view. In anterior view, almost half the length of the mesioventral surface is occupied by a leaf-shaped wear facet. A thick enamel layer covers the ventral surface of the canine; this layer is crossed by several very deep furrows parallel to the main axis of the tooth. A thinner enamel layer is also preserved on the distal face, and is particularly visible at the edge between the distal and dorsal surfaces; it is not crossed by longitudinal furrows.

The maxillary fragment IPS107057 (Fig. 2) includes well-preserved and little worn teeth from C1 to M2. The canine has a completely different morphology from the two described above. It is much shorter, not visibly curved, with a labiolingually flattened crown. In labial view, it shows a triangular shape and a faint serration along the mesial and especially distal margins. A crest-like tubercle develops at the distal margin close to the cervix; this tubercle is visibly separated from the rest of the crown by a deep vertical groove on the lingual side. All these features (associated to the absence of any supracanine flange in the preserved portion of the maxilla) allow referral of this specimen to a young adult female individual.

The cranium IPS107041a (Fig. 2) preserves the P3–M3 series on both sides (only the right M1 is missing), but the teeth are heavily worn and very difficult to describe in detail. The only exception is the M3 (see below).

The aforementioned maxilla IPS107057 (Fig. 2) is the only specimen in which the premolar series P1–P4 is fully preserved. A short diastema separates the C1 from the P1. The latter has an elongated outline in occlusal view, with a constriction in the middle and a greater breadth in the distal part. Three main cusps are visible, connected by small sharp crests and aligned along the sagittal axis of the tooth. The mesial cusp is the smallest and lowest. The central one is the largest and exhibits a triangular shape in labial view. The distal cusp is slightly higher and larger than the mesial one. Labially and lingually to the distal cusp, the crown reaches the maximum breadth and, distally to the cusp, it develops a cingulum-like distal prolongation which overlaps the mesial part of the P2 in occlusal view. The P2 has a roughly rectangular occlusal outline. The main cusp is the high and pointed paracone, located in mesiolabial position. A very small prestyle is visible at the mesial margin of the crown near the cervix; it is only visible in labial view, being covered by the distal portion of the P1 in occlusal view (see

above). A strong crest, running from the paracone tip toward the mesiolingual corner of the tooth, is connected to a well-developed primocone. The distal edge of the paracone is characterized by serrations, corresponding to subvertical furrows on the labial wall of the premolar. In the distolingual corner of the crown, a rounded protocone is present, delimited mesially and distally by small cusplets and separated labially by the rest of the crown by a deep longitudinal groove. The overall shape of the P3 is similar to that of the P2, with the following exceptions: the paracone is more distally positioned, almost in the middle of the crown; mesially, the prestyle and primocone are connected by a cingulum-like ridge which hosts some smaller cusplets; besides the crest connecting the paracone and primocone, another strong crest runs from the paracone to the protocone, delimiting mesially the deep distal valley; and the distal portion of the tooth is wider than the mesial in occlusal view. The P4 has a roughly squared occlusal outline, with a more rounded lingual margin. The large paracone is positioned along the labial margin slightly mesially to the midpoint, and forms the labial cutting edge with the lower metacone, from which it is separated by a fine transverse furrow. The mesial part of the cutting edge is formed by the serrated mesial margin of the paracone, which ends mesially with a small protoprestyle. On the lingual side, the protocone is as wide but lower than the paracone. Their apices are almost aligned. Between these two cusps, there are a rounded and distinct prestyle and a smaller preconule. Conversely, between the protocone and metacone, there is a deep valley (profossa), delimited distally by a transversal ridge formed by several accessory cusplets. Two other P4 (IPS107051a and IPS20134; Fig. 3) are present in the collection, but their advanced stage of wear prevents their detailed description. However, their overall morphology, including the position and shape of the main cusps, fits that described for the P4 of IPS107057.

The M1 in the maxilla IPS107057 (Fig. 2) is moderately worn. It has a figure-eight shape in occlusal view, with the mesial portion smaller than the distal one and a constriction between them. The four main cusps (paracone and protocone mesially, metacone and tetracone distally) are conical and very similar in size, with the two labial cusps (paracone and metacone) slightly larger than the two lingual ones. The enamel is thick and characterized by several invaginations (grooves or *Furchen* of Hünemann, 1968). Between the four main cusps, at about the middle of the occlusal surface, a tetrapreconule is present. It is relatively large, but still smaller than the main cusps. A mesial cingulum and a distal cingulum develop at

the mesial and distal margins of the tooth, respectively. Both host some accessory cusplets. A preconule is visible at about the middle of the mesial cingulum and a pentapreconule just mesially to the distal cingulum, between the distolingual corners of the metacone and tetracone. A small ectoconule is visible close to the labial cervix between the paracone and metacone. Another ectoconule is present on the lingual margin, just distally to the constriction between the main lobes of the molar. The isolated right M1 crown IPS107056 (Fig. 3) exhibits the same general morphology, but lacks the mesiolingual part. The incomplete M1 IPS107051b, found in association with the aforementioned P4 IPS107051a, is almost completely worn out.

The M2 of IPS107057 (Fig. 2) is very similar in morphology to the M1, but larger. Moreover, in the M2 the difference in width between the mesial and distal lobes is less marked than in the M1. The lower stage of wear allows recognizing a number of small accessory cusplets surrounding all the main cusps as well as those aligned along the cingula.

The best preserved M3 is the isolated right crown IPS107058 (Fig. 3). The wear stage is intermediate. The occlusal outline is roughly triangular, with a wide mesial lobe, a slightly narrower central lobe, and a considerably narrower distal lobe. The first two are separated by a labiolingual constriction similar to those seen in M1 and M2. Conversely, the third lobe is separated from the second by a narrow lingual constriction and a very marked labial step. The arrangement and size of the four main cusps, and the tetrapreconule between them, are similar to those described for the other molars. On the other hand, the M3 does not show a mesial cingulum, but the preconule is much more developed than previously described. The distal lobe is almost completely occupied by a rounded heptacone, delimited mesially by three distinct small cusps: a pentacone mesiolabially, a pentapreconule mesially, and a hexacone mesiolingually. Another accessory cusp is visible mesially to the pentapreconule, separated by the tetrapreconule by a shallow hypofossa. The same structures are seen in the left and right M3 preserved in the cranium IPS107041a, although in a more advanced stage of wear.

Specimen IPS107044a is a right dI2 (Fig. 3). It is overall smaller than the I2 IPS107043 described above. The crown is drop-shaped in occlusal view and shows an oblique cervix in labial and lingual views. The entire crown is inclined with respect to the root with an angle of about 45° and it forms a bulging distal prolongation that develops beyond the distal edge of the root. The labial and lingual surfaces of the crown are smooth.

The right maxillary fragment IPS107055 (Fig. 3) includes well-preserved dP3 and dP4. The dP3 is drop-shaped in occlusal view. It shows a very low prestyle at the mesial margin. The prestyle is connected to the paracone by a sharp crest. The paracone stands out as the largest cusp. It is pointed and triangular in labial view. A transverse valley separates the paracone from the metacone and protocone, located at the same level in the distal part of tooth. The protocone is slightly larger than the metacone. Distally to them, a faint cingulum is present. The dP4 is superficially similar to the M1 in overall shape. It has a rectangular occlusal outline with a constriction in the middle. The four main cusps are conical and very close in size. The distal cingulum is much more developed than the mesial one.

4.1.4. Lower teeth

No lower incisors are available in the Vallparadis collection. The left hemimandible IPS107041c preserves a complete lower canine, while in the right one (IPS107041b) the canine crown is broken at about half length (Fig. 2). These canines are massive and extend dorsally and laterally. Their apex is oriented slightly caudally. Due to the considerable development of these tusks and the advanced

wear stage of the postcanine dentition (also observable in the upper teeth of the associated cranium IPS107041a), we can confidently assign the cranium and mandible to an adult male individual. The canines are verrucosic (see Section 5.1). Enamel covers the labial and lingual sides of the crown, which are also crossed by a longitudinal furrow along the midline. The isolated male lower canines IPS13818, IPS107047, and IPS107054 (Fig. 3) show the same features.

The p1 is only preserved in the left hemimandible IPS107041c, in which it is positioned very close to the distal margin of the canine. It has an elliptical occlusal outline. The state of preservation is poor, but it seems to have only a single main cusp in the middle.

Again, the p2 is only present in the left hemimandible IPS107041c (the two roots of the p2 are also visible on the right side). The preservation is not good, as there is a fracture separating the mesial and distal portions of the tooth. The occlusal outline is labiolingually narrow, with a certain widening in the distal half.

The p3 is still visible in both hemimandibles and better preserved in the right one. The tooth is drop-shaped when observed in occlusal view, due to the widening of the distal half. The main cusps are not recognizable due to the advanced wear. Only the main cusp, namely the protoconid, is visible at the center of the occlusal surface. When observed in labial view, the tooth shows an almost horizontal occlusal edge, that is, all the cusps have been worn out at the same level. A vertical furrow in the distal half of the crown allows recognizing the separation between metaconid and hypoconid. A small stylid is visible on the distolingual wall of the p3, both in the left and right sides.

The same description applies to the p4. The occlusal surface is almost flat, but in this case, it is still possible to recognize the main cusps, namely the paraconid mesially (corresponding to a labiolingual narrowing of the occlusal wearing facet), the wide protoconid and metaconid which coalesced in the middle of the tooth, and the subtriangular hypoconid distally. When compared to the p3, the occlusal outline of the p4 is more ovoidal.

The m1 and m2 are impossible to describe due to the very advanced wear stage (the m1 is almost completely worn out on the right hemimandible).

The m3 is instead well preserved on both hemimandibles, IPS107041b-c (Fig. 2), and further represented by two isolated complete specimens, IPS107049 and IPS107052 (Fig. 3) and a partial tooth (IPS107050) that lacks the distal portion. In occlusal view, the m3 is elongated and distally tapered, with a straight mesial edge and a rounded distal outline. The two constrictions that separate the three lobes are not deep. The enamel appears very thick in all cusps in which it is exposed. The occlusal pattern formed by the deep grooves in the main cusps is complex. Mesially, the metaconid is slightly larger than the protoconid, and both are larger than the hypoconid and entoconid. A faint mesial cingulum is visible only in IPS107052. The hypopreconulid is large, about one third of the main cusps and has a rounded/rhomboidal occlusal outline. The third lobe is long and massive and is composed by four main cusps arranged in a cross. Mesially, the pentapreconulid is slightly larger than the aforementioned hypopreconulid and a pentaectoconulid is present on its labial side. The pentaconid, hexaconid, and heptaconid are similar in size and larger than the pentapreconulid. In moderately worn teeth (IPS107052), the heptaconid is composed by a main central cuspid and two smaller cusplets at the sides.

4.2. Comparisons

In the literature, European Early Pleistocene suines have mostly been attributed to *S. strozzi*, at least for fossil remains dated to until the Jaramillo subchron; from this interval onwards (i.e., from the beginning of the Epivillafranchian), suid remains have been

assigned to *S. scrofa* (with the remarkable exception of the Arda River sample; see the Introduction). For this reason, if we limited ourselves to a determination merely based on biochronological assumptions, the VCS remains should be referred to *S. scrofa*. However, the morphological features of the fossils from VCS lead to different conclusions.

Several characters observed in the craniomandibular and dental specimens described above clearly fit the morphology of *S. strozzi*. Cherin et al. (2018) highlighted the main morphological differences between *S. strozzi* and *S. scrofa*. Regarding the cranium, the following *S. strozzi*-like characters can be observed in IPS107041a from VCS (Fig. 2; Appendix 1): relatively narrow postorbital constriction, large nuchal crest relative to the greatest frontal width, drooping ventral outline of the zygomatic arch in lateral view, thickened zygomatic arch in dorsal view, deep and low pre-orbital fossa, and relatively high and narrow occipital region (although the evaluation of the last character may have been biased by some kind of diagenetic deformation). The similarities above are well appreciated by comparing IPS107041a with the lectotype cranium of *S. strozzi* (IGF 4242) from the Upper Valdarno (Azzaroli, 1954). As for the mandible, the most significant character is the shape of the labial margin in dorsal view, which shows a longitudinal swelling with a major convexity in the middle, like in *S. strozzi*; also, the wide angle formed by the mental prominence in labial view is a character already observed in *S. strozzi* (Cherin et al., 2018). In particular, morphological similarities between the mandible from VCS and that from the Arda River (Bona and Sala, 2016) are remarkable. Very interesting characters are also seen in the teeth. Like in *S. strozzi*, the p1 is relatively well developed and positioned very close to the lower canine, styles/stylids are present in the upper/lower premolars, the enamel exposed in the wearing facets of the molars is thick and forms complex occlusal patterns, with deep grooves. However, the most diagnostic characters are observed in the male lower canines: they are very long, with enamel on the labial and lingual surfaces, and above all they display the verrucosic condition (see Section 5.1 for a discussion of the importance of this character). In light of the analysis of discrete morphological features, an attribution of the VCS material to *S. strozzi* is well supported.

As for the postcranial skeleton, there is unfortunately not enough literature data to recognize significant differences between *S. scrofa* and *S. strozzi*. Detailed descriptions of the nearly complete skeleton of *S. strozzi* from Senèze (France) are in Azzaroli (1954) and some more information on calcaneum morphology are in Cherin et al. (2019). Unfortunately, the VCS postcranial sample (Table 1) does not include bones among those considered diagnostic by the aforementioned authors (e.g., morphology of the atlas and humerus of *S. strozzi* in Azzaroli, 1954). For this reason, the attribution of the VCS postcranial sample to *S. strozzi*—although extremely probable given the close stratigraphic association with the craniodental remains—should be taken with caution, pending the discovery of new Early Pleistocene postcranial material of *Sus* in Europe.

Regarding the morphometric comparisons, it is worth approaching the problem from a broader perspective. Numerous taxonomic determinations of Pleistocene suid remains have been carried out in the past mainly based on size (e.g., Ambrosetti et al., 1979; Faure and Guérin, 1983; Van der Made, 1999; Van der Made et al., 2017). The common opinion that emerges from these past works is that, especially in the chronological range of interest for this article (i.e., late Early and early Middle Pleistocene), the earlier form *S. strozzi* could be distinguished from *S. scrofa* by larger dimensions. As shown above, the two species are in fact distinguishable above all on the basis of qualitative morphological

characters, which however are often difficult to observe in the absence of sufficiently complete craniomandibular remains. Among these characters, the morphology of the lower canine stands out, but we will discuss it in detail in Section 5.1.

In Fig. 5, we consider the dimensions (maximum length vs. maximum width) of the m3 to make comparisons between *Sus* species. As already shown by Cherin et al. (2018), the size of the m3—in association with craniomandibular and dental morphological characters—is useful to discriminate *S. strozzi* from the Pliocene species *S. arvernensis* (note the complete separation of the metric ranges of the two species). Conversely, the huge size range of the extant wild boar virtually encompasses almost completely those of *S. arvernensis* and *S. strozzi*. This range has been obtained thanks to the comprehensive work by Albarella et al. (2009), who collected morphological and morphometric data from skeletal elements (mainly mandibles, lower teeth, and humeri) of almost 1500 wild boar individuals from across the world. Their work evidenced a number of geographic trends in the intraspecific variation of *S. scrofa* across its geographic range, mainly concerning (1) the differentiation of insular forms, which occupy the lower left part of the graph in Fig. 5 (in this regard, note also the position of the range of early Holocene wild boars from Japan) and (2) the existence of S–N and W–E clines (in fact, the right upper part of the range is occupied by the large wild boars from northeastern Russia). Albarella et al. (2009) also compared the body size of extant wild boars with that obtained from archeozoological remains from the Mesolithic of Europe. The dimensional range of these individuals (about 100 specimens) is again included into that of recent forms. Conversely, those reconstructed for Middle Pleistocene forms from Britain (Lister et al., 2010) and late Middle–early Late Pleistocene forms from Germany (Hünemann, 1975, 1977, 1978) fall in the upper right part of the graph, thus also incorporating the individuals of *S. strozzi* remaining outside the range of modern *S. scrofa*. In light of these results, it is obvious that purely dimensional criteria are not sufficiently diagnostic for taxonomic purposes, mainly due to the enormous dimensional intraspecific variation shown by *S. scrofa*.

4.3. Phylogenetic analysis

The phylogenetic analysis produced two equally parsimonious phylogenetic trees of 142 steps, with consistency index of 0.426, rescaled consistency index of 0.268, and retention index of 0.621. The strict consensus tree is shown in Fig. 6, with node support indicated by Bremer and bootstrap values. The distribution of character states in the most parsimonious trees is reported in Appendix 2.

As already detailed discussed in Cherin et al. (2018), after the early divergence of the Miocene primitive genus *Microstonyx*, the suine clade splits into two main clades. The first (African clade) includes the *Kolpochoerus*–*Hylochoerus* and *Metridiochoerus*–*Phacochoerus* groups. The second (Eurasian clade) includes the genera *Potamochoerus* and *Sus*, although the position of the former taxon in the tree does not fit previous studies based on morphological (Geraads, 2004; Souron et al., 2015) or molecular (Wu et al., 2006; Gongora et al., 2011) data and is probably the result of the presence of several plesiomorphic anatomical characters that make *Potamochoerus* superficially similar to *Sus* in many features (Groves and Grubb, 1993; Cherin et al., 2018).

The topology of the *Sus* clade clearly shows a separation between the wild boar and other members of the genus. *Sus scrofa*, which is characterized by a scrofic lower canine, is the most basal species and is the sister-group of a clade composed by extant and extinct species, all characterized by verrucosic lower canine. This topology agrees with those obtained by molecular analyses

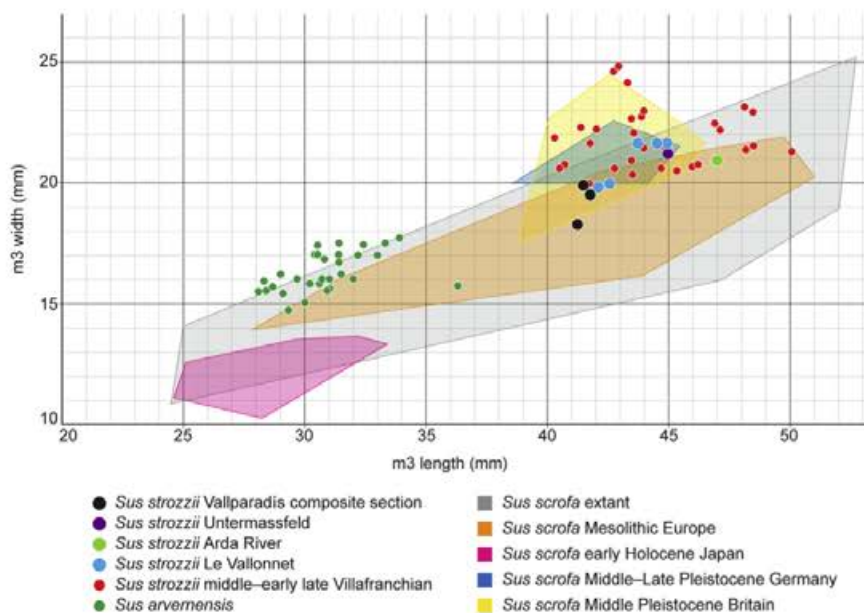


Fig. 5. Scatter plot of width versus length of the m3 of Epivillafranchian *Sus strozzi* analyzed in this paper, compared with measurements of middle–early late Villafranchian *S. strozzi*, Pliocene *S. arvernensis*, and extinct and extant *S. scrofa*. Sources of data: *S. strozzi* Arda River - Bona and Sala (2016); middle–early late Villafranchian *S. strozzi* - Titov (2000), Cherin et al. (2018); Pliocene *S. arvernensis* - Cherin et al. (2018); extant *S. scrofa* - Albarella et al. (2009) (range obtained from a sample of about 550 m3 from the entire geographic range of the species, i.e., Eurasia and North Africa); Mesolithic *S. scrofa* - Albarella et al. (2009) (range obtained from a sample of about 100 m3 from different European areas); early Holocene *S. scrofa* from Japan - Kawamura et al. (2017) (range obtained from a sample of about 100 m3 from Tsudupisuki-abu Cave); Middle–Late Pleistocene *S. scrofa* from Germany - Hünermann (1975, 1977, 1978); Middle Pleistocene *S. scrofa* from Britain - Lister et al. (2010).

(Gongora et al., 2011; Frantz et al., 2013; Ai et al., 2015), according to which *S. scrofa* is the basal member of the *Sus* radiation—see also the tree in Frantz et al. (2016), which accounts for both molecular and morphological data. The ancestral status of the Pliocene *S. arvernensis* with respect to *S. strozzi* and ISEA pigs has been proposed by many authors (Azzaroli, 1954, 1975; Berdondini, 1992; Pickford, 2012; Pickford and Obada, 2016) and is supported by our phylogenetic analysis. Besides the early branching of *S. arvernensis*, the phylogenetic relationships between the other verrucosic pigs are not fully resolved. The tree shows a polytomy which includes *Sus barbatus*, *S. verrucosus*, a clade grouping *S. celebensis* and *Sus brachygnathus*, and a clade formed by *S. strozzi* and the suine from the Vallparadis Section. The latter sister-group relationship is the most interesting result for the aims of this paper. We interpret it as an additional evidence of the taxonomic attribution of the VCS sample to *S. strozzi*. Actually, the separation of the two clades in the tree is supported only by one autapomorphy of the Vallparadis pig, that is, a slightly lower complexity of enamel figures exposed at the occlusal surface in the molars (character 41). However, the sample from Vallparadis is quite restricted, so that a proper evaluation of this character might be biased by the low number of molars available. Moreover, character 41 has a rescaled retention index of 0.28 and a homoplasy index of 0.6, showing that it is quite homoplastic in our analysis. Consequently, this difference is not sufficient to justify a taxonomic separation between the Vallparadis pig and the other known specimens referred to *S. strozzi*.

5. Discussion

5.1. The taxonomic importance of the lower canine morphology in suines

The difference between scrofic and verrucosic lower canines has been recognized as a diagnostic character for the taxonomic

distinction between suine species since the beginning of the XXth Century (Stehlin, 1899–1900). The wild boar is the only living species of *Sus* that shows a scrofic condition, that is, in the cross section of the lower canine crown (especially in males), the lingual side is the longest, and the distal side is longer than the labial. Conversely, in pigs with verrucosic morphology, the labial and lingual sides of the lower canine are similar in length and are broader than the distal one. This morphology is present in extant pigs living in ISEA (Hardjasmita, 1987; Cherin et al., 2018)—e.g., the Javan warty pig *S. verrucosus*, the bearded pig *S. barbatus*, the Sulawesi warty pig *S. celebensis*, and the Visayan warty pig *Sus cebifrons*, and their fossil relatives (*S. arvernensis* and *S. strozzi* from Europe, and *S. brachygnathus* and *Sus macrognathus* from Indonesia and surrounding areas).

Fig. 7 shows the relationship between the lingual/labial and distal/labial ratios. Our data show a clear separation between scrofic (i.e., *S. scrofa*) and verrucosic (i.e., *S. strozzi* and extant verrucosic ISEA pigs) species, along both axes. In particular, a significant difference in the canine distal/labial ($F_{1,118} = 346.2$, $p < 0.001$) and lingual/labial ($F_{1,118} = 283.6$, $p < 0.001$) ratios is recovered between scrofic and verrucosic canine types (Fig. 8), indicating that both ratios are diagnostic characters to separate the two groups of suines.

The PCA also showed clear separation between the two suine groups along PC1, which explained 86% of the total variance, while within-group phenotypic variation was represented along PC2, explaining 14% of the total variance (Fig. 9).

5.2. Quaternary suines from China

Quaternary Chinese species of *Sus*, which were excluded from our phylogenetic analysis for the reasons explained in Section 2.3, are problematic. *Sus lydekkeri* from northern China and *Sus peii* from southern China are both recorded from the Early–Middle

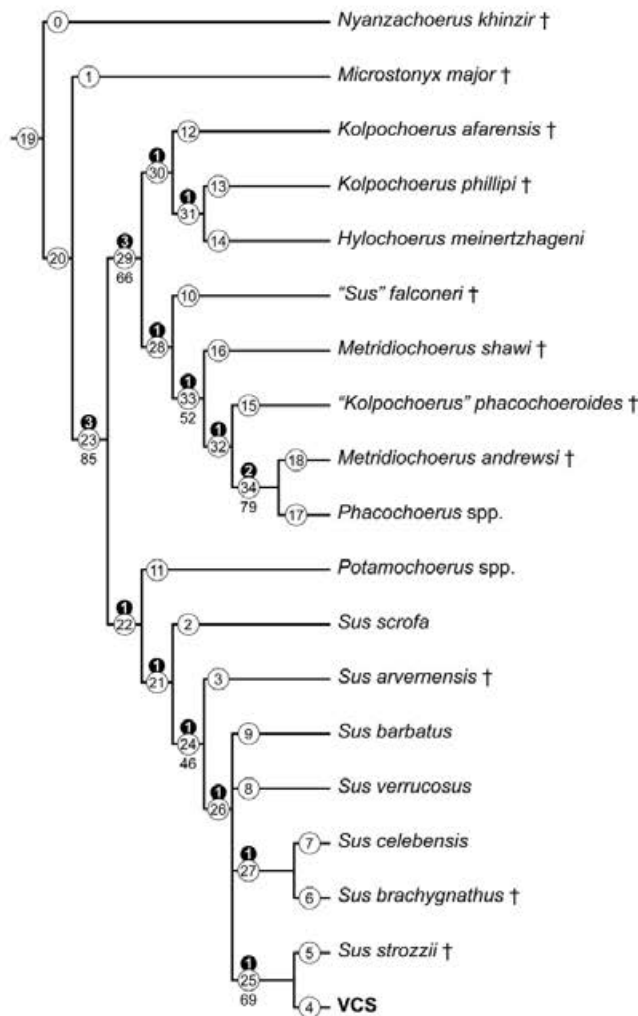


Fig. 6. Strict consensus tree showing the phylogenetic relationships between selected extant and extinct (†) Suinae. Node numbers in white circles, Bremer support in black circles above node numbers, bootstrap values below node numbers. Bootstrap values are only reported when $\geq 50\%$. VCS, *Sus* from the Vallparadis composite section.

Pleistocene and are the only species represented by relatively rich samples (Han et al., 1975; Han, 1987; Liu et al., 2017). They share numerous morphological features and were approximately as large as the European *S. strozzii* (Liu et al., 2017). However, they are also described in some respects as morphologically similar to *S. scrofa*, of which they have been claimed as putative ancestors (Dong et al., 2006, 2013). *Sus lydekkeri*, in particular, has even been considered as an extinct subspecies of *S. scrofa* by Fujita et al. (2000). All these hypotheses were questioned by the phylogenetic results by Cherin et al. (2018), according to which *S. lydekkeri* would occupy an intermediate position between *S. scrofa* and verrucosic pigs. Fujita et al. (2000) defined the morphology of the lower canine of *S. lydekkeri* from the type locality (Loc. 1 of Zhoukoudian) as “intermediate”, that is, with almost equally short labial and distal sides, and longer lingual side. On the other hand, the most complete skull of *S. lydekkeri* discovered to date (NNMO HY13-58.1-2 from Yangshuizhan in Nihewan Basin; Liu et al., 2017) undoubtedly shows verrucosic lower canines. Moreover, looking at lower canine measurements of *S. lydekkeri* published by Liu et al. (2017), it is noteworthy that for samples from some other northern Chinese

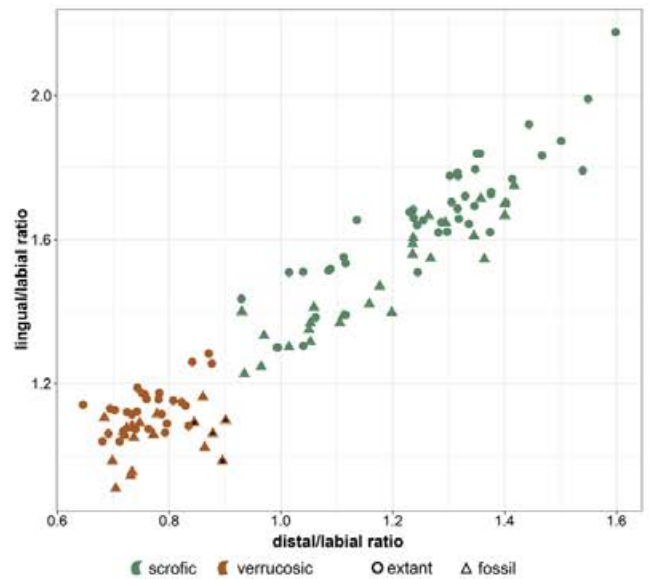


Fig. 7. Scatter plot of the distal/labial and lingual/labial ratios for the scrofic (green) and verrucosic (orange) lower canine types. Extant and fossil specimens are represented by different symbols. Specimens from Vallparadis composite section are indicated by a black asterisk inside the symbol. Raw data are in Appendix 3. (For interpretation of the references to color in this figure legend, the reader is referred to the Web version of this article.)

sites, the proportions turn out to be scrofic (distal/labial ratio > 1 and lingual/labial ratio > 1.3). Similar discrepancies exist for *S. peii*. Its lower canine is described as verrucosic by Fujita et al. (2000). Similarly, the two lower canines of *S. peii* from Sanhe Cave described by Dong et al. (2013) are verrucosic (distal/labial ratio equal to 0.75 and 0.79 in V18402.26 and V18402.27, respectively). Conversely, Dong (2008: 244) reported “If based on the lower canine pattern, [...] *S. peii* and *S. lydekkeri* are “scrofa” type (Fistani, 1996)”. However, *S. peii* is never mentioned by Fistani (1996).

As mentioned above, *S. lydekkeri* and *S. peii* are mainly reported from northern and southern China, respectively. However, there is “some overlap of the two species along certain areas of the Yangtze” (Liu et al., 2017: 32). Both are substantially known based on dentognathic remains, with the only remarkable exceptions of the skulls NNMO HY13-58.1-2 from the Early Pleistocene of Yangshuizhan (mentioned above; Liu et al., 2017) and IVPP C/C.383 from the Middle Pleistocene of Zhoukoudian Loc. 1 (Young, 1932), referred to *S. lydekkeri*. For these reasons, we cannot rule out that the hypodigms of the two species have been mixed at least in some cases, or that parts of them should be referred to other species. A comprehensive review of the Chinese record of *Sus* spp. would be welcome, especially in light of the present work on the morphology of the lower canine, which would easily allow discriminating between scrofic and verrucosic forms.

5.3. Epivillafranchian *Sus* from the Iberian Peninsula

With the exception of VCS, *S. strozzii* is not reported with certainty from any Epivillafranchian Iberian site (Madurell-Malapeira et al., 2014, 2019a). With reference to the earliest levels of the Atapuerca cave complex, two fragmented deciduous premolars of *Sus* sp. were found at Sima del Elefante TE9c (ca. 1.3–1.1 Ma; Huguet et al., 2017). Therefore, these scanty remains may represent the earliest record of suids in Europe at the beginning of the Epivillafranchian. Younger undescribed material assigned to *S. cf. scrofa*

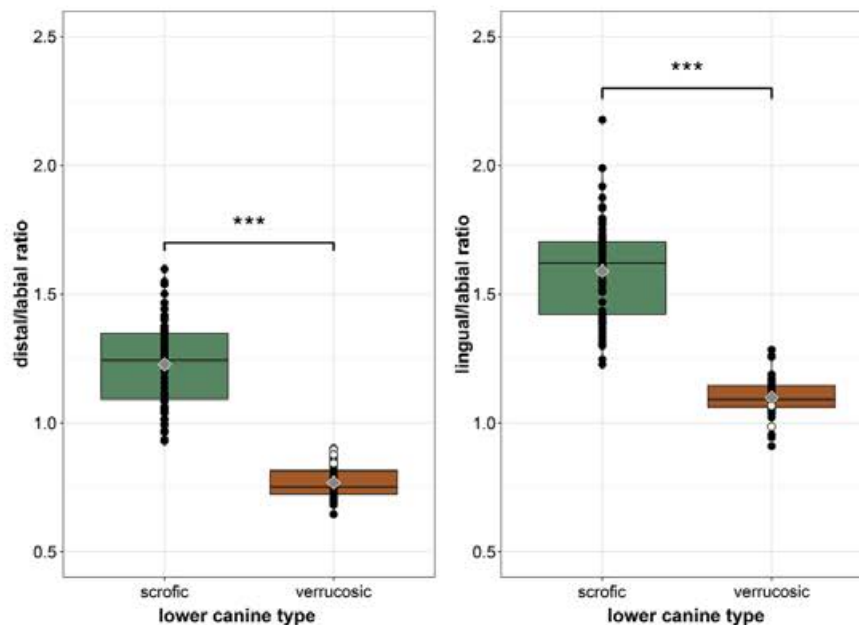


Fig. 8. Boxplots of the distal/labial and lingual/labial ratios for the scrofic (green) and verrucosic (orange) lower canine types. Horizontal line: median value; box: interquartile range (IQR); upper whisker: values less than or equal to 1.5 * IQR; lower whisker: values greater than or equal to 1.5 * IQR. The grey square represents the mean value for each canine type. Specimens from Vallparadis composite section are indicated by open circles. In the right boxplot, two Vallparadis specimens (IPS13818 and IPS107047) are covered by the mean value symbol. The asterisks indicate a $p < 0.001$ from the analysis of variance (ANOVA). Raw data are in Appendix 3. (For interpretation of the references to color in this figure legend, the reader is referred to the Web version of this article.)

was also listed by Rodríguez et al. (2011) from Gran Dolina TD3–4–5 (ca. 1.0 Ma). Finally, two isolated teeth (p3 and M1) attributed to *S. scrofa* were reported from Gran Dolina TD6 (Van der Made, 1999) and TD8 (Van der Made et al., 2017), respectively. The two units are close in age to the Early-Middle Pleistocene boundary (ca. 0.8–0.7 Ma; Rodríguez et al., 2011). In both cases, taxonomic attribution is merely based on size, which we do not consider reliable based on our analysis. In particular, the M1 from TD8 is very similar in size to the homologous teeth from VCS, i.e., falling within the lower size range of *S. strozzi*.

Julià Bruguès and Suc (1980) reported a suid m3 (IPS34657) from Bòbila Ordis (ca. 1.2–1.0 Ma). However, according to Agustí et al. (2018), it is difficult to ascertain the stratigraphic provenance of this material. Anyway, regardless of its age, in our opinion this single molar can only be referred to *Sus* sp. Vallverdu et al. (2014) mentioned the presence of *S. strozzi* from locality EF at Barranc de la Boella (ca. 1.0 Ma), but they did not describe the fossils. The same sample was attributed to *S. scrofa* by Martínez-Navarro et al. (2015), but a more recent revision of the scanty specimens available supports their assignment to *S. strozzi* (Madurell-Malapeira et al., 2019).

5.4. Epivillafranchian *Sus* from France

The richest suid sample from the French Epivillafranchian comes from Vallonnet Cave, in the southeastern part of the country. Recent dating of the archeopaleontological deposits through U–Pb methods, coupled with paleomagnetic constraints, provided an age of 1.2–1.1 Ma (Michel et al., 2017). Therefore, the site can be correlated with the lower part of the VCS. The suid record (Fig. 10) from Le Vallonnet consists of a left mandibular fragment with p2–m3 (MPRM B2.BC3.32), a right maxillary fragment with P4–M3 (MPRM B4.R13520), some isolated upper and lower teeth including an almost complete male lower canine (MPRM B7.BH8.10341), and

few postcranial remains (Moullé, 1992). After a first mention as *Sus* sp. in the preliminary work by de Lumley et al. (1988), the material was studied in greater depth by Moullé (1992) and referred to *S. strozzi* based on morphological and morphometric comparison. Moullé et al. (2006) preferred a more conservative allocation to *Sus* sp., given the small sample size. The morphology (Fig. 10) and dimensions (Appendix 4) of the teeth from Le Vallonnet fit those from VCS. The male lower canine MPRM B7.BH8.10341 is typically verrucosic (distal/labial ratio = 0.86). Consequently, we confirm the attribution of the Vallonnet material to *S. strozzi*.

The nearly coeval or slightly younger French sites of Sainzelles, Soleilhac (Palombo and Valli, 2004), Bois-de-Riquet (Bourguignon et al., 2016), Saint-Prest (Guérin et al., 2003), and Durfort (Aguilar et al., 2009) did not yield any suid remains. Tsoukala and Guérin (2016) mentioned the occurrence of *S. scrofa priscus* from Chàlon-Saint-Cosme and Ceysaguet, but without any details about the samples. On the contrary, concerning Ceysaguet (whose age is well constrained at ca. 1.2 Ma; Mourer-Chauviré and Bonifay, 2018), the possible presence of *S. strozzi* was reported by Bonifay and Brugal (1996). A single M3 from Abbeville, Carpentier quarry (Early-Middle Pleistocene boundary) was referred to *S. scrofa priscus* by Antoine et al. (2015), although the same authors stated that the tooth was “initially attributed to *Sus* cf. *strozzi* (det. A.M. Moigne)” (Antoine et al., 2015: 86). Given the scarcity of the available remains, we opt for a generic attribution to *Sus* sp. for the Abbeville material.

5.5. Epivillafranchian *Sus* from Germany

Untermassfeld near the town of Meiningen (Thuringia, central Germany) is one of the richest Early Pleistocene paleontological sites in Europe. Discovered in 1978, it has yielded to date more than 14,500 fossils of large mammals and smaller vertebrates in excellent state of preservation (Kahlke, 2006). The recognition of the

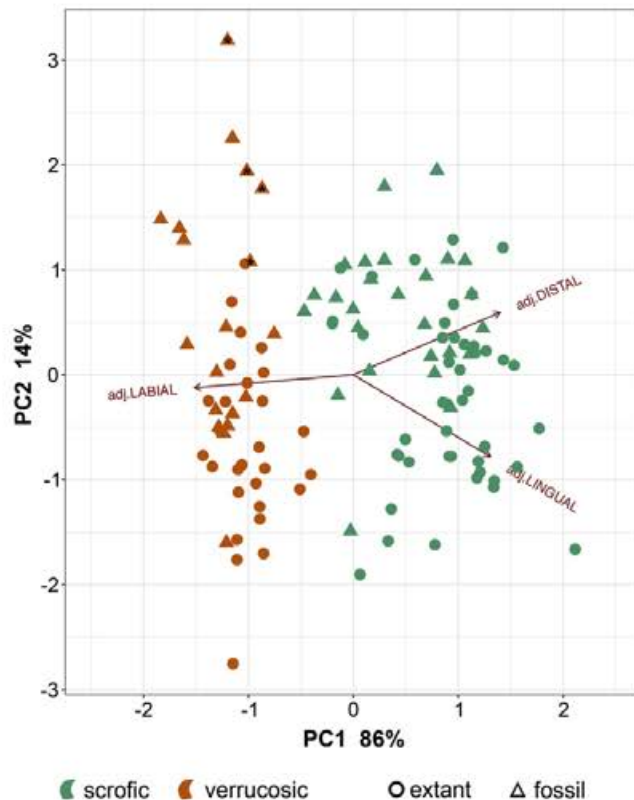


Fig. 9. Principal component analysis (PCA) of the three lower canine measurements corrected by their geometric mean (Mosimann shape variables). The first and second axis explain respectively 86% and 14% of the phenotypic total variance. The arrows indicate the direction of change for the three lengths, with the scrofic canines having relatively longer distal and lingual sides and the verrucosic canines having relatively shorter labial sides. Specimens from Vallparadis composite section are indicated by a black asterisk inside the symbol.

Epivillafranchian as a formal biochron (sensu Lindsay, 1990) is mainly based on the study of the Untermassfeld collection, which is considered as the “principal reference material for the large mammal fauna of the Epivillafranchian”, interpreted as “a separate chronostratigraphical unit wedged between the Villafranchian and the Galerian biochrons” (Kahlke, 2006: 111).

With reference to this time interval, the suid sample from Untermassfeld is second only to that of VCS in terms of richness, being composed of 18 craniomandibular and dental specimens (Guérin and Faure, 1997). The material was referred by the latter authors to *S. scrofa priscus*, of which it would represent the earliest occurrence in Europe. The collection includes a damaged juvenile cranium (IQW, 1985/20509) and a juvenile mandible (IQW, 1980/16539). According to Guérin and Faure (1997), the cranium is morphologically closer to that of *S. scrofa* than to that of *S. strozzi* because of the “widely spaced temporal ridges and the transversally depressed nuchal crest” (Guérin and Faure, 1997: 376–377). However, we do not consider this criterion as diagnostic, because the morphology of the dorsal neurocranium is strictly related to ontogeny in suines, as we have abundantly observed in osteological collections of extant species. It is predictable that, in a young individual, the parietal area is wider because the temporal ridges have not yet reached their full development. In adult individuals, the temporal ridges and nuchal crest tend to become stouter and the temporal ridges to approach each other, narrowing the parietal region. As for the teeth, Guérin and Faure (1997) found

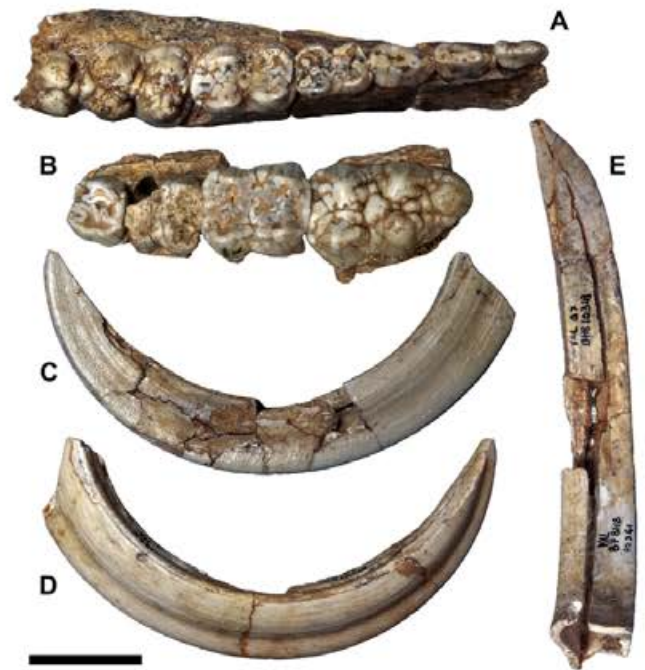


Fig. 10. *Sus strozzi* from the Le Vallonnet (France). A, Left mandibular fragment with p2–m3 MPRM B2.BC3.32 in occlusal view; B, Right maxillary fragment with P4–M3 MPRM B4.R13520 in occlusal view; C–E, Left c1 MPRM B7.BH8.10341 in labial (C), lingual (D), and distal (E) views. Scale bar: 30 mm.

size similarities between the Untermassfeld suine and *S. strozzi*, while they defined the simply built cheek teeth as indicators of a primitive form of *S. scrofa*. On the other hand, they stated that “the main cusp and cingulum morphology is more complicated than that of *Sus strozzi*” (Guérin and Faure, 1997: 379). Cherin et al. (2018) verified that the complexity of enamel figures exposed at the occlusal surface of upper and lower molars is higher in *S. strozzi* than in *S. scrofa*. Therefore, as far as they are described by Guérin and Faure (1997), the cheek teeth from Untermassfeld fit better with the typical morphology of *S. strozzi*. Finally, and most importantly, Guérin and Faure (1997) defined the well-preserved adult lower canine IQW 1984/19622 (Fig. 11) as scrofic. However, based on our measurements, the tooth is undoubtedly verrucosic (distal/labial ratio = 0.70). Therefore, we refer the Untermassfeld sample to *S. strozzi*.

To date, there are no other German sites coeval to Untermassfeld (i.e., close to Jaramillo in age). Two younger sites, Dorn-Dürkheim 3 and Mauer, both close to the Early-Middle Pleistocene boundary, respectively yielded no suid remains (Franzen et al., 2000) and only two isolated teeth (right M1 or M2 SMNS 31193 and right m2 SMNS, 18000) referable to *Sus* sp. The wild boar *S. scrofa* appears in the German record in the early Middle Pleistocene at Mosbach 2 (Middle Level of Sands according to Kahlke, 1961). The rich sample from the site comprises craniomandibular, dental, and postcranial, including also one adult male mandible (NHM:MZ PW1955/1119; Fig. 11) and four isolated lower canines (NHM:MZ PW1961/349, NHM:MZ PW1957/524, NHM:MZ PW1955/309, NHM:MZ PW1956/123), all showing a clearly scrofic morphology (distal/labial ratio ≈ 1.3). The few isolated molars from the coeval (or slightly older) localities of Süssenborn and Voigtstedt were referred to *S. scrofa priscus* by Hünemann (1969) and Hünemann (1965), respectively, but are too fragmentary for a determination to species rank.

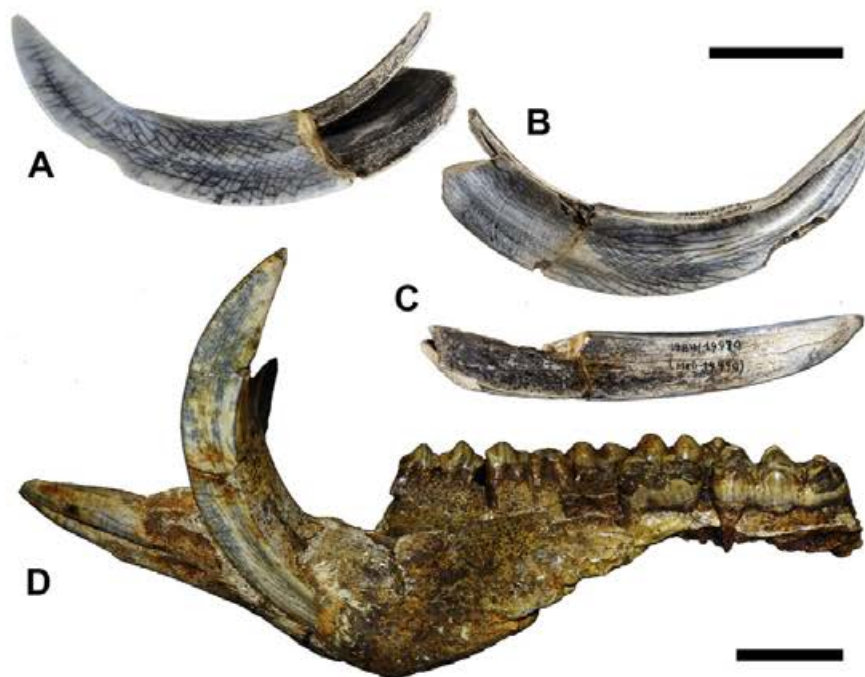


Fig. 11. Pleistocene *Sus* from Germany. A–C, Left c1 IQW 1984/19622 of *Sus strozzi* from Untermassfeld (Epivillafranchian) in labial (A), lingual (B), and distal (C) views (photos by Susann Doering); D, Mandible NHM:MZ PW1955/1119 of *Sus scrofa* from Mosbach 2 (early Middle Pleistocene) in left lateral view (photo by Bastian Lischewsky). Scale bars: 30 mm.

5.6. Epivillafranchian *Sus* from Italy

The best preserved Italian suid sample from the Epivillafranchian period is from the Frantoio locality, Arda River (northern Italy), dated to ca. 0.99 Ma (Bona and Sala, 2016). The sample consists of an almost complete mandible (MCCA Vt090) and an isolated upper incisor (MCCA Vt143). As already confirmed by Cherin et al. (2018), this material is clearly referable to *S. strozzi* based on mandibular and tooth morphology. This is here supported by the calculated distal/labial ratio of 0.78 for the Arda River specimen.

Several other Italian localities close in age to the Jaramillo subchron did not yield any suid remains. Among these, we can mention Colle Curti in the northern Apennine (Coltorti et al., 1998), Monte Peglia in Umbria (Sardella and Iurino, 2012 and references therein), and the upper layers of Lefte near Bergamo (Breda and Marchetti, 2007). Only isolated teeth, which we can only attribute to *Sus* sp., come from Castagnone (Piedmont; ca. 1.0 Ma; Siori and Sala, 2007) and Pagliare di Sassa (Abruzzo; ca. 0.8 Ma; Palombo et al., 2010). As for the slightly older site of Madonna della Strada (Abruzzo; ca. 1.2 Ma), suid remains were collected (Maccagno, 1962), but have never been described or figured, and are presumably lost (Magri et al., 2010).

The case of the Slivia (Trieste) is noteworthy. The fossil assemblage from this site was first described by Ambrosetti et al. (1979) and then revised by Bon et al. (1992). Initially considered as Middle Pleistocene in age (Ambrosetti et al., 1979), the Slivia assemblage was later designated as a reference for the homonymous Faunal Unit of the Italian biochronological framework (Gliozzi et al., 1997). The fauna is slightly younger than the Early-Middle Pleistocene boundary (Masini and Sala, 2007), and therefore it can be correlated with the uppermost part of the VCS. It includes only three suid teeth, referred to *S. cf. scrofa* by Ambrosetti et al. (1979) and to *S. scrofa* by Bon et al. (1992). The fragmented male lower canine MCSNT Vpa 2112 is typically verrucosic (distal/labial

ratio = 0.68), although given the scarcity of the sample we prefer to attribute the material to *S. cf. strozzi*.

5.7. Epivillafranchian *Sus* from eastern Europe

Epivillafranchian suines from eastern Europe are very rare. Vereshchagin (1957) reported a fragmentary mandible and a calcaneum from the latest Early Pleistocene (ca. 1.1–0.8 Ma) of Tsimbal, Taman Peninsula (Russia), which he allocated to a new species, *Sus tamanensis*. According to Alekseeva (1977), *S. tamanensis* is very close to (if not a junior synonym of) *S. strozzi*. In particular, Alekseeva (1977) stated that the Taman mandible has a very strong mental prominence, which is a typical character of *S. strozzi* according to Cherin et al. (2018).

The Epivillafranchian (ca. 1.0 Ma) of Somssich Hill 2 (Hungary) only yielded two isolated teeth (a deciduous upper premolar and a permanent lower premolar), referred to *Sus* sp. (Gasparik and Pazonyi, 2018).

The case of Kozarnika Cave (Bulgaria) is still puzzling. The very long sequence exposed in the cave probably spans from the Early to the Late Pleistocene (Guadelli et al., 2005). However, the age of the lower portion (yielding Lower Paleolithic archeological evidence) is debated. Guadelli et al. (2005) divided these deposits into three biozones, from bottom to top: biozone B2-2 (from 1.4 to 1.2 to 0.9 Ma), biozone B2-1 (0.8–0.6 Ma), and biozone B1 (0.6–0.4 Ma). Sirakov et al. (2010) redated the lowermost layers to 1.6–1.4 Ma, while according to Kahlke et al. (2011), the biozone B2-2 should be closer to 1.2 than to 1.4 Ma. Completely different results were achieved by paleomagnetic analysis by Muttoni et al. (2017), according to which the lowermost layers of the cave would record the Early-Middle Pleistocene boundary (ca. 0.78 Ma), thus making of Middle Pleistocene age the entire Lower Paleolithic interval of the section. These layers (Biozones B2-2 and B2-1) yielded several remains of a large-sized suine, which was referred (without detailed descriptions) to *S. cf. strozzi* by Guadelli et al. (2005) and to *Sus* sp.

by Sirakov et al. (2010). Unfortunately, conflicting chronological interpretations and the lack of detailed published descriptions and measurements of the pig remains make it impossible at the moment to discern which species of *Sus* is present in the basal part of Kozarnika Cave.

Several craniomandibular, dental, and postcranial remains of *Sus* are reported from the renowned site of Gombaszög (Slovakia), chronologically referred to the late Biharian (Early-Middle Pleistocene boundary; Wagner and Gasparik, 2014). Kretzoi (1938) initially referred the material to *S. scrofa priscus* and some years later to *Sus* sp. (Kretzoi, 1956). We had access to the only measurable male lower canine (HNHM V.59.926), which turned out to be scrofic (labial/distal ratio = 0.83). Therefore, the presence of the wild boar in Gombaszög is here confirmed, possibly representing one of the earliest occurrences of this species in Europe.

5.8. Biochronological, paleobiogeographical, and paleoecological implications

The implications of our results for the European biochronological framework and the paleobiogeography of Quaternary suines are remarkable (Fig. 12). The attestation of the occurrence of *S. strozzi* in Europe during the Epivillafranchian, at least until the end of the Early Pleistocene, indicates the reappearance of this species in this continent after a long period of (apparent) absence (late late Villafranchian; ca. 1.8–1.2 Ma). At the moment, it is not possible to verify whether the reappearance of *S. strozzi* was due to a dispersal from still unknown European refuge areas, or to a new dispersal wave from the East. In this regard, a review of the material

from eastern Europe would be needed. If the dating of some sites such as Kozarnika Cave and Tsimbal, and the taxonomic attribution of suine fossils to *S. strozzi* were confirmed, these would represent the earliest Epivillafranchian records of this species in Europe, thus supporting the hypothesis of a dispersal of the species from East to West. This reconstruction fits the occurrence of *S. strozzi* in the Levant just during the late late Villafranchian “suid gap” in Europe (in particular, in the site of ‘Ubeidiya in Israel dated at 1.6–1.3 Ma; Geraads et al., 1986; Martínez-Navarro et al., 2009, 2012).

The late survival of *S. strozzi* in Europe, even up to the beginning of the Middle Pleistocene, was almost prophetically hypothesized by Faure and Guérin (1983), but never confirmed by later authors. On the contrary, in recent decades, there has been a widespread opinion that after the “suid gap”, the arrival of *S. scrofa* in Europe marked the beginning of the Epivillafranchian (Kahlke et al., 2011; Bellucci et al., 2015; Martínez-Navarro et al., 2015). Our results show that (1) *S. scrofa* cannot be interpreted as a biochronological marker for the beginning of the Epivillafranchian, for which other bioevents must be considered (e.g., the first occurrences in Europe of *Megaloceros savini* or *Bison schoetensacki*; Madurell-Malapeira et al., 2019a and references therein); (2) pending new discoveries from the latest Villafranchian “suid gap”, the re-entry of *S. strozzi* in Europe is another Epivillafranchian marker. Our review highlights that, most likely, the replacement of *S. strozzi* by *S. scrofa* occurred in correspondence to, or soon thereafter, the Early-Middle Pleistocene boundary. In fact, we confirm the presence of the wild boar in several earliest Middle Pleistocene European sites, such as Mosbach (Germany; see Section 5.5), West Runton and Pakefield (Britain; Lister et al., 2010; see also Appendix 3), Gombaszög

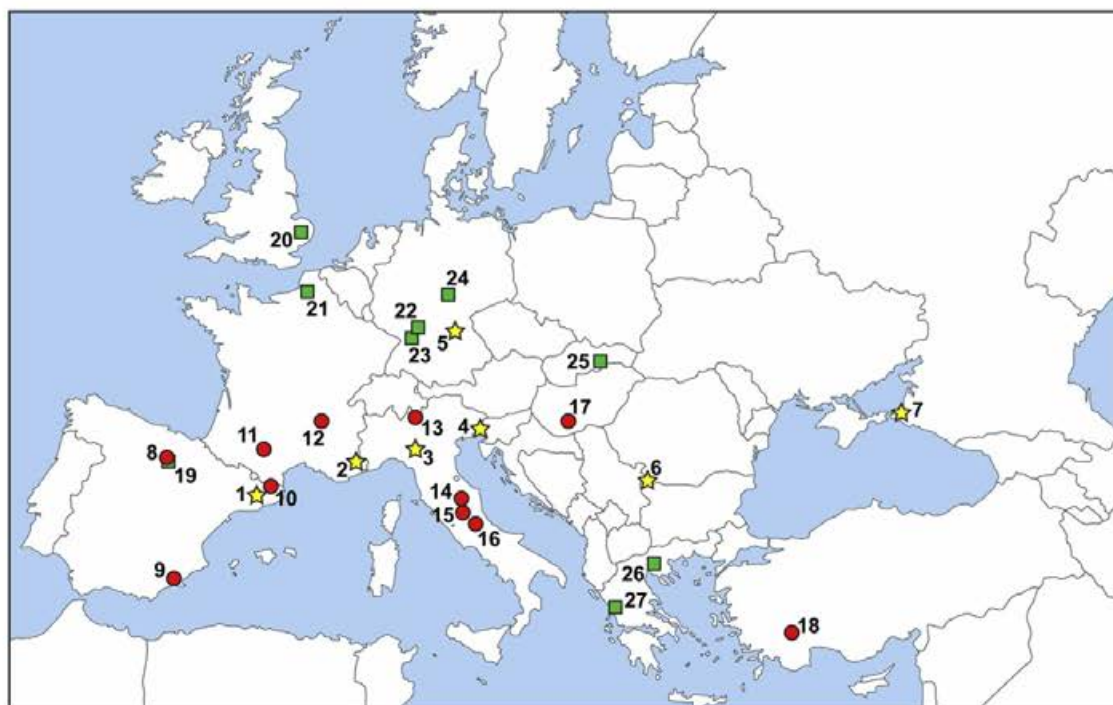


Fig. 12. Map of the Epivillafranchian–earliest Galerian records of *Sus* in Europe. Yellow stars, Epivillafranchian (latest Early Pleistocene) sites with *Sus strozzi*; red circles, selected Epivillafranchian sites with *Sus* sp. or no suine record; green squares, earliest Galerian (early Middle Pleistocene) with *Sus* sp. or *Sus scrofa*. 1, Vallparadis composite section; 2, Le Vallonnet; 3, Arda River; 4, Slivia (*S. cf. strozzi*); 5, Untermassfeld; 6, Kozarnika Cave B2-2 and B2-1 (*S. cf. strozzi*; debated chronology); 7, Tsimbal, Taman Peninsula (*S. “tamanensis”*); 8, Atapuerca Sima del Elefante TE9 and Gran Dolina TD3-5 (*Sus* sp.); 9, Cueva Victoria; 10, Incarcal; 11, Dürfort; 12, Ceyssaguet; 13, Leffe; 14, Colle Curti; 15, Monte Peglia; 16, Madonna della Strada (*Sus* sp.); 17, Somssich Hill 2 (*Sus* sp.); 18, Kobacas; 19, Atapuerca Gran Dolina TD6-8 (*Sus* sp.); 20, West Runton and Pakefield (*S. scrofa*); 21, Abbeville (*Sus* sp.); 22, Mosbach 2 (*S. scrofa*); 23, Mauer (*Sus* sp.); 24, Süssenborn (*S. scrofa*); 25, Petralona (*S. scrofa*; debated chronology); 26, Kyparissia (*S. scrofa*). Map from https://d-maps.com/carte.php?num_car=2232&lang=en. (For interpretation of the references to color in this figure legend, the reader is referred to the Web version of this article.)

(Slovakia; see Section 5.7), and Kyparissia (Greece; Athanassiou et al., 2018), among others.

The paleoenvironmental implications of our results are also interesting. The VCS is of crucial importance for the understanding of one of the major ecological transitions of the recent geological past, namely the Early-Middle Pleistocene Transition (EMPT; ca. 1.4–0.4 Ma), also known as the “Mid-Pleistocene Revolution” (Head and Gibbard, 2005; Strani et al., 2019). This global-scale phenomenon included the progressive replacement of low-amplitude 41 kyr climate cycles by high-amplitude 100 kyr cycles, the increase in long-term average global ice volume, and the establishment of marked asymmetry in global ice volume cycles (Head and Gibbard, 2005; Maslin and Ridgwell, 2005). In particular, the most extreme glacial period in this time span (the “0.9 Ma event”) seems to occur during Marine Isotope Stage (MIS) 24 and MIS 22. Northern Hemisphere ice volumes increased substantially, with severe effects on ecosystem structures especially at higher latitudes (Head and Gibbard, 2015). The effects of these environmental changes were probably milder in Mediterranean Europe, although some changes in the composition of animal and plant communities were also recorded (Kahlke et al., 2011; Head and Gibbard, 2015; Magri and Palombo, 2013). With an age spanning from 1.2 to 0.6 Ma, the VCS is one of the few available European successions in which the core of the EMPT can be analyzed (Madurell-Malapeira et al., 2010, 2017). Mesowear and microwear analyses performed on a large sample of VCS ungulates indicate that, before the “0.9 Ma event”, the area was dominated by open dry grasslands characterized by a certain seasonality (Strani et al., 2019), in agreement with data from other southern European coeval sites. After the 0.9 Ma cooling, the wear analysis suggests more humid conditions and greater expansion of woodlands, again in accordance to what is recorded in other Mediterranean sites. However, the relative abundance of seasonal mixed feeders in the post-Jaramillo VCS assemblages, indicates an even more marked seasonality than before the cooling event (Strani et al., 2019 and references therein).

Sus species have a wide ecological tolerance (Groves, 1981; Spitz, 1986). In particular, the wild boar, *S. scrofa*, is found in a huge variety of habitats throughout Eurasia, from steppe to forests, from semiarid environments to wetlands. Its diet is quantitatively dominated by plant matter (up to 96% in the annual cycle) but can comprise occasionally animal resources, especially depending on seasonal availability (Keuling et al., 2017 and references therein). Wild boars can tolerate temperatures spanning from –50 °C to 50 °C. The main limiting factors seem to be the availability of water and especially the snow coverage, which should not exceed 40–50 cm during winter (Groves, 1981). Similarly, ISEA verrucosic pigs are found in many different habitats within their range. Among them, *S. verrucosus* prefers mixed age oak forests interspersed with grasslands below 800 m in altitude (Blouch, 1993; Semiadi et al., 2016); *S. barbatus* is found in forests virtually with no elevation limits, and in peat swamp and mangrove forests (Caldecott et al., 1993; Luskin et al., 2017); *S. celebensis* is extremely adaptable and occurs from rainforest and swamp to open grasslands, even above 2500 m a.s.l. (MacKinnon, 1981; Burton and Macdonald, 2008); *S. philippensis* was formerly abundant from sea-level up to at least 2800 m, in virtually all habitats, before anthropogenic reduction of its range (Rabor, 1986; Heaney et al., 1991); *S. cebifrons* originally lived in primary and secondary forest from sea-level to mossy forest at 1600 m a.s.l. (Heaney et al., 1998; Meijaard et al., 2017). Paleocological information on *S. strozzii* is limited. According to Azzaroli (1954), *S. strozzii* would be similar to the extant *S. celebensis* in the relative shortness of limbs and metapodials in particular. These features, coupled with other skeletal characters and an overall massive body, would have resulted in very robust animal unsuitable for fast running. Moreover, the enlarged

morphology of the carpus might suggest an adaptation to soft, perhaps swampy soils (Azzaroli, 1954). Similar morphological adaptations can be also found in the African *Potamochoerus*, which also share with *S. strozzii* some features of the cervical vertebrae, humerus, and femur (Azzaroli, 1954). Both species of extant *Potamochoerus* live in a variety of ecosystems, but mostly occur in thick forests, with *Potamochoerus porcus* which prefers relatively more humid conditions (Melletti et al., 2017) than *Potamochoerus larvatus* (Seydack, 2017). These data would suggest a greater preference of *S. strozzii* for humid environments compared to *S. scrofa* (Faure and Guérin, 1983; Iannucci et al., 2020). On the contrary, the aforementioned paleoecological reconstructions available for the Vallparadis area would suggest that *S. strozzii* could tolerate very heterogeneous ecological conditions, since we find its remains in layers that precede (EVT12) and postdate (EVT7, CDRD7) the “0.9 Ma event”.

These results call for future detailed works on the paleoecology of *S. strozzii* (and other fossil suids) by using approaches and methods that are independent of morphology, such as biogeochemistry and dental microwear analysis.

6. Conclusions

The *Sus* record from the VCS, although relatively scarce when compared with those of other large mammals from the same site (e.g., hippo or deer), is the richest in Europe during the latest Early Pleistocene. Suid remains were recovered from layer EVT12, which is correlated with the Jaramillo subchron (1.07–0.99 Ma; MIS31), and from the nearly coeval layers EVT7 and CDRD7, referred to post-Jaramillo end-Matuyama times (ca. 0.86 Ma; MIS21; Madurell-Malapeira et al., 2010, 2014, 2017). On the basis of morphological and phylogenetic data, the suid from the VCS is clearly referable to *S. strozzii*. Among various morphological features, we stress the importance of the morphology of male lower canine as a very diagnostic character to distinguish *S. strozzii* (showing verrucosic canine) from *S. scrofa* (showing scrofic canine). On the contrary, we point out that linear measurements of individual cheek teeth are of little taxonomic value, especially in light of the great dental size intraspecific variation shown by some species of *Sus*, in particular *S. scrofa*. On the other hand, new research could be aimed at identifying significant differences in the morphology of the teeth (in particular m3, most represented in the fossil record) through shape analysis and/or geometric morphometrics. These approaches were successfully used to identify different suine species in ISEA (Cucchi et al., 2009) and to distinguish *S. scrofa* populations (e.g., wild versus domestic) (Price and Evin, 2019 and references therein).

The recognition of *S. strozzii* in Vallparadis prompted the revision of the suid Epivillafranchian and early Galerian records from other European localities provided in this paper. This led to the identification of *S. strozzii* in several additional sites, such as Le Vallonnet (France), Untermassfeld (Germany), Arda River (Italy), and probably Slivia (Italy), Taman Peninsula (Russia), and Kozarnika (Bulgaria). In some cases, our revision led to the redetermination of the available material, referred in the past to *S. scrofa* on the basis of characters we consider undiagnostic.

Contrary to what was previously believed, the latest Villafranchian “suid gap” in Europe was not followed by the arrival of *S. scrofa*, but by a reappearance of *S. strozzii*, probably thanks to a new dispersal wave from the East. The substitution of this last species by *S. scrofa* did not occur before the Early-Middle Pleistocene boundary.

Declaration of competing interest

The authors declare that they have no known competing financial interests or personal relationships that could have appeared to influence the work reported in this paper.

CRedit authorship contribution statement

Marco Cherin: Conceptualization, Methodology, Formal analysis, Investigation, Writing - original draft, Writing - review & editing, Visualization, Funding acquisition. **David M. Alba:** Methodology, Formal analysis, Writing - review & editing, Supervision, Funding acquisition. **Marco Crotti:** Methodology, Software, Formal analysis. **Sofia Menconero:** Visualization. **Pierre-Élie Moullé:** Resources. **Leonardo Sorbelli:** Conceptualization, Formal analysis, Writing - review & editing, Visualization, Funding acquisition. **Joan Madurell-Malapeira:** Conceptualization, Investigation, Resources, Writing - original draft, Writing - review & editing, Supervision, Project administration, Funding acquisition.

Acknowledgements

This work has been funded by the Agencia Estatal de Investigación–European Regional Development Fund of the European Union (CGL2016-76431-P and CGL2017-82654-P, AEI/FEDER-UE) and the Generalitat de Catalunya (CERCA Program). M.C. and L.S. were partially funded by the Erasmus + programme. D.M.A. and J.M.M. are members of consolidated research group 2017 SGR 116 (AGAUR, Generalitat de Catalunya). We sincerely thank Gerald Utschig (IQW) for the invaluable help, Costantino Buzi for suggestions, and the following colleagues for providing pictures, measurements, and/or information on *Sus* fossils from various European localities: Deborah Arbuta for Slivia (Italy); Athanassios Athanassiou for Kyparissia (Greece); Marzia Breda and Simon Parfitt for Pakefield, Boxgrove, and West Runton (UK); Giorgio Carnevale, Alberto Mottura, and Maria Stella Siori for Castagnone (Italy); Glenda Cruickshanks for Pakefield (UK); Thomas Engel and Rainer Brocke for Mosbach (Germany); Jean-Luc Guadelli for Kozarnika Cave (Bulgaria); Alessio Iannucci, Mihály Garsparik, and Raffaele Sardella for Gombaszög (Slovakia); Suzanne Jiquel for Lunel-Viel (France); Stéphane Madelaine for Pech de l'Azé and Combe Grenal (France); Anne-Marie Moigne for Cueva del Ángel (Spain) and Orgnac 3 (France); Benedetto Sala for Isernia (Italy); Antoine Souron for various French sites; Reinhard Ziegler for Mauer (Germany). We kindly thank Bastian Lischewsky (NHM:MZ) and Susann Doering (IQW) for the beautiful photographs. Comments by Antoine Souron and an anonymous reviewer helped to significantly improve the manuscript. We acknowledge The Willi Hennig Society for the use of TNT.

Appendix A. Supplementary data

Supplementary data to this article can be found online at <https://doi.org/10.1016/j.quascirev.2020.106234>.

References

- Aguilar, J.P., Antoine, P.-O., Bonnet, A., Crochet, J.-Y., Michaux, J., 2009. Compléments à la faune pléistocène de Durfort (Gard, Sud de la France). *Bull. Soc. Hist. Nat. Toulouse* 145, 55–58.
- Agusti, J., Leroy, S.A.G., Lozano-Fernández, I., Julià, R., 2018. Joint vegetation and mammalian records at the early Pleistocene sequence of Bòvila Ordis (Banyoles-Besalu Basin, NE Spain) and their bearing on early hominin occupation in Europe. *Palaebiodivers. Palaeoenvir.* 98, 653–662.
- Ai, H., Fang, X., Yang, B., Huang, Z., Chen, H., Mao, L., Zhang, F., Zhang, L., Cui, L., He, W., Yang, J., Yao, X., Zhou, L., Han, L., Li, J., Sun, S., Xie, X., Lai, B., Su, Y., Lu, Y., Yang, H., Huang, T., Deng, W., Nielsen, R., Ren, J., Huang, L., 2015. Adaptation and possible ancient interspecies introgression in pigs identified by whole-genome sequencing. *Nat. Genet.* 47, 217–225.
- Albarella, U., Dobney, K., Rowley-Conwy, P., 2009. Size and shape of the Eurasian wild boar (*Sus scrofa*), with a view to the reconstruction of its Holocene history. *Environ. Archaeol.* 14, 103–136.
- Alekseeva, L.I., 1977. The theriofauna of the early Anthropogene of eastern Europe. *Trudy Instituta Geologii i Geofiziki Akademiya Nauk SSSR* 300, 1–214.
- Ambrosetti, P., Bartolomei, G., De Giulii, C., Ficarelli, G., Torre, D., 1979. La breccia ossifera di Slivia (Aurisina - Sistiana) nel Carso di Trieste. *Boll. Soc. Paleontol. Ital.* 18, 207–220.
- Antoine, P., Moncel, M.-H., Locht, J.-L., Limondin-Lozouet, N., Auguste, P., Stotzel, E., Dabkowski, J., Voinchet, P., Bahain, J.-J., Falguères, C., 2015. Dating the earliest human occupation of Western Europe: new evidence from the fluvial terrace system of the Somme basin (Northern France). *Quat. Int.* 370, 77–99.
- Athanassiou, A., Michailidis, D., Vlachos, E., Tourloukis, V., Thompson, N., Harvati, K., 2018. Pleistocene vertebrates from the Kyparissia lignite mine, megalopolis basin, S. Greece: Testudines, Aves, Suiformes. *Quat. Int.* 497, 178–197.
- Azzaroli, A., 1954. Revisione della fauna dei terreni fluvio-lacustri del Valdarno Superiore. V. Filogenesi e biologia di *Sus strozzi* e di *Sus minor*. *Palaentogr. Ital.* 48, 41–76.
- Azzaroli, A., 1975. Remarks on the Pliocene Suidae of Europe. *Z. Säugetierkunde* 40, 355–367.
- Bellucci, L., Sardella, R., Rook, L., 2015. Large mammal biochronology framework in Europe at Jaramillo: the Epivillafranchian as a formal biochron. *Quat. Int.* 389, 84–89.
- Berdondini, E., 1992. Suids from the early villafranchian of villafranca d'Asti and China. *Rendiconti Lincei. Sci. Fis. Nat.* 9, 109–124.
- Blouch, R.A., 1993. The Javan warty pig (*Sus verrucosus*). In: Oliver, W.L.R. (Ed.), *Pigs, Peccaries, and Hippos: Status Survey and Conservation Action Plan*. IUCN, Gland, Switzerland, pp. 129–136.
- Bon, M., Piccoli, G., Sala, B., 1992. La fauna pleistocenica della Breccia di Slivia (Carso Triestino) nella collezione del Museo Civico di Storia Naturale di Trieste. *Atti Mus. Civ. Stor. Nat. Trieste* 44, 33–51.
- Breda, M., Marchetti, M., 2007. Pleistocene mammal faunas from the Leffe Basin (Bergamo, Northern Italy): revision and new data. *Cour. Forsch.-Inst. Senckenberg* 259, 61–77.
- Bona, F., Sala, B., 2016. Villafranchian-galerian mammal faunas transition in Southwestern Europe. The case of the late early Pleistocene mammal fauna of the Frantoio locality, Arda River (Castell'Arquato, Piacenza, northern Italy). *Geobios* 49, 329–347.
- Bonifay, M.F., Brugal, J.P., 1996. Biogéographie et biostratigraphie des grandes faunes du Pléistocène inférieur et moyen en Europe du Sud: apport des gisements français. *Paléol.* 8, 19–30.
- Bourguignon, L., Crochet, J.-Y., Capdevila, R., Ivorra, J., Antoine, P.-O., Agusti, J., Barsky, D., Blain, H.-A., Boulbes, N., Bruxelles, L., Claude, J., Cochard, D., Filoux, A., Firmat, C., Lozano-Fernández, I., Magniez, P., Pelletier, M., Rios-Garzaiz, J., Testu, A., Valensi, P., De Weyer, L., 2016. Bois-de-Riquet (Lézignan-la-Cèbe, Hérault): a late Early Pleistocene archeological occurrence in southern France. *Quat. Int.* 393, 24–40.
- Burton, J.A., Macdonald, A.A., 2008. Variation in distribution and abundance of large mammals in lore lindu national Park, central Sulawesi, Indonesia. *Malay. Nat. J.* 61, 295–305.
- Cabrera, L., Calvet, F., 1996. Onshore neogene record in NE Spain: Vallès-Penedès and el Camp half-grabens (NW mediterranean). In: Friend, P.F., Dabrio, C.J. (Eds.), *Tertiary Basins of Spain. The Stratigraphic Record of Crustal Kinematics: World and Regional Geology*. 6. Cambridge University Press, Cambridge, pp. 97–105.
- Caldecott, J.O., Blouch, R.A., Macdonald, A.A., 1993. The Bearded pig (*Sus barbatus*). In: Oliver, W.L.R. (Ed.), *Pigs, Peccaries, and Hippos: Status Survey and Conservation Action Plan*. IUCN, Gland, Switzerland, pp. 136–145.
- Cherin, M., Sorbelli, L., Crotti, M., Iurino, D.A., Sardella, R., Souron, A., 2018. New material of *Sus strozzi* (Suidae, Mammalia) from the early Pleistocene of Italy and a phylogenetic analysis of suines. *Quat. Sci. Rev.* 194, 94–115.
- Cherin, M., Azzaroli, B., Breda, M., Brobia Ansoleaga, A., Buzi, C., Pandolfi, L., Pazzaglia, F., 2019. Large mammal remains from the early Pleistocene site of Podere San Lorenzo (Perugia, central Italy). *Riv. Ital. Paleontol. Stratigr.* 125, 489–515.
- Coltorti, M., Albanelli, A., Bertini, A., Ficarelli, G., Laurenzi, M.A., Napoleone, G., Torre, D., 1998. The Colle Curti mammal site in the Colfiorito area (Umbria-Marche Apennine, Italy): geomorphology, stratigraphy, paleomagnetism and palynology. *Quat. Int.* 47/48, 107–116.
- Cucchi, T., Fujita, M., Dobney, K., 2009. Dispersal in Island South East Asia: molar shape analysis of *Sus* remains from niah caves, Sarawak. *Int. J. Osteoarchaeol.* 19, 508–530.
- De Giulii, C., Masini, F., Torre, D., 1986. The latest villafranchian faunas of Italy: the Pirro Nord fauna (Apricena, Gargano). *Palaentogr. Ital.* 74, 51–62.
- de Lumley, H., Kahlke, H.D., Moigne, A.M., Moullé, P.E., 1988. Les faunes de grands mammifères de la grotte du Vallonnet. *L'Anthropologie* 92, 465–495.
- de Serres, M., 1835–1839. *Recherches sur les Ossements Humatiles des Cavernes de Lunel-Viel*. Boehm et Cie, Montpellier, p. 275.
- Dong, W., 2008. Early Pleistocene suid (mammal) from the Dajushan, Huainan, Anhui Province (China). *Vertebr. Palasiat.* 46, 233–246.
- Dong, W., Jin, C., Zheng, L., Sun, C., Lü, J., Xu, Q., 2006. Artiodactyla from the Jinpendong site at Wuhu, Anhui Province. *Acta Anthropol. Sin.* 25, 161–171.

- Dong, W., Jin, C., Wang, Y., Xu, Q., Qin, D., Sun, C., Zhang, L., 2013. New materials of early Pleistocene *Sus* from Sanhe cave, Chongzuo, Guangxi, South China. *Acta Anthropol. Sin.* 32, 63–76.
- Duval, M., Bahain, J.-J., Falguères, C., García, J., Guilarte, V., Grün, R., Martínez, K., Moreno, D., Shao, Q., Voinchet, P., 2015. Revisiting the ESR chronology of the early Pleistocene hominin occupation at Vallparadís (Barcelona, Spain). *Quat. Int.* 389, 213–223.
- Faure, M., Guérin, C., 1983. *Sus strozzi* et *Sus scrofa*, deux mammifères artiodactyles, marqueurs des paléoenvironnements. *Palaeogeogr. Palaeoclimatol. Palaeoecol.* 48, 215–228.
- Fistani, A.B., 1996. *Sus scrofa priscus* (Goldfuss, de Serres) (Mammalia, Artiodactyla, Suidae) from the middle Pleistocene layers of Gajtan 1 site, southeast of Shkoder (north Albania). *Ann. Paleontol.* 82, 177–229.
- Forsyth-Major, C., 1881. Studi sugli avanzi pliocenici del genere *Sus* (*Sus strozzi* Menegh.). *Atti Soc. Tosc. Sc. Nat. Proc. Verb.* 2, 227.
- Frantz, L., Schraiber, J., Madsen, O., Megens, H.J., Semiadi, G., Meijaard, E., Li, N., Crooijmans, R.P.M.A., Archibald, A.L., Slatkin, M., Schook, L.B., Larson, G., Groenen, M.A.M., 2013. Genome sequencing reveals fine scale diversification and reticulation history during speciation in *Sus* (Suidae: Cetartiodactyla). *Genome Biol.* 14, R107.
- Frantz, L., Meijaard, E., Gongora, J., Haile, J., Groenen, M.A.M., Larson, G., 2016. The evolution of Suidae. *Ann. Rev. Anim. Biosci.* 4, 3.1–3.25.
- Franzen, J.L., Gliozzi, E., Jelinek, T., Scholger, R., Weidenfeller, M., 2000. Die spätpleistozäne Fossilagerstätte Dorn-Dürkheim 3 und ihre Bedeutung für die Rekonstruktion der Entwicklung des rheinischen Flußsystems. *Senckenberg. Lethaea* 80, 305–353.
- Freudenthal, M., 1971. Neogene vertebrates from the Gargano peninsula, Italy. *Scripta Geol.* 3, 1–10.
- Fujita, M., Kawamura, Y., Murase, N., 2000. Middle Pleistocene wild boar remains from NT cave, Niimi, Okayama prefecture, west Japan. *J. Geosci.* 43, 57–95.
- Gasparik, M., Pázoný, P., 2018. The macromammal remains and revised faunal list of the Somssich Hill 2 locality (late Early Pleistocene, Hungary) and the Epivillafranchian faunal change. *Fragm. Palaeontol. Hung.* 35, 153–178.
- Geraads, D., 2004. New skulls of *Kolpochoerus phacochoeroides* (Suidae: Mammalia) from the late Pliocene of Ahl al Oughlam, Morocco. *Palaeontol. Afr.* 40, 69–83.
- Geraads, D., Guérin, C., Faure, M., 1986. Les suidés du Pléistocène ancien d'Oubeidiyeh (Israël). *Mem. Travaux Cent. Rech. Fr. Jerus.* 5, 93–105.
- Gliozzi, E., Abbazzi, L., Argenti, P., Azzaroli, A., Caloi, L., Capasso Barbato, L., Di Stefano, G., Esu, D., Ficarelli, G., Girotti, O., Kotsakis, T., Masini, F., Mazza, P., Mezzabotta, C., Palombo, M.R., Petronio, C., Rook, L., Sala, B., Sardella, R., Zanolida, E., Torre, D., 1997. Biochronology of selected mammals, molluscs and ostracods from the middle Pliocene to the late Pleistocene in Italy. *Riv. Ital. Paleontol. Stratigr.* 103, 369–388.
- Goldfuss, A., 1823. Osteologische Beiträge zur Kenntnis verschiedener Säugethiere der Vorwelt. *Nova Acta Academiae Caesareae Leopoldino-Carolinae, naturae curiosum* 11, 1–482.
- Goloboff, P.A., Catalano, S.A., 2016. TNT version 1.5, including a full implementation of phylogenetic morphometrics. *Cladistics* 32, 221–238.
- Gongora, J., Cuddahee, R.E., Do Nascimento, F., Palgrave, C.J., Lowden, S., Ho, S.Y.W., Simond, D., Damayanti, C.S., White, D.J., Tay, W.T., Randi, E., Klingel, H., Rodrigues-Zarate, C.J., Allen, K., Moran, C., Larson, G., 2011. Rethinking the evolution of extant sub-Saharan African suids (Suidae, Artiodactyla). *Zool. Scripta* 40, 327–335.
- Gray, J.E., 1821. On the natural arrangement of vertebrate animals. *London Med. Reposit.* 15, 296–310.
- Groves, C., 1981. Ancestors for the pigs: taxonomy and phylogeny of the genus *Sus*. *Technical Bulletin N° 3 of the Department of Prehistory*. In: Research School of Pacific Studies Canberra. Australian National University Press, p. 96.
- Groves, C., Grubb, P., 1993. The suborder Suiformes. In: Oliver, W.L.R. (Ed.), *Pigs, Peccaries, and Hippos: Status Survey and Conservation Action Plan*. IUCN, Gland, Switzerland, pp. 1–4.
- Guadelli, J.-L., Sirakov, N., Ivanova, S., Sirakova, S.V., Anastassova, E., Courtaud, P., Dimitrova, I., Djabarska, N., Fernandez, P., Ferrier, C., Fontugne, M., Gambier, D., Guadelli, A., Iordanova, D., Iordanova, N., Kovatcheva, M., Krumov, I., Leblanc, J.-C., Mallye, J.-B., Marinska, M., Miteva, V., Popov, V., Spassov, R., Taneva, S., Tisera-Laborde, N., Tsanova, T., 2005. Une séquence du Paléolithique inférieur au Paléolithique récent dans les Balkans: la grotte Kozarnika à Orechets (Nord-Ouest de la Bulgarie). *Br. Archaeol. Rep. Int. Ser.* 1364, 87–103.
- Guérin, C., Faure, M., 1997. The wild boar (*Sus scrofa priscus*) from the post-Villafranchian lower Pleistocene of Untermassfeld. In: Kahlke, R.D. (Ed.), *Das Pleistozän von Untermassfeld bei Meiningen (Thüringen)*. Teil 1, vol. 40. Monographien des Römisch-Germanischen Zentralmuseums Mainz, pp. 375–383.
- Guérin, C., Dewolf, Y., Lauridou, J.P., 2003. Révision d'un site paléontologique célèbre: Saint-Prest (Chartres, France). *Geobios* 36, 55–82.
- Han, D., IVPP, 1987. Artiodactyla fossils from luechong *Gigantopithecus* cave in Guangxi. In: *Memoirs of Institute of Vertebrate Paleontology and Paleoanthropology, Academia Sinica*, vol. 18. Science Press, Beijing, pp. 135–208.
- Han, D., Xu, C., Yi, G., 1975. The Quaternary mammalian fossils from Bijishan, liuzhou, Guangxi. *Vertebr. Palasiat.* 13, 250–256.
- Hardjasmita, H.S., 1987. Taxonomy and phylogeny of the Suidae (Mammalia) in Indonesia. *Scripta Geol.* 85, 1–68.
- Head, M.J., Gibbard, P.L., 2005. Early–Middle Pleistocene transitions: an overview and recommendation for the defining boundary. In: Head, M.J., Gibbard, P.L. (Eds.), *Early–Middle Pleistocene Transitions: The Land–Ocean Evidence*. Special Publications 247. Geological Society, London, pp. 1–18.
- Head, M.J., Gibbard, P.L., 2015. Early–Middle Pleistocene transitions: linking terrestrial and marine realms. *Quat. Int.* 389, 7–46.
- Heaney, L.R., Gonzales, P.C., Uzzurum, R.C.B., Rickart, E.A., 1991. The mammals of Cataduanes Island: implications for the biogeography of small land-bridge islands in the Philippines. *Proc. Biol. Soc. Wash.* 104, 399–415.
- Heaney, L.R., Balete, D.S., Dollar, M.L., Alcalá, A.C., Dans, A.T.L., Gonzales, P.C., Ingle, N.R., Lepiten, M.V., Oliver, W.L.R., Ong, P.S., Rickart, E.A., Tabaranza Jr., B.R., Uzzurum, R.C.B., 1998. A synopsis of the mammalian fauna of the Philippine Islands. *Fieldiana Zool.* 88, 1–61.
- Huguet, R., Vallverdú, J., Rodríguez-Álvarez, X.P., Terradillos-Bernal, M., Bargalló, A., Lombera-Hermida, A., Menéndez, L., Modesto-Mata, M., Van der Made, J., Soto, M., Blain, H.-A., García, N., Cuenca-Bescós, G., Gómez-Merino, G., Pérez-Martínez, R., Expósito, I., Allué, E., Rofes, J., Burjachs, F., Canals, A., Bennisar, M., Nuñez-Lahuerta, C., Bermúdez de Castro, J.M., Carbonell, E., 2017. Level TE9c of Sima del Elefante (Sierra de Atapuerca, Spain): a comprehensive approach. *Quat. Int.* 433, 278–295.
- Hünemann, K.A., 1965. Die Suiden-Reste (Artiodactyla, Mammalia) des Altpleistozäns von Voigtstedt in Thüringen. *Pal. Abh. Abt. A* 2, 427–432.
- Hünemann, K.A., 1968. Die Suidae (Mammalia, Artiodactyla) aus den Ditherienensanden (Unterpliozän = Pont) Rheinheßens (Südwestdeutschland). *Schweiz. Palaeontol. Abh.* 86, 1–96.
- Hünemann, K.A., 1969. *Sus scrofa priscus* Goldfuss im Pleistozän von Süssenborn bei Weimar. *Pal. Abh. Abt. A* 3, 611–616.
- Hünemann, K.A., 1975. *Sus scrofa* Linné aus dem Pleistozän von Weimar-Ehringsdorf. *Pal. Abh.* 23, 251–263.
- Hünemann, K.A., 1977. *Sus scrofa* L. aus dem Jungpleistozän von Taubach bei Weimar in Thüringen. *Quartärpaläontologie* 2, 225–235.
- Hünemann, K.A., 1978. Das Wildschwein (*Sus scrofa* L.) aus dem Jungpleistozän von Burgtonna in Thüringen. *Quartärpaläontologie* 3, 123–127.
- Iannucci, A., Gasparik, M., Sardella, R., 2020. First report of *Sus strozzi* (Suidae, Mammalia) from the Early Pleistocene of Hungary (Dunaalmás) and species distinction based on deciduous teeth. *Sci. Nat.* 107, 5.
- Julià Brugués, R., Suc, J.-P., 1980. Analyse pollinique des dépôts lacustres du Pléistocène inférieur de Banyoles (Banolas, site de la Bobila Ordís - Espagne): un élément nouveau dans la reconstitution de l'histoire paléoclimatique des régions méditerranéennes d'Europe occidentale. *Geobios* 13, 5–19.
- Kahlke, H.D., 1961. Revision der Säugetierfaunen der klassischen deutschen Pleistozän-Fundstellen von Süssenborn, Mosbach und Taubach. *Geologie* 10, 493–525.
- Kahlke, R.D., 2006. Untermassfeld – a late Early Pleistocene (Epivillafranchian) fossil site near Meiningen (Thuringia, Germany) and its position in the development of the European mammal fauna. *Br. Archaeol. Rep. Int. Ser.* 1578, 1–144.
- Kahlke, R.D., García, N., Kostopoulos, D.S., Lacombar, F., Lister, A.M., Mazza, P.P.A., Spassov, N., Titov, V.V., 2011. Western Palaeoartic palaeoenvironmental conditions during the Early and early Middle Pleistocene inferred from large mammal communities, and implications for hominin dispersal in Europe. *Quat. Sci. Rev.* 30, 1368–1395.
- Kuss, S.E., 1961. Ein Beitrag zur Pliocän-Fauna von Herxheim/Pfalz. *Ber. Naturf. Ges. Freiburg* 61, 145–148.
- Kawamura, A., Kawamura, Y., Namiki, M., 2017. Early Holocene wild boar remains from Tsudupisuki-abu cave on Miyako Island of the southern Ryukyus, Japan. *Quat. Int.* 455, 18–29.
- Keuling, O., Podgórski, T., Monaco, A., Melletti, M., Merta, D., Albricht, M., Genov, P.V., Gethöffer, F., Vetter, S.G., Jori, F., Scalera, R., Gongora, J., 2017. Chapter 21: Eurasian wild boar *Sus scrofa* (Linnaeus, 1758). In: Melletti, M., Meijaard, E. (Eds.), *Ecology, Conservation and Management of Wild Pigs and Peccaries*. Cambridge University Press, Cambridge, pp. 202–233.
- Kretzoi, M., 1938. Die Raubtiere von Gombaszög nebst einer Übersicht der Gesamtfauuna. *Ann. Mus. Nat. Hung. Pars Min. Geol. Palaeont.* 31, 88–157.
- Kretzoi, M., 1956. Die altpleistozänen Wirbeltierfaunen des Villányer Gebirges. *Geol. Hung. ser. Palaeontologica* 27, 1–264.
- Kütke, K., 1933. Study of *Sus scrofa mosbachensis* from the Mosbach sand (Quaternary) and comparison with recent forms. *Nitzbl. Hesse Geol. L.-Amt Darmstadt* 14, 117–124.
- Lindsay, E.H., 1990. The setting. In: Lindsay, E.H., Fahlbusch, V., Mein, P. (Eds.), *European Neogene Mammalian Chronology*. Springer, New York, pp. 1–14.
- Linnaeus, C., 1758. *Systema Naturae Per Regna Tria Naturae, Secundum Classes, Ordines, Genera, Species, Cum Characteribus, Differentiis, Synonymis, Locis*. Tomus I. Laurentius Salvus, Stockholm, p. 338.
- Lister, A.M., Parfitt, S.A., Owen, F.J., Collinge, S.E., Breda, M., 2010. Metric analysis of ungulate mammals in the early Middle Pleistocene of Britain, in relation to taxonomy and biostratigraphy II: Cervidae, Equidae and Suidae. *Quat. Int.* 228, 157–179.
- Liu, W.H., Dong, W., Zhang, L.M., Zhao, W.J., Li, K.Q., 2017. New material of early Pleistocene *Sus* (Artiodactyla, Mammalia) from Yangshuizhan in Nihewan Basin, north China. *Quat. Int.* 434, 32–47.
- Luskin, M., Ke, A., Meijaard, E., Gumal, M., Kawanishi, K., 2017. *Sus Barbatus* (Errata version Published in 2018). The IUCN Red List of Threatened Species 2017 e.T41772A123793370. <https://dx.doi.org/10.2305/IUCN.UK.2017-3.RLTS.T41772A44141317.en>.
- Maccagno, A.M., 1962. *L'Elephas meridionalis* nesi di Contrada Madonna della Strada, Scoppito (AQ). *Atti Acc. Sci. Fis. Mat. Napoli* s. 3 (4), 38–129.
- MacKinnon, J., 1981. The Distribution and Status of Wild Pigs in Indonesia. Report to IUCN/SSC Pigs and Peccaries Specialist Group, p. 9.
- Madurell-Malapeira, J., Minwer-Barakat, R., Alba, D.M., Garcés, M., Gómez, M.,

- Aurell-Garrido, J., Ros-Montoya, S., Moyà-Solà, S., Berástegui, X., 2010. The Vallparadis section (Terrassa, Iberian Peninsula) and the latest Villafranchian faunas of Europe. *Quat. Sci. Rev.* 29, 2972–2982.
- Madurell-Malapeira, J., Ros-Montoya, S., Espigares, M.P., Alba, D.M., Aurell-Garrido, J., 2014. Villafranchian large mammals from the Iberian Peninsula: Paleogeography, paleoecology and dispersal events. *J. Iber. Geol.* 40, 167–178.
- Madurell-Malapeira, J., Alba, D., Espigares, M., Vinuesa, V., Palmqvist, P., Martínez-Navarro, B., Moyà-Solà, S., 2017. Were large carnivores and great climatic shifts limiting factors for hominin dispersals? Evidence of the activity of *Pachyrocata brevirostris* during the Mid-Pleistocene Revolution in the Vallparadis Section (Valles-Penedès Basin, Iberian Peninsula). *Quat. Int.* 431, 42–52.
- Madurell-Malapeira, J., Sorbelli, L., Bartolini Lucenti, S., Ruffi, I., Prat-Vericat, M., Ros-Montoya, S., Espigares, M.P., Martínez-Navarro, B., 2019a. The Iberian latest Early Pleistocene: glacial pulses, large carnivores and hominins. In: Martínez-Navarro, B., Palmqvist, P., Espigares, M.P., Ros-Montoya, S. (Eds.), *Libro de Resúmenes XXXV Jornadas de la Sociedad Española de Paleontología*, pp. 155–159.
- Magri, D., Palombo, M.R., 2013. Early to middle Pleistocene dynamics of plant and mammal communities in South west Europe. *Quat. Int.* 288, 63e72.
- Madurell-Malapeira, J., Sorbelli, L., Ros-Montoya, S., Martínez-Navarro, B., Vallverdú, J., Pineda, A., Rosas, A., Huguet, R., Cáceres, I., García-Taberner, A., López-Polín, L., Ollé, A., Saladié, P., 2019b. Acheulian tools and Villafranchian taxa: the latest early Pleistocene large mammal assemblage from Barranc de la Boella (NE Iberian peninsula). In: Martínez-Navarro, B., Palmqvist, P., Espigares, M.P., Ros-Montoya, S. (Eds.), *Libro de Resúmenes XXXV Jornadas de la Sociedad Española de Paleontología*, pp. 161–166.
- Magri, D., Di Rita, F., Palombo, M.R., 2010. An Early Pleistocene interglacial record from an intermontane basin of central Italy (Scoppito, L'Aquila). *Quat. Int.* 225, 106–113.
- Martínez-Navarro, B., Belmaker, M., Bar-Yosef, O., 2009. The large carnivores from 'Ubeidiya (early Pleistocene, Israel): biochronological and biogeographical implications. *J. Hum. Evol.* 56, 514–524.
- Martínez-Navarro, B., Belmaker, M., Bar-Yosef, O., 2012. The bovid assemblage (Bovidae, Mammalia) from the Early Pleistocene site of 'Ubeidiya, Israel: biochronological and paleoecological implications for the fossil and lithic bearing strata. *Quat. Int.* 267, 78–97.
- Martínez-Navarro, B., Madurell-Malapeira, J., Ros-Montoya, S., Espigares, M.P., Medin, T., Hortola, P., Palmqvist, P., 2015. The Epivillafranchian and the arrival of pigs into Europe. *Quat. Int.* 389, 131–138.
- Masini, F., Sala, B., 2007. Large- and small-mammal distribution patterns and chronostratigraphic boundaries from the Late Pliocene to the Middle Pleistocene of the Italian peninsula. *Quat. Int.* 160, 43–56.
- Maslin, M.A., Ridgwell, A.J., 2005. Mid-Pleistocene revolution and the 'eccentricity myth'. In: Head, M.J., Gibbard, P.L. (Eds.), *Early–Middle Pleistocene Transitions: the Land–Ocean Evidence*. Special Publications 247. Geological Society, London, pp. 19–34.
- Meijaard, E., Oliver, W.R.T., Leus, K., 2017. *Sus Cebifrons*. The IUCN Red List of Threatened Species 2017 e.T21175A44139575. <https://dx.doi.org/10.2305/IUCN.UK.2017-3.RLTS.T21175A44139575.en>.
- Melletti, M., Breuer, T., Huffman, B.A., Turkalo, A.K., Mirabile, M., Maisels, F., 2017. Chapter 13: red river Hog *Potamochoerus porcus* (Linnaeus, 1758). In: Melletti, M., Meijaard, E. (Eds.), *Ecology, Conservation and Management of Wild Pigs and Peccaries*. Cambridge University Press, Cambridge, pp. 134–149.
- Michel, V., Shen, C.C., Woodhead, J., Hu, H.M., Wu, C.C., Moullé, P.-É., Khatib, S., Cauche, D., Moncel, M.-H., Valensi, P., Chou, Y.M., Gallet, S., Echassoux, A., Orange, F., de Lumley, H., 2017. New dating evidence of the early presence of hominins in Southern Europe. *Sci. Rep.* 7, 10074.
- Minwer-Barakat, R., Madurell-Malapeira, J., Alba, D.M., Aurell-Garrido, J., De Esteban-Trivigno, S., Moyà-Solà, S., 2011. Pleistocene rodents from the Torrent de Vallparadis section (Terrassa, northeastern Spain) and biochronological implications. *J. Vertebr. Paleontol.* 31, 849–865.
- Montgelard, C., Catzeflis, F., Douzery, E., 1997. Phylogenetic relationships of artiodactyls and cetaceans as deduced from the comparison of cytochrome b and 12S rRNA mitochondrial sequences. *Mol. Biol. Evol.* 14, 550–559.
- Moullé, P.-É., 1992. Les grands mammifères du Pléistocène inférieur de la grotte du Vallonet (Roquebrune-Cap-Martin, Alpes-Maritimes). Étude paléontologique des Carnivores, Equidés, Suidés et Bovidés. Unpublished PhD thesis. Muséum National d'Histoire Naturelle, Paris.
- Moullé, P.-É., Lacombat, F., Echassoux, A., 2006. Apport des grands mammifères de la grotte du Vallonet (Roquebrune-Cap-Martin, Alpes-Maritimes, France) à la connaissance du cadre biochronologique de la seconde moitié du Pléistocène inférieur d'Europe. *L'Anthropologie* 110, 837–849.
- Mourer-Chauviré, C., Bonifay, M.-F., 2018. The birds from the early Pleistocene of Ceyssaguet (Lavoûte-sur-Loire, Haute-loire, France): description of a new species of the genus *Aquila*. *Quaternaire* 29, 183–194.
- Muttoni, G., Sirakov, N., Guadelli, J.-L., Kent, D.V., Scardia, G., Monesi, E., Zerbini, A., Ferrara, E., 2017. An early Brunhes (<0.78 Ma) age for the Lower Paleolithic tool-bearing Kozarnika cave sediments, Bulgaria. *Quat. Sci. Rev.* 178, 1–13.
- Palombo, M.R., Valli, A.M.F., 2004. Remarks on the biochronology of mammalian faunal complexes from the Pliocene to the Middle Pleistocene in France. *Geol. Rom.* 37, 145–163.
- Palombo, M.R., Mussi, M., Agostini, S., Barbieri, M., Di Canzio, E., Di Rita, F., Fiore, I., Iacumin, P., Magri, D., Speranza, F., Tagliacozzo, A., 2010. Human peopling of Italian intramontane basins: the early Middle Pleistocene site of Pagliare di Sassa (L'Aquila, central Italy). *Quat. Int.* 223–224, 170–178.
- Pazzaglia, F., Barchi, M.R., Buratti, N., Cherin, M., Pandolfi, L., Ricci, M., 2013. Pleistocene calcareous tufa from the Ellera basin (Umbria, central Italy) as a key for an integrated paleoenvironmental and tectonic reconstruction. *Quat. Int.* 292, 59–70.
- Pickford, M., 2012. Ancestors of Broom's pigs. *Trans. Roy. Soc. S. Afr.* 67, 17–35.
- Pickford, M., Obada, T., 2016. Pliocene suids from musaitu and Dermenji, Moldova: implications for understanding the origin of African *Kolpochoerus* van Hoepen & van Hoepen, 1932. *Geodiversitas* 38, 99–134.
- Price, M.D., Evin, A., 2019. Long-term morphological changes and evolving human-pig relations in the northern Fertile Crescent from 11,000 to 2000 cal. BC. *Archaeol. Anthropol. Sci.* 11, 237–251.
- R Core Team, 2019. *R: A Language and Environment for Statistical Computing*. R Foundation for Statistical Computing, Vienna, Austria. <https://www.R-project.org>.
- Rabor, D.S., 1986. Guide to the Philippine Flora and Fauna. Natural Resources Management Centre, Ministry of Natural Resources and University of the Philippines, p. 195.
- Remondino, F., El-Hakim, S., 2006. Image-based 3D modeling: a review. *Photogram. Method* 21, 269–291.
- Riechelmann, S., Richter, D.K., Lybs, M., Fietzke, J., 2014. Eine ungewöhnliche Sinterabfolge in der Heinrichshöhle von Hemer (Nordrhein-Westfalen). *Mitt. Verb. Höhlen. Karstforscher* 60, 91–96.
- Rodríguez, J., Burjachs, F., Cuenca-Bescós, G., García, N., Van der Made, J., Pérez González, A., Blain, H.-A., Expósito, I., López-García, J.M., García Antón, M., Allué, E., Cáceres, I., Huguet, R., Mosquera, M., Ollé, A., Rosell, J., Parés, J.M., Rodríguez, X.P., Díez, C., Rofes, J., Sala, R., Saladié, P., Vallverdú, J., Bennisar, M.L., Blasco, R., Bermúdez de Castro, J.M., Carbonell, E., 2011. One million years of cultural evolution in a stable environment at Atapuerca (Burgos, Spain). *Quat. Sci. Rev.* 30, 1396–1412.
- Sardella, R., Iurino, D.A., 2012. The latest early Pleistocene sabertoothed cat *Homotherium* (Felidae, Mammalia) from Monte Peglia (Umbria, central Italy). *Boll. Soc. Paleontol. Ital.* 51, 15–22.
- Semiadi, G., Rademaker, M., Meijaard, E., 2016. *Sus verrucosus*. The IUCN Red List of Threatened Species 2016 e.T21174A44139369. <https://dx.doi.org/10.2305/IUCN.UK.2016-1.RLTS.T21174A44139369.en>.
- Seydack, A.H.W., 2017. Chapter 12: Bushpig *Potamochoerus larvatus* (F. Cuvier, 1822). In: Melletti, M., Meijaard, E. (Eds.), *Ecology, Conservation and Management of Wild Pigs and Peccaries*. Cambridge University Press, Cambridge, pp. 122–133.
- Siori, M.S., Sala, B., 2007. The mammal fauna from the late early Biharian site of Castagnone (northern monferrato, Piedmont, NW Italy). *Geobios* 40, 207–217.
- Sirakov, N., Guadelli, J.-L., Ivanova, S., Sirakova, S., Boudadi-Maligne, M., Dimitrova, I., Fernandez, P., Ferrier, C., Guadelli, A., Iordanova, D., Iordanova, N., Kovatcheva, M., Krumov, I., Leblanc, J.-C., Miteva, V., Popov, V., Spassov, N., Taneva, S., Tsanova, T., 2010. An ancient continuous human presence in the Balkans and the beginnings of human settlement in western Eurasia: a Lower Pleistocene example of the Lower Paleolithic levels in Kozarnika cave (North-western Bulgaria). *Quat. Int.* 223, 94–106.
- Souron, A., Boissier, J.R., White, T.D., 2015. A new species of the suid genus *Kolpochoerus* from Ethiopia. *Acta Palaeontol. Pol.* 60, 79–96.
- Spitz, F., 1986. Current state of knowledge of wild boar biology. *Pig News Inf.* 7, 171–175.
- Stehlin, H.G., 1899–1900. Über die Geschichte des Suiden Gebisses. *Abhandlungen der Schweizerischen Paläontologischen Gesellschaft Zürich* 26/27, 1–527.
- Strani, F., DeMiguel, D., Alba, D.M., Moyà-Solà, S., Bellucci, L., Sardella, R., Madurell-Malapeira, J., 2019. The effects of the "0.9 Ma event" on the Mediterranean ecosystems during the Early-Middle Pleistocene transition as revealed by dental wear patterns of fossil ungulates. *Quat. Sci. Rev.* 210, 80–89.
- Swofford, D.L., 2002. PAUP*. Phylogenetic Analysis Using Parsimony (*and Other Methods). Version 4. Sinauer Associates, Sunderland, p. 142.
- Titov, V.V., 2000. *Sus* (Suidae, Mammalia) from the upper Pliocene of the north-eastern part of the Azov region. *Paleontol. J.* 34, 203–210.
- Tsoukala, E., Guérin, C., 2016. The Rhinocerotidae and Suidae of the middle Pleistocene from Petralona cave (Macedonia, Greece). *Acta Zool. Bulg.* 68, 243–264.
- Vallverdú, J., Saladié, P., Rosas, A., Huguet, R., Cáceres, I., Mosquera, M., García-Taberner, A., Estalrich, A., Lozano-Fernández, I., Pineda-Alcalá, A., Carrancho, Á., Villalain, J.J., Bourlés, D., Braucher, R., Lebatard, A.-E., Vialta, J., Esteban-Nadal, M., Bennisar, M.L., Bastir, M., López-Polín, L., Ollé, A., Vergés, J.M., Ros-Montoya, S., Martínez-Navarro, B., García, A., Martinell, J., Expósito, I., Burjachs, F., Agustí, J., Carbonell, E., 2014. Age and date for early arrival of the Acheulian in Europe (Barranc de la Boella, la Canonja, Spain). *PLoS One* 9, e103634.
- Van der Made, J., 1996. Listriodontinae (Suidae, Mammalia), their evolution, systematics and distribution in time and space. *Contrib. Tert. Quat. Geol.* 33, 3–254.
- Van der Made, J., 1999. Ungulates from Atapuerca TD6. *J. Hum. Evol.* 37, 389–413.
- Van der Made, J., Rosell, J., Blasco, R., 2017. Faunas from Atapuerca at the Early–Middle Pleistocene limit: the ungulates from level TD8 in the context of climatic change. *Quat. Int.* 433, 296–346.
- Vereshchagin, N.K., 1957. Mammal fossils from the lower Quaternary strata of the tcham peninsula. *Tr. Zool. Inst. Akad. Nauk SSSR* 22, 47–49.
- Von den Driesch, A., 1976. A guide to the measurement of animal bones from

- archaeological sites. Peabody Museum Bull. 1, 1–137.
- Wagner, J., Gasparik, M., 2014. Research history of Pleistocene faunas in Gombasek quarry (Slovakia), with comments to the type specimen and the type locality of *Ursus deningeri gombaszogensis* Kretzoi, 1938. *Fragm. Palaeontol. Hung.* 31, 125–143.
- Wu, G.S., Pang, J.F., Zhang, Y.P., 2006. Molecular phylogeny and phylogeography of Suidae. *Zool. Res.* 27, 197–201.
- Young, C., 1932. On the *Artiodactyla* from the *Sinanthropus* site at Chouk'outien. *Pal. Sinica s. C* 8, 1–158.

Distribution of character states for nodes in the most parsimonious trees.

Node	Character(state transformations)
<u>1</u>	7(0>1), 9(0>1)
2	6(1>0), 7(0>1), 32(1>0) , 46(0>1)
<u>3</u>	23(0>1)
<u>4</u>	41(2>1)
<u>6</u>	20(1>0) , 25(1>0) , 50(1>0)
7	19(0>1), 46(0>1)
<u>8</u>	7(0>1), 8(1>0) , 15(0>1) , 51(1>2)
<u>9</u>	6(1>0) , 13(1>0) , 14(1>0) , 33(0>1) , 46(0>1) , 51(1>2)
<u>10</u>	11(0>1) , 12(0>1) , 13(2>1) , 14(1>0) , 45(1>0)
<u>11</u>	5(0>2) , 11(0>1) , 24(0>1)
<u>13</u>	15(1>2) , 27(1>0)
<u>14</u>	2(0>1) , 3(1>0) , 4(2>1) , 8(1>0) , 9(0>1) , 11(0>1) , 14(1>0) , 29(0>1) , 30(1>0) , 34(0>1) , 35(0>1) , 36(0>1) , 37(0>1) , 44(0>1) , 48(0>1)
<u>15</u>	2(0>1) , 3(1>0) , 48(0>1)
<u>17</u>	1(1>0) , 13(2>0)
<u>18</u>	7(0>1)
21	13(2>1) , 15(1>0)
22	3(1>0) , 4(1>0) , 12(0>1)
23	33(1>02) , 39(1>0) , 47(1>0) , 51(0>1)
24	5(0>1) , 26(0>1) , 39(0>1) , 45(1>0)
25	8(1>0) , 15(0>1) , 28(0>1)
26	41(0>2)
27	17(1>0) , 23(0>1) , 31(0>1)
28	8(1>2) , 21(1>2) , 38(0>1) , 50(0>1)
29	0(1>0) , 23(0>1) , 28(0>1) , 41(0>1)
30	5(0>1) , 10(0>1) , 16(0>1) , 20(1>0)
31	7(0>1) , 40(0>1) , 43(0>1)
32	29(0>1) , 44(0>1) , 51(1>2)
33	30(1>0) , 37(0>1)
34	11(0>1) , 12(0>1) , 18(1>0) , 35(0>1)

Node numbers refer to nodes in the strict consensus tree (Fig. 6). Terminal nodes are underlined.

Appendix 3 - Lower canine comparative measurements

Species	Extant/Fossil	ID	Locality	labial_sn	labial_dx	lingual_sn	lingual_dx	distal_sn	distal_dx	LAB mean	LIN mean	DIS mean	DISLAB	LINLAB	Source of data	
<i>Sus strozzi</i>	F	IPS13018	VCS Cal Guardiola (Spain)	20.2	-	22.2	-	18.2	-	20.22	22.20	18.22	0.90	1.10	original data	
<i>Sus strozzi</i>	F	IPS107047	VCS Valparadis Estacio (Spain)	18.9	-	20.6	-	16.0	-	18.90	20.64	15.97	0.84	1.09	original data	
<i>Sus strozzi</i>	F	IPS107054	VCS Valparadis Estacio (Spain)	19.8	-	21.0	-	17.4	-	19.77	20.98	17.36	0.88	1.06	original data	
<i>Sus strozzi</i>	F	IPS107041b-c	VCS Valparadis Estacio (Spain)	19.0	20.0	18.8	19.7	17.1	17.8	19.49	19.21	17.45	0.90	0.99	original data	
<i>Sus strozzi</i>	F	MCCA V030	Ardè River (Italy)	20.1	20.5	22.5	22.8	15.8	16.0	20.30	22.05	15.80	0.76	1.12	Bona and Sala (2016)	
<i>Sus strozzi</i>	F	MFRM 87 89H 103M1	La Valsotina (France)	21.5	-	25.0	-	18.5	-	21.50	25.00	18.50	0.86	1.16	original data	
<i>Sus strozzi</i>	F	RDU 577	Liventovka (Russia)	25.0	-	26.4	-	18.0	-	25.00	26.40	18.00	0.72	1.06	Tsiv (2000)	
<i>Sus strozzi</i>	F	IGF 4006	Olivola (Italy)	27.6	-	27.2	-	19.3	-	27.57	27.17	19.26	0.70	0.99	original data	
<i>Sus strozzi</i>	F	IGF 4007	Olivola (Italy)	24.1	23.4	25.3	26.5	17.3	18.2	23.74	25.90	17.74	0.75	1.09	original data	
<i>Sus strozzi</i>	F	SRAU 337647	Paristala (Italy)	22.0	-	22.5	-	19.0	-	22.00	22.50	19.00	0.86	1.02	original data	
<i>Sus strozzi</i>	F	IOW 1984/19622	Untermaasfeld (Germany)	22.0	-	20.0	-	15.5	-	22.00	20.00	15.50	0.70	0.91	original data	
<i>Sus strozzi</i>	F	IGF 3969	Upper Valdarno (Italy)	25.8	-	27.4	-	18.5	-	25.76	27.44	18.49	0.72	1.07	original data	
<i>Sus strozzi</i>	F	IGF 3970	Upper Valdarno (Italy)	29.2	27.5	30.3	29.8	22.0	21.9	28.38	30.03	21.91	0.77	1.06	original data	
<i>Sus strozzi</i>	F	IGF 3968	Upper Valdarno (Italy)	-	26.9	-	28.2	-	18.8	28.88	28.21	19.81	0.74	1.05	original data	
<i>Sus strozzi</i>	F	IGF 3959	Upper Valdarno (Italy)	-	28.9	-	31.3	-	21.2	28.85	31.26	21.17	0.73	1.08	original data	
<i>Sus strozzi</i>	F	IGF 3951	Upper Valdarno (Italy)	-	28.9	-	27.3	-	21.1	28.85	27.25	21.10	0.73	0.94	original data	
<i>Sus strozzi</i>	F	IGF 424 (ectotype)	Upper Valdarno (Italy)	31.0	30.9	29.5	29.7	20.8	24.7	30.95	29.56	22.71	0.73	0.95	original data	
<i>Sus strozzi</i>	F	IGF 417	Upper Valdarno (Italy)	27.1	-	29.2	-	19.6	-	27.11	29.20	19.63	0.72	1.08	original data	
<i>Sus cf. strozzi</i>	F	MCSNT Vpa 2112	Silva (Italy)	15.0	-	21.0	-	13.0	-	15.00	21.00	13.00	0.68	1.11	Deborah Arbù	
<i>Sus scrofa</i>	F	HO Burg E 2817	Burgloma (Germany)	17.0	-	21.2	-	16.4	-	17.00	21.20	16.40	0.96	1.25	Hünemann (1978)	
<i>Sus scrofa</i>	F	Z3701	Colles 1 (Abruzzo)	20.0	-	20.0	-	18.0	-	20.00	20.00	18.00	0.92	1.42	Fastini (1995)	
<i>Sus scrofa</i>	F	HNHM V 59 928	Gombáč (Slovakia)	18.8	-	26.3	-	22.6	-	18.83	26.32	22.56	1.20	1.40	Alexis Iannucci	
<i>Sus scrofa</i>	F	IGF 6654V	Grota Cucigliana (Italy)	13.0	-	20.9	-	16.1	-	12.99	20.85	16.06	1.24	1.61	original data	
<i>Sus scrofa</i>	F	ISEM nia	Lunel-Viel (France)	23.1	-	30.1	-	23.5	-	23.14	30.13	23.47	1.01	1.30	original data	
<i>Sus scrofa</i>	F	NHM-MZ Pw1959/1119	Mosbach (Germany)	17.0	17.0	27.0	26.0	21.0	21.0	17.00	26.50	21.00	1.24	1.56	Thomas Engel	
<i>Sus scrofa</i>	F	NHM-MZ Pw1961/349	Mosbach (Germany)	-	15.0	-	25.0	-	15.00	25.00	21.00	1.40	1.67	Thomas Engel		
<i>Sus scrofa</i>	F	NHM-MZ Pw1967/524	Mosbach (Germany)	14.0	-	24.0	-	19.0	-	14.00	24.00	19.00	1.36	1.71	Thomas Engel	
<i>Sus scrofa</i>	F	NHM-MZ Pw1955/309	Mosbach (Germany)	-	17.0	-	25.0	-	20.0	17.00	25.00	20.00	1.18	1.47	Thomas Engel	
<i>Sus scrofa</i>	F	NHM-MZ Pw1959/123	Mosbach (Germany)	-	12.0	-	21.0	-	12.00	21.00	17.00	1.42	1.79	Thomas Engel		
<i>Sus scrofa</i>	F	OJA-NT 00033	NT Cave (Japan)	-	12.9	-	21.5	-	16.3	-	12.90	21.50	16.30	1.26	1.67	Fujita et al. (2000)
<i>Sus scrofa</i>	F	PK1CC	Pakefield (UK)	18.0	15.0	24.0	20.0	18.0	16.50	22.00	16.00	0.97	1.33	Glanda Cruickshanks		
<i>Sus scrofa</i>	F	PEC 1606	Peiratsos (Greece)	15.7	-	24.4	-	20.0	-	15.74	24.36	19.95	1.27	1.55	Evangela Tsoukala	
<i>Sus scrofa</i>	F	IGF 4721	Ponte alla Nave (Italy)	12.7	13.3	20.6	21.3	17.0	18.0	13.01	20.95	17.50	1.35	1.61	original data	
<i>Sus scrofa</i>	F	IOW 1968/9952	Taubach (Germany)	10.0	-	17.0	-	14.0	-	10.00	17.00	14.00	1.40	1.70	Hünemann (1977)	
<i>Sus scrofa</i>	F	IOW 1968/9953	Taubach (Germany)	19.0	-	25.0	-	20.0	-	19.00	25.00	20.00	1.05	1.32	Hünemann (1977)	
<i>Sus scrofa</i>	F	IOW 1968/9957	Taubach (Germany)	17.0	-	27.0	-	21.0	-	17.00	27.00	21.00	1.24	1.56	Hünemann (1977)	
<i>Sus scrofa</i>	F	IOW 1968/9958	Taubach (Germany)	17.0	-	27.0	-	22.0	-	17.00	27.00	22.00	1.29	1.65	Hünemann (1977)	
<i>Sus scrofa</i>	F	IOW 1968/9960	Taubach (Germany)	19.0	-	26.0	-	21.0	-	19.00	26.00	21.00	1.11	1.37	Hünemann (1977)	
<i>Sus scrofa</i>	F	IOW 1968/9965	Taubach (Germany)	19.0	-	26.0	-	21.0	-	19.00	26.00	21.00	1.11	1.37	Hünemann (1977)	
<i>Sus scrofa</i>	F	IOW 1968/11962	Taubach (Germany)	17.0	-	24.0	-	18.0	-	17.00	24.00	18.00	1.06	1.41	Hünemann (1977)	
<i>Sus scrofa</i>	F	IOW 1968/9951	Taubach (Germany)	11.0	-	17.0	-	15.0	-	11.00	17.00	15.00	1.36	1.55	Hünemann (1977)	
<i>Sus scrofa</i>	F	IOW 1968/9956	Taubach (Germany)	19.0	-	27.0	-	22.0	-	19.00	27.00	22.00	1.16	1.42	Hünemann (1977)	
<i>Sus scrofa</i>	F	IOW 1968/9959	Taubach (Germany)	18.0	-	25.0	-	20.0	-	18.00	25.00	20.00	1.11	1.39	Hünemann (1977)	
<i>Sus scrofa</i>	F	IOW 1968/9963	Taubach (Germany)	19.0	-	27.0	-	22.0	-	19.00	27.00	22.00	1.16	1.42	Hünemann (1977)	
<i>Sus scrofa</i>	F	IOW 1968/9964	Taubach (Germany)	20.0	-	27.0	-	21.0	-	20.00	27.00	21.00	1.05	1.35	Hünemann (1977)	
<i>Sus scrofa</i>	F	IOW 1968/11951	Taubach (Germany)	19.0	-	26.0	-	20.0	-	19.00	26.00	20.00	1.05	1.37	Hünemann (1977)	
<i>Sus scrofa</i>	F	IOW Ehr. 1968/9697 (4651)	Weimar-Ehrngedorf (Germany)	23.0	22.8	28.7	27.5	21.6	21.2	22.90	28.10	21.40	0.93	1.23	original data	
<i>Sus barbatus</i>	F	NHM 365H C.R.	ISEA	19.0	18.4	21.2	20.5	14.3	13.2	18.73	20.88	13.74	0.73	1.12	original data	
<i>Sus barbatus</i>	F	NHM10 4.5 158	ISEA	21.7	21.4	23.3	23.6	17.7	16.6	21.53	23.45	17.14	0.80	1.09	original data	
<i>Sus barbatus</i>	F	NHM 92 535	ISEA	15.8	16.4	18.7	17.9	13.0	13.7	16.06	18.28	13.32	0.83	1.14	original data	
<i>Sus barbatus</i>	F	NHM 0.3.30.12	ISEA	16.2	16.5	20.8	20.2	14.3	14.3	16.33	20.51	14.31	0.88	1.26	original data	
<i>Sus barbatus</i>	F	NHM 9.4.1.507	ISEA	19.0	19.3	23.3	23.6	14.6	14.7	19.17	20.80	14.63	0.76	1.07	original data	
<i>Sus barbatus</i>	F	NHM 374H C.R.	ISEA	21.4	21.0	24.8	23.5	13.7	13.6	21.17	24.16	13.68	0.65	1.14	original data	
<i>Sus barbatus</i>	F	NHM 32.3.7.1	ISEA	20.1	20.7	23.1	23.7	16.7	16.8	20.38	23.41	16.76	0.82	1.15	original data	
<i>Sus barbatus</i>	F	NHM 1892.9.4.16	ISEA	22.4	22.4	23.8	23.8	15.7	15.4	22.44	23.81	15.52	0.69	1.06	original data	
<i>Sus barbatus</i>	F	NHM 0.3.30.10	ISEA	19.7	20.7	22.8	23.8	16.1	16.0	20.22	23.31	16.33	0.81	1.15	original data	
<i>Sus barbatus</i>	F	NHM 375H C.R.	ISEA	18.8	18.4	24.0	23.8	16.4	16.0	18.58	23.85	16.18	0.87	1.28	original data	
<i>Sus barbatus</i>	F	NHM 97 6.25.1	ISEA	21.7	21.6	24.5	25.6	16.4	16.6	21.68	25.08	16.47	0.76	1.16	original data	
<i>Sus barbatus</i>	F	NHM 32.3.7.1	ISEA	20.4	20.7	23.7	22.7	14.0	14.9	20.56	23.17	14.45	0.70	1.13	original data	
<i>Sus barbatus</i>	F	NHM 367H C.R.	ISEA	22.3	22.4	23.9	23.6	18.0	17.4	22.36	23.77	17.72	0.79	1.06	original data	
<i>Sus barbatus</i>	F	NHM 90 6.25.10	ISEA	23.5	22.6	29.8	28.3	19.5	19.4	23.07	29.07	19.41	0.84	1.26	original data	
<i>Sus barbatus</i>	F	NHM 95 11.5.8	ISEA	20.2	20.4	23.7	24.6	15.5	14.7	20.33	24.16	15.11	0.74	1.19	original data	
<i>Sus barbatus</i>	F	NRM 591468	ISEA	21.8	22.3	24.5	22.9	15.9	16.8	22.04	23.67	16.31	0.74	1.07	original data	
<i>Sus cebifrons</i>	F	NHM 1992 319	ISEA	16.1	14.2	16.7	16.2	12.9	12.5	15.19	16.44	12.68	0.83	1.08	original data	
<i>Sus cebifrons</i>	F	NHM 1992 323	ISEA	13.2	12.3	15.4	14.5	10.1	9.8	12.74	14.95	9.97	0.78	1.17	original data	
<i>Sus cebifrons</i>	F	NHM 86 187	ISEA	15.3	15.3	17.0	17.6	10.6	10.7	15.29	17.29	10.62	0.69	1.13	original data	
<i>Sus cebifrons</i>	F	NHM 1992 325	ISEA	11.8	12.0	14.0	13.6	9.8	9.1	11.93	13.79	9.32	0.78	1.16	original data	
<i>Sus celebensis</i>	F	NRM 592837	ISEA	15.3	-	15.9	-	10.9	-	15.25	15.85	10.85	0.71	1.04	original data	
<i>Sus celebensis</i>	F	NHM 597987	ISEA	17.0	16.9	18.7	19.3	13.1	12.1	16.96	19.03	12.59	0.74	1.12	original data	
<i>Sus verrucosus</i>	F	NHM 20 11 14.6	ISEA	21.5	21.2	22.5	21.8	14.8	14.2	21.30	22.15	14.50	0.68	1.04	original data	
<i>Sus verrucosus</i>	F	NHM 9.1.5.817	ISEA	17.2	17.2	19.0	19.3	13.7	13.3	17.17	19.15	13.51	0.79	1.12	original data	
<i>Sus verrucosus</i>	F	NHM 55 4.2.3	ISEA	18.7	18.2	20.5	20.8	13.5	13.2	18.43	20.65	13.36	0.72	1.12	original data	
<i>Sus verrucosus</i>																

Appendix 4 - Comparative tooth measurements (in mm) of *Sus strozzi* from VCS, Le Vallonnet and Untermassfeld

Site	ID	Side	P2		P3		P4		M1		M2		M3		M1-M3 L		p2		p3		p4		m1		m2		m3		m3-m3 L							
			L	W	L	W	L	W	L	W	L	W	L	W	L	W	L	W	L	W	L	W	L	W	L	W	L	W		L	W					
VCS	IPS137041a	right	14.1	-	12.8	14.6	-	-	-	-	-	24.2	22.5	23.9	37.9	24.7	22.4	77.0																		
VCS	IPS137057	right	13.7	12.0	12.9	15.8	16.5	18.0	20.0	23.2	23.1	22.8	38.2	24.1	22.4	79.8																				
Le Vallonnet	MPRAM B4.R13520	right	13.7	10.0	14.4	13.0	12.4	15.7	19.5	16.1	17.0	26.0	21.2	21.0																						
Untermassfeld	ICW 1585/20509	-			14.1	15.8	18.4	-	17.9	25.3	21.6	22.7	41.8	25.3	22.8	84.1																				
VCS	IPS20134	left			12.6	14.5																														
VCS	IPS137053	left			11.4	12.7	-	15.0	-																											
Untermassfeld	ICW 1585/20709	right	15.0	7.0																																
Untermassfeld	ICW 1585/20709	right			16.0	12.0																														
Untermassfeld	ICW 1584/20310	right			17.0	12.5	17.5	13.0	14.5																											
VCS	IPS137056	right					19.9	15.9	-																											
Le Vallonnet	MPRAM B4.R13524	left					19.3	16.9	17.7																											
Le Vallonnet	MPRAM AB.B2.327	left					19.7	16.0	17.9																											
Le Vallonnet	MPRAM R13569	right					19.7	14.8	15.1																											
Le Vallonnet	MPRAM CB.B1.3823	left								26.4	21.8	23.2																								
Le Vallonnet	MPRAM B4.R13525	left								26.0	21.9	22.4																								
Le Vallonnet	MPRAM 26.2032.452	left								24.4	22.5	23.4																								
Le Vallonnet	MPRAM AB.B2.327	left								36.2	21.6	23.1																								
Le Vallonnet	MPRAM 27.Z96.291	right								26.9	20.3	22.9																								
VCS	IPS137058	right																																		
Untermassfeld	ICW 1584/19965	left																																		
Le Vallonnet	MPRAM AE.AG.100.7629	left								40.2	25.6	24.5																								
VCS	IPS137042b	right																																		
VCS	IPS137043c	left																																		
Le Vallonnet	MPRAM 97.B48.10341	left																																		
Le Vallonnet	MPRAM B4.R13619	left																																		
Le Vallonnet	MPRAM B4.R13618	right																																		
Le Vallonnet	MPRAM B4.R13527	left																																		
Le Vallonnet	MPRAM A2.A47.7806	right																																		
Le Vallonnet	MPRAM 97.B48.10402	right																																		
VCS	IPS137052	left																																		
VCS	IPS137049	left																																		
VCS	IPS137050	right																																		
Le Vallonnet	MPRAM R13518	right																																		
Le Vallonnet	MPRAM B4.R13526	left																																		
Le Vallonnet	MPRAM B4.R13528	left																																		
Le Vallonnet	MPRAM B4.R13524	left																																		

L, length; W, width; M1, distal width; Wm, mesial width. Estimated values are in italics.

Chapter S2

Supplementary material of the paper:

Sorbelli, L., Cherin, M., Kostopoulos, D.S., Sardella, R., Mecozzi, B., Plotnikov, V., Prat-Vericat, M., Azzarà, B., Bartolini-Lucenti, S. and Madurell-Malapeira, J., 2023. Earliest bison dispersal in Western Palearctic: Insights from the *Eobison* record from Pietrafitta (Early Pleistocene, central Italy). *Quaternary Science Reviews*, 301: 107923.

DOI: <https://doi.org/10.1016/j.quascirev.2022.107923>

Refer to chapter 4.

Supplementary material of: “Earliest bison dispersal in Western Palearctic: insights from the *Eobison* record from Pietrafitta (Early Pleistocene, Central Italy)”

Leonardo Sorbelli^{a,*}, Marco Cherin^b, Dimitris Kostopoulos^c, Raffaele Sardella^d, Beniamino Mecozzi^d, Valerii Plotnikov^e, Maria Prat-Vericat^a, Beatrice Azzarà^b, Saverio Bartolini-Lucenti^{a,f}, Joan Madurell-Malapeira^{a,f}

^a*Institut Català de Paleontologia Miquel Crusafont, Universitat Autònoma de Barcelona, Edifici ICTA-ICP, c/ Columnes s/n, Campus de la UAB, 08193, Cerdanyola del Vallès, Barcelona, Spain.*

^b*Dipartimento di Fisica e Geologia, Università degli Studi di Perugia, Via A. Pascoli, 06123 Perugia, Italy*

^c*Laboratory of Geology and Paleontology, School of Geology, Aristotle University of Thessaloniki, 54124, Thessaloniki, Greece.*

^d*PaleoFactory, Dipartimento di Scienze della Terra, Sapienza Università di Roma, Piazzale A. Moro 5, 00185 Roma, Italy.*

^e*Academy of Sciences of the Republic of Sakha (Yakutia), 677007 Yakutsk, Lenin ave. 33, Russia.*

^f*Dipartimento di Scienze della Terra, Università di Firenze, 50121 Firenze, Italy*

* Corresponding author.

E-mail address: leonardo.sorbelli@icp.cat

Supplementary Table 1. List of *Bison (Eobison) degiulii* specimens from Pietrafitta.

ID	Element
SABAP UMB 20. 1.6802/4	Basioccipital
SABAP UMB 20. 1.6803/2	Basioccipital
SABAP UMB 19. 2.1178	Cranium
SABAP UMB 19. 2.1179	Cranium
SABAP UMB 20. 1.6802/16	Frontal fragment
SABAP UMB 20. 1.6802/3	Nasals
SABAP UMB 21. 4.1177	Occipital
SABAP UMB 20. 1.6803/3	Petrosal bone
SABAP UMB 21. 4.1373	Petrosal bone
SABAP UMB 20. 1.6802/2	Premaxilla and maxilla
SABAP UMB 20. 1.6802/5	Horn-core
SABAP UMB 20. 1.6803/1	Horn-core
SABAP UMB 20. 1.7345	Horn-core
SABAP UMB 21. 4.1179	Horn-core
SABAP UMB 21. 4.1222	Horn-core
SABAP UMB 21. 4.1323	Horn-core
SABAP UMB 130074	Hemimandible
SABAP UMB 1.30075	Hemimandible
SABAP UMB 20. 1.6805/1	Hemimandible
SABAP UMB 20. 1.6805/2	Hemimandible
SABAP UMB 20. 1.6809	Hemimandible
SABAP UMB 20. 1.7339	Hemimandible
SABAP UMB 20. 1.7340	Hemimandible
SABAP UMB 20. 1.7341	Hemimandible
SABAP UMB 20. 1.7342	Hemimandible
SABAP UMB 21. 4.1168	Hemimandible
SABAP UMB 21. 4.1224	Hemimandible
SABAP UMB 21. 4.1235	Hemimandible
SABAP UMB 21. 4.1236	Hemimandible
SABAP UMB 21. 4.1298	Hemimandible
SABAP UMB 21. 4.1327	Hemimandible
SABAP UMB 21. 4.1376	Hemimandible
SABAP UMB 20.1.7343	Incisor
SABAP UMB 20. 1.7368	Incisor
SABAP UMB 20. 1.7369	Incisor
SABAP UMB 20. 1.7370	Incisor
SABAP UMB 21. 4.1214	Incisor
SABAP UMB 21. 4.1447	Incisor
SABAP UMB 21. 4.1448	Incisor
SABAP UMB 21. 4.1449	Incisor
SABAP UMB 20. 1.6802/15	P2
SABAP UMB 20. 1.7361	P2

SABAP UMB 21. 4.1452	P2
SABAP UMB 20. 1.6802/13	P3
SABAP UMB 20. 1.6802/14	P3
SABAP UMB 20. 1.7354	P3
SABAP UMB 20. 1.7356	P3
SABAP UMB 20. 1.7357	P3
SABAP UMB 20. 1.7358	P3
SABAP UMB 20. 1.7359	P3
SABAP UMB 20. 1.6802/12	P4
SABAP UMB 20. 1.6804/7	P4
SABAP UMB 20. 1.6804/8	P4
SABAP UMB 20. 1.7351	P4
SABAP UMB 20. 1.7353	P4
SABAP UMB 21. 4.1230	P4
SABAP UMB 22. 41.4887	P4
SABAP UMB 21. 4.1233	Upper premolar
SABAP UMB 20. 1.6802/11	M1
SABAP UMB 20. 1.6804/5	M1
SABAP UMB 20. 1.6804/6	M1
SABAP UMB 20. 1.7350	M1
SABAP UMB 21. 4.1326	M1
SABAP UMB 22. 41.4888	M1
SABAP UMB 20. 1.7352	M1/M2
SABAP UMB 20. 1.6802/10	M2
SABAP UMB 20. 1.6804/3	M2
SABAP UMB 20. 1.6804/4	M2
SABAP UMB 20. 1.7346/2	M2
SABAP UMB 20. 1.7348	M2
SABAP UMB 20. 1.7349	M2
SABAP UMB 21. 4.1229	M2
SABAP UMB 21. 4.1325	M2
SABAP UMB 21. 4.1446	M2
SABAP UMB 22. 41.4889	M2
SABAP UMB 20. 1.6802/8	M3
SABAP UMB 20. 1.6802/9	M3
SABAP UMB 20. 1.6804/1	M3
SABAP UMB 20. 1.6804/2	M3
SABAP UMB 20. 1.6806	M3
SABAP UMB 20. 1.7346/1	M3
SABAP UMB 20. 1.7347	M3
SABAP UMB 21. 4.1232	Upper molar
SABAP UMB 21. 4.1450	p2
SABAP UMB 20. 1.7366	p3
SABAP UMB 21. 4.1231	m1/m2
SABAP UMB 21. 4.1228	m1/m2

SABAP UMB 20. 1.7362	m2
SABAP UMB 20. 1.7363	m2
SABAP UMB 20. 1.7364	m2
SABAP UMB 20. 1.7365	m2
SABAP UMB 21. 4.1227	m3
SABAP UMB 21. 4.1239	m3
SABAP UMB 20. 1.7367	Lower molar
SABAP UMB 21. 4.1451	Molar
SABAP UMB 21. 4.1330	Tooth fragment
SABAP UMB 20. 1.7344	Root fragments
SABAP UMB 20.1.6802/1	Atlas
SABAP UMB 21. 4.1314	Atlas
SABAP UMB 21. 4.1164	Cervical vertebra
SABAP UMB 21. 4.1165	Cervical vertebra
SABAP UMB 22. 4.247/11	Scapula
SABAP UMB 22. 4.247/12	Scapula
SABAP UMB 21. 4.1139	Humerus
SABAP UMB 21. 4.1142	Humerus
SABAP UMB 21. 4.1144	Humerus
SABAP UMB 21. 4.1319	Humerus
SABAP UMB 21. 4.1336	Humerus
SABAP UMB 21. 4.1337	Humerus
SABAP UMB 21. 4.1338	Humerus
SABAP UMB 21. 4.1374	Humerus
SABAP UMB 21. 4.1440	Humerus
SABAP UMB 22. 4.247/2	Humerus
SABAP UMB 22. 4.247/3	Humerus
SABAP UMB 22. 4.886/1	Humerus
SABAP UMB 22. 4.247/9	Radius-ulna
SABAP UMB 22. 4.247/10	Radius-ulna
SABAP UMB 21. 4.1137	Radius-ulna
SABAP UMB 21. 4.1143	Radius-ulna
SABAP UMB 22. 4.886/2	Radius-ulna
SABAP UMB 22. 4.886/3	Radius-ulna
SABAP UMB 21. 4.1141	Radius
SABAP UMB 21. 4.1176	Radius
SABAP UMB 21. 4.1322	Radius
SABAP UMB 21. 4.1341	Radius
SABAP UMB 21. 4.1422	Radius
SABAP UMB 21. 4.1329	Ulna
SABAP UMB 21. 4.1383	Magnum
SABAP UMB 21. 4.1388	Magnum
SABAP UMB 22. 4.247/4	Magnum
SABAP UMB 21. 4.1421	Magnum
SABAP UMB 21. 4.1423	Magnum

SABAP UMB 21. 4.1424	Magnum
SABAP UMB 22. 41.4890	Magnum
SABAP UMB 22. 41.4891	Magnum
SABAP UMB 22. 41.4892	Magnum
SABAP UMB 20. 1.7329/2	Pyramidal
SABAP UMB 21. 4.1287	Pyramidal
SABAP UMB 21. 4.1300	Pyramidal
SABAP UMB 21. 4.1301	Pyramidal
SABAP UMB 21. 4.1318	Pyramidal
SABAP UMB 21. 4.1379	Pyramidal
SABAP UMB 21. 4.1384	Pyramidal
SABAP UMB 21. 4.1406	Pyramidal
SABAP UMB 21. 4.1430	Pyramidal
SABAP UMB 21. 4.1285	Scaphoid
SABAP UMB 21. 4.1303	Scaphoid
SABAP UMB 21. 4.1381	Scaphoid
SABAP UMB 21. 4.1386	Scaphoid
SABAP UMB 21. 4.1391	Scaphoid
SABAP UMB 21. 4.1401	Scaphoid
SABAP UMB 21. 4.1415	Scaphoid
SABAP UMB 21. 4.1429	Scaphoid
SABAP UMB 21. 4.1441	Scaphoid
SABAP UMB 22. 41.4893	Scaphoid
SABAP UMB 21. 4.1286	Semilunar
SABAP UMB 21. 4.1302	Semilunar
SABAP UMB 21. 4.1380	Semilunar
SABAP UMB 21. 4.1385	Semilunar
SABAP UMB 21. 4.1392	Semilunar
SABAP UMB 21. 4.1407	Semilunar
SABAP UMB 21. 4.1408	Semilunar
SABAP UMB 21. 4.1409	Semilunar
SABAP UMB 21. 4.1427	Semilunar
SABAP UMB 21. 4.1428	Semilunar
SABAP UMB 22. 41.4894	Semilunar
SABAP UMB 21. 4.1288	Unciform
SABAP UMB 21. 4.1289	Unciform
SABAP UMB 21. 4.1382	Unciform
SABAP UMB 21. 4.1387	Unciform
SABAP UMB 21. 4.1404	Unciform
SABAP UMB 21. 4.1405	Unciform
SABAP UMB 21. 4.1425	Unciform
SABAP UMB 21. 4.1426	Unciform
SABAP UMB 130038	Metacarpal
SABAP UMB 20. 1.7324	Metacarpal
SABAP UMB 20. 1.7325	Metacarpal

SABAP UMB 20. 1.7326	Metacarpal
SABAP UMB 20. 1.7329/1	Metacarpal
SABAP UMB 22. 4.247/7	Metacarpal
SABAP UMB 22. 4.247/8	Metacarpal
IGF 1011	Metacarpal
SABAP UMB 21. 4.1299	Rib
SABAP UMB 21. 4.1375	Rib
SABAP UMB 21. 4.1170	Ribs
SABAP UMB 21. 4.1171	Ribs
SABAP UMB 21. 4.1180	Ribs
SABAP UMB 21. 4.1172	Vertebra
SABAP UMB 21. 4.1173	Vertebra
SABAP UMB 21. 4.1175	Vertebra
SABAP UMB 21. 4.1181	Vertebra
SABAP UMB 21. 4.1182	Vertebra
SABAP UMB 21. 4.1183	Vertebra
SABAP UMB 21. 4.1184	Vertebra
SABAP UMB 21. 4.1185	Vertebra
SABAP UMB 21. 4.1186	Vertebra
SABAP UMB 21. 4.1192	Vertebra
SABAP UMB 21. 4.1193	Vertebra
SABAP UMB 21. 4.1194	Vertebra
SABAP UMB 21. 4.1195	Vertebra
SABAP UMB 21. 4.1196	Vertebra
SABAP UMB 21. 4.1221	Vertebra
SABAP UMB 21. 4.1248	Vertebra
SABAP UMB 21. 4.1260	Vertebra
SABAP UMB 21. 4.1293	Vertebra
SABAP UMB 21. 4.1295	Vertebra
SABAP UMB 21. 4.1321	Vertebra
SABAP UMB 21. 4.1328	Vertebra
SABAP UMB 21. 4.1416	Vertebra
SABAP UMB 21. 4.1417	Vertebra
SABAP UMB 21. 4.1418	Vertebra
SABAP UMB 21. 4.1419	Vertebra
SABAP UMB 21. 4.1439	Vertebra
SABAP UMB 21. 4.1458	Vertebra
SABAP UMB 22. 4.886/4	Vertebra
SABAP UMB 22. 4.886/5	Vertebra
SABAP UMB 19. 2.1177	Hemipelvis
SABAP UMB 21. 4.1136	Hemipelvis
SABAP UMB 21. 4.1138	Hemipelvis
SABAP UMB 22. 4.886/6	Hemipelvis
SABAP UMB 21. 4.1140	Femur
SABAP UMB 21. 4.1146	Femur

SABAP UMB 21. 4.1147	Femur
SABAP UMB 21. 4.1149	Femur
SABAP UMB 21. 4.1191	Femur
SABAP UMB 21. 4.1226	Femur
SABAP UMB 21. 4.1237	Femur
SABAP UMB 21. 4.1315	Femur
SABAP UMB 21. 4.1377	Femur
SABAP UMB 21. 4.1378	Femur
SABAP UMB 22. 4.247/5	Femur
SABAP UMB 22. 4.247/6	Femur
SABAP UMB 22. 4.886/7	Femur
SABAP UMB 21. 4.1265	Patella
SABAP UMB 21. 4.1266	Patella
SABAP UMB 22. 4.886/8	Patella
SABAP UMB 21. 4.1145	Tibia
SABAP UMB 21. 4.1148	Tibia
SABAP UMB 21. 4.1190	Tibia
SABAP UMB 21. 4.1197	Tibia
SABAP UMB 21. 4.1198	Tibia
SABAP UMB 21. 4.1339	Tibia
SABAP UMB 22. 4.247/13	Tibia
SABAP UMB 22. 4.247/14	Tibia
SABAP UMB 21. 4.1290	Malleolus
SABAP UMB 21. 4.1396	Malleolus
SABAP UMB 21. 4.1397	Malleolus
SABAP UMB 21. 4.1398	Malleolus
SABAP UMB 21. 4.1399	Malleolus
SABAP UMB 21. 4.1400	Malleolus
SABAP UMB 21. 4.1459	Malleolus
SABAP UMB 130142	Astragalus
SABAP UMB 21. 4.1151	Astragalus
SABAP UMB 21. 4.1187	Astragalus
SABAP UMB 21. 4.1240	Astragalus
SABAP UMB 21. 4.1241	Astragalus
SABAP UMB 21. 4.1242	Astragalus
SABAP UMB 21. 4.1243	Astragalus
SABAP UMB 21. 4.1244	Astragalus
SABAP UMB 21. 4.1331	Astragalus
SABAP UMB 21. 4.1332	Astragalus
SABAP UMB 21. 4.1359	Astragalus
SABAP UMB 22. 4.886/9	Astragalus
SABAP UMB 130028	Calcaneum
SABAP UMB 21. 4.1150	Calcaneum
SABAP UMB 21. 4.1152	Calcaneum
SABAP UMB 21. 4.1257	Calcaneum

SABAP UMB 21. 4.1324	Calcaneum
SABAP UMB 21. 4.1340	Calcaneum
SABAP UMB 21. 4.1368	Calcaneum
SABAP UMB 21. 4.1369	Calcaneum
SABAP UMB 22.4.244	Calcaneum
SABAP UMB 22. 4.247/1	Calcaneum
SABAP UMB 22. 4.886/10	Calcaneum
SABAP UMB 22. 41.4895	Calcaneum
SABAP UMB 21. 4.1153	Cubonavicular
SABAP UMB 21. 4.1162	Cubonavicular
SABAP UMB 21. 4.1166	Cubonavicular
SABAP UMB 21. 4.1188	Cubonavicular
SABAP UMB 21. 4.1245	Cubonavicular
SABAP UMB 21. 4.1247	Cubonavicular
SABAP UMB 21. 4.1296	Cubonavicular
SABAP UMB 21. 4.1333	Cubonavicular
SABAP UMB 21. 4.1389	Cubonavicular
SABAP UMB 22. 4.886/11	Cubonavicular
SABAP UMB 21. 4.1209	Cuneiform
SABAP UMB 21. 4.1246	Cuneiform
SABAP UMB 21. 4.1258	Cuneiform
SABAP UMB 21. 4.1297	Cuneiform
SABAP UMB 21. 4.1390	Cuneiform
SABAP UMB 21. 4.1410	Cuneiform
SABAP UMB 21. 4.1411	Cuneiform
SABAP UMB 21. 4.1412	Cuneiform
SABAP UMB 21. 4.1413	Cuneiform
SABAP UMB 22. 41.4896	Cuneiform
SABAP UMB 21. 4.1263	Small cuneiform
SABAP UMB 21. 4.1282	Small cuneiform
SABAP UMB 21. 4.1456	Small cuneiform
SABAP UMB 21. 4.1291	Pisiform
SABAP UMB 21. 4.1393	Pisiform
SABAP UMB 21. 4.1394	Pisiform
SABAP UMB 21. 4.1395	Pisiform
SABAP UMB 21. 4.1431	Pisiform
SABAP UMB 21. 4.1283	Tarsal
SABAP UMB 21. 4.1210	Sesamoid
SABAP UMB 21. 4.1211	Sesamoid
SABAP UMB 21. 4.1212	Sesamoid
SABAP UMB 21. 4.1213	Sesamoid
SABAP UMB 21. 4.1259	Sesamoid
SABAP UMB 21. 4.1261	Sesamoid
SABAP UMB 21. 4.1262	Sesamoid
SABAP UMB 21. 4.1277	Sesamoid

SABAP UMB 21. 4.1278	Sesamoid
SABAP UMB 21. 4.1284	Sesamoid
SABAP UMB 21. 4.1310	Sesamoid
SABAP UMB 21. 4.1312	Sesamoid
SABAP UMB 21. 4.1434	Sesamoid
SABAP UMB 21. 4.1435	Sesamoid
SABAP UMB 21. 4.1436	Sesamoid
SABAP UMB 21. 4.1437	Sesamoid
SABAP UMB 21. 4.1438	Sesamoid
SABAP UMB 21. 4.1454	Sesamoid
SABAP UMB 21. 4.1216	Distal Sesamoid
SABAP UMB 21. 4.1217	Distal Sesamoid
SABAP UMB 21. 4.1218	Distal Sesamoid
SABAP UMB 21. 4.1281	Distal Sesamoid
SABAP UMB 21. 4.1304	Distal Sesamoid
SABAP UMB 21. 4.1305	Distal Sesamoid
SABAP UMB 21. 4.1432	Distal Sesamoid
SABAP UMB 21. 4.1433	Distal Sesamoid
SABAP UMB 21. 4.1453	Distal Sesamoid
SABAP UMB 21. 4.1219	Carpal-Tarsal indet.
SABAP UMB 21. 4.1220	Carpal-Tarsal indet.
SABAP UMB 21. 4.1264	Carpal-Tarsal indet.
SABAP UMB 21. 4.1308	Carpal-Tarsal indet.
SABAP UMB 21. 4.1309	Carpal-Tarsal indet.
SABAP UMB 21. 4.1313	Carpal-Tarsal indet.
SABAP UMB 21. 4.1334	Carpal-Tarsal indet.
SABAP UMB 21. 4.1335	Carpal-Tarsal indet.
SABAP UMB 20. 1.7328	Metatarsal
SABAP UMB 20. 1.7330	Metatarsal
SABAP UMB 20. 1.7331	Metatarsal
SABAP UMB 20. 1.7332	Metatarsal
SABAP UMB 20. 1.7333	Metatarsal
SABAP UMB 20. 1.7334	Metatarsal
SABAP UMB 20. 1.7335	Metatarsal
SABAP UMB 20. 1.7336	Metatarsal
SABAP UMB 20. 1.7337	Metatarsal
SABAP UMB 20. 1.7338	Metatarsal
SABAP UMB 21. 4.1189	Metatarsal
SABAP UMB 21. 4.1215	Metatarsal
SABAP UMB 22. 4.247/15	Metatarsal
SABAP UMB 21. 4.1163	Metapodial
SABAP UMB 21. 4.1238	Metapodial
SABAP UMB 21. 4.1320	Metapodial
SABAP UMB 21. 4.1360	Metapodial
SABAP UMB 21. 4.1361	Metapodial

SABAP UMB 21. 4.1362	Metapodial
SABAP UMB 21. 4.1363	Metapodial
SABAP UMB 21. 4.1364	Metapodial
SABAP UMB 21. 4.1365	Metapodial
SABAP UMB 21. 4.1366	Metapodial
SABAP UMB 21. 4.1367	Metapodial
SABAP UMB 21. 4.1403	Metapodial
SABAP UMB 21. 4.1279	Vestigial metatarsal
SABAP UMB 21. 4.1280	Vestigial metatarsal
SABAP UMB 21. 4.1455	Vestigial metatarsal
SABAP UMB 20. 1.6808/1	Proximal phalanx
SABAP UMB 20. 1.6808/2	Proximal phalanx
SABAP UMB 21. 4.1154	Proximal phalanx
SABAP UMB 21. 4.1155	Proximal phalanx
SABAP UMB 21. 4.1156	Proximal phalanx
SABAP UMB 21. 4.1157	Proximal phalanx
SABAP UMB 21. 4.1158	Proximal phalanx
SABAP UMB 21. 4.1199	Proximal phalanx
SABAP UMB 21. 4.1200	Proximal phalanx
SABAP UMB 21. 4.1201	Proximal phalanx
SABAP UMB 21. 4.1202	Proximal phalanx
SABAP UMB 21. 4.1203	Proximal phalanx
SABAP UMB 21. 4.1223	Proximal Phalanx
SABAP UMB 21. 4.1249	Proximal phalanx
SABAP UMB 21. 4.1250	Proximal phalanx
SABAP UMB 21. 4.1316	Proximal phalanx
SABAP UMB 21. 4.1342	Proximal phalanx
SABAP UMB 21. 4.1343	Proximal phalanx
SABAP UMB 21. 4.1344	Proximal phalanx
SABAP UMB 21. 4.1345	Proximal phalanx
SABAP UMB 21. 4.1346	Proximal phalanx
SABAP UMB 21. 4.1347	Proximal phalanx
SABAP UMB 21. 4.1348	Proximal phalanx
SABAP UMB 21. 4.1371	Proximal phalanx
SABAP UMB 21. 4.1372	Proximal phalanx
SABAP UMB 21. 4.1444	Proximal phalanx
SABAP UMB 22. 4.245	Proximal phalanx
SABAP UMB 22. 4.886/12	Proximal phalanx
SABAP UMB 22. 4.886/13	Proximal phalanx
SABAP UMB 20. 1.6808/3	Intermediate phalanx
SABAP UMB 20. 1.6808/4	Intermediate phalanx
SABAP UMB 21. 4.1159	Intermediate phalanx
SABAP UMB 21. 4.1160	Intermediate phalanx
SABAP UMB 21. 4.1161	Intermediate phalanx
SABAP UMB 21. 4.1204	Intermediate phalanx

SABAP UMB 21. 4.1205	Intermediate phalanx
SABAP UMB 21. 4.1206	Intermediate phalanx
SABAP UMB 21. 4.1207	Intermediate phalanx
SABAP UMB 21. 4.1208	Intermediate phalanx
SABAP UMB 21. 4.1251	Intermediate phalanx
SABAP UMB 21. 4.1252	Intermediate phalanx
SABAP UMB 21. 4.1255	Intermediate phalanx
SABAP UMB 21. 4.1274	Intermediate phalanx
SABAP UMB 21. 4.1275	Intermediate phalanx
SABAP UMB 21. 4.1276	Intermediate phalanx
SABAP UMB 21. 4.1317	Intermediate phalanx
SABAP UMB 21. 4.1349	Intermediate phalanx
SABAP UMB 21. 4.1350	Intermediate phalanx
SABAP UMB 21. 4.1351	Intermediate phalanx
SABAP UMB 21. 4.1352	Intermediate phalanx
SABAP UMB 21. 4.1353	Intermediate phalanx
SABAP UMB 21. 4.1442	Intermediate phalanx
SABAP UMB 22. 4.246	Intermediate phalanx
SABAP UMB 22. 4.886/14	Intermediate phalanx
SABAP UMB 22. 4.886/15	Intermediate phalanx
SABAP UMB 22. 4.886/16	Intermediate phalanx
SABAP UMB 20. 1.6808/5	Distal phalanx
SABAP UMB 20. 1.6808/6	Distal phalanx
SABAP UMB 21. 4.1174	Distal phalanx
SABAP UMB 21. 4.1253	Distal phalanx
SABAP UMB 21. 4.1254	Distal phalanx
SABAP UMB 21. 4.1256	Distal phalanx
SABAP UMB 21. 4.1354	Distal phalanx
SABAP UMB 21. 4.1355	Distal phalanx
SABAP UMB 21. 4.1356	Distal phalanx
SABAP UMB 21. 4.1357	Distal phalanx
SABAP UMB 21. 4.1358	Distal phalanx
SABAP UMB 22. 4.886/21	Distal phalanx
SABAP UMB 22. 4.886/20	Distal phalanx
SABAP UMB 22. 4.886/19	Distal phalanx
SABAP UMB 22. 4.886/18	Distal phalanx
SABAP UMB 22. 4.886/17	Distal phalanx
SABAP UMB 22. 41.4897	Distal phalanx
SABAP UMB 21. 4.1234	Phalanx indet.
SABAP UMB 21. 4.1292	Phalanx indet.
SABAP UMB 21. 4.1306	Phalanx indet.
SABAP UMB 21. 4.1311	Phalanx indet.
SABAP UMB 21. 4.1370	Phalanx indet.
SABAP UMB 21. 4.1402	Phalanx indet.
SABAP UMB 21. 4.1443	Phalanx indet.

SABAP UMB 21. 4.1267	Caudal vertebra
SABAP UMB 21. 4.1268	Caudal vertebra
SABAP UMB 21. 4.1269	Caudal vertebra
SABAP UMB 21. 4.1270	Caudal vertebra
SABAP UMB 21. 4.1271	Caudal vertebra
SABAP UMB 21. 4.1272	Caudal vertebra
SABAP UMB 21. 4.1273	Caudal vertebra
SABAP UMB 21. 4.1445	Caudal vertebra
SABAP UMB 21. 4.1414	Fragments
SABAP UMB 20. 1.6802/6	Fragments
SABAP UMB 20. 1.6802/7	Fragments
SABAP UMB 20. 1.6803/4	Fragments
SABAP UMB 21. 4.1169	Fragments
SABAP UMB 21. 4.1294	Fragments
SABAP UMB 21. 4.1457	Fragments
SABAP UMB 22. 4.886/22	Fragments

Supplementary Table 2. Abbreviations of the measurements shown in Fig. S1.

Measurement	Abbreviations
Anterior articular facet width (atlas)	AAW
Abaxial hemicondyle thickness (metapodials)	ABETl
Abaxial hemicondyle thickness (metapodials)	ABETm
Axial hemicondyle thickness (metapodials)	AETm
Articular surface length	AL
Width of anterior processes (basioccipital)	APW
Articular surface thickness	AT
Distance between bregma and akrocranium (temporo-parietal)	BAW
Body length (calcaneum)	BLB
Minimum length (calcaneum)	BLmin
Body minimum height (calcaneum)	CBHmin
Body minimum width (calcaneum)	CBWmin
<i>Capitis femoris</i> thickness (femur)	CFT
<i>Capitis femoris</i> width (femur)	CFW
<i>Collum scapulae</i> length (scapulae)	CSL
Condylar width (occipital)	CW
Distal diaphysis thickness (metapodials)	DDT
Distal diaphysis width (metapodials)	DDW
Distal end articular thickness (limb bones)	DEAT
Distal end articular width (limb bones)	DEAW
Distal end thickness (limb bones)	DET
Distal end thickness of the lateral trochlear crest (metapodials and femur)	DETI
Distal end thickness of the medial trochlear crest (metapodials and femur)	DETM
Distal end width (limb bones)	DEW
Diaphysis thickness at midshaft (limb bones)	DT
Diaphysis minimum thickness (limb bones)	DTmin
Distal trochlear width (astragalus)	DTW
Diaphysis width at midshaft (limb bones)	DW
Diaphysis minimum width (limb bones)	DWmin
Distance from supraorbital foramen to akrocranium (frontals)	FFLmin
Maximum distance between the supraorbital foramina (frontals)	FFW
Length from Nasion to akrocranium (frontals)	FLmax
Frontal length from Nasion to Bregma (frontals)	FLmin
Foramen magnum height (occipital)	FMH
Foramen magnum width (occipital)	FMW
Width of the postorbital constriction (frontals)	FWmin
Glenoid cavity length (scapula)	GL
Glenoid cavity maximum length (scapula)	Gmax
Glenoid process length (scapulae)	GPL
Great trochanter thickness (femur)	GTT
Glenoid cavity width (femur)	GW
Height	H
Anteroposterior diameter at the base (horn)	HAP

Distance between the anterior margins of the bases (horn)	HBWmax
Distance between the posterior margins of the bases (horn)	HBWmin
Dorsoventral diameter at the base (horn)	HDV
Chord length following the maximum curve (horn)	HLmax
Distance from the base to the tip (horn)	HLmin
Maximum height (calcaneum)	Hmax
Distance between the horncore anterior margin and the orbit (frontals)	HOD
Angle between the mid-line of the horncore and the sagittal of the skull (cranium)	HS°
Intertemporal bridge height (occipital)	IBH
Intertemporal bridge width (occipital)	IBW
Left	L
Lateral length (astragalus)	Ll
Medial length (astragalus)	Lm
Maximum length	Lmax
Minimum length (astragalus)	Lmin
Height of the corpus at the first molar (mandible)	MIH
Height of the corpus at the third molar (mandible)	M3H
Malleolar facet length (tibia)	MFL
Malleolar facet width (tibia)	MFW
Molar row length (mandible)	MRL
Mastoid width (occipital)	MW
Cubo-navicular articular facet length (calcaneum)	NCFL
Occipital squama maximum height (occipital)	OSHmax
Occipital squama minimum height (occipital)	OSHmin
Olecranon fossa width (humerus)	OW
Height of the corpus at the second premolar (mandible)	P2H
Posterior articular facet width (atlas)	PAW
Proximal end articular thickness (limb bones)	PEAT
Proximal end articular width (limb bones)	PEAW
Proximal end thickness (limb bones)	PET
Proximal end width (limb bones)	PEW
Proximo-lateral facet oblique diameter (metatarsal)	PFOl
Próximo-medial facet oblique diameter (metatarsal)	PFOm
Proximo-lateral articular facet width (metacarpal)	PFWl
Proximo-medial facet width (metacarpal)	PFWm
Width of posterior processes (basioccipital)	PPW
Premolar row length (mandible)	PRL
Proximal trochlear width (astragalus)	PTW
Postcornual width (temporo-occipital)	PW
Right	R
Width of the rotula articulation	RAW
Oblique length of the sole (distal phalanx)	SOL
<i>Sustentaculum tali</i> height (calcaneum)	STH
<i>Sustentaculum tali</i> thickness (calcaneum)	STT
Thickness	T
<i>Tuber calcanei</i> height (calcaneum)	TCaH
Trochlea crest height (humerus)	TCrH

<i>Tuber calcanei</i> width (calcaneum)	TCW
Lateral trochlear height (humerus)	THl
Medial trochlear height (humerus)	THm
Lateral thickness (astragalus)	Tl
Medial thickness (astragalus)	Tm
Length of the teeth row (mandible)	TRL
Trochlea thickness of the lateral epicondyle (humerus)	TTl
Trochlea thickness of the medial epicondyle (humerus)	TTm
Intertrochlear width (astragalus)	TTW
Trochlear lateral articulation width (humerus)	TWl
Trochlear medial articulation width (humerus)	TWm
Maximum width	Wmax
Minimum width	Wmin

Supplementary Table 3. Measurements (mm) of the teeth of *Bison (Eobison) degiulii* from Pietrafitta.

Estimated measurements are in italics. Abbreviations as in Fig. S1 and Table S2.

ID Specimen	Tooth	Side	L	W
SABAP UMB 20. 1.6802/15	P2	R	16.6	14.1
SABAP UMB 20. 1.7361	P2	L	16.1	14.0
SABAP UMB 21. 4.1452	P2	R	18.6	13.3
SABAP UMB 20.1. 6802/13	P3	R	18.1	16.7
SABAP UMB 20.1. 6802/14	P3	L	16.7	21.7
SABAP UMB 20. 1.7354	P3	L	17.8	<i>14.1</i>
SABAP UMB 20. 1.7356	P3	R	19.8	<i>14.4</i>
SABAP UMB 20. 1.7357	P3	R	18.4	16.2
SABAP UMB 20. 1.7358	P3	L	16.8	19.8
SABAP UMB 20. 1.7359	P3	R	16.3	20.1
SABAP UMB 20.1. 6802/12	P4	R	17.3	20.3
SABAP UMB 20. 1.6804/7	P4	R	17.7	22.8
SABAP UMB 20. 1.6804/8	P4	L	17.2	23.6
SABAP UMB 20. 1.7351	P4	L	17.8	22.2
SABAP UMB 20. 1.7353	P4	?	-	-
SABAP UMB 21. 4.1230	P4	R	16.4	20.6
SABAP UMB 20. 1.6802/11	M1	R	22.9	24.8
SABAP UMB 20. 1.6804/5	M1	L	24.4	26.9
SABAP UMB 20. 1.6804/6	M1	R	24.3	26.5
SABAP UMB 20. 1.7350	M1	R	22.7	24.5
SABAP UMB 21. 4.1326	M1	R	27	25.5
SABAP UMB 22. 41.4888	M1	L	24.6	26.3
SABAP UMB 20. 1.6802/10	M2	L	26.1	25.7
SABAP UMB 20. 1.6804/3	M2	R	27.4	27.1
SABAP UMB 20. 1.6804/4	M2	L	27.5	27.6
SABAP UMB 20. 1.7346/2	M2	R	25.0	25.6
SABAP UMB 20. 1.7348	M2	R	27.5	25.8
SABAP UMB 20. 1.7349	M2	L	28.0	26.3
SABAP UMB 21. 4.1229	M2	R	28.2	25.0
SABAP UMB 21. 4.1325	M2	R	27.6	26.0
SABAP UMB 21. 4.1446	M2	R	28.6	29.0
SABAP UMB 22. 41.4889	M2	L	26.8	24.8
SABAP UMB 20. 1.6802/8	M3	R	28.4	26.3
SABAP UMB 20. 1.6802/9	M3	L	30.0	25.8
SABAP UMB 20. 1.6804/1	M3	L	29.1	28.8
SABAP UMB 20. 1.6804/2	M3	R	29.0	28.5
SABAP UMB 20. 1.6806	M3	L	27.6	27.0
SABAP UMB 20. 1.7346/1	M3	R	26.7	25.1
SABAP UMB 20. 1.7347	M3	L	26.0	27.3
SABAP UMB 20. 1.6805/2a	p2	L	12.1	8.4
SABAP UMB 20. 1.6805/1a	p2	R	13.1	8.3
SABAP UMB 20. 1.6809/1	p2	L	12.2	

SABAP UMB 20. 1.7340/1	p2	R	11.1	8.0
SABAP UMB 20. 1.7341/1	p2	R	13.0	9.0
SABAP UMB 20. 1.7342/1	p2	L	12.3	8.7
SABAP UMB 130074/1	p2	R	13.0	8.3
SABAP UMB 21. 4.1450	p2	L	12.0	8.5
SABAP UMB 20. 1.7362	p3	L	23.0	11.8
SABAP UMB 20. 1.6805/2b	p3	L	19.5	11.4
SABAP UMB 20. 1.6805/1b	p3	R	19.5	12.2
SABAP UMB 20. 1.6809/2	p3	L	18.5	11.0
SABAP UMB 20. 1.7340/2	p3	R	15.7	9.8
SABAP UMB 20. 1.7341/2	p3	R	18.9	11.3
SABAP UMB 20. 1.7342/2	p3	L	17.5	11.1
SABAP UMB 130074/2	p3	R	19.3	11.0
SABAP UMB 21. 4.1235/1	p3	R	19.5	10.3
SABAP UMB 20. 1.6805/1c	p4	R	20.9	12.6
SABAP UMB 20. 1.7339/1	p4	R	21.4	12.6
SABAP UMB 20. 1.6809/3	p4	L	24.6	12.1
SABAP UMB 20. 1.7340/3	p4	R	18.0	12.3
SABAP UMB 20. 1.7341/3	p4	R	21.4	12.0
SABAP UMB 20. 1.7342/3	p4	L	20.5	11.7
SABAP UMB 130074/3	p4	R	21.9	12.5
SABAP UMB 1.30075/1	p4	L	21.7	13.2
SABAP UMB 21. 4.1235/2	p4	R	22.9	11.6
SABAP UMB 21. 4.1236/1	p4	R	20.5	11.6
SABAP UMB 20. 1.6805/2c	m1	L	21.2	15.5
SABAP UMB 20. 1.6805/1d	m1	R	20.8	15.7
SABAP UMB 20. 1.7339/2	m1	R	23.0	15.3
SABAP UMB 20. 1.7341/4	m1	R	21.8	15.5
SABAP UMB 20. 1.7342/4	m1	L	22.5	15.5
SABAP UMB 130074/4	m1	R	22.9	15.3
SABAP UMB 1.30075/1	m1	L	22.9	16.3
SABAP UMB 21. 4.1236/2	m1	R	22.9	14.3
SABAP UMB 21. 4.1231	m1/m2	R	26.8	16.4
SABAP UMB 20. 1.7362	m2	L	27.2	17.7
SABAP UMB 20. 1.7363	m2	L	27.1	16.2
SABAP UMB 20. 1.7364	m2	L	23.4	15.2
SABAP UMB 20. 1.7363	m2	L	27.4	16.0
SABAP UMB 20. 1.6805/2d	m2	L	25.9	18.9
SABAP UMB 20. 1.6805/1e	m2	R	27.1	17.2
SABAP UMB 20. 1.7339/3	m2	R	27.0	16.6
SABAP UMB 20. 1.6809/5	m2	L	24.8	15.3
SABAP UMB 20. 1.7340/4	m2	R	23.5	16.0
SABAP UMB 20. 1.7341/5	m2	R	26.1	17.0
SABAP UMB 20. 1.7342/5	m2	L	25.8	16.0
SABAP UMB 130074/5	m2	R	27.2	16.3
SABAP UMB 1.30075/1	m2	L	28.3	16.7
SABAP UMB 21. 4.1236/3	m2	R	25.0	14.7

SABAP UMB 21. 4.1228	m2/m1	R?	-	20.2
SABAP UMB 20. 1.6805/2e	m3	L	37.8	18.8
SABAP UMB 20. 1.6805/1f	m3	R	37.6	17.4
SABAP UMB 20. 1.7339/4	m3	R	36.6	16.5
SABAP UMB 20. 1.7340/5	m3	R	38.3	16.1
SABAP UMB 20. 1.7341/6	m3	R	37.2	16.2
SABAP UMB 20. 1.7342/6	m3	L	36.3	16.2
SABAP UMB 130074/6	m3	R	38.4	15.3
SABAP UMB 1.30075/	m3	L	39.2	16.3
SABAP UMB 21. 4.1227	m3	R	37.4	16.4
SABAP UMB 21. 4.1239	m3	R	36.6	15.5

Supplementary Table 4. Comparative dental measurements (mm) of M1, M2, M3, and m3 in selected *Leptobos* and *Bison* s.l. samples. Abbreviations as in Fig. S1 and Table S2. Data taken from: ^aDuvernois and Guérin (1989); ^bBukshiamidze (2005); ^cMoya Solà (1987); ^dthis work; ^eMasini (1989); ^fKostopoulos et al. (2018); ^gAsperen and Kahlke (2017); ^hBrugal (1995); ⁱMoullé (1992); ^jSorbelli et al. (2021a); ^kVasiliev (2008).

Taxon	Locality	Statistics	LMI	WMI	LM2	WM2	LM3	WM3	Lm3	Wm3
<i>Leptobos merlei</i> ^a	St. Vallier (France)	Mean (N)	19.5 (4)	23.4 (4)	24.0 (4)	25.6 (4)	27.0 (4)	24.9 (4)	38.3 (2)	17.5 (2)
		Min-Max	18.0–20.5	21.0–25.5	22.0–26.0	24.5–28.0	25.5–29.0	24.0–26.5	37.5–39	17.5–17.5
		SD	1.08	1.88	1.63	1.60	1.58	1.18	1.1	
<i>Leptobos etruscus</i> ^a	Senéze, Upper Valdarno (France, Italy)	Mean (N)	19.9 (26)	23.2 (29)	25.1 (30)	23.5 (30)	29.2 (27)	23.5 (27)	39 (56)	16.3 (56)
		Min-Max	17.0–23.0	17.5–27.0	20.0–28.0	16.0–28.5	25.0–34.0	17–28.0	34.5–45	13–19.5
		SD	1.6	1.9	2.3	3.1	2.3	2.6	2.1	1.4
<i>B. (Eobison) georgicus</i> ^b	Dmamisi (Georgia)	Mean (N)	23 (4)	25.4 (4)	27.2	26.0	30.1	27.4	39.5	13.9
		Min-Max	20.3–28.8	24.2–26	25.3–29	25–27.3	27.8–31.3	27.1–28.9	37.9–42.4	13–15.1
		SD	3.4	3.3	1.9	1.0	1.7	0.5	42.4	15.1
<i>B. (Eobison) sp.</i> ^c	Venta Micena (Spain)	Mean (N)	25.9 (11)	20.9 (11)	28.7 (9)	25.9 (11)	29.7 (10)	21.8 (9)	38.9 (14)	15.6 (15)
		Min-Max	22.8–27.2	19.3–23.0	26.2–30.9	22.8–27.2	27.4–32.3	21–23.3	37.3–42.4	13.9–17.5
		SD	1.34	1.7	1.6	1.3	1.9	1.3	1.5	0.9
<i>B. (Eobison) deginilii</i> ^d	Pietrafitta (Italy)	Mean (N)	24.3 (5)	25.6 (5)	27.3 (9)	26.5 (9)	28.1 (7)	27 (7)	37.6 (10)	16.5 (10)
		Min-Max	22.7–27.0	24.5–26.9	25–28.6	25.0–29.0	26.0–30.0	25.1–28.8	36.3–39.2	15.3–18.8
		SD	1.7	1.0	1.1	1.4	1.4	1.4	0.9	1
<i>B. (Eobison) deginilii</i> ^e	Pirro (Italy)	Mean (N)	20.4 (7)	23.3 (7)	23.3 (6)	24.7 (6)	26.2 (10)	23.5 (10)	34.3 (1)	15.0 (1)
		Min-Max	19.6–22.2	21.0–26.0	22.0–26.0	23.9–25.3	23.0–28.4	21.2–25.5		
		SD	1.0	1.5	1.5	0.6	1.9	1.1		
<i>B. (Eobison) deginilii</i> ^f	Mygdonia Basin (Greece)	Mean (N)	26.2 (18)	24.2 (18)	29.8 (22)	24.9 (22)	30.8 (22)	23.9 (22)	40 (10)	17 (10)
		Min-Max	22.0–33.9	19.3–28.0	25–35.9	19.5–29.6	27.9–33	18–29.1	37.1–45.1	15.1–18.1
		SD	4.0	2.7	2.5	3.3	1.3	3.3	2.4	0.9
<i>B. (Eobison) cf. deginilii</i> ^d	Capena (Italy)	Mean (N)	23.2 (2)	25.3 (1)	26.7 (2)	22.3 (1)	28.6 (2)	21.8 (1)	39.5 (1)	16.4 (1)
		Min-Max	22.7–23.6		28.3–28.9					
		SD	0.6		0.4					
<i>B. (Poephagus) menneri</i> ^g	Untermassfeld (Germany)	Mean (N)	26.9 (16)	20.7 (16)	31.2 (17)	20.6 (17)	31.7 (13)	21 (13)	41.4 (20)	15.9 (22)
		Min-Max	22.7–30.6	17.0–25.2	27.7–35.0	17–26.3	30.2–34.3	16.8–23.8	38–45.3	13.2–18.7
		SD	3.1	2.9	1.9	3.2	1.2	2.1	2.1	1.7

<i>B. (Bison) schoetensacki</i> ^{g, h, i, j}	Durfort, Le Vallonnet,	Mean (N)	28.4 (54)	23 (44)	31.1 (63)	23.6 (54)	32.7 (58)	25.1 (50)	42.6 (52)	17.9 (52)
	Süsselnborn, Isernia, Vallparadis	Min-Max	20.6-34.5	16.5-29.2	23.3-35.7	17.5-30.5	23.5-40.3	18.4-31.5	37.8-49.8	14.7-21
	(France, Germany, Italy, Spain)	SD	3.4	3.3	2.6	3.0	2.8	2.8	2.4	1.5
<i>B. (Bison) prisicus prisicus</i> ^g	Taubach	Mean (N)	33 (15)	23.3 (15)	35.9 (14)	25.5 (14)	38.1 (4)	24.2 (4)	48.6 (18)	18.8 (19)
	(Germany)	Min-Max	30.2-35.3	21.1-28.2	33.8-38.3	22.3-29.6	36.1-40.0	20.7-26.5	44.0-53.7	16.0-21.5
		SD	1.5	2.1	1.4	2.4	1.7	2.6	3.1	2.9
<i>B. (Bison) prisicus prisicus</i> ^k	Krasny Yar, R-W	Mean (N)	25.3 (10)	27.5 (10)	31.2 (11)	28.1 (9)	33.1 (8)	28.2 (6)	46.8 (58)	19.9 (68)
	(Russia)	Min-Max	20.5-32	24.7-33.0	26.5-34.7	23.0-31.0	29.0-37.0	24.0-30.5	42-53.5	16-22.5

Supplementary Table 5. Measurements (mm) of the hemimandibles of *Bison (Eobison) degiulii* from Pietrafitta. Abbreviations as in Fig. S1 and Table S2.

ID Specimen	Side	TRL	MRL	PRL	P2H	MIH	M3H
SABAP UMB 20. 1.6805/2	L	145.0	89.2	55.2	-	59.6	46
SABAP UMB 20. 1.6805/1	R	142.6	89.1	53.4	74.2	-	43.6
SABAP UMB 20. 1.7339	R	-	86.0	-	61.9	52.0	-
SABAP UMB 20. 1.6809	L	-	-	55.7	-	41.0	33.2
SABAP UMB 20. 1.7340	R	132.1	88.8	45.6	-	47.0	35.8
SABAP UMB 20. 1.7341	R	144.8	88.7	55.3	65.2	52.0	41.4
SABAP UMB 20. 1.7342	L	139.5	86.6	53.4	70.0	52.0	38.1
SABAP UMB 130074	R	148.0	94.7	52.6	73.4	56.7	-
SABAP UMB 130075	L	-	94.2	-	66.1	50.0	-

Supplementary Table 6. Principal component analysis of crania using six selected variables (see Section 3 in the main text and Fig. 9). Eigenvalue and % variance of the PCs and coefficients of each variable for each PC are shown. Abbreviations as Table 1.

	PC 1	PC 2	PC 3	PC 4	PC 5	PC 6
Eigenvalue	0.01975	0.003426	0.002557	0.001933	0.001403	6.53E-20
% Variance	67.943	11.785	8.7981	6.6487	4.8249	2.25E-16
msIBW	0.84355	-0.24305	0.048119	-0.056924	-0.239	0.40825
msCW	-0.014523	0.022855	0.5209	0.40254	0.63184	0.40825
msFMW	-0.35892	-0.72025	-0.42201	0.059933	0.063753	0.40825
msMW	0.078591	0.55012	-0.59037	-0.22958	0.35111	0.40825
msOSHmax	-0.23781	0.3415	-0.0035191	0.52965	-0.61613	0.40825
msPPW	-0.31089	0.048821	0.44688	-0.70562	-0.19156	0.40825

Supplementary Table 7. Measurements (mm) of the atlas of *Bison (Eobison) degiulii* from Pietrafitta. Abbreviations as in Fig. S1 and Table S2.

ID Specimen	Wmax	Lmax	PAW	AAW	H
SABAP UMB 20. 1.6802/1	182.9	126.4	107.1	112.4	-
SABAP UMB 21. 4.1314	-	-	-	-	95.6

Supplementary Table 8. Measurements (mm) of the scapulae of *Bison (Eobison) degiulii* from Pietrafitta. Abbreviations as in Fig. S1 and Table S2.

ID Specimen	Side	GL	GLmax	GW	CSL
SABAP UMB 22. 4.247/11	L	75.3	85.0	60.5	65.0
SABAP UMB 22. 4.247/12	S	79.30	90.80	61.1	68.7

Supplementary Table 9. Measurements (mm) of the humeri of *Bison (Eobison) deginili* from Pietrafitta. Abbreviations as in Fig. S1 and Table S2.

ID Specimen	Side	Lmax	DEW	DEAW	OW	TWm	TWI	DET	TTm	TTI	THm	TCH	THI
SABAP UMB 21. 4.1139	R	-	92.5	86.2	34.1	56.6	28.8	-	-	-	55.5	47.5	37.6
SABAP UMB 21. 4.1144	L	-	101.7	89.5	34.9	62.8	27.7	81.0	-	-	49.2	49.6	39.0
SABAP UMB 21. 4.1336	R	-	-	82.9	-	55.8	27.7	-	-	-	50.2	47	37.6
SABAP UMB 21. 4.1337	L	-	-	74.6	-	50.9	25.3	-	-	-	47.2	42.8	33.5
SABAP UMB 21. 4.1338	R	-	-	75.5	-	47.2	23.9	-	-	-	55.5	46.9	-
SABAP UMB 22. 4.247/2	R	365.0	95.3	84.3	33.3	56.0	25.4	93.1	91.7	61.0	51.7	46.5	36.1

Supplementary Table 10. Comparative measurements (mm) of the humerus in selected *Leptobos* and *Bison* s.l. samples. Abbreviations as in Fig. S1 and Table S2. Data taken from: ^aMasini (1989); ^bRodrigo (2011); ^cBukshianidze (2005); ^dthis work; ^eSher (1997); ^fMoullé (1992); ^gSala (1986); ^hSorbelli et al. (2021a); ⁱVasiliev (2008).

Taxon	Locality	Statistics			DEAW	TWm	TTm	TTI	THm
		Mean	Min-Max	SD					
<i>Leptobos</i> gr. LSEM ^{a, b}	Les Écouaires, St. Vallier	76.9 (16)	70.8 (6)	48.2 (6)	76.7 (14)	54.1 (6)	46.7 (17)		
	Montopoli, Villarroya	65.0-89.9	65.7-77.0	45.0-51.3	67.7-85.3	47.6-61.3	41.0-52.2		
	(France, Italy, Spain)	8.2	4.8	2.6	6.4	5.8	4.1		
<i>Leptobos</i> etruscus ^{a, b}	Senèze, Matassino,	85.7 (21)	79.9 (17)	54.5 (17)	81.7 (20)	58.5 (16)	51.2 (22)		
	Olivola, Fonélas-1	68.8-94.2	64.5-85.0	41.7-57.6	62.3-90.0	48.6-63.0	39.9-55.8		
	(France, Italy, Spain)	6.5	4.5	3.6	7.5	3.1	3.7		
<i>Bison</i> (<i>Eobison</i>) <i>georgicus</i> ^c	Dmanisi	93.0 (4)	81.9 (4)	63.9 (4)	87.3 (4)	57.7 (3)	49.7 (4)		
	(Georgia)	91.3-95.4	78.4-84.4	54.5-58.3	81.6-91.9	55.4-59.1	48.6-50.9		
		1.9	2.6	1.7	4.6	2.0	1.3		
<i>Bison</i> (<i>Eobison</i>) <i>degninii</i> ^d	Pietrafitta	96.5 (3)	82.2 (6)	54.9 (6)	91.7 (1)	61.0 (1)	51.6 (5)		
	(Italy)	92.5-101.7	74.6-89.5	47.2-62.8	-	-	47.2-55.5		
		4.7	5.9	5.3	-	-	3.4		
<i>Bison</i> (<i>Eobison</i>) <i>degninii</i> ^a	Pirro Nord	81.3 (5)	80.7 (3)	62.1 (1)	-	29.8 (2)	50.8 (2)		
	(Italy)	74.1-91.6	74.5-92.0	53.7-70.5	-	-	43.7-57.9		
		7.4	9.8	11.9	-	-	10.0		
<i>B.</i> (<i>Eobison</i>) <i>degninii</i> ^d	Mygdonia Basin	103.2 (6)	93.9 (7)	62.2 (6)	99.4 (6)	69.7 (6)	58.3 (6)		
	(Greece)	95.6-116.6	80.6-101.4	59.9-64.2	92.5-103.9	66.0-73.2	50.5-67.0		
		7.2	7.2	1.4	4.7	3.0	5.4		
<i>B.</i> (<i>Poephagus</i>) <i>menneri</i> ^c	Untermassfeld (Germany)	104.1 (24)	94.8 (30)	-	-	-	60.1 (28)		
		90.0-120.0	85.0-104.5	-	-	-	52.0-68.0		
		8.6	6.0	-	-	-	4.6		
<i>B.</i> (<i>Bison</i>) <i>schoentensaefti</i> ^{f, g, h}	Le Valkonnet, Isernia,	-	102.6 (25)	65.8 (5)	105.7 (1)	68.6 (2)	58.3 (5)		
	Vallparadis,	-	87.9-113.0	60.5-72.0	-	65.2-72.0	52.0-70.0		
	(France, Italy, Spain)	-	6.9	4.7	-	4.8	6.9		
<i>B.</i> (<i>Bison</i>) <i>priscus</i> ⁱ	Krasny Yar, R-W	119.7 (60)	108.9 (69)	-	118.1 (62)	-	68.0 (73)		
	(Russia)	43.0-69.0	94.0-124.5	-	102.3-132.0	-	59.0-76.7		
		-	-	-	-	-	-		

Supplementary Table 11. Measurements (mm) of the radii of *Bison (Eobison) degiulii* from Pietrafitta. Estimated measurements are in italics. Abbreviations as in Fig. S1 and Table S2.

ID Specimen	Side	Lmax	PEW	PEAW	PET	PEAT	DWmin	DW	DTmin	DT	DEW	DEAW	DET	DEAT
SABAP UMB 21. 4.1137	R	317.5	91.2	86.1	50.4	43.6	50.2	53.6	30.5	33.0	91.6	83.2	56.7	-
SABAP UMB 21. 4.1143	L	325.0	94.0	-	51.0	45.2	-	-	-	-	-	-	-	-
SABAP UMB 21. 4.1141	R	-	86.5	81.5	47.4	42.0	50.0	51.5	30.0	32.8	-	-	-	-
SABAP UMB 21. 4.1176	L	-	82.9	66.9	-	-	-	-	-	-	86.9	74.4	-	-
SABAP UMB 22. 4.247/9	R	330.0	85.4	79.8	48.0	43.0	50.2	51.4	29.3	32.0	84.5	77.0	58.0	49.1
SABAP UMB 22. 4.247/10	L	330.0	89.2	80.9	48.9	42.5	55.1	58.2	30.2	31.8	78.9	75.8	56.0	55.0

Supplementary Table 12. Comparative measurements (mm) of the radius of selected *Leptobos* and *Bison* s.l. samples. Abbreviations as in Fig. S1 and Table S2. Data taken from: ^aMasini (1989); ^bRodrigo (2011); ^cTong et al., 2016; ^dBukshianidze (2005); ^eMoya-Solà (1987); ^fthis work; ^gSher (1997); ^hBrugal (1995); ⁱMoullé (1992); ^jSorbelli et al. (2021a); ^kPrat et al. (2003); ^lVercoutère and Guerin (2010); ^mSala (1986); ⁿCastañón (2017); ^oCroitor (2010); ^pEmpel and Roskož (1963).

Taxon	Locality	Statistics	Lmax	PEW	PEAW	PET	PEAT	DW	DEW	DET
<i>Leptobos</i> gr. LSEM ^{a, b}	Les Étaouaires, St. Vallier Montopoli, Villarroya (France, Italy, Spain)	Mean (N)	311.4 (19)	77.0 (19)	72.0 (19)	41.6 (13)	39.0 (8)	45.0 (15)	73.6 (17)	50.2 (15)
		Min-Max	288.0-326.0	68.5-86.5	63.7-78.1	36.2-47.7	34.0-44.5	38.4-50.0	64.0-81.5	40.3-60.0
		SD	12.0	5.7	5.4	3.5	4.1	4.1	4.8	5.5
<i>Leptobos etruscus</i> ^{a, b}	Senèze, Matassino, Olivola, Fonelas-1 (France, Italy, Spain)	Mean (N)	300.4 (9)	85.3 (20)	77.8 (18)	44.6 (19)	43.5 (9)	38.2 (13)	74.4 (15)	50.9 (13)
		Min-Max	260.2-319.0	77.2-92.6	70.0-83.2	37.0-48.0	39.2-48.0	24.4-54.0	62.1-84.7	38.8-62.2
		SD	20.2	4.5	3.8	3.2	3.1	11.9	6.6	6.9
<i>B. (Eobison) palaeosinensis</i> ^c	Nihowan Basin (China)	Mean (N)	335.0 (1)	91.8 (2)	83.1 (2)	-	-	-	92.0 (1)	-
		Min-Max	-	84.0-99.5	75.0-91.2	-	-	-	-	-
		SD	-	11.0	11.5	-	-	-	-	-
<i>B. (Eobison) georgicus</i> ^d	Dmanisi (Georgia)	Mean (N)	302.0 (2)	91.7 (3)	81.6 (3)	48.5 (3)	43.0 (3)	51.8 (3)	71.6 (3)	59.0 (3)
		Min-Max	300.0-304.0	90.1-93.3	79.8-82.6	47.6-49.6	40.7-44.3	50.7-52.7	51.8-82.9	56.9-62.9
		SD	2.8	1.6	1.5	1.0	2.0	1.0	17.2	3.4
<i>B. (Eobison) sp.</i> ^e	Venta Micena (Spain)	Mean (N)	277.0 (3)	71.6 (8)	-	37.2 (8)	-	42.2 (3)	63.3 (5)	43.0 (5)
		Min-Max	267.8-282.6	65.2-76.3	-	34.5-40.3	-	42.0-42.4	57.0-69.2	40.2-48.0
		SD	8.0	4.2	-	2.0	-	0.2	4.5	3.0
<i>B. (Eobison) degiulii</i> ^f	Pietrafitta (Italy)	Mean (N)	325.6 (4)	88.2 (6)	79 (5)	49.1 (5)	43.3 (5)	53.7 (4)	85.5 (4)	56.9 (3)
		Min-Max	317.5-330.0	82.9-94.0	66.9-86.1	47.4-51.0	42.0-45.2	51.4-58.2	78.9-91.6	56.0-58.0
		SD	5.9	4.1	7.2	1.5	1.2	3.2	5.3	1.0
<i>B. (Eobison) degiulii</i> ^f	Mydonia Basin (Greece)	Mean (N)	335 (4)	87.6 (7)	80.6 (7)	48.4 (7)	43.4 (6)	48.2 (6)	80.4 (5)	53.4 (5)
		Min-Max	318.0-357.0	85.0-91.2	76.3-84.6	43.6-51.0	41.3-46.8	44.2-53.7	76.5-85.2	50.3-56.0
		SD	17.3	2.0	3.0	2.7	2.2	3.5	3.2	2.6
<i>B. (Eobison) cf. degiulii</i> ^f	Capena (Italy)	Mean (N)	327.6 (1)	92.9 (1)	-	-	-	54.8 (1)	86.8 (1)	-
		Mean (N)	384.5 (13)	104.3 (24)	94.9 (24)	-	49.1 (24)	57.6 (17)	98.8 (13)	-
<i>B. (Prophogus) menneri</i> ^g	Untermassfeld (Germany)	Min-Max	350.0-418.0	91.5-118.0	83.0-106.5	-	43.0-57.0	49.0-65.5	89.0-110.0	-
		SD	22.5	7.5	6.5	-	4.1	5.4	6.9	-

<i>B. (Bison) schoetensacki</i> ^{h, i, j}	Durfort, Le Vallonnet,	Mean (N)	372.6 (12)	105.2 (20)	96.3 (21)	54.0 (14)	48.9 (20)	60.4 (12)	97.8 (12)	62.5 (12)
	Mauer, Vallparadis	Min-Max	339.1-390.0	94.4-115.0	86.9-107	46.5-63.0	40.5-57.0	50.6-64.2	89-102.8	46.0-77.0
	(France, Germany, Italy)	SD	15.0	5.0	5.1	3.9	5.2	3.8	3.9	8.7
<i>B. (Bison) priscus</i> ssp. ^{k, l, m, n, o}	Habarra, Romain-La-Roche,	Mean (N)	370.2 (30)	111.9 (42)	103 (43)	66.1 (33)	51.0 (6)	60.7 (12)	98.4 (32)	71.4 (5)
	Cava Filo, Kiputz IX, Tiraspol	Min-Max	327.0-405.0	92.0-126.0	80.3-117.5	50.5-110.0	45.0-46.0	47.0-75.0	77.0-120.0	63.0-79.0
	(France, Italy, Spain, Ukraine)	SD	20.4	9.5	8.4	15.8	4.6	9.4	10.4	6.0
<i>B. (Bison) bonasus</i> P	Białowieża	Mean (N)	343.4 (36)	92.3 (36)	-	46.9 (36)	-	-	82.4 (36)	57.7
	(Poland)	Min-Max	291.0-392.0	80.0-111.0	-	42.0-54.0	-	-	71.0-100.0	47.0-72.0
		SD	21.8	8.2	-	3.3	-	-	7.8	5.9

Supplementary Table 13. Measurements (mm) of the carpals and tarsals of *Bison* (*Eobison*) *degiulii* from Pietrafitta. Estimated measurements are in italics. Abbreviations as in Fig. S1 and Table S2.

ID Specimen	Element	Side	L	W	T
SABAP UMB 21. 4.1209	Cuneiform	L	15.6	25.3	41.7
SABAP UMB 21. 4.1246	Cuneiform	L	16.0	23.2	38.6
SABAP UMB 21. 4.1258	Cuneiform	R	<i>16.2</i>	23.2	-
SABAP UMB 21. 4.1297	Cuneiform	R	19.9	24.2	40.4
SABAP UMB 21. 4.1390	Cuneiform	L	16.5	24.3	40.8
SABAP UMB 21. 4.1410	Cuneiform	R	18.4	27.7	42.4
SABAP UMB 21. 4.1411	Cuneiform	R	16.5	26.5	42.9
SABAP UMB 21. 4.1412	Cuneiform	L	17.1	26.4	42.2
SABAP UMB 21. 4.1413	Cuneiform	L	19.0	22.9	39.6
SABAP UMB 21. 4.1209	Cuneiform	L	15.6	25.3	41.7
SABAP UMB 21. 4.1246	Cuneiform	L	16.0	23.2	38.6
SABAP UMB 21. 4.1258	Cuneiform	R	<i>16.2</i>	23.2	-
SABAP UMB 21. 4.1297	Cuneiform	R	19.9	24.2	40.4
SABAP UMB 22. 41.4896	Cuneiform	R	16.6	27.2	42.4
SABAP UMB 21. 4.1383	Magnum	R	23.3	41.4	36.9
SABAP UMB 21. 4.1388	Magnum	R	25.8	38.1	38.8
SABAP UMB 21. 4.1421	Magnum	L	28.2	43.2	39.2
SABAP UMB 21. 4.1423	Magnum	L	24.5	44.2	38.6
SABAP UMB 21. 4.1424	Magnum	R	23.7	44.1	39.4
SABAP UMB 22. 4.247/4	Magnum	R	24.5	41.7	37.7
SABAP UMB 22. 41.4890	Magnum	DX	26.4	-	37.1
SABAP UMB 22. 41.4891	Magnum	DX	26.3	38.0	36.4
SABAP UMB 22. 41.4892	Magnum	SX	24.9	42.0	38.1
SABAP UMB 21. 4.1290	Malleolus	R	30.1	19.8	40.2
SABAP UMB 21. 4.1396	Malleolus	L	30.3	21.9	42.1
SABAP UMB 21. 4.1397	Malleolus	L	33.5	22.2	43.5
SABAP UMB 21. 4.1398	Malleolus	L	26.9	16.8	33.2
SABAP UMB 21. 4.1399	Malleolus	L	27.5	27.0	36.9
SABAP UMB 21. 4.1400	Malleolus	R	28.1	17.7	37.5
SABAP UMB 21. 4.1459	Malleolus	R	32.7	19.2	38.8
SABAP UMB 20. 1.7329/2	Pyramidal	L	50.5	26.7	43.8
SABAP UMB 21. 4.1287	Pyramidal	R	47.1	24.8	39.4
SABAP UMB 21. 4.1300	Pyramidal	L	-	24.4	39.5
SABAP UMB 21. 4.1301	Pyramidal	R	49.2	26.0	40.0
SABAP UMB 21. 4.1318	Pyramidal	R	43.7	24.3	38.7
SABAP UMB 21. 4.1379	Pyramidal	R	-	22.5	<i>34.9</i>
SABAP UMB 21. 4.1384	Pyramidal	R	49.0	23.7	40.0
SABAP UMB 21. 4.1406	Pyramidal	L	40.1	22.5	35.6
SABAP UMB 21. 4.1430	Pyramidal	R	-	19.8	-
SABAP UMB 21. 4.1285	Scaphoid	L	42.0	32.5	47.0
SABAP UMB 21. 4.1303	Scaphoid	R	37.0	33.2	48.3

SABAP UMB 21. 4.1381	Scaphoid	R	40.0	28.4	42.5
SABAP UMB 21. 4.1386	Scaphoid	R	-	30.0	-
SABAP UMB 21. 4.1391	Scaphoid	L	35.0	26.5	44.1
SABAP UMB 21. 4.1401	Scaphoid	R	36.5	30.6	46.5
SABAP UMB 21. 4.1429	Scaphoid	L	45.0	31.0	47.0
SABAP UMB 21. 4.1441	Scaphoid	R	38.7	34.5	51.4
SABAP UMB 22. 41.4893	Scaphoid	L	39.7	33.3	47.6
SABAP UMB 21. 4.1286	Semilunar	R	34.5	36.0	40.7
SABAP UMB 21. 4.1302	Semilunar	L	35.8	32.2	48.8
SABAP UMB 21. 4.1380	Semilunar	R	36.1	39.81	42.4
SABAP UMB 21. 4.1385	Semilunar	R	32.5	28.0	39.0
SABAP UMB 21. 4.1392	Semilunar	L	31.4	33.9	39.9
SABAP UMB 21. 4.1407	Semilunar	R	33.3	31.5	42.0
SABAP UMB 21. 4.1408	Semilunar	R	35.6	31.9	43.2
SABAP UMB 21. 4.1409	Semilunar	L	-	32.0	-
SABAP UMB 21. 4.1427	Semilunar	L	35.2	35.7	44.7
SABAP UMB 21. 4.1428	Semilunar	R	34.8	35.5	43.3
SABAP UMB 21. 4.1288	Unciform	L	26.7	31.2	34.7
SABAP UMB 21. 4.1289	Unciform	R	26.9	30.4	34.4
SABAP UMB 21. 4.1382	Unciform	R	26.1	32.2	34.8
SABAP UMB 21. 4.1387	Unciform	R	24.9	30.2	35.5
SABAP UMB 21. 4.1404	Unciform	L	23.8	26.7	28.9
SABAP UMB 21. 4.1405	Unciform	R	27.9	32.9	32.5
SABAP UMB 21. 4.1425	Unciform	L	28.4	34.7	36.5
SABAP UMB 21. 4.1426	Unciform	R	28.5	34.4	37.2

Supplementary Table 14. Principal component analysis of metacarpals using seven selected variables (see Section 3 and Fig. 9). Eigenvalue and % variance of the PCs and coefficients of each variable for each PC are shown. Abbreviations as in Table 1.

	PC 1	PC 2	PC 3	PC 4	PC 5	PC 6	PC 7
Eigenvalue	0.00359497	0.000471576	0.000376779	0.000291477	0.000196987	0.00012557	8.11E-15
% Variance	71.084	9.3245	7.4501	5.7634	3.895	24.829	1.60E-11
msLmax	-0.8102	-0.19676	-0.16936	-0.20672	-0.30088	-0.0074193	0.37796
msPET	-0.062886	0.17589	0.83697	-0.15927	0.16086	0.2655	0.37796
msPEW	0.23734	0.2769	0.1089	0.038811	-0.41525	-0.73372	0.37796
msDT	-0.0088787	-0.43998	0.043104	0.7786	0.22862	-0.056019	0.37796
msDW	0.44846	-0.58928	-0.13709	-0.53008	0.093526	0.016061	0.37796
msDEtm	-0.079196	0.46998	-0.39308	-0.10228	0.67467	-0.099135	0.37796
msDEW	0.27536	0.30325	-0.28943	0.18093	-0.44155	0.61473	0.37796

Supplementary Table 15. Measurements (mm) of the pelvis of *Bison (Eobison) degiulii* from Pietrafitta.

Abbreviations as in Table S2.

ID Specimen	Side	Lmax	SB	SH	LFO	LA	LAR
SABAP UMB 19. 2.1177	L	-	-	-	-	82.9	62.2
SABAP UMB 21. 4.1136	R	523.0	23.5	58.5	108.0	86.3	75.5
SABAP UMB 21. 4.1138	R	540.0	21.8	57.2	114.4	88.3	69.4

Supplementary Table 16. Measurements (mm) of the femurs of *Bison (Eobison) degiulii* from Pietrafitta. Estimated measurements are in italics. Abbreviations as in Fig. S1 and Table S2.

ID Specimen	Side	Lmax	Lm	PEW	CFW	CFT	GTT	DWmin	DTmin	DEW	DETm	DETI	RAW
SABAP UMB 21. 4.1140	R	450.0	430.0	-	56.6	53.6	-	-	-	-	-	-	57.0
SABAP UMB 21. 4.1146	R	-	-	-	-	-	-	-	-	-	130	-	51.9
SABAP UMB 21. 4.1147	R	455.0	435.0	145.8	58.0	58.3	83.4	44.3	54.7	114.5	140.3	113.0	59
SABAP UMB 21. 4.1149	L	457	425.0	139.0	55.7	58.2	85.4	50.9	50.8	-	-	113.1	59.2
SABAP UMB 21. 4.1315	L	-	-	-	52.5	52.9	-	-	-	-	-	-	-
SABAP UMB 21. 4.1377	R	-	-	-	-	49.9	-	-	-	-	-	-	-
SABAP UMB 21. 4.1378	R	-	-	-	52.0	50.0	-	-	-	-	-	-	-
SABAP UMB 21. 4.1191	L	-	-	-	-	-	-	-	-	-	-	-	57.0
SABAP UMB 22. 4.247/5	R	-	443.0	144.0	60.7	54.3	-	-	-	-	<i>139.3</i>	-	-
SABAP UMB 22. 4.247/6	L	461.0	437.0	133.6	60.6	54.0	-	-	-	100.0	139.2	113.0	60.0

Supplementary Table 17. Comparative measurements (mm) of the femur in selected *Leptobos* and *Bison* s.l. samples. Abbreviations as in Fig. S1 and Table S2. Data taken from: ^aMasini (1989); ^bRodrigo (2011); ^cthis work; ^dSher (1997); ^eVasiliev (2008); ^fEmpel and Roskoz (1963).

Taxon	Locality	Statistics	Lmax	Lm	PEW	CFT	GTT	DWmin	DTmin	DEW	DETm
<i>Leptobos etruscus</i> ^{a, b}	Senèze, Olivola (France, Italy)	Average (N)	409.7 (3)	400.3 (3)	129.8 (3)	48.0 (3)	-	-	-	97.9 (7)	128.6 (6)
		Min-Max	381.5-424.5	376.0-415.0	118.5-139.0	44.5-50.5	-	-	-	-	83.5-108.0
<i>B. (Eobison) degiulii</i> ^c	Pietrafitta (Italy)	Average (N)	455.8 (4)	434.0 (5)	140.6 (4)	53.9 (8)	84.4 (2)	47.6 (2)	52.8 (2)	107.3 (2)	137.2 (4)
		Min-Max	450.0-461.0	425-443	133.6-145.8	49.9-58.3	83.4-85.4	44.3-50.9	50.8-54.7	100.0-114.5	130.0-140.3
		SD	4.6	6.9	5.5	3.2	1.4	4.7	2.8	10.3	4.8
<i>B. (Eobison) degiulii</i> ^a	Pirro Nord (Italy)	Average (N)	367.5 (1)	352 (1)	105.1 (2)	47.8 (2)	59.5 (2)	36.6 (2)	41.5 (2)	91.4 (2)	122.5 (2)
		Min-Max	-	-	104.6-105.5	47.5-48.0	58.9-60.0	34.6-38.5	38.5-44.5	88.0-94.7	121.0-123.9
		SD	-	-	0.6	0.4	0.8	2.8	4.2	4.7	2.1
<i>B. (Poephobos) memeri</i> ^d	Untermassfeld (Germany)	Average (N)	430.0 (1)	-	130.0 (1)	-	-	40 (1)	-	108.8 (5)	143.0 (4)
		Min-Max	-	-	-	-	-	-	-	99.0-118.0	135.0-154.0
		SD	-	-	-	-	-	-	-	7.9	9.1
<i>B. (Bison) priscus priscus</i> ^e	Krasny Yar, R-W	Average (N)	533.9 (8)	488.6 (11)	181.9 (10)	-	98.7 (8)	54.9 (22)	61.5 (21)	138.2 (16)	175.0 (6)
		SD	-	-	-	-	-	-	-	-	-

(Russia)	Min-Max	504.0-564.0	450.0-515.0	163.5-199.0	-	83.0-111.5	47.0-60.0	56.0-67.0	120.0-154.0	168.5-182.8
Białowieża	Average (N)	455.2 (32)	432.2 (32)	134.5 (31)	56.0 (32)	73.3 (31)	42.3 (32)	49.1 (32)	111.8 (32)	135.3 (32)
(Poland)	Min-Max	404.0-515.0	386.0-487.0	119.0-156.0	50.0-64.0	60.0-89.0	36-48	41.0-58.0	100.0-133.0	122.0-155.0
	SD	30.4	27.1	11.0	3.7	7.7	3.7	4.4	8.7	8.7

Supplementary Table 18. Measurements (mm) of the tibiae of *Bison (Eobison) degiulii* from Pietrafitta. Estimated measurements are in italics. Abbreviations as in Fig. S1 and Table S2.

ID Specimen	Side	Lmax	PEW	PET	Dwmin	Dtmin	DEW	DEAW	DET	DEAT	MFW	MFT
SABAP UMB 19. 2.1176	L	425.0	115.8	122.7	47.2	38.9	74.8	67.6	58.4	50.2	14.0	34.0
SABAP UMB 21. 4.1145	L	429.0	127.5	115.0	46.9	39.2	71.6	62.1	58.0	50.9	16.3	33.5
SABAP UMB 21. 4.1148	R	-	-	108.0	-	-	-	-	-	-	-	-
SABAP UMB 21. 4.1339	R	-	-	-	-	-	71.0	60.0	-	-	14.2	33.8
SABAP UMB 21. 4.1190	R	-	123.6	-	45.4	38.7	74.4	63.1	56.1	44.1	16.5	34.8
SABAP UMB 22. 4.247/13	L	430.0	-	-	45.2	36.5	68.3	59.0	57.8	48.2	14.6	31.8
SABAP UMB 22. 4.247/14	R	-	110.8	-	-	-	-	-	-	-	-	-

Supplementary Table 19. Comparative measurements (mm) of the tibia in selected *Leptobos* and *Bison* s.l. samples. Abbreviations as in Fig. S1 and Table S2. Data taken from: ^aMasini (1989); ^bRodrigo (2011); ^cTong et al., 2016; ^dBukshianidze (2005); ^eMoya-Solà (1987); ^fthis work; ^gSher (1997); ^hBrugal (1995); ⁱMoullé (1992); ^jSala (1986); ^kSorbelli et al. (2021a); ^lPrat et al. (2013); ^mVercoutère and Guerin (2010); ⁿFlerov (1976); ^oCastañes (2017); ^pVasiliev (2008); ^qEmpel and Roskož (1963).

Taxon	Locality	Statistics	Lmax	PEW	PET	Dwmin	Dtmin	DEW	DET	
<i>Leptobos</i> gr. LSEM ^{a,b}	St.-Vallier, Les Étouaires, Pantalla, Villarroja (France, Italy, Spain)	Mean (N)	-	-	-	41.4 (7)	33.0 (7)	62.8 (19)	53.1 (17)	
		Min-Max	-	-	-	37.7-44.2	29.8-35.6	55.7-73.9	47.9-62.8	
		SD	-	-	-	2.7	2.0	4.3	4.0	
<i>Leptobos etruscus</i> ^{a,b}	Senèze, Olivola (France, Italy)	Mean (N)	412.0 (2)	96.1 (11)	90.1 (5)	47.5 (13)	35.8 (14)	65.5 (23)	52.1 (22)	
		Min-Max	407.0-417.0	79.0-118.0	75.0-100.0	45.1-51.1	29.3-41.0	56.2-71.6	44.7-58.4	
		SD	7.1	11.4	9.7	2.0	3.1	4.2	4.0	
<i>B. (Eobison) polacensis</i> ^c	Nihowan Basin (China)	Mean (N)	403.0 (4)	106.3 (4)	-	47.8 (4)	-	73.8 (4)	56.0 (4)	
		Min-Max	346.0-446.0	98.0-120.0	-	45.0-51.0	-	70.0-78.0	53.0-58.0	
		SD	42.1	10.5	-	3.2	-	3.9	2.4	
<i>B. (Eobison) georgicus</i> ^d	Dmanisi (Georgia)	Mean (N)	-	-	-	-	-	71.2 (2)	55.2 (2)	
		Min-Max	-	-	-	-	-	-	70.2-72.3	
		SD	-	-	-	-	-	-	1.6	
<i>B. (Eobison) sp.</i> ^e	Venta Micena (Spain)	Mean (N)	385.0 (2)	99.8 (2)	-	48.3 (2)	43.6 (2)	60.7 (4)	46.1 (4)	
		Min-Max	366.0-404.0	93.6-106.0	-	44.6-52.0	37.2-50	60.0-62.2	41.2-51.7	
		SD	26.9	8.8	-	5.2	9.1	1.0	4.4	
<i>B. (Eobison) degiulii</i> ^f	Pietrafitta (Italy)	Mean (N)	427.0 (2)	122.3 (3)	115.2 (3)	46.5 (3)	38.9 (3)	73.0 (4)	57.5 (3)	
		Min-Max	425.0-429.0	115.8-127.5	108.0-122.7	45.4-47.2	38.7-39.2	71.0-74.8	56.1-58.4	
		SD	2.8	6.0	7.4	1.0	0.3	1.9	1.2	
<i>B. (Eobison) degiulii</i> ^g	Pirro Nord (Italy)	Mean (N)	351.0 (1)	96.5 (1)	90.0 (1)	48.2 (1)	36 (1)	79.0 (1)	50.9 (1)	
		Mean (N)	468.8 (4)	129.7 (3)	-	-	-	-	84.0 (25)	62.0 (23)
		Min-Max	439.0-505.0	122.0-142.0	-	-	-	-	74.0-94.0	55.0-67.0
<i>B. (Bison) schoentensacki</i> ^{h,i,j,k}	Durfort, Le Vallonnet, Mauer, Isernia, Vallparadis (France, Germany, Italy, Spain)	Mean (N)	29.2	8.8	-	-	-	5.4	3.8	
		Mean (N)	-	-	-	55.5 (12)	39.5 (6)	84.2 (23)	62.3 (23)	
		Min-Max	-	-	-	46.5-68.0	33.4-42.3	69.3-92.3	50.6-70.0	
SD	-	-	-	5.3	3.2	6.1	3.2	5.1		

<i>B. (Bison) priscus</i> spp. ^{j, l, m, n, o}	Habarra, Romain-La-Roche,	Mean (N)	448.2 (21)	133.7 (24)	129.0 (4)	55.6 (10)	-	85.0 (38)	63.4 (11)
	Taubach, Cava Filo, Kiputz IX (France, Germany, Italy, Spain)	Min-Max SD	399.0-535.0 30.6	120.0-155.0 8.7	115.0-143.0 12.4	50.0-63.0 5.1	-	68.0-104.0 7.7	57.0-76.0 6.2
<i>B. (Bison) priscus priscus</i> ^p	Krasny Yar, R-W (Russia)	Mean (N)	459.4 (16)	136.4 (16)	123.1 (14)	-	43.5 (70)	85.8 (92)	65.0 (87)
	Białowieża (Poland)	Min-Max Mean (N) Min-Max SD	430.0-496.0 403.0 (4) 346.0-446.0 42.1	122.0-150.0 106.3 (4) 98.0-120.0 10.5	110.5-134.5 - - -	- 47.8 (4) 45.0-51.0 3.2	- - - -	73.0-98.2 73.8 (4) 70.0-78.0 3.9	56.5-75.4 56.0 (4) 53.0-58.0 2.4

Supplementary Table 20. Measurements (mm) of cubonaviculars of *Bison (Eobison) degiulii* from Pietrafitta. Abbreviations as in Fig. S1 and Table S2.

ID Specimen	Side	L	W	T
SABAP UMB 21. 4.1245	L	-	66.8	51.4
SABAP UMB 21. 4.1247	R	-	64.1	56.6
SABAP UMB 21. 4.1296	R	40.2	62.44	58.3
SABAP UMB 21. 4.1333	R	-	59.1	47.6
SABAP UMB 21. 4.1389	L	-	62.0	50.0
SABAP UMB 21. 4.1153	L	45.9	66.3	61.7
SABAP UMB 21. 4.1162	R	-	-	-
SABAP UMB 21. 4.1166	R	48.5	68.3	62.7
SABAP UMB 21. 4.1188	L	42.0	67.6	60.0
SABAP UMB 22. 4.886/11	L	-	67.6	-

Supplementary Table 21. Comparative measurements (mm) of the cubonavicular in selected *Leptobos* and *Bison* s.l. samples. Abbreviations as in Fig. S1 and Table S2. Data taken from: ^aMasini (1989); ^bRodrigo (2011); ^cMoyà Solà (1987); ^dthis work; ^eSher (1997); ^fBrugal (1995); ^gMoullé (1992); ^hSala (1986); ⁱSorbelli et al. (2021a); ^jVasiliev (2008); ^kEmpel and Roskoz (1963).

Taxon	Locality	Statistics	L	W	T
<i>Leptobos</i> gr. LSEM ^{a, b}	St.-Vallier, Les Étouaires,	Average (N)	37.3 (20)	60.6 (30)	57.4 (30)
	Montopoli, Villarroya	Min-Max	32.1-42.3	51.5-66.5	48.0-63.3
	(France, Italy, Spain)	SD	3.2	4.3	4.2
<i>Leptobos etruscus</i> ^{a, b}	Senèze, Olivola	Average (N)	34.4 (6)	59.6 (23)	58.3 (23)
	(France, Italy)	Min-Max	30.1-39.3	52.5-67.3	48.8-66.4
		SD	3.6	4.5	5.9
<i>B. (Eobison) sp.</i> ^c	Venta Micena	Average (N)	29.3 (5)	58.4 (5)	52.5 (5)
	(Spain)	Min-Max	24.5-34.9	52.6-65.1	48.4-57.7
		SD	4.0	5.2	4.7
<i>B. (Eobison) degiulii</i> ^d	Pietrafitta	Average (N)	44.2 (4)	64.9 (9)	56 (8)
	(Italy)	Min-Max	40.2-48.5	59.1-68.3	47.6-62.7
		SD	3.8	3.2	5.7
<i>B. (Poephagus) menneri</i> ^e	Untermassfeld	Average (N)	52.7 (32)	72.9 (34)	67.4 (35)
	(Germany)	Min-Max	43.0-60.0	65.5-84.0	58.5-85.0
		SD	4.3	5.7	5.8
<i>B. (Bison) schoetensacki</i> ^{f, g, h, i}	Durfort, Le Vallonnet,	Average (N)	55.8 (5)	75.6 (14)	69.1 (16)
	Isernia, Vallparadis	Min-Max	45.0-58.8	66.7-84	60.7-78.0
	(France, Italy, Spain)	SD	8.4	4.8	4
<i>B. (Bison) priscus priscus</i> ^j	Krasny Yar, R-W	Average (N)	-	80.5 (61)	76.3 (57)
	(Russia)	Min-Max	-	68.2-91.4	61.0-84.0
		SD	-	-	-
<i>B. (Bison) bonasus</i> ^k	Białowieża	Mean (N)	48.9 (31)	66.4 (31)	62.2 (31)
	(Poland)	Min-Max	42.0-58.0	60.0-76.0	55.0-73.0
		SD	4.9	4.8	4.9

Supplementary Table 22. Measurements (mm) of the astragali of *Bison (Eobison) degiulii* from Pietrafitta. Abbreviations as in Fig. S1 and Table S1.

ID Specimen	Side	Ll	Lm	Lmin	Tl	Tm	PTW	TTW	DTW
SABAP UMB 130142	R	80.4	72.9	-	42.9	44.5	50.0	-	51.9
SABAP UMB 21. 4.1151	L	77.1	72.0	60.5	43.0	44.8	51.6	43.2	51.5
SABAP UMB 21. 4.1187	L	75.5	69.5	59.5	44.7	44.9	47.7	45.6	53.2
SABAP UMB 21. 4.1240	L	64.9	60.3	51.0	34.8	35.7	40.6	38.1	42.1
SABAP UMB 21. 4.1241	L	-	72.0	-	-	43.7	-	-	49.9
SABAP UMB 21. 4.1242	R	76.7	72.4	61.7	42.0	45.4	42.7	44.5	49.2
SABAP UMB 21. 4.1243	L	78.5	71.8	60.1	45.0	45.5	50.5	48.9	52.5
SABAP UMB 21. 4.1244	L	76.5	74.8	61.6	43.0	45.6	47.0	44.0	48.0
SABAP UMB 21. 4.1331	R	77.1	70.8	60.6	44.8	45.4	47.7	46.6	51.6
SABAP UMB 21. 4.1332	R	70.8	65.0		40.0	40.5	43.0	42.9	46.0
SABAP UMB 21. 4.1359	R	67.8	63.0	53.2		38.2	46.0	43.0	47.1
SABAP UMB 22. 4.886/9	R	78.5	72.2	61.0	46.2	47.8	49.8	45.8	54.5

Supplementary Table 23. Comparative measurements (mm) of the astragalus in selected *Leptobos* and *Bison* s.l. samples. Abbreviations as in Fig. S1 and Table S2. Data taken from: ^aMasini (1989); ^bRodrigo (2011); ^cTong et al. (2016); ^dBukshianidze (2005); ^eMoyà-Solà (1987); ^fthis work; ^gCroitro (2010); ^hSher (1997); ⁱBrugal (1995); ^jMoullé (1992); ^kSala (1986); ^lSorbelli et al. (2021a); ^mFlerov (1976); ⁿPrat et al. (2013); ^oVercoutère and Guérin (2010); ^pEmpel and Roskoz (1963).

Taxon	Locality	Measure	Ll	Tm	PTW	DTW
<i>Leptobos</i> gr. LSEM ^{a, b}	Les Étouaires, St. Vallier, Montopoli, Villarroya (France, Italy, Spain)	Mean (N)	72.2 (47)	40.0 (44)	46.3 (44)	47.0 (46)
		Min-Max	65.0-77.3	35.1-45.8	37.0-52.8	38.2-54
		SD	3.3	3.0	4.3	3.7
<i>Leptobos etruscus</i> ^{a, b}	Senèze, Matassino, Olivola, Upper Valdarno (France, Italy)	Mean (N)	70.4 (41)	38.80 (42)	43.8 (36)	45.5 (40)
		Min-Max	60.5-76.7	32.5-43.7	32.7-51.8	34.0-52.5
		SD	4.1	2.7	3.4	3.9
<i>B. (Eobison) palaeosinensis</i> ^c	Nihowan Basin (China)	Mean (N)	78.0 (3)	-	-	50.7 (3)
		Min-Max	74.0-80.0	-	-	46.0-53.0
		SD	3.5	-	-	4.0
<i>B. (Eobison) georgicus</i> ^d	Dmanisi (Georgia)	Mean (N)	78.9 (1)	-	50.3 (1)	52.5 (1)
		Min-Max	71.5 (15)	-	-	47.2 (17)
		SD	66.6-77.0	-	-	40-53.7
<i>B. (Eobison) sp.</i> ^e (Moyà-Solà, 1987)	Venta Micena (Spain)	Mean (N)	71.5 (15)	-	-	47.2 (17)
		Min-Max	66.6-77.0	-	-	40-53.7
		SD	3.5	-	-	3.6
<i>B. (Eobison) degiulii</i> ^f	Pietrafitta (Italy)	Mean (N)	74.5 (11)	43.1 (12)	46.7 (11)	49.4 (12)
		Min-Max	64.9-80.4	35.7-45.6	40.6-51.6	42.1-53.2
		SD	5.0	3.4	3.6	3.3
<i>B. (Eobison) degiulii</i> ^a (Masini, 1989)	Pirro Nord (Italy)	Mean (N)	73.8 (11)	42.1 (11)	46.8 (11)	48.7 (11)
		Min-Max	67.1-79.8	39.0-46.8	41.3-49.7	44.3-53.3
		SD	4.0	2.2	2.7	3.0
<i>B. (Eobison) degiulii</i> ^f	Mygdonia basin (Greece)	Mean (N)	78.9 (8)	45.0 (8)	53.1 (8)	52.7 (8)
		Min-Max	73.9-87.2	41.0-48.9	47.6-59.7	46.7-59.5
		SD	4.6	3.1	4.3	4.0
<i>B. (Poephagus) menneri</i> ^h (Sher, 1997)	Untermassfeld (Germany)	Mean (N)	85.8 (33)	-	57.6 (34)	56.2 (35)
		Min-Max	78.5-95.5	-	52.0-66.0	50.5-64.5
		SD	4.1	-	3.7	3.8
<i>B. (Bison) schoetensacki</i> ^{i, j, k, l} (This paper)	Durfort, Le Vallonnet, Mauer, Isernia, Vallparadis (France, Germany, Italy, Spain)	Mean (N)	89.0 (43)	48.8 (38)	57.0 (24)	59.1 (46)
		Min-Max	78.9-100.0	34.0-56.5	45.5-65.5	59.1-65.4
		SD	4.8	4.2	5.5	3.7
<i>B. (Bison) priscus</i> ssp. ^{k, m, n, o} (Brugal, 1995)	Taubach, Habarra, Romain-La-Roche, Cava Filo, Kiputz IX (France, Germany, Italy, Spain)	Mean (N)	93.4 (64)	53.1 (40)	60.8 (12)	63.3 (63)
		Min-Max	80.5-105.0	44.0-60.0	57.0-66.0	52-76.0
		SD	6.1	3.7	2.3	6.3
<i>B. (Bison) bonasus</i> ^{a, b}	Białowieża (Poland)	Mean (N)	77.0 (39)	45.1 (39)	-	54.4 (39)
		Min-Max	67.0-87.0	38.0-51.0	-	47.0-63.0
		SD	4.7	3.2	-	3.5

Supplementary Table 24. Measurements (mm) of the calcanei of *Bison* (*Eobison*) *degiulii* from Pietrafitta. Estimated measurements are in italics. Abbreviations as in Fig. S1 and Table S2.

ID Specimen	Side	Lmax	BLB	BLmin	Hmax	Wmax	HST	SIT	TCaH	TCW	MFL	MFW	NCFL	CBWmin	CBHmin
SABAP UMB 130028	R	155.0	116.3	89.4	70.0	50.1	58.6	31.9	55.0	38.3	39.0	18.6	42.5	24.9	45.7
SABAP UMB 21. 4.1150	R	137.8	96.0	-	63.6	-	-	-	-	-	28.9	16.6	41.1	-	-
SABAP UMB 21. 4.1152	R	159.8	<i>118.0</i>	98.0	64.5	55.7	-	31.8	55.6	41.7	32	18.6	39.4	25.6	49.7
SABAP UMB 21. 4.1257	?	-	-	-	-	-	-	26.3	-	-	-	-	-	-	-
SABAP UMB 21. 4.1324	L	-	-	90.1	-	54.0	49.5	33.2	45.7	38.3	-	-	-	24.2	43
SABAP UMB 21. 4.1340	L	154.8	116.9	90.8	57.6	55.2	46.7	28.9	48.4	42.7	33.4	16.4	38.9	23.5	43.9
SABAP UMB 21. 4.1368	L	-	-	-	-	-	-	21.2	-	-	-	-	-	19.0	-
SABAP UMB 22. 4.244	L	156.1	114.7	91.7	58.7	50.0	50.8	31.9	49.7	40.7	27.6	16.7	42.2	30.2	43.9
SABAP UMB 22. 4.247/1	L	152.0	116.7	92.3	58.8	53.9	52.4	32.0	48.3	40.3	28.6	16.6	40.4	26.5	45.2
SABAP UMB 22. 4.886/10	L	-	116.3	89.5	-	52.3	54.0	31.8	49.1	38.9	-	-	-	23.1	45.3
SABAP UMB 22. 41.4895	L	-	-	-	65.5	55.0	-	-	-	-	33.2	18.3	-	23.5	-

Supplementary Table 25. Comparative measurements (mm) of the calcaneum in selected *Leptobos* and *Bison* s.l. samples. Abbreviations as in Fig. S1 and Table S2. Data taken from: ^aMasini (1989); ^bRodrigo (2011); ^cTong et al. (2016); ^dMoyà-Solà (1987); ^ethis work; ^fSher (1997); ^gBrugal (1995); ^hMoullé (1992); ⁱSorbelli et al. (2021a); ^jVasiliev (2008); ^kEmpel and Roskoz (1963).

Taxon	Locality	Statistics	Lmax	Hmax	Wmax	TCaH	TCW
<i>Leptobos</i> gr. LSEM ^{a, b}	Les Étozières, St. Vallier, Montopoli (France, Italy)	Mean (N)	145.5 (6)	62.2 (6)	49.6 (7)	43.1 (7)	34.6 (7)
		Min-Max	126.0-155.5	50.4-81.0	43.2-57.0	37.2-47.5	30.0-38.6
<i>Leptobos etruscus</i> ^a	Senèze, Casa Fraia, Matassino, Olivola, (France, Italy)	SD	11.9	10.6	5.2	4.0	3.7
		Mean (N)	149.2 (14)	58.8 (20)	51.1 (17)	43.3 (18)	37.7 (18)
<i>B. (Eobison) palaeosinensis</i> ^c	Nihewan Basin (China)	Min-Max	134.0-159.1	49.8-62.8	42.4-59.0	38.2-47.3	32.7-42.1
		SD	9.0	3.1	4.4	3.0	3.1
<i>B. (Eobison) sp.</i> ^d	Venta Micena (Spain)	Mean (N)	146.3 (4)	-	47 (4)	-	-
		Min-Max	136-160	-	44-53	-	-
<i>B. (Eobison) degnallii</i> ^e	Pietrafita (Italy)	SD	10	-	4.1	-	-
		Mean (N)	151.7 (3)	-	-	-	25.1 (3)
<i>B. (Eobison) degnallii</i> ^a	Pirro Nord (Italy)	Min-Max	148.0-158.0	-	-	-	23.0-27.4
		SD	5.5	-	-	-	2.2
<i>B. (Poephagus) menneri</i> ^f	Untermassfeld (Germany)	Mean (N)	152.6 (6)	62.7 (7)	53.3 (8)	50.5 (6)	40.3 (6)
		Min-Max	137.8-159.8	57.6-70.0	50.0-55.7	45.7-55.6	38.3-42.7
<i>B. (Bison) schoetensacki</i> ^{g, h, i}	Durfort, Le Vallonnnet, Vallparadis (France, Spain)	SD	7.7	4.5	2.2	4.0	1.8
		Mean (N)	140.8 (2)	58.2 (2)	45.2 (2)	44.2 (2)	36.5 (2)
<i>B. (Bison) prisacus prisacus</i> ^j	Krasny Yar, R-W (Russia)	Min-Max	138.5-143.0	57.2-59.2	41.3-49.0	42.0-48.0	34.5-39.5
		SD	3.2	1.4	5.4	3.3	2.7
<i>B. (Bison) bonasus</i> ^k	Białowieża (Poland)	Mean (N)	177.1 (21)	70.0 (20)	59.1 (21)	52.4 (21)	44.9 (20)
		Min-Max	163.5-189.0	61.0-79.6	53.4-68.3	47.8-59.3	39.5-49.5
<i>B. (Bison) prisacus prisacus</i> ^j	Krasny Yar, R-W (Russia)	SD	7.7	4.8	4.0	3.1	3.1
		Mean (N)	170.5 (10)	70.3 (12)	56.8 (12)	50.4 (9)	43.2 (7)
<i>B. (Bison) prisacus prisacus</i> ^j	Białowieża (Poland)	Min-Max	155.0-189.4	66.5-73.5	50.0-62.0	46.5-53.2	38.3-46.9
		SD	10.3	2.3	4.2	2.3	3.0
<i>B. (Bison) prisacus prisacus</i> ^j	Białowieża (Poland)	Mean (N)	188.3 (23)	74.8 (50)	65.1 (44)	52.4 (4)	49.6 (24)
		Min-Max	163.0-201.0	66.0-85.7	56.0-75.0	46.0-57.0	39.5-54.6
<i>B. (Bison) bonasus</i> ^k	Białowieża (Poland)	Mean (N)	159.8 (33)	-	56.0 (28)	43.2 (33)	40.0 (33)
		Min-Max	142.0-181.0	-	49.0-66.0	37.0-50.0	34.0-50.0
		SD	11.3	-	5.4	3.6	4.3

Supplementary Table 26. Comparative measurements (mm) of the metatarsal in selected *Leptobos* and *Bison* s.l. samples. Abbreviations as in Fig. S1 and Table S2. Data taken from: ^aMasini (1989); ^bRodrigo (2011); ^cGarrido (2008); ^dBukshianidze (2005); ^ethis work; ^fManiakas and Kostopoulos (2017); ^gKostopoulos et al. (2018); ^hSher (1997); ⁱBrugal (1994); ^jMoullé (1992); ^kSchertz (1936); ^lSala (1986); ^mBreda et al. (2021a); ⁿBreda et al. (2010); ^oVercoutère and Guérin (2010); ^pPrat et al. (2003); ^qCastañón et al. (2012); ^rEmpel and Roskož (1963).

Taxon	Locality	Statistics	Lmax	PEW	PET	DW	DT	DEW	DET
<i>Leptobos elatus</i> ^{a,b}	Les Étouaires, Villarroja (France, Spain)	Mean (N)	285.7 (24)	49.5 (38)	48.2 (31)	32.1 (23)	31.7 (17)	54.9 (24)	34.6 (23)
		Min-Max	267.2-297.0	45.0-56.8	42.3-53.7	28.5-34.6	28.8-34.5	49.2-63.3	31.9-37.9
		SD	7.3	3.0	2.7	2.1	1.8	3.6	1.5
<i>Leptobos etruscus</i> ^{a,b,c}	Senèze, Matassino, Olivola (France, Italy)	Mean (N)	267.7 (29)	50.1 (47)	49.2 (45)	33.3 (39)	32.8 (37)	55.5 (37)	34.6 (36)
		Min-Max	240.0-290.5	45.3-55.7	43.0-54.0	28.6-38.2	27.6-37.8	47.1-60.5	29.7-38.8
		SD	13.0	3.2	3.3	2.8	2.8	3.8	2.2
<i>B. (Eobison) palaeosinensis</i> ^{a,c}	Nihowan Basin (China)	Mean (N)	256.9 (7)	51.3 (7)	50.7 (6)	32.2 (2)	33.2 (2)	59.4 (7)	31.6 (1)
		Min-Max	237.0-280.0	46.5-57.0	45.0-60.0	31.4-31.9	30.9-35.5	52.5-67.0	-
		SD	18.2	4.8	6.3	1.1	3.3	5.8	-
<i>B. (Eobison) sp.</i> ^d	Venta Micena (Spain)	Mean (N)	264.7 (15)	48.5 (23)	51.1 (24)	34.5 (19)	32.8 (20)	34.4 (20)	57.3 (20)
		Min-Max	240.9-286.2	45.0-53.9	43.5-59.4	29.6-37.7	27.4-38.0	29.5-38.3	50.2-63.8
		SD	12.9	3.7	4.4	2.5	3.3	2.2	4.0
<i>B. (Eobison) degiulii</i> ^e	Pietrafita (Italy)	Mean (N)	276.5 (10)	57 (7)	50.1 (6)	37.3 (8)	36.5 (7)	61.1 (11)	37.3 (12)
		Min-Max	250.3-296.0	47.8-64.5	35.9-56.8	34.5-42.8	33.3-40.6	52.9-71.3	33.5-41.2
		SD	17.6	5.8	8.6	2.8	2.4	5.3	2.6
<i>B. (Eobison) degiulii</i> ^{a,e}	Pirro Nord (Italy)	Mean (N)	252.9 (2)	53.8 (5)	53.1 (4)	34.6 (1)	42.6 (2)	59.3 (2)	34.5 (1)
		Min-Max	246.8-259.0	50.6-58.8	49.0-56.4	-	32.4-52.7	59.2-59.3	-
		SD	8.6	4.2	3.4	-	14.4	0.1	-
<i>B. (Eobison) degiulii</i> ^f	Mygdonia Basin (Greece)	Mean (N)	275.5 (10)	55.3 (16)	55.0 (17)	34.3 (15)	35.2 (14)	63.8 (12)	39.3 (12)
		Min-Max	261.3-286.9	51.1-62.1	51.4-64.0	31.1-38.1	31.9-40.3	59.5-70.6	36.9-40.9
		SD	8.4	2.9	3.5	2.3	2.6	3.2	1.2
<i>B. (Eobison) cf. degiulii</i> ^{a,c}	Capena (Italy)	Mean (N)	267.8 (1)	56.7 (1)	58.0 (1)	39.7 (1)	36.8 (1)	66.0 (1)	37.0 (1)
		Mean (N)	315.0 (18)	64.0 (18)	61.7 (18)	41.3 (18)	41.0 (17)	72.8 (19)	45.1 (19)
		Min-Max	301.4-329.0	56.9-72.3	53.8-68.6	35.6-47.3	35.7-45.2	64.5-80.0	39.5-50.6
<i>B. (Pocplogus) menneri</i> ^{d,g}	(Germany)	SD	9.5	4.5	4.9	3.9	3.1	4.8	2.8

		Mean (N)	287.7 (27)	62.4 (30)	59.7 (30)	41.1 (24)	40.4 (24)	70.5 (28)	42.3 (21)
<i>B. (Bison) schoetensocki</i> ^{d, e, h, i, j, k, l, m}	Durfort, Le Vallonnet, Mauer, Sissemborn,	Min-Max	260.0-323.0	53.0-82.0	48.6-69.0	33.6-53.0	33.6-47.0	61.3-85.0	34.5-47.3
	Vallparadis, Cromer Forest bed (France, Germany, Spain, UK)	SD	15.6	6.0	4.8	4.2	3.7	6.8	3.7
<i>B. (Bison) prisacus</i> ^{d, j, k, n, o, p}	Romain-La-Roche, Roter berg, Taubach,	Mean (N)	289.0 (43)	65.4 (47)	62.3 (17)	42.9 (33)	43.6 (14)	78.8 (46)	45.3 (33)
	Cava Filo, Habarna, Kiputz IX, Joint Minor Cave (France, Germany, Italy, Spain, UK)	Min-Max	254.6-318.3	51.0-79.0	56.0-68.0	36.5-53.9	33.7-51.9	68.5-91.0	38.9-51.5
<i>B. (Bison) bonasus</i> ^q	Bialowicza (Poland)	Mean (N)	263.5 (36)	59.0 (36)	54.1 (36)	-	-	63.2 (36)	42.0 (36)
		Min-Max	242.0-288.0	52.0-69.0	48.0-63.0	-	-	56.0-72.0	38.0-48.0
	SD	10.9	5.0	4.1	-	-	4.6	2.8	

Supplementary Table 27. Principal component analysis of metatarsals using seven selected variables (see Section 3 and Fig. 9). Eigenvalue and % variance of the PCs and coefficients of each variable for each PC are shown. Abbreviations as in Table 1.

	PC 1	PC 2	PC 3	PC 4	PC 5	PC 6	PC 7
Eigenvalue	0.00148352	0.000553658	0.00040309	0.000359229	0.000158925	0.000122487	7.93E-15
% Variance	48.152	17.971	13.083	11.666	51.584	39.757	2.57E-11
mv Lmax	-0.88239	-0.058484	-0.036863	0.057929	-0.2216	0.14591	0.37796
mv PET	0.050947	0.40536	0.23537	-0.79111	0.029613	-0.089971	0.37796
mv PEW	0.20854	-0.16965	-0.12751	0.12667	-0.53584	-0.68224	0.37796
mv DT	0.14508	-0.058862	0.809	0.39353	0.11606	0.099089	0.37796
mv DW	0.16084	-0.76727	-0.19639	-0.27216	0.2999	0.19999	0.37796
mv DETm	-0.039181	0.34412	-0.35354	0.30632	0.66133	-0.28462	0.37796
mv DEW	0.35616	0.30479	-0.33007	0.17882	-0.34946	0.61184	0.37796

Supplementary Table 28. Measurements (mm) of the phalanges of *Bison (Eobison) degiulii* from Pietrafitta. Estimated measurements are in italics. Abbreviations as in Fig. S1 and Table S2.

ID Specimen	Element	Lmax	Wmax	Tmax	PEAW	PEAT	DEW	DET	SOL
SABAP UMB 20. 1.6808/1	Proximal phalanx	75.0	31.7	34.6	30.3	27.7	22.8	28.2	-
SABAP UMB 20. 1.6808/2	Proximal phalanx	69.3	29.3	35.2	-	-	21.5	25.4	-
SABAP UMB 21. 4.1199	Proximal phalanx	79.2	34.7	41.7	31.1	32.4	30.0	30.5	-

Page 277: Fig. S1 Measurements taken in this work: a1–3, Cranium; b1–2, Atlas; c, Tooth; d, Mandible; e, Pelvis; f1–4, Humerus; g1–5 Metapodials; h1–4, Tibia; i1–5, Femur; j1–4, Radius; k1–4, Phalanges; l1–2, Semilunar; m1–2, Scaphoid; n1–2, Cubonavicular; o1–2, Scapula; p1–2, Malleolus; q1–2, Cuneiform; r1–2, Unciform; s1–2, Magnum; t1–2, Pyramidal; u1–2, Astragalus; v1–2, Calcaneum. Elements drawn not in scale. Abbreviations are explained in Table S2.

Page 278: Fig. S2 Humeri and radius-ulnae of *Bison (Eobison) degiulii* from Pietrafitta. a, Left humerus SABAP UMB 21. 4.1144 in anterior (a1) and posterior (a2) views; b, Right humerus SABAP UMB 22. 4.247/2 in anterior (b1), posterior (b2), and lateral (b3) views; c, Left radius-ulna SABAP UMB 22. 4.247/10 in anterior (c1), posterior (c2), and medial (c3) views; d, Right radius-ulna SABAP UMB 21. 4.1137 in anterior (d1), lateral (d2), posterior (d3) views; Scale bar: 100 mm.

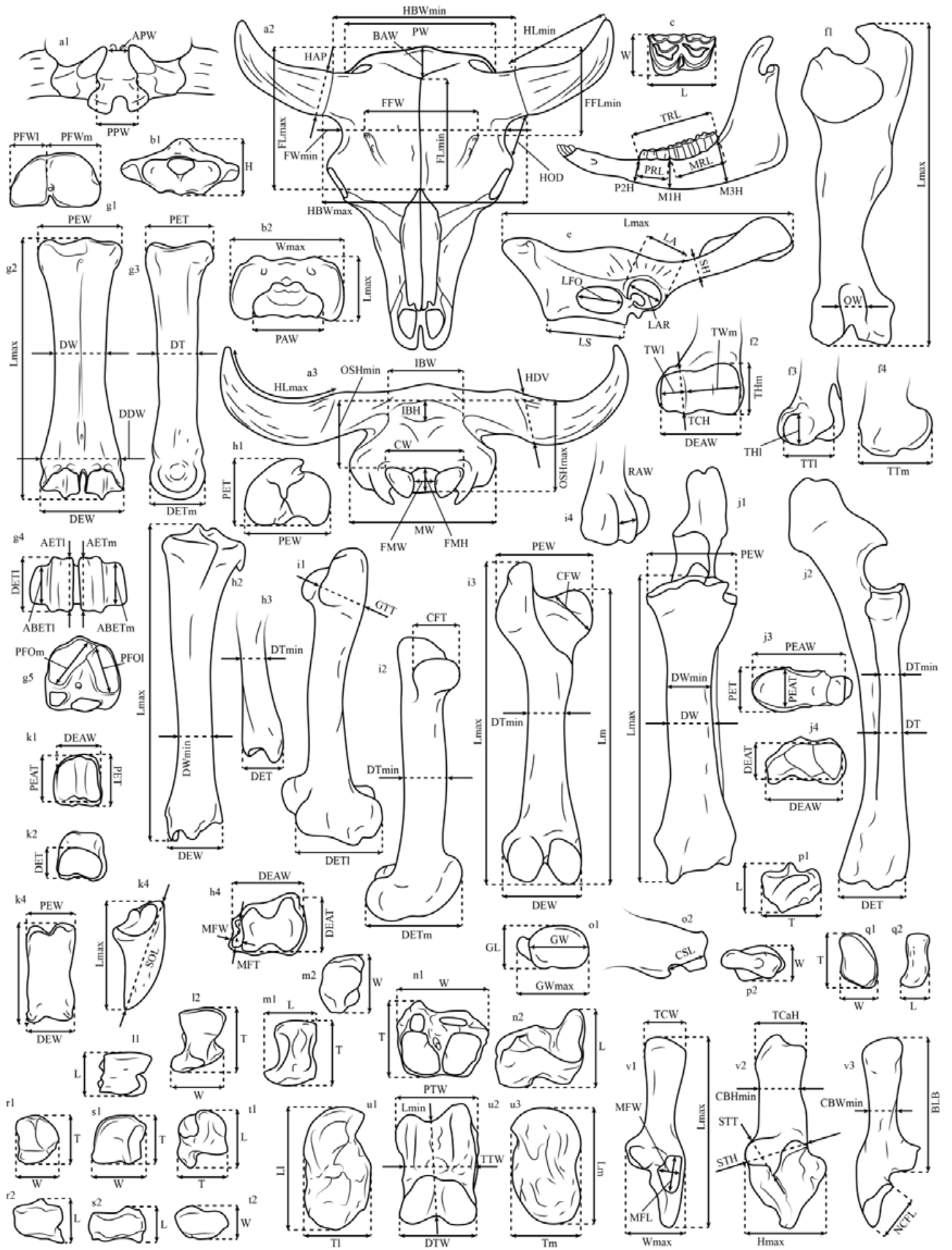
Page 279: Fig. S3 Carpal bones of *Bison (Eobison) degiulii* from Pietrafitta. a, Left pyramidal SABAP UMB 21. 4.1406 in lateral (a1) and medial (a2) views; b, Right pyramidal SABAP UMB 21. 4.1287 in lateral (b1) and medial (b2) views; c, Right semilunar SABAP UMB 21. 4.1407 in proximal (c1) and distal (c2) views; d, Right semilunar SABAP UMB 21. 4.1286 in proximal (d1) and distal (d2) views; e, Left unciform SABAP UMB 21. 4.1425 in proximal (e1) and distal (e2) views; f, Right unciform SABAP UMB 21. 4.1289 in proximal (f1) and distal (f2) views; g, Right pisiform in medial view; h, Left pisiform in medial view; i, Left scaphoid SABAP UMB 21. 4.1381 in proximal (i1) and lateral (i2) views; j, Right scaphoid SABAP UMB 21. 4.1401 in proximal (j1) and lateral (j2) views; k, Left magnum-trapezoid SABAP UMB 21. 4.1423 in distal (k1) and proximal (k2) views; l, Right magnum-trapezoid SABAP UMB 21. 4.1424 in distal (l1) and proximal (l2) views. Scale bar: 50 mm.

Page 280: Fig. S4 Pelvis and hindlimb bones of *Bison (Eobison) degiulii* from Pietrafitta. a, Right hemipelvis SABAP UMB 21. 4.1138 in lateral view; b, Right hemipelvis SABAP UMB 21. 4.1136 in lateral view; c, Left patella SABAP UMB 21. 4.1265 in anterior (c1) and posterior (c2) views; d, Left femur SABAP UMB 21. 4.1149 in distal (d1), anterior (d2), medial (d3), and posterior (d4) views; e, Right tibia SABAP UMB 21. 4.1148 in anterior (e1), medial (e2), posterior (e3), lateral (e4) and distal (e5) views; f, Left tibia SABAP UMB 19. 4.1176 in anterior (f1), proximal (f2), distal (f3), posterior (f4), lateral (f5), and medial (f6) views. Scale bar: 100 mm.

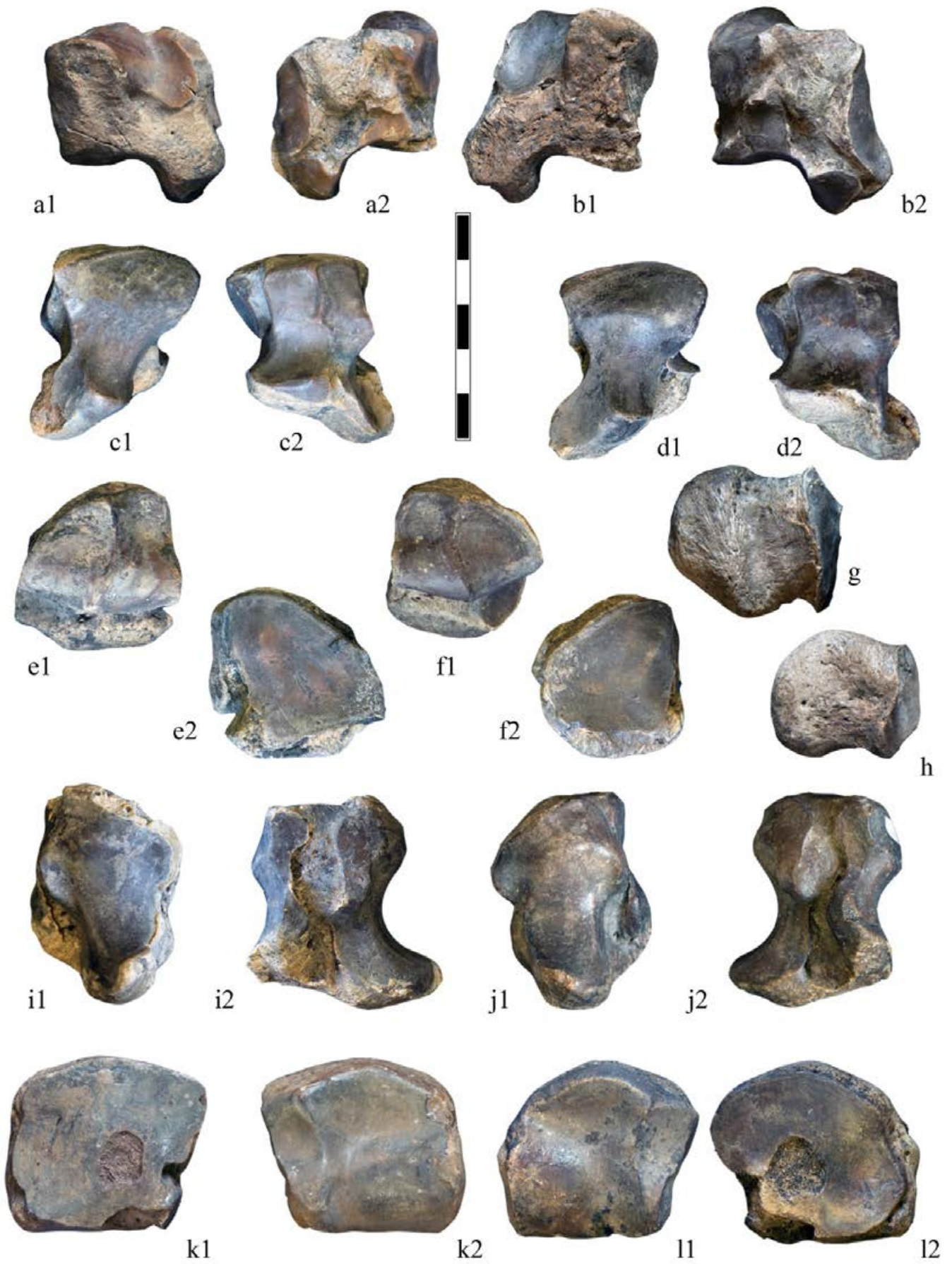
Page 281: Fig. S5 Tarsal bones of *Bison (Eobison) degiulii* from Pietrafitta. a, Right astragalus SABAP UMB 130142 in anterior (a1), posterior (a2), and lateral (a3) views; b, Right astragalus SABAP UMB 21. 4.1242 in anterior (b1), posterior (b2), and lateral (b3) views; c, Left calcaneum SABAP_UMB 22. 4.244 in medial (c1) and anterior (c2)

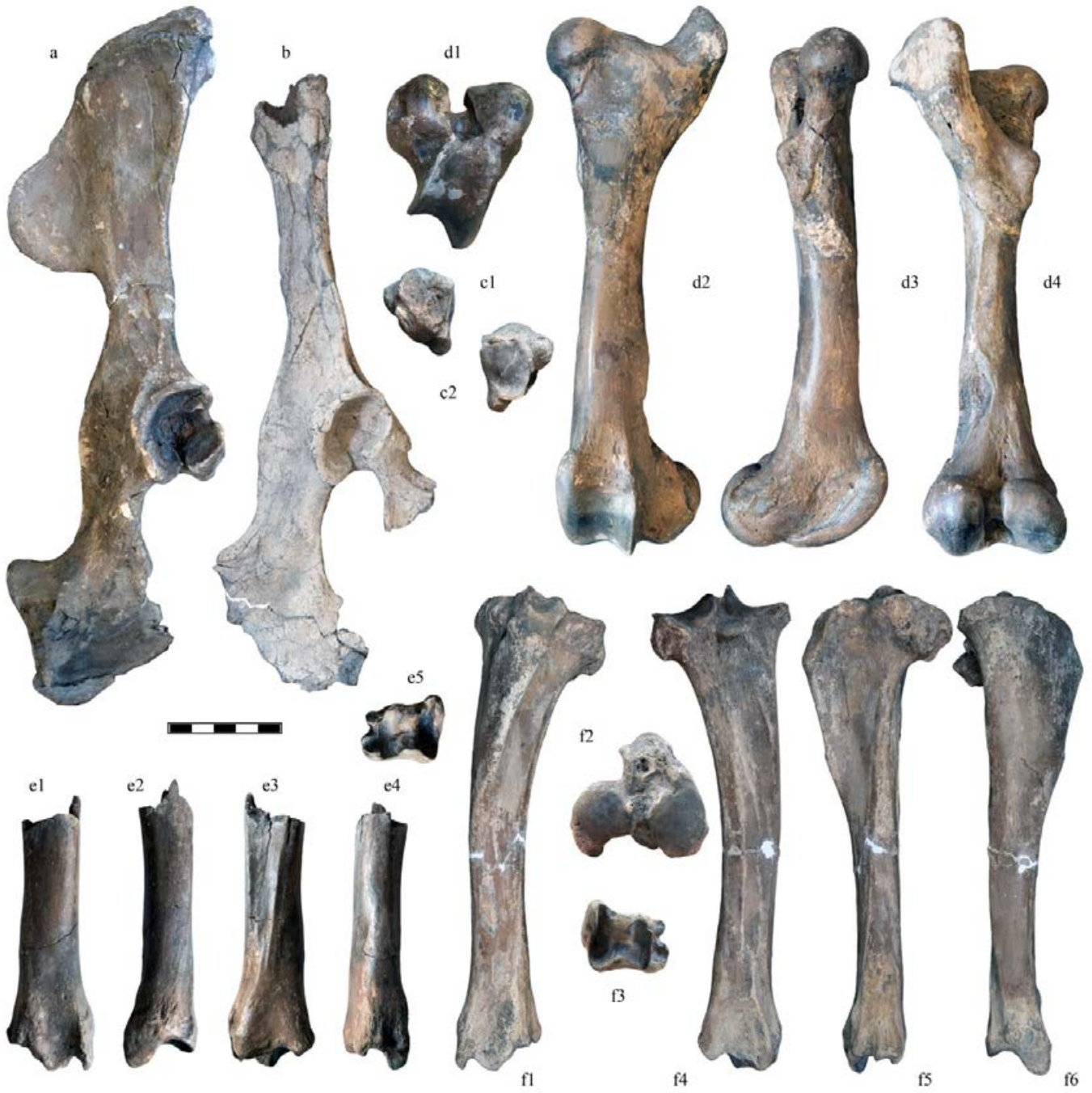
views; d, Right calcaneum SABAP UMB 130028 in anterior (d1) and posterior (d2) views; e, Left cubonavicular SABAP UMB 21. 4.1153 in proximal (e1), anterior (e2), distal (e3), and lateral (e4) views; f, Right cubonavicular SABAP UMB 21. 4.1247 in proximal (f1), anterior (f2), distal (f3), and lateral (f4) views; g, Left cuneiform SABAP UMB 21. 4.1413 in proximal (g1) and medial (g2) views; h, Right cuneiform SABAP UMB 21. 4.1411 in proximal (h1) and medial (h2) views; j, Right malleolus SABAP UMB 21. 4.1290 in medial (j1) and distal (j2) views; k, Left malleolus SABAP UMB 21. 4.1411 in proximal (k1) and distal (k2) views. Scale bar: 50 mm.

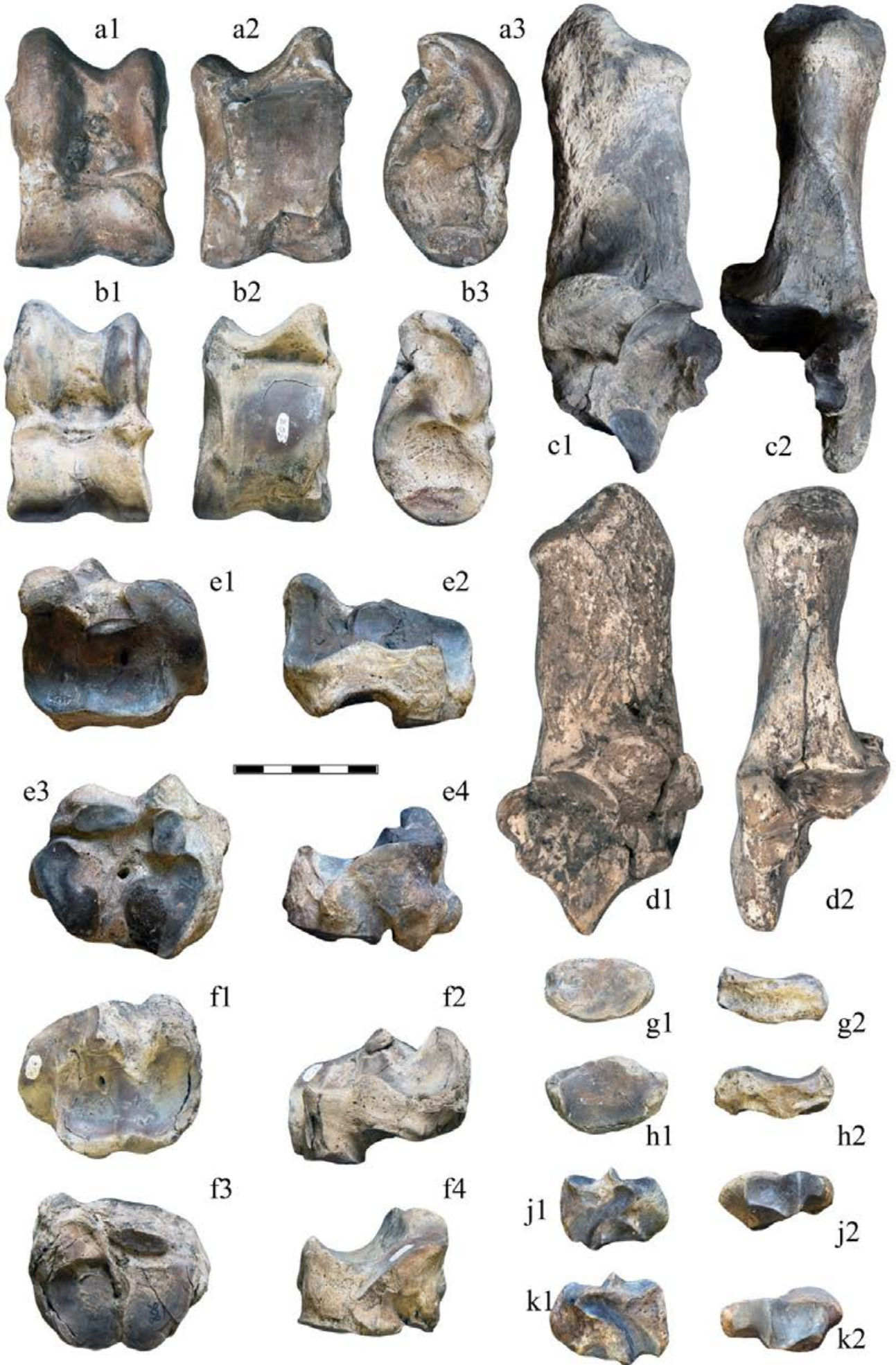
Page 282: Fig. S6 Phalanges and sesamoids of *Bison (Eobison) degiulii* from Pietrafitta. a, Right proximal phalanx SABAP UMB 21. 4.1158 in anterior (1), axial (2), proximal (3) and distal (4) views; b, Left proximal phalanx SABAP UMB 20. 1.6808/1 in anterior (1), axial (2), proximal (3) and distal (4) views; c, Right intermediate phalanx SABAP UMB 20. 1.6808/4 in in anterior (1), axial (2), proximal (3) and distal (4) views; d, Right intermediate phalanx SABAP UMB 21. 4.1274 in anterior (1), axial (2), proximal (3) and distal (4) views; e, sesamoid SABAP UMB 21. 4.1436 in anterior (1) and lateral (2) views; f, sesamoid SABAP UMB 21. 4.1453 in anterior (1) and posterior (2) views. g, Right distal phalanx SABAP UMB 21. 4.1254 in abaxial (1), proximal (2), posterior (3) and anterior (4) views; h, Right distal phalanx SABAP UMB 21. 4.1256 in abaxial (1), proximal (2), posterior (3) and anterior (4) views. Scale bar: 50 mm.

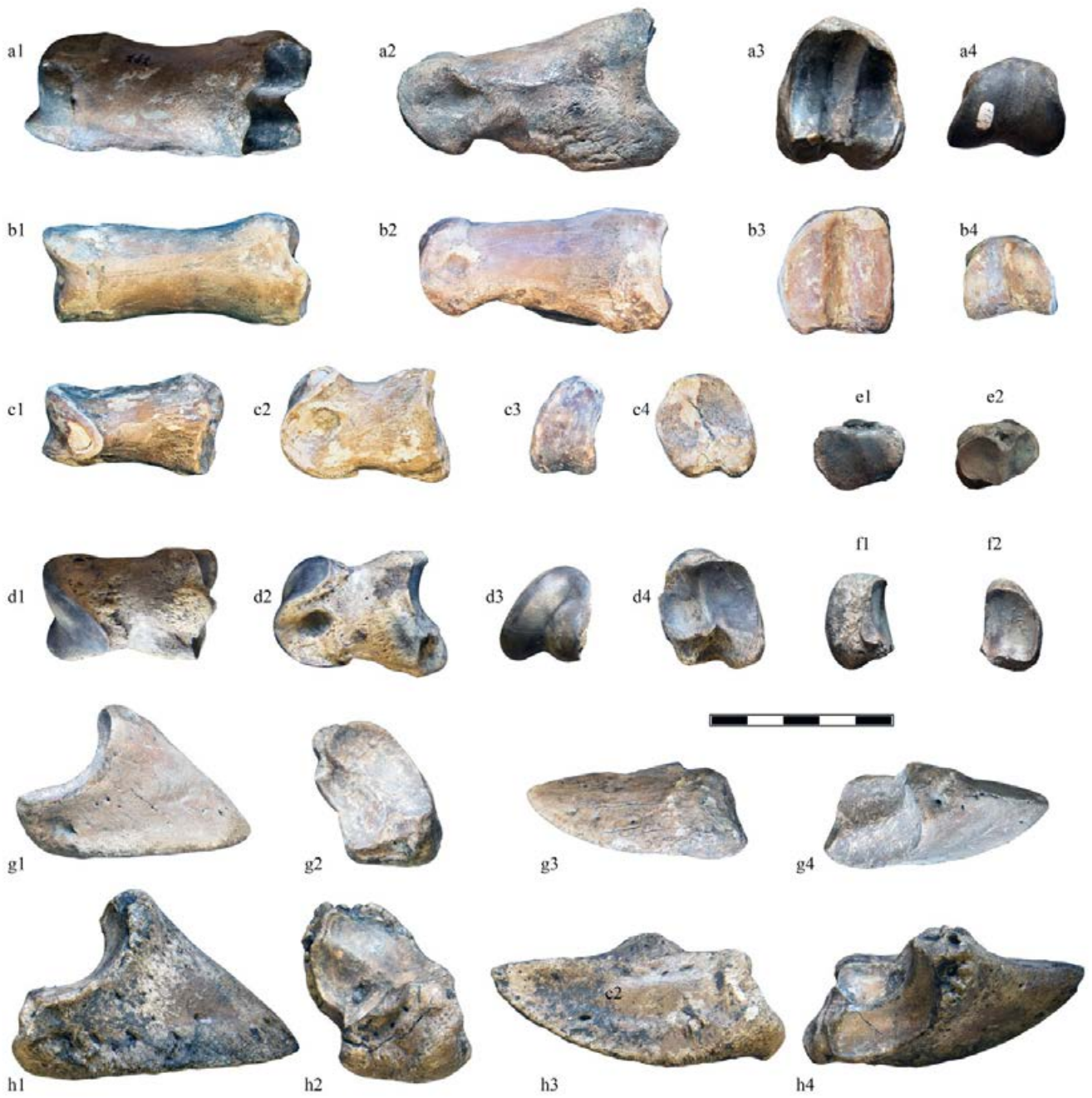












Chapter S3

Supplementary material of the paper:

Sorbelli, L., Alba, D.M., Cherin, M., Moullé, P.É., Brugal, J.P. and Madurell-Malapeira, J., 2021. A review on *Bison schoetensacki* and its closest relatives through the early-Middle Pleistocene transition: Insights from the Vallparadís Section (NE Iberian Peninsula) and other European localities. *Quaternary Science Reviews*, 261: 106933.

DOI: <https://doi.org/10.1016/j.quascirev.2021.106933>

Refer to chapter 5.

SUPPLEMENTARY MATERIAL OF

A review on *Bison schoetensacki* and its closest relatives through the Early-Middle Pleistocene Transition: insights from the Vallparadis Section (NE Iberian Peninsula) and other European localities

Leonardo Sorbelli^a, David M. Alba^a, Marco Cherin^b, Pierre-Élie Moullé^c, Jean-Philip Brugal^d, Joan Madurell-Malapeira^{a*}

^a Institut Català de Paleontologia Miquel Crusafont, Universitat Autònoma de Barcelona, Edifici ICTA-ICP, c/ Còlumbes s/n, Campus de la UAB, 08193 Cerdanyola del Vallès, Barcelona,

Spain

^b Dipartimento di Fisica e Geologia, Università degli Studi di Perugia, Via A. Pascoli, 06123 Perugia, Italy

^c Musée de Préhistoire Régionale de Menton, 06500 Menton, France

^d Aix-Marseille Université, CNRS, Minist. Culture, UMR 7269 Lampaosa, MMSH, 13094 Aix-en-Provence cedex 2, France

* Corresponding author.

E-mail address: joan.madurell@icp.cat (J. Madurell-Malapeira).

Table S1. List of *Bison schoetensacki* specimens from Vallparadis Estacio (EVT) and Cal Guardiola (CGR) layers.

ID	Anatomical element	Layer	ID	Anatomical element	Layer	ID	Anatomical element	Layer	ID	Anatomical element	Layer	ID	Anatomical element	Layer
IPS93141	Astragalus	CGR07	IPS92970	Horn core	EVT7	IPS14985	Metacarpal	CGR07	IPS92958	Cubonavicular	EVT10	IPS91545	Pyramidal	EVT7
IPS93249	Astragalus	EVT7	IPS50672	Humerus	CGR04	IPS15002	Metacarpal	CGR07	IPS92984	Indeterminate fragments	EVT7	IPS92961	Pyramidal	EVT10
IPS93250	Astragalus	EVT7	IPS92928	Humerus	EVT7	IPS107626	Metacarpal	EVT12	IPS92985	Indeterminate fragments	EVT7	IPS13570	Radius	CGR02
IPS93251	Astragalus	EVT7	IPS92929	Humerus	EVT7	IPS107635	Metacarpal	EVT12	IPS14304	Pelvis fragment	CGR02	IPS39893	Radius	CGR02
IPS93252	Astragalus	EVT7	IPS114549	Humerus	EVT7	IPS107636	Metacarpal	EVT12	IPS14977	Proximal phalanx	CGR07	IPS48775	Radius	CGR07
IPS93253	Astragalus	EVT12	IPS114568	Humerus	EVT7	IPS118115	Metacarpal	EVT12	IPS61879	Proximal phalanx	CGR03	IPS92914	Radius	EVT7
IPS118120b	Astragalus	EVT12	IPS107620	Humerus	EVT12	IPS118116	Metacarpal	EVT12	IPS92924	Proximal phalanx	EVT10	IPS92915	Radius	EVT7
IPS93266	Autopodial fragment	EVT10	IPS92981	Long bone fragment	EVT12	IPS17761	Metapodial distal fragment	CGR07	IPS92925	Proximal phalanx	EVT7	IPS92916	Radius	EVT7
IPS114551	Axis	EVT7	IPS92968	Mandible	EVT12	IPS18517	Metapodial distal fragment	CGR07	IPS92926	Proximal phalanx	EVT10	IPS92918	Radius	EVT7
IPS11896	Calcaneum	CGR02	IPS92978	Mauilla	EVT7	IPS92959	Metapodial distal fragment	EVT10	IPS92927	Proximal phalanx	EVT7	IPS92919	Radius	EVT7
IPS93244	Calcaneum	EVT7	IPS796	Metacarpal	CGR07	IPS18430	Metatarsal	CGR07	IPS107624	Proximal phalanx	EVT12	IPS92920	Radius	EVT7
IPS93245	Calcaneum	EVT7	IPS92905	Metacarpal	CGR07	IPS92906	Metatarsal	EVT7	IPS114554	Proximal phalanx	EVT7	IPS107616	Radius	EVT12
IPS93246	Calcaneum	EVT7	IPS92907	Metacarpal	EVT10	IPS92930	Metatarsal	EVT12	IPS118118	Proximal phalanx	EVT12	IPS107617	Radius	EVT12
IPS93247	Calcaneum	EVT7	IPS92908	Metacarpal	EVT7	IPS92931	Metatarsal	EVT7	IPS118119	Proximal phalanx	EVT12	IPS107628	Radius	EVT12
IPS93248	Calcaneum	EVT7	IPS92909	Metacarpal	EVT12	IPS92932	Metatarsal	EVT12	IPS16776	Intermediate phalanx	CGR02	IPS118111	Radius	EVT12
IPS118120a	Calcaneum	EVT12	IPS92910	Metacarpal	EVT12	IPS92933	Metatarsal	EVT7	IPS40612	Intermediate phalanx	CGR02	IPS92922	Scapula	EVT7
IPS93263	Capitotrapezoid	EVT10	IPS92911	Metacarpal	EVT7	IPS92934	Metatarsal	EVT7	IPS107621	Intermediate phalanx	EVT12	IPS107637	Scapula	EVT12
IPS107615	Cervical vertebra	EVT12	IPS92912	Metacarpal	EVT7	IPS92935	Metatarsal	EVT7	IPS118114	Intermediate phalanx	EVT12	IPS92960	Semilunar	EVT10
IPS93269	Cranial fragments	EVT12	IPS92913	Metacarpal	EVT12	IPS92936	Metatarsal	EVT7	IPS39742	Discal phalanx	CGR02	IPS92965	Cuneiform	EVT10
IPS93271	Cranial fragments, horn core	EVT10	IPS13547	Metacarpal	CGR07	IPS92937	Metatarsal	EVT12	IPS41397	Discal phalanx	CGR02	IPS92994	M2 and M3	EVT10
IPS93272	Cranial fragments	EVT10	IPS13911	Metacarpal	CGR02	IPS92938	Metatarsal	EVT12	IPS92967	Discal phalanx	EVT10	IPS92954	Thoracic vertebra	EVT3
IPS93280	Indeterminate fragments	EVT12	IPS13928	Metacarpal	CGR07	IPS92939	Metatarsal	EVT7	IPS107623	Discal phalanx	EVT12	IPS92955	Thoracic vertebra	EVT7
IPS93282	Indeterminate fragments	EVT12	IPS14102	Metacarpal	CGR07	IPS107634	Metatarsal	EVT12	IPS107625	Discal phalanx	EVT12	IPS92956	Thoracic vertebra	EVT3
IPS93283	Indeterminate fragments	EVT12	IPS14702	Metacarpal	CGR07	IPS114552	Metatarsal	EVT7	IPS107622	Discal phalanx	EVT12	IPS118117	Thoracic vertebra	EVT12
IPS93273	Hemimandible	EVT7	IPS114815	Metacarpal	CGR07	IPS114553	Metatarsal	EVT7	IPS118112	Discal phalanx	EVT12	IPS92940	Tibia	EVT7
IPS93277	Hemimandible	EVT7	IPS114917	Metacarpal	CGR02	IPS92957	Cubonavicular	EVT10	IPS118113	Discal phalanx	EVT12	IPS92942	Tibia	EVT7

ID	Anatomical element	Layer	ID	Anatomical element	Layer	ID	Anatomical element	Layer	ID	Anatomical element	Layer
IPS93043	Tibia	EVT7	IPS93040	m1 or m2	EVT7	IPS93018	M3	EVT7	IPS93002	Upper molar	EVT7
IPS9307618	Tibia	CGR02	IPS93041	m1 or m2	EVT7	IPS93021	M3	EVT7	IPS93003	M2	EVT7
IPS114546	Tibia	EVT12	IPS93042	m1	EVT7	IPS93023	M3	EVT3	IPS93046	Upper molar	EVT7
IPS114555	p3	EVT7	IPS93047	M1	EVT7	IPS93033	M3	EVT7	IPS93057	Upper molar	EVT7
IPS93006	p3	EVT7	IPS92991	M2	EVT10	IPS93043	m3	EVT7	IPS92986	P2	EVT7
IPS93050	p3	EVT7	IPS92990	m2	EVT7	IPS20182	M3	CGR07	IPS92996	P3	EVT10
IPS93054	p3 or dp4	EVT7	IPS93005	M2	EVT7	IPS93000	Cheek tooth	EVT7	IPS92998	P3	EVT7
IPS92997	dp4	EVT7	IPS93014	m2	EVT7	IPS93026	Cheek tooth	EVT7	IPS93012	P3 or P4	EVT7
IPS93008	dp4	EVT7	IPS93019	m2	EVT7	IPS93052	Cheek tooth	EVT7	IPS92995	P4	EVT10
IPS93037	dp4	EVT7	IPS93022	M2	EVT7	IPS93053	Cheek tooth	EVT7	IPS93013	P4	EVT3
IPS114965	dp4	CGR07	IPS93032	M2	EVT7	IPS93035	Lower cheek tooth	EVT7	IPS93015	p4	EVT7
IPS93063	i1	EVT12	IPS93027	m1	EVT7	IPS93001	Lower molar	EVT7	IPS93020	P4	EVT7
IPS93064	i1	EVT12	IPS93030	m2	EVT7	IPS93024	Lower molar	EVT7	IPS93045	p4	EVT7
IPS93062	i2	EVT12	IPS93044	m2	EVT7	IPS93031	Lower molar	EVT10	IPS93049	P4	EVT7
IPS93065	i3	EVT12	IPS92988	M2	EVT7	IPS93048	Lower molar	EVT7	IPS93056	p4	EVT7
IPS92992	M1	EVT10	IPS93007	M3	EVT7	IPS93061	Lower molar	EVT7	IPS13557	P4	CGR07
IPS93017	M1	EVT6	IPS93028	M3	EVT7	IPS13681	Lower molar	CGR02	IPS92921	Ulna	EVT12
IPS93036	M1	EVT7	IPS93028	M3	EVT7	IPS93004	Lower premolar	EVT7	IPS107616	Ulna	EVT12
IPS93039	m1 or m2	EVT7	IPS93034	M2	EVT7	IPS93058	Lower premolar	EVT7	IPS114545	Ulna	EVT12
IPS93009	m2	EVT7	IPS92993	M3	EVT10	IPS93051	Indeterminate tooth	EVT7	IPS114548	Ulna	EVT7
IPS93016	M1	EVT6	IPS92987	m3	EVT7	IPS93055	Indeterminate tooth	EVT7	IPS92962	Unciform	EVT10
IPS93029	M1	EVT7	IPS92989	m3	EVT7	IPS93059	Indeterminate tooth	EVT7	IPS92964	Unciform	EVT7
IPS93038	M2	EVT7	IPS93011	M3	EVT7	IPS93060	Indeterminate tooth	EVT7			

Table S2. Comparative dental measurements (mm) of m3, M1, M2, and M3 in selected *Leptobos* and *Bison* s.l. samples. Abbreviations: L, length; W, width.

Taxon (source) of data	Locality	Statistics	m3L	m3W	M1L	M1W	M2L	M2W	M3L	M3W	
<i>Leptobos etruscus</i> (Duvernois and Guérin, 1989)	Senèze (France)	Mean	41.0	16.1	20.1	23.1	26.3	23.6	29.8	22.8	
		Minimum	37.5	13.5	18.5	20.0	20.5	28.5	28.0	34.0	
		Maximum	45.0	19.5	22.5	27.0	19.5	28.5	18.5	27.5	
		SD	2.3	1.8	1.3	2.2	2.6	3	1.8	2.5	
		N	10	11	7	7	8	8	10	10	
<i>Bison (Eobison) georgicus</i> (Bukshianiძე, 2005)	Dmanisi (Georgia)	Mean	40.5	15.3			29.0	26.0	30.1	27.4	
		Minimum	37.9	13.0					28.9	27.1	
		Maximum	43.3	18.0						31.3	27.8
		SD	2.4	2.2						1.7	0.5
		N	5	5			1	1	1	2	2
<i>Bison</i> sp. (Moyà Solà, 1987)	Venta Micena (Spain)	Mean	38.9	15.6	25.9	20.9	28.7	25.9	29.7	21.8	
		Minimum	37.3	13.9	22.8	19.3	26.2	22.8	27.4	21	
		Maximum	42.4	17.5	27.2	23.0	30.9	27.2	32.3	23.3	
		SD	1.5	0.9	1.34	1.7	1.6	1.3	1.9	1.3	
		N	14	15	11	11	9	11	10	9	
<i>Bison (Eobison) degiulii</i> (Masini, 1989)	Pirro Nord/Capena (Italy)	Mean	34.3	15.0	20.4	23.3	23.3	24.7	20.3	23.2	
		Minimum			19.6	21.0	22.0	23.9	16.5	21.2	
		Maximum			22.2	26.0	26.0	25.3	27.6	24.6	
		SD			1	1.5	1.5	0.6	3.4	0.9	
		N			1	7	7	6	6	10	10
<i>Bison (Eobison) cf. degiulii</i> (Kostopoulos et al., 2018)	Mygdonia basin (Greece)	Mean	40	17.0	26.2	24.2	29.8	24.9	30.8	23.9	
		Minimum	37.1	15.1	22.0	19.3	25.0	19.5	27.9	18.0	
		Maximum	45.1	18.1	33.9	28.0	35.9	29.6	33.0	29.1	
		SD	2.4	0.9	4.0	2.7	2.6	3.3	1.3	3.3	
		N	16	16	18	18	22	22	22	22	
<i>Bison menneri</i> (van Asperen and Kahle, 2017)	Untermassfeld (Germany)	Mean	41.4	16.0	26.9	20.7	31.2	20.6	31.7	21	
		Minimum	22.7	17.0	22.7	17	27.7	17	30.2	16.8	
		Maximum	45.3	18.7	30.6	25.2	35	26.3	34.3	23.9	
		SD	2.1	1.7	3.1	2.9	1.9	3.2	1.2	2.1	
		N	20	22	16	16	17	17	13	13	
<i>Bison schoetensacki</i> (Moulié, 1992)	Le Vallonnet (France)	Mean	41.5	18.4	28.1	26.1	30.7	28.1	32.0	29.9	
		Minimum	37.8	17.2	23.0	16.5	28.5	25.0	29.5	26.6	
		Maximum	43.5	18.9	32.2	29.2	33.3	30.5	35.3	31.5	
		SD	1.8	0.6	3.1	3.3	1.4	1.8	1.8	2.3	
		N									

<i>Bison schoetensocki</i> (This paper)	Vallparadis Composite Section (Spain)	N	7	7	18	12	11	8	8	4
		Mean	41.7	17.5	23.3	25.1	27.4	25.5	28.7	25.5
		Minimum	38.2	16.3	20.6	23.4	24.7	20.4	23.5	24.2
		Maximum	46.5	18.4	27.0	26.8	32.3	28.8	32.3	27.6
		SD	3.0	1.0	2.4	1.3	2.2	2.6	2.7	1.3
<i>Bison schoetensocki</i> (van Asperen and Kahle, 2017)	Süssenborn (Germany)	N	5	5	8	8	12	12	9	9
		Mean	43.5	16.5	30.1	21.3	32.1	22.1	34.2	23.6
		Minimum	39.4	14.7	26.9	17.9	28.3	17.5	29.0	18.4
		Maximum	47.6	19.0	34.5	25.5	35.7	27.2	40.3	28
		SD	2.4	1.1	2	2	1.8	1.9	2.2	2.2
<i>Bison schoetensocki</i> (Breda et al., 2010)	Cromer Forest-bed (various localities; England)	N	17	18	28	24	43	37	30	26
		Mean	39.8	18.0	29.3	26.2	29.0	27.0	33.0	26.2
		Minimum	36.0	16.2	28.6	26.0			32.0	24.0
		Maximum	43.1	21.0	30.0	26.4			34.0	28.0
		SD	2.2	1.2	1	0.3			0.7	1.9
<i>Bison cf. priscus</i> (Breda et al., 2010)	Westbury (England)	N	9	13	2	2	1	1	1	6
		Mean	44.6	19.5	29.5	26.3	33.2	28.1	33.4	28.0
		Minimum	41.0	16.1	26.0	23.0	31.6	26.8	30.0	26.3
		Maximum	49.7	21.9	33.5	29	35	29.3	37.0	30.2
		SD	2.6	1.9	2.5	1.6	1.3	1.1	2	1.4
<i>Bison schoetensocki</i> (This paper)	Isernia la Pineta (Italy)	N	8	8	17	17	8	7	14	13
		Mean	42.5	19.0					32.6	26.4
		Minimum	39.0	16.0					29.9	22.3
		Maximum	49.8	21.0					36.0	29.6
		SD	2.3	1.2					1.6	2.3
<i>Bison priscus</i> (van Asperen and Kahle, 2017)	Taubach (Germany)	N	21	21					11	11
		Mean	48.6	18.8	33	23.3	35.9	25.5	38.1	24.2
		Minimum	44.0	16.0	30.2	21.1	33.8	22.3	36.1	20.7
		Maximum	53.7	21.5	35.3	28.2	38.3	29.6	40.0	26.5
		SD	3.1	2.9	1.5	2.1	1.4	2.4	1.7	2.6
<i>Bison priscus</i> (Vasiliev, 2008)	Krasny Yar, R-W (Russia)	N	18	19	15	15	14	14	4	4
		Mean	46.8	19.9	25.3	27.5	31.2	28.1	33.1	28.2
		Minimum	42	16	20.5	24.7	26.5	23.0	29.0	24.0
		Maximum	53.5	22.5	32.0	33.0	34.7	31.0	37.0	30.5
		SD								
		N	58	68	10	10	11	9	8	6

Table S3. Z-scores values for length (L) and width (W) of m3, M1, M2, M3 of the VCS sample compared with selected *Leptobos* and *Bison* s.l. species.

Tooth	ID	<i>Leptobos etruscus</i> (Senèze)		<i>Bison</i> sp. (Venta Micena)		<i>Bison</i> (Fobison) <i>degiulii</i> (Pirro)		<i>Bison</i> (Fobison) <i>degiulii</i> (Mygdonia basin)		<i>Bison schoetensacki</i> (Le Vallonnet)		<i>Bison menneri</i> (Untermassfeld)		<i>Bison schoetensacki</i> (Süssenborn)		<i>Bison prisus</i> (Taubach)	
		L	W	L	W	L	W	L	W	L	W	L	W	L	W	L	W
m3	IPS93043	0.39	0.83	2.01	2.30	0.82	0.59	0.24	-1.36	0.24	0.97	0.24	0.97	-0.65	1.00	-2.18	-0.40
m3	IPS92977	-1.22	0.11	-0.47	0.80	-0.75	-0.79	-1.74	-3.65	-1.53	0.21	-1.53	0.21	-2.18	-0.19	-3.39	-0.84
m3	IPS92973	0.31	1.28	1.88	3.22	0.74	1.44	0.13	0.05	0.15	1.45	0.15	1.45	-0.73	1.73	-2.25	-0.13
m3	IPS92987	2.40	1.28	5.10	3.22	2.77	1.44	2.69	0.05	2.44	1.45	2.44	1.45	1.26	1.73	-0.68	-0.13
m3	IPS92989	-0.31	0.33	0.94	1.26	0.14	-0.36	-0.62	-2.94	-0.52	0.44	-0.52	0.44	-1.31	0.17	-2.71	-0.71
	Mean	0.31	0.77	1.89	2.16	0.75	0.47	0.14	-1.57	0.16	0.90	0.16	0.90	-0.72	0.89	-2.24	-0.44
	Minimum	-1.22	0.11	-0.47	0.80	-0.75	-0.79	-1.74	-3.65	-1.53	0.21	-1.53	0.21	-2.18	-0.19	-3.39	-0.84
	Maximum	2.40	1.28	5.10	3.22	2.77	1.44	2.69	0.05	2.44	1.45	2.44	1.45	1.26	1.73	-0.68	-0.13
	STD	1.33	0.53	2.05	1.11	1.29	1.02	1.63	1.70	1.46	0.57	1.46	0.57	1.26	0.88	1.00	0.33
	N	5	5	5	5	5	5	5	5	5	5	5	5	5	5	5	5
M1	IPS92992	4.02	1.12	-0.52	2.83	-0.25	0.51	-0.94	-0.16	-0.55	1.65	-0.55	1.65	-2.42	2.15	-5.22	1.08
M1	IPS93016	5.59	0.49	0.97	1.99	0.25	-0.01	-0.30	-0.58	0.11	1.17	0.11	1.17	-1.42	1.46	-3.88	0.41
M1	IPS93017	3.62	1.25	-0.90	3.01	1.68	0.62	-1.11	-0.07	-0.71	1.75	-0.71	1.75	-2.67	2.30	-5.55	1.23
M1	IPS93029	1.42	1.65	-2.99	3.55	1.62	0.96	-2.01	0.20	-1.63	2.06	-1.63	2.06	-4.06	2.75	-7.41	1.66
M1	IPS93036	0.71	0.31	-3.66	1.75	0.67	-0.15	-2.30	-0.70	-1.92	1.04	-1.92	1.04	-4.51	1.26	-8.01	0.22
M1	IPS93047	0.39	0.13	-3.96	1.51	0.25	-0.30	-2.43	-0.82	-2.05	0.90	-2.05	0.90	-4.71	1.07	-8.28	0.03
	Mean	2.62	0.83	-1.84	2.44	3.23	1.06	-1.51	-0.36	-1.12	1.43	-1.12	1.43	-3.30	1.83	-6.39	0.77
	Minimum	0.39	0.13	-3.96	1.51	0.25	-0.30	-2.43	-0.82	-2.05	0.90	-2.05	0.90	-4.71	1.07	-8.28	0.03
	Maximum	5.59	1.65	0.97	3.55	2.27	0.25	-0.30	0.20	0.11	2.06	0.11	2.06	-1.42	2.75	-3.88	1.66
	STD	2.09	0.60	1.98	0.81	2.78	0.88	0.86	0.40	0.87	0.46	0.87	0.46	1.32	0.67	1.77	0.64
	N	6	6	6	6	6	6	6	6	6	6	6	6	6	6	6	6
M2	IPS92988	-0.19	0.57	-1.77	-0.45	1.69	1.09	-1.55	-1.56	-2.78	1.47	-2.78	1.47	-3.49	1.69	-7.04	-0.08
M2	IPS92991	0.70	1.74	-0.37	2.16	3.25	6.97	-0.65	0.42	-1.59	2.57	-1.59	2.57	-2.22	3.56	-5.43	1.36
M2	IPS92994	0.23	1.34	-1.10	1.27	2.44	4.95	-1.12	-0.26	-2.21	2.19	-2.21	2.19	-2.89	2.92	-6.27	0.87
M2	IPS93005	0.51	1.54	-0.67	1.72	2.91	5.96	-0.85	0.08	-1.85	2.38	-1.85	2.38	-2.50	3.24	-5.78	1.11
M2	IPS93003	-0.54	0.50	-2.32	-0.60	1.08	0.76	-1.91	-1.67	-3.25	1.40	-3.25	1.40	-3.99	1.59	-7.66	-0.16
M2	IPS93022	1.17	-0.80	0.37	-3.51	4.07	-5.79	-0.18	-3.87	-0.97	0.18	-0.97	0.18	-1.56	-0.49	-4.60	-1.76

M2	IPS93032	0.78	1.24	-0.24	1.04	3.39	4.45	-0.57	0.74	-1.70	-0.43	-1.49	2.10	-2.11	2.76	-5.30	0.74
M2	IPS93034	-1.17	0.03	-3.29	-1.64	-0.01	-1.59	-2.54	-0.36	-5.20	-2.46	-4.07	0.96	-4.88	0.84	-8.78	-0.73
M2	IPS93038	-0.23	0.84	-1.83	0.15	1.62	2.43	-1.59	0.38	-3.52	-1.11	-2.83	1.72	-3.55	2.12	-7.11	0.25
	Mean	0.14	0.78	-1.25	0.02	2.27	2.14	-1.22	0.32	-2.85	-1.21	-2.34	1.66	-3.02	2.03	-6.44	0.18
	Minimum	-1.17	-0.80	-3.29	-3.51	-0.01	-5.79	-2.54	-1.12	-5.20	-3.87	-4.07	0.18	-4.88	-0.49	-8.78	-1.76
	Maximum	1.17	1.74	0.37	2.16	4.07	6.97	-0.18	1.20	-1.00	0.42	-0.97	2.57	-1.56	3.56	-4.60	1.36
	STD	0.74	0.81	1.16	1.80	1.29	4.05	0.74	0.74	1.32	1.36	0.98	0.76	1.05	1.28	1.32	0.99
	N	9	9	9	9	9	9	9	9	9	9	9	9	9	9	9	9
M3	IPS20182	0.45	1.29	0.48	3.21			-0.13	0.64	-0.78	-1.75	-0.96	2.36	-1.63	1.09	-4.51	0.69
M3	IPS29993	0.34	1.94	0.37	4.43			-0.28	1.12	-0.89	-1.03	-1.14	3.11	-1.73	1.82	-4.63	1.31
M3	IPS29994	0.68	1.90	0.70	4.35			0.18	1.09	-0.56	-1.08	-0.62	3.07	-1.45	1.77	-4.27	1.27
M3	IPS93007	-1.41	0.77	-1.28	2.21			-2.63	0.25	-2.61	-2.33	-3.79	1.76	-3.14	0.49	-6.49	0.18
M3	IPS93011	-1.02	0.60	-0.91	1.91			-2.10	0.13	-2.22	-2.50	-3.19	1.57	-2.82	0.31	-6.07	0.03
M3	IPS93018	-1.13	1.29	-1.02	3.21			-2.25	0.64	-2.33	-1.75	-3.37	2.36	-2.92	1.09	-6.19	0.69
M3	IPS93021	-0.40	1.17	-0.32	2.98			-1.26	0.55	-1.61	-1.88	-2.25	2.22	-2.32	0.95	-5.41	0.57
M3	IPS93023	-3.56	0.89	-3.32	2.44			-5.50	0.34	-4.72	-2.19	-7.05	1.90	-4.88	0.63	-8.77	0.30
M3	IPS93028	1.41	0.69	1.39	2.06			1.16	0.19	0.17	-2.41	0.49	1.66	-0.86	0.40	-3.49	0.11
M3	IPS93033	-1.58	1.49	-1.44	3.59			-2.85	0.79	-2.78	-1.52	-4.05	2.60	-3.28	1.31	-6.67	0.88
	Mean	-0.62	1.20	-0.53	3.04			-1.57	0.57	-1.83	-1.84	-2.59	2.26	-2.50	0.99	-5.65	0.60
	Minimum	-3.56	0.60	-3.32	1.91			-5.50	0.13	-4.72	-2.50	-7.05	1.57	-4.88	0.31	-8.77	0.03
	Maximum	1.41	1.94	1.39	4.43			1.16	1.12	0.17	-1.03	0.49	3.11	-0.86	1.82	-3.49	1.31
	STD	1.44	0.48	1.36	0.90			1.92	0.36	1.41	0.52	2.18	0.55	1.16	0.54	1.52	0.46
	N	10	10	10	10			10	10	10	10	10	10	10	10	10	10

Table S4. Measurements (mm) of the vertebrae of *Bison schoetensocki* from Vallparadis Estació (EVT) layers. Abbreviations: ant, anterior; CL, centrum length; CH, centrum height; CW, centrum width; NSL, neural spine length; NSW, neural spine width; post, posterior; SCW, spinal canal width.

ID Specimen	Layer	Element	CL	CH ant.	CW ant.	CH post.	CW post.	SCW ant.	SCW post.	NSW	NSL
IPS92954	EVT3	Thoracic vertebra	63.5	50.4	56.4	44.2	46.7	29.2	35.2	50.2	>400
IPS92956	EVT3	Thoracic vertebra	70.8	44.8	55.4	45.5	54.0	27.7	30.0	53.2	
IPS118117	EVT12	Thoracic vertebra	73.7	74.1	54.4		47.3	21.0	22.3	40.6	73.7
IPS107615	EVT12	Cervical vertebra	60.5	45.1	35.6	55.0	51.0	17.6	14.6		
IPS114551	EVT7	Axis	145.4	44.8	106.7	69.0	53.9	28.5	27.2		

Table S5. Measurements (mm) and descriptive statistics of the scapulae of *Bison schoetensacki* from Vallparadís Estació (EVT) layers. Abbreviations: CSL, *collum scapulae* length; GL, glenoid cavity length; GPL, glenoid process length; GW, glenoid cavity width; L, left; R, right.

ID Specimen	Layer	Side	GL	GW	GPL	CSL
IPS107637	EVT12	R	75.1	62.2	83.3	67.4
IPS92922	EVT7	L	60.5	60.5	84	75.9
		Mean	75.1	61.4	83.7	71.6
		Minimum	60.5	60.5	83.3	67.4
		Maximum	62.2	84	75.9	
		SD	0.5	6	1.2	
		N	1	2	2	2

Table S6. Comparative measurements (mm) of the scapula in selected *Bison* s.l. samples. Abbreviations: CSL, *collum scapulae* length; GL, *glenoid cavity* length; GPL, *glenoid process* length; GW: *glenoid cavity* width.

Taxon	Locality	Statistics	GL	GW	GPL
<i>Bison menneri</i> (Sher, 1997)	Untermassfeld (Germany)	Mean	70.6	60.9	84.5
		Minimum	67.5	55	80.5
		Maximum	70.0	70.0	92.5
		SD	3.8	6.0	4.7
<i>Bison schoetensacki</i> (Moullé, 1992)	Le Vallonnet (France)	N	4	4	4
		Mean	78.2	59.9	88.4
		Minimum	78.1	58.0	86.8
		Maximum	78.3	61.8	89.9
<i>Bison schoetensacki</i> (This paper)	Vallparadis composite section (Spain)	SD	0.1	2.7	2.2
		N	2	2	2
		Mean	75.1	61.4	83.7
		Minimum		60.5	83.3
<i>Bison schoetensacki</i> (Sala, 1986)	Mauer (Germany)	Maximum	62.2	84.0	
		SD	0.5	6.0	
		N	1	2	2
		Mean	88.0	71.5	103.5
<i>Bison priscus</i> (Sala, 1986)	Cava Filo (Italy)	Minimum	84.0	68.0	101.0
		Maximum	92.0	75.0	106.0
		SD	5.7	5.0	3.5
		N	2	2	2
<i>Bison priscus</i> (Vasiliev, 2008)	Krasny Yar, R-W (Russia)	Mean	83.9	63.7	97.4
		Minimum	69.0	51.0	76.0
		Maximum	98.5	75.0	115
		SD	13.2	9.2	15.9
<i>Bison priscus</i> (Vasiliev, 2008)	Taradanovo, W1-2 (Russia)	N	5	5	5
		Mean	88.8	70.6	104.9
		Minimum	74.5	60.5	84.5
		Maximum	100.0	84.2	126
<i>Bison priscus</i> (Vasiliev, 2008)	Taradanovo, W1-2 (Russia)	SD			
		N	33	33	33
		Mean	89.0	70.5	103.2
		Minimum	78.0	56.0	87.5
<i>Bison priscus</i> (Vasiliev, 2008)	Taradanovo, W1-2 (Russia)	Maximum	96.5	81.8	117
		SD			
		N	42	46	40

Table S7. Measurements (mm) and descriptive statistics of the humeri of *Bison schoetensoeki* from Vallparadis Estació (EVT) and Cal Guardiola (CGR) layers. Abbreviations: DDT, distal diaphysis thickness; DDW, distal diaphysis width; DEAW, distal epiphysis articular width; DEW, distal epiphysis width; DET, distal epiphysis thickness; L, left; OW, oleocranon fossa width; R, right; TCH, trochlea crest height; THl, lateral trochlear height; THm, medial trochlear height; TTm, trochlea thickness (medial epicondyle); TTI, trochlea thickness (lateral epicondyle); TWl, trochlear lateral articular width; TWm, trochlear medial articular width.

ID Specimen	Layer	Side	DDW	DDT	DEW	DEAW	OW	TWm	TWl	DET	TTm	TTI	THm	TCH	THI
IPSS0672	CGRD4	R	58.1	64.5	111.3	105.0	28.8	72.0	33.0	95.3	105.7	72.0	70.0	52.2	44.0
IPS92928	EVT7	R	50.0	56.2	100.0	92.3	34	65.3	27.0				57.8	49.5	41.3
IPS92929	EVT7	R	48.4				35.4								
IPS107620	EVT12	L	42.1	50.7	93.0	89.2	21.0	60.5	28.7			65.2	54.5	48.5	41.7
IPS114568	EVT7	R	60.1	65.8	98.1	95.3	37.5	68.8	26.5				57.0	53.4	43.2
IPS114549	EVT7	L	50.2	57.1	101.7	87.9		62.4	25.5				52.0	49.1	36
		Mean	51.5	58.9	100.8	93.9	31.3	65.8	28.1	95.3	105.7	68.6	58.3	50.6	41.3
		Minimum	42.1	50.7	93.0	87.9	21.0	60.5	25.5			65.2	52	48.5	36
		Maximum	60.1	65.8	111.2	105	37.5	72.0	33			72.0	70.0	53.4	44.1
		SD	6.6	6.3	6.7	6.8	6.6	4.7	23.0			4.8	7.0	2.1	3.1
		N	6	5	5	5	5	5	5	1	1	2	5	5	5

Table S8. Comparative measurements (mm) of the humerus in selected *Leptobos* and *Bison* s.l. samples. Abbreviations: DEAW, distal epiphysis articular width; DEW, distal epiphysis width; THl, lateral trochlear height; THm, medial trochlear height; TTI, trochlea thickness (lateral epicondyle); TTm, trochlea thickness (medial epicondyle); TWm, trochlear medial articulation width.

Taxon	Locality	Statistics	DEW	DEAW	TWm	TTm	TTI	THm	THl
<i>Leptobos etruscus</i> (Masini, 1989)	Matassino/Olivola (Italy)	Mean	88.0	79.7	55.6	83.6	57.7	52.3	39.3
		Minimum	82.9	64.5	53	68	48.6	43	33
		Maximum	91.5	85	58.6	88.7	63	55.8	42.4
		SD	2.8	4.5	1.6	5.8	3.6	3.2	2.9
<i>Bison (Bison) poloecsinensis</i> (Tong et al., 2016)	Shanshenmiaozui (China)	Mean	93.0	16	15	10	14	14	16
		N	1						
<i>Bison (Bison) georgicus</i> (Bukhianiidze, 2005)	Dmanisi (Georgia)	Mean	93.0	81.9	63.9	87.3	57.7	49.7	34.8
		Minimum	91.3	78.4	54.5	81.6	55.4	48.6	31.6
		Maximum	95.4	84.8	91.8	91.9	59.1	50.9	37.2
		SD	1.9	2.7	15.7	4.6	2.1	1.3	2.4
<i>Bison (Bison) degiulii</i> (Masini, 1989)	Pirro Nord (Italy)	Mean	80.0	75.5	5	4	3	4	4
		N	1	1					
<i>Bison menneri</i> (Sher, 1997)	Untermassfeld (Germany)	Mean	104.1	94.8			1	60.1	
		Minimum	90.0	85.0				52.0	
		Maximum	120	104.5				68.0	
		SD	8.6	6.0				4.6	
<i>Bison schoetensocki</i> (Moullé, 1992)	Le Vallonnet (France)	N	24	30				28	
		Mean		103.3					
		Minimum		92.0					
		Maximum		113.0					
<i>Bison schoetensocki</i> (This paper)	Vallparadis Composite Section (Spain)	SD		6.9					
		N		12					
		Mean	100.8	93.9	65.8	105.7	68.6	58.3	41.3
		Minimum	93.0	87.9	60.5		65.2	52.0	36
<i>Bison schoetensocki</i> (Sala, 1986)	Mauer (Germany)	Maximum	111.3	105.0	72.0		72.0	70.0	44
		SD	6.7	6.8	4.7		4.8	7.0	3.1
		N	5	5	5	1	2	5	5
		Mean		94.5					
<i>Bison schoetensocki</i> (Sala, 1986)	Isermia (Italy)	Minimum		93.0					
		Maximum		96.0					
		SD		2.1					
		N		2					
<i>Bison schoetensocki</i> (Sala, 1986)	Isermia (Italy)	Mean		105.2					
		Minimum		96.0					

<i>Bison aff. priscus</i> (Sher, 1997)	Tiraspol (Ukraine)	Maximum	108			
		SD	3.8			
		N	9			
		Mean	117.7	115.7		
		Minimum	114.0	111.5		
<i>Bison priscus</i> (Sher, 1997)	North-East Siberia (Russia)	Maximum	120.0	118.0		
		SD				
		N	3	3		
		Mean	112.5	100.4	63.5	
		Minimum	100.0	90.0	56.0	
<i>Bison priscus</i> (Vasiliev, 2008)	Krasny Yar, R-W (Russia)	Maximum	125.0	111.0	68.0	
		SD	9.3	7.2	4.0	
		N	15	15	15	
		Mean	119.7	108.9	79.6	118.1
		Minimum	99.3	94.0	68.7	102.3
<i>Bison priscus</i> (Sala, 1986)	Cava Filo (Italy)	Maximum	135.5	124.5	90	76.7
		SD				
		N	63	69	56	73
		Mean	118.3	107.3		
		Minimum	106.0	97.0		
<i>Bison priscus</i> (Castaños, 2012)	Kiputz IX (Spain)	Maximum	124.0	115.0		
		SD	8.3	7.8		
		N	4	4		
		Mean	107.4	99.7		
		Minimum	93.0	85.5		
<i>Bison bonasus</i> (Empel and Roskoz, 1963)	Warsaw (Czech Republic)	Maximum	115.0	111.5		
		SD	8.6	7.0		
		N	6	20		
		Mean		89.4		
		Minimum		81.0		
		101.0				
		SD	7.2			
		N	39			

Table S9. Stampfli's trochlea index for selected species of *Leptobos* and *Bison* s.l.

Taxon	Stampfli's trochlea index
<i>Leptobos etruscus</i> , Matassino/Olivola (Masini, 1989)	range: 28.4–35.4; mean = 31.4; N = 16
<i>Bison</i> (<i>Eobison</i>) <i>georgicus</i> , Dmanisi (Bukshianidze, 2005)	range: 29.6–31.3; mean = 30.6; N = 4
<i>Bison menneri</i> , Untermassfeld (Sher, 1997)	range: 28.7–34.4; mean = 31.5; N = 16
<i>Bison schoetensacki</i> , VCS (this paper)	range: 27.8–32.2; mean = 29.9; N = 5
<i>Bison</i> aff. <i>priscus</i> , Tiraspol (Sher, 1997)	mean = 27.8; N = 1
<i>Bison priscus</i> , Siberia (Sher, 1997)	range: 27.8–34.0; mean = 30.4; N = 15
<i>Bos primigenius</i> , Rhine Gravels (Martin, 1987)	range: 26.5–29.4; mean = 28.0; N = 10

Table S10. Lehmann trochlear index for selected species of bovids.

Taxon	Lehmann trochlear index
<i>Leptobos etruscus</i> , Matassino/Olivola (Masini, 1989)	range: 66.2–80.4; mean = 75.3; N = 15
<i>Bison (Eobison) georgicus</i> , Dmanisi (Bukshianidze, 2005)	range: 62.1–76.4; mean = 70; N = 4
<i>Bison menneri</i> , Untermassfeld (Sher, 1997)	range: 66.2–87; mean = 72.7; N = 24
<i>Bison schoetensacki</i> , VCS (this paper)	range: 62.9–76.5; mean = 71.2; N = 5
<i>Bison priscus</i> (Martin, 1987)	range: 63.4–72.4; mean = 67.1; N = 14
<i>Bos primigenius</i> (Martin, 1987)	range: 65.7–73.1; mean = 69.2; N = 10

Table S11. Measurements (mm) and descriptive statistics of the radii of *Bison schoetensacki* from Vallparadís Estació (EVT) and Cal Guardiola (CGR) layers.

Abbreviations: DEAT, distal end articular thickness; DEATmin, distal end articular thickness (not considering the distal end of ulna); DEAW, distal end articular width; DET, distal end maximum thickness; DEW, distal end width; DT, diaphysis thickness (midshaft); DTmin, diaphysis minimum thickness; DW, diaphysis width (midshaft); DWmin, diaphysis minimum width; L, left; Lmax, maximum length; PEAT, proximal end articular thickness; PEATl, lateral facet articular thickness (proximal end); PEAW, proximal end articular width ; PET, proximal end thickness; PEW, proximal end width; R, right.

ID Specimen	Layer	Side	Lmax	PEW	PEAW	PET	PEAT	PEATl	DWmin	DWm	DTmin	DTm	DEW	DEAW	DET	DEAT	DEATmin
IPS48775	CGRD2	R	380.0	107.6	99.1	54.8	47.2	30.7	59.8	63.9	37.7	38.6					
IPS39893a	CGRD2	R	384.5			63.0	53.0		62.0	62.9	38.1	38.9	102.7	97.0	69.2	66.1	44.2
IPS13570	CGRD2	R		107.9	100.7	52.4	47.2	29.7									
IPS92914	EVT7	L	363.7	102.9	91.9	49.5	42.2	29.8	56.6	58.0	28.0	30.5	94.5	92.5	46.0	44.5	33.5
IPS92915	EVT7	R		102.8	94.5	57.6	49.6	30.5	60.0		35.5						
IPS92916	EVT7	L											101.3	90.4	48.5	44.5	39.5
IPS92918	EVT7	L		99.9	91.8	50.9	47.5	28.4									
IPS92919	EVT7	R	339.1	96.2	86.9	46.5	41.0	25.5	49.8	50.6	27.5	32.8	89.0	78.1	61.4	51.0	36.6
IPS92920	EVT7	R		104.0	95.4	54.0	48.4	29.5	57.5	60.0	35.1	36.4					
IPS107617	EVT12	L	357.2	101.8	92.7	52.3	46.3	32.7	59.4	62.8	34.1	35.4	96.9	88.9	60.1	57.0	50.8
IPS107628	EVT12	R	376.9	106.4	99.5	53.9	47.2	34.0	55.3	60.4	35.3	36.5	97.5	90.8	67.3	56.7	47.9
IPS107616	EVT12	R	360.4	102.6	94.1	54.0	48.8	33.9	56.8	63.9	34.8	36.0	97.1	90.6	64.0	54.6	48.9
IPS118111	EVT12	R	383.0	110.1	97.6	55.1	46.9	36.8	63.1	64.2	36.0	40.8	102.8	88.3	77.0	63.0	54.0
	Mean		368.1	103.8	94.9	53.7	47.1	31.0	58.0	60.4	37.2	36.1	97.6	89.8	61.3	54.4	43.6
	Minimum		339.1	96.2	86.9	46.5	41.0	25.5	49.8	50.6	27.5	30.5	89.0	78.1	46.0	44.5	33.5
	Maximum		384.5	110.1	100.7	63	53	36.8	63.1	64.2	67.4	40.8	102.8	97.0	77.0	66.1	54.0
	SD		15.8	4.0	4.1	4.1	3.1	3.1	3.8	4.0	10.6	3.0	4.4	5.1	9.8	7.4	7.2
	N		8	11	11	12	12	11	10	11	11	10	9	9	9	9	9

Table S12. Comparative measurements (mm) of the radius of selected *Leptobos* and *Bison* s.l. samples. Abbreviations: DET, distal end maximum thickness; DW, diaphysis width (midshaft); Lmax, maximum length; PEAT, proximal end articular thickness; PEAW, proximal end articular width; PET, proximal end maximum thickness; PEW, proximal end maximum width.

Taxon	Locality	Statistics	Lmax	PEW	PEAW	PET	PEAT	DW	DEW	DET
<i>Leptobos etruscus</i> (Masini, 1989)	Matassino/Olivola (Italy)	Mean	297.4	84.7	77.5	41.6	43.5	47.3	76.7	53.0
		Minimum	273.0	77.2	70.0	39.2	39.2	42.0	66.2	47.0
		Maximum	308.5	92.6	83.2	48.0	48.0	53.6	84.7	56.9
		SD	16.5	4.9	4.0	10.6	3.1	4.3	5.4	3.4
		N	4	15	15	16	9	5	8	6
<i>Bison (Eobison) polbeosinensis</i> (Tong et al., 2016)	Shanshenmiaozui (China)	Mean	335	91.8	83.1				92.0	
		Minimum		84.0	75.0					
		Maximum		99.5	91.2					
		SD		11.0	11.5					
		N	1	2	2					1
<i>Bison (Eobison) georgicus</i> (Bukshianidze, 2005)	Dmanisi (Georgia)	Mean	302	91.7	81.6	48.5	43.0	51.8	81.6	59.0
		Minimum	300.0	90.1	79.8	47.6	40.7	50.7	80.2	62.9
		Maximum	304.0	93.3	82.6	49.6	44.3	52.7	82.9	62.9
		SD	1.9	2.7	15.7	1.2	4.6	2.1	1.3	2.4
		N	4	4	5	4	4	3	4	4
<i>Bison</i> sp. (Moyà-Solà, 1987)	Venta Micena (Spain)	Mean	277.0	71.6		37.2		42.2	63.3	43.0
		Minimum	267.8	65.2		34.5		42.0	57.0	40.2
		Maximum	282.6	76.3		40.3		42.4	69.2	48.0
		SD	8.0	4.2		2.0		0.2	4.5	3.0
		N	3	8		8		3	5	5
<i>Bison (Eobison) cf. degiulii</i> (Kostopoulos, 1997)	Mygdonia basin (Greece)	Mean	300.0	84.3		47.8		48.0	79.7	47.0
		Minimum		80.6		44.8		47.7		
		Maximum		88.0		50.8		48.3		
		SD								
		N	1	2	2	2	1	2	1	1
<i>Bison menneri</i> (Sher, 1997)	Untermassfeld (Germany)	Mean	384.5	104.3	94.9		49.1	57.6	98.8	
		Minimum	350.0	91.5	83.0		43.0	49.0	89.0	350.0
		Maximum	418.0	118.0	106.5		57.0	65.5	110.0	418.0

<i>Bison priscus</i> (Vasiliev, 2008)	Krasny Yar, R-W (Russia)	Maximum	393.0	120.5	107.5	58.5	63.5	111.0
		SD	20.2	6.8	5.2	4.0	5.0	8.7
		N	16	16	16	16	16	15
		Mean	389.9	115.9	107.1	60.3	66.1	110.6
		Minimum	343.0	100.0	94.0	50.0	51.8	93.2
		Maximum	427.0	142.0	130.0	71.5	86.0	132.5
<i>Bison priscus</i> (Vasiliev, 2008)	Taradanovo, W1-2 (Russia)	SD						
		N	40	61	62	49	40	46
		Mean	374.4	106.9	99.5	55.0	59.6	95.8
		Minimum	351.8	98.5	94.0	51.5	49.1	82.3
		Maximum	400.3	121.7	108.7	60.7	71	111.2
		SD						
<i>Bison priscus</i> (Vasiliev, 2008)	Krasny Yar, W2 (Russia)	SD						
		N	6	11	11	12	6	16
		Mean	366.0	107.8	100.3	56.6	55.6	90.9
		Minimum		126.4	116.5	65.0	58.5	98.0
		Maximum		94.0	86.0	48	50.7	84.0
		SD						
<i>Bison priscus</i> (Sala, 1986)	Cava Filo (Italy)	N	1	4	3	5	5	3
		Mean	389.0	107.2	100.7	51		
		Minimum	388.0	92.0	86.0	45		
		Maximum	390.0	125.0	114.0	56		
		SD	1.4	13.8	11.5	4.6		
		N	2	6	6	6		
<i>Bison priscus</i> (Castaños, 2014)	Kigutz IX (Spain)	Mean	363.3	106.7	99.0		53.6	94.4
		Minimum	327.0	96.5	91.0		47.0	77.0
		Maximum	405.0	117.5	110.0		61.5	114
		SD	23.1	6.6	5.7		4.4	8.3
		N	10	17	17		10	23
		Mean	343.4	92.3		46.9		82.4
<i>Bison bonasus</i> (Empel and Roskoz, 1963)	Warsaw (Czech Republic)	Minimum	291.0	80.0		42.0		71.0
		Maximum	392.0	111.0		54.0		100.0
		SD	21.8	8.2		3.3		7.8
		N	36	36		36		36

Table S13. Measurements (mm) and descriptive statistics of the ulnae of *Bison schoetensacki* from Vallparadis Estació (EVT) and Cal Guardiola (CGR) layers.

Abbreviations: AL, articular surface length; AT, articular surface thickness; L, left; Lmax, maximum length; OL, olecranon length; OTmin, olecranon minimum thickness; R, right; Wmax, maximum width (on the coronoid process).

ID Specimen	Layer	Side	Lmax	OL	OTmin	Wmax	AL	AT
IPS39893	CGR-D2	Right	482.4	150.3	81.6		52.7	31.1
IPS92921	EVT7	Right				57.5	51.3	30.1
IPS107616	EVT12	Right	469.6	135.2	78.8	57.5	49.39	31.6
IPS107617	EVT12	Left	470.7	133.4	77.6	55.1	50.9	30.3
IPS107628	EVT12	Right				60.8		
IPS118111	EVT12	Right				58	55	30
		Mean	474.2	139.6	79.3	57.8	51.8	30.6
		Minimum	469.6	133.4	77.6	55.1	49.4	30
		Maximum	482.4	150.3	81.6	60.8	55	31.6
		SD	5.8	7.6	1.7	1.8	1.9	0.7
		N	3	3	3	5	5	5

Table S14. Comparative measurements (mm) of the ulna in selected *Bison* s.l. Abbreviations: AL, articular surface length; AT, articular surface thickness; Lmax, maximum length; OL, olecranon length; OTmin, olecranon minimum thickness; PAT, processus anconaeus thickness; Wmax, maximum width (on the coronoid process).

Taxon	Locality	Statistics	Lmax	OL	OTmin	Wmax	AL	AT
<i>Bison</i> (<i>Eobison</i>) <i>polacostinensis</i> (Tong et al., 2016)	Shanshenmiaozui (China)	Mean	495.0	>104.0				
		N	1	11				
<i>Bison</i> (<i>Eobison</i>) <i>georgicus</i> (Bukhianidze, 2005)	Dmanisi (Georgia)	Mean	465	148.4	90.2	57.6		
		N	1	1				
<i>Bison menneri</i> (Sher, 1997)	Untermaßfeld (Germany)	Mean	420.0	133.0	84.0	53.0		
		Minimum	509.0	165.0	105.0	66.0		
		Maximum	32.2	12.4	6.7	3.7		
		SD	6	9	11	13		
<i>Bison schoetensodói</i> (This paper)	Vallparadis Composite Section (Spain)	Mean	474.2	139.6	79.3	57.8	51.8	30.6
		Minimum	469.6	133.4	77.6	55.1	49.4	30.0
		Maximum	482.4	150.3	81.6	60.8	55.0	31.6
		SD	5.8	7.6	1.7	1.8	1.9	0.7
<i>Bison aff. priscus</i> (Sher, 1997)	Tiraspol (Ukraine)	Mean	3	3	3	5	5	5
		N	196.0	126.0				
<i>Bison priscus</i> (Sher, 1997)	Taubach (Germany)	Mean		166.0	119.2	>70.0		
		Minimum		114.3				
		Maximum		124.0				
		SD		6.9				
<i>Bison priscus</i> (Sher, 1997)	North-East Siberia (Russia)	N	1	1	2	1		
		Mean	157.0	100.5	62.3			
		Minimum	138.0	80.5	55.5			
		Maximum	195.0	128.5	75.0			
<i>Bison priscus</i> (Vasiliev, 2008)	Krasny Yar, R-W (Russia)	SD	17.6	14.0	5.9			
		N	12	13	13			
		Mean	487.9	154.9	110.8			64.4
		Minimum	464	135.5	85.5			52.7
		Maximum	515.5	173.5	123.3			77
		SD						
		N	9	23	43			44

Table S15. Measurements (mm) of the carpals and tarsals of *Bison schoetensacki* from Vallparadís Estació (EVT) layers. Abbreviations: L, left; R, right; L, length; R, right; T, thickness; W, width.

ID Specimen	Layer	Element	Side	L	W	T
IPS92963	EVT10	Capitatotrapezoid	L	49.0	45.5	29.0
IPS91545	EVT7	Pyramidal	R	45.0	28.4	50.9
IPS92961	EVT10	Pyramidal	L	45.8	26.7	49.9
IPS92960	EVT10	Semilunar	L	32.9	39.0	48.2
IPS92962	EVT10	Unciform	L	30.6	38.2	39.2
IPS92964	EVT7	Unciform	L	27.4	32.9	37.3
IPS92957	EVT7	Cubonavicular	R	51.2	74.2	68.5
IPS92958	EVT3	Cubonavicular	R	45.0	73.6	68.0
IPS92965	EVT10	Cuneiform	R	20.0	27.4	40.0

Table S16. Comparative measurements (mm) of the metacarpal in selected *Leptobos* and *Bison* s.l. samples. Abbreviations: DET, distal epiphysis thickness; DEW, distal epiphysis width; DT, diaphysis thickness (midshaft); DW, diaphysis width (midshaft); L, left; Lmax, maximum length; PET, proximal epiphysis thickness; PEW, proximal epiphysis width; R, right.

Taxon	Locality	Measures	Lmax	PEW	PET	DW	DT	DEW	DET
<i>Leptobos etruscus</i> (Masini, 1989)	Senèze /Olivola (France/Italy)	Mean	250.5	62.4	40.6	38.9	27.8	63.1	34.6
		Minimum	242.0	55	36.7	32.7	21.5	55.3	29.7
		Maximum	265.5	66.8	42.8	43.7	31.5	67.3	37.2
		SD	5.8	3	1.7	3.5	2.5	3.2	1.9
		N	16	17	17	16	16	17	18
<i>Bison (Eobison) palaeosinensis</i> (Tong et al., 2016) (Masini, 1989)	Various localities of China	Mean	227.7	64.4	40.4	39.4	30.6	63.9	34.6
		Minimum	207.0	56.0	35.0			58.8	34.2
		Maximum	248.1	73.8	47.5			65.2	34.9
		SD	12.9	6.8	5.3			2.2	0.3
		N	7	7	3	1	1	6	3
<i>Bison (Eobison) georgicus</i> (Bukhianidze, 2005)	Dmanisi (Georgia)	Mean	244.2	66.9	42.1	39.8	29.2	65.5	35.0
		Minimum	231.3	62.8	37.7	34.3	25.8	61.0	33.2
		Maximum	256.6	70.5	45.4	44.4	31.6	72.0	36.9
		SD	10.3	3.1	2.8	4.2	2.5	4.0	1.6
		N	3	4	4	3	3	4	4
<i>Bison</i> sp. (Maniakas and Kostopoulos, 2017a)	Venta Micena (Spain)	Mean	225.6	58.5	36.6	35.3	26.9	60.1	33.0
		Minimum	208.2	52.3	32.8	31.4	24.1	53.5	30.0
		Maximum	248.7	69.5	46.5	44.2	32.1	69.1	36.3
		SD	10.0	4.6	3.3	3.6	2.1	4.7	1.6
		N	30	43	44	31	30	36	35
<i>Bison (Eobison) degiulii</i> (Masini, 1989)	Pirro Nord/Capena (Italy)	Mean	221.1	63.8	40.1	40.0	28.0	64.4	33.4
		Minimum	210.0	58.0	35.5	29.8	25.0	62.1	29.3
		Maximum	230.0	69.5	44.1	46.2	30.1	66.5	37.3
		SD	8.6	4.6	3.1	6.4	2.1	1.6	2.5
		N	5	7	6	4	4	6	7
<i>Bison (Eobison) cf. degiulii</i> (Kostopoulos et al., 2018)	Mygdonia basin (various localities) (Greece)	Mean	238.5	67.4	40.1	42.4	29.4	70.3	39.3
		Minimum	220.7	57.7	32.9	31.8	23.5	59.5	34.4
		Maximum	258.1	78.3	48.4	51.2	35.2	88.8	48.2
		SD	10.4	4.8	3.0	5.0	2.8	6.5	3.0
		N							

Bison menneri (Sher, 1997); Maniakas and Kostopoulos, 2017a)	Untermassfeld (Germany)	N	19	24	24	23	23	22	22
		Mean	276.5	77.0	46.5	44.8	32.8	75.6	38.2
		Minimum	255.8	64.4	39.3	35.3	27.8	65.4	29.5
		Maximum	296.0	91.4	52.6	57.7	39.0	86.0	47.3
		SD	10.1	5.6	3.2	4.6	3.0	6.2	5.8
		N	37	50	48	43	40	41	38
Bison schoetensocki (This paper)	Le Vallonnet (France)	Mean	261.7	82.3	48.9	53.6	35.6	75.2	42.0
		Minimum	245.0	74.7	45.0	43.0	31.0	66.2	37.5
		Maximum	271.0	89.0	51.5	64.0	42.0	83.7	46.5
		SD	9.2	5.3	2.3	6.9	3.8	6.4	2.5
		N	8	6	6	9	9	15	15
Bison schoetensocki (This paper)	Vallparadis Composite Section (Spain)	Mean	241.7	77.6	46.1	48.8	33.7	77.2	41.2
		Minimum	228.9	67.7	41.3	36.3	27.9	66.7	35.3
		Maximum	262.7	85.1	51.5	53.9	46.6	83.4	45.9
		SD	10.8	5	2.7	5.0	4.1	5.9	3.7
		N	11	18	17	15	15	10	10
Bison schoetensocki (Brugal, 1995)	Durfort (France)	Mean	247.2	77.1	46.2	47.7	32.4	77.2	41.9
		Minimum	239.0	69.2	41.3	42.4	28.7	67.5	38.0
		Maximum	250.0	81.3	50.0	53.0	35.0	82.3	43.4
		SD	3.9	5.2	3.5	4.3	2.6	6.1	2
		N	6	6	6	6	6	6	
Bison schoetensocki (Maniakas and Kostopoulos, 2017a)	Süsslenborn (Germany)	Mean	246.1	77.7	45.0	46.3	32.1	75.6	42.7
		Minimum	238.3	69.6	37.6	40.8	28.0	65.9	35.8
		Maximum	253.7	85.2	49.7	50.5	36.4	81.8	52.4
		SD	7.7	5.9	4.3	3.1	3.1	6.2	5.2
		N	5	10	10	9	9	7	6
Bison schoetensocki (Sala, 1987; this paper)	Cromer Forest-bed formation (Various localities (United Kingdom)	Mean	247.6	78.2	48.3			78.6	42.8
		Minimum	225.0	70.0	42.0			67.0	40.0
		Maximum	263.0	89.0	56.0			87.2	46.0
		SD	10.7	6.4	4.4			5.8	1.9
		N	11	11	8		12	7	7
Bison schoetensocki (Maniakas and Kostopoulos, 2017a)	Isernia La Pineta (Italy)	Mean			52.2			80	43.3
		Minimum			52.2			79.2	43.2
		Maximum			52.2			80.8	43.4
		SD						0.8	0.1
		N		1			2	2	
Bison schoetensocki (Schertz, 1936b; this paper)	Mauer (Germany)	Mean	265.4	83.7	49.0	49.2	33.5	79.1	42.9
		Minimum	250.4	71.8	43.5	46.7	30.3	70.7	36.8

<i>Bison cf. schoetensocki</i> (Schertz, 1936b; this paper)	Maximum	277.0	93.0	53.0	55.5	37.0	88.5	50.0
	SD	8.5	6.4	3.3	3.2	3.0	6.7	5.1
	N	12	10	9	6	6	11	6
Mosbach (Germany)	Mean	256	84.5	48.9	49.9	32.6	42.4	33.2
	Minimum	241.1	72.0	43.4	43.3	30.2	40.1	30.3
	Maximum	277.8	97.3	56.4	55.1	35.1	46.0	36.3
	SD	11.3	6.9	3.3	5.2	2.5	2.1	3.0
	N	22	18	19	4	4	6	3
	Mean	265.1	92.6	54.1	58.2	36.7	93.9	47.5
<i>Bison aff. priscus</i> (Sher, 1997)	Minimum	252.7	80.5	49.0	46.6	33.7	81.0	43.5
	Maximum	276.0	10.0	64.0	67.6	38.7	99.0	51.6
	SD	6.4	6.2	4.1	5.7	1.9	5.3	4.0
Tiraspol (Ukraine)	N	9	11	11	8	8	8	7
	Mean	270.9	89.0	56.2	54.4	37.0	90.1	47.4
	Minimum	251.4	71.4	47.4	42.3	30.6	78.3	41.8
<i>Bison priscus</i> (Maniakas and Kostopoulos, 2017a)	Maximum	286.5	100.9	62.9	61.6	42.0	98.1	51.4
	SD	10.6	8.9	5.1	6.6	3.6	6.9	3.2
	N	8	8	8	8	8	10	10
<i>Bison priscus</i> (This paper)	Mean	248.8	87.6	52.4	55.9	36.2	85.8	45.7
	Minimum	232	75.5	44	45	31	75.5	37
	Maximum	263	102	63	63	42	97	51.5
Châtillon-Saint-Jean (France)	SD	7	8.3	5.2	6.3	3.5	8.4	3.1
	N	26	26	26	26	26	7	26
	Mean	257.4	87.8	51.1	57.0	36.0	86.5	45.5
<i>Bison priscus</i> (Vercoûtère and Guérin, 2010)	Minimum	238.5	80.5	50.0	53.5	33.0	80.5	44.0
	Maximum	279	95.0	52.5	59.5	42.5	90.0	47.0
	SD	15.4	4.9	1.1	2.2	3.8	2.9	1.1
Cava Filo (Italy)	N	6	5	4	4	4	6	4
	Mean	240.7	84.1	47.5			91.0	47.8
	Minimum	232.0	79.0	43.0			80.0	44.0
North Sea seabed	Maximum	260.0	93.0	50.0			99.0	53.0
	SD	10.0	4.6	2.4			5.9	2.8
	N	6	6	6			6	6
<i>Bison priscus</i> (Sala, 1986)	Mean	238.2	82.3	48.2	50.7	34.0	83.8	44.0
	Minimum	226.0	72.0	43.0	41.0	30.0	75.0	40.0
	Maximum	248.0	96.0	55.0	59.0	40.0	95.0	48.0
<i>Bison priscus</i> (Drees, 2005)	SD	6.3	6.7	3.2	6.3	29.0	6.7	2.2
	N	15	15	15	15	15	15	15

<i>Bison priscus</i> (Sher, 1997)	North-East Siberia (Russia)	Mean	222.1	80.3	45.8	49.1	32.5	82.8
		Minimum	206.0	68.5	39.0	38.7	28.0	71.0
		Maximum	235.0	90.5	51.5	62.0	37.0	95.0
		SD	8.5	6.5	3.5	6.2	2.7	6.8
		N	29	29	29	29	29	29
<i>Bison priscus</i> (Maniakas and Kostopoulos, 2017a)	Various localities of England (United Kingdom)	Mean	225.8	81.9	46.3	50.8	33.0	79.2
		Minimum	209.7	69.4	40.8	43.2	27.6	69
		Maximum	241.3	90.8	52.8	56.2	36.6	88.2
		SD	9.3	7.0	3.5	4.4	3.1	6.4
		N	9	9	9	9	9	9
<i>Bison priscus</i> (Vasiliev, 2008)	Krasny Yar, R-W (Russia)	Mean	240.5	85.5	49.6	53.0	34.4	87.1
		Minimum	215.2	71.5	40.8	42.0	28.5	73.7
		Maximum	280.0	98.0	59.0	63.0	43.0	99.0
		SD						
		N	64	68	69	69	70	63
<i>Bison priscus priscus</i> (Vasiliev, 2008)	Taradanovo, W1-2 (Russia)	Mean	236.0	89.0	46.4	48.1	32.1	44.5
		Minimum	220.3	69.8	38.3	40.2	28.5	72.2
		Maximum	254.5	95.4	55.6	61.5	40.7	93.0
		SD						
		N	31	34	34	36	36	40
<i>Bison priscus</i> (Vasiliev, 2008)	Chumysh, Q3 (Russia)	Mean	237.9	84.0	48.8	52.6	34.0	85.7
		Minimum	218.0	71.3	40.7	41.2	28.8	71.2
		Maximum	260.6	99.0	58.8	65.0	39.8	99.6
		SD						
		N	57	52	51	56	55	57
<i>Bison priscus</i> (Vasiliev, 2008)	Krasny Yar, W2 (Russia)	Mean	237.4	83.0	47.4	50.9	33.3	83.8
		Minimum	226.5	73.0	42.6	41.0	29.3	72.0
		Maximum	246.0	95.0	53.0	60.8	36.8	94.0
		SD						
		N	8	10	8	9	10	8
<i>B. priscus</i> (Vasiliev 2008)	Kurtak, Q3 (Russia)	Mean	236.8	84.6	48.7	52.2	33.7	85.4
		Minimum	213.4	73.4	40	41.2	26.8	74.0
		Maximum	251	101.5	60	65.1	39.5	104.4
		SD						
		N	63	65	65	70	70	75
<i>Bison priscus</i> (Bibikova, 1950)	Ukraine, Q3 (Ukraine)	Mean	228.6	78.3	46.0	47.7	31.5	81.3
		Minimum	206.2	69.5	40.2	40.7	27.7	71.5
		Maximum	245.4	90.4	52.6	57.8	36.8	98.1
		SD						
		N	62	62	62	62	62	62

<i>Bison</i> sp. (This paper)	Siréjol cave (France)	SD	78	73	74	75	75	67	64
		N	223.2	73.6	44.3	43.4	30.1	75.3	40
		Mean	210.5	64.2	39.5	36	25.8	69	37.7
		Minimum	231	86	51.4	47	32.5	80.8	43.2
		Maximum	5.8	5.7	3.7	3.1	2	4.1	1.8
<i>Bison priscus</i> (Castaños et al., 2012)	Kiputz IX (Spain)	N	15	14	15	15	15	15	14
		Mean	236.9	80.7		48.9		87.9	46.4
		Minimum	217.0	60.0		39.5		78.0	41.5
		Maximum	254.0	96.5		57.0		101.5	52.0
		SD	11.9	7.9		5.2		7.5	3.1
<i>Bison bonasus</i> (Reshetov and Sukhanov, 1979)	Unknown	N	14	22	14	14		14	14
		Mean	210.0	70.5	41.4	39.5	25.9	66.5	38.2
		Minimum	201.0	62.0	37.3	32.0		60.0	34.6
		Maximum	225.0	79.0	45.8	49.0		75.0	42.4
		SD							
<i>Bos primigenius</i> (Brugal, 1985)	Lunel Viel (France)	N	35	35	35	35	35	35	35
		Mean	254.4	82.5	50.5	52.0	36.2	84.5	45.1
		Minimum	241.1	69.6	41.7	40.0	29.5	70.7	38.9
		Maximum	271.5	95.2	59.3	66.0	42.2	99.2	52.2
		SD							
N	60	71	71	60	60	57	54		

Table S17. Ratio (%) between distal diaphysis width (DDW) and distal maximum width (DEW) in metacarpals of various species of bovids.

Taxon	DDW/DEW*100
<i>Leptobos etruscus</i> , Olivola/ Senèze (Masini, 1989)	range: 89.2–98.3; mean = 95; N = 17
<i>Bison</i> (Eobison) <i>georgicus</i> , Dmanisi (Bukshianidze, 2005)	range: 94.0–103.4; mean = 98.7; N = 4
<i>Bison</i> sp., Venta Micena (Maniakas and Kostopoulos, 2017a)	range: 92.5–101.5; mean = 97; N = 32
<i>Bison</i> (Eobison) <i>degiulii</i> , Piro Nord/Capena (Masini, 1989)	range: 98.2–101.7; mean = 99.7; N = 3
<i>Bison</i> (Eobison) cf. <i>degiulii</i> , Mygdonia Basin (Kostopoulos et al., 2018)	range: 92.2–99.9; mean = 96.2; N = 21
<i>Bison menneri</i> , Untermassfeld (Sher, 1997)	range: 92.8–102.7; mean = 98.8; N = 21
<i>Bison schoetensacki</i> , Vallparadis Composite Section (This paper)	range: 91.5–97.5; mean = 94.8; N = 8
<i>Bison schoetensacki</i> , Süssenborn (Maniakas and Kostopoulos, 2017a)	range: 93.6–99.8; mean = 96.9; N = 6
<i>Bison schoetensacki</i> , Dürfort (Brugal, 1995)	range: 94.7–98.7; mean = 95.8; N = 6
<i>Bison priscus</i> , Romain-la-Roche (Vercoutère and Guérin, 2010)	range: 93.3–98.9; mean = 95.3; N = 4
<i>Bison priscus</i> , Taubach (Sher, 1997)	range: 89.3–98.5; mean = 93.9; N = 9
<i>Bison priscus</i> , UK (Maniakas and Kostopoulos, 2017a)	range: 98.1–102.6; mean = 99.4; N = 8
<i>Bos primigenius</i> Romain-la-Roche (Vercoutère and Guérin, 2010)	range: 87.8–101.4; mean = 93.6; N = 9
<i>Bos primigenius</i> Lunel Viel (Brugal, 1985)	mean = 92.4; N: 57

Table S18. Ratio (%) between width of the lateral facet (PFWl) and width of the medial facet (PFWm) of the proximal epiphysis in metacarpals of various species of bovids.

Taxon	PFWl/ PFWm*100
<i>Leptobos etruscus</i> Olivola/Senèze (Masini, 1989)	range: 71.6–98; mean = 81.3; N = 18
<i>Bison (Eobison) palaeosinensis</i> China (Masini, 1989)	mean = 86.5; N = 1
<i>Bison (Eobison) georgicus</i> , Dmanisi (Bukshianidze, 2005)	range :67.3–75; mean = 71.1; N = 4
<i>Bison</i> sp., Venta Micena (Masini, 1989)	range:67.7–70.2; mean = 68.9; N = 2
<i>Bison (Eobison) degiulii</i> , Pirro Nord/Capena (Masini, 1989)	range:68.5–74.8; mean = 72.3; N = 4
<i>Bison menneri</i> , Untermassfeld (Sher, 1997)	mean = 72.3; N = 24
<i>Bison schoetensacki</i> , Vallparadis Composite Section (This paper)	range: 62.3–82.9; mean = 71.4; N = 16
<i>Bison priscus</i> , Ukraine/Germany (Sher, 1997)	mean = 69.7; N = 18
<i>Bos primigenius</i> Ukraine/Germany (Sher, 1997)	mean = 69; N = 21

Table S19. Principal component analysis of metacarpals using seven selected variables (see Section 3 and Fig. 10). Eigenvalue and % variance of the PCs and coefficient of each variables for each PC. Abbreviations as in Table 4.

	PC 1	PC 2	PC 3	PC 4	PC 5	PC 6	PC 7
Eigenvalue	0.00258538	0.000585286	0.000427393	0.000408312	0.000188404	0.000116617	8.56E-16
% variance	59.966	13.575	99.131	94.705	43.699	27.049	1.98E-11
mv Lmax	-0.83086	-0.17921	-0.27416	0.14799	-0.19284	0.021075	0.37796
mv PET	-0.0095925	0.29015	0.37141	0.62507	0.4779	0.12578	0.37796
mv PEW	0.21969	0.26208	0.10576	0.1438	-0.55811	-0.62996	0.37796
mv DT	-0.0059032	-0.53122	0.64735	-0.39292	0.036922	-0.010008	0.37796
mv DW	0.45535	-0.52992	-0.53669	0.20786	0.18901	-0.044997	0.37796
mv DETI	-0.054462	0.43139	-0.25535	-0.59101	0.46217	-0.19998	0.37796
mv DEW	0.22578	0.25673	-0.058324	-0.1408	-0.41504	0.73809	0.37796

Table S20. Principal component analysis of metacarpals following Scott and Barr (2004) (see Section 3 and Fig. 10). Eigenvalue and % variance of the PCs and coefficient of each variables for each PC. Abbreviations as in Table 4.

	PC 1	PC 2	PC 3	PC 4	PC 5	PC 6	PC 7	PC 8
Eigenvalue	0.00275304	0.000667232	0.000518681	0.000387236	0.000199621	7.89E+00	5.73E+00	4.76E+00
% variance	58.456	14.167	11.013	82.222	42.386	16.745	12.174	10.108
re Lmax	0.81739	0.36269	-0.083492	0.36791	-0.22368	0.061456	0.015739	0.06288
re DW	-0.44093	0.38381	0.072559	0.73961	0.26044	0.13508	0.13271	0.048037
re DT	0.043998	0.61013	0.44117	-0.50562	0.25478	0.14236	0.25699	0.15587
re DETI	0.2263	-0.33029	0.32148	0.13645	0.2538	-0.13944	0.60295	-0.51992
re DETm	0.18711	-0.48411	0.30725	0.13375	0.27791	0.31828	-0.001039	0.66317
re DEW	-0.09344	0.026324	-0.041165	0.039192	-0.24246	-0.70443	0.43037	0.49711
re PEW	-0.15322	-0.058333	-0.26866	-0.081916	-0.47145	0.58365	0.57248	0.059988
re PET	0.13075	0.036564	-0.72215	-0.13122	0.62812	-0.010199	0.19897	0.092827

Table S21. Pairwise comparison results based on MANOVA ($p < 0.05$) for seven raw selected variables of metacarpals of several *Bison* s.l. and *Leptobos etruscus* samples. *Leptobos etruscus*: samples from Olivola and Senèze; *B. (Eobison) sp.*: sample from Venta Micena; *B. (Eobison) cf. degiulii*: sample from Mygdonia Basin; *B. menneri*: sample from Untermassfeld; *B. schoetensacki*: samples from Le Vallonnet, Durfort, Süßenborn, Mauer; *B. priscus priscus*: samples from Taubach, Châtillon-Saint-Jean, Romain-la-Roche; *B. priscus mediator*: samples from UK (several sites, see Fig. 9), North Sea seabed. Abbreviations are given in Table 4. Values of $p < 0.05$ are in bold.

	<i>Eobison</i> sp.	<i>Eobison</i> cf. <i>degiulii</i>	<i>Bison menneri</i>	<i>Bison schoetensacki</i>	VCS	<i>Bison priscus priscus</i>	<i>Bison priscus mediator</i>
<i>Leptobos etruscus</i>	<0.001	<0.001	<0.001	<0.001	<0.001	<0.001	<0.001
<i>Eobison</i> sp.		<0.001	<0.001	<0.001	<0.001	<0.001	<0.001
<i>Eobison</i> cf. <i>degiulii</i>			<0.001	0.001	0.045	<0.001	<0.001
<i>Bison menneri</i>				<0.001	<0.001	<0.001	<0.001
<i>Bison schoetensacki</i>					0.075	<0.001	<0.001
VCS						0.03	0.011
<i>Bison priscus priscus</i>							<0.001

Table S22. Measurements (mm) and descriptive statistics of the tibiae of *Bison schoetensacki* from Vallparadis Estació (EVT) and Cal Guardiola (CGR) layers. Abbreviations: DEAAW, distal epiphysis astragalus articulation width; DEAT, distal epiphysis articulation thickness; DEAW, distal epiphysis articular width; DET, distal epiphysis thickness; DEW, distal epiphysis width; DTmin, minimum diaphysis thickness; DWmin, minimum diaphysis width; L, left; MFT, malleolar facet thickness; MFW, malleolar facet width; R, right.

ID Specimen	Layer	Side	DWmin	DTmin	DEW	DEAW	DEAAW	DET	DEAT	MFW	MFT
IPS107618	CGRD2	R	56.7	39.2	89.6	78.6	58.7	60.9	53.4	19.3	
IPS92940	EVT7	R			74.4	68.9	54.2	51.9	45.3	13.5	34.8
IPS92942	EVT7	R	54.0	40.4	81.7	74.9	57.2	59.4	51.7	16.8	34
IPS92943	EVT7	L	46.5	33.4	69.3	61.5	50.2	50.6	44.6	11.0	24.5
IPS114546	EVT12	R			92.3	80.6	58.0	69.9	60.5	18.7	41.8
		Mean	52.4	37.7	81.5	72.9	55.7	58.5	51.1	15.8	33.8
		Minimum	46.5	33.4	69.3	61.5	50.2	50.6	44.6	11.0	24.5
		Maximum	56.7	40.4	92.3	80.6	58.7	69.9	60.5	19.3	41.8
		SD	5.3	3.7	9.8	7.8	3.5	7.8	6.5	3.5	7.1
		N	3	3	5	5	5	5	5	5	4

Table S23. Comparative measurements (mm) of the tibia in selected *Leptobos* and *Bison* s.l. samples. Abbreviations: DET, distal epiphysis thickness; DEW, distal epiphysis width; DTmin, minimum diaphysis thickness; DWmin, minimum diaphysis width.

Taxon	Locality	Measures	DWmin	DTmin	DEW	DET
<i>Leptobos etruscus</i> (Duvernois and Guérin, 1989)	Senèze (France)	Mean	46.8	34.3	68.0	57.0
		Minimum	44.5	33.0	61.0	56.0
		Maximum	48.5	36.5	72.0	57.0
		SD	1.8	1.7	6.1	
<i>Bison (Eobison) polibosinensis</i> (Tong et al., 2016)	Various localities of China	N	4	4	3	2
		Mean	47.8		73.8	56.0
		Minimum	45.0		70.0	53.0
		Maximum	51.0		78.0	58.0
<i>Bison (Eobison) georgicus</i> (Bukshianidze, 2005)	Dmanisi (Georgia)	SD	3.2		3.9	2.5
		N	4		4	4
		Mean			71.2	55.1
		Minimum			70.2	54.7
<i>Bison</i> sp. (Maniakas and Kostopoulos, 2017a)	Venta Micena (Spain)	Maximum			72.3	55.6
		SD			1.6	0.6
		N			2	2
		Mean			60.7	46.1
<i>Bison menneri</i> (Sier, 1997)	Untermassfeld (Germany)	Minimum			60	41.2
		Maximum			62.2	51.7
		SD			1	4.4
		N			4	4
<i>Bison schoetensocki</i> (Moullé, 1992)	Le Vallonnet (France)	Mean			84.0	62.0
		Minimum			74.0	55.0
		Maximum			94.0	67.0
		SD			5.4	3.5
<i>Bison schoetensocki</i> (This paper)	Vallparadis Composite Section (Spain)	N			23	23
		Mean	56.9		82.9	62.2
		Minimum	51.0		76.3	57.2
		Maximum	68.0		89.8	64.4
<i>Bison schoetensocki</i> (This paper)	Durfort (France)	SD	7.6		5.8	3.3
		N	4		4	4
		Mean	52.4		81.5	58.5
		Minimum	46.5		69.3	50.6
<i>Bison schoetensocki</i> (This paper)	Durfort (France)	Maximum	56.7		92.3	69.9
		SD	5.3		9.8	7.8
		N	3		3	5
		Mean			82.7	67.4

(Brugal, 1995)		Minimum Maximum SD N	81.4 84.0 1.8 2	66.7 68.0 0.9 2
<i>Bison schoetensacki</i> (Sala, 1986)	Isernia la Pineta (Italy)	Mean Minimum Maximum SD N	86.9 79.0 91.0 5.4 4	63.3 57.0 67.0 4.4 4
<i>Bison</i> spp. (Sier, 1997)	Mauer (Germany)	Mean Minimum Maximum SD N	56.9 53.0 60.5 5.3 2	61.9 56.0 64.0 2.5 7
<i>Bison</i> aff. <i>priscus</i> (Sier, 1997)	Tiraspol (Ukraine)	Mean Minimum Maximum SD N	92.8 89.0 94.0 2.2 4	69.5 64.0 73.0 3.4 4
<i>Bison priscus</i> (Sala, 1986)	Cava Filo (Italy)	Mean Minimum Maximum SD N	54.5 46.0 62.0 5.7 6	59.3 56.0 64.5 3.5 5
<i>Bison priscus</i> (Vasiliev, 2008)	Krasny Yar, R-W (Russia)	Mean Minimum Maximum SD N	43.5 36.3 54.5 70 42.6	65.0 56.5 75.4 87 63.9
<i>Bison priscus priscus</i> (Vasiliev, 2008)	Taradanovo, W1-2 (Russia)	Mean Minimum Maximum SD N	38.0 45.7 94.6 12 31	69.0 58.0 27

Table S24. Measurements (mm) and descriptive statistics of the astragali of *Bison schoetensacki* from Vallparadis Estació (EVT) and Cal Guardiola (CGR) layers. Abbreviations: DTW, distal trochleae width; LI, lateral length; Lm, medial length; Lmin, minimum length; PTW, proximal trochleae width; TI, lateral thickness; Tm, medial thickness; TTW, intertrochlear width.

ID Specimen	Layer	Side	LI	Lm	Lmin	TI	Tm	PTW	TTW	DTW
IPS39141	CGRD7	R	90.1	83.4	71.5	45.6	50.8	60	48.4	60.1
IPS92949	EVT7	R	84.4	77.2	66.0	46.0	42.7	49.4	44.2	52.1
IPS92950	EVT7	R	78.9	73.1	60.8	43.3	42.1	45.6	42.9	51.5
IPS92951	EVT7	R	81.9	76.6	64.5	44.5	44.0	45.5	49.0	52.8
IPS92952	EVT7	R	82.4	74.1	63.1	44.6	48.1	51.8	50.1	55.0
IPS92953	EVT12	L	90.9	80.8	68.7	48.3	51.0	54.8	54.9	61.0
IPS118120b	EVT12	L	85.2	76.8	67.0	45.6	48.3	56.8	50.8	56.9
		Mean	84.8	77.4	65.9	45.8	46.3	52.0	48.6	55.6
		Minimum	78.9	73.1	60.8	43.3	42.1	45.5	42.9	51.5
		Maximum	90.9	83.4	71.5	48.3	51.0	60.0	54.9	61.0
		SD	4.4	3.6	3.6	1.9	3.7	5.5	4.0	3.8
		N	7	7	7	7	7	7	7	7

Table S25. Comparative measurements (mm) of the astragalus in selected *Leptobos* and *Bison* s.l. samples. Abbreviations: DTW, distal trochleae width; U, lateral length; Lm, medial length; PTW, proximal trochleae width; TI, lateral thickness.

Taxon	Measures	U	Lm	TI	PTW	DTW
<i>Leptobos etruscus</i> (Masini, 1989)	Mean	71.5	39.2	38.2	43.6	46.2
	Minimum	67.2	35.0	35.0	39.7	42.0
	Maximum	76.7	43.7	42.0	48.0	52.0
	SD	2.9	2.5	2.3	2.3	3.2
	N	18	18	18	18	18
<i>Bison (Eobison) palaeosinensis</i> (Tong et al., 2016)	Mean	78.0				50.7
	Minimum	74.0				46.0
	Maximum	80.0				53.0
	SD	3.5				4.0
	N	3				3
<i>Bison (Eobison) georgicus</i> (Bukshianidze, 2005)	Mean	78.9			50.3	52.5
	N	1			1	1
	Mean	71.5				47.2
	Minimum	66.6				40.0
	Maximum	77.0				53.7
<i>Bison sp.</i> (Moyà-Solà, 1987)	SD	3.5				3.6
	N	15				17
	Mean	73.4	42.1	40.6	46.8	48.7
	Minimum	67.1	39	36.7	41.3	44.3
	Maximum	79.8	46.8	44.0	49.7	53.3
<i>Bison (Eobison) degiulii</i> (Masini, 1989)	SD	4.1	2.2	2.2	2.7	3.1
	N	10	10	10	9	10
	Mean	79.1				52.6
	Minimum	73.5				46.4
	Maximum	87.1				60.3
<i>Bison (Eobison) cf. degiulii</i> (Croitor, 2016)	SD	4.7				4.2
	N	8				8
	Mean	85.8			57.6	56.2
	Minimum	78.5			52.0	50.5
	Maximum	95.5			66.0	64.4
<i>Bison menneri</i> (Sher, 1997)	SD	4.1			3.7	3.8
	N	33			34	35

<i>Bison schoetensacki</i> (Moullé, 1992)	Le Vallonnet (France)	Mean	86.7	49	48.2	60.1
		Minimum	83.7	46.5	46.5	56.8
		Maximum	90.0	51.9	52.1	65.4
		SD	2.1	2.1	1.7	2.9
<i>Bison schoetensacki</i> (This paper)	Vallparadis Composite Section (Spain)	N	6	6	8	7
		Mean	84.8	77.4	45.8	55.6
		Minimum	78.9	73.1	43.3	45.4
		Maximum	90.9	83.4	48.3	60.0
<i>Bison schoetensacki</i> (Brugal, 1995)	Durfort (France)	SD	4.4	3.6	1.9	5.5
		N	7	7	7	7
		Mean	83.1	46.5	45.4	55.4
		Minimum	69.8	41.2	39.0	48.5
<i>Bison schoetensacki</i> (Maniakas and Kostopoulos, 2017)	Isernia la Pineta (Italy)	Maximum	89.6	49.0	48.5	60.0
		SD	7.4	2.9	3.4	4.3
		N	6	6	6	6
		Mean	92.3	52.6	51.6	60.5
<i>Bison schoetensacki</i> (Sher, 1997)	Mauer (Germany)	Minimum	87.7	49.0	49.6	54.2
		Maximum	99.5	56.5	54.8	65.5
		SD	3.3	2.6	1.7	3.3
		N	11	6	7	12
<i>Bison cf. schoetensacki</i> (Sher, 1997)	Mosbach (Germany)	Mean	91.0	48.6	49.7	60.0
		Minimum	85.0	34.0	43.0	55.0
		Maximum	100.0	55.0	53.5	65.0
		SD	4.4	5.3	3.3	3.3
<i>Bison aff. priscus</i> (Sher, 1997)	Tiraspol (Ukraine)	N	14	14	15	15
		Mean	94.2	51.3	51.6	60.0
		Minimum	88.5	47.0	49.0	53.0
		Maximum	99.5	57.0	55.5	66.0
<i>Bison priscus</i> (Vercoutère and Guérin, 2010)	Romain-la-Roche (France)	SD	5.0	4.4	2.5	5.7
		N	5	4	5	5
		Mean	97.8			62.8
		Minimum	92.8			59.8
<i>Bison priscus</i> (Vercoutère and Guérin, 2010)	Romain-la-Roche (France)	Maximum	105.3			66.0
		SD	6.6			3.1
		N	3			3
		Mean	94.1	54.9	53.1	60.8
<i>Bison priscus</i> (Vercoutère and Guérin, 2010)	Romain-la-Roche (France)	Minimum	91.0	52.5	51.0	57.0
		Maximum	91.0	52.5	51.0	57.0

<i>Bison priscus</i> (Sala, 1986)	Cava Filo (Italy)	Maximum	100.0	57.0	57.0	66.0	69.5
		SD	3.1	1.6	1.7	2.3	3.1
		N	12	12	12	12	12
	Krasny Yar, R-W (Russia)	Mean	88.5	49.8	49.8		58.5
		Minimum	86.0	46	47.8		52.0
		Maximum	90.7	52	51.2		62.6
		SD	2.4	3.3	1.8		5.7
		N	3	3	3		3
		Mean	91.5	52	51.7		60.5
	Taradanovo, W1-2 (Russia)	Minimum	82.0	46.5	46.0		53.2
		Maximum	102.5	58.0	56.7		67.3
		SD					
N		68	60	67		69	
Mean		88.5	49.6	48.9		57.0	
Minimum		76.2	42.5	41.7		47.5	
<i>Bison bonasus</i> (Empel and Roskoz, 1963)	Warsaw (Polonia)	Maximum	104	55.3	57.7		63.6
		SD					
		N	139	95	134		125
	Warsaw (Polonia)	Mean	77.0	45.1			54.4
		Minimum	67.0	38.0			47.0
		Maximum	87.0	51.0			63.0
SD	4.7	3.3			3.5		
N	39	39			39		

Table S26. Measurements (mm) and descriptive statistics of the calcanei of *Bison schoetensacki* from Vallparadis Estació (EVT) and Cal Guardiola (CGR) layers. Abbreviations: Lmax, maximum length; BLm, minimum length (medial view); BLP, calcaneum body length (posterior view); CBHmin, calcaneum body minimum height; CBWmin, calcaneum body minimum width; Hmax, maximum height; HST, height at sustentaculum tali level; HTC, height of tuber calcanei; L, left; MFL, malleolar facet length; MFW, malleolar facet width; NCFL, cubonavicular articular facet length; R, right; STT, sustentaculum tali thickness; Wmax, maximum width; WTC, width of tuber calcanei.

ID Specimen	Layer	Side	Lmax	BLP	BLm	Hmax	Wmax	HST	STT	HTC	WTC	MFL	MFW	NCFL	CBWmin	CBHmin
IPS13936	CGR-D2	R	189.4	139.1	110.3	72.5	60.0	69.9	33.0	52.2	46.9	34.5	21.1	48.9	25.4	50.1
IPS92944	EVT7	R	166.6	125.4	102.9	66.7	58.0	58.3	35.6	52.1	40.4	32.0	19.0	48.0	26.0	44.8
IPS92945	EVT7	R	160.8	115.3	92.7	68.5	51.2	61.9	33.7	49.2	38.3	32.9	17.7	48.0	21.6	46.3
IPS92946	EVT7	R	174.4	126.3	102.2	69.9	52.0	63.1	33.0	51.6	43.4	31.0	16.0	49.3	31.3	46.4
IPS92947	EVT7	R	169.6	123.6	100.5	73.5	59.0	62.9	35.7	47.3	43.7	32.4	20.1	46.7	26.6	47.2
IPS92948	EVT7	L	177.6	129.1	103.8	70.8	55.0	64.0	33.0	53.2	45.6	32.8	19.6	50.5	28.7	47.4
IPS-118120	EVT12	R	170.8	131.0	102.1	69.3	58.7		34.9	50.6	44.0	32.7	18.8	48.5	25.3	45.0
		Mean	172.7	127.1	102.1	70.2	56.3	63.4	34.1	50.9	43.2	32.6	18.9	48.5	26.4	46.8
		Minimum	160.8	115.3	92.7	66.7	51.2	58.3	33.0	47.3	38.3	31	16	46.7	21.6	44.8
		Maximum	189.4	139.1	110.3	73.5	60.0	69.9	35.7	53.2	46.9	34.5	21.1	50.5	31.3	50.1
SD			9.1	7.3	5.2	2.3	3.5	3.8	1.2	2.1	3.0	1.1	1.7	1.2	3.0	1.8
N			7	7	7	7	7	6	7	7	7	7	7	7	7	7

Table S27. Comparative measurements (mm) of the calcaneus in selected *Leptobos* and *Bison* s.l. samples. Abbreviations: BLP, calcaneum body length (posterior view); Hmax, maximum height; HTC, height of tuber calcanei; Lmax, maximum length; Wmax, maximum width; WTC, width of tuber calcanei.

Taxon	Locality	Measures	Lmax	BLP	Hmax	Wmax	HTC	WTC
<i>Leptobos etruscus</i> (Masini, 1989)	Olivola (Italy)	Mean	149.7	104.9	58.9	51.1	43.5	38.2
		Minimum	134.0	100.0	54.7	43.2	39.0	34.0
		Maximum	159.1	123.5	62.2	59.0	47.0	42.1
		SD	9.3	7.3	2.4	4.2	2.9	2.6
		N	10	14	11	13	12	12
<i>Bison (Eobison) palaeosinensis</i> (Tong et al., 2016)	Various localities of China	Mean	146.3			47.0		
		Minimum	136.0			44.0		
		Maximum	160.0			53.0		
		SD	10.0			4.1		
		N	4			4		
<i>Bison</i> sp. (Moyà-Solà, 1987)	Venta Micena (Spain)	Mean	151.7					25.1
		Minimum	148.0					23.0
		Maximum	158.0					27.4
		SD	5.5					2.2
		N	3					3
<i>Bison (Eobison) degliuili</i> (Masini, 1989)	Pirro Nord (Italy)	Mean	140.8	109.4	58.2	45.2	44.2	36.5
		Minimum	138.5	103.0	57.2	41.3	42.0	34.5
		Maximum	143.0	119.2	59.2	49.0	48.0	39.5
		SD	3.2	8.6	1.4	5.4	3.3	2.7
		N	2	3	2	2	2	3
<i>Bison mienneri</i> (Sher, 1997)	Untermassfeld (Germany)	Mean	177.1		70.0	59.2	52.4	44.6
		Minimum	163.5		61.0	53.4	47.8	37
		Maximum	189.0		79.6	68.3	59.3	49.5
		SD	7.9		5.0	4.2	3.1	3.5
		N	21		20	20	21	21
<i>Bison schoetensocki</i> (Moullé, 1992)	Le Vallonnet (France)	Mean	158.0			50.0	48.5	
		Minimum	155.0				46.5	
		Maximum	161.0				50.5	
		SD	4.2				2.8	
		N	2				1	2
<i>Bison schoetensocki</i> (This paper)	Vallparadis Composite Section (Spain)	Mean	172.7	127.1	70.2	56.3	50.9	43.2
		Minimum	160.8	115.3	66.7	51.2	47.3	38.3
		Maximum	189.4	139.1	73.5	60.0	53.2	46.9

<i>Bison schoetensocki</i> (Brugal, 1995)	SD	9.1	7.3	2.3	3.5	2.1	3.0
	N	7	7	7	7	7	7
	Mean	180.0	123.1	70.6	59.4		
	Minimum		120.0	66.5	54.0		
	Maximum		130.2	73.0	62.0		
<i>Bison priscus</i> (Maniakas and Kostopoulos, 2017a)	SD	4.1	2.5	2.5	3.7		
	N	1	5	5	4		
	Mean	199.3		81.8	74.0	63.0	52.9
	Minimum	185.0		79.6	69.9	59.5	50.5
	Maximum	206.0		83.6	77.1	65.5	54.0
<i>Bison priscus</i> (Vercoutère and Guérin, 2010)	SD	8.3		1.8	3.0	2.3	1.4
	N	4		4	4	4	4
	Mean	190.0		78.3	66.7	54.0	48.7
	Minimum	187.0		75.0	63.0	51.0	48.0
	Maximum	195.0		82.0	71.0	57.0	49.0
<i>Bison priscus</i> (Vasiliev, 2008)	SD	3.6		3	4	4.2	0.6
	N	4		4	3	2,00	3
	Mean	188.3		74.8	65.1	52.4	49.6
	Minimum	163.0		66.0	56.0	46.0	39.5
	Maximum	201.0		85.7	75.0	57.0	54.6
<i>Bison priscus</i> (Vasiliev, 2008)	SD						
	N	23		50.0	44	25	24
	Mean	186.3		73.3	64.4	52.1	50.3
	Minimum	170		65.2	51.3	44.3	42.7
	Maximum	210		82.7	74	59	58
<i>Bos primigenius</i> (Brugal, 1985)	SD						
	N	53.0		77	69.0	51.0	53.0
	Mean	179.1		71.5	63.1		
	Minimum	164.5		61.8	54.6		
	Maximum	199.3		81.1	77.3		
<i>Bison bonasus</i> (Empel and Roskož, 1963)	SD						
	N	35.0		80	35		
	Mean	159.8			56.0	43.2	40.0
	Minimum	142.0			49.0	37.0	34.0
	Maximum	181.0			66.0	50.0	50.0
	SD	11.3			5.4	3.6	4.3
	N	33			28	33	33

Table S28. Comparative measurements (mm) of the metatarsal in selected *Leptobos* and *Bison* s.l. samples. Abbreviations: DEW, distal epiphysis width; DET, distal epiphysis thickness; DW, diaphysis width (midshaft); DT, diaphysis thickness (midshaft); Lmax, maximum length; PET, proximal epiphysis thickness; PEW, proximal epiphysis width.

Taxon	Locality	Statistics	Lmax	PEW	PET	DW	DT	DEW	DET
<i>Leptobos etruscus</i> (Masini, 1989)	Senèze/Olivola (France/Italy)	Mean	273.8	50.4	50.1	34.2	33.8	55.1	35.0
		Minimum	258.0	46.4	45.0	31.3	29.5	50.2	32.0
		Maximum	290.5	55.7	53.5	37.4	36.3	59.0	37.3
		SD	8.6	2.7	2.6	2.1	2.1	2.7	1.8
<i>Bison (Fobison) palaeosinensis</i> (Tong et al., 2016; Masini, 1989)	Various localities of China	N	16	16	16	16	15	15	10
		Mean	256.2	51.1	50.9	32.2	33.2	59.4	32.8
		Minimum	237.0	46.5	45.0	31.4	30.9	52.5	31.6
		Maximum	280.0	57.0	60.0	32.9	35.5	67.0	34.0
<i>Bison</i> sp. (Maniakas and Kostopoulos, 2017a)	Venta Micena (Spain)	SD	19.8	4.6	6.1	1.1	3.3	6.4	1.7
		N	6	6	6	2	2	6	2
		Mean	264.7	51.1	48.5	32.8	34.5	57.3	34.4
		Minimum	240.9	43.5	45.0	27.4	29.6	50.2	29.5
<i>Bison (Fobison) degiulii</i> (Masini, 1989)	Pirro/Capena (Italy)	Maximum	286.2	59.4	53.9	38.0	37.7	63.8	38.3
		SD	12.9	4.4	3.7	3.3	2.5	4.0	2.2
		N	15	24	23	20	19	20	20
		Mean	257.3	52.8	54.3	37.1	34.7	57.9	34.9
<i>Bison (Fobison) cf. degiulii</i> (Kostopoulos et al., 2018)	Mygdonia basin (Various localities) (Greece)	Minimum	246.8	50.9	52.3	34.6	32.4	51.7	32.9
		Maximum	267.8	56.7	58	39.5	36.8	66.0	37
		SD	14.9	3.4	3.2	2.5	2.2	5.4	1.5
		N	2	3	3	3	3	5	5
<i>Bison memneri</i> (Sher, 1997; Maniakas and Kostopoulos 2017a)	Untermassfeld (Germany)	Mean	275.5	55.3	55.0	34.3	35.2	63.7	39.3
		Minimum	261.2	51.1	51.4	31.1	31.9	59.5	36.9
		Maximum	286.9	62.1	64	38.1	40.3	70.6	40.9
		SD	8.4	2.9	3.5	2.3	2.6	3.2	1.2
<i>Bison schoetensacki</i>	Le Vallonnet (France)	N	10	16	17	15	14	12	12
		Mean	315.0	64.0	61.7	41.3	41.0	72.8	45.1
		Minimum	301.4	56.9	53.8	35.6	35.7	64.5	39.5
		Maximum	329	72.3	68.6	47.3	45.2	80	50.6
		SD	9.5	4.5	4.9	3.9	3.1	4.8	2.8
		N	18	18	18	18	17	19	19
		Mean	298.0	69.8	61.3			77.7	48.7

<i>Bison priscus</i> (Maniakas and Kostopoulos, 2017a)	Taubach (Germany)	SD	15	5.9	5.6	4.1	7.2	
		N	6	6	6	6	6	
		Mean	284.2	65.5	62.8	46.7	46.7	80.1
		Minimum				41.1	41.4	72.4
		Maximum				53.9	51.9	89.3
		SD				6.6	5.3	6.9
<i>Bison priscus priscus</i> (Vercoutère and Guérin, 2010)	Romain-la-Roche (France)	N	1	1	1	3	5	
		Mean	305.8	71.5	66.0	47.3	48.7	76.2
		Minimum	298.0	70.0	64.0	46.0	47.0	75.0
		Maximum	314.0	73.0	68.0	48.0	50.0	77.5
		SD	8.0	2.1	2.8	1.2	1.5	1.3
		N	3	2	2	3	3	3
<i>Bison priscus</i> (Sala, 1986)	Cava Filo (Italy)	Mean	294.3	65.2	63.3		83.3	
		Minimum	281.0	61.0	56.5		73.0	
		Maximum	308.0	74.0	68.0		89.0	
		SD	10.4	5	4.2		5.4	
		N	6	6	6		6	
		Mean	266.4	58.5	58.0	36.6		79.7
<i>Bison priscus</i> (Sher, 1997)	North East Siberia (Russia)	Minimum	254.0	51.5	53.5	29.5	70.5	
		Maximum	283.0	69.5	66	48.0	78.5	
		SD	7.2	4.7	3.8	4.5	5.6	
		N	25	25	24	25	6	
		Mean	279.8	65.3	60.6	42.6	40.5	75.0
		Minimum	254.6	57.7	56.0	37.5	33.7	69.5
<i>Bison priscus</i> (Maniakas and Kostopoulos, 2017a)	Various localities of England (United Kingdom)	Maximum	302.1	70.2	67.1	49.1	79.8	
		SD	13.4	4.1	3.6	4.2	3.9	
		N	8	8	8	8	8	
		Mean	296.7	66.6	64.6	44.4	42.0	77.7
		Minimum	278.3	56.8	55.5	34.7	38.0	68.3
		Maximum	314.0	75.4	70.5	50.2	47.0	86.7
<i>Bison priscus</i> (Vasiliev, 2008)	Krasny Yar, R-W (Russia)	SD						
		N	30	43	41	36	42	
		Mean	293.4	65.7	63.4	41.7	42.1	76.6
		Minimum	264.0	56.2	56.0	34.3	36.4	67.5
		Maximum	309.0	73.2	68.5	47.5	46.4	84.0
		SD						
<i>B. priscus priscus</i> (Vasiliev, 2008)	Taradanovo, W1-2 (Russia)	N	33	38	37	38	43	
		Mean						
		Minimum						
		Maximum						
		SD						
		N						

<i>Bison priscus</i> (Vasiliev, 2008)	Krasny Yar, WZ	Mean	286.3	59.6	57.3	36.8	38.3	73.8	42.1
		Minimum	285.5	57.8	55.0	32.8	32.0	71.2	41.5
		Maximum	287.0	61.3	59.2	38.8	41.0	76.4	44.0
		SD							
		N	2	5	5	4	4	3	3
<i>Bison priscus</i> (Castaños et al., 2012)	Kiputz IX (Spain)	Mean	296.5	65.8		42.6		81.2	45.9
		Minimum	268.0	51		36.5		70	40.5
		Maximum	318.0	79		51.0		91	51.5
		SD	16.3	6.9		5.7		7.4	3.8
		N	12	23		12		12	12
<i>Bison bonasus</i> (Empel and Roskoz, 1963)	Warsaw (Polonia)	Mean	260.9	58.0	53.2			62.0	41.5
		Minimum	242.0	47.0	44.0			51.0	36.0
		Maximum	288.0	69.0	63.0			72.0	48.0
		SD	11.1	5.4	4.3			5.3	2.9
		N	39	39	39			39	39
<i>Bos primigenius</i> (Brugal, 1985)	Lunel Viel (France)	Mean	288.4	66.5	64.8	44.8	45.1	77.4	38.4
		Minimum	263.7	53.4	54.8	35.7	38.3	68.0	32.0
		Maximum	312.7	78.7	74.6	55.0	52.7	89.3	42.7
		SD							
		N	52	92	92	63	63	52	54

Table S29. Ratio (%) between distal diaphysis width (DDW) and distal maximum width (DEW) in metatarsals of various species of bovids.

Taxon	DDW/DEW*100
<i>Leptobos etruscus</i> (Masini, 1989)	range: 94.2–101.3; mean = 98.2; N = 14
<i>Bison</i> sp. Venta Micena (Maniakas and Kostopoulos, 2017a)	range: 95.1–100.0; mean = 97; N = 19
<i>Bison</i> (<i>Eobison</i>) <i>degjuli</i> (Masini, 1989)	range: 93.3–96.7; mean = 95; N = 2
<i>Bison</i> (<i>Eobison</i>) cf. <i>degjuli</i> (Kostopoulos et al., 2018)	range: 93.8–106.8; mean = 98.6; N = 12
<i>Bison menneri</i> (Sher, 1997)	range: 96.4–105.4; mean = 99.8; N = 19
<i>Bison schoetensocki</i> Vallparadis Composite Section (This paper)	range: 90.8–103.3; mean = 98.7; N = 8
<i>Bison schoetensocki</i> Süssenborn (Maniakas and Kostopoulos, 2017a)	range: 94.8–98.8; mean = 97.6; N = 6
<i>Bison schoetensocki</i> Dürfort (Brugal, 1995)	range: 97.1–102.9; mean = 99.9; N = 3
<i>Bison priscus</i> Taubach (Sher, 1997)	range: 93.9–96.9; mean = 95.2; N = 8
<i>Bison priscus</i> Romain-la-Roche (Vercoutère and Guérin, 2010)	range: 101.3–108.0; mean = 105.7; N = 3
<i>Bison priscus</i> UK (Maniakas and Kostopoulos, 2017a)	range: 95.7–99.7; mean = 97.4; N = 8
<i>Bos primigenius</i> Romain-la-Roche (Vercoutère and Guérin, 2010)	range: 91.7–98.6; mean = 95.7; N = 3
<i>Bos primigenius</i> (Brugal, 1985)	average: 93.7; N = 52

Table S30. Principal component analysis of metatarsals using seven selected variables (see Section 3 and Fig. 10). Eigenvalue and % variance of the PCs and coefficient of each variables for each PC. Abbreviations as in Table 4.

	PC 1	PC 2	PC 3	PC 4	PC 5	PC 6	PC 7
Eigenvalue	0.00104894	0.00055803	0.000459951	0.000312436	0.00015311	0.000110268	9,84E-15
% variance	39.692	21.116	17.404	11.822	57.936	41.725	3,73E-12
mv Lmax	0.81154	-0.35556	-0.13103	-0.10965	-0.19147	0.079202	0.37796
mv PET	-0.020849	0.15944	-0.13173	-0.525	0.73203	-0.049449	0.37796
mv PEW	-0.2466	0.039901	-0.17232	-0.20579	-0.43866	-0.7282	0.37796
mv DT	-0.10104	-0.062571	0.9035	-0.10061	-0.087596	0.09437	0.37796
mv DW	-0.42049	-0.66638	-0.20568	0.3781	0.18127	0.13469	0.37796
mv DETI	0.20422	0.50097	0.014653	0.70483	0.19835	-0.16767	0.37796
mv DEW	-0.22677	0.3842	-0.2774	-0.14187	-0.39393	0.63706	0.37796

Table S31. Principal component analysis of metatarsals following Scott and Barr (2004) (see Section 3 and Fig. 10). Eigenvalue and % variance of the PCs and coefficient of each variables for each PC. Abbreviations as in Table 4.

	PC 1	PC 2	PC 3	PC 4	PC 5	PC 6	PC 7	PC 8
Eigenvalue	0.00107108	0.000679073	0.000467574	0.000233519	0.00014504	8.62E+00	3.97E+00	2.76E+00
% variance	38.951	24.695	17.004	84.921	52.745	31.359	14.453	10.025
re Lmax	0.90652	0.12343	-0.049579	0.30502	-0.20162	0.1265	-0.097363	0.036869
re DW	-0.046536	0.82418	-0.3662	-0.083114	0.30869	0.04473	0.061286	0.2766
re DT	0.1545	0.24712	0.79638	-0.46758	-0.023953	0.10068	0.13179	0.18476
re DETI	0.23835	-0.28778	-0.23494	-0.26483	0.35307	0.26888	0.72778	-0.091805
re DETm	0.18033	-0.32507	-0.23471	-0.39033	0.012315	-0.42979	-0.16882	0.66408
re DEW	-0.23325	-0.14062	0.028346	0.31295	-0.2064	0.6256	0.091064	0.62033
re PEW	-0.075716	0.13996	0.097497	0.35516	-0.35665	-0.53833	0.63182	0.15112
re PET	0.052133	-0.12875	0.32958	0.48462	0.75424	-0.1835	-0.061169	0.17586

Table S32. Pairwise comparison results based on MANOVA ($p < 0.05$) for seven raw selected variables of metatarsals of several *Bison* s.l. and *Leptobos etruscus* samples. *L. etruscus*: samples from Olivola, Senèze; *B. (Eobison) sp.*: sample from Venta Micena; *B. (Eobison) cf. degiulii*: sample from Mygdonia Basin; *B. menneri*: sample from Untermassfeld; *B. schoetensacki*: samples from Le Vallonnet, Durfort, Süßenborn, Mauer; *B. priscus priscus*: samples from Taubach, Romain-la-Roche; *B. priscus mediator*: samples from UK (several sites); see Fig. 9). Abbreviations are given in Tables 2 and 4. Values of $p < 0.05$ are in bold.

	<i>Eobison</i> sp.	<i>Eobison</i> cf. <i>degiulii</i>	<i>Bison menneri</i>	<i>Bison schoetensacki</i>	VCS	<i>B. priscus priscus</i>	<i>B. priscus mediator</i>
<i>Leptobos etruscus</i>	0.08	0.007	<0.001	0.001	0.025	0.044	<0.001
<i>Eobison</i> sp.		0.041	<0.001	0.00	0.085	0.086	<0.001
<i>Eobison</i> cf. <i>degiulii</i>			<0.001	0.226	0.437	0.32	0.016
<i>Bison menneri</i>				0.006	0.002	0.016	<0.001
<i>Bison schoetensacki</i>					0.274	0.594	0.179
VCS						0.769	0.075
<i>B. priscus priscus</i>							0.567

Table S33. Measurements (mm) of the phalanges of *Bison schoetensacki* from Vallparadis Estació (EVT) and Cal Guardiola (CGR) layers. Abbreviations: DET, distal end thickness; DEW, distal end width; Lmax, maximum length; PEAT, proximal end articular thickness; PEAW, proximal end articular width; SLmax, maximum length of the sole; SOL, oblique length of the sole; SW, width at the middle; Tmax, maximum thickness; Wmax, maximum width; Wmin, minimum width.

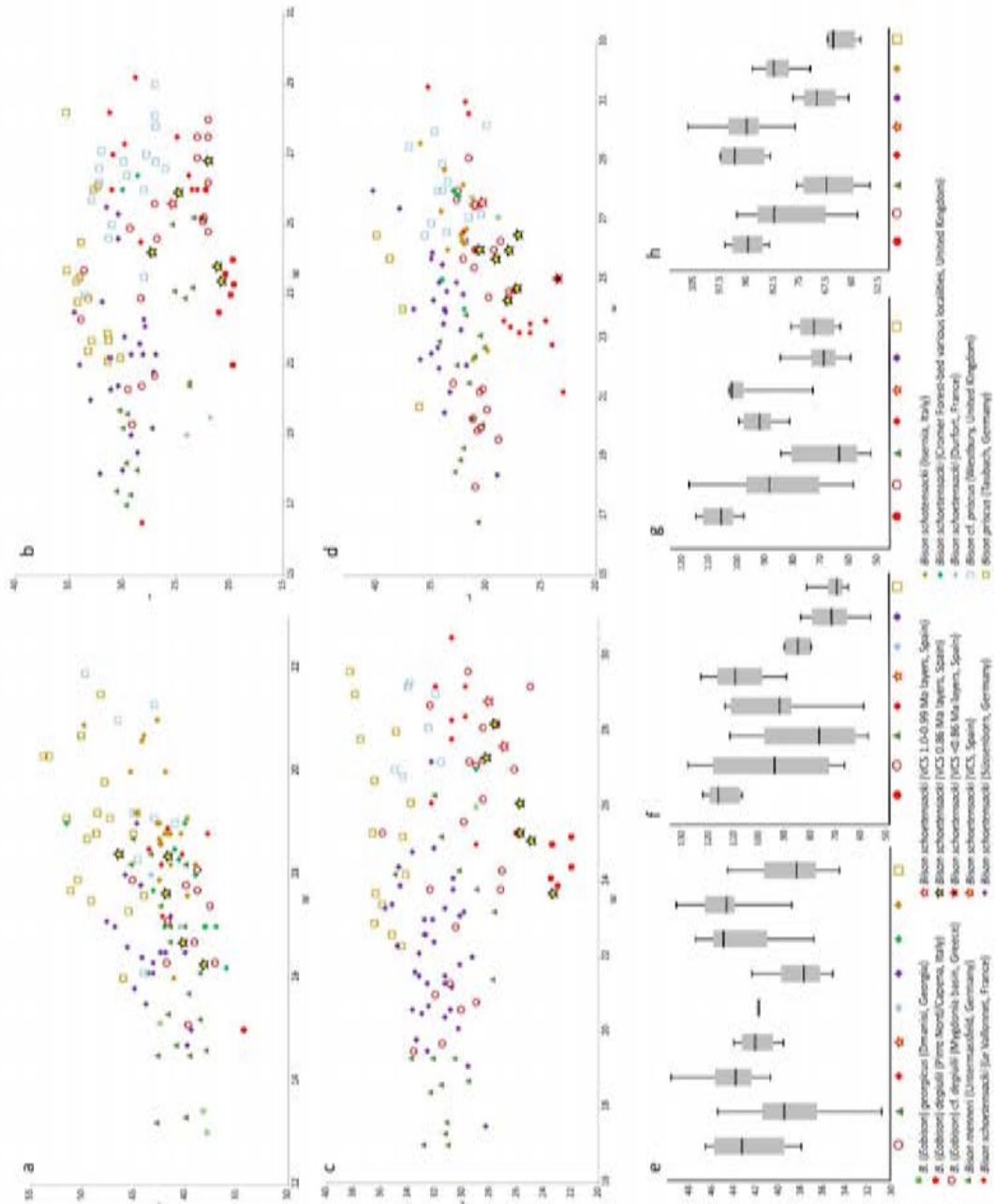
ID Specimen	Layer	Element	Lmax	Wmax	Tmax	PEAW	PEAT	DEW	DET	Wmin	SLmax	SOL	SW
IPS14977	CGRD7	Proximal phalanx	71.6	35.7	42.3	32.1	29.4	31.1	26.7	30.2			
IPS61879	CGRD3	Proximal phalanx	77.8	33.9	40.0	30.7	28.7	32.7	27.0	29.9			
IPS92924	EVT10	Proximal phalanx	71.0	38.8	43.1	36.6	30.5	37.1	27.3	33.8			
IPS92925	EVT7	Proximal phalanx	74.8	39.7	42.6	34.8	33.9	35.0	28.5	30.0			
IPS92926	EVT10	Proximal phalanx	77.7	34.7	42.7	32.5	28.9	31.9	24.0	32.0			
IPS92927	EVT7	Proximal phalanx	72.7	35.0	39.5	30.4	29.3	32.4	25.2	27.9			
IPS107621	EVT12	Proximal phalanx	74.0	35.5	38.8	32.1	28.7	32.9	26.2	32.1			
IPS114554	EVT7	Proximal phalanx	83.5	39.1	43.7	34.2	35.7	36.9	28.2	34.5			
IPS118118	EVT12	Proximal phalanx	77.2	39.4	43.1	34.1	35.7	27.2	38.1	35.6			
IPS118119	EVT12	Proximal phalanx	73.4	41.5	46.5	35.0	38.2	29.1	41.7	36.8			
IPS16778	CGRD2	Intermediate phalanx	57.0	43.4	46.8	41.7	32.6	34.7	42.3	35.0			
IPS40612	CGRD2	Intermediate phalanx	50.0	40.9	47.4		27.6						
IPS107624	EVT12	Intermediate phalanx	55.0	40.4	40.5	37.0	30.6	28.8	36.4	31.6			
IPS118114	EVT12	Intermediate phalanx	50.2	41.1	47.0	39.5	31.1	38.5	36.0	33.6			
IPS39142	CGRD2	Distal phalanx	92.8	45.1	49.6	33.2					89.0	74.7	34.3
IPS41597	CGRD2	Distal phalanx	97.6	48.9	51.0	34.0	44.0				97.5	76.8	35.1
IPS107622	EVT12	Distal phalanx	95.0	37.5	43.4	32.1	35.7				94.8	80.9	30.0
IPS107623	EVT12	Distal phalanx	95.9	50.7	47.3	33.5	39.8				95.5	80.6	36.9
IPS107625	EVT12	Distal phalanx	83.2	42.0	46.4	27.3	33.5				80.5	70.4	30.9
IPS118112	EVT12	Distal phalanx	72.8	33.0	46.2	29.2	38.3				79.8	69.0	29.2
IPS118113	EVT12	Distal phalanx	92.4	41.5	52.1	36.2	43.2				86.3	86.3	33.0

Table S34. Sexual dimorphism in various samples of *Bison* s.l.. We computed the difference (%) between male and female of four selected metacarpal measurements following the equation given by Schertz (1936b) (equation in Section 3 of the main text). Abbreviations: DEW, distal end width; DW, diaphysis width; Lmax, maximum length; PEW, proximal end width.

Taxa	Variable	Female mean values (mm)	Male mean values (mm)	Difference %
<i>Bison menneri</i> , Untermassfeld (Sher, 1997; Maniakas and Kostopoulos, 2017a)	Lmax	272.8	283.3	3.7
	PEW	74.1	84.3	12.1
	DW	42.5	51.6	17.7
	DEW	71.8	83.4	14.0
<i>Bison schoetensacki</i> , Le Vallonnet (This paper)	Lmax	253.7	266.4	4.8
	PEW	74.7	85.1	12.2
	DW	49.8	59.1	15.9
	DEW	70.8	82.8	14.5
<i>Bison schoetensacki</i> , EVT12 (VCS) (This paper)	Lmax	229.7	234.7	2.1
	PEW	78.6	79.1	12.5
	DW	37.3	50.4	25.9
	DEW	66.7	79.1	15.7
<i>Bison schoetensacki</i> , Süssenborn (Maniakas and Kostopoulos, 2017a)	Lmax	239.5	252.7	5.2
	PEW	71.1	81.1	12.3
	DW	43.9	47.7	7.8
	DEW	67.9	78.7	13.7
<i>Bison schoetensacki</i> , Durfort (Brugal, 1995)	Lmax	242.5	249.5	2.8
	PEW	69.8	80.8	13.7
	DW	42.4	50.4	15.9
	DEW	68.7	81.4	15.7
<i>Bison priscus</i> , Châtillon-Saint-Jean (This paper)	Lmax	244.7	251.9	2.8
	PEW	79	93.8	15.8

<i>Bison priscus</i> North Sea (Drees, 2005)	DW	49	60.9	19.7
	DEW	77.3	92.2	16.2
	Lmax	235.2	241.9	2.8
	PEW	78.6	88.3	13.1
	DW	45.6	56.7	19.6
	DEW	78.4	90.0	12.4
	Lmax	236.7	243.0	2.6
	PEW	78.6	89.8	12.5
	DW	46.1	57.7	20.0
	DEW	80.1	91.5	12.4
<i>Bison priscus</i> Krasny Yar, R–W, (Vasiliev, 2008)	Lmax	205.0	215.0	4.7
	PEW	67.0	74.0	9.5
	DW	35.0	44.0	20.5
Extant <i>Bison bonasus</i> (Reshetov and Sukhanov, 1979)	DEW	63.0	70.0	10.0
	Lmax	203	211.6	4.1
	PEW	64.2	75.1	14.5
Extant <i>Bison</i> spp. (Lewis et al., 2005)	DW	36.9	48.6	24.1
	DEW	63.6	75.1	15.3

Figure S1. a-d, Bivariate plots of length (L) vs width (W) of m3 (a), M1 (b), M2 (c), and M3 (d) in several *Bison* s.l. species. e-h, Box-plots of W/L% of m3 (e), M1 (f), M2 (g), and M3 (h) in several *Bison* s.l. species.



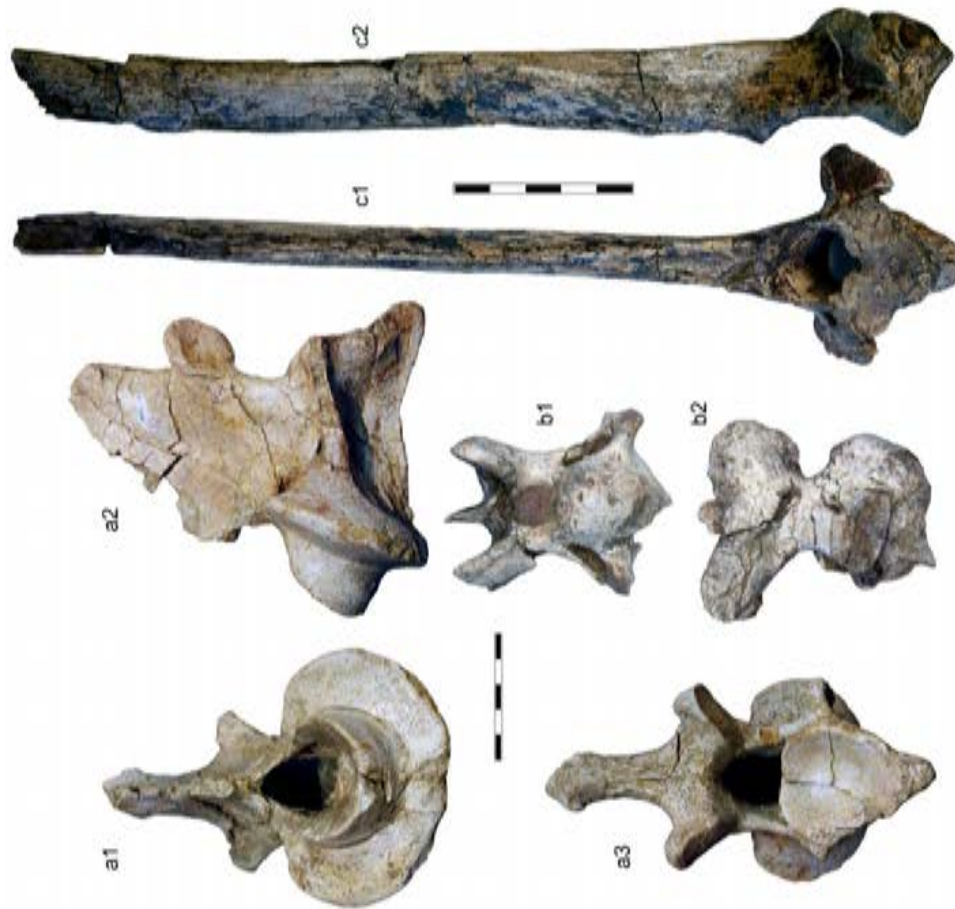


Figure S2. Vertebral remains of *Bison schoetensacki* from the Vallparadis Composite Section. a, Axis IPS114451 in anterior (1), left lateral (2), and posterior (3) views; b, Cervical vertebra IPS107605 in anterior (1) and right lateral (2) views; c, Thoracic vertebra IPS92954 in anterior (1) and right lateral (2) views. Scale bar: 100 mm.

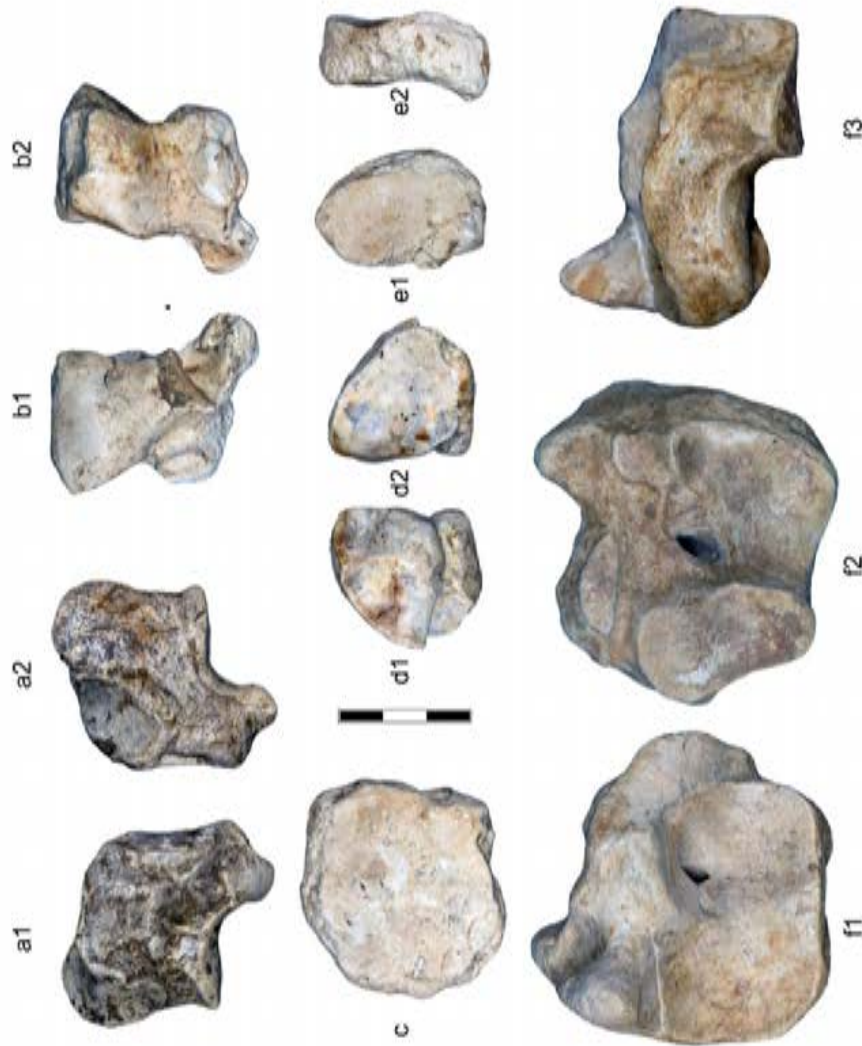
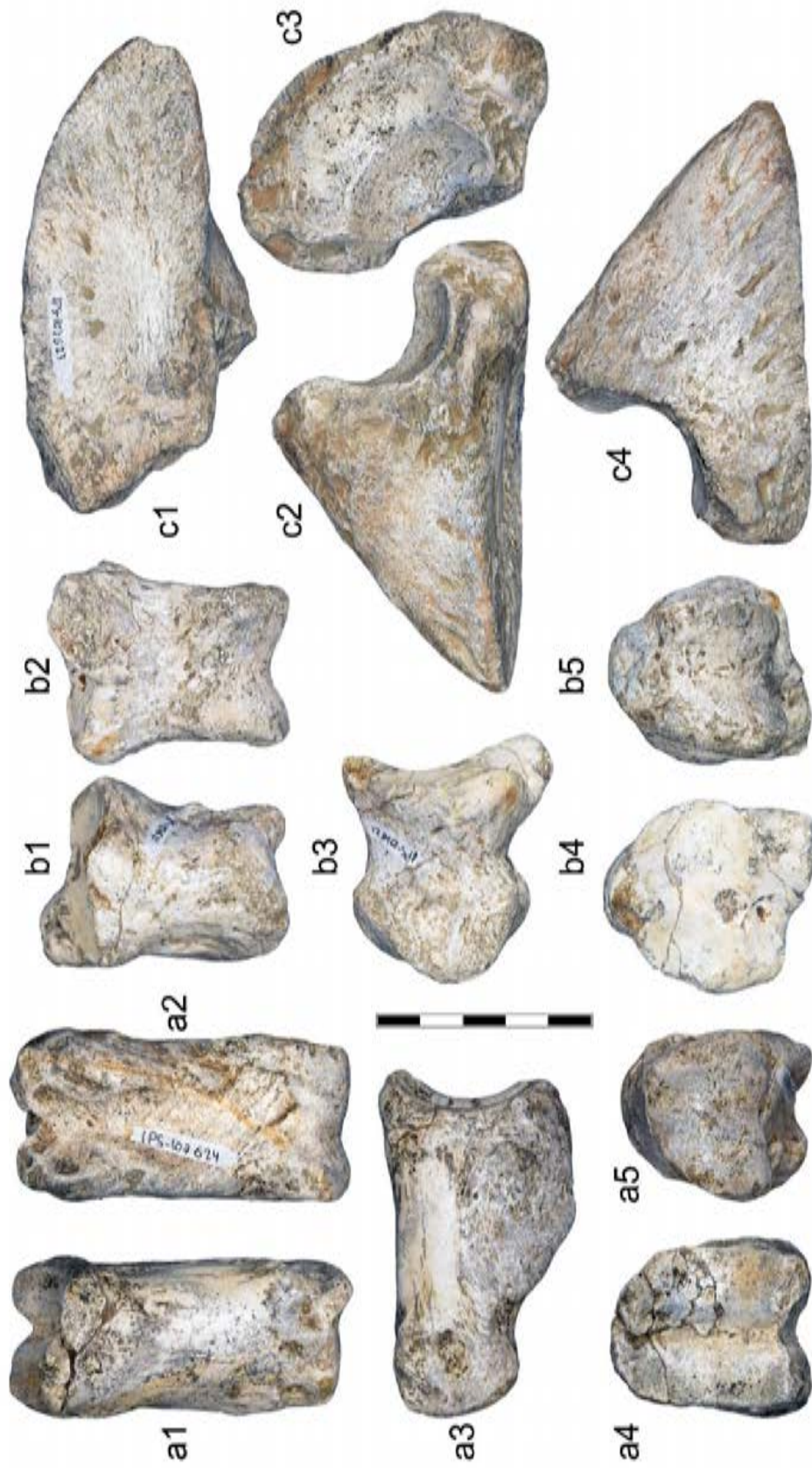


Figure S3. Carpals and tarsals of *Bison schoetensocki* from the Vallparadis Composite Section. a, Right pyramidal IPS91545 in medial (1) and lateral (2) views; 2, Right semilunar IPS92960 in proximal (1) and distal (2) views; c, Left capitotrapezoid IPS92963 in distal view; d, Left unciform in proximal (1) and distal (2) views; e, Right cuneiform (IPS92965) in distal (1) and medial (2) views; f, Left cubonavicular in proximal (1), distal (2), and anterior (3) views. Scale bar: 30 mm.



Supplementary Figure 4. Phalanges of *Bison schoetensocki* from the Vallparadis Composite Section: a, Left proximal phalanx IPS107624 in anterior (1), posterior (2), lateral (3), proximal (4), and distal (5) views; b, Right intermediate phalanx IPS107621 in anterior (1), posterior (2), lateral (3), proximal (4), and distal (5) views; c, Right distal phalanx IPS107623 in posterior (1), medial (2), proximal (3), and lateral (4) views. Scale bar: 50 mm.

Supplementary references

- Castaños, J., Castaños, P., Murelaga, X. and Alonso-Olazabal, A., 2012. Kiputz IX: un conjunto singular de bisonte esteparrio (*Bison priscus* Bojanus, 1827) del Pleistoceno Superior de la Península Ibérica. *Ameghiniana* 49, 247–261.
- Empel, W. and Roskosz, T., 1963. Das Skellett der Gliedmassen des Wisents, *Bison bonasus* (Linnaeus, 1758) *Acta Theriol.* 7, 259–297.
- Duvernois, M.P. and Guérin, C., 1989. Les Bovidae (Mammalia, Artiodactyla) du Villafranchien Supérieur d'Europe Occidentale. *Geobios* 22, 339–379.
- Martin, T., 1987. Artunterschiede an den Langknochen großer Artiodactyla des Jungpleistozäns Mitteleuropas. *Cour. Forsch.-inst. Senck.* 96, 1–121.
- Reshetov V.Yu., Sukhanov V.B. 1979 Postcranial skeleton. In: V.E. Sokolov (Ed.), *European Bison—Morphology, Systematics, Evolution*, Ecology, Nauka, Moscow (1979), 142–173 (in Russian)

ACKNOWLEDGEMENTS

This thesis was conducted thanks to the AGAUR (Agència de Gestió d'Ajuts Universitaris i de Recerca) FI pre-doctoral grant by the Generalitat de Catalunya (2019 FI_B 00579) with the support of the “Secretariat d'Universitats i de Recerca from the Generalitat de Catalunya” and the European Social Fund. The works produced in this thesis were possible thank to the consolidated research group 2021 SGR 00620 (AGAUR, Generalitat de Catalunya), the MINECO project “The Cenozoic primates from the Iberian Peninsula and their contribution to the reconstruction of the evolutionary history of the group” (PID2020-116908GB-I00), the “Projecte de recerca quadriennal en materia d'arqueologia i paleontologia” (Generalitat de Catalunya): “La Transició Pleistocè inferior mitjà a Catalunya” (CLT009/18/00070) and the Generalitat de Catalunya (CERCA Programme).

I want to thank the coordinator of the PhD program in Geology from the Universitat Autònoma de Barcelona Prof. Joan Reche, for his constant help during the years of my PhD. I am grateful also to the Comitè de Seguiment de doctorat including Prof. M. Luisa Arboleya, Prof. Mercè Corbella and Prof. Marc Furió. I want to thank also Dr. Asier Gómez Olivencia and Prof. Dimitris Kostopoulos for the international doctorate mention.

During these years I had the pleasure to work with many people. I want to thank them for the direct (and indirect) support that they gave me in the creation of this thesis.

First of all, my two directors Dr. Joan Madurell-Malapeira and Dr. Marco Cherin. Both were my mentors and (each one in his own way) taught me all I know about being a palaeontologist and doing science. Since my first steps in the world of academia they gave me all the support that a stubborn and anxious student could need. The fieldworks, the infinite brainstorming, and the discoveries in which we participated together created a bond that is stronger than a simple professional relationship. Having the pleasure of doing what you love with someone that shares the same passion as yours is something special. Thank you, Joan and Marco.

My academic tutor and co-director of the thesis Prof. Salvador Moyà Solà for his constant support during these years and his infinite patience during the painfully bureaucratic procedures. My, more experienced, colleagues with whom I have had hours and hours of talks about palaeontology (and not only): Prof. Dimitris Kostopoulos, Prof. Raffaele Sardella, Prof. Dawid Adam Iurino, Prof. Massimo Delfino, Prof. Giorgio Carnevale, Prof. Bienvenido Martínez-Navarro, Prof. Jean-Philippe Brugal, Prof. David Alba, Prof. Lorenzo Rook, Prof. Marzia Breda, Prof. Faysal Bibi, Prof. Luca Bellucci, Prof. Luca Pandolfi, Dr. Bruno Gómez de Soler, Dr. Gerard Campeny Vall-Llosera, Dr. Saverio Bartolini Lucenti, Dr. Andrea Villa, Dr. Beniamino Mecozzi, Dr. Flavia Strani, Dr. Omar Cirilli, Dr.

Alessio Iannucci and, special mention, Beatrice Azzarà who will be Dr. soon and with whom I shared many years of studies (and deadlines). These palaeontologists come from different places, but all share the same passion.

I would like to acknowledge the effort given by all the co-authors and the reviewers of the manuscripts in this compendium and to all the curators and technicians which provided the data that I manage these years. In particular, I am deeply grateful to the passionate work of Dr. Paola Romi (Soprintendenza Archeologia, Belle Arti e Paesaggio per l'Umbria), without her, the amazing collection of bovid from Pietrafitta would be not part of this thesis.

The ICP has been my second home for many years. I will always be grateful to the people that helped me in this period. David and his enlightening lesson of statistics during the cigarette pause and his “italiano perfetto”, Enric for his aid in the bureaucratic mess that is our world, the great restoration team of the ICP (special mention to Marina, Almu y Ana) which prepared most of the fossils presented here, Josep and Jordi for helping me in finding all the fossils stored in the deep “dungeons” of the ICP, Manel & Manel for the precious help during the long periods of excavation. Judit, Sole, Raef, Fortu, Isaac, Arnau, Àngel, Marc, Júlia, Pere and all the researchers and technicians who passed by the ICP during these years and ended up being part of my life as a palaeontologist.

I want to thank all my colleagues and mates from these PhD years in Barcelona. I will never forget our moments spent together: the excavations, the “covfefe”, the cinemas (in and out of home) and the beers at the Villa. Oriol, Alessandro, Rafel, Andrea, Carmen, Guillem, Chabi, Teresa, Raquel, Claudia, Vic, Isa(aaa)ac, Georgina, Jordi, Kelly, Shub, Sharrah, Anabel and Laura. You are my friends.

My mates, Florian and Guillem. I hate you and I love you. I will miss our philosophical chats at night.

A special thank you to my “sisters” Maria and Sílvia for everything we have done together. We are a trio and our office will always be the best office in the world. A big chunk of my whole life in Barcelona is made by you two and it is something that will be there forever.

I also thank my friends from Perugia, i freghi di F&F e quelli del GS. You know me. I am here, at this moment, because I am just the results of our interactions of the last 32 years.

Lastly, I want to thank my family, this thesis is for you. Ma' and Pa'. You gave me all I needed to follow my dreams. For my mother, being able to cope with my ability to miss every deadline and for my father, always there for speaking about our favourite movies and series. For my sister Marzia, when I have some time (and you too) we play videogames together, I promise. I hope you three will be always happy.

The very last who I wanted to thank is someone who entered in my life and made me understand that I could be a better person. You remind me every day that there is always something good to find. You are an amazing

palaeontologist, and I don't think this thesis would be finished without you (literally). Thank you Elpiniki. You are the best dancer in the world!

These (almost) four years of PhD taught me a lot of things. Too many maybe and I am lucky that my awful memory will help me erasing some of them. Few, however, are stuck somewhere in my brain, and they will always remind me that nothing is certain, everything is a construct, and all is a huge, unbearable mess. Nothing really matters and that's why it's worth studying.

Animale (s.m.): Organismo che richiede un gran numero di altri animali per il proprio sostentamento, dimostrando così in modo inoppugnabile quanto siano generosi i disegni della Provvidenza nel preservare la vita delle sue creature

-Ambrose Bierce "Il Dizionario del Diavolo"